# Halogenation of polypnictogen ligand complexes

Dissertation

zur Erlangung des

DOKTORGRADES DER NATURWISSENSCHAFTEN

(DR. RER. NAT.)

der Fakultät Chemie und Pharmazie

der Universität Regensburg


vorgelegt von

**Anna Garbagnati**

aus Omegna

im Jahr 2022

Diese Arbeit wurde angeleitet von Prof. Dr. Manfred Scheer.

Promotionsgesuch eingereicht am: 03.03.2022

Tag der mündlichen Prüfung: 14.04.2022

Vorsitzender: Prof. Dr. Patrick Nürnberger

Prüfungsausschuss: Prof. Dr. Manfred Scheer

Prof. Dr. Henri Brunner

Prof. Dr. Frank-Michael Matysik

Universität Regensburg

Statutory declaration

I hereby declare in lieu of oath that I have prepared the present work without undue help from third parties and without using any aids other than those specified; the data and concepts taken directly or indirectly from other sources are marked with a reference to the literature.

Anna Garbagnati

This thesis was elaborated within the period from September 2017 and March 2022 in the Institute of Inorganic Chemistry at the University of Regensburg, under the supervision of Prof. Dr. Manfred Scheer.

List of Publications:

A. Garbagnati, M. Seidl, G. Balázs, M. Scheer.

“Halogenation of Diphosphorus Complexes”

*Inorg. Chem*. **2021**, *60*, 5163–5171.

A. Garbagnati, M. Seidl, G. Balázs, M. Scheer.

“Halogenation of the Hexaphosphabenzene Complex

$[(Cp^*Mo)_2(\mu,\eta^6{:}\eta^6\text{-}P_6)]$ – Snapshots on the Reaction Progress”

*Chem.Eur. J. **2022**, e202200669.*

A. Garbagnati, M. Seidl, M. Piesch, G. Balázs, M. Scheer.

“Halogenation of heterobimetallic triple-decker complexes containing $P_5$ and $As_5$ middle deck”

*Polyhedron,* **2022**, *221*, 115854.

A. Garbagnati, M. Seidl, M. Piesch, G. Balázs, M. Scheer.

“Halogenation and nucleophilic quenching of pnictogen-containing cations. Two routes to E-X bond formation in cobalt triple-decker complexes (E = As, P; X = F, Cl, Br, I) ”

*Chem. Eur. J.* **2022**, e202201026.

*To Nicolò,*

*Marta*

*and Michela,*

*my guiding light.*

## Preface

Some of the presented results have already been published during the preparation of this thesis (*vide supra*). The corresponding citations are given at the beginning of the respective chapters.

Each chapter includes a list of authors. At the beginning of each chapter the individual contribution of each author is described.

To ensure uniform design of this work, all chapters are subdivided into “Introduction”, “Results and Discussion”, “Conclusion”, “References” and “Supporting information”. Furthermore, all chapters have the same text settings and numeration of compounds. The depicted molecular structures may differ in their style. A general introduction together with the objectives of this thesis are given at the beginning. In addition, a comprehensive conclusion of this work is presented at the end of this thesis.

# Contents

# 1 Introduction

## 1.1 Phosphorus

Phosphorus is the 15th element of the periodic table and it was originally discovered in the middle of the 17th century, in the city of Hamburg, by the German alchemist Hennig Brand.[1] Brand isolated white phosphorus in 1669 by a process which requires the evaporation of urine followed by the heating of the residue in exclusion of air until a glowing material was formed.[2] The alchemist called the substance cold fire ("kaltes Feuer") or, affectionately, "mein Feuer" because he truly believed that he was in possession of elemental "fire", one of the four Aristotelian elements (earth, water, air and fire).[1,2] The new glowing element was then named phosphorus, from the Greek word phosphoros, meaning "light bringer or bearer".[3]

Over 300 years later, phosphorus still represents the main topic of an active research area and it is omnipresent in everyday life. Despite being found in small amounts in the Earth crust (0.09 wt%) and not being readily bioavailable, phosphorus plays an essential role in biological systems. It is present in the skeleton and teeth in form of hydroxylapatite ($Ca_5(PO_4)_3(OH)$), in the phosphate esters bridges that binds the helix strands of DNA and in the ATP, the most abundant biomolecule in nature, fundamental for the metabolism of biological systems.[4] In addition, synthetic organophosphorus compounds are widely used in the chemical, pharmaceutical and agricultural industries [5] and white phosphorus is well known for its past application in military warfare.[6] Due to its wide application, the industrial production of white phosphorus exceeds 500000 tons annually. The natural source of this element is the mineral apatite (phosphate rock), salts of phosphoric acids with the formula $Ca_{10}(PO_4)_6(X_2)$ (X = OH, F, Cl, Br).[7] The industrial synthesis of white phosphorus proceeds *via* reduction of apatite with quartz sand and coke in an electric furnace (Scheme 1).[5]

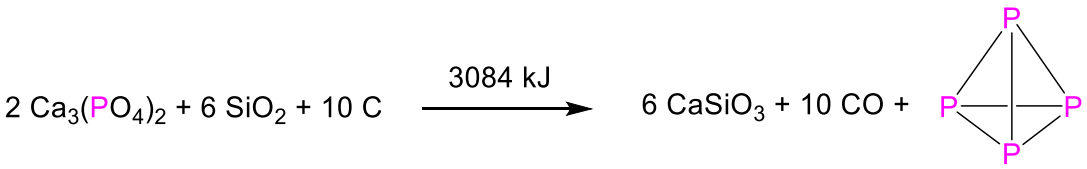


**Scheme 1.** Industrial synthesis of white phosphorus.

Elemental phosphorus exists in three basic allotropic modifications: white, red, and black, which differ significantly in their chemical and physical properties. The structure of white phosphorus is well known, a $P_4$ tetrahedral molecule with P-P single bonds between the atoms (Figure 1, a).[8] The $P_4$ bond lengths are examined by various techniques (X-ray

(2.199 - 2.212 Å)[9,10,11], Raman spectroscopy (2.2228(5) Å)[12], electron diffraction (2.1994(3) Å)[13] and DFT calculations (2.194 Å)[14]). Therefore, the approximate value of 2.21 Å is the standard reference value for a P-P single bond.

The $P_4$ molecule of white phosphorus exists in three different crystalline phases (α, β, γ). The α-P phase is the one that the molecule has at ambient temperature and pressure (cubic structure). By Raman spectroscopy investigations of solid $P_4$ from 12 K up to room temperature, two phase transitions could be observed, at 80 K and 193 K, respectively. The first one is the γ→β transition and it is irreversible. The second one, at approximately 193 K (-78°C), corresponds to the reversible β↔α transition.[15a, b]

The P-P bonds of the tetrahedral $P_4$ are weak (200 $kJ \cdot mol^{-1}$) and this leads to a low activation barrier towards the oxidation. On the other hand, the P-O bonds of combustion products are stronger (330 to 650 $kJ \cdot mol^{-1}$), releasing energy during their formation. These are the reasons why this form of the element is widely pyrophoric, spontaneously combusting upon exposure to air.[16] A possible solution to this problem was presented in 2006 by Mal *et. al,* showing a way to render $P_4$ molecules air-stable and water-soluble *via* their incorporation in self-assemble tetrahedral capsules.[17]

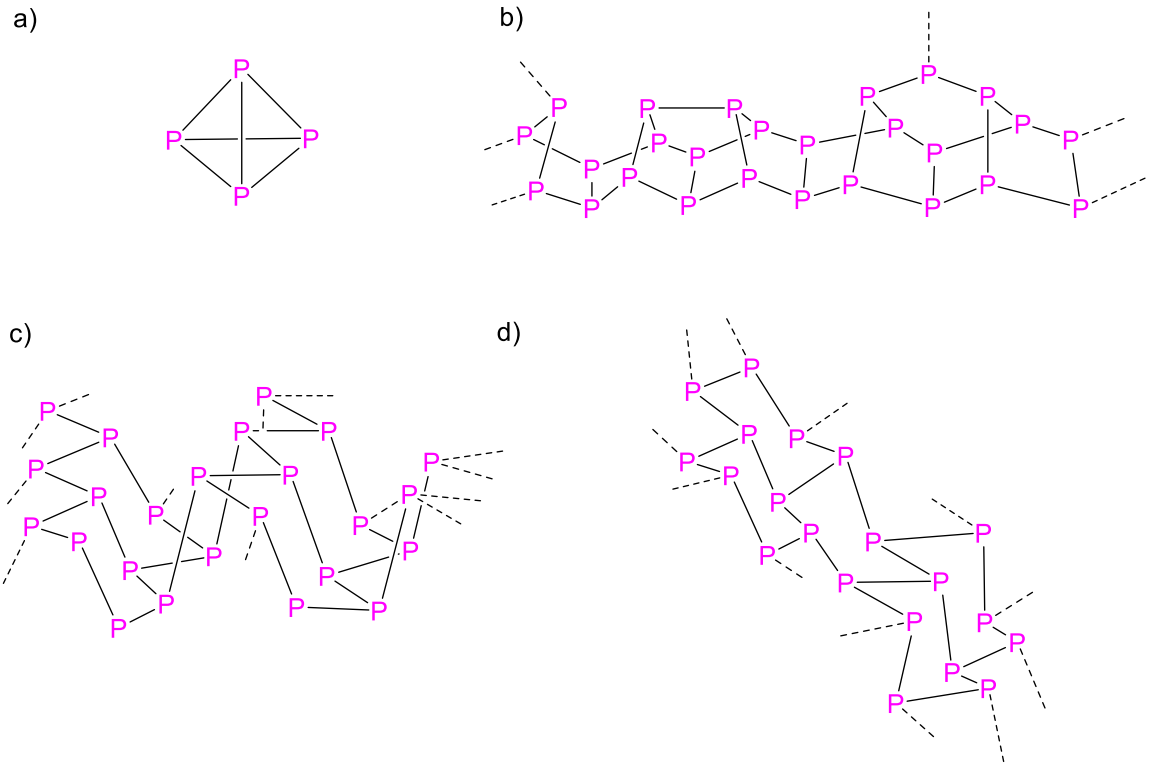


**Figure 1.** Selected examples of allotropic modification of phosphorus. a) $P_4$ tetrahedral modification of white phosphorus; b) Violet or Hittorf's phosphorus; c) orthorhombic black phosphorus; d) rhombohedral black phosphorus.

When white phosphorus is heated or irradiated by UV light, it is transformed into the amorphous red phosphorus, whose structure is considered to be a polymeric network of different building units.[18] This allotrope is commercially available, and it is known as “type I”. By additional annealing, four crystalline phases are formed, labelled as “types II-V’’ red phosphorus.[8] Among these phases, phase IV and V could be structurally characterized. The first to be discovered was phase V in 1865, by Hittorf and in 1969 its crystal structure was elucidated by Thurn and Krebs.[8,18] This modification was named Hittorf’s or Violet phosphorus. It is described as an arrangement of two units, a $P_8$ and a $P_9$ group, linked covalently to each other through two further P atoms to form an infinite, tube-like structure of pentagonal cross-sections (Figure 1, b). The tubes are connected perpendicularly to each other and form layers.[19] In 2005, the crystal structure of phase IV red phosphorus could be characterized by single crystal X-ray diffraction and transmission electron microscopy methods, showing a closer relation to the modification of Hittorf’s phosphorus. This new modification was named Fibrous red phosphorus and it is characterized by a parallel disposition of the connected tubes, contrarily to the violet phosphorus in which they run perpendicularly. The tubes in the Fibrous phosphorus may also be interpreted as zigzag-shaped double chains, which form a corrugated ladder.[18]

The thermodynamically most stable allotrope of the element at room temperature is black phosphorus. It was produced for the first time in 1914 by Bridgman under high pressure at 200°C. In 1981 crystals of black phosphorus were produced by melting red phosphorus at high temperature and pressure.[20] This modification has an orthorhombic crystal structure, in normal conditions, and consists of a layered material in which individual atomic layers are stacked together by van der Waals interactions and can be therefore compared to graphite. In every single layer, each P atom is covalently bonded with the three adjacent ones to form a honeycomb structure. This monolayer black phosphorus, known as “phosphorene”, is a semiconductor.[21] This modification undergoes two reversible structural transitions at room temperature by increasing the pressure. The first transition is from the orthorhombic (Figure 1, c) to the hexagonal (rhombohedral) black phosphorus, which has the same structural motif as grey arsenic (Figure 1, d). On further increase of pressure, the arsenic-type pattern is replaced by a simple cubic one. These transitions go in the opposite direction when the pressure is decreased.[22] Together with the semiconducting properties of this modification, there are possible applications in different fields, such as regenerative medicine and anticancer application.[23]

## 1.2 Activation of white phosphorus by transition metals

The development of a controlled way to activate white phosphorus, to convert it directly to the widely used organophosphorus compounds, is highly desirable. The production of the latter is still based on the chlorination of white phosphorus into $PCl_3$, $PCl_5$ or $POCl_3$, followed by their functionalization with alcohols, Grignard or organolithium reagents (Scheme 2, right). Since this reaction is of great industrial relevance, the ideal would be to have a sustainable and environmentally friendly process. Therefore, the production of stoichiometric amounts of waste (HCl, LiCl, MgClX) and the use of extremely toxic and corrosive chlorine gas represents the main problem.[5,24]

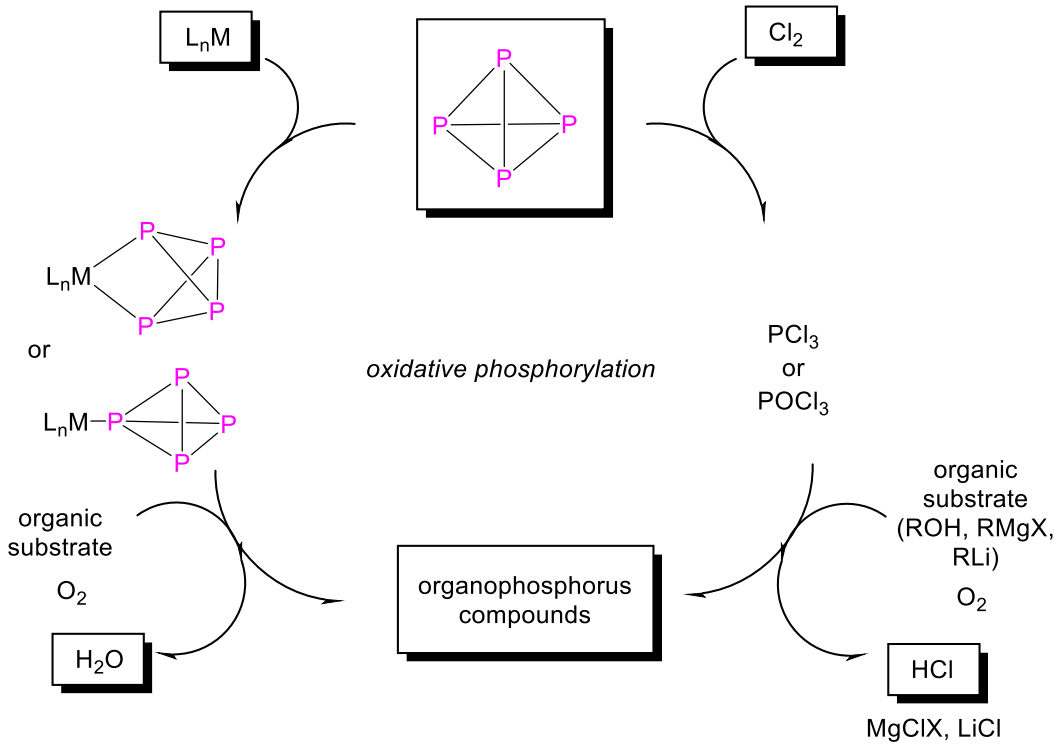


**Scheme 2.** right) Classical process used for industrial $P_4$ activation; left) Possible homogeneous catalytic pathway inspired by the principle of green chemistry, with production of water instead of HCl as side product. This shows the key role of the metal fragment {$L_nM$}.

Until now, the activation of $P_4$ was carried out with the use of heterocyclic carbenes,[25] highly nucleophilic main group compounds[26] and early- and late-transition metal fragments.[5,24,27] The latter is a high interest research field based on the idea that it is possible to eventually find catalytic methods that convert $P_4$ directly to organophosphorus derivatives, by investigating the fundamental reactivity of $P_4$ towards reactive metal centres (Scheme 2, left). The ideal catalyst would be a suitable transition metal complex able to cause the selective oxidative phosphorylation reaction.

The activation of white phosphorus in the presence of unsaturated metal fragments consists in the controlled and consecutive cleavage of P-P bonds within the $P_4$ tetrahedron, which normally proceeds under thermolytic or catalytic conditions. This process may follow different degradation pathways, which always starts from the formation of the "$P_4$ butterfly" species and whose further cleavage leads to cyclic, branched, or linear $P_n$ fragments (Scheme 3). These fragments are in turn stabilized by transition metal or main group compounds.

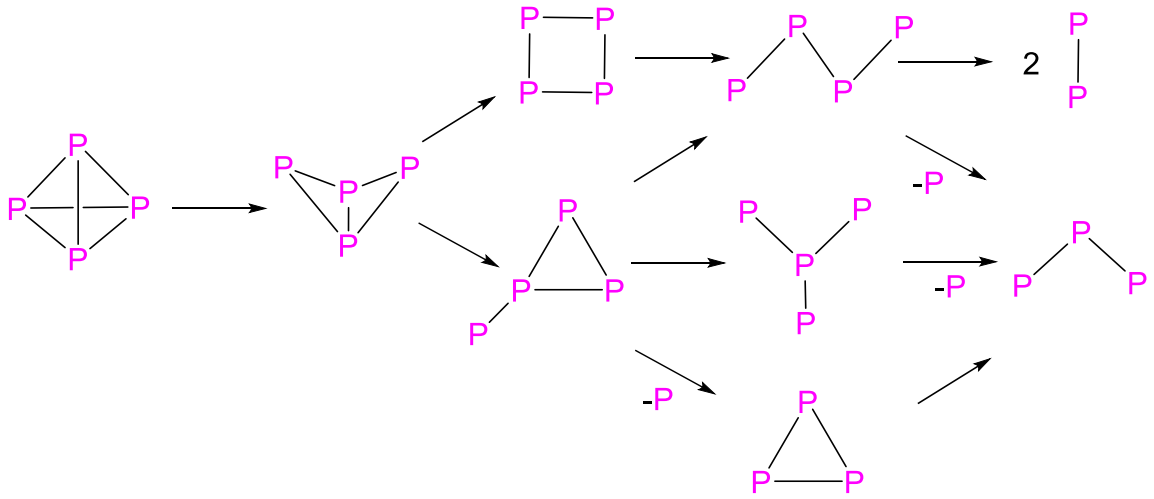


**Scheme 3.** Different degradation pathways in the process of $P_4$ activation. Only the $P_n$ backbones of the fragments are shown while the substituents and the charges are omitted for clarity.

$P_4$ activation represents a way to synthesize a variety of complexes containing the versatile $P_n$ units (n = 1-4). Compounds with n ≥ 5 are also known and they may be formed as the result of aggregation of smaller fragments. The most significant examples in this category are the compounds containing aromatic *cyclo*-$P_5$ and *cyclo*-$P_6$ ligands, which represent the inorganic analogue of cyclopentadiene and benzene, respectively, based on the isolobal relationship between P and CH. Figure 2 summarizes a selection of significant structural motifs of $P_n$ ligand complexes (n = 1-4, n ≥ 5), which are ordered based on the number of P atoms incorporated. In the following part, some relevant examples of these complexes are discussed.[5,24]

The first example of a $P_n$-ligand complex dates back to 1971, when Lindsell and Ginsberg described the compound $[Rh(PPh_3)_2Cl(\eta^2\text{-}P_4)]$, bearing an intact $P_4$ molecule bonded to a rhodium atom.[28] In 2002 Krossing *et. al*. discovered that it must be regarded as a tetraphosphabicyclobutane with two covalent P-Rh bonds instead.[29] For the category of n = 1, the P atom could be terminal (Figure 2), like in the phosphido-complex $[Mo(P)(NRAr)_3]$ (**I**, R = $C(CD_3)_2CH_3$, Ar = 3,5-$C_6H_3Me_2$),[30] bridged between two to four metal fragments (Figure 2) like in $[\{CpW(CO)_2\}\{Cr(CO)_5\}_2(\mu_3\text{-}P)]$ (**II**, Cp = $\eta^5\text{-}C_5H_5$) [31], or at the vertex of a

trigonal pyramidal molecule (Figure 2), where the base is occupied by three metal fragments (*e.g.* $[Mo_nW_{(3-n)}(CO)_6(\mu_3\text{-}P)]$, **III**, n= 0-3).[32] For n = 2, the $P_2$ ligand can be bridged, as a dumbbell between two or four metal fragments (Figure 2), as in the tetrahedrane complex $[\{CrCp(CO)_2\}_2(\mu,\eta^2\text{-}P_2)]$ (**IV**)[33] or in the square planar $\{Co_2(CO)_6(\mu,\eta^2\text{-}P_2)[M(CO)_5]_2\}$ (**V**, M = Cr, W),[34] respectively. For n = 3, the most common structural motif of the ligand is represented by a *cyclo*-$P_3$ unit (Figure 2), that can be part of a sandwich complex ($[(Cp''Ni)(\eta^3\text{-}P_3)]$, **VI**, Cp'' = $\eta^5$-1,3-$tBu_2C_5H_3$)[35] or of a triple-decker complex like in $[K][(Cp'''Ni)_2(\mu,\eta^3\text{:}\eta^3\text{-}P_3)]$ (**VII**, Cp''' = $\eta^5$-1,2,4-$tBu_3C_5H_2$)[36].

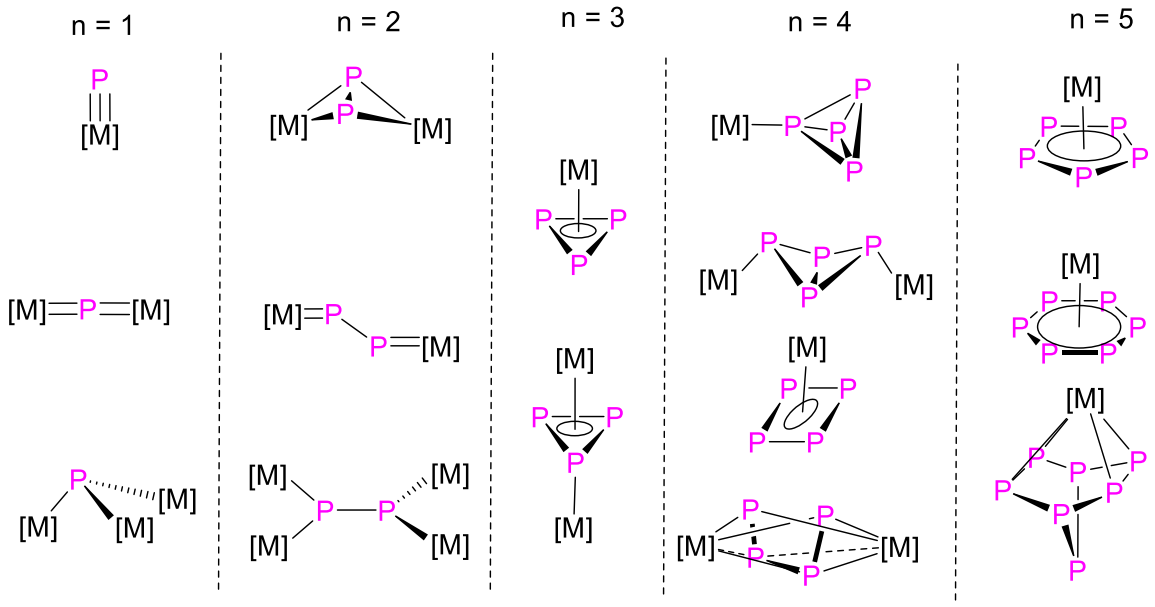


**Figure 2.** Selection of significant structural motifs of $P_n$ ligand complexes (n = 1-4, n ≥ 5). [M] = transition-metal complex fragment.

Alternatively, the $P_3$ unit could be present as an allylic ligand, such as in the heterobimetallic triple decker complex $[(Cp'''Co)(Cp'''Ni)(\mu,\eta^3\text{:}\eta^3\text{-}P_3)]$ (**VIII**).[37] For n = 4, the $P_4$ unit could be present as an intact tetrahedron (Figure 2), as in the compound $[CpRu(PPh_3)_2(\eta^1\text{-}P_4)][PF_6]$,[38] as a *cyclo*-$P_4$ unit (Figure 2) like in the sandwich complex $[Cp'''Co(\eta^4\text{-}P_4)]$ (**IX**),[39] or as a butterfly motif (Figure 2), like in the complex $[\{Cp'''Fe(CO)_2\}_2(\mu,\eta^1\text{:}\eta^1\text{-}P_4)]$ (**X**).[40] For n = 5 and n = 6, the most significant examples, as already mentioned, are the complexes with the aromatic *cyclo*-$P_5$ and *cyclo*-$P_6$ ligands (Figure 2), present either in sandwich or triple-decker complexes. The most known example of sandwich complex is pentaphosphaferrocene (n = 5, $[Cp^*Fe(\eta^5\text{-}P_5)]$, **XI**, Cp* = $\eta^5$-$C_5Me_5$),[41] the inorganic analogue of ferrocene, while with n = 6, several triple-decker complexes are known, with the middle deck being the inorganic analogue of benzene. Among the latter, there are the complexes $[(Cp^*M)_2(\mu,\eta^6\text{:}\eta^6\text{-}P_6)]$ (**XII**, M = Mo;[42] **XIII**, M = V[43]). A plethora of $P_n$-ligand complexes has been synthesized so far, the examples

presented here are only a selection, for a complete list it is possible to consult the reviews about $P_4$ activation.[5, 7, 8, 24, 27]

## 1.3 Arsenic

Arsenic is the 33rd element of the periodic table and one hypothesis about its discovery is attributed to the Bishop of Regensburg Albert Magnus, who reduced Arsenic trioxide ($As_2O_3$) around the year 1250. The element's name comes from the Greek word *arsenios*, which means "virile", "audacious" or "brave" and it was used to refer to the mineral orpiment ($As_2S_3$). For decades arsenic compounds were used to treat diseases of different nature, but the element is mainly known to the general public for its toxic properties.[44] It can cause a variety of adverse health effects to human after acute or chronical exposure. Arsenic is cumulative in plant and animal tissues and therefore can also be found in the human body, whose total amount is approximately 3-4 mg. Contrarily to phosphorus, this element is found abundantly in the earth's crust, being the 20th element (terrestrial abundance: 1.5-3 $mg \cdot kg^{-1}$ considering natural and anthropogenic source). It is a component of more than 245 minerals, mainly in the form of arsenates or sulfides, which are converted to arsenic oxides by the watering of rocks, entering in this way the arsenic cycle. Arsenic is used for several applications like as desiccants and food preservatives, feed additives, drugs, insecticides, and herbicides.[45]

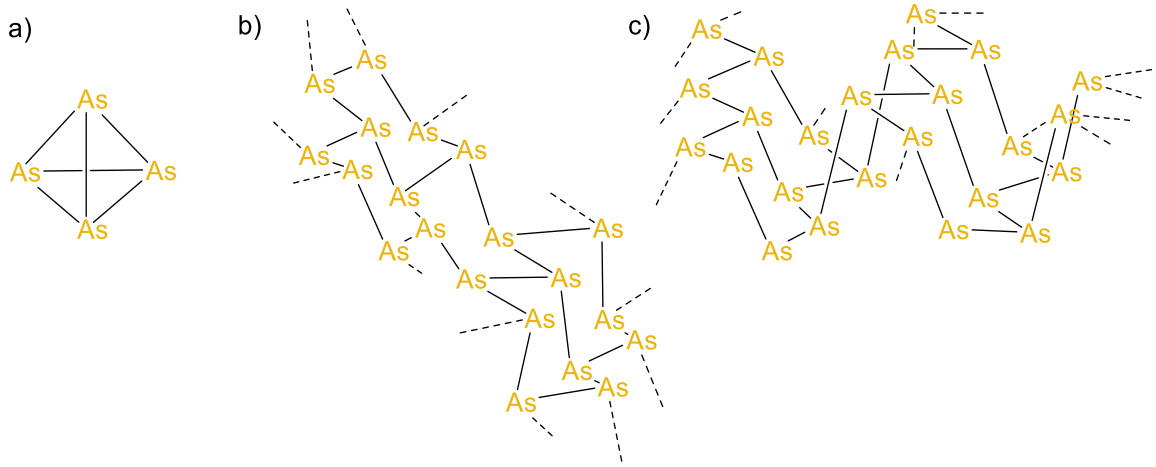


**Figure 3.** Selected examples of allotropic modification of arsenic. a) $As_4$ tetrahedral modification; b) grey arsenic (rhombohedral); c) orthorhombic black arsenic.

In the solid state, arsenic is present in four allotropic modifications: grey (or metallic), amorphous black, orthorhombic black and yellow arsenic. The latter is composed by tetrahedral $As_4$ molecules, being the heavier homologue of white phosphorus (Figure 3, a). Contrarily to $P_4$, the tetrahedron represents the most unstable modification. Yellow arsenic gradually converts into the grey modification at room temperature and this

conversion is accelerated by exposure to light. $As_4$ shows a very poor solubility at ambient conditions and nevertheless represents the only soluble form. Due to the extreme instability of yellow arsenic, its crystal structure could not be elucidated.[44] The tetrahedral structure in the gas phase was determined by electron diffraction experiments, with As-As distances of 2.44 Å[46] and 2.435(4) Å.[47] The synthesis of yellow arsenic was reported for the first time in 1867 by Bettendorf and it is based on the condensation of $As_4$ vapours, deriving from the heating of grey arsenic, which afterwards are quenched in $CS_2$.[48]

The thermodynamically most stable allotrope of the element is grey arsenic which has a rhombohedral structure. This modification is made by arsenic layers which in turn are formed by $As_6$ rings in chair conformation (Figure 3, b), analogously to the modification of the rhombohedral black phosphorus (cf. Figure 2).[49] The condensation of arsenic vapour onto heated surfaces leads to the formation of amorphous black arsenic, which in turn can be converted to the orthorhombic black modification by its crystallization in the presence of mercury vapours. Orthorhombic black arsenic is called the “cousin” of black phosphorus because it has a similar puckered orthorhombic structure (Figure 3, c) and is also an excellent layer semiconductor.[50]

## 1.4 Activation of yellow arsenic by transition metals

Compared to the activation of white phosphorus, much less is known about the reactivity of yellow arsenic towards transition metal complexes, mainly due to its high instability and toxicity. Nevertheless, several polyarsenic ligands could be prepared and stabilized by the coordination sphere of transition metals. Analogously to $P_4$, $As_4$ activation consists in subsequent reductive cleavage of the As-As bonds in a degradation process that may follow different pathways (the pathways illustrated in figure 2 for $P_4$ could be applied also to $As_4$). Herein some significant examples of $As_n$-ligand complexes are presented. The first As-containing compound is $[Co(CO)_3(\eta^3\text{-}As_3)]$ and it was synthesized in 1969 by Dahl.[51] With n = 1, the As ligand might be terminal, like in the complex $[(N_3N)W(As)]$ (**XIV**).[52] For n = 2, analogously to complex **IV**, one possible structural motif is with the $As_2$ ligand as a dumbbell between two metal fragments, to form a tetrahedrane complex, like $[\{MoCp^*(CO)_2\}_2(\mu,\eta^{\,2}\text{-}As_2)]$ (**XV**).[53] For the structure containing an $As_3$ unit, the most common modification is a *cyclo*-$As_3$, present both in sandwich, like the first As compound discovered,[51] and triple-decker complexes, like in $[(Cp^*Fe)(Cp'''Co)(\mu,\eta^3\text{:}\eta^3\text{-}As_3)]$ (**XVI**).[54] When n = 4, the $As_4$ unit could be present as an intact tetrahedron in the final complex, like in $[(Ph_3P)Au(\eta^2\text{-}As_4)]$ (**XVII**),[55] where the $As_4$ molecule is transferred to the Au atom, to which is side-on coordinated. Alternatively, it could be found as a *cyclo*-$As_4$ unit like in the triple-decker complex $[(Cp'''Fe)_2(\mu,\eta^4\text{:}\eta^4\text{-}As_4)]$ (**XVIII**),[56] or as a butterfly motif, like in

the organo-substituted compound $Cp^{PEt}{}_2As_4$ (**XIX**, $Cp^{PEt} = C_5(4\text{-}EtC_6H_4)_5$).[57] Analogously to what was observed with phosphorus, the aggregation of multiple As atoms may result in the formation of $As_n$-compounds, where n ≥ 5. With n = 5, the most known complex is the pentaarsaferrocene [Cp*Fe($\eta^5$-$As_5$)] (**XX**),[58] the heavier homologue of pentaphosphaferrocene which bears the aromatic *cyclo*-$As_5$ unit. The ligand can also be found as middle deck, like in the cationic complex $[(Cp^{Bn}Fe)_2(\mu,\eta^5{:}\eta^5\text{-}As_5)][BF_4]$ (**XXI**, $Cp^{Bn} = C_5(CH_2(C_6H_5)_5)$).[56] With n = 6, there are complexes with the *cyclo*-$As_6$ unit, known as hexaarsabenzene ligand, like the heavier homologue of the triple decker **XII**, $[(Cp^{R}Mo)_2(\mu,\eta^6{:}\eta^6\text{-}As_6)]$ ($Cp^R$ = Cp*, $C_5Me_4Et$, **XXII**, **XXIII**).[59] The aggregation of $As_n$ fragments may also result in the formation of even bigger As units, like in the complex $[(Cp^*Ru)_2(As_8I_6)]$ (**XXIV**), resulted from the iodination of [Cp*Fe($\eta^5$-$As_5$)], where, together with a bridging $AsI_2$ ligand, an $As_7$ cage unit is formed.[60]

## 1.5 Halogens

The elements of the group 17 of the periodic table, fluorine, chlorine, bromine, iodine, and astatine are known with the name *halogens*, from the Greek *hals*, “salt” and *gennan*, “to generate” because they are literally the salt formers. Fluorine and chorine are poisonous gases, their names come from the words *fluoros*, “flowing” and *chloros*, “yellowish, or light green”, referring to the color of the gas. Bromine is a volatile and toxic red liquid, while iodine is a volatile solid. The original Greek words used to name them mean “stink” and “violet colored”, respectively. Astatine is a radioactive element, and it is present in negligible amount in nature because all its isotopes in the natural series have half-lives of less than one minute. Reasonably, its name comes from the world “unstable”.[49,61] The distribution of the halogens varies from element to element. All of them form diatomic molecules ($F_2$, $Cl_2$, $Br_2$, $I_2$, $At_2$) and, due to their reactivity, they are not present in nature in their elemental state but rather in the form of their negative ions, $X^-$ (with the exception of the mineral Antozonite, originally known as “stinkspat”, which is characterized by the presence of multiple inclusions in which elemental $F_2$ is encapsulated).[62] One of their sources are the large halide mineral deposits (especially for NaCl, KCl and $CaF_2$, also iodide minerals can be found, but they are less abundant). The main source for bromine and chlorine is represented by the ocean because their halides (*e.g.* NaCl, NaBr) are well soluble. The halogens are stronger oxidants, and amongst them, fluorine is the most reactive as shown by the trend of oxidation potential (E°), which decreases through the group. ($F^-$ > $Cl^-$ >$Br^-$ >$I^-$). The properties of these elements, high ionization energy, electronegativity and electron affinity are summarized in table 1.

**Table 1.** Representative properties of the halogens.

| Property | F | Cl | Br | I | At |
|---|---|---|---|---|---|
| **Covalent radio/Å** | 0.71 | 0.99 | 1.14 | 1.33 | 1.40 |
| **Ionic radio/Å** | 1.31 | 1.81 | 1.96 | 2.20 | - |
| **1st Ionization energy/(kJ·mol$^{-1}$)** | 1681 | 1251 | 1139 | 1008 | 926 |
| **Pauling Electronegativity** | 4.0 | 3.2 | 3.0 | 2.6 | 2.2 |
| **Electron affinity/(kJ·mol$^{-1}$)** | 328 | 349 | 325 | 295 | 270 |
| **E°($X_2$,$X^-$)/V** | +3.05 | +1.36 | +1.09 | +0.54 | - |

The semi reaction of a redox process in which the halogen is reduced (Scheme 4) is favored by a high electron affinity.

$$1/2\ X_2(g) + e^- \longrightarrow X^-(aq)$$

**Scheme 4.** Semi reaction of a redox process which shows the reduction of a halogen X.

The oxidation potential of fluorine is higher than the one of chlorine (despite its lower electron affinity) because of the small enthalpy of dissociation of $F_2$ and thanks to the high enthalpy of formation for the ionic complexes bearing the small $F^-$ ion (the hydration enthalpy is enhanced for small ions).[61] Even though they are marked as less reactive than fluorine, the heavier halogens are still amongst the most reactive elements. In general, the reaction of $X_2$ with compounds containing M-M, M-H or M-C bonds (M = metal or non-metal) results in the formation of M-X bonds. The reactivity is enhanced when the conditions promote the generation of halogen atoms, but this does not mean that all the reactions proceed always in this way.[49]

Halogens may also be used for the activation (or in this case the term degradation is more suited) of white phosphorus. Normally, the halogens oxidize $P_4$ to form $PX_3$ or $PX_5$ derivatives. The conversion of $P_4$ into $PCl_3$ is still widely used as a fundamental step in the industrial synthesis of organophosphorus compounds (*vide supra*).[8] In the next paragraph, an overview of the halogenation of coordinated $P_4$ and of pnictogen containing compounds is presented.

## 1.6 Halogenation of $E_n$ ligand complexes (E = P, As)

The halogenation of $P_4$ is not a new research field, if we consider that one of the first publication on this topic was released in 1897.[63]

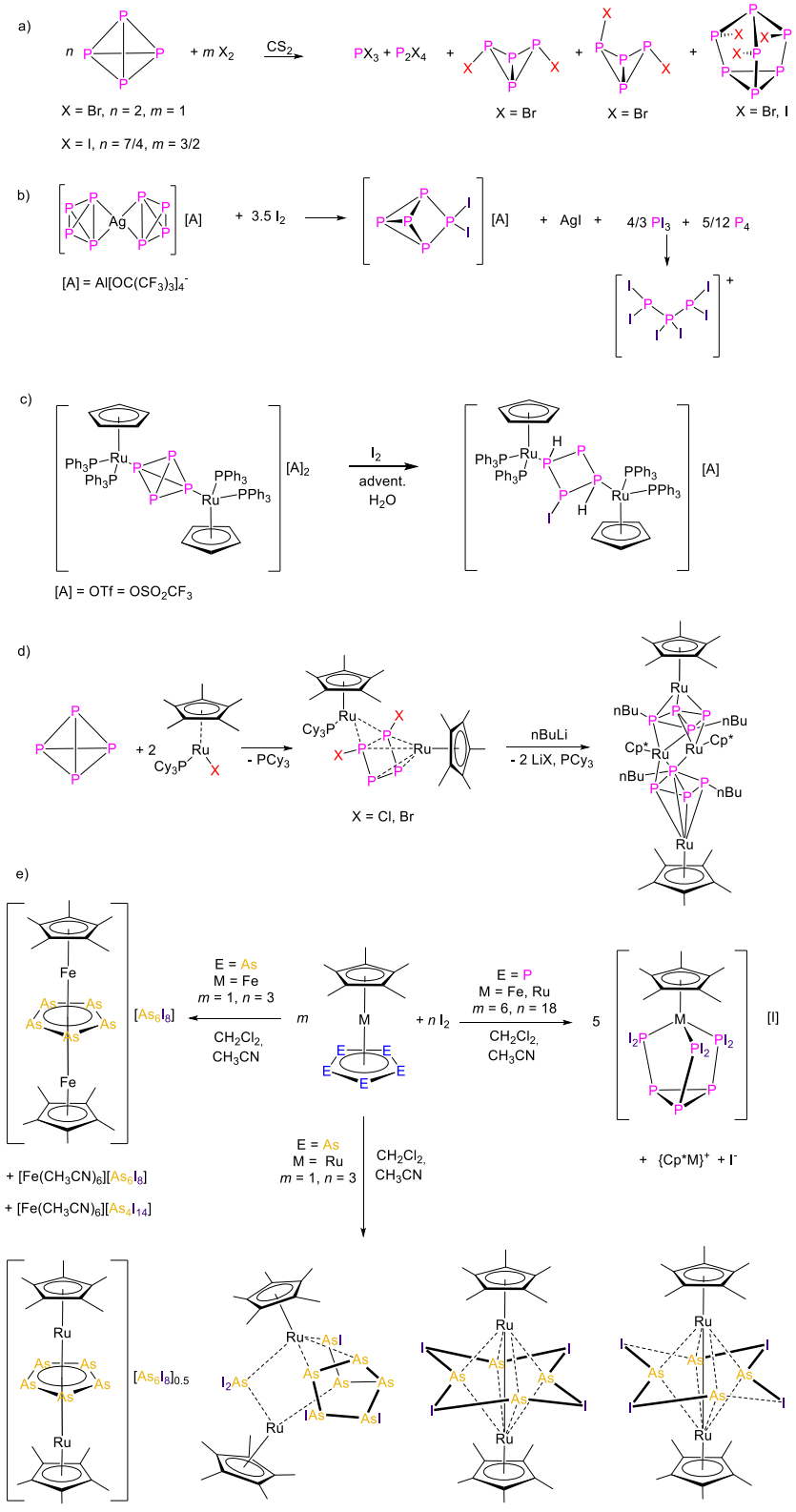


**Scheme 5.** Selected examples of halogenation of polypnictogen compounds.

The reaction between phosphorus and iodine was initially investigated by means of iodine color comparisons with standard solutions, in 1940.[64] In 2018, Mealli *et. al.* described in detail the mechanism of the complete iodination of white phosphorus to four equivalents of $PI_3$, based on DFT calculations. What emerged from this study was that each step of the reaction is better described as a concerted reaction, rather than a redox process.[65] Further investigations on the same reaction were conducted in 2021 by Manca *et. al.*, this time with coordinated white phosphorus, in the complex [Cp*Ru(dppe)($\eta^1$-$P_4$)]. The study demonstrated the key role of the metal since the proposed mechanism differs significantly from the concerted one. In this case, the main role of the Ru atom was to enhance the basicity of the phosphorus, affecting its reactivity towards the $I_2$ molecule.[66] In 1994, Tattershall *et. al.* performed a $^{31}$P NMR investigation of the halogenation of white phosphorus.[67] They discovered that, together with $PI_3$ or $P_2I_4$, the reaction between $P_4$ and $I_2$ leads to the formation of the cage species $P_7I_3$. The same was observed for the Br case and when Br or Cl were involved. Additionally, the butterfly halides species $P_4XY$ (X = Cl, Br; Y = Cl, Br) could also be identified (Scheme 5, a).

Synthetic access to halogenated phosphorus compounds was given for example by the group of Krossing *et. al.* who showed that the reaction between coordinated $P_4$ in the complex [Ag($\eta^2$-$P_4$)$_2$][TEF] (TEF$^-$ = Al{OC($CF_3$)$_3$}$_4$) with $I_2$ at -78 °C leads to the binary phosphorus rich cation $[P_5I_2]^+$. At -40 °C the reaction proceeds further to give $[P_3I_6]^+$, the first subvalent P-X cation (Scheme 5, b).[68] On the base of all these investigations, the question arose about the possibility to apply the halogenation of $P_n$-ligand complexes as a new synthetic approach to form novel polyphosphorus fragments. However, only later in 2012, Barbaro *et. al* presented the first example for the iodine activation of coordinated white phosphorus, in the presence of adventitious water. The resulting monocation [{CpRu($PPh_3$)$_2$}$_2$(μ,$\eta^1$:$\eta^1$-$P_4H_2I$)]$^+$ bears the elusive 1,3-dihydride-2-iodidecyclotetra-phosphane anion $[P_4H_2I]^-$, which in turn is the precursor of the unprecedented 1,3-dihydride-2,4-bicyclotetraphosphane [1,1,0] ($P_4H_2$), easily obtained from the iodide dissociation (Scheme 5, c).[69] After this discovery, the interest in the field has increased greatly since the halogenation represents an additional reactivity in achieving a better and deeper understanding in the nature of phosphorus-metal bonds. As mentioned before, the final goal of the study of $P_4$ activation is to find the conditions for its catalytic conversion to the organophosphorus derivatives. In this context, a study on the ruthenium mediated halogenation of white phosphorus was published in 2019, describing the role of the metal in the synthesis of the complex [(RuCp*)$_2$($PCy_3$)(μ,$\eta^2$:$\eta^4$-$P_4X_2$)] bearing the unprecedented $P_4X_2$ moiety (X = Cl, Br, Scheme 5, d).[70] Afterwards, a study on the iodination of [Cp*M($\eta^5$-$E_5$)] (M = Fe, Ru; E = P, As) showed that this approach can be a powerful tool for the

synthesis of new polyphosphorus fragments as well as for their heavier congeners, even if the results are predictably different moving from P to As (Scheme 5, e).[60] To conclude, the halogenation of coordinated white phosphorus is an open research field that can be applied to the whole plethora of known $E_n$-ligand complexes and helps in understanding the reactivity of $P_4$. Furthermore, the formation of the P-X bond could eventually be used for further derivatization/functionalization.

## 1.7 References


[1] M. E. Weeks, *J. Chem. Educ*. **1932**, *9*, 16-21.
[2] F. Krafft, *Angew. Chem. Int. Edit*. **1969**, *8*, 660-671.
[3] J. E. Brady, *General chemistry: principles and structure*. Hoboken: Wiley; **1990**.
[4] G. M. Filippelli, *Elements* **2008**, *4*, 89-95.
[5] C. M. Hoidn, D. J. Scott, R. Wolf, *Chem. Eur. J*. **2021**, *27*, 1886-1902.
[6] U. Aviv, R. Kornhaber, M. Harats, J. Haik, *Disaster and Mil Med*, **2017**, *3*, 6.
[7] B. M. Cossairt, N. A. Piro, C. C. Cummins, *Chem. Rev*. **2010**, *110*, 4164-4177.
[8] M. Scheer, G. Balázs, A. Seitz, *Chem. Rev*. **2010**, *110*, 4236-4256.
[9] A. Simon, H. Borrmann, J. Horakh, *Chem. Ber*. **1997**, *130*, 1235.
[10] H. Okudera, R. E. Dinnebier, A. Simon, *Z. Kristallogr. Cryst. Mater*. **2005**, *220*.
[11] A. Simon, H. Borrmann, H. Crauber, *Phosphorus and Sulfur* **1987**, *30*, 507-510
[12] N. J. Brassington, H. G. M. Edwards, D. A. Long, *J. Raman Spectrosc*. **1981**, *11*, 346.
[13] B. M. Cossairt, C. C. Cummins, A. R. Head, D. L. Lichtenberger, R. J. F. Berger, S. A. Hayes, N. W. Mitzel, G. Wu, *J. Am. Chem. Soc*. **2010**, *132*, 8459.
[14] M. Haser, O. Treutler, *J. Chem. Phys.* **1995**, *102*, 3703.
[15] H. Östmark, S. Wallin, N. Hore, O. Launila, *J. Chem. Phys*. **2003**, *119*, 5918-1922.
[16] F. S. Dainton, *Trans. Faraday Soc*. **1947**, *43*, 244.
[17] P. Mal, B. Breiner, K. Rissanen, J. Nitschke, *Science* **2009**, *324*, 1697-1699.
[18] M. Ruck,D. Hoppe, B. Wahl, P. Simon, Y. Wang, G. Seifert, *Angew. Chem. Int. Ed*. **2005**, *44*, 7616-7619.
[19] H. Thurn, H. Krebs*, Angew. Chem. Int. Ed.* **1966**, *5*, 1047-1048.
[20] A. Morita, *Appl. Phys. A*, **1986**, *39*, 227-242.
[21] L. Li, Y. Yu, G. J. Ye, Q. Ge, X. Ou, H. Wu, D. Feng, X. H. Chen, Y. Zhang, *Nature Nanotech.* **2014**, *9*, 372-377.
[22] J. Jamieson, *Science*, **1963**, *139*, 1291-1292.
[23] M. Raucci, I. Fasolino, M. Caporali, M. Serrano-Ruiz, A. Soriente, M. Peruzzini, L. Ambrosio, *ACS Appl. Mater. Interfaces*, **2019**, *11*, 9333-9342.
[24] M. Caporali, L. Gonsalvi, A. Rossin, M. Peruzzini, *Chem. Rev.* **2010**, *110*, 4178-4235.
[25] J. D. Masuda, W. W. Schoeller, B. Donnadieu, G. Bertrand, *Angew. Chem. Int. Ed.* **2007**, *46*, 7052-77055.
[26] A. R. Fox, R. J. Wright, E. Rivard, P.P Power, *Angew. Chem. Int. Ed.* **2005**, *44*, 7729-7733.
[27] M Peruzzini, L. Gonsalvi, A. Romerosa, *Chem. Soc. Rev.* **2005**, *34*, 1038-1047.
[28] A. P. Ginsberg, W. E. Lindsell, *J. Am. Chem. Soc.* **1971**, *93*, 2082-2084.
[29] I. Krossing, L. van Wüllen, *Chem. Eur. J.* **2002**, *8*, 700-711.
[30] C. E. Laplaza, W. M. Davis, C. C. Cummins, *Angew. Chem. Int. Ed. Engl.* **1995**, *34*, 2042-2044.
[31] G.Huttner, U. Weber, B. Sigwarth, O. Scheidsteger, H. Lang, L. Zsolnai, *J. Organomet. Chem*. **1985**, *282*, 331-348.
[32] J. E. Davies, M. C. Klunduk, M. J. Mays, P. R. Raithby, G. P. Shields, P. K. Tompkin, *Dalton Trans.* **1997**, 715-720.
[33] L. Y. Goh, C. K. Chu, R. C. S. Wong and T. W. Hambley, *J. Chem. Soc. Dalton Trans.* **1990**, 977-982.
[34] H. Lang, L. Zsolnai and G. Huttner, *Angew. Chem. Int. Ed*. **1983**, *22*, 976-977.
[35] O. J. Scherer, T. Dave, J. Braun, G. Wolmershäuser, *J. Organomet. Chem.* **1988**, *350*, C20-C24.
[36] E. Mädl, G. Balázs, E. V. Peresypkina, M. Scheer*, Angew. Chem. Int. Ed.* **2016**, *55*, 7702-7707.
[37] M. Piesch, F. Dielmann, S. Reichl, M. Scheer, *Chem. Eur. J.* **2020**, *26*, 1518-1524.
[38] M. Di Vaira, P. Frediani, S. S. Costantini, M. Peruzzini, P. Stoppioni, *Dalton Trans*. **2005**, 2234-2236.
[39] F. Dielmann, A. Y. Timoshkin, M. Piesch, G. Balázs, M. Scheer, *Angew. Chem.* **2017**, *129*, 1693-1698.
[40] C. Schwarzmaier, A. Y. Timoshkin, G.Balázs, M. Scheer, *Angew. Chem. Int. Ed*. **2014**, *53*, 9077-9081.
[41] O. J. Scherer, T. Brück, *Angew. Chem. Int. Ed. Engl*. **1987**, *26*, 59.
[42] O. J. Scherer, H. Sitzmann, G. Wolmershäuser, *Angew. Chem.* **1987**, *97*, 358-359.
[43] O. J. Scherer, J. Schwalb, H. Swarowsky, G. Wolmershäuser, W. Kaim, R. Gross, *Chem. Ber.* **1988**, *121*, 443-449.
[44] M. Seidl, G. Balázs, M. Scheer, *Chem. Rev*. **2019**, *119*, 8406-8434.
[45] B. K. Mandal, K. T. Suzuki, *Talanta*, **2002**, *58*, 201-235.

[46] L. R. Maxwell, S. B. Hendricks, V. M. Mosley, *J. Chem. Phys.* **1935**, *3*, 699-709.
[47] Y. Morino, T. Ukaji, T. Ito, *Chem. Soc. Jpn*. **1966**, *39*, 64-71.
[48] A. Bettendorff, *Justus Liebigs Ann. Chem.* **1867**, *144*, 110-114.
[49] N. N. Greenwood, A. Earnshaw, *Chemistry of the Elements, 2nd ed.*; Elsevier, **1998**.
[50] N. Antonatos, J. Luxa, J. Sturala, *Nanoscale*, **2020**, *12*, 5397-5401.
[51] A. S. Foust, M. S. Foster, L. F. Dahl, *J. Am. Chem. Soc.* **1969**, *91*, 5631-5633.
[52] M. Scheer, J. Müller, M. Häser, *Angew. Chem. Int. Ed. Engl.* **1996**, *35*, 2492-2496.
[53] O. J. Scherer, H. Sitzmann, G. Wolmershäuser, *J. Organomet. Chem.* **1986**, *309*, 77-86.
[54] M. Piesch, M. Scheer, *Organometallics*, **2020**, *39*, 4247-4252.
[55] C. Schwarzmaier, M. Sierka, M. Scheer, *Angew. Chem. Int. Ed.* **2013**, *52*, 858−861.
[56] M. Schmidt, A. E. Seitz, M. Eckhardt, G. Balazs, E. V. Peresypkina, A. V. Virovets, F. Riedlberger, M. Bodensteiner, E. M. Zolnhofer, K. Meyer, M. Scheer, *J. Am. Chem. Soc.* **2017**, *139*, 13981-13984.
[57] S. Heinl, G. Balazs, A. Stauber, M. Scheer, *Angew. Chem. Int. Ed.* **2016**, *55*, 15524-15527.
[58] O. J. Scherer, C. Blath, G. Wolmershäuser, *J. Organomet. Chem.* **1990**, *387*, C21-C24.
[59] O. J. Scherer, H. Sitzmann, G. Wolmershäuser, *Angew. Chem. Int. Ed. Engl.* **1989**, *28*, 212-213.
[60] H. Brake, E. V. Peresypkina, A. V. Virovets, M. Piesch, W. Kremer, L. Zimmermann, C. Klimas, M. Scheer *Angew. Chem. Int. Ed.* **2020**, *59*, 16241-16246.
[61] P. Atkins, T. Overton, J. Rourke, M. Weller, F. Armstrong, *Shriver and Atkins' Inorganic Chemistry, 5th ed.*; Oxford University Press, **2010**.
[62] R. Vochten, E. Esmans and W. Vermeirsch,*Chemical Geology*, **1977**, 20.
[63] Besson, *Compl. Rend*. **1897**, *124*, 1349.
[64] D. Wyllie, M. Ritchie, E. B. Ludlam, *J. Chem. Soc*. **1940**, 583-587.
[65] C. Mealli, A. Ienco, M. Peruzzini, G. Manca, *Dalton Trans*. **2018**, *47*, 394-408.
[66] G. Manca, A. Ienco, *Inorg. Chimica Acta*, **2021**, *517*, 1202-1205.
[67] B.W. Tattershall, N.L. Kendall *Polyhedron* **1994**, *13*, 1517-1521.
[68] I. Krossing, J. Chem. Soc. *Dalton Trans.* **2002**, 505-512.
[69] P. Barbaro, C. Bazzicalupi, M. Peruzzini, S. Seniori Costantini, P. Stoppioni, *Angew. Chem. Int. Ed.* **2012**, *51*, 8628-8631.
[70] M. Bispinghoff, Z. Benkő, H. Grützmacher, F. Delgado Calvo, M. Caporali, M. Peruzzini, *Dalton Trans.* **2019**, *48*, 3593-3600.

# 2 Research Objectives

The redox chemistry of [Cp*Fe($\eta^5$-$P_5$)] was studied by our group, showing that in general the oxidation led to the formation of a new P-P bond. After, the iodination of [Cp*M($\eta^5$-$E_5$)] (M = Fe, Ru; E = P, As)] was investigated, proving that it is a powerful tool for the synthesis of new halogen functionalized $E_n$ ligand complexes (E = P, As). This demonstrates that the iodination and the "classical" oxidation can afford different results and therefore being considered as complementary tools for the synthesis of new polypnictogen complexes. A comparable result was obtained with the oxidation of [{CpMo$(CO)_2$}$_2$($\mu$,$\eta^2$:$\eta^2$-$P_2$)], which dimerized after a new P-P bond formation. Due to the similarity of the reactivity of these compounds towards oxidation, a comparison between their reaction behavior towards halogens was missing. Additionally, the latter investigation was limited to $I_2$, but no reactivity studies towards the other halogens or halogen sources have been performed. Therefore, the first object of this work was:

- Investigation of the reactivity of [{CpMo$(CO)_2$}$_2$($\mu$,$\eta^2$:$\eta^2$-$P_2$)] towards halogens ($I_2$, $Br_2$) and halogen sources ($PBr_5$, $PCl_5$).

Based on the obtained results, we were interested in expanding the investigation of the reactivity of halogens towards different $P_n$ ligand complexes, whose redox properties have already been elucidated. Accordingly, the next object was:

- Investigation of the reactivity of the triple-decker complex [(Cp*Mo)$_2$($\mu$,$\eta^6$:$\eta^6$-$P_6$)] towards halogens ($I_2$, $Br_2$) and halogen sources ($PBr_5$, $PCl_5$).

Finally, we were interested in how the nature of the $E_n$ ligand and of the pnictogen atom involved could affect the outcome of the reaction. Thus, we wanted to explore a possible alternative way to obtain E-X bonds without using the harsh conditions required for halogenation reactions. Therefore, the next objectives were:

- Investigation of the halogenation of the triple-decker complexes [(Cp'''Co)$_2$($\mu$,$\eta^2$:$\eta^2$-$E_2$)$_2$] (E = P, As) bearing two independent $E_2$ units and exploration of the possibility of quenching the cations of [(Cp'''Co)$_2$($\mu$,$\eta^4$:$\eta^4$-$E_4$)][TEF]$_2$ (E = P, As) with nucleophilic halides;

- Investigation of the reactivity of the heterobimetallic triple-decker complexes [(Cp*Fe)(Cp'''Co)(μ,η$^5$:η$^4$-)$E_5$] (E = P, As) towards halogens ($I_2$, $Br_2$) and halogen sources ($PCl_5$).

## Preface

The following chapter has already been published: The article is reprinted with permission from Garbagnati, A.; Seidl, M.; Balázs, G.; Scheer. M. Halogenation of diphosphorus complexes. *Inorg. Chem*. **2021**, *60*, 5163-5171. 

## Authors

Anna Garbagnati, Michael Seidl, Gábor Balázs, Manfred Scheer.

## Author contribution

A. Garbagnati prepared the manuscript and performed the synthesis and characterization of the herein presented compounds. G. Balázs performed all DFT calculations and contributed to the corresponding parts in the manuscript and the Supporting Information and revised the manuscript. Michael Seidl did the refinement of the solid-state structures. M. Scheer supervised the research and revised the manuscript.

## Acknowledgement

This work was comprehensively supported by Deutsche Forschungsgemeinschaft (DFG) within the project Sche 384/36-1. We thank Rudolf Weinzierl and Matthias Ackermann for the EPR measurements.

3. Halogenation of diphosphorus complexes

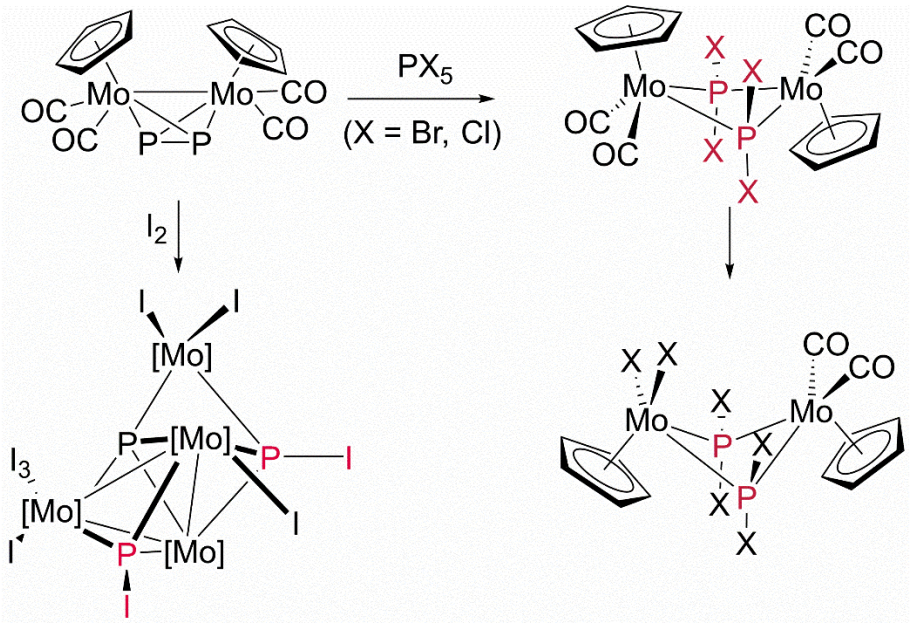

# 3 Halogenation of Diphosphorus Complexes

***Abstract:*** *A systematic study of diverse halogenation reactions of the tetrahedral $Mo_2P_2$ ligand complex [{CpMo(CO)$_2$}$_2$(μ,η$^2$:η$^2$-P$_2$)] (**1**) is reported. By reacting **1** with different halogenating agents, a series of complexes such as [(CpMo)$_4$(μ$_4$-P)(μ$_3$-PI)$_2$(μ-I)(I)$_3$(I$_3$)] (**2**), [{CpMo(CO)$_2$}$_2$(μ-PBr$_2$)$_2$] (**3a**), [{CpMo(CO)$_2$}(CpMoBr$_2$)(μ-PBr$_2$)$_2$] (**4a**), [{CpMo(CO)$_2$}$_2$(μ-PCl$_2$)$_2$] (**3b**), [{CpMo(CO)$_2$}(CpMoCl$_2$)(μ-PCl$_2$)$_2$] (**4b**) were obtained. Whereas the reaction of **1** towards various bromine and chlorine sources leads to similar results, a different behaviour is observed in the reaction with iodine in which **2** is formed. The products were comprehensively characterized by spectroscopic methods, single crystal X-ray diffraction and the electronic structures of **2**, **3a** and **4a** were elucidated by DFT calculations.*

## 3.1 Introduction

The transformation of $P_4$ is an active research area because $P_4$ is the starting material for most phosphorus-containing compounds, which are widely used in chemical, pharmaceutical, detergent, agricultural and food industries.[1] The controlled functionalization of $P_4$ by stoichiometric or catalytic reactions is still widely investigated in order to achieve the breakthrough in this area.[2] So far, the functionalization of white phosphorus has been carried out by means of nucleophilic main group compounds[3,4] and early and late transition metal complexes.[2b,c] The latter generate transition metal complexes containing either coordinated intact $P_4$ or different polyphosphorus ($P_n$) units. These complexes are of particular interest since the activity of the metal can be used in concert with that of organic reagents in order to obtain organophosphorus derivatives.[5] However, this approach needs insight into the reaction behaviour of the phosphorus-metal bond.[1] An example for the reactivity studies of polyphosphorus complexes is their redox chemistry.[6] The oxidation of polyphosphorus ligand complexes leads to a distortion of the ligand, especially when triple decker complexes are used,[7] or to a P-P bond formation.[8] Another form of oxidation in a more classical sense is the halogenation, which, however, presents a far more aggressive way since the elimination of single P atoms could proceed under the formation of $PX_3$ (X = Cl, Br, I). White phosphorus is usually oxidized by halogens to form $PX_3$ or $PX_5$.[2d] Several investigations of the halogenation of $P_4$ were done in the past. In 1994, Tattershall *et al.* reported a series of products resulting from the reaction of

$P_4$ with $I_2$, $Br_2$ or ICl that were identified by NMR spectroscopy (Scheme 1a).[9] In 2001, Krossing *et al.* reported the synthesis of $P_5X_2^+$,[10] the first subvalent binary P-X cation, by halogenating $P_4$ or $[Ag(P_4)_2]^+$ and afterwards also $PX_4^+$, $P_2X_5^+$ (X = Br, I) (Scheme 1b),[11] all of them salts of the nonoxidizing, weakly coordinating anion $Al(OR)_4^-$ [R = $C(CF_3)_3$]. The first example of the halogenation of polyphosphorus compounds was reported by Stoppioni *et al.* by the reaction of $[\{CpRu(PPh_3)_2\}_2(\mu,\eta^1{:}\eta^1\text{-}P_4)](OTf)_2$ with $I_2$ in the presence of traces of water, resulting in the monocation $[\{CpRu(PPh_3)_2\}_2(\mu,\eta^1{:}\eta^1\text{-}P_4H_2I)]^+$.[12] Another recent result is the ruthenium-mediated halogenation of white phosphorus reported by Peruzzini *et. al.*[13] In their study, they present a two-step synthesis for the conversion of the $P_4$ unit inside a ruthenium complex into new $P_4R_2$ ligands. In a first step, the bimetallic complex $[RuCp^*(PCy_3)(\mu,\eta^2{:}\eta^4\text{-}P_4X_2)RuCp^*]$ (X = Cl, Br; Scheme 1c), which features a planar $P_4X_2$ moiety as a ligand, is formed. In the second step, the subsequent functionalization of this $P_4X_2$ moiety was performed by the exchange of the halide substituents with organic groups using alkyl lithium reagents such as *n*BuLi. An additional application of the halogenation of white phosphorus is its implementation in the catalytic synthesis of triarylphosphates from $P_4$ and phenols under aerobic conditions and in the presence of different Fe(III) catalysts and iodine.[14] Here, the reaction of $P_4$ with $I_2$ leads to the formation of $PI_3$, which is considered to be crucial for the sustainment of this catalytic reaction.

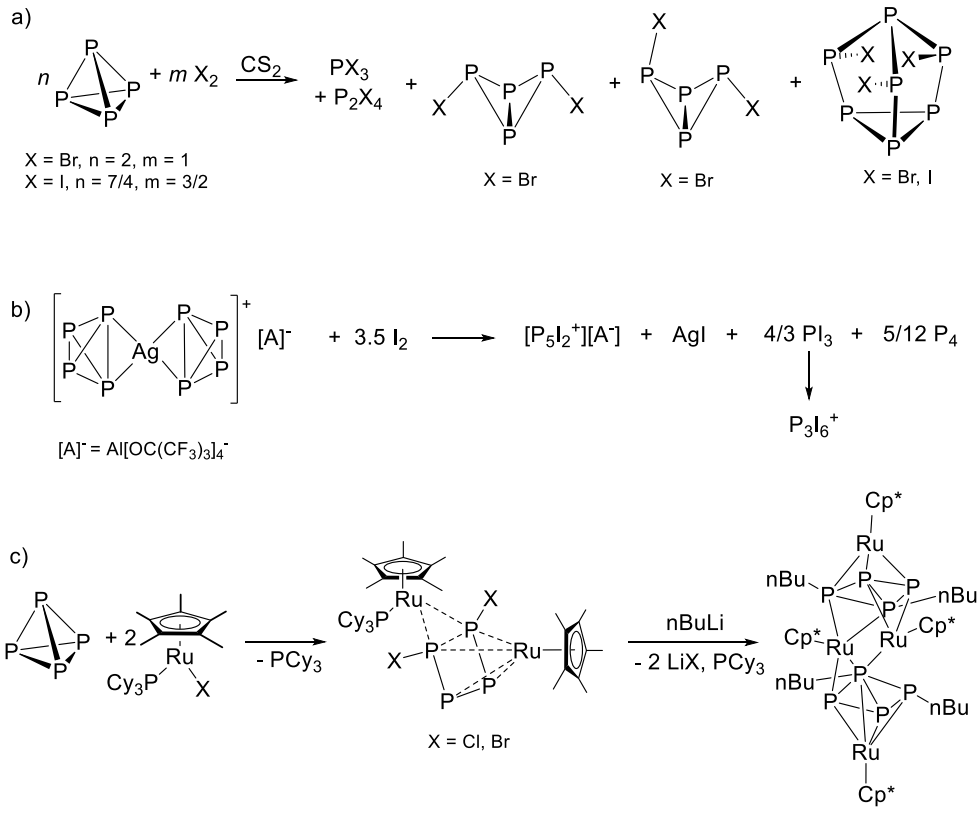


**Scheme 1.** Selected examples of halogenation of white phosphorus.

In view of these studies, the question arises whether the halogenation of polyphosphorus units, which are already coordinated in complexes, could lead to a new synthetic approach to functionalized phosphorus derivatives. After having successfully studied the iodation of pentaphosphametallocenes,[15] the question about the usability of different halogen sources in a general manner arises because the use of molecular $X_2$ (X = Cl, Br) would be too harsh and lead most likely to the decomposition of the starting material. Herein, we report on a systematic study of the reactivity of [{CpMo(CO)$_2$}$_2$(μ,η$^2$:η$^2$-P$_2$)][16] (**1**) towards halogens and halogen sources such as $PBr_5$ and $PCl_5$. Complex **1** was chosen as a mimic of $P_4$ because it is an isolobal analogue in which two vertices of $P_4$ are replaced by Mo complex fragments to increase the stability of the starting material.

## 3.2 Results and discussion

When **1** is reacted with one equivalent of $I_2$, in the $^{31}$P NMR spectrum of the reaction solution, signals of unreacted **1** and [CpMo(CO)$_2$(η$^3$-P$_3$)] (δ = −351 ppm) can be detected indicating that **1** is only partially decomposed, without any other diamagnetic products being formed (cf. Figure S1). When **1** is reacted with two equivalents of $I_2$, the $^{31}$P NMR spectrum of the reaction solution is empty, indicating the full conversion of **1** into paramagnetic compounds. No diamagnetic species, like $PI_3$ or $P_2I_4$ are formed.[17]

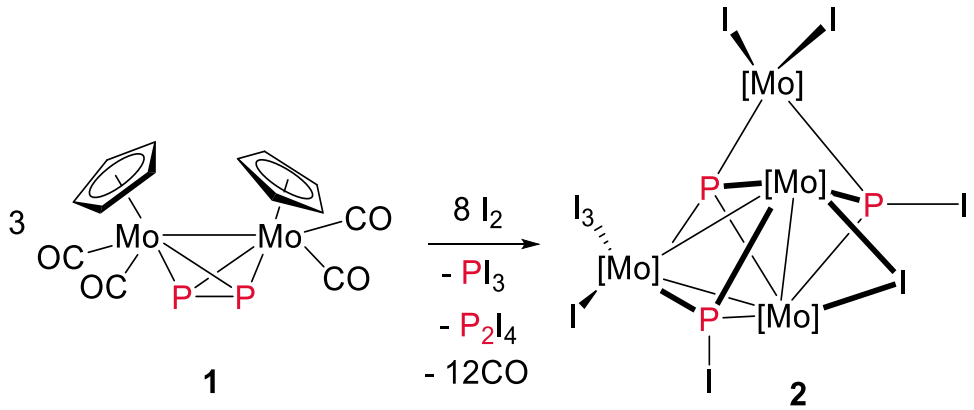


**Scheme 2.** Reaction of [{CpMo(CO)$_2$}$_2$(μ,η$^2$:η$^2$-P$_2$)] (**1**) with $I_2$.

The addition of an excess of $I_2$ to a solution of **1** in dichloromethane at room temperature resulted in an immediate color change, from bright red to dark brown. After work-up, the paramagnetic compound [(CpMo)$_4$(μ$_4$-P)(μ$_3$-PI)$_2$(μ-I)(I)$_3$(I$_3$)] (**2**) was isolated as black crystals in a crystalline yield of 19% (Scheme 2). The $^{31}$P NMR spectrum of the reaction mixture showed four singlets at 174.1 ppm, 102.6 ppm, −125.4 ppm, and −168.8 ppm (cf. Figure S2). While the first two can be attributed to $PI_3$ and $P_2I_4$, respectively, the other two

cannot be assigned to any known compound. Since no signal of the starting material was observed, full conversion of **1** can be assumed. Obviously, by this reaction, all CO ligands in **1** are eliminated and partly replaced by iodine followed by the aggregation of the formed intermediates leading to **2**, whose solid state structure was determined by single crystal X-ray diffraction (Figure 1). After work-up of the reaction and crystallisation of **2**, a few crystals of the compound $[(CpMo)_2(\mu\text{-}I)_4][I_3]$ (**5**), which was mentioned by Gordon *et. al.,*[18] could be isolated and now characterized by X-ray diffraction (cf. SI).

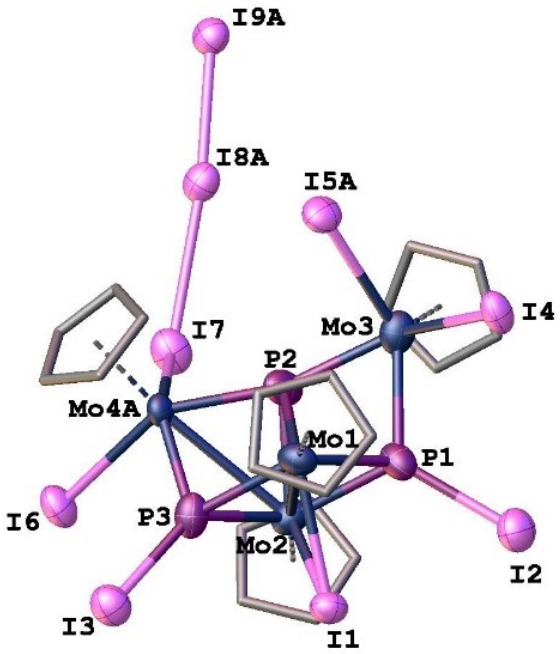


**Figure 1.** Molecular structure of **2** with thermal ellipsoids at 50% probability level. Hydrogen atoms and the free iodine molecules are omitted for clarity.

In the solid state, **2** forms a tetranuclear complex in which every CpMo moiety is bound to at least one I and two or more P atoms. Additionally, three out of four CpMo units are connected by Mo-Mo bonds (except for Mo3 which is only bonded via bridging $\mu_4$-P and $\mu_3$-PI ligands). The Mo-P bond lengths vary from 2.261(12) Å (for Mo4A-P3) to 2.523(8) Å (for Mo1-P2). With 2.568(12) Å, the long P1···P2 distance can be considered as an interaction of two P atoms (*vide infra*). Slightly shorter P-P distances of 2.4285(8) Å, but still representing a P-P bond, were reported for the complex $[(LCu)_2(\mu,\eta^2{:}\eta^2\text{-}P_4)]$ (L = $[\{N(C_6H_3i\text{Pr}_2\text{-}2,6)C(Me)\}_2CH]$).[19] The P3···P1 (3.958(12) Å) and the P3···P2 (3.117(11) Å) distances are considerably longer indicating that there is no bond between these atoms. Both the NMR as well as the X-band EPR spectra of isolated **2** are silent, suggesting a paramagnetic complex in a triplet spin state. In order to clarify the electronic structure of **2**, DFT calculations were performed.

**Table 1.** Relative energies (kJ·mol$^{-1}$) of [(CpMo)$_4$(μ$_4$-P)(μ$_3$-PI)2(μ-I)(I)$_3$(I$_3$)] (**2**) in different spin states calculated using different functionals together with the def2-TZVP basis set.

| | BP86 | TPSS | TPSSh | B3LYP | PBE0 | B97-D |
|---|---|---|---|---|---|---|
| **unrestricted singlet** | 0.0 | 0.0 | 6.4 | 18.5 | 14.3 | 9.3 |
| **triplet** | 5.0 | 2.9 | 0.0 | 0.0 | 0.0 | 0.0 |
| **quintet** | 57.5 | 62.8 | 52.2 | 25.1 | 38.9 | 36.0 |
| **septet** | 95.9 | 104.1 | 78.5 | 23.3 | 46.9 | 52.1 |

The geometry was optimized for different spin states using the B3LYP functional together with the def2-TZVP basis set. The calculations indicate that the ground state of **2** is the triplet spin state and the unrestricted singlet and the quintet spin states are higher in energy with 18.5 kJ·mol$^{-1}$ and 25.1 kJ·mol$^{-1}$, respectively. One has to note that the relative energy of the different spin states of **2** depends on the functional used (Table 1). The Natural Population Analysis (NPA) of **2** in the triplet spin state shows that the spin density is mainly localized on Mo3 (1.83e) with only minor spin density on Mo2 (0.13e). The singly occupied natural orbitals and spin density distribution are depicted in figure 2.

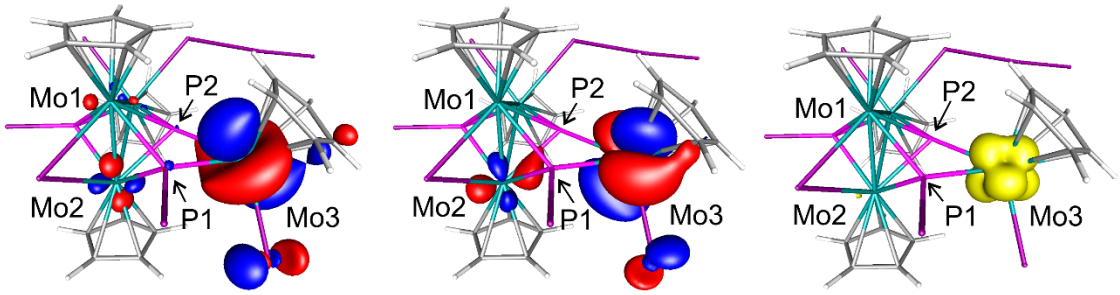


**Figure 2.** Occupied α spin natural orbitals without occupied ß counterpart (left and middle) and spin density in **2** (right).

**2** can be best described as being built from a Mo$_3$P$_3$ core, which is held together by Mo-Mo and Mo-P bonds. Moderate mixing of phosphorus atomic orbitals into the orbitals building the Mo-Mo bonds is observed (especially for Mo4A-Mo2 and Mo1-Mo2; labeling according to Figure 1) indicating some degree of delocalized four-center two-electron bond character. To this unit, a CpMoI$_2$ fragment, containing the two unpaired electrons, is bonded via the atoms P1 and P2. The coordination geometry of P2 is strongly distorted from the tetrahedral geometry with a Mo4A-P2-Mo3 angle of 161.9(5)°. This distortion is also reflected by the orbitals involved in the bonding to Mo. While the bonding of P2 to Mo1 and Mo2 is realized over sp$^3$ orbitals (sp$^{3.08}$ and sp$^{3.78}$, respectively), the bonding to

Mo4A and Mo3 is realized over sp orbitals ($sp^{1.11}$ and $sp^{0.82}$, respectively). The Wiberg bond indices (WBIs) of 0.71, 0.49 and 0.45 for the Mo1-Mo2, Mo4A-Mo2 and Mo1-Mo2 bonds correlate with the corresponding bond lengths. The P1···P2 distance is relatively long (2.568(12) Å), indeed the WBI of 0.16 indicates only a weak interaction. No direct orbital overlap between the atoms P1 and P2 was detected, only delocalized orbitals over the Mo1-Mo2-P1-P2 unit. The WBIs of the Mo-P bonds vary between 0.77 and 0.92 indicating the presence of Mo-P single bonds.

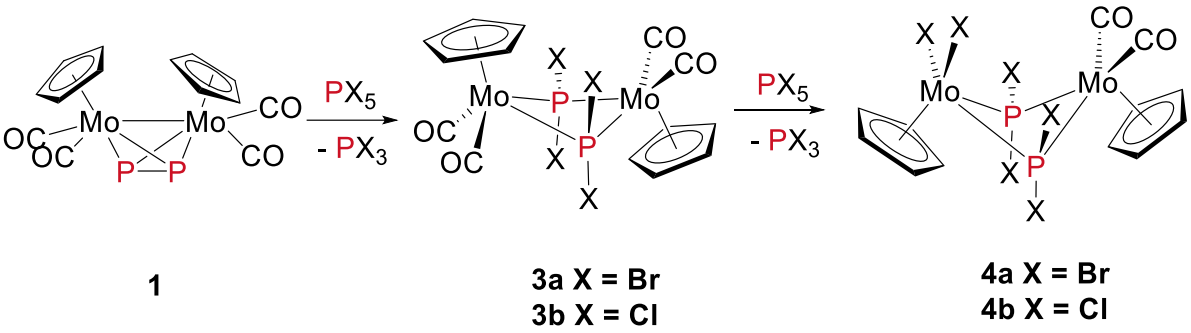


**Scheme 3.** Reaction of [{CpMo(CO)$_2$}$_2$(μ,η$^2$:η$^2$-P$_2$)] (**1**) with PX$_5$.

Since we were interested in a systematic study of the reactivity of [{CpMo(CO)$_2$}$_2$(μ,η$^2$:η$^2$-P$_2$)] (**1**) towards different halogen sources, we reacted **1** with two equivalents of $PBr_5$ (as a bromine source) at room temperature and, after workup, [{CpMo(CO)$_2$}$_2$(μ-PBr$_2$)$_2$] (**3a**) was isolated in 29% yield (Scheme 3).[20] The $^{31}$P NMR spectrum of the reaction mixture after seven hours showed, together with the signal of **1**, two additional singlets at 229.2 ppm and 200.4 ppm (cf. Figure S10) corresponding to $PBr_3$ and **3a**, respectively, indicating a partial conversion of the starting complex **1** (Scheme 3). After seven days at room temperature, the $^{31}$P NMR spectrum of the reaction solution showed, in addition to the signal of **3a**, the formation of [{CpMo(CO)$_2$}(CpMoBr$_2$)(μ-PBr$_2$)$_2$] (**4a**; singlet at 301.2 ppm), but no more signal of **1**, indicating the full conversion of the latter and the formation of **4a** after **3a** (cf. Figure S11). It can therefore be concluded that the reaction of **1** with $PBr_5$ proceeds first with the halogenation of the P atoms, forming the $PBr_2$ bridging ligands of **3a**, followed by the halogenation of one of the metal atoms, resulting in the $CpMoBr_2$ units of **4a**. When the reaction was performed directly with an excess of $PBr_5$ (6 equivalents) at room temperature, an immediate color change was observed and, after workup, [{CpMo(CO)$_2$}(CpMoBr$_2$)(μ-PBr$_2$)$_2$] (**4a**) was isolated in 54% yield (Scheme 3). The $^{31}$P NMR spectrum of this reaction mixture showed, among traces of **3a**, the formation of **4a** and $PBr_3$ (singlets at 301.2 ppm, 229.2 ppm, respectively) as well as one additional singlet at −101.1 ppm indicating a full conversion of the starting complex **1** (cf. Figure S12). The signal at −101.1 ppm was already detected in the $^{31}$P NMR spectrum of pure $PBr_5$ (cf.

Figure S23). Since in solution $PBr_5$ is mainly dissociated into $PBr_3$ and $Br_2$,[21] its main signal at 225 ppm is the signal of $PBr_3$. The one at −101.1 ppm could not be undoubtedly assigned, but, due to its chemical shift, one can assume that it belongs to a small molecule in which the P nucleus is surrounded by more than three halogens such as undissociated $PBr_5$ and is therefore denoted $PBr_x$.[22] The formation of $PBr_3$ suggests that part of **1** is completely brominated to $PBr_3$ and probably $CpMoBr_4$ or $[(CpMo)_2(\mu\text{-}Br_4)]$ are formed.[23] The reaction of **1** with $Br_2$ leads to the formation of the same products as with $PBr_5$. The main difference is the formation of $PBr_3$, which appears, as a side product of the reaction, only when at least three equivalents of bromine are used. In addition, the reaction of **1** with two equivalents of bromine leads to a full conversion of **1** into **3a**, while, under the same conditions, with $PBr_5$, only a partial conversion of **1** into **3a** was observed.[24] Reacting **1** with six or more equivalents of bromine leads to immediate precipitation of **4a** (*vide infra*), and formation of $PBr_3$ and $PBr_x$ (cf. Figure S18).

These results show a completely different reactivity of **1** towards $Br_2$ as compared to the observed reactivity of **1** towards $I_2$. While **1** reacts with $I_2$ under elimination of all CO ligands, followed by the aggregation of the formed species under elimination of $PI_3$ and $P_2I_4$, with $Br_2$, only the two CO ligands at one Mo center are replaced, leading to the stable compound **4a**.

In order to investigate the possibility of further halogenation of **1**, we refluxed a solution of **1** with six equivalents of $PBr_5$. Under these conditions, the formed **4a** is not stable and decomposes, because when **4a** was refluxed alone in acetonitrile for two hours decomposition occurred.[25] One way to control the outcome of the reaction is the stoichiometry; however, the influence of the temperature has to be investigated. **1** was reacted with six equivalents of $Br_2$ and a variable temperature $^{31}P\{^1H\}$ NMR measurement was recorded between 193 K and 300 K (cf. Figure S22). Already at 193K, the color changes and the formation of a precipitate of **4a** in the NMR tube was observed. In the $^{31}P\{^1H\}$ NMR spectrum at 193K two main signals corresponding to $PBr_x$ and $PBr_3$ (-101.1 ppm and 229.2 ppm, respectively) appear, indicating a full conversion of **1**. Neither **3a** nor **4a** are detected until room temperature is reached, where the signal of **4a** is observed due to its redissolution. The absence of the signal of the hexa-brominated product at low temperature can be explained by the fact that it is precipitated and cannot be detected until room temperature reached. Therefore, one can conclude that the best way to control the reaction between **1** and $Br_2$ is the stoichiometry, which allows the formation of **3a** (with two equivalents of $Br_2$) or directly **4a** (when six equivalents of $Br_2$ are used).

Since the reactivity of **1** towards $I_2$ and bromine sources, respectively, is very different, we investigated the reactivity of **1** towards chlorine. To avoid the use of chlorine gas we chose $PCl_5$ as chlorinating agent. Surprisingly, the reactivity of **1** towards $PCl_5$ is very similar to that of **1** towards $PBr_5$, leading to the chlorinated derivatives **3b** and **4b** (Scheme 3).

To compare this reactivity with the one towards bromine, **1** was reacted with one (two or three) equivalents of $PCl_5$ and followed up via NMR spectroscopy. In all cases, the $^{31}P$ NMR spectrum of the reaction mixture showed, although with different ratios, three singlets corresponding to **4b** (337.1 ppm), **3b** (236.3 ppm) and $PCl_3$ (220.9 ppm). When three equivalents of $PCl_5$ were used, **1** was not detectable, indicating full conversion to **3b**, **4b** and $PCl_3$. All attempts to isolate pure **3b** failed since it is always formed in a mixture with **4b**, even when the reaction is performed at low temperatures. The addition of six equivalents of $PCl_5$ to a solution of **1** resulted in an immediate color change. After workup, [{CpMo(CO)$_2$}(CpMoCl$_2$)(μ-PCl$_2$)$_2$] (**4b**) was isolated in a yield of 91% (Scheme 3). The $^{31}P$ NMR spectrum of the reaction mixture is comparable to the one discussed for **4a**, showing the full conversion of **1** into **4b** and $PCl_3$. The $^{1}H$ NMR spectrum of **4b** shows two signals for the two nonequivalent Cp rings, one singlet at 5.6 ppm and one triplet at 5.5 ppm, due to the coupling of the protons of one Cp ligand with the two phosphorus atoms ($^3J_{PH}$ = 2.14 Hz) (cf. Figure S24). This is also comparable with the $^{1}H$ NMR spectrum of **4a** which reveals two signals for the two nonequivalent Cp rings, one singlet at 5.7 ppm and one triplet at 5.6 ppm, which is due to the coupling of the protons of one Cp ligand with the two phosphorus atoms ($^3J_{PH}$ = 2.45 Hz) (cf. Figure S7). In the $^{31}P$ NMR spectrum of **4a**, the $^3J_{PH}$ coupling could not be detected due to the slightly broadened signal ($\omega_{½}$ = 16.5 Hz) (cf. Figure S8). In order to substitute all CO ligands of **1** with chlorine, the reaction mixture was refluxed in toluene for two hours. Contrary to **4a**, **4b** was stable at these conditions, neither further halogenation with $PCl_5$ nor decomposition occurred. Even though the reactivity of **1** towards $Br_2$ and $Cl_2$ sources is very similar, there is a significant difference in the yield (54% for **4a** *versus* 91% for **4b**) when **1** is reacted with $PX_5$ (X = Cl, Br). To better explain these results, we compared the amount of $PX_3$ formed in the reaction mixture using $PPh_3$ as an internal standard of the NMR study. While around 80% of $PBr_3$ comes from $PBr_5$ and 20% of it from **1** (cf. Figure S6), all $PCl_3$ comes from $PCl_5$ (cf. Figure S27). This is in line with the observation that **4a** is less stable than **4b** and partly decomposes under the formation of $PBr_3$. The main difference in the $PX_5$ reagents lies in their dissociation in solution. While $PBr_5$ dissociates into $PBr_3$ and $Br_2$, $PCl_5$ stays intact.[21]

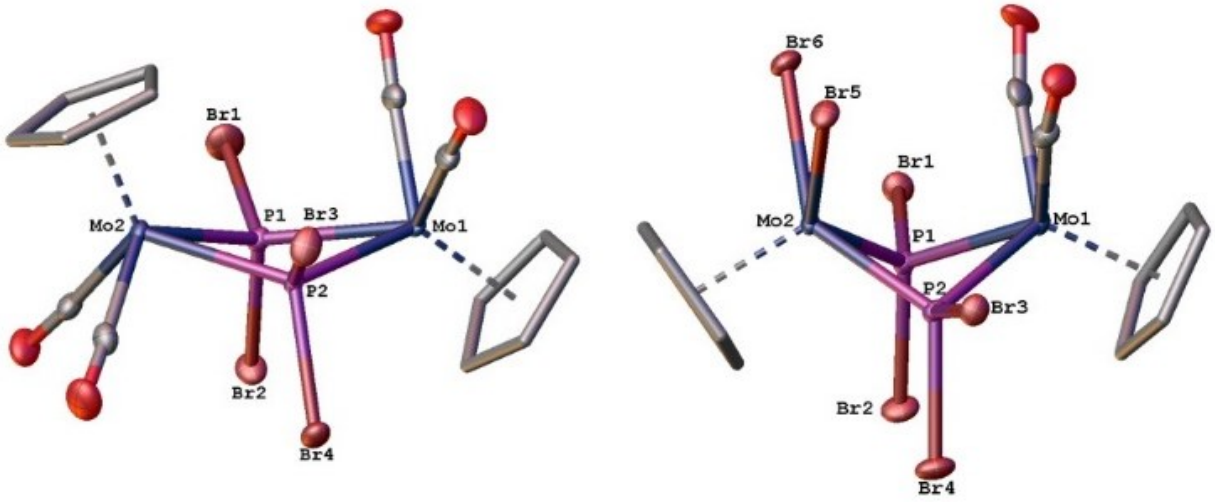


**Figure 3.** Molecular structure of **3a** (on the left) and **4a** (on the right) with thermal ellipsoids at 50% probability level. The hydrogen atoms are omitted for clarity. Selected bond lengths and angles: **3a**: Mo1-P1: 2.4769(8) Å, Mo1-P2: 2.4641(8) Å, Mo1-P2-Mo2: 122.26(3)°, Mo2-P1-Mo1: 112.34(3)°; **4a**: Mo1-P1: 2.4323(5) Å, Mo1-P2: 2.4265(3) Å, Mo2-P1: 2.365(3) Å, Mo2-P2: 2.356(3) Å, Mo1-P2-Mo2: 86.86(9)°, Mo1-P1-Mo2: 86.50(9)°.

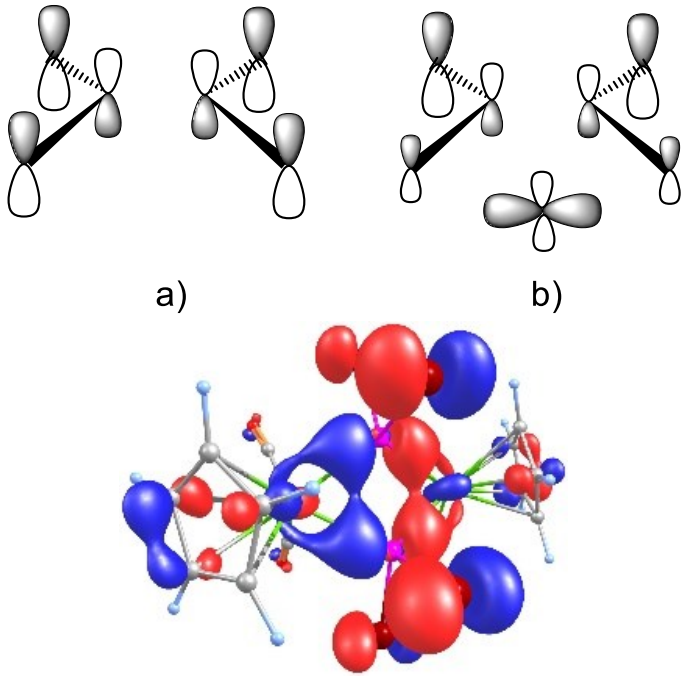


**Figure 4.** Orbital combinations of the $PBr_2$ fragments in a) **3a** and b) **4a**. Isosurface of the HOMO-5 orbital in **3a** on the right.

Single crystals of **3a** suitable for X-ray structure analysis could be obtained from a $CH_2Cl_2$ solution at −80°C. In the solid state, **3a** forms a dinuclear complex in which the $CpMo(CO)_2$ fragments are connected by two bridging $PBr_2$ ligands (Figure 3). The Cp ligands are oriented in *trans* position to each other and only the former $P_2$ unit is brominated, but no CO ligand on the Mo center is substituted. The Mo-P distances are similar to each other

and vary between 2.4564(8) Å and 2.4769(8) Å. The P1···P2 distance amounts to 2.5856(11) Å indicating that there is no bond between these atoms, just as there is none between the two Mo atoms, with a Mo1···Mo2 distance of 4.0980(3) Å. The central four-membered ring in **3a** is not planar, as shown by the folding angle of 147.48(9)°.

In the solid state, **4a** forms a dinuclear complex built from a $CpMo(CO)_2$ and a $CpMoBr_2$ unit which are connected via two bridging $PBr_2$ ligands (Figure 3). The central $Mo_2P_2$ four-membered ring is not planar, as shown by the folding angle of 120.89(2)°. In contrast to the structure of **3a**, the Cp ligands are oriented in *cis* position to each other. The Mo-P distances involving Mo1 (2.4323(5) Å for Mo1-P1 and 2.4265(3) Å for Mo1-P2) are slightly longer than the corresponding distances between Mo2 and the P atoms (2.3650(3) Å for Mo2-P1 and 2.3560(3) Å for Mo2-P2). The P1···P2 distance is 2.9429(4) Å indicating that there is no bond between these atoms, just as there is no bond between the two Mo atoms, with a Mo1···Mo2 distance of 3.2887(5) Å. The Mo1···Mo2 distance in **4a** (3.2887(5) Å) lies below the sum of the van der Waals radii of Mo (4.12 Å).[26] The main difference in the structures of **3a** and **4a** are the relative orientation of the Cp ligands, the folding angle of the central $Mo_2P_2$ core as well as the slightly different Mo···Mo distances (*vide supra*).

The molecular structure of **4b** could be determined by single crystal X-ray diffraction and it is isostructural to **4a** (Figure 5). The P1···P2 (2.9157(8) Å) as well as the Mo1···Mo2 distance (3.2736(11) Å) are similar to the corresponding distances found in **4a** (*vide supra*). The central $Mo_2P_2$ four-membered ring is not planar, as shown by the folding angle of 120.70(8)°.

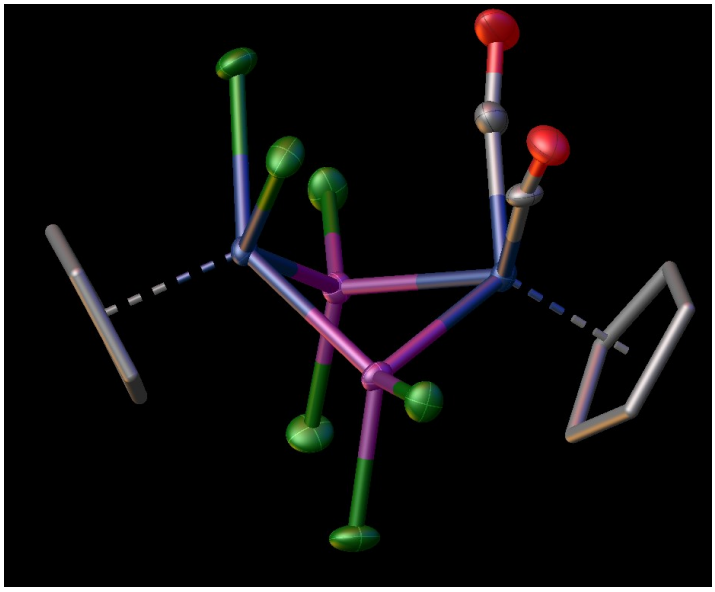

**Figure 5.** Molecular structure of **4b** with thermal ellipsoids at 50% probability level. The hydrogen atoms are omitted for clarity. Selected bond lengths and angles: Mo1-P1: 2.426(3) Å, Mo1-P2: 2.407(3) Å, Mo2-P1: 2.351(3) Å, Mo2-P2: 2.344(3) Å, Mo1-P2-Mo2: 87.08(9)°, Mo1-P1-Mo2: 86.49(8)°.

DFT calculations reproduce well the geometric parameters of **3a** and **4a**. The shorter P1···P2 interaction in **3a** compared to **4a** is mainly based on the in-phase combination of the π-type orbitals of the two $PBr_2$ groups (Figure 4), which represents mainly the bromine lone pairs, but with roughly 10% contribution of phosphorus per $PBr_2$ fragment. The molecular orbital representing this interaction is depicted in Figure 4. In contrast, in **4a** the same π-type orbital of the $PBr_2$ unit shows a strong in-phase combination with a Mo d orbital, leading to a Mo-P bonding overlap but not to a bonding interaction between the two phosphorus atoms (Figure 4).

## 3.3 Conclusions

In conclusion, we showed that the reactivity of the $P_2$ ligand complex [{$CpMo(CO)_2$}$_2$($\mu,\eta^2:\eta^2$-$P_2$)] (**1**) towards different halogen sources ($I_2$, $Br_2$, $PBr_5$ and $PCl_5$), differs depending on the used halogen. While the reaction of **1** with chlorine or bromine sources is similar, the reaction of **1** with $I_2$ is completely different. In the latter case, a complete substitution of the CO ligands in **1** by iodine and the formation of the paramagnetic tetranuclear complex [$(CpMo)_4(\mu_4\text{-}P)(\mu_3\text{-}PI)_2(\mu\text{-}I)(I)_3(I_3)$] (**2**) in a triplet spin state occurred. In the reactions of **1** with brominating or chlorinating agents, two tetra-halogenated complexes with the formula [{$CpMo(CO)_2$}$_2$($\mu$-$PX_2$)$_2$] **3a,b** (X = Br, Cl) are initially formed, as a result of the halogenation on the P atoms. Afterwards, a replacement of the carbonyl ligands on one Mo atom by the halogen atoms occurs and two hexa-halogenated complexes with the formula [{$CpMo(CO)_2$}($CpMoX_2$)($\mu$-$PX_2$)$_2$] **4a,b** (X = Br, Cl) are formed. Considering the choice of the halogen sources, the used $PCl_5$ avoids chlorine gas and is comparable with the reactivity of $PBr_5$. By comparing $PBr_5$ with $Br_2$, even though the products obtained in the reaction with **1** are the same, there are nonetheless some differences. Under the same conditions, $Br_2$ leads to a full conversion of **1** into the tetrabrominated compound [{$CpMo(CO)_2$}$_2$($\mu$-$PBr_2$)$_2$] (**3a**), in contrast to the only partial conversion observed for $PBr_5$. Moreover, the formation of $PBr_3$, as a result of the complete halogenation of **1**, is only observed when at least three equivalents of bromine are used, while it is already detected when one equivalent of $PBr_5$ is used (not derived from $PBr_5$ itself).

In this study, we presented four unprecedented complexes containing bridging $PX_2$ ligands, which are of potential interest because of their further ability to be functionalized on the P atoms by replacing the halogens with a linker or other organic groups via classic organic reactions. Future investigations will focus on the reactivity of other polyphosphorus complexes, as well as on other compounds containing the heavier pnictogen congeners.

## 3.4 References


[1] D. E. C. Corbridge, *Phosphorus: Chemistry, Biochemistry and Technology, 6th Edition*, CRC Press, Boca Raton, FL, **2013**.

[2] a)C. M.Hoidn, D. J. Scott, R. Wolf, *Chem. Eur. J.* **2021**, *27*, 1886-1902; b) B. M. Cossairt, N. A.Piro, C. C. Cummins, *Chem. Rev*. **2010**, *110*, 4164–4177; c) M. Caporali, L. Gonsalvi, A. Rossin, M. Peruzzini, *Chem. Rev.* **2010**, *110*, 4178 – 4235; d) M. Scheer, G. Balázs, A. Seitz, *Chem. Rev*. **2010**, *110*, 4236–4256; e) for a recent catalytic transformation of P4 cf.:U. Lennert, P. B. Arockiam, V. Streitferdt, D. J. Scott, Ch. Rödl, R. M. Gschwind, R. Wolf, *Nat. Cat.* **2019**, *2*, 1101-1106.

[3] J. D. Masuda, W. W. Schoeller, B. Donnadieu, G. Bertrand, *Angew. Chem.* **2007**, *119*, 7182-7185.

[4] A. R. Fox, R. J. Wright, E. Rivard, P. P. Power, *Angew. Chem.* **2005**, *117*, 7907-7911.

[5] M. Serrano-Ruiz, A. Romerosa, P. Lorenzo-Luis, *Eur. J. Inorg. Chem.* **2014**, 1587–1598.

[6] for reduction chemistry cf.: a) M. Piesch, Ch. Graßl, M. Scheer, *Angew. Chem. Int. Ed.* **2020**, *59*, 7154-7160, b) E. Mädl, G. Balázs, E. V. Peresypkina, M. Scheer, *Angew. Chem. Int. Ed.* **2016**, *55*, 7702–7707; c) M. Piesch, M. Seidl, M. Scheer, *Chem. Sci*. **2020**, *11*, 6745-6751.

[7] M. Fleischmann, F. Dielmann, G. Balázs, M. Scheer, *Chem. Eur. J*. **2016**, *22*, 15248-15251.

[8] a) M. Butovskiy, G. Balázs, M. Bodensteiner, E. V. Peresypkina, A. V. Virovets, J. Sutter, M. Scheer, *Angew. Chem. Int. Ed*, **2013**, *52*, 2972-2976; b) L. Dütsch, M. Fleischmann, S. Welsch, G. Balázs, W. Kremer, M. Scheer, *Angew. Chem. Int. Ed*. **2018**, *57*, 3256-3261.

[9] B. W. Tattershall, N. L. Kendall, *Polyhedron* **1994**, *13*, 1517-1521.

[10] I. Krossing, I.Raabe, *Angew. Chem. Int. Ed.* **2001**, *40*, 4406-4409.

[11] M. Gonsior, I. Krossing, L. Müller, I. Raabe, M. Jansen, L. V. Wüllen, *Chem. Eur. J*. **2002**, *8*, 4475-4492. Compounds containing the PCl4+ cation, have been earlier reported c.f.: J. Shamir, S. Luski, A. Bino, S. Cohen, D. Gibson, *Inorg. Chem*. **1985**, *24*, 2301-2309.

[12] P. Barbaro, C. Bazzicalupi, M. Peruzzini, S. Seniori Costantini, P. Stoppioni, *Angew. Chem. Int. Ed*. **2012**, *51*, 8628-8631.

[13] M. Bispinghoff, Z. Benkő, H. Grützmacher, F. Delgado Calvo, M. Caporali, M. Peruzzini, *Dalton Trans*. **2019**, *48*, 3593-3600.

[14] K. M. Armstrong, P. Kilian, *Eur. J. Inorg. Chem.* **2011**, 2138-2147.

[15] H. Brake, E. V. Peresypkina, A. V. Virovets, M. Piesch, W. Kremer, L. Zimmermann, Ch. Klimas, M. Scheer, *Angew. Chem. Int. Ed.* **2020**, *59*, 16241-16246.

[16] O. J. Scherer, H. Sitzmann, G. Wolmershäuser, *J. Organomet. Chem.* **1984**, *268*, C9-C12.

[17] Complex **2** cannot be detected spectroscopically since it is NMR- and EPR-silent.

[18] J. C. Gordon, V. T. Lee, R. Poli, *Inorg. Chem*. **1993**, *32*, 4460-4463.

[19] F. Spitzer, M. Sierka, M. Latronico, P. Mastrorilli, A. V. Virovets, M. Scheer, *Angew. Chem. Int. Ed.* **2015**, *54*, 4392-4396.

[20] When **1** is reacted with one equivalent of $PBr_5$, after six hours the yield of **3a** (calculated via $^{31}$P-NMR with a capillary of $PPh_3$ as a standard, cf. Figure S9) is 28%.

[21] A. I. Popov, N. Skelly, J. *Am. Chem. Soc.* **1954**, *76*, 3916-3919.

[22] When **1** is reacted with a larger excess of $PBr_5$ (i.e. ten or one hundred equivalents) at room temperature, **4a** precipitates immediately, but, in both cases, the $^{31}$P NMR spectrum of the reaction solution shows two singlets at 228.9 ppm and at -101.1 ppm (corresponding to $PBr_3$ and $PBr_x$, respectively). In case of one hundred equivalents of $PBr_5$ being used, the ratio between the signal of $PBr_3$ and the signal at -101.1 ppm is higher compared to the one when ten equivalents are used, indicating that, even with a huge excess of halogen sources, **4a** could be directly obtained. However, when more than six equivalents of $PBr_5$ are used, there is a lot of unreacted halogenating agent left in solution. (cf. Figures S13-14).

[23] We do not have any evidence of the formation of $[CpMoBr_4]$ or $[(CpMo)_2(\mu\text{-}Br_4)]$. Note that the formation of the paramagnetic complex $[(Cp^*Mo)_2(\mu\text{-}I_4)]^+[I_3]^-$ in similar reactions was observed. (R. Poli, J. C. Gordon, J. U. Desai, A. L. Rheingold, J. *Chem. Soc*, *Chem. Comm* **1991**, 1518.) EPR spectroscopy was performed for the reaction solution of **1** with two equivalents of $PBr_5$ and of **1** with six equivalents of $PBr_5$, but in both cases no signal was detected, indicating that no paramagnetic products detectable with EPR are formed.

[24] When **1** is reacted with one equivalent of $Br_2$, the $^{31}$P NMR spectrum of the reaction solution shows, after eight hours, two singlets at -43.2 ppm and at 200.4 ppm, corresponding to **1** and **3a**, respectively. This indicates that there is only a partial conversion of **1** into **3a**, and no side products are detected (cf. Figure S15). When **1** is reacted with two equivalents of $Br_2$, the $^{31}$P NMR spectrum of the reaction solution shows, after eight hours, only one singlet at 200.4 ppm, indicating a full conversion of **1** into **3a** and no formation of $PBr_3$ or any other diamagnetic product (cf.Figure S16). When **1** is reacted with three equivalents of $Br_2$, after seven hours, three singlets are detected in the $^{31}$P-NMR spectra of the reaction solution at 200.4 ppm (**3a**), 229.0 ppm ($PBr_3$) and at 301.3 ppm (**4a**), indicating a full conversion of **1** (cf. Figure S17). When **1** is reacted with six equivalents of bromine, **4a** precipitates immediately, while the $^{31}$P NMR spectrum of the reaction solution shows two singlets at 229.0 ppm and at -101.1 ppm corresponding to $PBr_3$ and $PBr_x$ respectively (cf. Figure S18). When **1** is reacted

with ten or one hundred equivalents of bromine, the same signals as observed in the case of $PBr_5$ are detected in the $^{31}P$ NMR spectra. In summary, the minimum amount of $Br_2$ needed to achieve a full conversion of **1** into **3a** is two equivalents, while, with three equivalents, both **3a** and **4a** are detected. The formation of $PBr_3$ also with pure bromine proves that it derives from the complete halogenation of **1**.

[25] When **4a** was refluxed in $CH_3CN$, it was found not to be stable and to undergo decomposition. Therefore, we investigated what happens when the reaction is performed directly under reflux. When **1** is reacted with six equivalents of $PBr_5$ and refluxed for two hours in acetonitrile, the $^{31}P$ NMR spectrum of the reaction solution shows two singlets at 235.5 ppm and -94.5 ppm, corresponding to $PBr_3$ and $PBr_x$, respectively (cf. Figure S20). When **1** is reacted with one equivalent of $PBr_5$ and refluxed for two hours in acetonitrile, the $^{31}P$ NMR spectrum of the reaction solution shows two signals at 232.8 ppm ($PBr_3$) and -355.7 ppm, the latter cannot be attributed (cf. Figure S21). Since **1** is stable at this temperature, while **4a** undergoes decomposition, it is reasonable to assume that a halogenation to form **4a** occurs, however, with the decomposition of the latter being faster than a possible further halogenation (cf. Figure S19).

[26] S. S. Batsanov, *Inorg. Mat*. **2001**, *37*, 871-885.

## 3.5 Supporting information

### General procedures

All manipulations were carried out under an inert atmosphere of dried nitrogen using standard Schlenk and glove box techniques. Solvents were dried using a MB SPS-800 device of the company MBRAUN. Deuterated solvents were freshly distilled under nitrogen from $CaH_2$ ($CD_2Cl_2$) and from Na/K alloy ($C_6D_6$).

NMR spectra were recorded on a Bruker Advance III 400 MHz NMR spectrometer. Chemical shifts were measured at room temperature and given in ppm; they are referenced to TMS for $^1H$ and 85% $H_3PO_4$ for $^{31}P$ as external standard. LIFDI-MS spectra (LIFDI = liquid injection field desorption ionization) were measured on a JEOL AccuTOF GCX. ESI-MS spectra (ESI = Electrospray ionization) were measured on an Agilent Q-TOF 6540 UHD. Elemental Analysis (CHN) was determined using a Vario micro cube instrument. The X-Band EPR measurements were carried out with a MiniScope MS400 device with a frequency of 9.44GHz and a rectangular resonator TE102 of the company Magnettech GmbH.

The compound [{$CpMo(CO)_2$}$_2$($\mu,\eta^2$:$\eta^2$-$P_2$)] (**1**) was synthesized according to literature procedure.[1] Phosphorous (V) chlorine was purchased from abcr, Phosphorous (V) bromine (95%) from Alfa Aesar, Iodine from Sigma-Aldrich and they all were used as received without any further purifications.

### Synthesis of [$(CpMo)_4(\mu_4$-P)($\mu_3$-PI)$_2$($\mu$-I)(I)$_3$($I_3$)] (2)

[{$CpMo(CO)_2$}$_2$($\mu,\eta^2$:$\eta^2$-$P_2$)] (**1**) (20 mg, 0.04 mmol, 1 eq) is dissolved in 10 mL of $CH_2Cl_2$. To this solution, a solution of $I_2$ (0.12 mmol, 30.70 mg, 3 eq) in 20 mL of $CH_2Cl_2$ is added. A change in color from bright orange to dark brown is immediately observed. The solution is stirred for 1 hour, then is filtered over celite and stored at room temperature. After two weeks [$(CpMo)_4(\mu_4$-P)($\mu_3$-PI)$_2$($\mu$-I)(I)$_3$($I_3$)] (**2**) crystallized as black crystals, suited for X-ray analysis.

**Yield 2**: 14 mg, 0.007 mmol, 18%

Both, the NMR as well as the X-band EPR spectra of isolated **2** are silent, suggesting a paramagnetic complex in triplet spin state (see computational details section).

**FD-MS** ($CH_2Cl_2$): 829.56 (100%, [$C_{10}H_{10}Mo_2I_4^+$])]; only a fragment could be detected.

**EA** calculated for $C_{20}H_{20}Mo_4P_3I_9$ (1886.84 g·mol$^{-1}$): C: 12.72, H: 1.07; found [%]: C:12.74, H: 0.94.

**Synthesis of [{CpMo(CO)$_2$}$_2$(μ-PBr$_2$)$_2$] (3a)**

[{CpMo(CO)$_2$}$_2$(μ,η$^2$:η$^2$-P$_2$)] (**1**) (20 mg, 0.04 mmol, 1 eq) is dissolved in 10 mL of $CH_2Cl_2$. To this solution, a solution of $PBr_5$ (34.71 mg, 0.08 mmol, 2 eq) in 10 mL of $CH_2Cl_2$ is added. A change in color from bright orange to dark brown is immediately observed. The solution is stirred for 1 hour. The solvent is removed *in vacuo*. The resulting brown residue is dissolved in 5 mL of $CH_2Cl_2$, layered by 10 mL of hexane and stored at -80°C. After two weeks [{CpMo(CO)$_2$}$_2$(μ-PBr$_2$)$_2$] (**3a**) crystallized as black blocks, suited for X-ray analysis.

**Yield 3a** 10 mg, 0.012 mmol, 29%

**$^1$H NMR** (400 MHz, $CD_2Cl_2$, 300K): δ [ppm] = 5.60 (s, 10 H, $C_5H_5$).

**$^{31}$P{$^1$H} NMR** (162 MHz, $CD_2Cl_2$, 300K): δ [ppm] = 200.38 (s, 2 P, ($P$Br$_2$)$_2$).

**$^{13}$C{$^1$H} NMR** (300 MHz, $CD_2Cl_2$, 300K): δ [ppm] = 98.46 (s, 5 C, $C_5H_5$).

**FD-MS** ($CH_2Cl_2$): 815.38 (100%, [**3a**$^+$]).

**EA** calculated for $C_{14}H_{10}Br_4Mo_2O_4P_2$ (815.49 g·mol$^{-1}$): C: 20.60, H: 1.24; found [%]: C: 19.78, H: 1.97

**ATR** (Germanium crystal): ν [cm$^{-1}$] = 1916, 1970 (CO).

**Synthesis of [{CpMo(CO)$_2$}(CpMoBr$_2$)(μ-PBr$_2$)$_2$] (4a)**

[{CpMo(CO)$_2$}$_2$(μ,η$^2$:η$^2$-P$_2$)] (**1**) (30 mg, 0.06 mmol, 1 eq) is dissolved in 15 mL of $CH_2Cl_2$. To this solution, a solution of $PBr_5$ (154.98 mg, 0.36 mmol, 6 eq) in 20 mL of $CH_2Cl_2$ is added. A change in color from bright orange to brown is observed, together with the formation of a light brown precipitate. The solution is stirred for 1 hour, then is filtered over celite and stored at room temperature. After two weeks [{CpMo(CO)$_2$}(CpMoBr$_2$)(μ-PBr$_2$)$_2$] (**4a**) crystallized as black blocks, suited for X-ray analysis.

**Yield 4a** 30 mg, 0.033 mmol, 54%

**$^1$H NMR** (400 MHz, $CD_2Cl_2$, 300K): δ [ppm] = 5.57 (t, 5 H, $^3J_{P,H}$ = 2.45 Hz, $C_5H_5$), 5.67 (s, 5 H, $C_5H_5$).

**$^{31}$P{$^1$H} NMR** (162 MHz, $CD_2Cl_2$, 300K): δ [ppm] = 301.23 (s, 2 P, ($P$Br$_2$)$_2$).

**$^{13}$C{$^1$H} NMR** (300 MHz, $CD_2Cl_2$, 300K): δ [ppm] = 97.27 (s, 5 C, $C_5H_5$) 103.40 (s, 5C, $C_5H_5$).

**ESI-MS** ($CH_3CN$): cation mode: *m/z* = 840.41 (3.72% [**M** - Br]$^+$).

**EA** calculated for $C_{12}H_{10}Br_6Mo_2O_2P_2$ (917.34 g·mol$^{-1}$): C: 15.68, H: 1.10; found [%]: C: 14.52, H: 1.38 (due to the high sensitivity of **4a** to moisture and air, it was not possible to obtain an exact elemental analysis, despite several attempts).

**ATR** (Germanium crystal): ν̃ [cm$^{-1}$] = 2015, 2077 (CO).

**Synthesis of [{CpMo(CO)$_2$}$_2$(μ-PCl$_2$)$_2$] (3b)**

[{CpMo(CO)$_2$}$_2$(μ,η$^2$:η$^2$-P$_2$)] (**1**) (20 mg, 0.04 mmol, 1 eq) is dissolved in 10 mL of $CH_2Cl_2$. To this solution, a solution of $PCl_5$ (50 mg, 0.24 mmol, 6 eq) in 15 mL of $CH_2Cl_2$ is added. A change in color from bright orange to brown is observed. The solution is stirred for 10 minutes. With these conditions is possible to observe **3b** via NMR spectroscopy but all attempts to isolate it failed since it is always formed in a mixture with **4b**.

**Yield 3b** (calculated via NMR) 21.35%

**$^1$H NMR** (400 MHz, $CD_2Cl_2$, 300K): δ [ppm] = 5.56 (s, 10 H, $C_5H_5$).

**$^{31}$P{$^1$H} NMR** (162 MHz, $CD_2Cl_2$, 300K): δ [ppm] = 236.29 (s, 2 P, ($P$Cl$_2$)$_2$).

**LIFDI-MS** (toluene): 637.65 (48%, [**3b**$^+$]).

**EA** All attempts to isolate **3b** failed since it is always formed in a mixture with **4b**, therefore it was not possible to obtain an exact elemental analysis.

**IR** ($CH_2Cl_2$): ν̃ [cm$^{-1}$] = 1932, 1981 (CO). (these bands are obtained from the solution of the crude reaction mixture and are assigned by comparison with the bands obtained from isolated **4b**).

**Synthesis of [{CpMo(CO)$_2$}(CpMoCl$_2$)(μ-PCl$_2$)$_2$] (4b)**

[{CpMo(CO)$_2$}$_2$(μ,η$^2$:η$^2$-P$_2$)] (**1**) (25 mg, 0.05 mmol, 1 eq) is dissolved in 15 mL of $CH_2Cl_2$. To this solution, a solution of $PCl_5$ (62.96 mg, 0.30 mmol, 6 eq) in 15 mL of $CH_2Cl_2$ is added. A change in color from bright orange to brown is observed, followed by the formation of a light brown precipitate. The solution is stirred for 1 hour and then is filtered over celite. The resulting bright yellow solution is stored at room temperature. A few hours later [{CpMo(CO)$_2$}(CpMoCl$_2$)(μ-PCl$_2$)$_2$] (**4b**) crystallized as brown blocks, suitable for X-Ray analysis.

**Yield 4b** 30 mg, 0.046 mmol, 92%

**$^1$H NMR** (400 MHz, $CD_2Cl_2$, 300K): δ [ppm] = 5.51 (t, 5 H, $^3J_{P,H}$ = 2.25 Hz, $C_5H_5$), 5.63 (s, 5 H, $C_5H_5$).

**$^{31}$P{$^1$H} NMR** (162 MHz, $CD_2Cl_2$, 300K): δ [ppm] = 337.13 (s, 2 P, ($P$Cl$_2$)$_2$).

**$^{13}C\{^{1}H\}$ NMR** (300 MHz, $C_6D_6$, 300K): δ [ppm] = 101.87 (s, 5 C, $C_5H_5$), 94.33 (s, 5 C, $C_5H_5$).

**FD-MS** (toluene):653.63 (100%, [**4b**$^+$]).

**EA** calculated for $C_{12}H_{10}Cl_6Mo_2O_2P_2$ (653.64 g·mol$^{-1}$): C: 22.03, H: 1.54; found [%]: C:22.14, H: 1.84.

**IR** ($CH_2Cl_2$): ν [cm$^{-1}$] = 2030, 2059 (CO).

## Selected NMR spectra

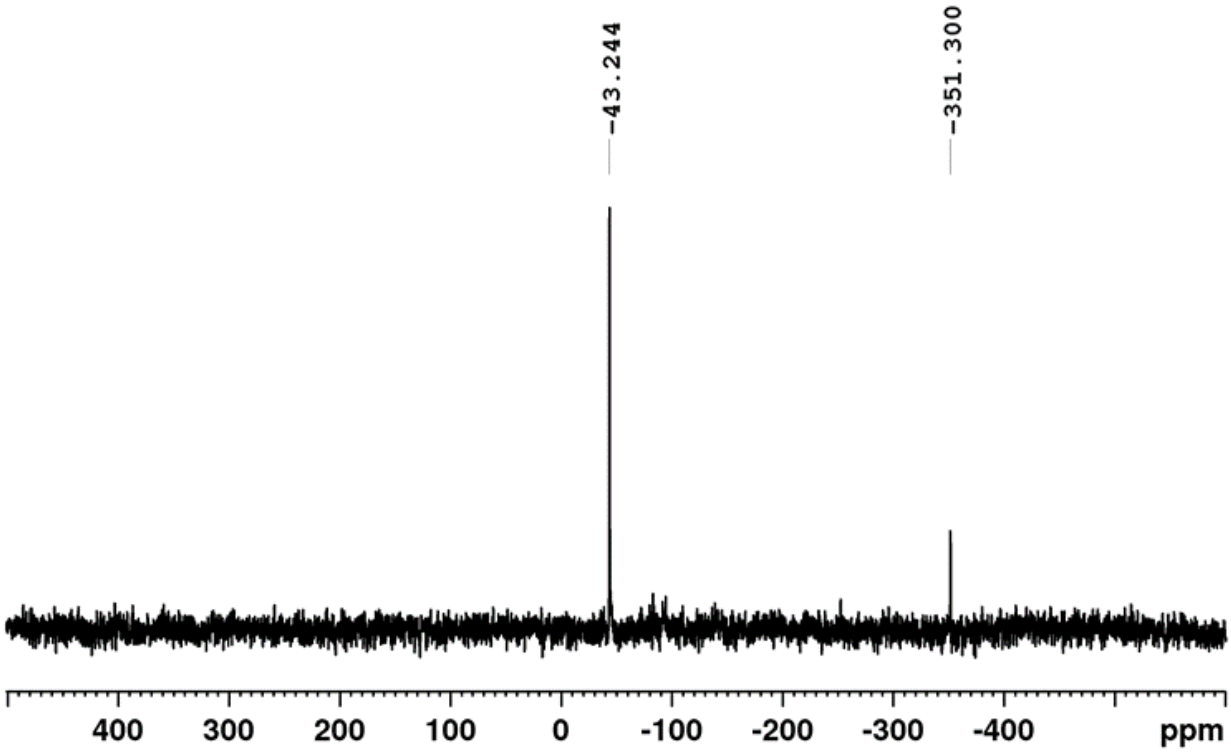


**Figure S 1.** $^{31}P\{1H\}$ NMR spectrum of the solution of the reaction between 1 (1 eq) and $I_2$ (1 eq) (C6D6 capillary, 300K).

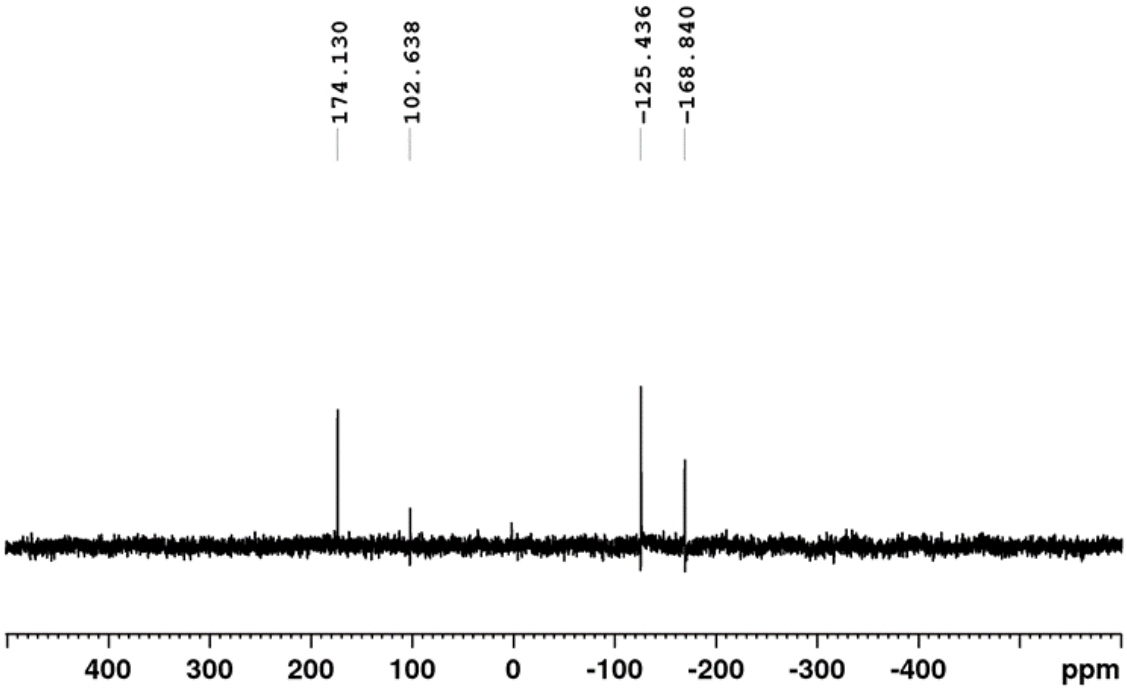


**Figure S 2.** $^{31}P\{^1H\}$ NMR spectrum of the solution of the reaction between **1** (1 eq) and $I_2$ (3 eq) ($C_6D_6$ capillary, 300K).

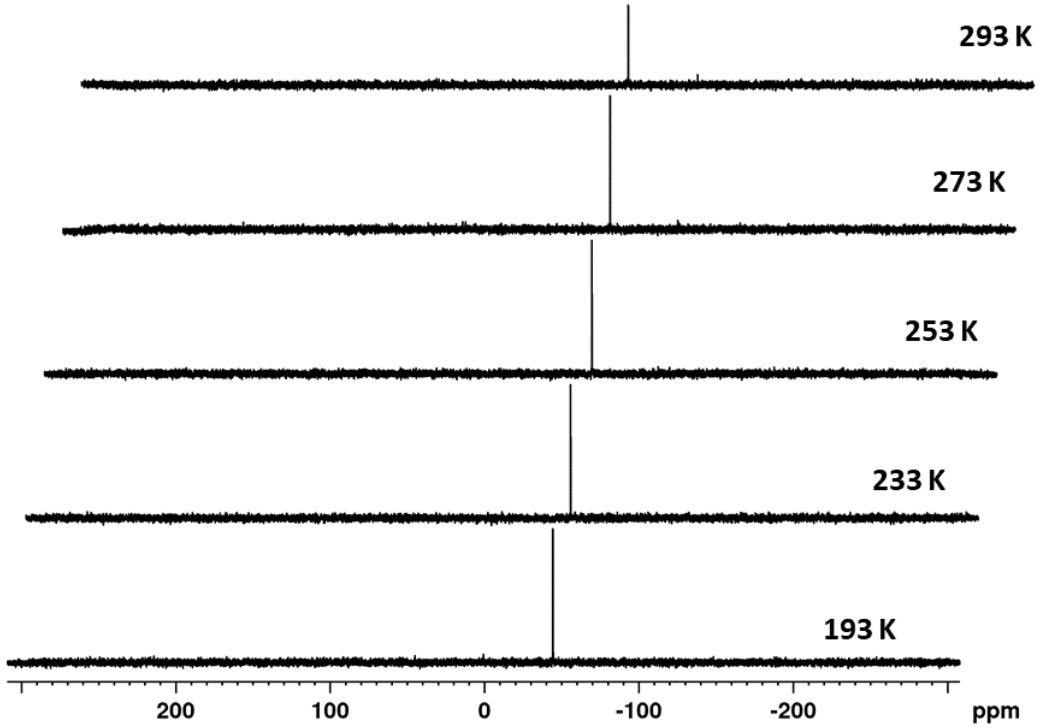


**Figure S 3.** VT $^{31}P\{^{1}H\}$ NMR spectra of the solution of the reaction between **1** (1eq) and $I_2$ (3 eq) ($CD_2Cl_2$).

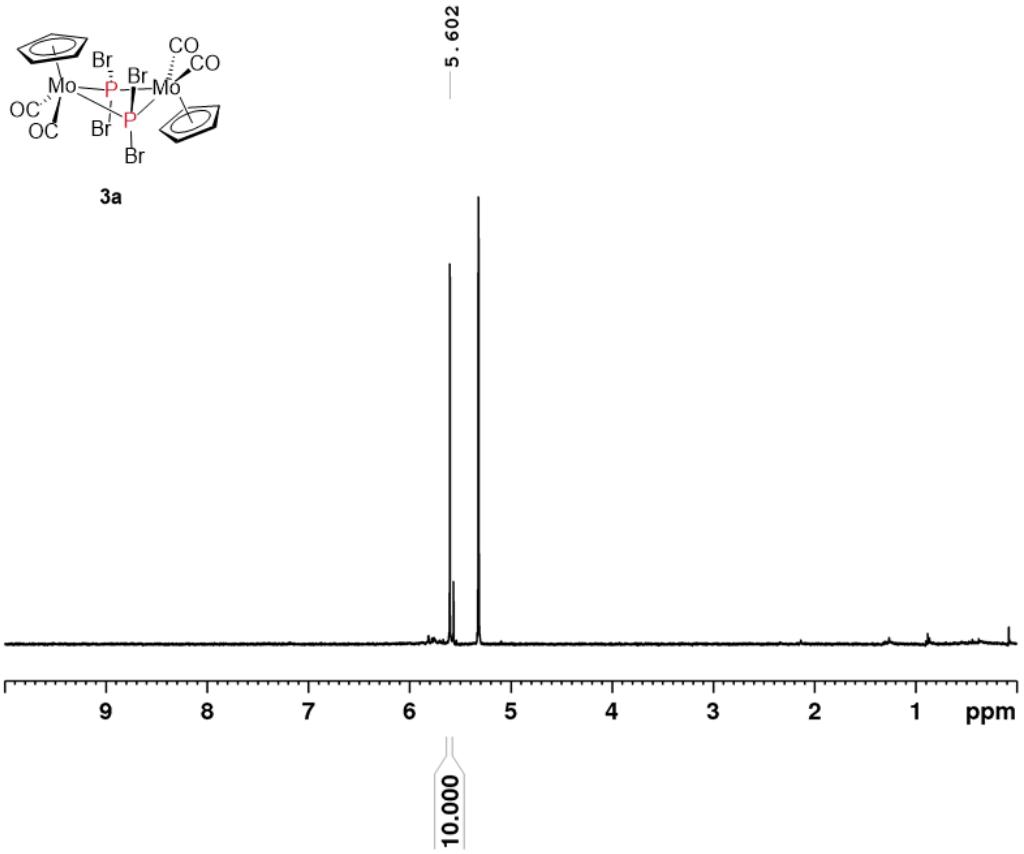


**Figure S 4.** $^{1}H$ NMR spectrum of compound **3a** ($CD_2Cl_2$, 300 K).

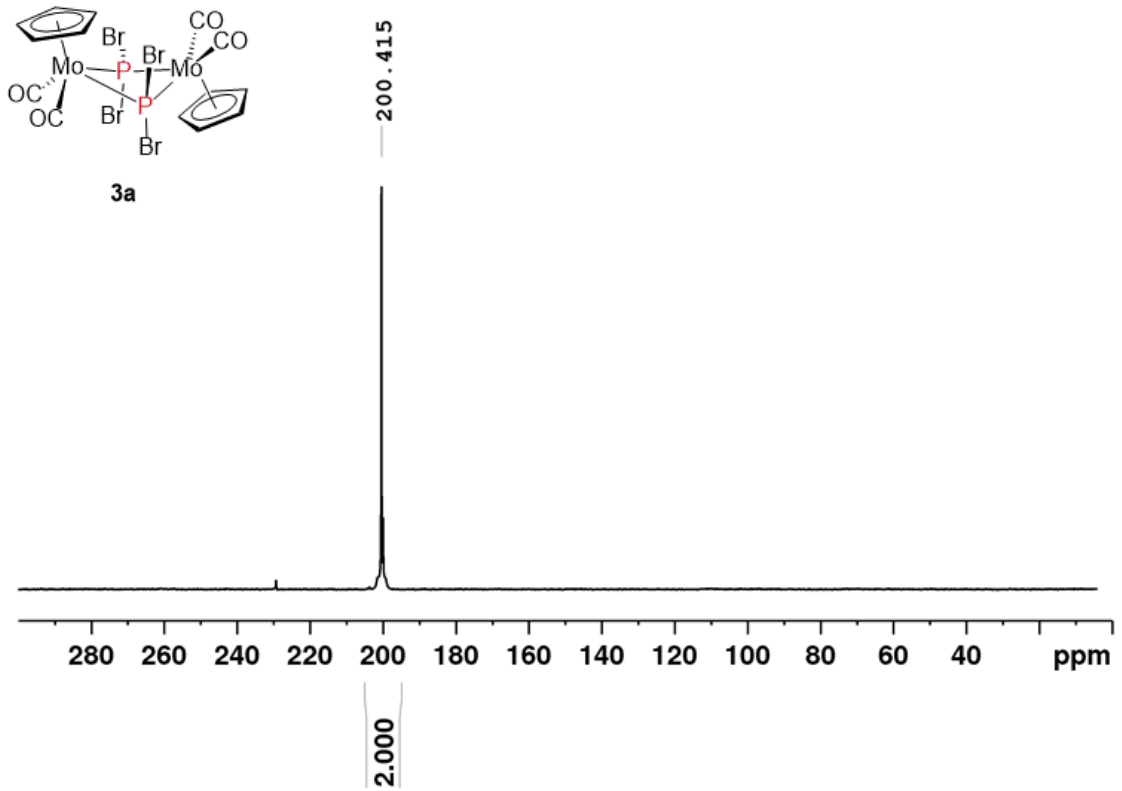


**Figure S 5.** $^{31}P\{^{1}H\}$ NMR spectrum of compound **3a** ($CD_2Cl_2$, 300 K).

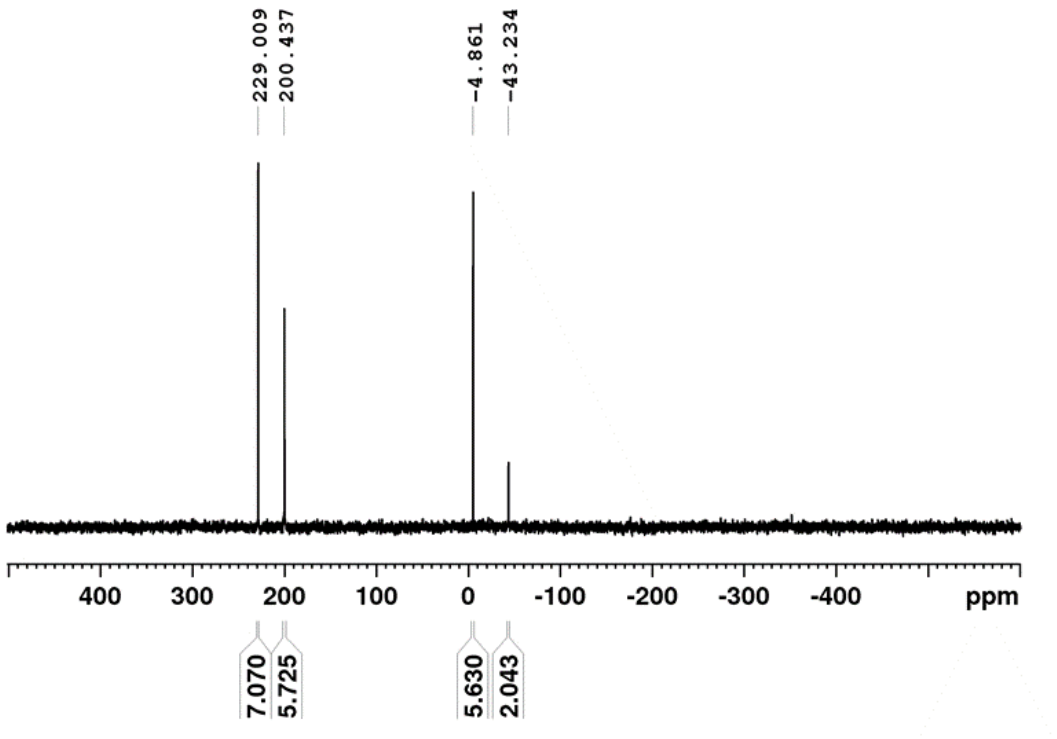


**Figure S 6.** $^{31}P\{^{1}H\}$ NMR spectrum of the reaction solution of **1** (1 eq) with $PBr_5$ (1 eq) and $PPh_3$ as a reference ($C_6D_6$ capillary, 300 K).

- mmol $PPh_3$ in the inner part of the Evans NMR tube: $8.0 \cdot 10^{-4}$
- mmol $PBr_5$ in the external part of the Evans NMR tube: $4.5 \cdot 10^{-3}$
- $\frac{PBr_5}{PPh_3} = \frac{4.5 \cdot 10^{-3}}{8.0 \cdot 10^{-4}} = 5.63$
- Integration $PPh_3 = 5.63$
- Integration $PBr_3 = 7.07$
- 5.63 out of 7.07 (**80%**) equals the amount of $PBr_3$ coming from $PBr_5$
- (7.07 – 5.63) = 1.44 (**20%**) equals the amount of $PBr_3$ coming from **1**

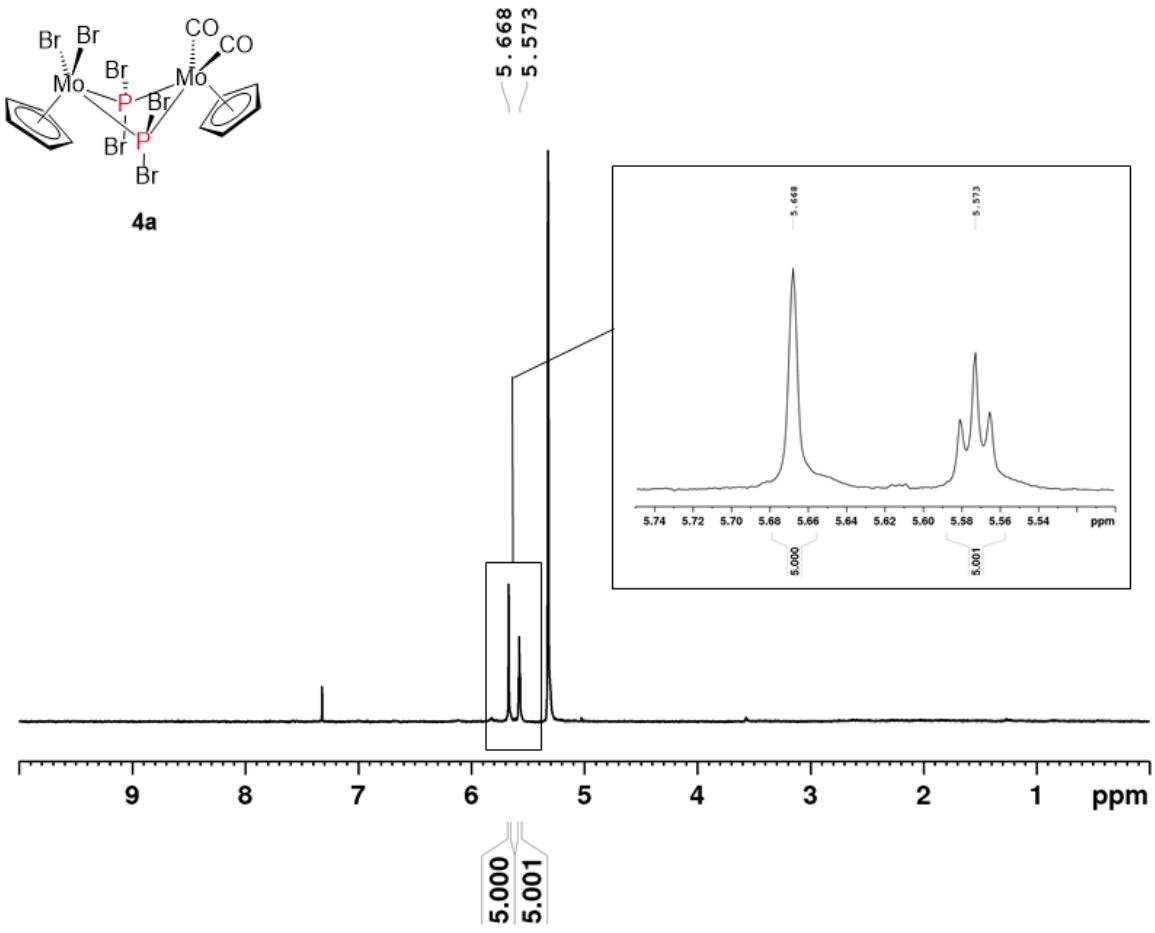


**Figure S 7.** $^1H$ NMR spectrum of compound **4a** ($CD_2Cl_2$, 300 K).

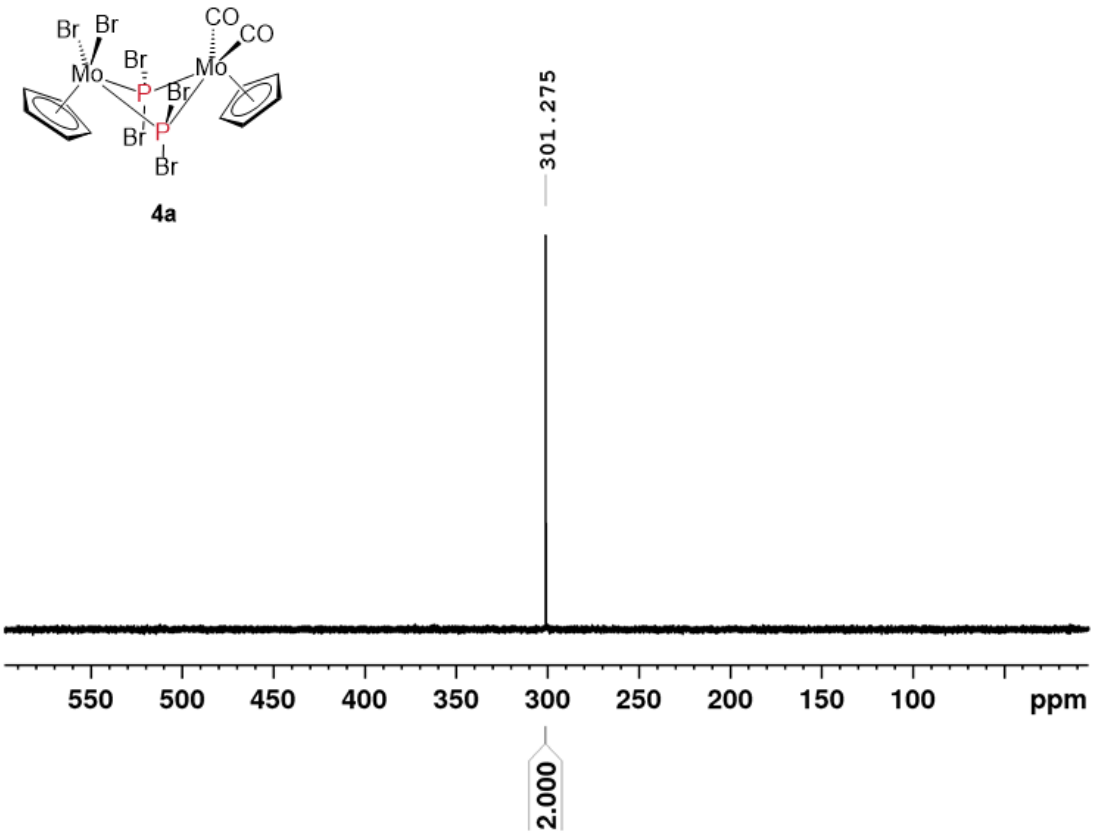


**Figure S 8.** $^{31}P\{^{1}H\}$ NMR spectrum of compound **4a** ($CD_2Cl_2$, 300 K).

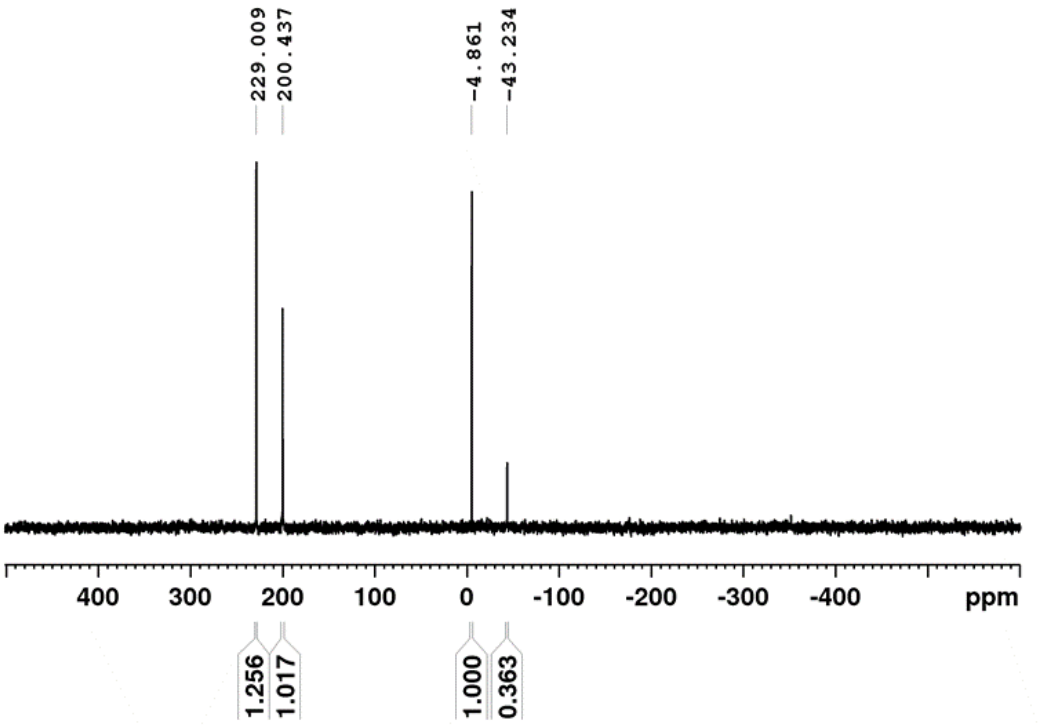


**Figure S 9.** $^{31}P\{^{1}H\}$ NMR spectrum of the solution of the reaction between **1** (1 eq) and $PBr_5$ (1 eq) ($C_6D_6$ capillary and $PPh_3$ as a reference δ =-4.9 ppm, 300K).

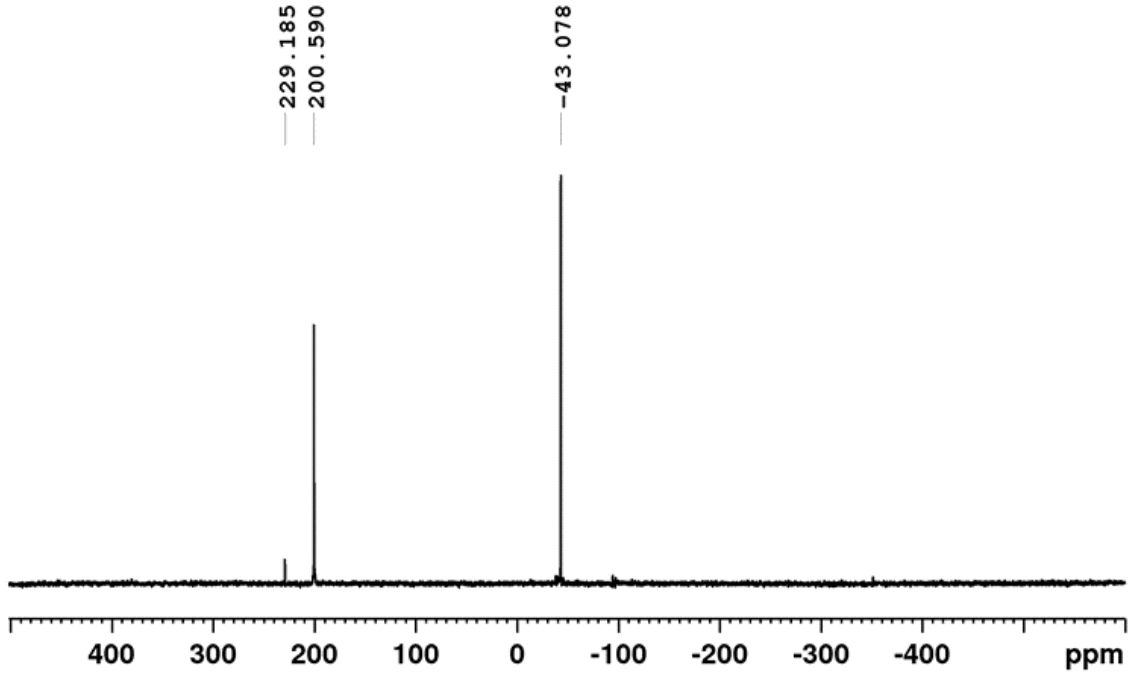


**Figure S 10.** $^{31}P\{^{1}H\}$ NMR spectrum of the solution of the reaction between **1** (1eq) and $PBr_5$ (2 eq) after seven hours ($C_6D_6$ capillary, 300K).

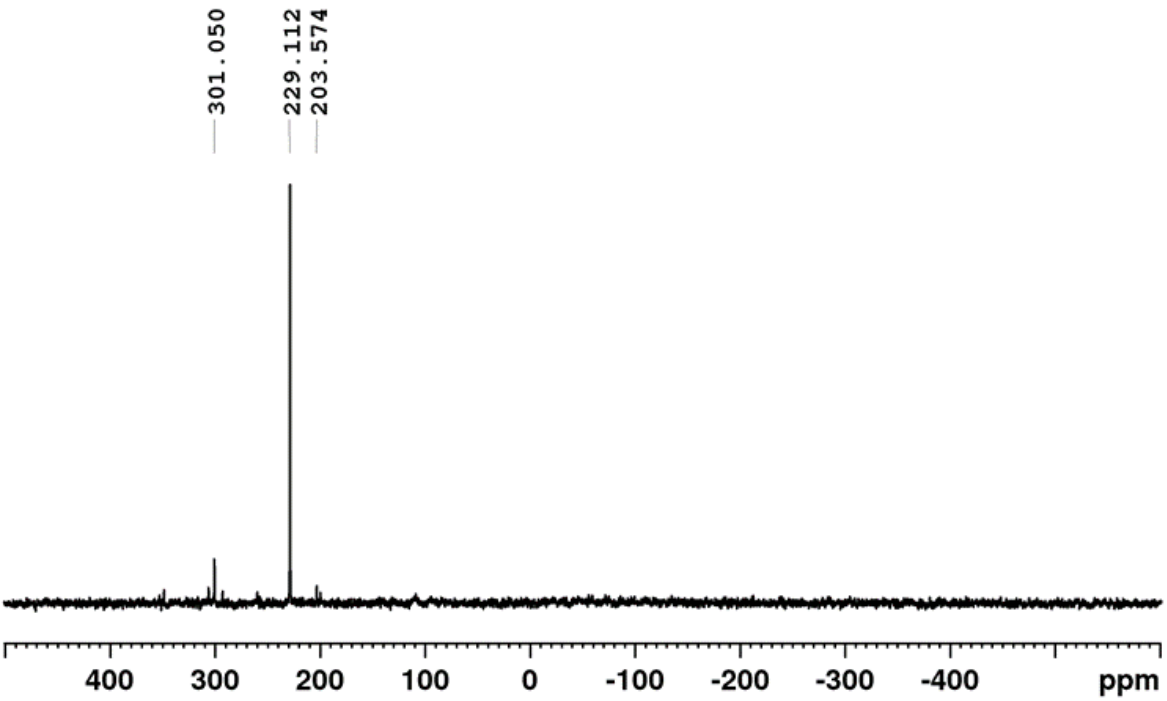


**Figure S 11.** $^{31}P\{^{1}H\}$ NMR spectrum of the solution of the reaction between **1** (1 eq) and $PBr_5$ (2 eq) after seven days ($C_6D_6$ capillary, 300K).

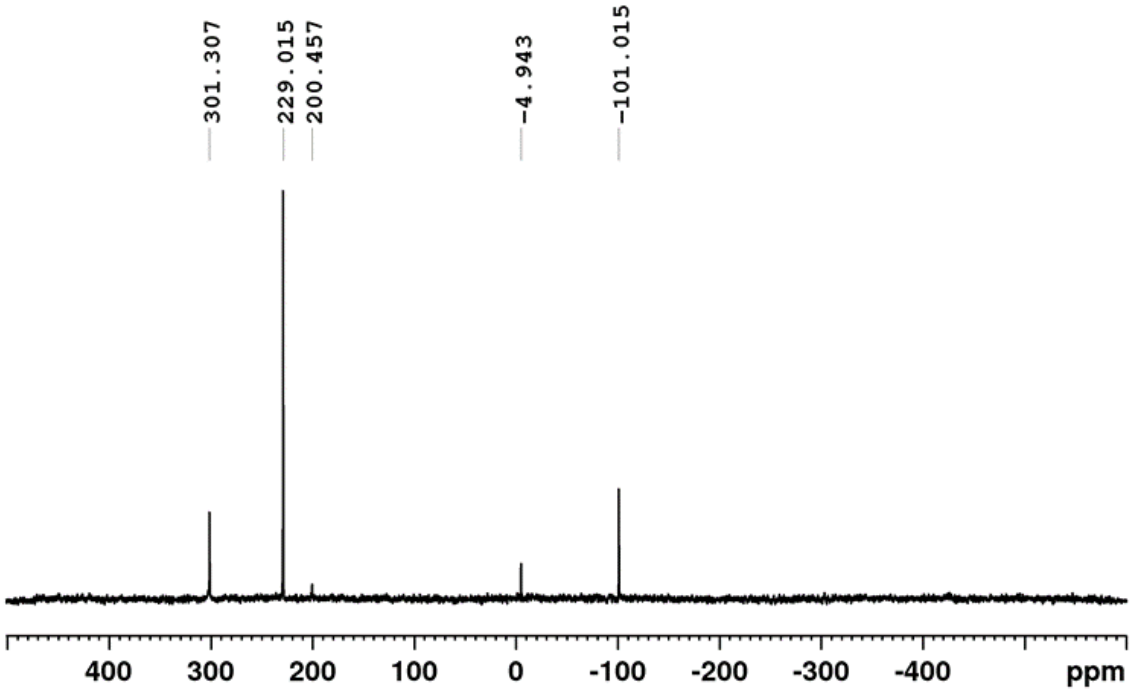


**Figure S 12.** $^{31}P\{^{1}H\}$ NMR spectrum of the solution of the reaction between **1** (1 eq) and $PBr_5$ (6 eq) ($C_6D_6$ capillary and $PPh_3$ as a reference δ =-4.9 ppm, 300K).

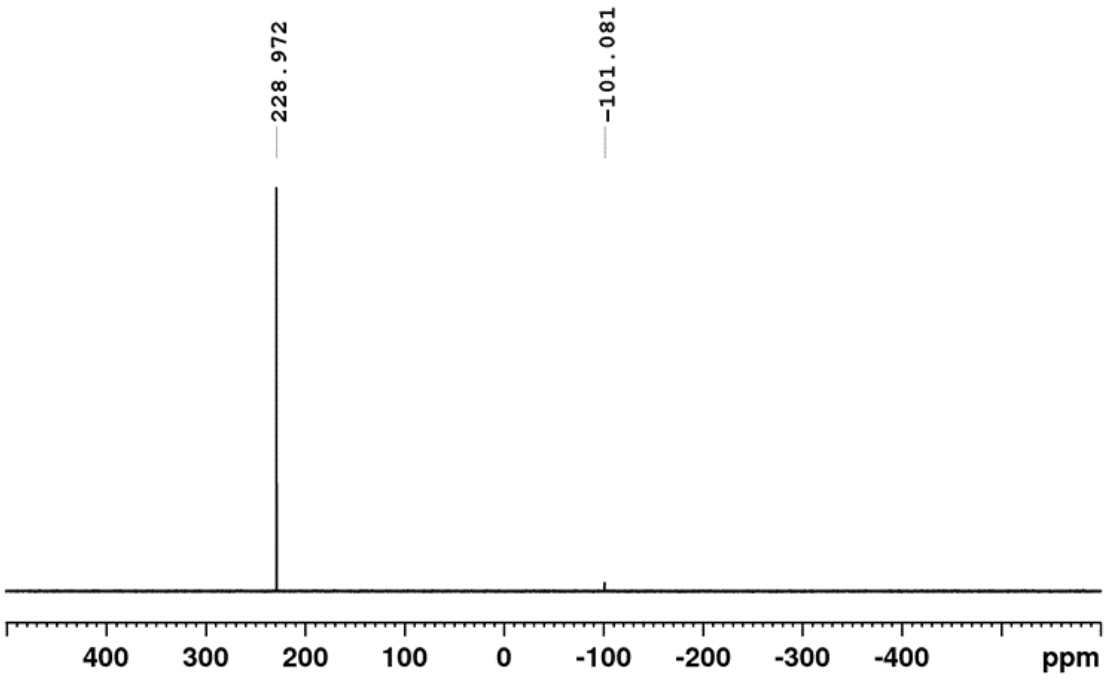


**Figure S 13.** $^{31}P\{^{1}H\}$ NMR spectrum of the solution of the reaction between **1** (1 eq) and $PBr_5$ (10 eq) ($C_6D_6$ capillary, 300K).

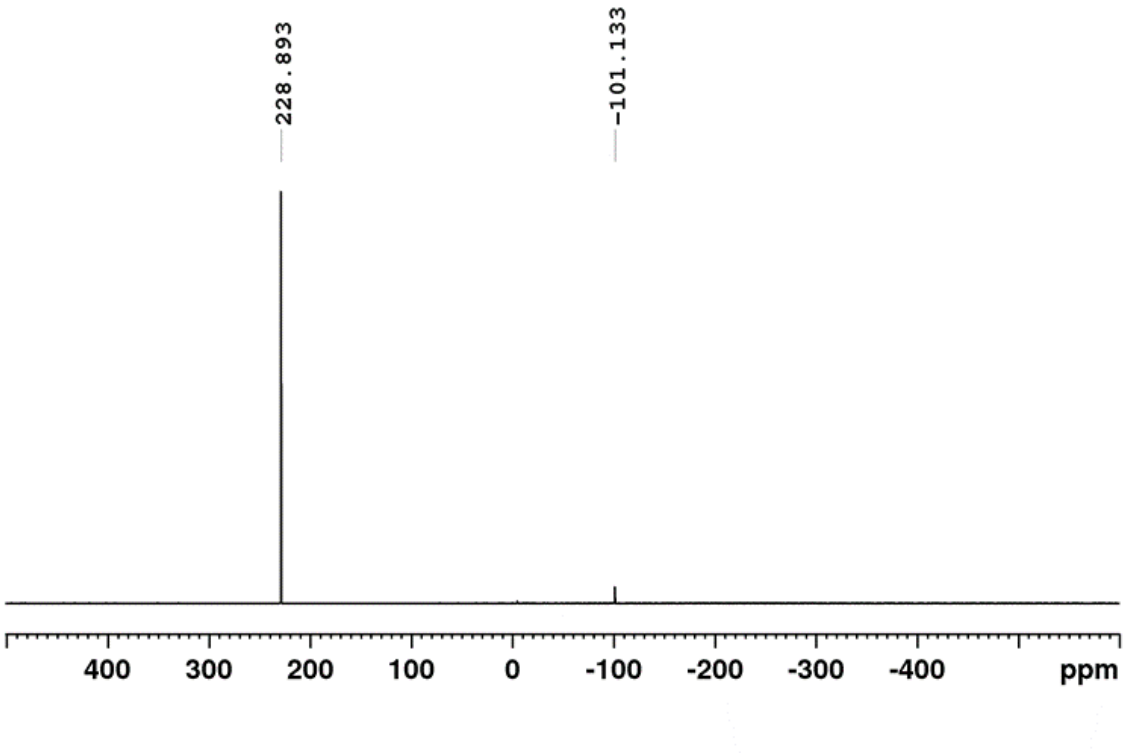


**Figure S 14.** $^{31}P\{^{1}H\}$ NMR spectrum of the solution of the reaction between **1** (1 eq) and $PBr_5$ (100 eq) ($C_6D_6$ capillary, 300K).

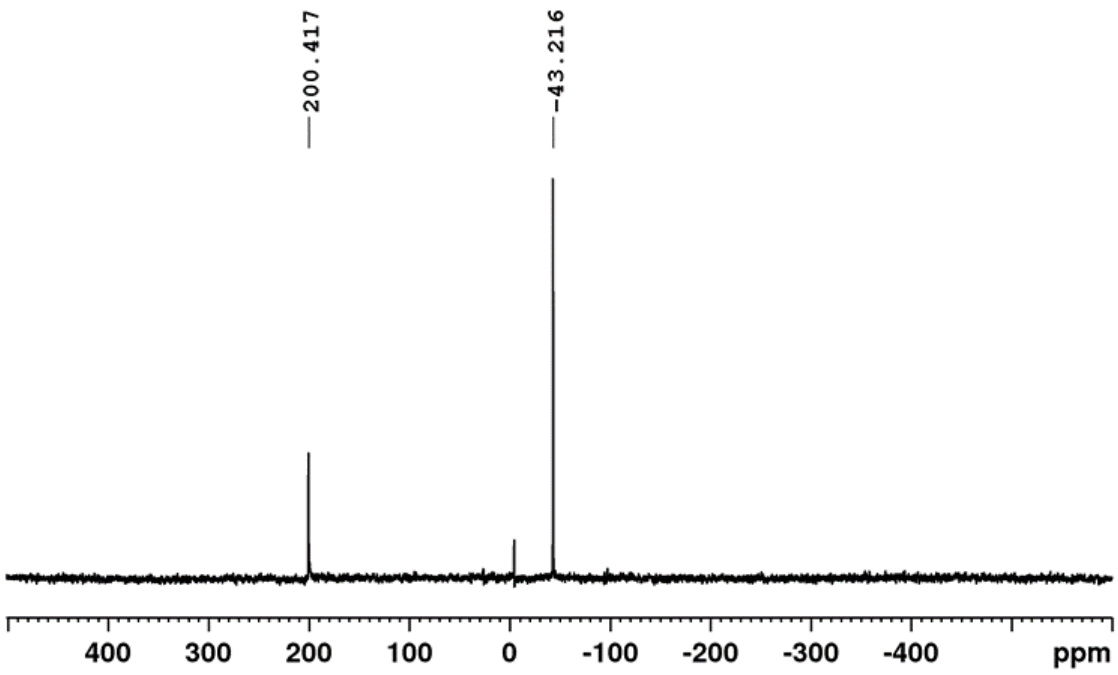


**Figure S 15.** $^{31}P\{^{1}H\}$ NMR spectrum of the solution of the reaction between **1** (1 eq) and $Br_2$ (1 eq) ($C_6D_6$ capillary, 300K).

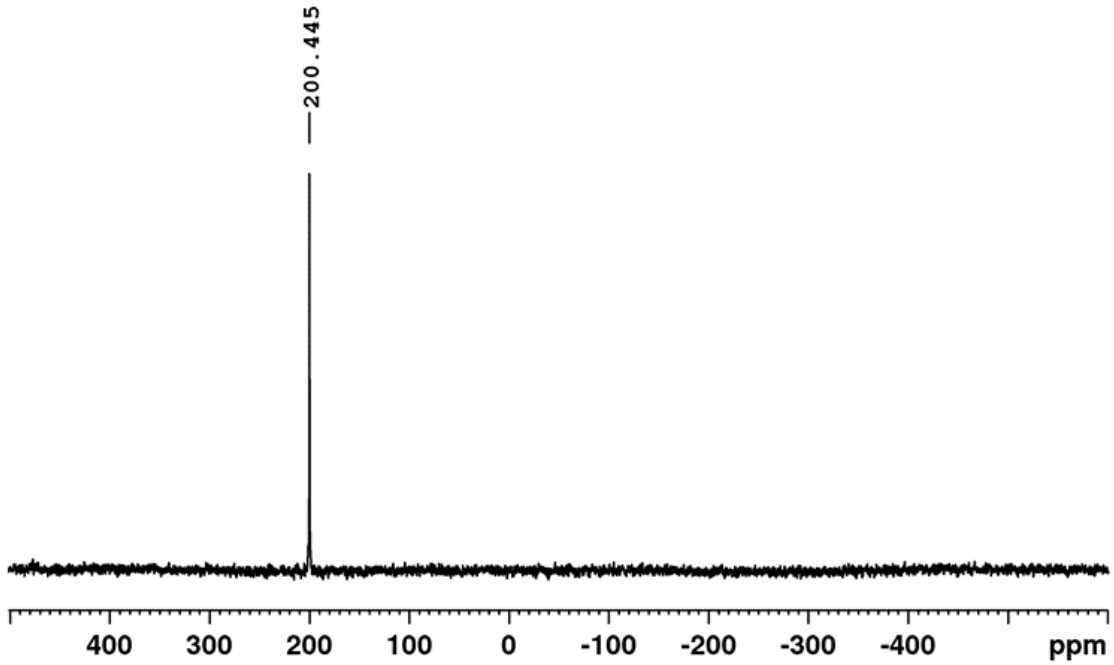


**Figure S 16.** $^{31}P\{^{1}H\}$ NMR spectrum of the solution of the reaction between **1** (1 eq) and $Br_2$ (2 eq) ($C_6D_6$ capillary, 300K).

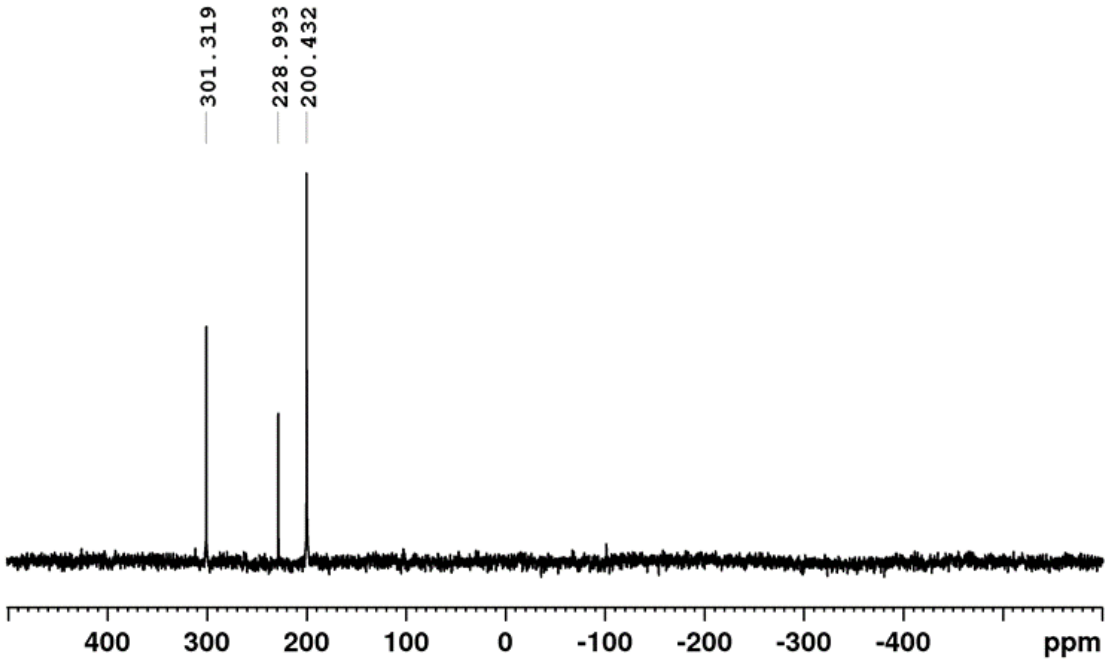


**Figure S 17.** $^{31}P\{^{1}H\}$ NMR spectrum of the solution of the reaction between **1** (1 eq) and $Br_2$ (3 eq) ($C_6D_6$ capillary, 300K).

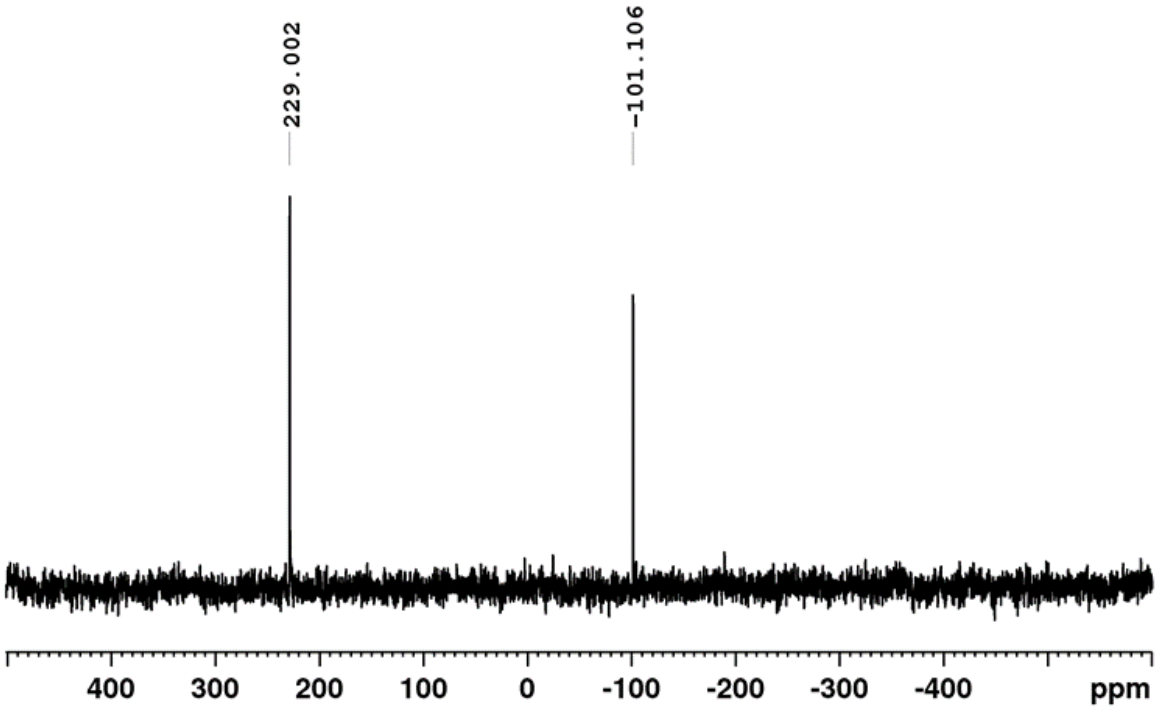


**Figure S 18.** $^{31}P\{^{1}H\}$ NMR spectrum of the solution of the reaction between **1** (1 eq) and $Br_2$ (6 eq) ($C_6D_6$ capillary, 300K).

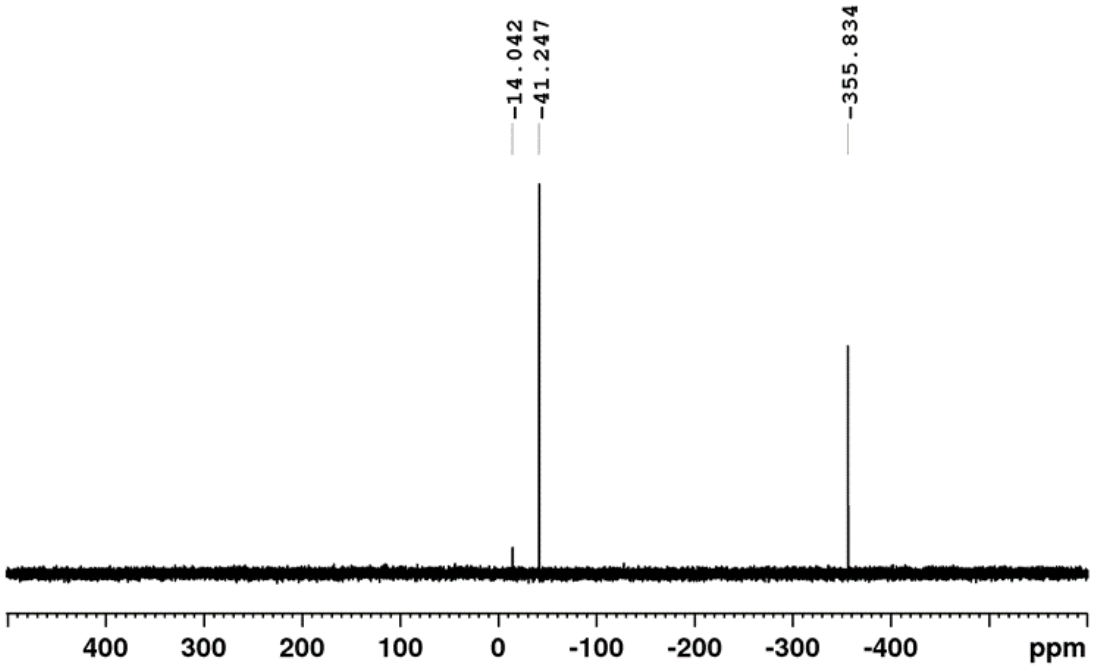


**Figure S 19.** $^{31}P\{^{1}H\}$ NMR spectrum of **4a** after 2 hours at reflux in $CH_3CN$ ($C_6D_6$ capillary, 300K).

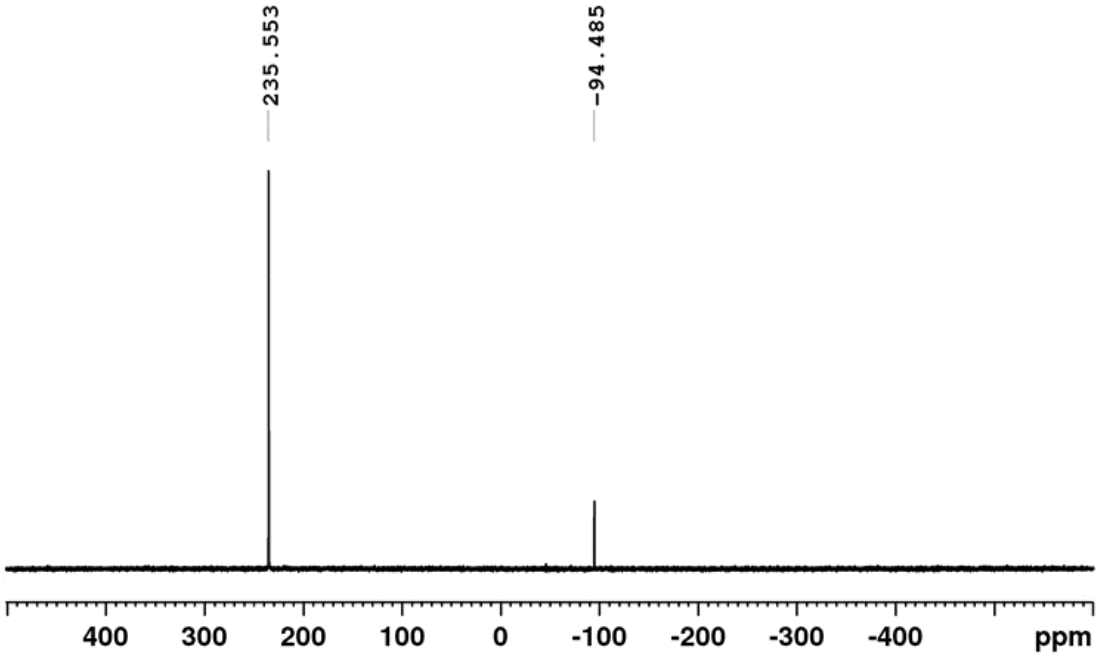


**Figure S 20.** $^{31}P\{^{1}H\}$ NMR spectrum of the solution of the reaction between **1** (1 eq) and $PBr_5$ (6 eq) after 2 hours at reflux in $CH_3CN$ ($C_6D_6$ capillary, 300K).

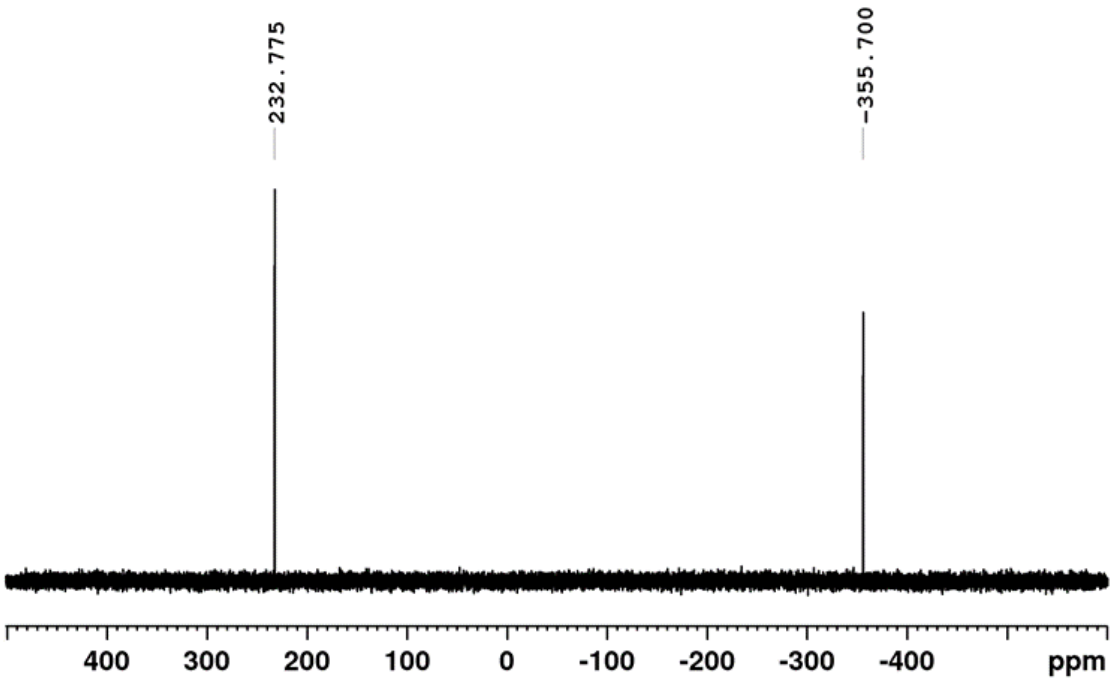


**Figure S 21.** $^{31}P\{^{1}H\}$ NMR spectrum of the solution of the reaction between **1** (1 eq) and $PBr_5$ (1 eq) after 2 hours at reflux in $CH_3CN$ ($C_6D_6$ capillary, 300K).

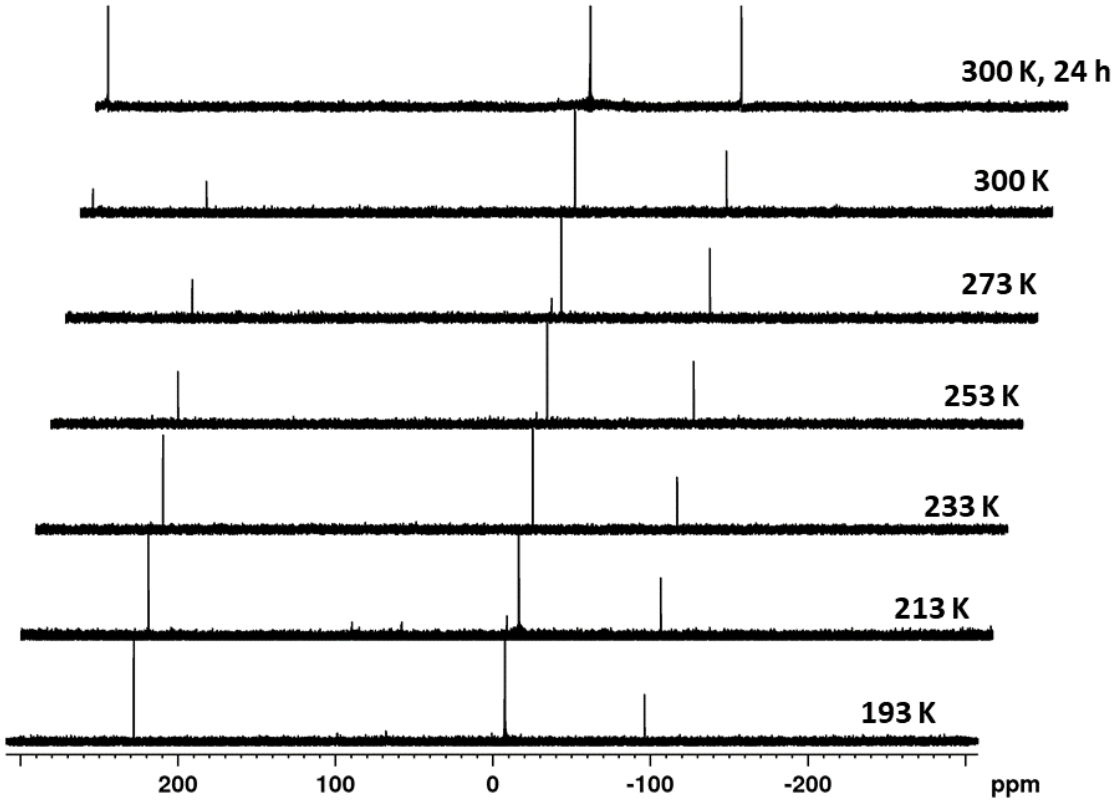


**Figure S 22.** VT $^{31}P\{^{1}H\}$ NMR spectra of the solution of the reaction between **1** (1 eq) and $Br_2$ (6 eq) in $CD_2Cl_2$ ($CD_2Cl_2$ and $PPh_3$ as a reference δ =-4.9 ppm).

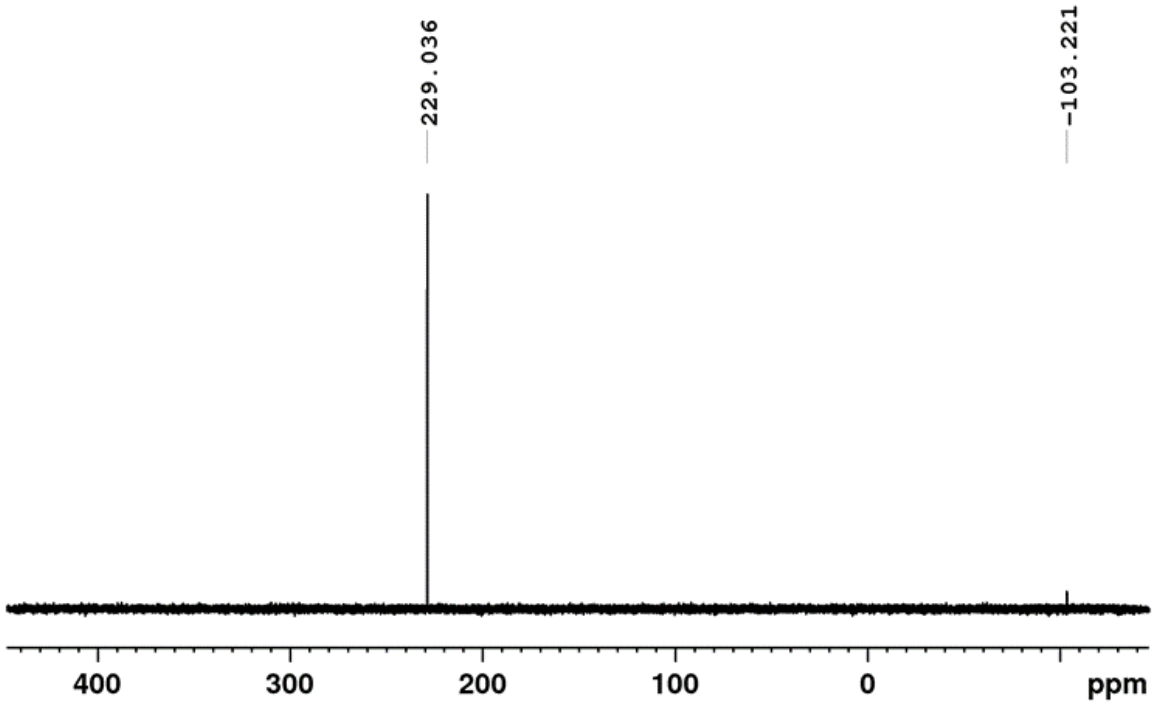


**Figure S 23.** $^{31}P\{^{1}H\}$ NMR spectrum of $PBr_5$ ($C_6D_6$, 300K).

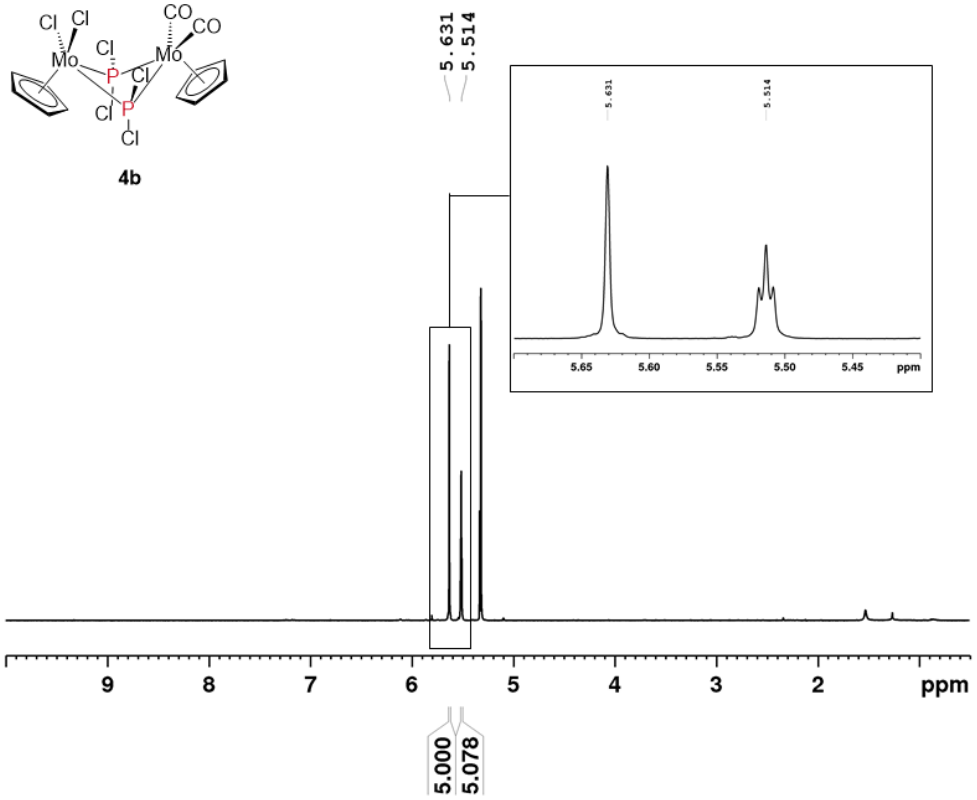


**Figure S 24.** $^{1}H$ NMR spectrum of compound **4b** ($CD_2Cl_2$, 300 K).

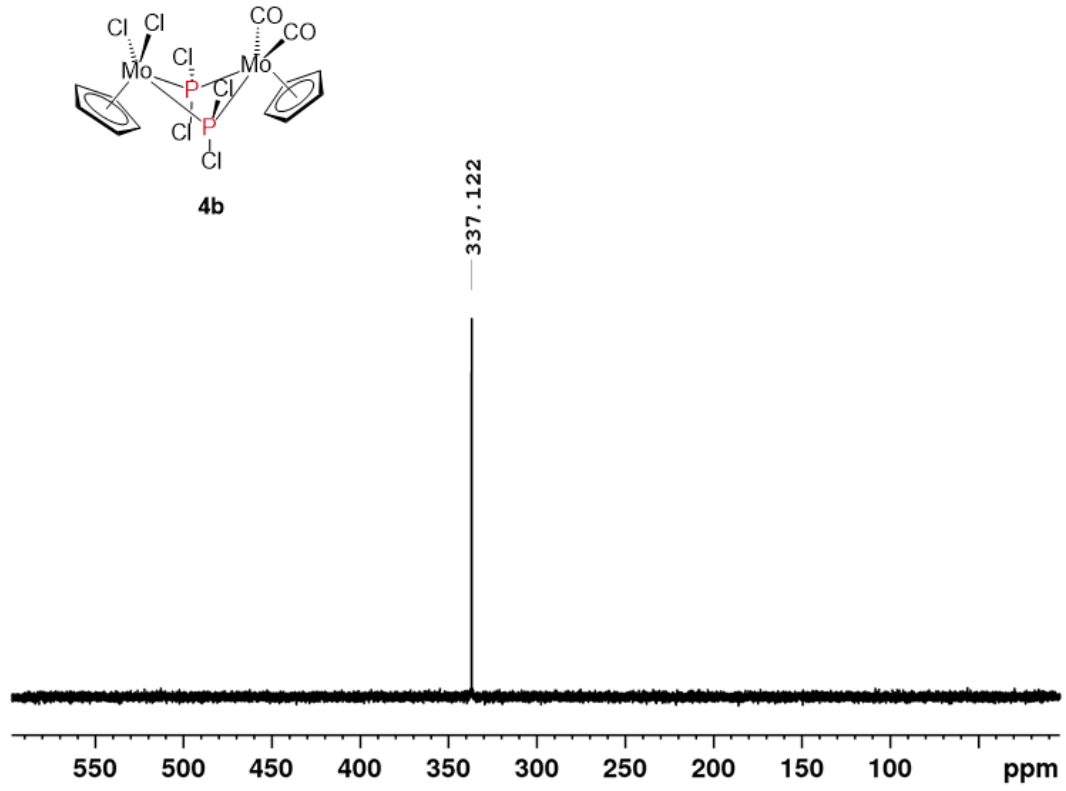


**Figure S 25.** $^{31}P\{^{1}H\}$ NMR spectrum of compound **4b** ($CD_2Cl_2$, 300 K).

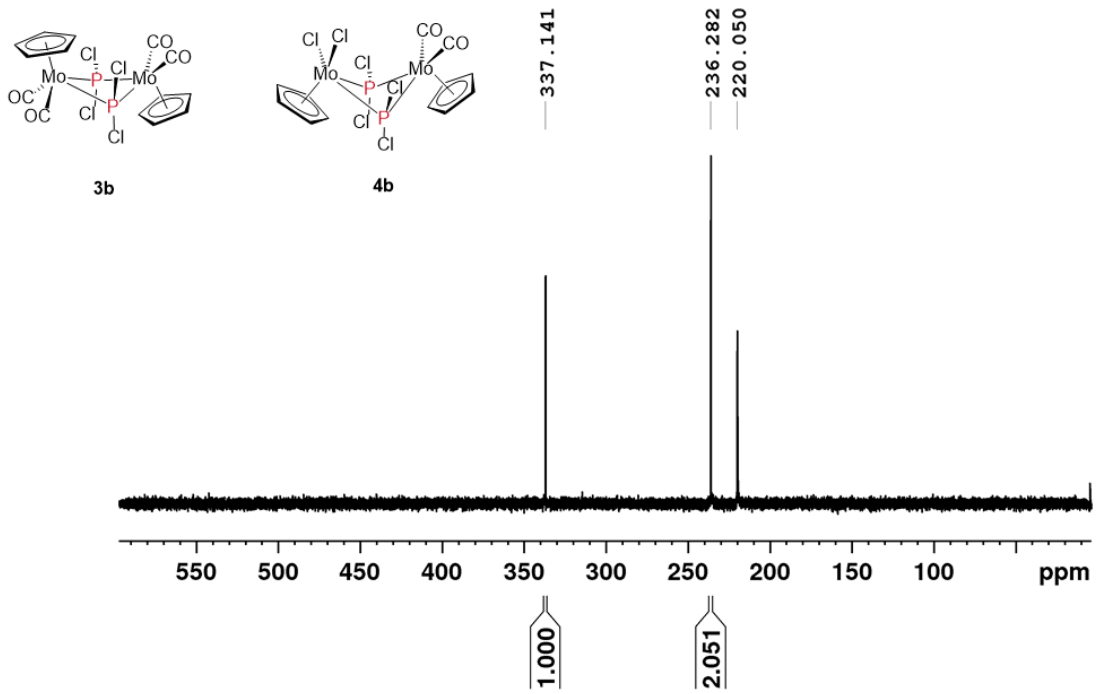


**Figure S 26.** $^{31}P\{^{1}H\}$ NMR spectrum, positive region, of the solution of the reaction between 1 *(1 eq)* and $PCl_5$ (1 eq) ($CD_2Cl_2$, 300 K).

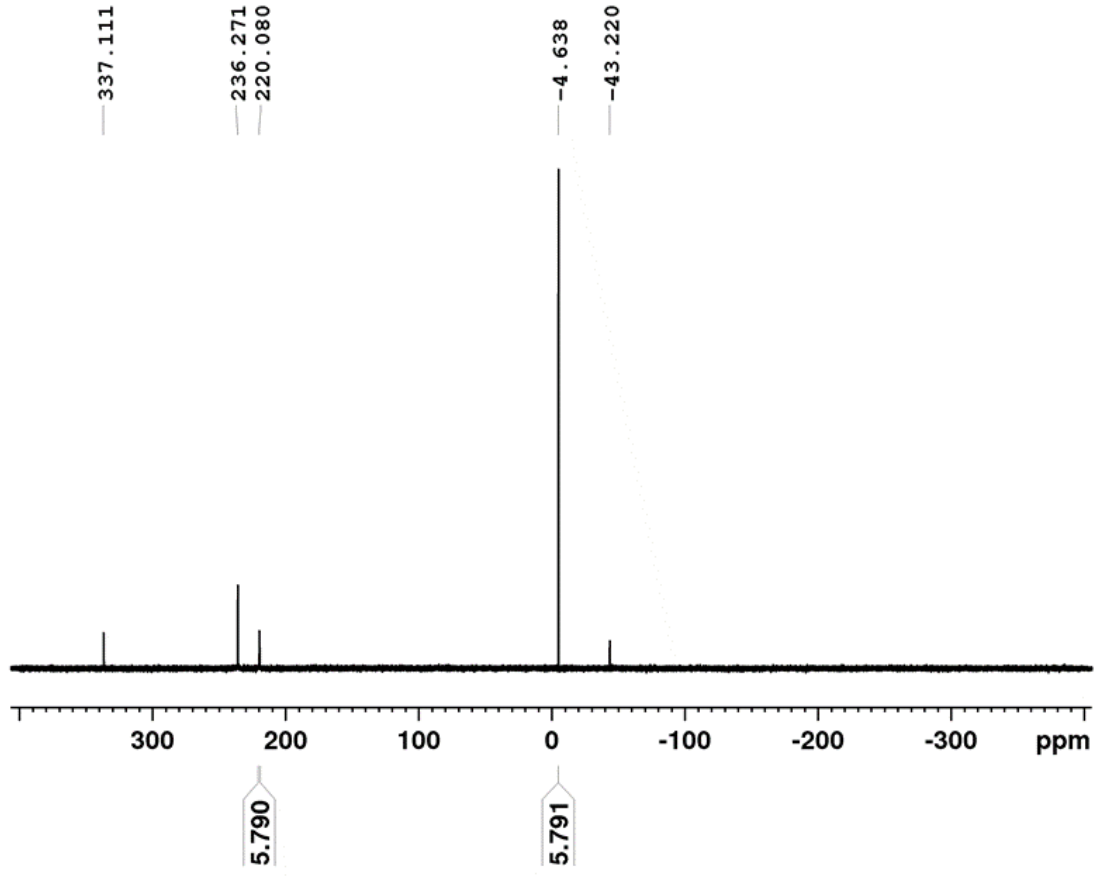


**Figure S 27.** $^{31}P\{^{1}H\}$ NMR spectrum of the reaction solution of **1** with $PCl_5$ and $PPh_3$ as a reference ($CD_2Cl_2$, 300 K).

- mmol $PPh_3$ in the inner part of the Evans NMR tube: $5.7 \cdot 10^{-4}$
- mmol $PCl_5$ in the Evans NMR tube: $3.33 \cdot 10^{-3}$
- $\frac{PCl_5}{PPh_3} = \frac{3.33 \cdot 10^{-3}}{5.7 \cdot 10^{-4}} = 5.79$
- Integration $PPh_3 = 5.79$
- Integration $PCl_3 = 5.79$
- 5.79 out of 5.79 (**100%**) equals the amount of $PCl_3$ coming from $PCl_5$
- No $PCl_3$ comes from **1**

**Crystallographic details**

The crystals were selected and mounted on a Gemini Ultra diffractometer equipped with an AtlasS2 CCD detector (**4b**, **5**),

on a GV50 diffractometer equipped with a TitanS2 detector (**2**, **3a**) and on a SuperNova diffractometer equipped with an Atlas detector (**4a**), respectively. All crystals were kept at a steady T = 123(1) K during data collection. Data collection and reduction were performed with **CrysAlispro** (Version 1.171.41.54a (**2**)[2], Version 1.171.38.46 (**4b**)[3], 1.171.39.37b (**3a**, **4a**), 1.171.39.46 (**5**))[4]. For the compounds (**3a**, **4a**, **4b**, **5**) a numerical absorption correction based on gaussian integration over a multifaceted crystal model and an empirical absorption correction using spherical harmonics as implemented in SCALE3 ABSPACK were applied. For compound **2** an analytical numeric absorption correction using a multifaceted crystal model based on expressions derived by R.C. Clark & J.S. Reid and an empirical absorption correction using spherical harmonics, implemented in SCALE3 ABSPACK scaling algorithm were applied.

Using **Olex2**[5], all structures were solved by **ShelXT**[6] and a least square refinement on $F^2$ was carried out with **ShelXL**[7]. All non-hydrogens atoms were refined anisotropically. Hydrogen atom positions were calculated geometrically and refined using the riding model.

The images showing the compounds **2**-**5** were generated using **Olex2**.[4]

**Compound 2**: The asymmetric unit contains one molecule of the complex $[(CpMo)_4(\mu_4\text{-}P)(\mu_3\text{-}PI)_2(\mu\text{-}I)(I)_4]$ and two only partly occupied $I_2$ molecules, which are additionally disordered over two positions (46:04; 12:12). One of these $I_2$ units (46% occupancy) forms with another I atom an $I_3$ unit. Further one of the four Mo atoms is disordered over two positions (67:33). The restraints SADI and SIMU were applied to describe these disorders. Additional, compound **2** was refined as a 2-component twin (BASF 0.51).

**Compound 3a**: The asymmetric unit contains one molecule of the complex $[CpMo(CO)_2(PBr_2)]_2$.

**Compound 4a**: The asymmetric unit contains one molecule of the complex $[CpMo(CO)_2(\mu_2\text{-}PBr_2)_2CpMoBr_2]$. The Cp ligand of the $[CpMo(CO)_2]$ fragment is disordered over two positions (66:34). To describe this disorder the SADI and SIMU restraints were applied. Further, compound **4a** was refined as a 2-component inversion twin (BASF: 0.18).

**Compound 4b**: The asymmetric unit contains one molecule of the complex $[CpMo(CO)_2(\mu_2\text{-}PCl_2)_2CpMoCl_2]$. The Cp ligand of the $[CpMo(CO)_2]$ fragment is disordered over two positions (57:43). To describe this disorder the SADI, ISOR and SIMU restraints

were applied. Further, compound **4b** was refined as a 2-component inversion twin (BASF: 0.42).

**Compound 5**: The asymmetric unit contains one quarter of the complex $[CpMo(I)_2]_2[I_3]$.

CCDC-2039393 (**2**), CCDC-2039394 (**3a**), CCDC-2039395 (**4a**), CCDC-2039396 (**4b**) and CCDC-2039397 (**5**) contain the supplementary crystallographic data for this paper. These data can be obtained free of charge at www.ccdc.cam.ac.uk/conts/retrieving.html (or from the Cambridge Crystallographic Data Centre, 12 Union Road, Cambridge CB2 1EZ, UK; Fax: + 44-1223-336-033; e-mail: deposit@ccdc.cam.ac.uk).

**Table S 1.** Crystallographic details of the compounds **2**, **3a**, **3b** and **4b**.

| **Compound** | **2** | **3a** | **4a** | **4b** |
|---|---|---|---|---|
| CCDC | 2039393 | 2039394 | 2039395 | 2039396 |
| Formula | $C_{20}H_{20}I_{8.48}Mo_4P_3$ | $C_{14}H_{10}Br_4Mo_2O_4P_2$ | $C_{12}H_{10}Br_6Mo_2O_2P_2$ | $C_{12}H_{10}Cl_6Mo_2O_2P_2$ |
| $D_{calc.}$/ g cm$^{-3}$ | 3.139 | 2.569 | 3.002 | 2.272 |
| $\mu$/mm$^{-1}$ | 65.336 | 20.225 | 25.457 | 20.141 |
| Formula Weight | 1813.14 | 815.68 | 919.48 | 652.72 |
| Color | black | dark black | dark black | light brown |
| Shape | block | block | block | plate |
| Size/mm$^3$ | 0.10×0.06×0.04 | 0.13×0.08×0.05 | 0.12×0.09×0.08 | 0.22×0.06×0.03 |
| $T$/K | 123(1) | 123.01(10) | 123(1) | 123 |
| Crystal System | monoclinic | monoclinic | orthorhombic | orthorhombic |
| Flack Parameter | -0.022(9) | - | - | - |
| Hooft Parameter | -0.0219(2) | - | - | - |
| Space Group | $P2_1$ | $P2_1/n$ | $Pna2_1$ | $Pna2_1$ |
| $a$/Å | 10.6325(4) | 10.74440(10) | 14.9697(3) | 14.5924(8) |
| $b$/Å | 12.4167(3) | 13.7134(2) | 9.1775(2) | 8.9657(4) |
| $c$/Å | 15.1106(5) | 14.3200(2) | 14.8058(3) | 14.5870(5) |
| $\alpha$/° | 90 | 90 | 90 | 90 |
| $\beta$/° | 105.956(4) | 91.6200(10) | 90 | 90 |
| $\gamma$/° | 90 | 90 | 90 | 90 |
| V/Å$^3$ | 1918.05(11) | 2109.10(5) | 2034.09(7) | 1908.43(15) |
| $Z$ | 2 | 4 | 4 | 4 |
| $Z'$ | 1 | 1 | 1 | 1 |
| Wavelength/Å | 1.54184 | 1.54184 | 1.54184 | 1.54184 |
| Radiation type | Cu K$_\alpha$ | Cu K$_\alpha$ | CuK$_\alpha$ | Cu K$_\alpha$ |
| $\Theta_{min}$/° | 3.042 | 4.465 | 5.655 | 5.792 |
| $\Theta_{max}$/° | 74.563 | 74.347 | 74.865 | 72.883 |
| Measured Refl's. | 13190 | 19909 | 13430 | 5703 |
| Ind't Refl's | 13190 | 4263 | 3808 | 2801 |
| Refl's with I > 2(I) | 12376 | 4205 | 3704 | 2606 |
| $R_{int}$ | 0.0832 | 0.0493 | 0.0615 | 0.0433 |
| Parameters | 398 | 235 | 264 | 264 |
| Restraints | 276 | 0 | 166 | 196 |
| Largest Peak | 1.991 | 0.812 | 1.042 | 1.083 |
| Deepest Hole | -0.955 | -1.261 | -0.799 | -1.022 |
| GooF | 1.084 | 1.096 | 1.088 | 1.040 |
| $wR_2$ (all data) | 0.1788 | 0.0753 | 0.0869 | 0.0991 |
| $wR_2$ | 0.1751 | 0.0748 | 0.0858 | 0.0970 |
| $R_1$ (all data) | 0.0659 | 0.0291 | 0.0387 | 0.0421 |
| $R_1$ | 0.0632 | 0.0285 | 0.0373 | 0.0388 |

**Table S 2.** Crystallographic details of the compound **5**.

| **Compound** | **5** |
|---|---|
| CCDC | 2039397 |
| Formula | $C_{10}H_{10}I_7Mo_2$ |
| $D_{calc.}$/ g cm$^{-3}$ | 3.824 |
| $\mu$/mm$^{-1}$ | 11.459 |
| Formula Weight | 1210.36 |
| Color | metallic dark brown |
| Shape | plate |
| Size/mm$^3$ | 0.08×0.08×0.02 |
| $T$/K | 123 |
| Crystal System | orthorhombic |
| Space Group | *Pbam* |
| $a$/Å | 8.6088(3) |
| $b$/Å | 14.8872(5) |
| $c$/Å | 8.2028(3) |
| $\alpha$/° | 90 |
| $\beta$/° | 90 |
| $\gamma$/° | 90 |
| V/Å$^3$ | 1051.28(6) |
| $Z$ | 2 |
| $Z'$ | 0.25 |
| Wavelength/Å | 0.71073 |
| Radiation type | Mo K$_\alpha$ |
| $\Theta_{min}$/° | 3.618 |
| $\Theta_{max}$/° | 32.199 |
| Measured Refl's. | 5848 |
| Ind't Refl's | 1832 |
| Refl's with I > 2(I) | 1557 |
| $R_{int}$ | 0.0353 |
| Parameters | 50 |
| Restraints | 0 |
| Largest Peak | 1.163 |
| Deepest Hole | -0.944 |
| GooF | 1.027 |
| $wR_2$ (all data) | 0.0506 |
| $wR_2$ | 0.0479 |
| $R_1$ (all data) | 0.0354 |
| $R_1$ | 0.0254 |

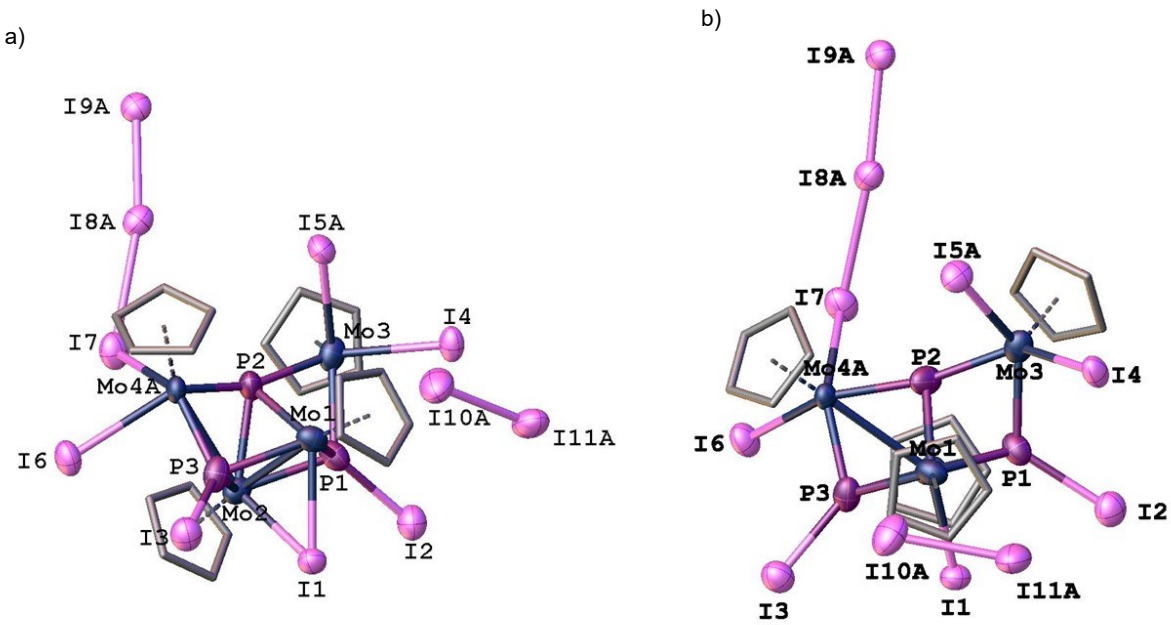


**Figure S 28.** Side (a) and front (b) view of the part 1 of the molecular structure of **2** with thermal ellipsoid at 50% probability level. The hydrogen atoms and the part 2 are omitted for clarity.

**Table S 3.** Selected bond lengths and angles of **2**

| Atom | Atom | Length/Å |
|---|---|---|
| Mo1 | Mo2 | 2.740(3) |
| Mo1 | P1 | 2.423(7) |
| Mo1 | P2 | 2.523(8) |
| Mo1 | P3 | 2.387(8) |
| Mo2 | P1 | 2.421(8) |
| Mo2 | P2 | 2.408(9) |
| Mo2 | P3 | 2.398(7) |
| Mo3 | P1 | 2.390(9) |
| Mo3 | P2 | 2.330(8) |
| Mo4A | P2 | 2.283(11) |
| Mo4A | P3 | 2.261(12) |
| P1 | P2 | 2.568(12) |
| I8A | I9A | 2.764(6) |

| Atom | Atom | Atom | Angle/° |
|---|---|---|---|
| P1 | Mo1 | P2 | 62.5(3) |
| P3 | Mo1 | P2 | 78.8(3) |
| P2 | Mo2 | P1 | 64.2(3) |
| P2 | Mo3 | P1 | 65.9(3) |
| P3 | Mo4A | P2 | 86.7(4) |
| P2 | Mo4A | Mo2 | 50.0(3) |
| Mo4A | P2 | Mo1 | 87.0(3) |
| Mo4A | P3 | Mo1 | 90.9(4) |
| Mo4A | P2 | Mo3 | 161.9(5) |

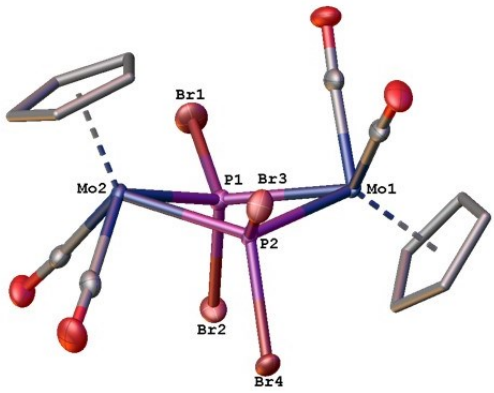


**Figure S 29:** Molecular structure of **3a** with thermal ellipsoid at 50% probability level. The hydrogen atoms are omitted for clarity.

**Table S 4.** Selected bond lengths and angles of **3a**

| Atom | Atom | Length/Å |
|---|---|---|
| Mo1 | P2 | 2.4641(8) |
| Mo1 | P1 | 2.4769(8) |
| Mo2 | P2 | 2.4714(8) |
| Mo2 | P1 | 2.4564(8) |
| Br2 | P1 | 2.2850(9) |
| Br3 | P2 | 2.2773(9) |
| Br4 | P2 | 2.2738(8) |
| Br1 | P1 | 2.2829(9) |
| P2 | P1 | 2.5856(11) |

| Atom | Atom | Atom | Angle/° |
|---|---|---|---|
| P2 | Mo1 | P1 | 63.11(3) |
| P1 | Mo2 | P2 | 63.30(3) |
| Mo1 | P2 | Mo2 | 112.26(3) |
| Mo1 | P2 | P1 | 58.69(3) |
| Mo2 | P2 | P1 | 58.07(3) |
| Mo1 | P1 | P2 | 58.20(3) |
| Mo2 | P1 | Mo1 | 112.34(3) |
| Mo2 | P2 | P1 | 58.07(3) |

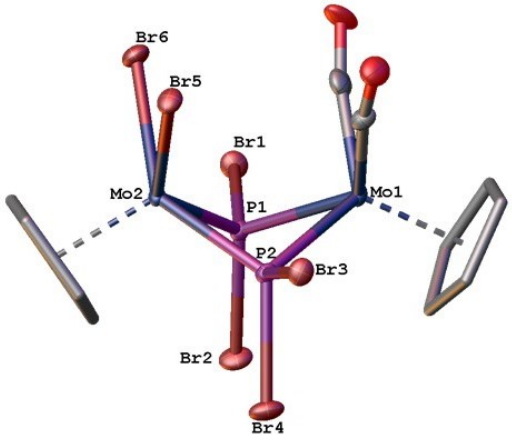


**Figure S 30:** Molecular structure of **4a** with thermal ellipsoid at 50% probability level. The hydrogen atoms and the second part of the disordered Cp ligand are omitted for clarity.

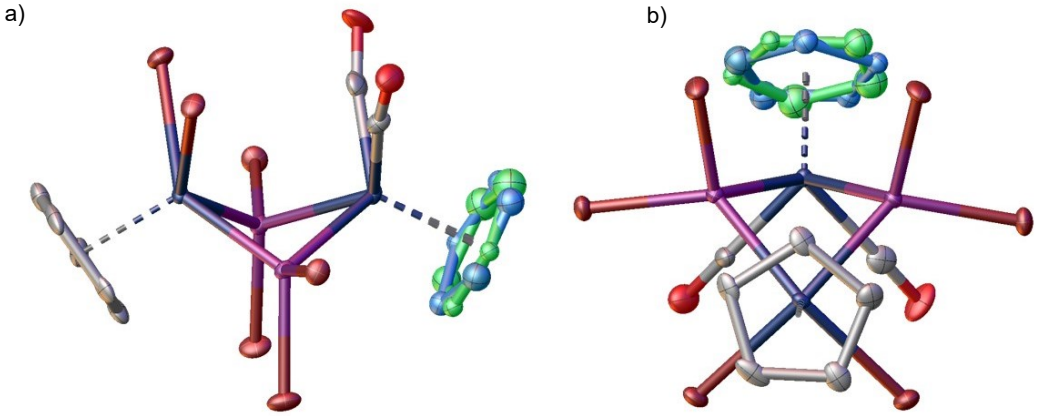


**Figure S 31.** Side (a) and front (b) view of the molecular structure of **4a** with thermal ellipsoid at 50% probability level. The disordered Cp ligand is highlighted blue (part 1) and green (part 2). The hydrogen atoms are omitted for clarity.

**Table S 5.** Selected bond lengths and angles of **4a**.

| Atom | Atom | Length/Å |
|---|---|---|
| Mo2 | P2 | 2.356(3) |
| Mo2 | P1 | 2.365(3) |
| Mo1 | P1 | 2.432(5) |
| Mo1 | P2 | 2.426(3) |
| Br1 | P1 | 2.238(3) |
| Br4 | P2 | 2.243(3) |
| Br2 | P1 | 2.239(3) |
| Br3 | P2 | 2.225(3) |

| Atom | Atom | Atom | Angle/° |
|---|---|---|---|
| P2 | Mo1 | P1 | 77.09(9) |
| Mo1 | P2 | Mo2 | 86.86(9) |
| Mo1 | P1 | Mo2 | 86.50(9) |

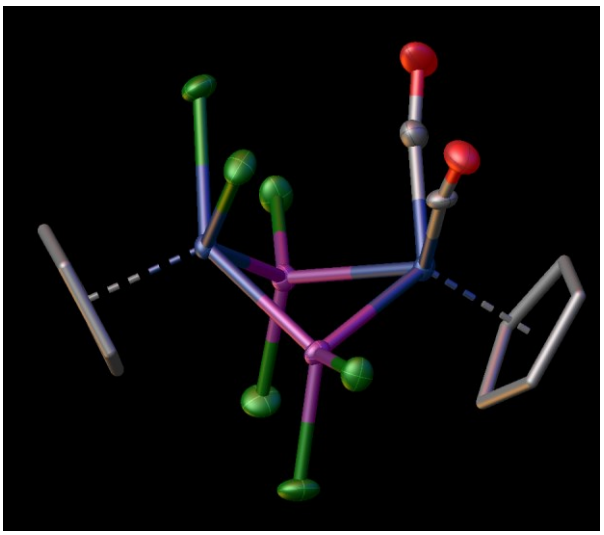

**Figure S 32.** Molecular structure of **4b** with thermal ellipsoid at 50% probability level. The hydrogen atoms and the second part of the disordered Cp ligand are omitted for clarity.

a) b)

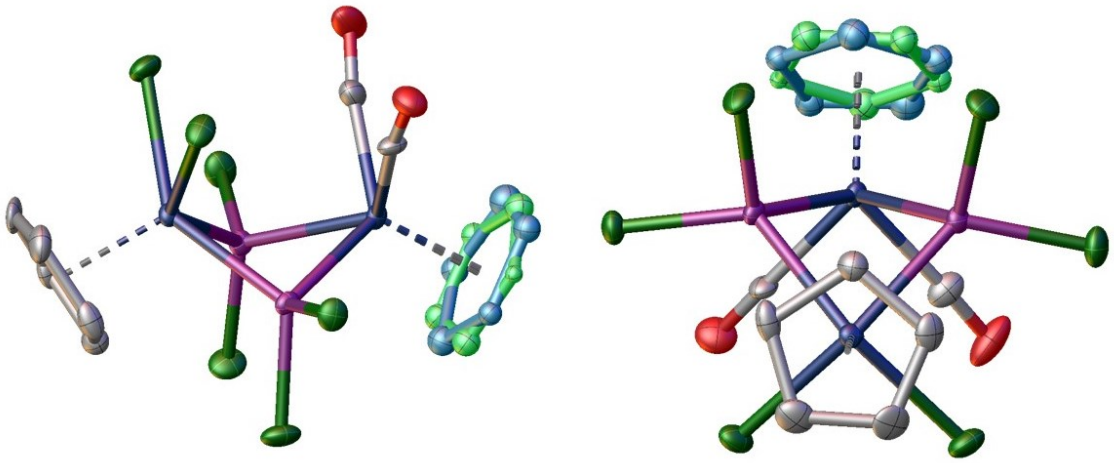

**Figure S 33.** Side (a) and front (b) view of the molecular structure of **4b** with thermal ellipsoid at 50% probability level. The disordered Cp ligand is highlighted blue (part 1) and green (part 2).

**Table S 6.** Selected bond lengths and angles of **4b.**

| Atom | Atom | Length/Å |
|---|---|---|
| Mo1 | P2 | 2.407(3) |
| Mo1 | P1 | 2.426(3) |
| Mo2 | P1 | 2.351(3) |
| Mo2 | P2 | 2.344(3) |
| P2 | Cl4 | 2.056(4) |
| P2 | Cl3 | 2.071(3) |
| Cl1 | P1 | 2.060(4) |
| P1 | Cl2 | 2.069(4) |

| Atom | Atom | Atom | Angle/° |
|---|---|---|---|
| P2 | Mo1 | P1 | 74.23(9) |
| Mo1 | P2 | Mo2 | 87.08(9) |
| Mo1 | P1 | Mo2 | 86.49(8) |

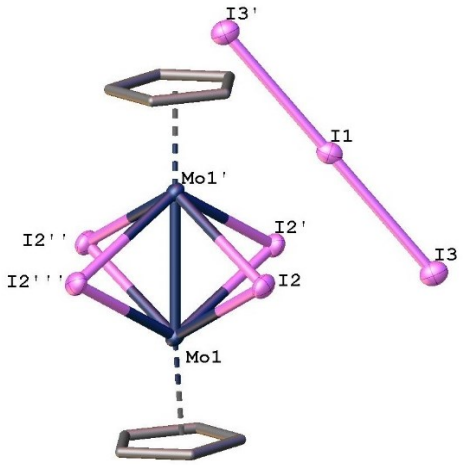


**Figure S 34.** Molecular structure of **5** with thermal ellipsoid at 50% probability level. The hydrogen atoms are omitted for clarity.

**Table S 7.** Selected bond lengths and angles of **5.**

| Atom | Atom | Length/Å |
|---|---|---|
| Mo1 | Mo1’ | 2.7032(8) |
| Mo1 | I2 | 2.7769(4) |
| I1 | I3 | 2.9319(4) |

| Atom | Atom | Atom | Angle/˚ |
|---|---|---|---|
| I3’ | I1 | I3 | 180.000(14) |
| I2 | Mo1 | I2”’ | 75.992(11) |
| Mo1 | I2 | Mo1’ | 58.225(15) |

## Computational details

All calculations for $[(CpMo)_4(\mu_4\text{-}P)(\mu_3\text{-}PI)_2(\mu\text{-}I)(I)_3(I_3)]$ (**2**) have been performed with the TURBOMOLE program package.[8,9] The geometry has been optimized in different spin states using the BP86,[10,11] B3LYP,[12,13] PBE0,[Error! Bookmark not defined.14,15] B97-D,[16] TPSS[17] and TPSSh[18] functionals together with the def2-TZVP[19,20] basis set (cf. Table 1). To speed up the geometry optimization the Resolution of Identity (RI)[20,21] and the Multipole Accelerated Resolution-of-the-Identity (MARI-J)[22] approximations has been used. The final energy of the molecules was determined by single point calculations without using the RI formalism.

The DFT calculations for compounds **3, 4a** and **3, 4b** have been performed with Gaussian 09[23] using the B3LYP functional together with the def2-TZVP basis set.

**$[(CpMo)_4(\mu_4\text{-}P)(\mu_3\text{-}PI)_2(\mu\text{-}I)(I)_3(I_3)]$ (2)**

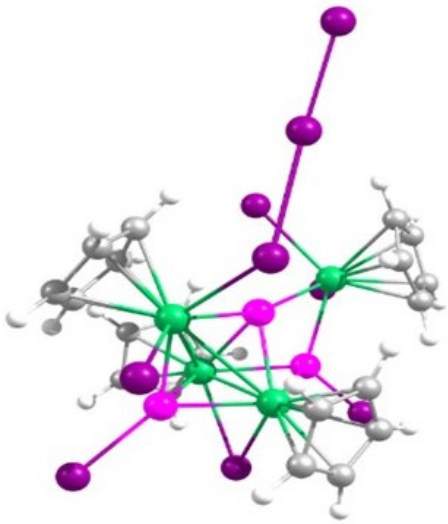

**Table S 8.** Relative energies ($kJ \cdot mol^{-1}$) of $[(CpMo)_4(\mu_4\text{-}P)(\mu_3\text{-}PI)_2(\mu\text{-}I)(I)_3(I_3)]$ (**2**) in different spin states calculated using different functionals together with the def2-TZVP basis set.

| | BP86 | TPSS | TPSSH | B3LYP | PBE0 | B97-D |
|---|---|---|---|---|---|---|
| **unrest. singl.** | 0.00 | 0.00 | 6.43 | 18.49 | 14.25 | 9.32 |
| **triplet** | 5.01 | 2.88 | 0.00 | 0.00 | 0.00 | 0.00 |
| **quintet** | 57.52 | 62.84 | 52.21 | 25.12 | 38.92 | 35.97 |
| **septet** | 95.85 | 104.05 | 78.45 | 23.34 | 46.88 | 52.05 |

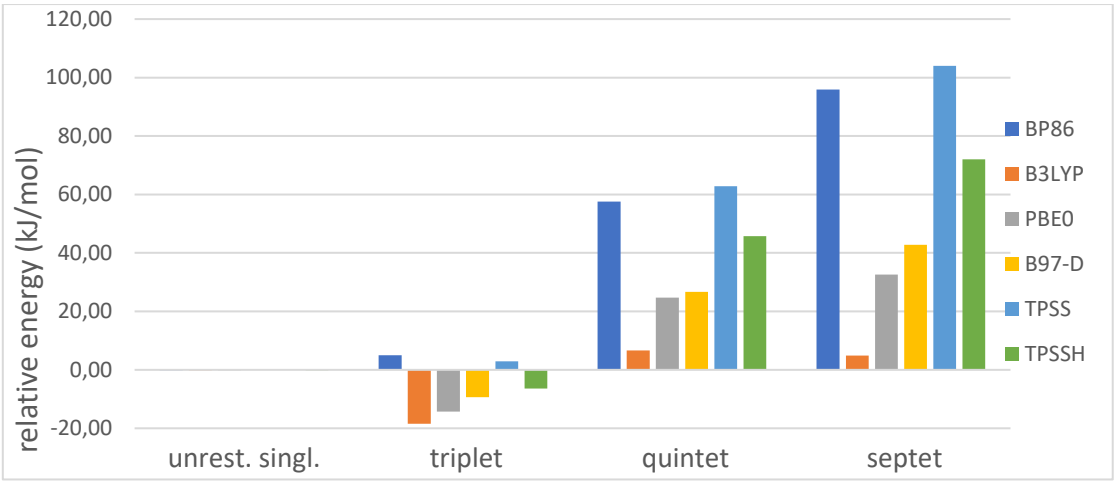


**Figure S 35.** Relative energies (kJ·mol$^{-1}$) of [(CpMo)$_4$(μ$_4$-P)(μ$_3$-PI)$_2$(μ-I)(I)$_3$(I$_3$)] (**2**) in different spin states calculated using different functionals together with the def2-TZVP basis set.

**Table S 9.** Cartesian coordinates of the optimised geometry of [(CpMo)$_4$(μ$_4$-P)(μ$_3$-PI)$_2$(μ-I)(I)$_3$(I$_3$)] (**2**) in unrestricted singlet spin state at the B3LYP/def2-TZVP level. Total energy = −4750.54510486619 a.u.; <S*S> = 0.00.

| Atom | x | y | z |
|---|---|---|---|
| Mo | -1.6691341 | -0.0046287 | 1.4372379 |
| Mo | -1.6619085 | 0.0595124 | -1.3142437 |
| Mo | 0.2121058 | 2.2451420 | 0.2542290 |
| Mo | 1.1669585 | -2.3063722 | -0.5798797 |
| P | -2.1051505 | 1.9493541 | 0.0979836 |
| P | 0.4118841 | -0.1021393 | 0.0954354 |
| P | -1.1971324 | -1.9980314 | 0.0238877 |
| I | -3.9055971 | 3.6083441 | -0.1132614 |
| I | -2.6981361 | -4.0526775 | 0.1762704 |
| I | -4.1306992 | -0.4753063 | 0.0606598 |
| I | -0.6182858 | 4.1079420 | 2.3464937 |
| I | 0.4470732 | -4.0005985 | -2.6819917 |
| I | 2.8658621 | -1.0582070 | -2.4726445 |
| I | 2.2859510 | 1.7275826 | 2.3484580 |
| I | 5.3582042 | 1.0310682 | 1.3591746 |
| I | 7.9887645 | 0.4824726 | 0.6501523 |
| C | -1.0202591 | 0.7032384 | 3.5751085 |
| C | -2.8905740 | -0.6041158 | 3.4014968 |
| C | -0.5997134 | -0.6491983 | 3.4307083 |
| C | -2.4385889 | 0.7304372 | 3.5551636 |
| H | -3.0540304 | 1.6103357 | 3.6444170 |
| C | -1.7617068 | -1.4576754 | 3.3276017 |
| C | -0.8205189 | 0.5306700 | -3.4420985 |
| C | -2.5232598 | 1.0193302 | -3.3190442 |
| H | -3.0686002 | 1.9491904 | -3.3125453 |
| C | -2.0467792 | -1.2317219 | -3.2722193 |
| C | -1.1201223 | 0.8561339 | -3.4720230 |
| C | -3.0884332 | -0.2760634 | -3.2153642 |

| Atom | x | y | z |
|---|---|---|---|
| H | -0.3806243 | 1.5560560 | 3.7125009 |
| H | -3.9178717 | -0.9228519 | 3.3362391 |
| H | 0.4208728 | -0.9875614 | 3.4590943 |
| H | -1.8011741 | -2.5287658 | 3.2130706 |
| H | 0.1515196 | -0.9760818 | -3.5699353 |
| H | -2.1520626 | -2.3024511 | -3.2151027 |
| H | -0.4129139 | 1.6434623 | -3.6568676 |
| H | -4.1354321 | -0.4947073 | -3.0898576 |
| C | 2.2238564 | 2.8612585 | -0.8936486 |
| H | 3.1461032 | 2.3412703 | -0.6937760 |
| C | 0.1862242 | 3.4190256 | -1.7880898 |
| C | 1.7411913 | 4.0182127 | -0.2233035 |
| C | 1.2629148 | 2.4797688 | -1.8474831 |
| C | 0.5001646 | 4.3788997 | -0.8043507 |
| C | 3.2323485 | -2.7201692 | 0.5085861 |
| C | 1.2641233 | -3.1960682 | 1.5787044 |
| C | 1.4806848 | -4.2174329 | 0.6139155 |
| H | 0.8470282 | -5.0688126 | 0.4358425 |
| C | 2.7121648 | -3.9165582 | -0.0519307 |
| H | 3.1604218 | -4.4882696 | -0.8459446 |
| C | 2.3416090 | -2.2769998 | 1.5088623 |
| H | -0.6943499 | 3.4335097 | -2.4055122 |
| H | 2.2278830 | 4.5288729 | 0.5897620 |
| H | 1.3699045 | 1.6327061 | -2.5020481 |
| H | -0.1189607 | 5.2085430 | -0.5099475 |
| H | 4.1315383 | -2.2120460 | 0.2058145 |
| H | 0.4311503 | -3.1483626 | 2.2565764 |
| H | 2.4635126 | -1.3771254 | 2.0896666 |

**Table S 10.** Cartesian coordinates of the optimised geometry of [(CpMo)$_4$(μ$_4$-P)(μ$_3$-PI)$_2$(μ-I)(I)$_3$(I$_3$)] (**2**) in triplet spin state at the B3LYP/def2-TZVP level. Total energy = −4750.55214680069 a.u.; <S*S> = 2.03.

| Atom | x | y | z | Atom | x | y | z |
|---|---|---|---|---|---|---|---|
| Mo | -1.6886549 | 0.0411364 | 1.3936624 | H | -0.2872294 | 1.4973190 | 3.6794629 |
| Mo | -1.7755657 | 0.1792134 | -1.3479962 | H | -3.9391171 | -0.8108181 | 3.3237679 |
| Mo | 0.1971779 | 2.2438580 | 0.2018025 | H | 0.3930557 | -1.0716904 | 3.3428866 |
| Mo | 1.2645246 | -2.4041062 | -0.4908133 | H | -1.8984794 | -2.5066753 | 3.1076852 |
| P | -2.1428385 | 2.0273773 | 0.1095969 | H | 0.2120179 | -0.6153816 | -3.5558962 |
| P | 0.3253684 | -0.1065435 | -0.0574132 | H | -1.8887626 | -2.2440630 | -3.2742814 |
| P | -1.2363818 | -1.8933115 | -0.0811059 | H | -0.7252617 | 1.9145651 | -3.6711322 |
| I | -3.9016794 | 3.7446468 | 0.0277417 | H | -4.1041760 | -0.7395601 | -3.1497398 |
| I | -2 .7150710 | -3.9830408 | 0.0812172 | C | 2.1694462 | 2.8140561 | -1.0153566 |
| I | -4.1913629 | -0.3969357 | 0.0699133 | H | 3.0675763 | 2.2334173 | -0.8862256 |
| I | -0.5207503 | 4.0823928 | 2.3618483 | C | 0.1249394 | 3.5302925 | -1.7778914 |
| I | 0.5048464 | -4.0422919 | -2.5879390 | C | 1.7918075 | 3.9667391 | -0.2750284 |
| I | 2.9529446 | -1.0224477 | -2.2461295 | C | 1.1390475 | 2.5347050 | -1.9338343 |
| I | 2.3162625 | 1.6265431 | 2.2213130 | C | 0.5478405 | 4.4242666 | -0.7741020 |
| I | 5.4141298 | 1.0500876 | 1.2479637 | C | 3.2930589 | -2.8379352 | 0.7199926 |
| I | 8.0755847 | 0.5908097 | 0.5878095 | C | 1.2736444 | -3.3816087 | 1.6629137 |
| C | -0.9665149 | 0.6768958 | 3.5360491 | C | 1.6088488 | -4.3975811 | 0.7331693 |
| C | -2.8970586 | -0.5412643 | 3.3739284 | H | 1.0130244 | -5.2647603 | 0.5022444 |
| C | -0.6108842 | -0.6874419 | 3.3500249 | C | 2.8600368 | -4.0595220 | 0.1486670 |
| C | -2.3828285 | 0.7670777 | 3.5465955 | H | 3.3750026 | -4.6222046 | -0.6124157 |
| H | -2.9559492 | 1.6714282 | 3.6674125 | C | 2.3138484 | -2.4124452 | 1.6506494 |
| C | -1.8097236 | -1.4421541 | 3.2509141 | H | -0.7861554 | 3.6222068 | -2.3425334 |
| C | -0.8161643 | -0.3052014 | -3.4608402 | H | 2.3481338 | 4.4113780 | 0.5321154 |
| C | -2.7227300 | 0.9938115 | -3.3736243 | H | 1.1594982 | 1.7211369 | -2.6353425 |
| H | -3.3902840 | 1.8400616 | -3.3752373 | H | -0.0042536 | 5.2740270 | -0.4122108 |
| C | -1.9311437 | -1.1689058 | -3.3257286 | H | 4.1972984 | -2.3049600 | 0.4777525 |
| C | -1.3110633 | 1.0304389 | -3.4994289 | H | 0.3901645 | -3.3666413 | 2.2779878 |
| C | -3.0988461 | -0.3697518 | -3.2634083 | H | 2.3698009 | -1.5106449 | 2.2385674 |

**Table S 11.** Cartesian coordinates of the optimised geometry of [(CpMo)$_4$(μ$_4$-P)(μ$_3$-PI)$_2$(μ-I)(I)$_3$(I$_3$)] (**2**) in quintet spin state at the B3LYP/def2-TZVP level. Total energy = −4750.54258024538 a.u.; <S*S> = 6.11.

| Atom | x | y | z | Atom | x | y | z |
|---|---|---|---|---|---|---|---|
| Mo | -1.7768317 | 0.0139544 | 1.3731729 | C | -1.5628435 | 0.8987222 | -3.5277301 |
| Mo | -2.0424195 | -0.0675485 | -1.4164554 | C | -3.2797023 | -0.6111877 | -3.3799025 |
| Mo | 0.4536313 | 2.3876441 | 0.4448489 | H | -0.3469122 | 1.4972348 | 3.6306523 |
| Mo | 1.2090265 | -2.3256873 | -0.5409121 | H | -4.0126690 | -0.7985525 | 3.3492190 |
| P | -1.8864540 | 1.9553128 | -0.0625704 | H | 0.3150679 | -1.0833794 | 3.3209459 |
| P | 0.1687054 | -0.0011826 | -0.1588993 | H | -1.9839511 | -2.5065232 | 3.1432164 |
| P | -1.2663767 | -1.9603164 | -0.0253214 | H | 0.0449989 | -0.6567585 | -3.6064022 |
| I | -3.5473603 | 3.7629189 | -0.3979641 | H | -1.9581343 | -2.4112350 | -3.4299681 |
| I | -2.6933043 | -4.0505217 | 0.2182219 | H | -1.0185752 | 1.8229196 | -3.6230455 |
| I | -4.3445945 | -0.3435015 | 0.1402023 | H | -4.2666351 | -1.0367798 | -3.2960668 |
| I | -0.4947573 | 4.1429037 | 2.4466108 | C | 2.3659269 | 2.7863044 | -0.8746113 |
| I | 0.4539160 | -4.0486302 | -2.5822501 | H | 3.2355333 | 2.1598446 | -0.7615033 |
| I | 2.8472148 | -0.9757360 | -2.3725487 | C | 0.3385859 | 3.5885980 | -1.5899960 |
| I | 2.3885633 | 1.5629274 | 2.4207766 | C | 2.0917175 | 3.9871661 | -0.1660580 |
| I | 5.5192890 | 1.1242781 | 1.3699970 | C | 1.2873579 | 2.5446118 | -1.7594029 |
| I | 8.1541019 | 0.7419511 | 0.6036662 | C | 0.8456910 | 4.4845548 | -0.6150223 |
| C | -1.0313600 | 0.6809921 | 3.4930353 | C | 3.2623144 | -2.6412259 | 0.6602222 |
| C | -2.9690905 | -0.5323879 | 3.3802536 | C | 1.2894261 | -3.3321555 | 1.6025538 |
| C | -0.6851440 | -0.6899495 | 3.3232811 | C | 1.6897684 | -4.3122940 | 0.6597441 |
| C | -2.4482314 | 0.7795991 | 3.5120843 | H | 1.1526818 | -5.2143839 | 0.4196337 |
| H | -3.0168545 | 1.6876386 | 3.6254938 | C | 2.9095814 | -3.8830151 | 0.0736711 |
| C | -1.8898319 | -1.4396361 | 3.2640228 | H | 3.4562239 | -4.3987489 | -0.6985052 |
| C | -1.0018629 | -0.4081573 | -3.5332754 | C | 2.2618443 | -2.2962078 | 1.5999414 |
| C | -2.9727921 | 0.7744851 | -3.4300445 | H | -0.5843844 | 3.7163352 | -2.1295165 |
| H | -3.6820685 | 1.5857308 | -3.3908714 | H | 2.7081030 | 4.4248992 | 0.6012065 |

| | | | | | | | |
|---|---|---|---|---|---|---|---|
| C | -2.0674886 | -1.3395909 | -3.4501431 | H | 1.2290215 | 1.7158777 | -2.4431866 |
| H | 0.3520904 | 5.3722762 | -0.2600515 | H | 0.4104212 | -3.3857283 | 2.2221379 |
| H | 4.1292556 | -2.0473516 | 0.4234642 | H | 2.2605700 | -1.4013077 | 2.1999488 |

**Table S 12.** Cartesian coordinates of the optimised geometry of $[(CpMo)_4(\mu_4\text{-}P)(\mu_3\text{-}PI)_2(\mu\text{-}I)(I)_3(I_3)]$ (**2**) in unrestricted singlet spin state at the TPSSH/def2-TZVP level. Total energy = −4750.72882957214 a.u.; <S*S> = 0.0.

| Atom | x | y | z | Atom | x | y | z |
|---|---|---|---|---|---|---|---|
| Mo | -1.6257568 | 0.0099527 | 1.4369618 | H | -0.3703064 | 1.6143831 | 3.6654092 |
| Mo | -1.6023113 | 0.0535813 | -1.2962978 | H | -3.8498796 | -0.9566927 | 3.2875441 |
| Mo | 0.1906331 | 2.2418105 | 0.2623694 | H | 0.4969192 | -0.9112232 | 3.4096142 |
| Mo | 1.1656095 | -2.2557295 | -0.6051073 | H | -1.6955074 | -2.5121488 | 3.1663010 |
| P | -2.1075735 | 1.9343571 | 0.0925872 | H | 0.1656244 | -1.0863650 | -3.5055604 |
| P | 0.4485644 | -0.0918266 | 0.1204448 | H | -2.1963996 | -2.3033694 | -3.1075326 |
| P | -1.1489495 | -1.9721357 | 0.0475011 | H | -0.2750743 | 1.5546033 | -3.6271377 |
| I | -3.9327857 | 3.5285472 | -0.1134486 | H | -4.0999437 | -0.3960492 | -3.0139276 |
| I | -2.6354223 | -4.0093612 | 0.2084259 | C | 2.1902460 | 2.8787384 | -0.8277494 |
| I | -4.0211804 | -0.4969568 | 0.0598709 | H | 3.1233438 | 2.3927953 | -0.5861403 |
| I | -0.6874696 | 4.0720176 | 2.3018461 | C | 0.1546833 | 3.3360536 | -1.7873766 |
| I | 0.3933105 | -3.9491526 | -2.6529677 | C | 1.6453768 | 4.0307930 | -0.1934973 |
| I | 2.8215368 | -1.0398541 | -2.5088645 | C | 1.2682259 | 2.4365278 | -1.7978782 |
| I | 2.1983171 | 1.7945724 | 2.3493508 | C | 0.4023819 | 4.3285327 | -0.8129408 |
| I | 5.1210408 | 0.8936808 | 1.4250446 | C | 3.2322964 | -2.6920203 | 0.4081860 |
| I | 7.6936304 | 0.1004263 | 0.7693664 | C | 1.2737423 | -3.0953586 | 1.5323652 |
| C | -0.9895012 | 0.7432445 | 3.5331240 | C | 1.4403352 | -4.1414633 | 0.5782238 |
| C | -2.8301227 | -0.6117381 | 3.3595692 | H | 0.7749698 | -4.9749550 | 0.4239198 |
| C | -0.5346213 | -0.6013199 | 3.3893906 | C | 2.6690332 | -3.8857346 | -0.1185927 |
| C | -2.4106110 | 0.7366512 | 3.5120442 | H | 3.0802665 | -4.4778889 | -0.9192594 |
| H | -3.0470893 | 1.6036890 | 3.5937164 | C | 2.3747967 | -2.2047831 | 1.4209102 |
| C | -1.6790679 | -1.4396082 | 3.2874309 | H | -0.7164848 | 3.2962777 | -2.4189224 |
| C | -0.7867873 | -0.5948939 | -3.3819792 | H | 2.0863609 | 4.5722836 | 0.6276517 |
| C | -2.4177004 | 1.0366052 | -3.2726562 | H | 1.4184021 | 1.5650053 | -2.4157116 |
| H | -2.9219184 | 1.9910383 | -3.2713542 | H | -0.2618767 | 5.1342363 | -0.5461816 |
| C | -2.0449282 | -1.2380626 | -3.1904103 | H | 4.1348791 | -2.2092349 | 0.0717396 |
| C | -1.0214064 | 0.8055158 | -3.4280232 | H | 0.4553279 | -3.0108230 | 2.2263700 |
| C | -3.0430967 | -0.2310359 | -3.1498042 | H | 2.5339183 | -1.2961351 | 1.9820424 |

**Table S 13.** Cartesian coordinates of the optimised geometry of $[(CpMo)_4(\mu_4\text{-}P)(\mu_3\text{-}PI)_2(\mu\text{-}I)(I)_3(I_3)]$ (**2**) in triplet spin state at the TPSSH/def2-TZVP level. Total energy = −4750.73127866544 a.u.; <S*S> = 2.02.

| Atom | x | y | z | Atom | x | y | z |
|---|---|---|---|---|---|---|---|
| Mo | -1.6481330 | 0.0542107 | 1.3870333 | C | -1.7421285 | -1.4289626 | 3.2015180 |
| Mo | -1.7276530 | 0.1869141 | -1.3313277 | C | -0.7743375 | -0.3948929 | -3.3784653 |
| Mo | 0.1802709 | 2.2316332 | 0.2120354 | C | -2.6010442 | 1.0251602 | -3.3494068 |
| Mo | 1.2703906 | -2.3698509 | -0.4970123 | H | -3.2156909 | 1.9117837 | -3.3765122 |
| P | -2.1458332 | 2.0222490 | 0.1137708 | C | -1.9463308 | -1.1845647 | -3.2304718 |
| P | 0.3582349 | -0.1041762 | -0.0459811 | C | -1.1849775 | 0.9685338 | -3.4583457 |
| P | -1.1884778 | -1.8660639 | -0.0735995 | C | -3.0642265 | -0.3092029 | -3.2108216 |
| I | -3.9212410 | 3.6885276 | 0.0754431 | H | -0.2690096 | 1.5423986 | 3.6335802 |
| I | -2.6551271 | -3.9373907 | 0.0769043 | H | -3.8844465 | -0.8327780 | 3.2679467 |
| I | -4.0892587 | -0.4137777 | 0.0686528 | H | 0.4592407 | -1.0157975 | 3.2853534 |
| I | -0.5686997 | 4.0373429 | 2.3310296 | H | -1.8161216 | -2.4947638 | 3.0480563 |
| I | 0.4777534 | -3.9621855 | -2.5752080 | H | 0.2363401 | -0.7704400 | -3.4442713 |
| I | 2.9354462 | -0.9805818 | -2.2164297 | H | -1.9730075 | -2.2595627 | -3.1433855 |
| I | 2.2373209 | 1.6557879 | 2.2187025 | H | -0.5406048 | 1.8086905 | -3.6491520 |
| I | 5.1971588 | 0.9877866 | 1.2252607 | H | -4.0934104 | -0.6101930 | -3.0952276 |
| I | 7.8142072 | 0.4439063 | 0.4936693 | C | 2.1500155 | 2.8281332 | -0.9367423 |
| C | -0.9342585 | 0.7078197 | 3.4906433 | H | 3.0645125 | 2.2821092 | -0.7612616 |
| C | -2.8463150 | -0.5448700 | 3.3252347 | C | 0.1004125 | 3.4409814 | -1.7792651 |
| C | -0.5539452 | -0.6524328 | 3.3019279 | C | 1.6987442 | 3.9768919 | -0.2283524 |

| | | | |
|---|---|---|---|
| C | -2.3543346 | 0.7746433 | 3.4995323 |
| H | -2.9424969 | 1.6716023 | 3.6141339 |
| C | 3.2821345 | -2.8301358 | 0.6599791 |
| C | 1.2553079 | -3.3074700 | 1.6312045 |
| C | 1.5490361 | -4.3412544 | 0.7024827 |
| H | 0.9198206 | -5.1881519 | 0.4784413 |
| C | 2.8065729 | -4.0443489 | 0.1014154 |
| H | 3.2936967 | -4.6247714 | -0.6663761 |
| C | 2.3251552 | -2.3678185 | 1.6000714 |
| C | 1.1607661 | 2.4851601 | -1.8824469 |
| C | 0.4489380 | 4.3702783 | -0.7754247 |
| H | -0.8026032 | 3.4759013 | -2.3651228 |
| H | 2.2047448 | 4.4542398 | 0.5950885 |
| H | 1.2328057 | 1.6442604 | -2.5515164 |
| H | -0.1565342 | 5.1968400 | -0.4417189 |
| H | 4.1967079 | -2.3215055 | 0.3993246 |
| H | 0.3742439 | -3.2579298 | 2.2500764 |
| H | 2.4102690 | -1.4579124 | 2.1753332 |

**Table S 14.** Cartesian coordinates of the optimised geometry of [(CpMo)$_4$(μ$_4$-P)(μ$_3$-PI)$_2$(μ-I)(I)$_3$(I$_3$)] (**2**) in quintet spin state at the TPSSH/def2-TZVP level. Total energy = −4750.71139308007 a.u.; <S*S> = 6.06.

| Atom | x | y | z |
|---|---|---|---|
| Mo | -1.7353693 | 0.0391615 | 1.3563599 |
| Mo | -1.9945103 | -0.0603500 | -1.4083787 |
| Mo | 0.4169338 | 2.3666612 | 0.4563908 |
| Mo | 1.2171747 | -2.2884082 | -0.5484532 |
| P | -1.8856872 | 1.9604278 | -0.0762796 |
| P | 0.2014738 | 0.0030827 | -0.1569926 |
| P | -1.2141682 | -1.9237072 | -0.0170473 |
| I | -3.5539215 | 3.7277516 | -0.4034948 |
| I | -2.6399964 | -3.9875566 | 0.2351396 |
| I | -4.2537186 | -0.3491550 | 0.1392689 |
| I | -0.5692949 | 4.1078284 | 2.4131827 |
| I | 0.4188339 | -3.9872194 | -2.5496165 |
| I | 2.8162362 | -0.9415315 | -2.3663535 |
| I | 2.3024335 | 1.5965051 | 2.4494854 |
| I | 5.2921244 | 1.0488741 | 1.3919810 |
| I | 7.8820589 | 0.5614794 | 0.5660960 |
| C | -1.0085990 | 0.7238388 | 3.4432770 |
| C | -2.9035783 | -0.5600858 | 3.3154527 |
| C | -0.6120291 | -0.6348766 | 3.2612614 |
| C | -2.4303229 | 0.7723301 | 3.4589715 |
| H | -3.0314562 | 1.6604539 | 3.5737050 |
| C | -1.7900638 | -1.4286956 | 3.1964596 |
| C | -0.9628887 | -0.5108694 | -3.4651775 |
| C | -2.8574237 | 0.8028442 | -3.4067501 |
| H | -3.5138411 | 1.6597645 | -3.3841631 |
| C | -2.0896137 | -1.3692204 | -3.3708960 |
| C | -1.4384043 | 0.8321617 | -3.4927474 |
| C | -3.2546016 | -0.5599558 | -3.3292732 |
| H | -0.3535151 | 1.5655033 | 3.5873895 |
| H | -3.9374640 | -0.8653320 | 3.2757577 |
| H | 0.4052042 | -0.9861381 | 3.2440216 |
| H | -1.8491900 | -2.4978155 | 3.0596964 |
| H | 0.0690826 | -0.8282216 | -3.5100222 |
| H | -2.0496885 | -2.4461291 | -3.3156115 |
| H | -0.8329438 | 1.7172580 | -3.6009762 |
| H | -4.2686730 | -0.9178382 | -3.2382565 |
| C | 2.3260864 | 2.7619006 | -0.8030441 |
| H | 3.1998849 | 2.1429874 | -0.6649754 |
| C | 0.2972589 | 3.5338491 | -1.5614530 |
| C | 2.0219367 | 3.9650786 | -0.1051638 |
| C | 1.2646150 | 2.5007655 | -1.7076057 |
| C | 0.7742552 | 4.4426780 | -0.5800848 |
| C | 3.2661988 | -2.6326301 | 0.5795947 |
| C | 1.2883779 | -3.2299888 | 1.5819279 |
| C | 1.6289668 | -4.2445662 | 0.6478940 |
| H | 1.0477101 | -5.1271752 | 0.4331075 |
| C | 2.8543382 | -3.8734370 | 0.0260088 |
| H | 3.3611745 | -4.4229370 | -0.7516950 |
| C | 2.2990613 | -2.2290900 | 1.5349278 |
| H | -0.6228703 | 3.6420799 | -2.1132168 |
| H | 2.6143260 | 4.4119419 | 0.6773636 |
| H | 1.2266503 | 1.6582974 | -2.3793531 |
| H | 0.2574725 | 5.3222624 | -0.2340512 |
| H | 4.1468654 | -2.0729250 | 0.3076998 |
| H | 0.4174756 | -3.2346601 | 2.2170169 |
| H | 2.3396231 | -1.3172516 | 2.1116940 |

## [{CpMo(CO)$_2$}$_2$(μ-PBr$_2$)$_2$] (3a)

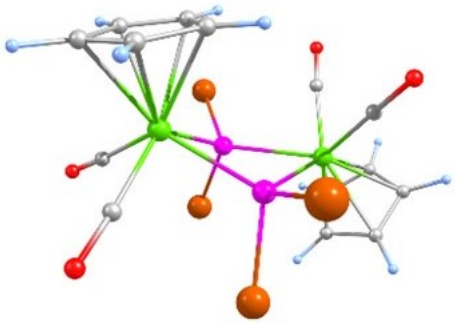

**Table S 15.** Cartesian coordinates of the optimised geometry of [{CpMo(CO)$_2$}$_2$(μ-PBr$_2$)$_2$] (**3a**) at the B3LYP/def2-TZVP level. Total energy = −11957.0057876 a.u..

| Atom | x | y | z | Atom | x | y | z |
|---|---|---|---|---|---|---|---|
| Mo | 1.669991000 | 0.925554000 | 0.314907000 | H | -2.456602000 | 1.835793000 | -0.737011000 |
| Mo | -1.821006000 | -1.217612000 | 0.419170000 | C | 3.669434000 | -0.252304000 | -0.129815000 |
| P | 0.230863000 | -1.037250000 | 1.034651000 | H | 3.635029000 | -1.264665000 | -0.493467000 |
| P | 0.202763000 | -0.135493000 | -1.463316000 | C | -1.785561000 | -2.241140000 | -2.126073000 |
| Br | 1.506994000 | -1.530860000 | -2.740360000 | C | -4.135279000 | -1.023844000 | -0.322259000 |
| Br | 1.549538000 | -2.917483000 | 1.101113000 | H | -4.774555000 | -1.842269000 | -0.609708000 |
| Br | -0.390870000 | -1.108303000 | 3.251497000 | C | 3.765476000 | 1.562207000 | 1.274110000 |
| Br | -0.463626000 | 1.219981000 | -3.202396000 | H | 3.811456000 | 2.170039000 | 2.163532000 |
| O | -1.837103000 | -2.834346000 | -3.104471000 | C | 3.716550000 | 0.144739000 | 1.234940000 |
| O | 0.317001000 | 2.229642000 | 2.816209000 | H | 3.724188000 | -0.515035000 | 2.087051000 |
| O | 0.281181000 | 3.517568000 | -0.753382000 | C | 3.694109000 | 0.923032000 | -0.929829000 |
| O | -1.796125000 | -4.176514000 | 0.614802000 | H | 3.681431000 | 0.956948000 | -2.006926000 |
| C | 0.776918000 | 1.704248000 | 1.904665000 | C | 3.751559000 | 2.041264000 | -0.058383000 |
| C | -1.759461000 | -3.094927000 | 0.239781000 | H | 3.785171000 | 3.076549000 | -0.357890000 |
| C | -3.673216000 | 0.020840000 | -1.174136000 | C | -2.910087000 | 0.453408000 | 0.946979000 |
| H | -3.883868000 | 0.126408000 | -2.225667000 | H | -2.426957000 | 0.926515000 | 1.786170000 |
| C | 0.753787000 | 2.534245000 | -0.395461000 | C | -3.647700000 | -0.759267000 | 0.990330000 |
| C | -2.925781000 | 0.932599000 | -0.382611000 | H | -3.835639000 | -1.350267000 | 1.871594000 |

## [{CpMo(CO)$_2$}(CpMoBr$_2$)(μ-PBr$_2$)$_2$] (4a)

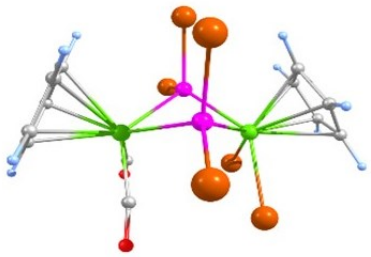

**Table S 16.** Cartesian coordinates of the optimised geometry of [{CpMo(CO)$_2$}(CpMoBr$_2$)(μ-PBr$_2$)$_2$] (**4a**) at the B3LYP/def2-TZVP level. Total energy = −16878.6432952 a.u.

| Atom | x | y | z | Atom | x | y | z |
|---|---|---|---|---|---|---|---|
| Mo | 1.580869000 | -0.180774000 | 1.008034000 | H | 0.801225000 | -0.895987000 | 3.826413000 |
| Mo | -0.887202000 | -0.362220000 | 1.361319000 | C | 2.364305000 | 1.602851000 | 2.249601000 |
| Br | -1.406746000 | -3.003533000 | 1.649350000 | H | 2.480535000 | 2.578775000 | 1.809292000 |
| Br | 1.453277000 | 2.900682000 | -1.784005000 | C | 3.379391000 | 0.612722000 | 2.352954000 |
| Br | -0.763435000 | 3.105064000 | 0.734599000 | H | 4.371037000 | 0.682800000 | 1.941999000 |
| Br | -2.185491000 | 0.167680000 | 2.444282000 | C | 1.185710000 | 1.088589000 | 2.864665000 |
| Br | 2.123513000 | -2.727239000 | 0.796309000 | H | 0.260668000 | 1.617130000 | 3.005041000 |
| Br | 3.455928000 | 0.021625000 | -0.799831000 | C | -2.158015000 | 0.757134000 | -2.976827000 |
| P | 0.450079000 | 1.478737000 | -0.310005000 | H | -1.697389000 | 1.382665000 | -3.724011000 |
| P | -0.707334000 | -0.909154000 | 1.078482000 | C | -3.221965000 | 0.075675000 | -1.059496000 |
| O | 1.366243000 | -0.266272000 | -3.567473000 | H | -3.683742000 | 0.089486000 | -0.086398000 |
| O | -0.165244000 | -3.410229000 | -1.738114000 | C | -2.671050000 | 1.194854000 | -1.729420000 |
| C | 0.634041000 | -0.266082000 | -2.697360000 | H | -2.642671000 | 2.203134000 | -1.351321000 |
| C | -0.364147000 | -2.315050000 | -1.505168000 | C | -3.054538000 | -1.063869000 | -1.887419000 |
| C | 2.836975000 | -0.509706000 | 3.004394000 | H | -3.394216000 | -2.061932000 | -1.663459000 |
| H | 3.343776000 | -1.442960000 | 3.175741000 | C | -2.394958000 | -0.645777000 | -3.081706000 |
| C | 1.477460000 | -0.232143000 | 3.314717000 | H | -2.166889000 | -1.266676000 | -3.932540000 |

## [{CpMo(CO)$_2$}$_2$(μ-PCl$_2$)$_2$] (3b)

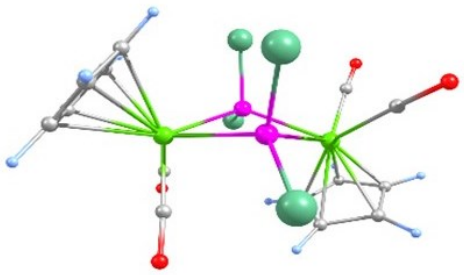

**Table S 17.** Cartesian coordinates of the optimised geometry of [{CpMo(CO)$_2$}$_2$(μ-PCl$_2$)$_2$] (**3b**) at the B3LYP/def2-TZVP level. Total energy = −3501.1892496 a.u.

| Atom | x | y | z | Atom | x | y | z |
|---|---|---|---|---|---|---|---|
| Mo | 1.722110000 | 0.847759000 | 0.286562000 | H | -2.421916000 | 1.748473000 | -0.768963000 |
| Mo | -1.752180000 | -1.297647000 | 0.448598000 | C | 3.693014000 | -0.370517000 | -0.173489000 |
| P | 0.282843000 | -1.097346000 | 1.011271000 | H | 3.636108000 | -1.382143000 | -0.536749000 |
| P | 0.255164000 | -0.197266000 | -1.484264000 | C | -1.673728000 | -2.319892000 | -2.153672000 |
| Cl | 1.458701000 | -1.470767000 | -2.656803000 | C | -4.072283000 | -1.129011000 | -0.362298000 |
| Cl | 1.499978000 | -2.817597000 | 1.077656000 | H | -4.703039000 | -1.953047000 | -0.652469000 |
| Cl | -0.288390000 | -1.142462000 | 3.042501000 | C | 3.839635000 | 1.441712000 | 1.229178000 |
| Cl | -0.356051000 | 1.060066000 | -3.065310000 | H | 3.906355000 | 2.048544000 | 2.117953000 |
| O | -1.694886000 | -2.913775000 | -3.133428000 | C | 3.760071000 | 0.025511000 | 1.190839000 |
| O | 0.369866000 | 2.132530000 | 2.800420000 | H | 3.762834000 | -0.634367000 | 2.042898000 |
| O | 0.330413000 | 3.431883000 | -0.801708000 | C | 3.736426000 | 0.804167000 | -0.974015000 |
| O | -1.654351000 | -4.254551000 | 0.586167000 | H | 3.717915000 | 0.838137000 | -2.051027000 |
| C | 0.832941000 | 1.621783000 | 1.881792000 | C | 3.825068000 | 1.920909000 | -0.103180000 |
| C | -1.647955000 | -3.172060000 | 0.210362000 | H | 3.878731000 | 2.955241000 | -0.403012000 |
| C | -3.617602000 | -0.079047000 | -1.211652000 | C | -2.867221000 | 0.359786000 | 0.912851000 |
| H | -3.826494000 | 0.025067000 | -2.263711000 | H | -2.394181000 | 0.838564000 | 1.754706000 |
| C | 0.807624000 | 2.455582000 | -0.429861000 | C | -3.593824000 | -0.859355000 | 0.952598000 |
| C | -2.881829000 | 0.839349000 | -0.417266000 | H | -3.781485000 | -1.451956000 | 1.83288900 |

## [{CpMo(CO)$_2$}(CpMoCl$_2$)(μ-PCl$_2$)$_2$] (4b)

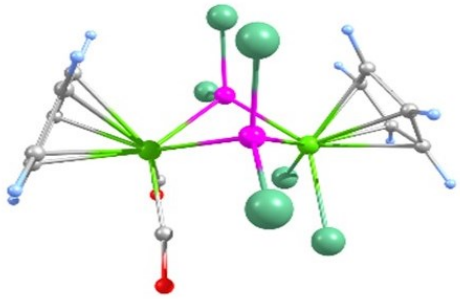

**Table S 18.** : Cartesian coordinates of the optimised geometry of [{CpMo(CO)$_2$}(CpMoCl$_2$)(μ-PCl$_2$)$_2$] (**4b**) at the B3LYP/def2-TZVP level. Total energy = −4194.9156358 a.u.

| Atom | x | y | z | Atom | x | y | z |
|---|---|---|---|---|---|---|---|
| Mo | 1.576536000 | -0.185980000 | 0.995818000 | H | 0.790830000 | -0.896154000 | 3.818728000 |
| Mo | -0.882979000 | -0.366544000 | 1.366258000 | C | 2.353926000 | 1.601003000 | 2.235104000 |
| Cl | -1.313128000 | -2.817857000 | 1.618626000 | H | 2.474137000 | 2.578252000 | 1.799055000 |
| Cl | -2.058033000 | 0.120921000 | 2.288795000 | C | 3.366987000 | 0.608318000 | 2.337562000 |
| Cl | -0.699806000 | 2.925185000 | 0.656996000 | H | 4.354305000 | 0.671539000 | 1.913795000 |
| Cl | 1.396411000 | 2.770666000 | -1.628948000 | C | 1.172870000 | 1.086505000 | 2.848077000 |
| Cl | 2.052257000 | -2.572825000 | 0.767525000 | H | 0.247699000 | 1.615662000 | 2.987252000 |
| Cl | 3.299704000 | -0.000096000 | -0.728137000 | C | -2.164087000 | 0.764369000 | -2.967653000 |
| P | 0.448483000 | 1.464875000 | -0.309134000 | H | -1.708397000 | 1.391104000 | -3.716810000 |
| P | -0.699796000 | -0.903148000 | 1.067563000 | C | -3.212705000 | 0.079280000 | -1.043436000 |
| O | 1.417490000 | -0.239015000 | -3.524519000 | H | -3.666233000 | 0.091785000 | -0.066410000 |
| O | -0.126666000 | -3.415628000 | -1.675585000 | C | -2.663247000 | 1.198912000 | -1.713366000 |
| C | 0.659257000 | -0.259335000 | -2.677114000 | H | -2.628357000 | 2.205448000 | -1.331065000 |
| C | -0.340507000 | -2.315833000 | -1.480130000 | C | -3.058464000 | -1.057136000 | -1.878503000 |
| C | 2.823814000 | -0.512846000 | 2.989265000 | H | -3.401621000 | -2.054460000 | -1.656665000 |
| H | 3.325702000 | -1.451616000 | 3.147984000 | C | -2.409486000 | -0.636506000 | -3.077411000 |
| C | 1.464808000 | -0.234173000 | 3.301881000 | H | -2.191705000 | -1.254673000 | -3.932881000 |

## References


[1] O. J. Scherer, H. Sitzmann, G. Wolmershäuser, *J. Organomet. Chem.* **1984**, *268*, C9-C12.
[2] CrysAlisPro Software System, Rigaku Oxford Diffraction, **2020**.
[3] CrysAlisPro Software System, Rigaku Oxford Diffraction, **2015**.
[4] CrysAlisPro Software System, Rigaku Oxford Diffraction, **2017**.
[5] O. V. Dolomanov, L. J. Bourhis, R. J. Gildea, J. A. K. Howard, H. Puschmann, *J. Appl. Cryst.* **2009**, *42*, 339-341.
[6] G. M. Sheldrick, *Acta Cryst.* **2015**, *A71*, 3-8.
[7] G. M. Sheldrick, *Acta Cryst.* **2015**, *C71*, 3-8.
[8] R. Ahlrichs, M. Bär, M. Häser, H. Horn, C. Kölmel, *Chem. Phys. Lett.* **1989**, *162*, 165–169.
[9] O. Treutler, R. Ahlrichs, *J. Chem. Phys.* **1995**, *102*, 346–354.
[10] A. D. Becke, *Phys. Rev. A*, **1988**, *38*, 3098.
[11] J. P. Perdew, *Phys. Rev. B* **1986**, *33*, 8822-8824; Erratum: J. P. Perdew, *Phys. Rev. B* **1986**, *34*, 7406.
[12] A. D. Becke, *J. Chem. Phys.* **1993**, *98*, 5648-5652.
[13] C. Lee, W. Yang, R. G. Parr, *Phys. Rev. B* **1988**, *37*, 785-789.
[14] J. P. Perdew, K. Burke, M. Ernzerhof, *Phys. Rev. Lett.* **1996**, *77*, 3865-3868; Erratum *Phys. Rev. Lett.* **1997**, *78*, 1396.
[15] J. P. Perdew, M. Ernzerhof, K. Burke, *J. Chem. Phys.* **1996**, *105*, 9982-9985.
[16] S. Grimme, *J. Comput. Chem.* **2006**, *27*, 1787-1799.
[17] J. Tao, J. P. Perdew, V. N. Staroverov, G. E. Scuseria, *Phys. Rev. Lett.* **2003**, *91*, 146401.
[18] V. N. Staroverov, G. E. Scuseria, J. Tao, J. P. Perdew, *J. Chem. Phys.* **2003**, *119*, 12129-12137.
[19] A. Schäfer, C. Huber, R. Ahlrichs, *J. Chem. Phys.* **1994**, *100*, 5829.
[20] K. Eichkorn, F. Weigend, O. Treutler, R. Ahlrichs, R *Theor. Chem. Acc.* **1997**, *97*, 119.
[21] K. Eichkorn, O. Treutler, H. Oehm, M. Häser, R. Ahlrichs, *Chem. Phys. Lett.* **1995**, *242*, 652–660.

[22] M. Sierka, A. Hogekamp, R. Ahlrichs, *J. Chem. Phys.* **2003**, *118*, 9136.
[23] Gaussian 09, Revision E.01, M. J. Frisch, G. W. Trucks, H. B. Schlegel, G. E. Scuseria, M. A. Robb, J. R. Cheeseman, G. Scalmani, V. Barone, B. Mennucci, G. A. Petersson, H. Nakatsuji, M. Caricato, X. Li, H. P. Hratchian, A. F. Izmaylov, J. Bloino, G. ZhengJ. L. Sonnenberg, M. Hada, M. Ehara, K. Toyota, R. Fukuda, J. Hasegawa, M. Ishida, T. Nakajima, Y. Honda, O. Kitao, H. Nakai, T. Vreven, Jr. J. A. Montgomery,J. E. Peralta, F. Ogliaro, M. Bearpark, J. J. Heyd, E. Brothers, K. N. Kudin, V. N. Staroverov, T. Keith, R. Kobayashi, J. Normand, K. Raghavachari, A. Rendell, J. C. Burant, S. S. Iyengar, J. Tomasi, M. Cossi, N. Rega, J. M. Millam, M. Klene, J. E. Knox, J. B. Cross, V. Bakken, C. Adamo, J. Jaramillo, R. Gomperts, R. E. Stratmann, O. Yazyev, A. J. Austin, R. Cammi, C. Pomelli, J. W. Ochterski, R. L. Martin, K. Morokuma, V. G. Zakrzewski, G. A. Voth, P. Salvador, J. J. Dannenberg, S. Dapprich, A. D. Daniels, O. Farkas, J. B. Foresman, J. V. Ortiz, J. Cioslowski, D. J. Fox, *Gaussian, Inc.*, Wallingford CT, **2013**.

## 4. Halogenation of the Hexaphosphabenzene Complex $[(Cp^*Mo)_2(\mu,\eta^6:\eta^6\text{-}P_6)]$ – Snapshots on the Reaction Progress

### Authors

Anna Garbagnati, Michael Seidl, Gábor Balázs, Manfred Scheer.

### Author contribution

A. Garbagnati prepared the manuscript and performed the synthesis and characterization of the herein presented compounds. G. Balázs performed all DFT calculations, contributed to the corresponding parts in the manuscript and the Supporting Information and revised the manuscript. M. Seidl did the refinement of the solid-state structures. M. Scheer supervised the research and revised the manuscript.

### Acknowledgement

This work was comprehensively supported by Deutsche Forschungsgemeinschaft (DFG) within the project Sche384/36-2. We thank Matthias Ackermann and Sabrina Dinauer for the EPR measurements.

4. Halogenation of the Hexaphosphabenzene Complex [(Cp*Mo)$_2$(μ,η$^6$:η$^6$-P$_6$)] – Snapshots on the Reaction Progress

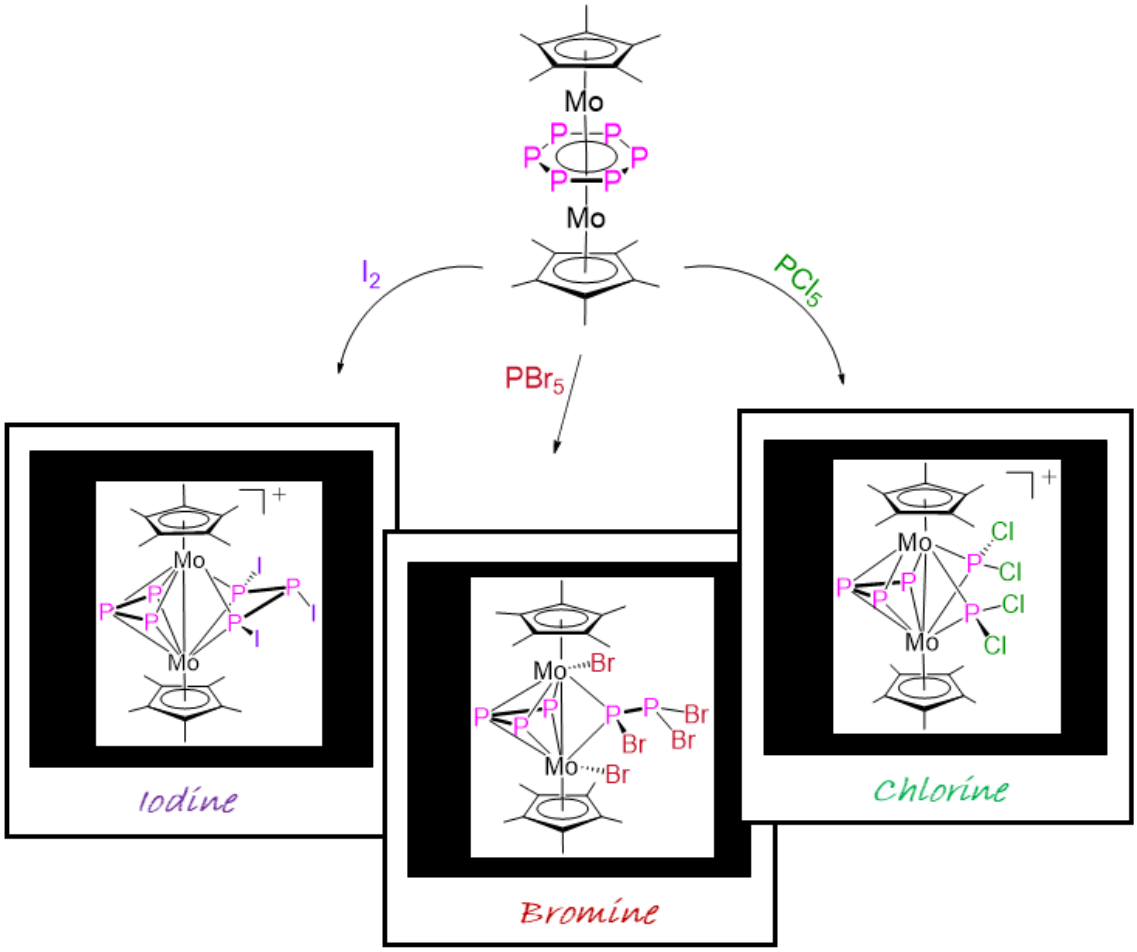

# 4 Halogenation of the hexaphosphabenzene Complex [(Cp*Mo)$_2$(μ,η$^6$:η$^6$-P$_6$)] – Snapshots on the reaction progress

***Abstract:*** *The oxidation of [(Cp*Mo)$_2$(μ,η$^6$:η$^6$-P$_6$)] (**1**) with halogens or halogen sources was investigated. The iodination afforded the ionic complexes [(Cp*Mo)$_2$(μ,η$^3$:η$^3$-P$_3$)(μ,η$^1$:η$^1$:η$^1$-P$_3$I$_3$)][X] (X = I$_3^-$, I$^-$) (**2**) and [(Cp*Mo)$_2$(μ,η$^4$:η$^4$-P$_4$)(μ-PI$_2$)][I$_3$] (**3**), while the reaction with PBr$_5$ led to the complexes [(Cp*Mo)$_2$(μ,η$^3$:η$^3$-P$_3$)(μ-Br)$_2$][Cp*MoBr$_4$] (**4**) [(Cp*MoBr)$_2$(μ,η$^3$:η$^3$-P$_3$)(μ,η$^1$-P$_2$Br$_3$)] (**5**) and [(Cp*Mo)$_2$(μ-PBr$_2$)(μ-PHBr)(μ-Br)$_2$] (**6**). The reaction of **1** with the far stronger oxidating agent PCl$_5$ was followed via time- and temperature-dependent $^{31}$P{$^1$H} NMR spectroscopy. One of the first intermediates detected at 193K was [(Cp*Mo)$_2$(μ,η$^3$:η$^3$-P$_3$)(μ-PCl$_2$)$_2$][PCl$_6$] (**8**) which rearranges upon warming to [(Cp*Mo)$_2$(μ-PCl$_2$)$_2$(μ-Cl)$_2$] (**9**), [(Cp*MoCl)$_2$(μ,η$^3$:η$^3$-P$_3$)(μ-PCl$_2$)] (**10**) and [(Cp*Mo)$_2$(μ,η$^4$:η$^4$-P$_4$)(μ,PCl$_2$)][Cp*MoCl$_4$] (**11**), which could be isolated at room temperature. All complexes were characterized by single-crystal X-ray diffraction, NMR spectroscopy and their electronic structures were elucidated by DFT calculations.*

## 4.1 Introduction

The halogenation of white phosphorus is the first step on an industrial scale to transform P$_4$ to organophosphorus derivatives. First publications on the halogenation of white phosphorus date back more than 120 years.[1,2] In 1940, *Wyllie et. al.* proved that the reaction of P$_4$ with I$_2$ leads to P$_2$I$_4$ or PI$_3$, depending on the used stoichiometry, while the reaction of P$_4$ with Br$_2$ leads to PBr$_3$.[3] Based on these results, in 1994, *Tattershall et al.* reported four series of compounds resulting from the reaction of P$_4$ with I$_2$, Br$_2$ or ICl that were identified by NMR spectroscopy.[4] Later on, *Stoppioni et. al.* presented the first example of a halogenation of coordinated white phosphorus in the coordination sphere of transition metal by iodine, which resulted in the monocation [{CpRu(PPh$_3$)$_2$}$_2$(μ,η$^1$:η$^1$-P$_4$H$_2$I)]$^+$).[5] In 2019, *Peruzzini et. al.* reported the ruthenium-mediated halogenation of white phosphorus, resulting in the complex [RuCp*(PCy$_3$)(μ,η$^2$:η$^4$-P$_4$Cl$_2$)RuCp*] bearing the unprecedented P$_4$Cl$_2$ moiety.[6] Recently, the stepwise degradation of white phosphorus coordinated to a Ru(II) complex upon the reaction with iodine was postulated

by DFT computations.[7] The key role of the metal was demonstrated since the proposed mechanism differs significantly from the concerted one that is valid for uncoordinated white phosphorus.[8] As an alternative access, $P_4$ moieties already converted to polyphosphorus complexes might be a valuable approach to functionalized polyphosphorus complexes.

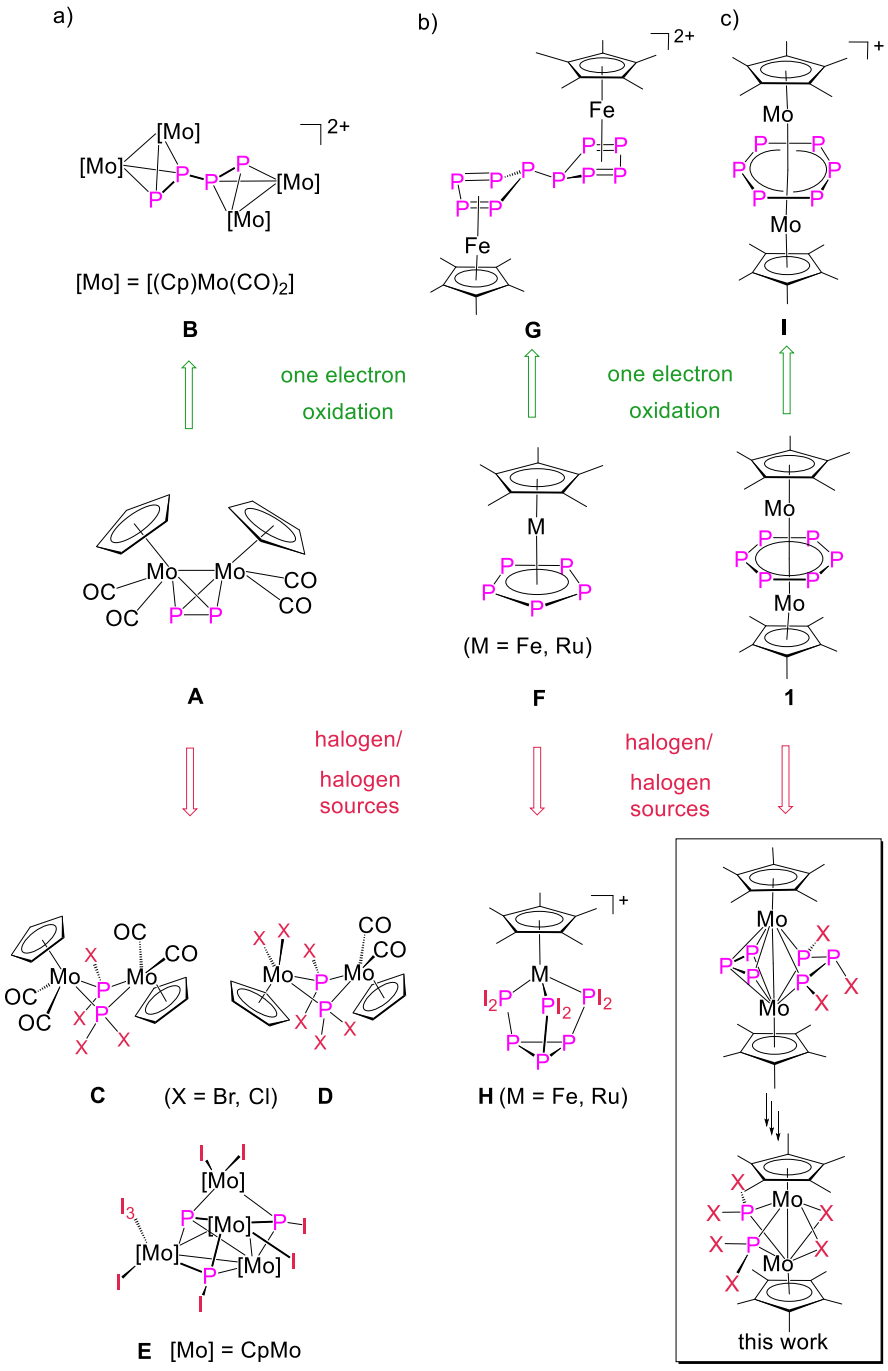


**Scheme 1** Selected examples of one-electron oxidations *versus* halogenation reactions of $P_n$-ligand complexes. Selected $P_n$ ligand complexes are a) the tetrahedrane [{CpMo(CO)$_2$}$_2$(μ,η$^2$:η$^2$-P$_2$)]; b) [Cp*M(η$^5$-E$_5$)] (M = Fe, Ru; E = P, As); c) [(Cp*Mo)$_2$(μ,η$^6$:η$^6$-P$_6$)].

## 4. Halogenation of the Hexaphosphabenzene Complex $[(Cp^*Mo)_2(\mu,\eta^6{:}\eta^6\text{-}P_6)]$ – Snapshots on the Reaction Progress

Our recent study on the iodination of the *cyclo*-$E_5$ complexes $[Cp^*M(\eta^5\text{-}E_5)]$ (M = Fe, Ru; E = P, As)[9] has shown that this is a powerful tool for the high-yield synthesis of new types of functionalized polypnictogen compounds (Scheme 1b, red arrow). By examining different halogen sources, the halogenation of the tetrahedrane compound $[\{CpMo(CO)_2\}_2(\mu,\eta^2{:}\eta^2\text{-}P_2)]$ proved to lead to very diverse reaction products (Scheme 1a, red arrow).[10]

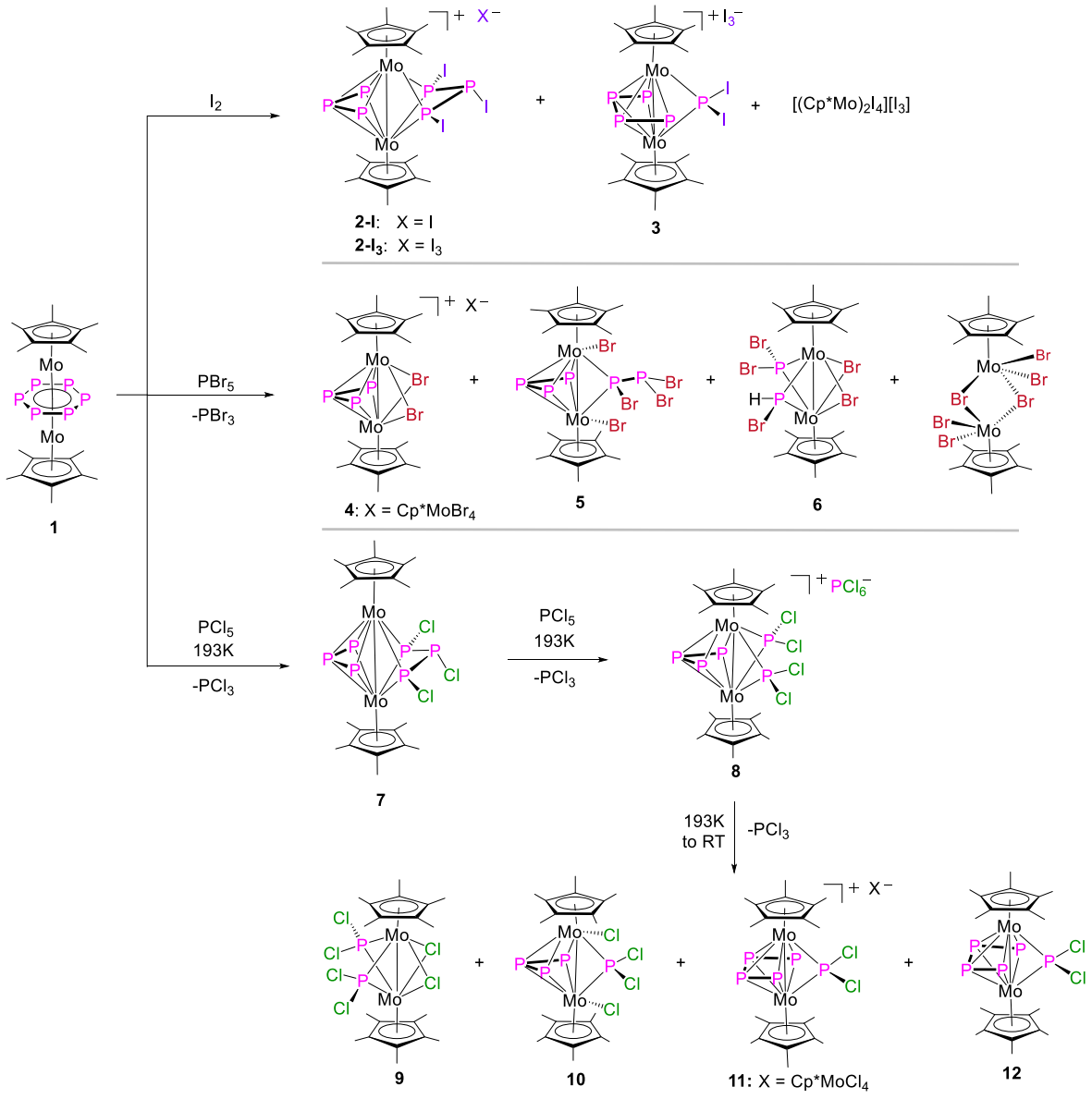


**Scheme 2** Reaction of $[(Cp^*Mo)_2(\mu,\eta^6{:}\eta^6\text{-}P_6)]$ with $I_2$, $PBr_5$ and $PCl_5$.

These studies clearly show the different reactivity of polyphosphorus complexes with oxidants such as halogens towards an alternative one-electron oxidation. Thus, the oxidation of $[\{CpMo(CO)_2\}_2(\mu,\eta^2{:}\eta^2\text{-}P_2)]$ leads selectively to the dicationic complex $[\{CpMo(CO)_2\}_4(\mu,\eta^2{:}\eta^2{:}\eta^2{:}\eta^2\text{-}P_4)]^{2+}$[11] (Scheme 1a, **B**), while the halogenation yields, depending on the used stoichiometry and halogen, **C** – **E** (Scheme 1a). Similarly, a

substantial difference in the one-electron oxidation of [Cp*Fe(η$^5$-P$_5$)] and its oxidation with halogens was realized. While the oxidation leads to the dicationic complex [(Cp*Fe)$_2$(μ,η$^{5:5}$-P$_{10}$)]$^{2+}$ (Scheme 1b, **G**),[12] the reaction with I$_2$ yields the nortricylane derivative **H** (Scheme 1b).[9] Since in triple-decker complexes the middle deck is stabilized by two metal fragments, a higher stability of the products in the reaction with halogens is expected, possibly enabling the identification of intermediates and their isolation along the reaction pathway.

Therefore, the redox-active compound [(Cp*Mo)$_2$(μ,η$^6$:η$^6$-P$_6$)] (**1**)[13] was chosen for a detailed study of its halogenation. The cyclo-voltammogram of this 28 VE complex reveals a reversible one-electron oxidation in which a 27 VE product results in a distorted *cyclo*-P$_6$ ligand in a bis-allylic arrangement (Scheme 1c, **I**).[14] Herein we report on the oxidation of the hexaphosphabenzene complex [(Cp*Mo)$_2$(μ,η$^6$:η$^6$-P$_6$)] (**1**) by halogens and halogen sources such as I$_2$, PBr$_5$ and PCl$_5$ as a novel synthetic approach to unprecedented halogen-functionalized complexes of the type [(Cp*Mo)$_2$P$_n$X$_m$] (n, m = 1, 2, 3; X = I, Br, Cl) revealing P$_n$X$_m$ middle decks.

## 4.2 Results and discussions

The reaction of **1** with an excess of iodine (6 equiv.) in CH$_2$Cl$_2$, followed by the layering of the reaction solution with *n*-pentane, leads to [(Cp*Mo)$_2$(μ,η$^3$:η$^3$-P$_3$)(μ,η$^1$:η$^1$:η$^1$-P$_3$I$_3$)][I$_3$] (**2-I$_3$**) as a red crystalline compound in 54% isolated yields (Scheme 2). When a stoichiometric amount of I$_2$ was used (3 equiv.), a few crystals of the similar complex **2-I** in which I$_3^-$ is replaced by I$^-$ as counterion were isolated. Redissolving the remaining precipitate of this reaction in CH$_2$Cl$_2$ and layering it with toluene afforded [(Cp*Mo)$_2$(μ,η$^4$:η$^4$-P$_4$)(μ-PI$_2$)][I$_3$] (**3**) as black blocks in a crystalline yield of 2% (Scheme 2). The ESI-MS spectrum of the latter reaction solution shows the molecular ion peak of **2** and **3**, together with the one of the paramagnetic complex [(Cp*Mo)$_2$(μ-I)$_4$][I$_3$]. The latter compound was already described by *Poli et. al*.[15] Possible other products as for instance PI$_3$ or P$_2$I$_4$ could not be detected in the $^{31}$P{$^1$H} NMR spectrum of the reaction solution which shows only the signals of **2** *(vide infra)*. The formation of **3** could not be ascertained by $^{31}$P NMR spectroscopy due it is paramagnetic nature. Since no signals of the starting material were detected, its full conversion can be assumed. The variable temperature (VT) $^{31}$P{$^1$H} NMR spectrum of this reaction solution recorded from −80°C to room temperature shows that the formation of **2** starts already at low temperatures, with **2** being the only P-containing diamagnetic product that could be detected. The spectra at higher temperatures are silent because **2** precipitates quickly from the solution already at low temperatures (cf. SI for VT-$^{31}$P{$^1$H} NMR) and the remaining products are paramagnetic.

## 4. Halogenation of the Hexaphosphabenzene Complex $[(Cp^*Mo)_2(\mu,\eta^6{:}\eta^6\text{-}P_6)]$ – Snapshots on the Reaction Progress

Our study of the halogenation of $[\{CpMo(CO)_2\}_2(\mu,\eta^2{:}\eta^2\text{-}P_2)]$ showed that the nature of the halogen ($I_2$ *vs*. $Br_2$) plays a decisive role regarding the type of the resulting compounds.[10] Hence, the reaction of $[(Cp^*Mo)_2(\mu,\eta^6{:}\eta^6\text{-}P_6)]$ (**1**) with $PBr_5$ as a bromine source was carried out. Due to the higher reactivity of bromine (towards Iodine), the reaction of **1** with an excess of $PBr_5$ (6 equiv.) in $CH_2Cl_2$ was carried out at −40°C and the reaction solution was slowly warmed up to –20°C. Precipitation of the concentrated reaction solution with cold *n*-pentane led to a green precipitate which was dissolved in THF and layered with toluene affording a few crystals of $[(Cp^*Mo)_2(\mu,\eta^3{:}\eta^3\text{-}P_3)(\mu\text{-}Br)_2][Cp^*MoBr_4]$ (**4**) (2% yield). The supernatant of the mother liquor was decanted off and, while warming up to room temperature, crystals of the neutral species $[(Cp^*MoBr)_2(\mu,\eta^3{:}\eta^3\text{-}P_3)(\mu\text{-}P_2Br_3)]$ (**5**) were formed in 17% yield. Performing the reaction under the same conditions but evaporating all volatiles at −10°C, washing the residue with *n*-pentane and toluene and finally recrystallizing from a mixture of $CH_2Cl_2$/*n*-pentane, crystals of $[(Cp^*Mo)_2(\mu\text{-}PBr_2)(\mu\text{-}PHBr)(\mu\text{-}Br)_2]$ (**6**) could be isolated (9% yield; Scheme 2). Additionally, also a few crystals of the known side product $[(Cp^*MoBr_2)_2(\mu\text{-}Br)_2]$[16] were isolated. The $^{31}P\{^1H\}$ NMR spectrum of the reaction solution shows, among the signals corresponding to **4**[17] and **6**, a broad singlet at 230 ppm corresponding to $PBr_3$ which overlaps with one of the two signals of **6**. Signals corresponding to **5** could not be detected in the $^{31}P$ NMR spectrum of the freshly prepared reaction solution, but were only detected after storing the sample at room temperature for five days. This indicates that **5** is not an initial product of the reaction of **1** with $PBr_5$. Preparing an NMR sample by mixing precooled solution of **1** and $PBr_5$ and performing a VT $^{31}P\{^1H\}$ NMR experiment (starting at −80°C) shows the formation of a very complex reaction mixture (cf. SI) from which no known complexes could be identified. By warming to room temperature, signals corresponding to **6** could be detected. Since the signal of $PBr_3$ is always detected when using $PBr_5$ as a reagent, the question arises which part of it results from the halogenation of **1**. $^{31}P$ NMR spectroscopic investigations showed that only about 30% of the $PBr_3$ results from $PBr_5$ while the remaining 70% follows from the bromination of **1** (cf. SI).

Against the background that the reaction of **1** towards a bromine source was predictably more complex than the one with iodine, the question arises as to what would be the difference in the reactivity towards an even stronger halogenating source as for instance chlorine. Therefore, a time-dependent $^{31}P\{^1H\}$ NMR study of the reaction of **1** with an excess of $PCl_5$ (6 equiv.) was carried out at 193 K (Figure 1a). The signal of **1** could not be detected, which proves that its conversion is completed already at 193 K after fifteen minutes. The first $^{31}P\{^1H\}$ NMR spectrum ($t_1$= 15 minutes) shows four resonances centred at δ = 420.8, 329.3, 145.1 and −361.7 ppm in a 1:2:2:1 integral ratio, corresponding to an

AMM'OO'X spin system (Figure 1a,b) which can be assigned to **7**, based on its similarity with **2** (*vide infra*). In addition, a singlet corresponding to $PCl_3$ (δ = 220.0 ppm) and a singlet at 6.5 ppm which could not be assigned were detected. **7** could not be isolated due to its high instability. Attempts to crystallize it led to the isolation of $[(Cp^*Mo)_2(\mu,\eta^3{:}\eta^3\text{-}P_3)(\mu\text{-}PCl_2)_2][PCl_6]$ (**8**) instead (74% yield, scheme 2).

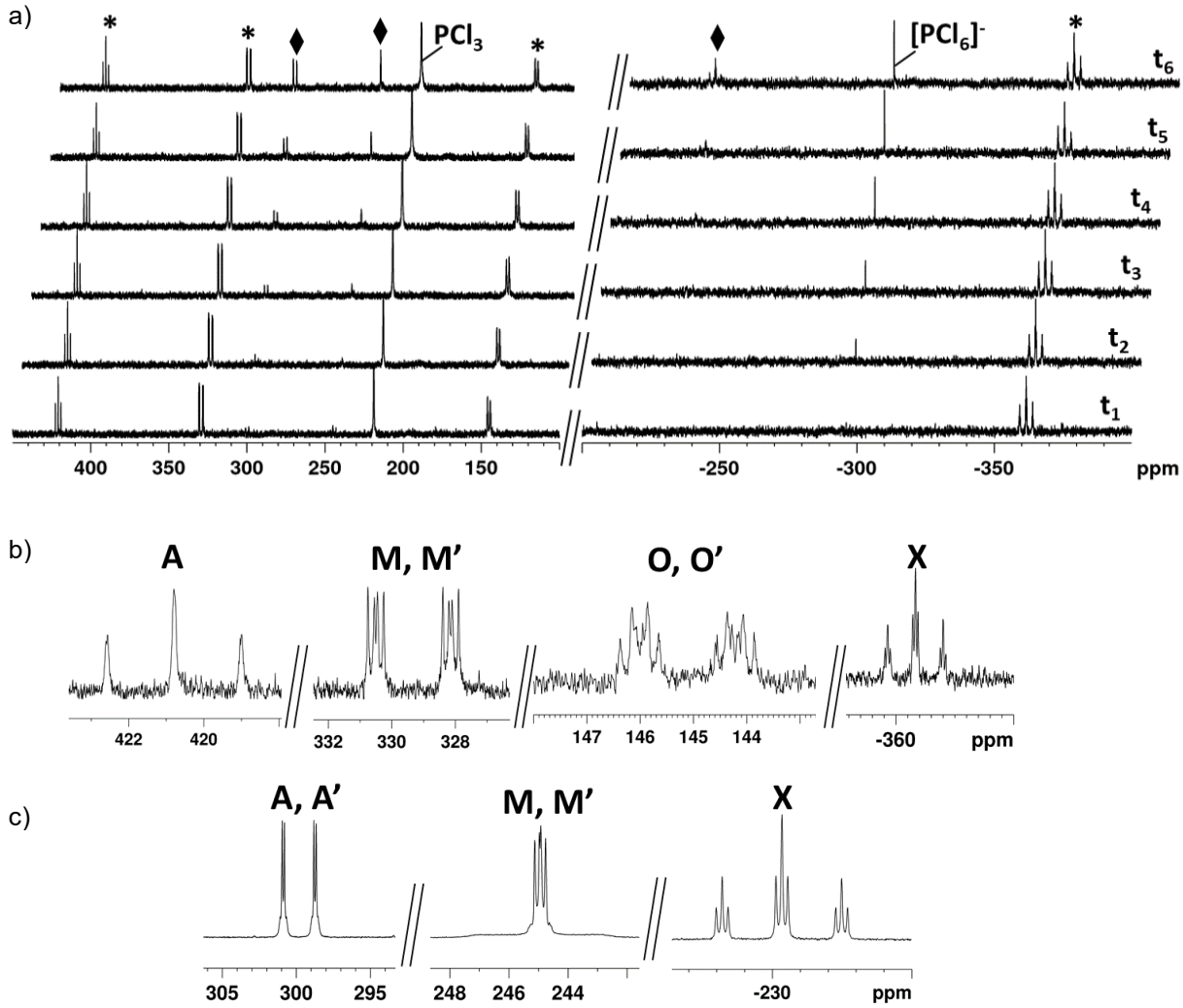


**Figure 1 a)** Time-dependent $^{31}P\{^1H\}$ NMR spectra of the reaction solution of **1** with $PCl_5$ at 193 K. * = **7**, ♦ = **8**; **b)** Selected signals of the $^{31}P\{^1H\}$ NMR spectrum of **7** ($CD_2Cl_2$, 193 K) **c)** Selected signals of the $^{31}P\{^1H\}$ NMR spectrum of **8** ($CD_2Cl_2$, 233 K).

Based on the $^{31}P$ NMR spectroscopic data, the first product of the reaction of **1** with $PCl_5$ is **7** which then converts to **8**, where its signals start to appear in the time-dependent NMR study after one hour ($t_2$ = 1 hour; figure 1a). Solutions of **8** in $CH_2Cl_2$ at room temperature are stable for less than one hour, afterwards the color of the solution starts to change from bright red to dark brown. Its decomposition can also be detected by NMR spectroscopy (cf. SI). The $^{31}P\{^1H\}$ NMR spectrum of the crystals of **8** dissolved in $CD_2Cl_2$

at room temperature reveals after seven hours its complete decomposition and formation of $[(Cp^*Mo)_2(\mu\text{-}PCl_2)_2(\mu\text{-}Cl)_2]$ (**9**), $[(Cp^*MoCl)_2(\mu,\eta^3{:}\eta^3\text{-}P_3)(\mu\text{-}PCl_2)]$ (**10**) and $PCl_3$ (Figure 2).

Moreover, the intensity of the signal corresponding to $PCl_3$ (220.2 ppm) increases with the temperature, while the one of $[PCl_6]^-$ decreases until it disappears completely at room temperature (cf. SI for VT $^{31}P\{^1H\}$ NMR). By performing the reaction of **1** with $PCl_5$ directly at room temperature, **9** and **10** can be isolated in 3% and 4% crystalline yield, respectively (Scheme 2). The $^{31}P\{^1H\}$ NMR spectrum of the reaction solution at 25°C shows the characteristic signals of **9** (δ = 317.2 ppm), **10** (*vide infra*) and $PCl_3$ (δ = 220.2 ppm) among other signals that could not be assigned (cf. SI). Roughly 78% of the $PCl_3$ originates from **1**, which reflects the low yields of **9** and **10**.[18] Attempts to isolate other products of the chlorination led to the isolation of the 30 VE cationic triple-decker compound $[(Cp^*Mo)_2(\mu,\eta^4{:}\eta^4\text{-}P_4)(\mu\text{-}PCl_2)][Cp^*MoCl_4]$ (**11**) (Scheme 2).

**11** is well soluble in $CD_2Cl_2$ but paramagnetic (cf. SI) and therefore could not be detected by NMR spectroscopy but was identified by single crystal X-ray diffraction analysis.

In the $^1H$ NMR spectrum of **11**, the signal of the anion $[Cp^*MoCl_4]^-$ in **11** could be detected at −13.9 ppm as a broad singlet ($\omega_{1/2}$ = 170 Hz), which is in line with the reported chemical shift.[19] When **1** was reacted with three equiv. of $PCl_5$, the neutral analogue of **11**, *i.e.* $[(Cp^*Mo)_2(\mu,\eta^4{:}\eta^4\text{-}P_4)(\mu\text{-}PCl_2)]$ (**12**), could be isolated in 10% yield.[20] The 31VE triple-decker complex **12** is paramagnetic, but no signals could be detected by EPR spectroscopy, probably due to its triplet spin state. Crystals of **11** were alternatively obtained by layering a solution of **8** with *n*-pentane in $CH_2Cl_2$ at room temperature after few days. Therefore, together with **9** and **10**, **11** represents another decomposition product of **8** (Scheme 2). Additional proof of this is provided by the $^1H$ NMR spectrum of crystals of **8** dissolved in $CD_2Cl_2$ which also shows, after 15 days at room temperature, the broad singlet of the counterion of **11**, $[Cp^*MoCl_4]^-$(cf. SI).[21]

The $^{31}P$ NMR spectra of **2** and **7** are very similar, both of them showing an AMM'OO'X spin system (cf. SI). The central phosphorus atom of the allylic-like $P_3$ unit ($P^X$) resonates at high field (−327 ppm for **2** and −362 ppm for **7**), while the peripheral P atoms ($P^M/P^{M'}$) resonate at lower field (349 ppm for **2** and 382 ppm for **7**) and show the largest $^1J_{PP}$ coupling constant (~380 Hz). Similar chemical shifts and coupling constants were found for the allylic-like $P_3$ unit in the complexes **5**, **10** and **8** (for details see SI), although **5** shows an ADHKX spin system (Figure 3, top) due to the chemically inequivalent peripheral P atoms of the allylic-like $P_3$ unit. The central P atom ($P^A$) of the $P_3X_3$ subunit resonates at low field (380 ppm for **2** and 421 ppm for **7**), while the peripheral P atoms ($P^O/P^{O'}$) resonate at moderately higher field (5 ppm for **2** and 145 ppm for **7**) and show a smaller $^1J_{PP}$ coupling

constant (~280 Hz; Figure 1b). Within the PBrPBr$_2$ unit of **5**, the $^1J_{PP}$ coupling of 420 Hz is rather large and an additional large coupling ($J_{PAPH}$ = 70 Hz) is observed within the P$_3$ unit. Similarly, P-P couplings can be detected between the PCl$_2$ and the P$_3$ units (up to 35 Hz) in **8** (Figure 1c) and **10** (up to 41 Hz, Figure 3, bottom). Additionally, the resonance signal of the $PCl_6^-$ anion in **8** is observed at −296 ppm in the $^{31}$P NMR spectrum. Compound **8** shows rather broad signals at room temperature, which sharpen by lowering the temperature to −40°C (Figure 1c).

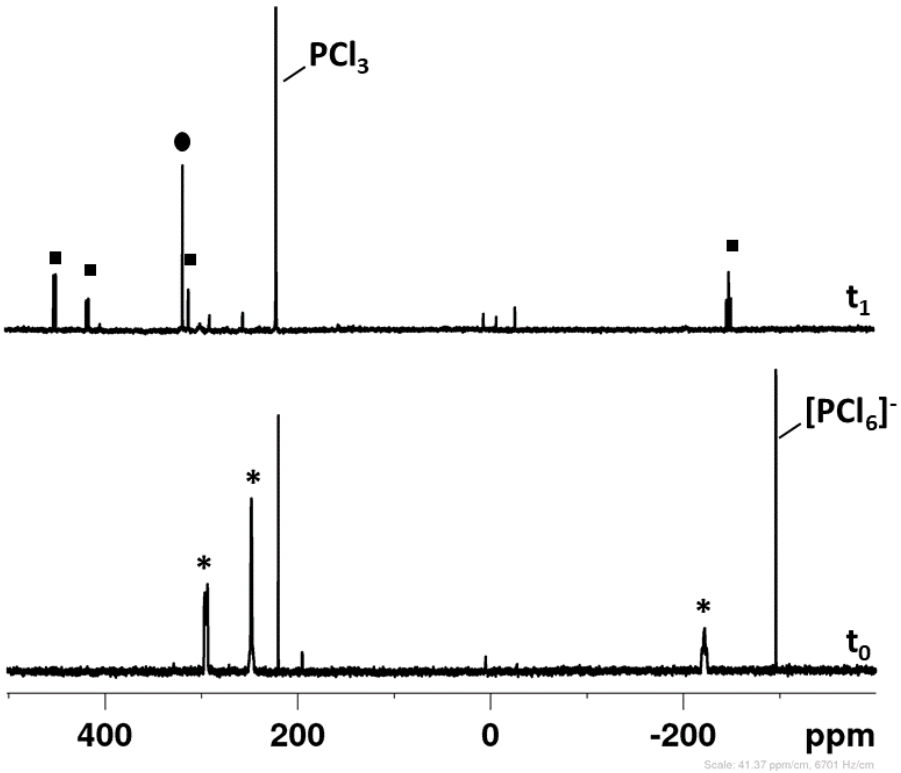


**Figure 2** $^{31}$P{$^1$H} NMR spectra of **8** at $t_0$ = 20 minutes and $t_1$ = 7 hours ($CD_2Cl_2$, 300 K). Whereas, after 20 minutes, only signals of **8** (*) and $PCl_3$ are visible, after 7 hours, its complete decomposition into **9** (●) and **10** (■) is detected.

The $^{31}$P{$^1$H} NMR spectrum of **6** shows two doublets with a coupling constant of 38 Hz, corresponding to the two nonequivalent phosphorus atoms. The signal at the highest field can be assigned to the PH ligand which splits into a doublet of doublets due to the coupling with the proton ($^1J_{PH}$ = 444 Hz, $^2J_{PH}$ = 5 Hz). For **9**, only one singlet was detected (cf. SI). The $^{31}$P NMR chemical shifts and coupling constants for all complexes were determined by iterative simulation of the experimental spectra (see SI).

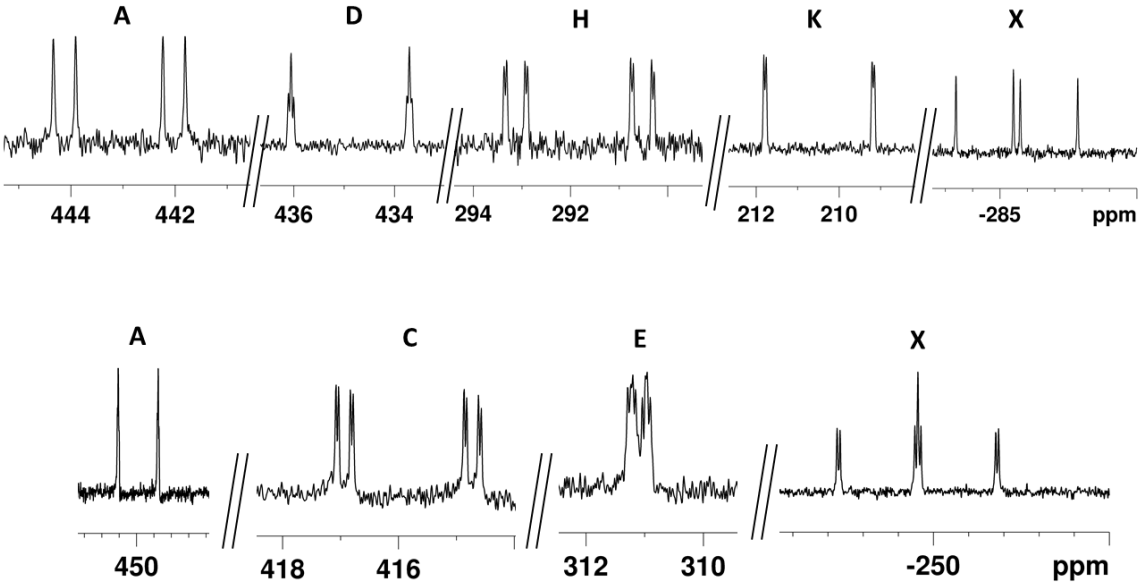


**Figure 3** Selected signals of the $^{31}P\{^1H\}$ NMR spectra of **5** (top) and **10** (bottom) ($CD_2Cl_2$, 300 K).

Apart from **7** which is extremely unstable even at low temperatures in solution and could not be isolated, the solid-state structures of all other products were determined by single crystal X-ray diffraction analysis (Figure 4), revealing that the halogenation of the 28VE *cyclo*-P$_6$-containing triple-decker complex [(Cp*Mo)$_2$(μ,η$^6$:η$^6$-P$_6$)] (**1**) leads to the formation of dinuclear monocations and neutral species which, in most cases, retain their triple-decker geometry. However, in some cases, degradation to [(Cp*MoBr$_2$)$_2$(μ-Br)$_2$], [(Cp*Mo)(I$_4$)]$^-$ or [Cp*MoX$_4$], the latter being observed as an anion in **4** and **11**, was detected. For all complexes, the Mo-Mo bond lengths are below the sum of their covalent radii (3.08 Å)[22] and longer than the corresponding distance in the neutral *cyclo*-P$_6$ complex **1** (2.647(1) Å)[13] and in the related monocation [(Cp*Mo)$_2$(μ,η$^6$:η$^6$-P$_6$)][FAl] ([FAl] = [FAl{OC$_6$F$_{10}$(C$_6$F$_5$)}$_3$], 2.661(8) Å).[14] They vary from 2.691(2) Å in **9** to 2.920(6) Å in **10**. The only exception is observed within **4** with a Mo-Mo distance of 2.579(6) Å. The Cp* ligand in the compounds **2-I$_3$**, **3**, **4**, **6**, **8**, **9** and **11** is almost coplanar, being only minimally tilted (tilt angle of 1° to 7°). In compounds **5** and **10**, the coplanarity of the ligands is lost, and the Cp* ligands are tilted by 40° and 38°, respectively.

The molecular structure of **2-I$_3$** shows an allylic-P$_3$ and a P$_3$I$_3$ ligand each of them bridging the two {Cp*Mo} fragments (Figure 4). In the P$_3$I$_3$ unit, the central P atom does not coordinate to molybdenum. Compared to the P-P bond lengths in **1**[13] (average: 2.171(3) Å and in the range of P-P single bonds (2.22 Å)[23]), the P3-P4 (2.139(5) Å) and P4-P5 (2.138(6) Å) distances are shortened. Similar bond lengths were observed for the cationic complex [(Cp*Mo)$_2$(μ,η$^6$:η$^6$-P$_6$)][FAl][14] whose *cyclo*-P$_6$ undergoes a bis-allylic distortion

upon one electron oxidation (average: 2.136(10) Å). The P1-P2 (2.216(5) Å) and the P1-P6 (2.220(5) Å) distances in the $P_3I_3$ ligand are longer than the one in **1**, but still in the range of a P-P single bond, while the distance between P2 and P6 with 2.459(5) Å is too long for a usual single bond, but considerably below the sum of the van der Waals radii (3.80 Å).[8] DFT calculations for compound **2-I$_3$** reproduce this distance (2.434 Å) well, but no bonding interaction could be detected (the Mayer bond order (BO) is lower than 0.1 and no orbital overlap occurs). The P···P distances between the two $P_3$ ligands are rather long (P2···P3 2.652(5) Å and P5···P6 2.665(5) Å). Nevertheless, DFT calculations indicate the presence of a P···P interaction as shown by BOs of 0.16 and 0.18 for P2···P3 and P5···P6, respectively (see also SI). A similar *cyclo*-$P_3I_3$ moiety was recently postulated by DFT computations as one of the intermediates involved in the last steps of the iodine-induced stepwise degradation of the $P_4$ ligand in [Cp*Ru(dppe)(η$^1$-P$_4$)],[7] but without any experimental evidences. Therefore, **2-I$_3$** represents the first example of an isolated polyphosphorus complex bearing a $P_3I_3$ ligand. The presence of an allylic $P_3$ ligand is recurrent among the products of the halogenation of **1**, as in **4**, **5**, **8** and **10**, which will be discussed together, therefore. In the allylic $P_3$ ligand of **4**, the P1-P2 (2.126(2) Å) and the P2-P3 (2.118(19) Å) bond lengths are shortened compared to the P-P bond lengths in **1** (average: 2.171(3) Å). In the case of **5**, the $P_3$ ligand is distorted (P3-P4 2.174(2) Å; P4-P5 2.128(2) Å) and additionally a $P_2Br_3$ ligand bridges between the two {Cp*MoBr} fragments in an *end-on* coordination mode with P-P bond lengths that are in the range of a P-P single bond (P1-P2 = 2.260(2) Å). Several diphosphines of the type $RP_2Br_3$ were reported, *e.g.* with R = $^t$Bu by *Baudler et al*,[24] R = $CCl_3$ [25] or R = CN,[26] but no $P_2Br_3$ unit as a ligand attached to a metal fragment is known. Thus, the one in **5** is the first reported example. The $P_3$ ligand in **8** is in line with what was observed for the analog $P_3$ units in **2-I$_3$**, **4** and **5**, with P2-P3 = 2.105(4) Å and P3-P4 = 2.101(4) Å. The average distance from this unit and the $PCl_2$ groups (2.663(7) Å) suggests the presence of P···P interactions between them. The solid-state structure of **10** is comparable to the one observed for **5**, with a distorted allylic $P_3$ ligand (P2-P3: 2.163(2) Å and P3-P4: 2.123(2) Å) bridging between two {Cp*MoCl} units. The short distance between the $P_3$ ligand and the $PCl_2$ group (P1-P2 = 2.577(19) Å) indicates an interaction which is also reflected in a rather large $^2J_{PP}$ coupling constant between these nuclei. The short P1···P2 distance (2.551 Å) is well reproduced by DFT calculations and is accompanied by a BO of 0.22 indicating the presence of a bonding interaction. The $P_n$ core of **10** is comparable to the one observed in compound [{Cp*V}$_2$(μ,η$^3$:η$^3$-P$_3$){μ-P(NHC$^{Me}$)}] resulting from the ring contraction of the vanadium analog of **1** ([(Cp*V)$_2$(μ,η$^6$:η$^6$-P$_6$)]) induced by $^{Me}$NHC.[27]

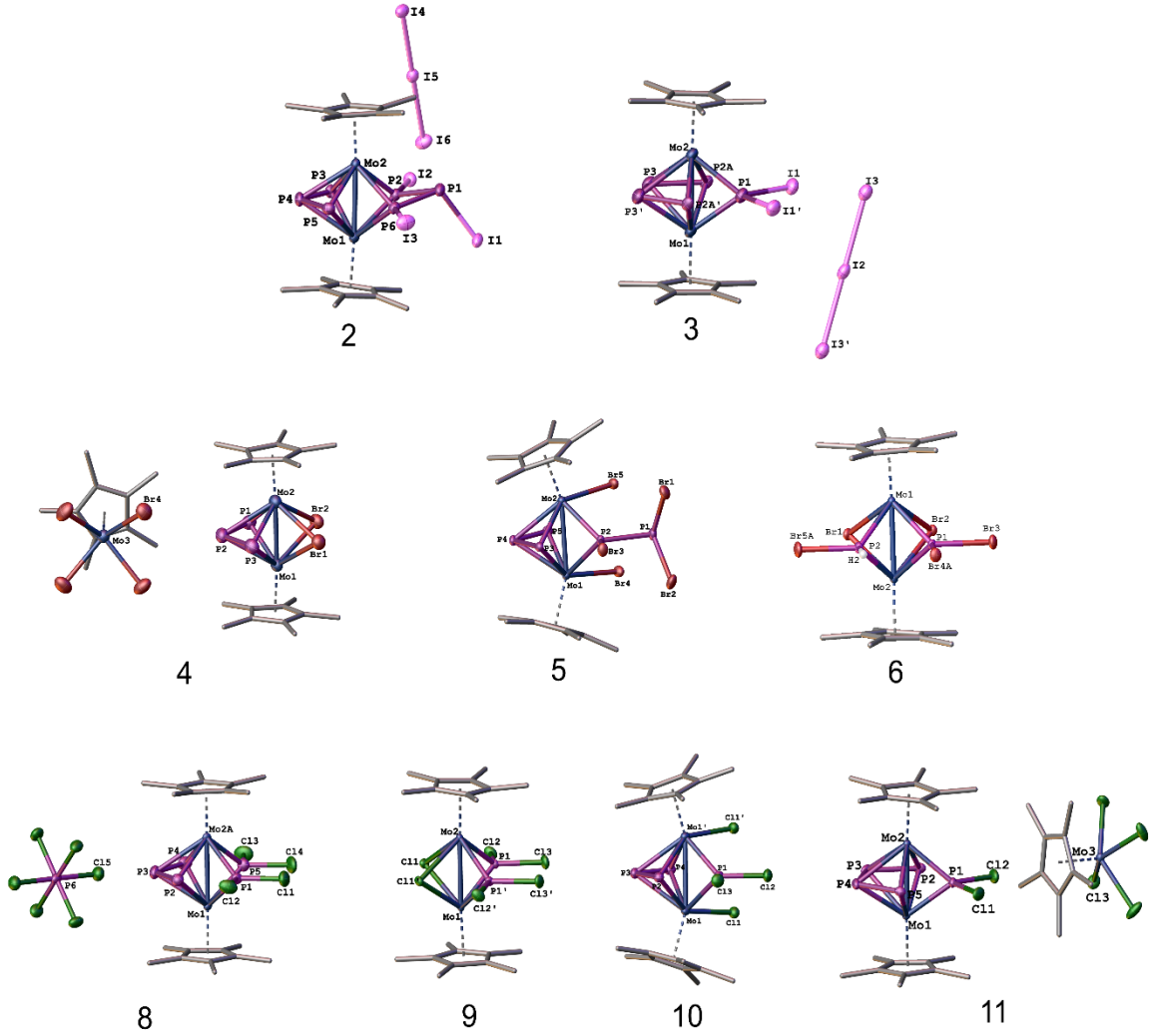


**Figure 4** Molecular structures of **2-I$_3$**, **3**, **4**, **5**, **6, 8**, **9**, **10** and **11** with thermal ellipsoids at 50% probability level. The hydrogen atoms are omitted for clarity. Selected bond lengths: **2I$_3$**: Mo1-Mo2: 2.722(15) Å, P1-P2: 2.216(5) Å, P1-P6: 2.220(5) Å, P3-P4: 2.139(5), P4-P5: 2.138(6) Å; **3**: Mo1-Mo2: 2.743(8) Å, P2A-P3A: 2.243(7) Å, P3-P3': 2.162(4); **4**: Mo1-Mo2: 2.579(6) Å, P1-P2: 2.126(2) Å, P2-P3: 2.118(19) Å; **5**: Mo1-Mo2: 2.919(7) Å, P1-P2: 2.260(2) Å, P3-P4: 2.174(2) Å, P4-P5: 2.128(2) Å; **6**: Mo1-Mo2: 2.709(3) Å; **8**: Mo1-Mo2: 2.728(2) Å, P2-P3: 2.105(4) Å, P3-P4: 2.101(4) Å; **9**: Mo1-Mo2: 2.691(2) Å; **10**: Mo1-Mo1': 2.920 (6) Å, P2-P3: 2.163 (2) Å, P3-P4 2.123 (3) Å; **11**: Mo1-Mo2: 2.759(4) Å, P2-P3: 2.210(9) Å, P4-P5: 2.197(8), P3-P4: 2.155(9) Å.

The solid-state structure of **3** reveals a *cisoid*-P$_4$ and a PI$_2$ bridging ligand separated from each other by 2.596(9) Å. The P2-P3 (= P2'-P3') (2.243(7) Å) and P3-P3' (2.162(4) Å) bond lengths in the *cisoid*-P$_4$ ligand all lie in the range of P-P single bonds. Therefore, it cannot be described as a tetraphosphabuta-1,3-diene-like ligand, contrary to the analog *cisoid*-P$_4$ ligands in complexes ([(Cp$^{BIG}$Fe)$_2$(μ,η$^4$:η$^4$-P$_4$)],[28] [(Cp''Fe)$_2$(μ,η$^4$:η$^4$-P$_4$)],[29] [{Cp$^R$Fe}$_2$(μ,η$^4$:η$^4$-P$_4$)] (Cp$^R$ = C$_5$H$_3$(SiMe$_3$)$_2$).[30] The *cisoid*-P$_4$ ligand as middle deck in the 30VE species **11** is similar to the one in **3** with two longer P-P bonds (P2-P3 = 2.210(9) Å,

P4-P5= 2.197(8) Å) and a shorter one (P3-P4 = 2.155(9) Å). The P1-P2 and the P1-P5 distances in **11** are 2.664(8Å) and 2.6591(7), respectively, indicating a P-P interaction (*vide infra*).

The solid-state structure of **6** contains only two P atoms, in the form of a $PBr_2$ and a PHBr bridging ligand, with a nonbonding distance between the two phosphorus atoms of 2.762(9) Å. A similar structure was observed for compound **9**, which bears two equivalent bridging $PCl_2$ ligands, separated from each other by 2.894(6) Å.

In order to investigate the bonding situation in complexes **2-12**, DFT calculations at the D4-TPSSh(CPCM)/def2-TZVP level were conducted.[31] The geometric parameters of the complexes are well reproduced, including the distances between the different $P_n$ units in the molecules. In all complexes **2-12**, a Mo-Mo bond was detected, being in line with the relatively short Mo-Mo distances. The Mayer bond order (BO) varies from 0.87 in **4** to 0.59 in **5** (Mo-Mo distances 2.574 and 2.892 Å in the optimized geometries, respectively). The intrinsic bonding orbitals [32] representing the Mo-Mo bond in **2** and the bonding within the $Mo_2P_3$ unit in **4** are depicted in Figure 5.

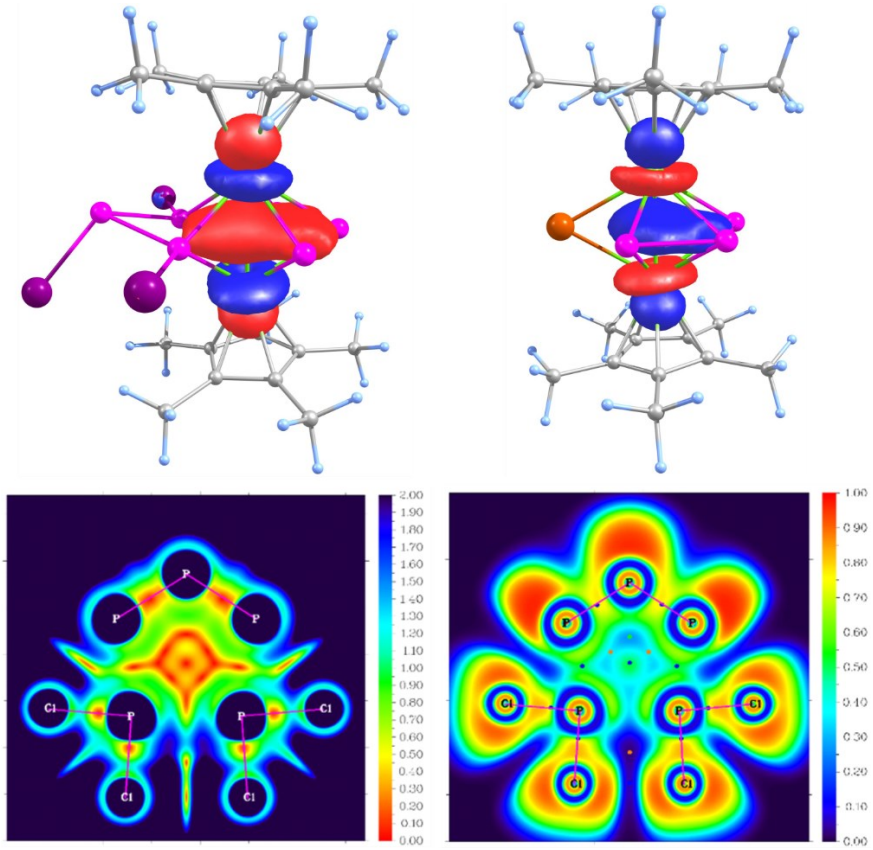


**Figure 5** Intrinsic Bonding Orbitals representing the Mo-Mo bond in **2** (top left) and **4** (top right) as well as the Interaction Region Indicator (IRI) plot in the plane defined by the phosphorus atoms (bottom left) and Electron Localization Function (ELF) plot (bottom right) in **8**. Blue dots represent (3,-1) critical points.

The NBO[33] analysis is in agreement with the IBO analysis, although only in **4** and **6** an Mo-Mo bond (Mo-Mo 2.579 Å (**4**) and 2.709 (**6**)) is predicted by the NBO analysis, while in the other complexes a nonbonding NBO on each Mo with an occupancy of approx. 1e is partitioned instead of an Mo-Mo bonding orbital. Although, the P2-P6 distance in **2** is rather short, no bonding interaction could be detected by DFT calculations. In contrast, bonding interactions were detected between P2-P3 (2.649 Å) and P5-P6 (2.628 Å) as shown by BOs of 0.16 and 0.18, respectively. Similar interactions were detected between P1-P2A in **3** (P1-P2A 2.623 Å, BO 0.17; singlet spin state), P2-P3 in **5** (2.594 Å, BO 0.17), P1-P2 in **8** (2.517 Å, BO 0.24), P1-P2 in **10** (2.551 Å, BO 0.22), P2-P3 in **11** (2,626 Å, BO 0.18; singlet spin state) and P2-P3 in **12** (2.665, BO 0.17). The Interaction Region Indicator (IRI)[34] clearly shows a bonding interaction between the $P_3$ and the $PCl_2$ units in **8**, among the expected bonds. A plot of IRI in the plane defined by the phosphorus atoms is depicted in figure 5 showing the regions with notable chemical bond interaction (orange) and areas where weak interactions occur (green). The Electron Localization Function (ELF)[35] and Localized Orbital Locator (LOL)[36] also support these interactions (see SI). Complexes **3** and **11** are paramagnetic in solutions at room temperature, however, DFT calculations show that the singlet spin state of the cation in **3** and **11** is with 90 and 102 kJ·mol$^{-1}$, respectively, more stable than the triplet spin state. The overall paramagnetic behavior of **11** might be due to the paramagnetic nature of the counter anions [Cp*MoCl$_4$]$^-$, having a triplet spin state as determined experimentally.[37]

## 4.3 Conclusions

In summary, we showed that the halogenation of [(Cp*Mo)$_2$(μ,η$^6$:η$^6$-P$_6$)] (**1**) proceeds *via* a very complex pathway leading to a plethora of complexes containing different $P_n$ units such as $P_4$, $P_3$ and $P_1$. An excess of halogens/halogen sources leads to phosphorus-free complexes of the type [Cp*MoX$_n$] (X = I, Br, Cl) as well as $PX_3$ (X = Br, Cl) as final reaction products. Additionally, we showed that besides iodination, which is known to be a powerful tool for the synthesis of new $P_n$ ligand complexes, bromination and chlorination can also be used for this purpose. Among the products of the iodination of the hexaphosphabenzene complex **1**, the novel compound **2** bearing an unprecedented $P_3I_3$ ligand could be isolated. With a bromine source, complex **5** could be isolated, representing the first example of a compound bearing a $P_2Br_3$ unit as a bridging ligand between two Mo centers.

Whereas the products of the one-electron oxidation of **1** showed only a distortion of the hexagonal geometry of the $P_6$ middle deck, the use of halogens or halogen sources as oxidating agents afforded a variety of new polyphosphorus compounds bearing

synthetically useful novel $P_nX_m$ units. As expected, the chemoselectivity of the reaction decreased with the enhancement of the oxidizing power of the halogen. However, with a strict control of the temperature it is possible to have a good control of the reaction even with a stronger oxidant such as the chlorine source $PCl_5$. First snapshots from the halogenation of the $P_6$ ligand complex were found, and even though the complete pathway could not be clarified, they gave useful information concerning the proceeding reaction. Thus, first an allylic fragmentation of the *cyclo*-$P_6$ unit occurs followed by the monohalogenation of the P atoms of one of the allylic $P_3$ units. Subsequently, a dihalogenation revealing $PX_2$ units occurs, which is followed by the removal of the P atoms as $PX_3$ moieties. Only afterwards, the second allylic-$P_3$ unit seems to be halogenated.

This study adds triple-decker complexes to the class of poly-phosphorus compounds that can be successfully halogenated. Therefore, future investigations will focus on the halogenation of heterobimetallic triple-decker compounds as well as of $E_n$ ligand derivatives that combine the features of triple-decker complexes and separate $E_n$ units. Moreover, since the halogenation reactions in general have shown to be a powerful tool for the generation of halogen functionalized polyphosphorus ligands, future studies will also focus on the use of these products for further derivatisations.

## 4.4 References


[1] J. A. Besson, *Compt. Rend*. **1897**, *124*, 1346-1349.
[2] R. Bouloch, *Compt. Rend.* **1905**, *141*, 256.
[3] D. Wyllie, M. Ritchie, E. B. Ludlom *J. Chem. Soc*. **1940**, 583-587.
[4] B.W. Tattershall, N.L. Kendall *Polyhedron* **1994**, *13*, 1517-1521.
[5] P. Barbaro, C. Bazzicalupi, M. Peruzzini, S. Seniori Costantini, P. Stoppioni, *Angew. Chem. Int. Ed*. **2012**, *51*, 8628-8631.
[6] M. Bispinghoff, Z. Benkő, H. Grützmacher, F. Delgado Calvo, M. Caporali, M. Peruzzini, *Dalton Trans.* **2019**, *48*, 3593-3600.
[7] G. Manca, A. Ienco, *Inorg. Chim. Acta*, **2021**, *517*, 120205.
[8] C. Mealli, A. Ienco, M. Peruzzini, G. Manca, *Dalton Trans.*, **2018**, *47*, 394.
[9] H. Brake, E. Peresypkina, A. V. Virovets, M. Piesch, W. Kremer, L. Zimmermann, Ch. Klimas, M. Scheer, *Angew. Chem. Int. Ed*. **2020**, *59*, *59*, 16241-16246.
[10] A. Garbagnati, M. Seidl, G. Balázs, M. Scheer, *Inorg. Chem*. **2021**, *60*, 5163–5171.
[11] L. Dütsch, M. Fleischmann, S. Welsch, G. Balázs, M. Scheer, *Angew. Chem. Int. Ed*. **2018**, *57*, 3256-3261.
[12] M. V. Butovskiy, G. Balázs, M. Bodensteiner, E. V. Peresypkina, A. V. Virovets, J. Sutter, Manfred Scheer, *Angew. Chem. Int. Ed*. **2013**, *52*, 2972 –2976.
[13] O. J. Scherer, H. Sitzmann, G. Wolmershäuser, *Angew. Chem. **1985,*** 97, 358-359; *Angew. Chem. Int. Ed. Engl.* **1985**, *24*, 351-353.
[14] M. Fleischmann, F. Dielmann, G. Balázs, M. Scheer, *Chem. Eur. J*. **2016**, *22*, 15248-15251.
[15] J. C. Gordon, V. T. Lee, R. Poli, *Inorg. Chem*. **1993**, *32*, 4460-4463
[16] J. U. Desai, J. C. Gordon, H. Kraatz, V. T. Lee, B. E. Waltermire, R. Poli, A. L. Rheingold, and C. B. White, *Inorg. Chem.* **1994**, *33*, 3752–3769.
[17] In the $^{31}$P-NMR spectrum of the reaction solution, only one of the two signals of **4** could be detected, probably due to its low concentration, whereas the characteristic signal of its counterion $[Cp^*MoBr_4]^-$ could be detected in the $^1$H NMR spectrum.
[18] Determined by $^{31}$P NMR spectroscopy (cf. SI).
[19] H.B. Kraatz, R.Poli, *J. Organomet. Chem.* **1994**, *475*, 167-175.

[20] Unfortunately, complex **12** could be obtained only once. All attempts to synthesize **12** in a targeted manner have failed so far.
[21] The use of a smaller number of equivalents of $PCl_5$ (1, 2 or 3 equiv.) did not lead to an improvement of the chemoselectivity and often resulted in the crystallization of the residual **1**, even though it was not detected in the $^{31}P$ NMR spectrum. The use of a large excess of the halogenating agent (10 equiv.) led e.g. to the isolation of the known compound [(Cp*MoCl)$_2$(μ-Cl)$_2$] in 14% crystalline yield; see: F. Abugideiri, G. A. Brewer, J. U. Desai, J. C. Gordon, R. Poli, *Inorg. Chem.* **1994**, *33*, *17*, 3745–3751.
[22] S. Alvarez, *Dalton Trans.*, **2013**, *42*, 8617–8636 .
[23] P. Pyykkç, M. Atsumi, *Chem. Eur. J*. **2009**, *15*, 12770–12779.
[24] M. Baudler, J. Hellmann, *Z. Anorg. Allg. Chemie*, **1982**, *490*, 11-18.
[25] P.L. Airey, *Z. Naturforsch*. **1969**, *24b*, 1393-1397.
[26] K.B. Dillon, A.W.G. Platt, T.C. Waddington, *Inorganic and Nuclear Chemistry Letters*, **1981**, *17*, 201-205.
[27] M. Piesch, S. Reichl, M. Seidl, G. Balázs, M. Scheer, *Angew. Chem. Int. Ed*. **2019**, *58*, 16563-16568.
[28] S. Heinl, G. Balázs, M. Scheer, *Phosphorus, Sulfur, and Silicon and the Related Elements*, *189*, **2014**, 1-9.
[29] Scherer, O. J.; Schwarz, G.; Wolmershäuser, *G. Z. Anorg. Allg. Chem.* **1996**, *622*, 951-957.
[30] Miluykov, V. A.; Sinyashin, O. G.; Lonnecke, P.; Hey-Hawkins, E. *Mendeleev Commun*. **2003**, *13*, 212-213.
[31] D4-TPSSh(CPCM)/def2-TZVP level: a) D4: E. Caldeweyher, S. Ehlert, A. Hansen, H. Neugebauer, S. Spicher, C. Bannwarth, S. Grimme, *J. Chem. Phys.* **2019**, *150*, 154122; b) TPSSh: J. Tao, J. P. Perdew, V. N. Staroverov, G. E. Scuseria, *Phys. Rev. Lett.* **2003**, *91*, 146401; V. N. Staroverov, G. E. Scuseria, J. Tao, J. P. Perdew, *J. Chem. Phys.* **2003**, *119*, 12129-12137; Erratum: *J. Chem. Phys.* **2004**, *121*, 11507-11507; c) CPCM: J. Tomasi, B. Mennucci, R. Cammi, *Chem. Rev.* **2005**, *105*, 2999-3094; d) def2-TZVP: F. Weigend, R. Ahlrichs, *Phys. Chem. Chem. Phys.* **2005**, *7*, 3297-3305.
[32] G. Knizia, *J. Chem. Theory Comput.* **2013**, *9*, 4834-4843.
[33] NBO 6.0. E. D. Glendening, J. K. Badenhoop, A. E. Reed, J. E. Carpenter, J. A. Bohmann, C. M. Morales, C. R. Landis, F. Weinhold (Theoretical Chemistry Institute, University of Wisconsin, Madison, WI, 2013); http://nbo6.chem.wisc.edu/
[34] T. Lu, Q. Chen, *Chemistry–Methods* **2021**, *1*, 231-239.
[35] a) C. F.-W. LU Tian, *Acta Phys. -Chim. Sin.* **2011**, *27*, 2786-2792; b) A. Savin, O. Jepsen, J. Flad, O. K. Andersen, H. Preuss, H. G. von Schnering, *Angew. Chem. Int. Ed. Engl.* **1992**, *31*, 187-188; c) A. D. Becke, K. E. Edgecombe, *J. Chem. Phys.* **1990**, *92*, 5397-5403.
[36] H. Jacobsen, Can. *J. Chem*. **2008**, *86*, 695-702.
[37] F. Abugideiri, G. A. Brewer, J. U. Desai,f J. C. Gordon, R. Poli, *Inorg. Chem.* **1994**, *33*, 3745-3751.

## 4.5 Supporting information

### General procedures

All manipulations were carried out under an inert atmosphere of dried nitrogen or argon using standard Schlenk and glove box techniques. Solvents were dried using a MB SPS-800 device of the company MBRAUN. Deuterated solvents were freshly distilled under Argon from $CaH_2$ ($CD_2Cl_2$) and from Na/K alloy ($C_6D_6$).

IR spectra were recorded on a Varian FTS-800 spectrometer.

NMR spectra were recorded on a Bruker Advance III 400 MHz NMR spectrometer. If not differently mentioned, the chemical shifts were measured at room temperature and given in ppm; they are referenced to TMS for $^1$H and 85% $H_3PO_4$ for $^{31}$P as external standard.

LIFDI-MS spectra (LIFDI = liquid injection field desorption ionization) were measured on a JEOL AccuTOF GCX. ESI-MS spectra (ESI = Electrospray ionization) were measured on an Agilent Q-TOF 6540 UHD. Elemental Analysis (CHN) was determined using a Vario micro cube instrument. The X-Band EPR measurements were carried out with a MiniScope MS400 device with a frequency of 9.44GHz and a rectangular resonator TE102 of the company Magnettech GmbH.

The compound [(Cp*Mo)$_2$(μ,η$^6$:η$^6$-P$_6$)] (**1**) was synthesized according to literature procedure.[1]

Phosphorous (V) chlorine was purchased from abcr, Phosphorous (V) bromine (95%) from Alfa Aesar, Bromine from ACROS Organics and Iodine from Sigma-Aldrich and they all were used as received without any further purifications.

**Synthesis of [(Cp*Mo)$_2$(μ,η$^3$:η$^3$-P$_3$)(μ,η$^1$:η$^1$ η$^1$: η$^1$:-P$_3$I$_3$)][I$_3$] (2-I$_3$)**

[(Cp*Mo)$_2$(μ,η$^6$:η$^6$-P$_6$)] (**1**) (20 mg, 0.031 mmol, 1 equiv.) is dissolved in 10 mL of $CH_2Cl_2$. To this solution, a solution of $I_2$ (24 mg, 0.186 mmol, 6 equiv.) in 10 mL of $CH_2Cl_2$ is added. A change in colour from bright red to dark red/brown is immediately observed. The solution is stirred for 1 hour, then is filtered over celite. The resulting dark red solution is layered with 50 mL of pentane and stored at room temperature. After a few days, [(Cp*Mo)$_2$(μ,η$^3$:η$^3$-P$_3$)(μ,η$^1$: η$^1$ η$^1$ η$^1$-P$_3$I$_3$)][I$_3$] (**2-I$_3$**) crystallized as clear orange plates, suitable for X-Ray analysis.

Yield **2-I$_3$**: 17 mg crystals (0.012 mmol, 54%)

Yield **2-I$_3$** powder (54%)

**$^1$H NMR** (400 MHz, $CD_2Cl_2$, 300K): δ [ppm] =2.09 (s, 10 H, $C_5(CH_3)_5$)

**$^{31}P\{^1H\}$ NMR** (162 MHz, $C_6D_6$ capillary/$CH_2Cl_2$, 300K): AMM'OO'X spin system. δ [ppm] = $\delta_A$ = 379.6 (t, 1 P), $\delta_M = \delta_{M'}$ = 349.3 (d, 2 P), $\delta_O = \delta_{O'}$ = 4.6 (m, 2 P), $\delta_X$ = -327.4 (m, 1 P). For coupling constants see Table S1.

**ESI-MS** ($CH_2Cl_2$): cation mode: *m/z* = 1028.60 (100%, [**2**$^+$])

**EA** calculated for $C_{20}H_{30}Mo_2P_6I_6$ (1413.3 g·mol$^{-1}$): C:17.04, H:2.15; found [%]: C: 17.30, H: 2.14

**Synthesis of $[(Cp^*Mo)_2(\mu,\eta^4{:}\eta^4\text{-}P_4)(\mu\text{-}PI_2)][I_3]$ (3)**

$[(Cp^*Mo)_2(\mu,\eta^6{:}\eta^6\text{-}P_6)]$ (**1**) (200 mg, 0.309 mmol, 1 equiv.) is dissolved in 25 mL of $CH_2Cl_2$. To this solution, a solution of $I_2$ (235 mg, 0.927 mmol, 3 equiv.) in 30 mL of $CH_2Cl_2$ is added. A change in colour from bright red to dark red/brown is immediately observed. The solution is stirred for 20 minutes and then the solvent removed *in vacuo*. The red/purple precipitate is washed with 10 mL of pentane and a red solution is removed with a cannula. The remaining precipitate is dissolved in 20 mL of $CH_2Cl_2$ and layered with 50 mL of toluene. $[(Cp^*Mo)_2(\mu,\eta^4{:}\eta^4\text{-}P_4)(\mu\text{-}PI_2)][I_3]$ (**3**) crystallized as metallic dark black block crystals, suitable for X-Ray analysis, within a few days.
Yield **3**: 10 mg (0.008 mmol, 2%)

**X-band EPR** (r.t, liquid) $g_{iso}$ = 1.974 (cf. EPR spectra).

**ESI-MS** ($CH_2Cl_2$): cation mode: *m/z* = 870.73 (72.9%, [**3**$^+$])

**EA** calculated for $C_{20}H_{30}Mo_2P_5I_5$ (1251.76 g·mol$^{-1}$): C:19.19, H:2.42; found [%]: C:18.42, H:2.13

**Synthesis of $[(Cp^*Mo)_2(\mu,\eta^3{:}\eta^3\text{-}P_3)(\mu\text{-}Br)_2][Cp^*MoBr_4]$ (4)**

$PBr_5$ (800 mg, 1.854 mmol, 6 equiv.) in 25 mL of $CH_2Cl_2$ is added to a stirred solution of $[(Cp^*Mo)_2(\mu,\eta^6{:}\eta^6\text{-}P_6)]$ (**1**) (200 mg, 0.309 mmol, 1 equiv.) in $CH_2Cl_2$ at -40°C .The colour of the reaction mixture turned from bright red to dark brown within a few seconds. The solution is stirred for 40 minutes allowing the temperature to rise slowly (final T = -20°C) and then the solvent is removed *in vacuo*. The green/brown residue was dissolved in 10 mL of $CH_2Cl_2$ and reprecipitated adding 30 mL of cold pentane. The obtained olive-green precipitate was dissolved in 15 mL of thf and layered by 30 mL of toluene. After a few days, **4** can be obtained in form of metallic red plates.
Yield **4**: 15 mg (0.012 mmol, 2%)

**$^1H$ NMR** (400 MHz, $CD_2Cl_2$, 300K): δ [ppm] = 2.06 (s, 10 H, $([\{C_5(CH_3)_5)Mo\}_2(P_3Br_2)]^+$), -19.04 (br. s, 5 H, $([C_5(CH_3)_5)MoBr_4]^-$)[2]

**$^{31}$P{$^1$H} NMR** (162 MHz, $CD_2Cl_2$, 300K): δ [ppm] = AA'X spin system δ [ppm]: $\delta_A = \delta_{A'}$ = 434.1 (d, 2P), $\delta_X$ = -62.6 (t, 1P). For coupling constants see Table S2.

**ESI-MS** ($CH_2Cl_2$): cation mode: *m/z* = 714.85 (100%, [**4**$^+$])

**EA** calculated for $C_{30}H_{45}Mo_3P_3Br_6(C_7H_8)_{0.5}$ (1311.97 g·mol$^{-1}$): C: 30.67, H: 3.76; found [%]: C: 30.40, H: 3.07

**Synthesis of [(Cp*MoBr)$_2$(μ,η$^3$:η$^3$-P$_3$)(μ,η$^1$:η$^1$-P$_2$Br$_3$)] (5)**

$PBr_5$ (400 mg, 0.926 mmol, 6 equiv.) in 15 mL of $CH_2Cl_2$ is added to a stirred solution of [(Cp*Mo)$_2$(μ,η$^6$:η$^6$-P$_6$)] (**1**) (100 mg, 0.154 mmol, 1 equiv.) in $CH_2Cl_2$ at -40°C. The colour of the reaction mixture turned from bright red to dark brown within a few seconds. The solution is stirred for 40 minutes allowing the temperature to rise slowly (final T = -20°C) and then the solvent is removed *in vacuo*. The green/brown residue was dissolved in 10 mL of $CH_2Cl_2$ and reprecipitated adding 30 mL of cold pentane. While the crystallization of the residue afforded **4**, the slow warm up of the mother liquor afforded dark red needles as crystals of **5**.

Yield **5**: 10 mg (0.010 mmol, 17%)

**$^1$H NMR** (400 MHz, $CD_2Cl_2$, 300K): δ [ppm] = 1.94 (s, 10 H, $C_5(CH_3)_5$)

**$^{31}$P{$^1$H} NMR** (162 MHz, $CD_2Cl_2$, 300K): ADHKX spin system δ [ppm] = $\delta_A$ = 443.1 (dd, 1 P), $\delta_D$ = 434.9 (m, 1 P), $\delta_H$ = 291.8 ppm (ddd, 1P), $\delta_K$ = 210.5 (dd, 1 P) $\delta_X$ = -285.6 (dd, 1 P). For coupling constants see Table S3.

**EI-MS** ($CH_2Cl_2$): cation mode: *m/z* = 683.83 (17.7%, [**5**$^+$]- $P_3Br_3$), 601.9 (10.3%, [**5**$^+$]- $P_3Br_4$), 584.9 (2.9%, [**5**$^+$]- $PBr_5$)

**EA** calculated for $C_{20}H_{30}Mo_2P_5Br_5(C_5H_{12})$ (1088.91 g·mol$^{-1}$): C: 27.58, H: 3.89; found [%]: C: 27.16, H: 3.06

**Synthesis of [(Cp*Mo)$_2$(μ-PBr$_2$)(μ-PHBr)(μ-Br)$_2$] (6)**

$PBr_5$ (997 mg, 2.316 mmol, 6 equiv.) in 25 mL of $CH_2Cl_2$ is added to a stirred solution of [(Cp*Mo)$_2$(μ,η$^6$:η$^6$-P$_6$)] (**1**) (250 mg, 0.386 mmol, 1 equiv.) in $CH_2Cl_2$ at -40°C .The colour of the reaction mixture turned from bright red to dark brown within a few seconds. The solution is stirred for two and a half hours allowing the temperature to rise slowly (final T = -10°C) and then the solvent is removed *in vacuo*. The precipitate is washed with pentane and toluene (fractions filtered off) and the remaining residue is concentrated in 10 mL of $CH_2Cl_2$ and reprecipitated overnight after the addition of 30 mL of cold hexane. The mother liquors are stored at -30°C allowing the crystallization of **6** as dark red blocks.

Yield **6**: calculated via NMR (9%)

**$^1$H NMR** (400 MHz, $CD_2Cl_2$, 300K): δ [ppm] = 6.67 (dd, 1H, $^1J_{PH}$ = 444 Hz, $^3J_{PH}$ = 5 Hz, P*H*), 2.11 (s, 10H, $C_5(CH_3)_5$).

**$^{31}$P{$^1$H} NMR** (162 MHz, $CD_2Cl_2$, 300K): AM spin system. δ [ppm] = $\delta_A$ = 307.1 (d, 1 P), $\delta_M$ = 230.2 (d, 1 P). For coupling constants see Table S4.

**$^{31}$P NMR** (162 MHz, $C_6D_6$ capillary in $CH_2Cl_2$, 300 K): AM spin system. δ [ppm] = $\delta_A$ = 307.1 (d, 1 P), $\delta_M$ = 223.94 (dd, 1P, $^1J_{PH}$ = 444 Hz).

**EI-MS** ($CH_2Cl_2$): cation mode: *m/z* = 731.89 (6.6%, [**6**$^+$] - $PBr_2$, - H), 683.93 (85.7%, [**6**$^+$] - 3 Br, - H), 601.99 (46.1%, [**6**$^+$] - 4 Br, - H)

**EA** calculated for $C_{20}H_{31}Mo_2P_2Br_5$ ($C_6H_{14}$) (1010.95 g·mol$^{-1}$): C: 30.89, H: 4.49; found [%]: C: 31.21, H: 4.39

**Synthesis of [(Cp*Mo)$_2$(μ,η$^3$:η$^3$-P$_3$)(μ-PCl$_2$)$_2$][PCl$_6$] (8)**

[(Cp*Mo)$_2$(μ,η$^6$:η$^6$-P$_6$)] (**1**) (200 mg, 0.309 mmol, 1 equiv.) and $PCl_5$ (386 mg, 1.854 mmol, 6 equiv.) are weighted together and dissolved in 20 mL of $CH_2Cl_2$ at -80°C (all the steps of this procedure are performed at -80°C, when this is not the case, it will be specified). The reaction mixture turned from bright red to bright green within a few seconds and is stirred for 10 minutes. Afterwards, 60 mL of hexane are slowly added to favour the precipitate formation and the reaction is stirred for additionally 30 minutes. The colourless solution is decanted off and the resulting olive-green precipitate is dissolved in 20 mL of $CH_2Cl_2$ and layered with 40 mL of hexane. The system is let warm up to approximately -60°C and when the green solution of $CH_2Cl_2$ turned bright orange, is stored at -80°C. After a few weeks, **8** crystallized as clear red blocks, suitable for X-Ray analysis.
Yield **8**: 228 mg (0.227 mmol, 74%)

**$^1$H NMR** (400 MHz, $CD_2Cl_2$, 233K): δ [ppm] = 2.23 ppm (s, 10H, $C_5(CH_3)_5$)

**$^{31}$P{$^1$H} NMR** (162 MHz, $CD_2Cl_2$, 233K): AA'MM'X spin system. δ [ppm]: $\delta_A$ = 299.9 (m, 1 P ), $\delta_{A'}$ = 299.8 (m, 1 P) $\delta_M$= 245.0 (m, 1 P) $\delta_{M'}$ = 244.9 (m, 1 P), $\delta_X$ = -230.3 (tt, 1 P), δ = -296.2 (s, 1 P, [*P*Cl$_6$]$^-$). For coupling constants see Table S6.

**ESI-MS** ($CH_2Cl_2$): cation mode: *m/z* = 758.81 (100%, [**8**$^+$])

**EA** due to the high sensitivity of **8** towards temperature, it was not possible to obtain an exact elemental analysis.

**Synthesis of [(Cp*Mo)$_2$(μ-PCl$_2$)$_2$(μ-Cl)$_2$] (9)**

[(Cp*Mo)$_2$(μ,η$^6$:η$^6$-P$_6$)] (**1**) (250 mg, 0.386 mmol, 1 equiv.) and $PCl_5$ (482 mg, 2.316 mmol, 6 equiv.) are weighted together and dissolved in 30 mL of $CH_2Cl_2$ at -40°C The reaction

mixture turned from bright red to dark brown within a few seconds and is stirred for 10 minutes. Afterwards, it is stirred for additional two hours at room temperature, then the solvent is removed *in vacuo*. The resulting dark red precipitate is washed with 2 x 10 mL of pentane and then dissolved in 15 mL of toluene, filtered, and layered with 30 mL of pentane. After a few days, **9** crystallized as dark red prisms, suitable for X-Ray analysis.
Yield **9**: 25 mg (0.034 mmol, 3 %)

**$^1$H NMR** (400 MHz, $CD_2Cl_2$, 300K): δ [ppm] = 2.07 (s, 10H, $C_5(CH_3)_5$)

**$^{31}$P{$^1$H} NMR** (162 MHz, $CD_2Cl_2$, 300K): δ [ppm] = 317.19 (s, 2 P)

**EI-MS** ($CH_2Cl_2$): cation mode: *m/z* = 737.86 (8.3%, [**9**$^+$])

**EA** calculated for $C_{20}H_{30}Mo_2P_2Cl_6$ (737.04 g·mol$^{-1}$): C:32.59, H: 4.10; found [%]: C:33.15, H:3.87

**Synthesis of [(Cp*MoCl)$_2$(μ,η$^3$:η$^3$-P$_3$)(μ-PCl$_2$)] (10)**
$PCl_5$ (482 mg, 2.316 mmol, 6 equiv.) in 20 mL of $CH_2Cl_2$ is added to a stirred solution of [(Cp*Mo)$_2$(μ,η$^6$:η$^6$-P$_6$)] (**1**) (250 mg, 0.386 mmol, 1 equiv.) in $CH_2Cl_2$ at -40°C. The colour of the reaction mixture turned from bright red to bright green, brown and finally red within a minute and it is stirred for 1 hour. Afterwards, it is stirred for additionally 10 minutes at room temperature, allowing the colour to change from brick red to berry red, then solvent is removed *in vacuo*. The resulting purple precipitate is washed with 2 x 10 mL of pentane and then dissolved in 15 mL of toluene, filtered, and layered with 30 mL of pentane. The solution is stored at -30°C and after a few days **10** crystallized as clear green plates, suitable for X-Ray analysis (when the dark berry red mother liquor was concentrated to half of its volume and put back at -30°C, crystals of **9** formed within 2 days).
Yield **10**: calculated via NMR (4 %)

**$^1$H NMR** (400 MHz, $CD_2Cl_2$, 300K): δ [ppm] = 1.92 (s, 10H, $C_5(CH_3)_5$)

**$^{31}$P{$^1$H} NMR** (162 MHz, $CD_2Cl_2$, 300K): δ [ppm] = ACEX spin system δ [ppm]: $\delta_A$ = 449.9 (m, 1P), $\delta_C$ = 415.8 (ddd, 1P), $\delta_E$ = 311.1 (m, 1P), $\delta_X$ = -249.6 (tt, 1P). For coupling constants see Table S7.

**EI-MS** ($C_7H_8$): cation mode: *m/z* = 555.95 (2.9%, [**10**$^+$] - $PCl_4$)

**EA** calculated for $C_{20}H_{30}Mo_2P_4Cl_4(C_7H_8)$ (820.22 g·mol$^{-1}$): C: 39.54, H: 4.67; found [%]: C: 40.74, H:4.08

**Synthesis of [(Cp*Mo)$_2$(μ,η$^4$:η$^4$-P$_4$) (μ-PCl$_2$)][Cp*MoCl$_4$] (11)**

$PCl_5$ (96 mg, 0.462 mmol, 6 equiv.) in 10 mL of $CH_2Cl_2$ is added to a stirred solution of [(Cp*Mo)$_2$(μ,η$^6$:η$^6$-P$_6$)] (**1**) (50 mg, 0.077 mmol, 1 equiv.) in $CH_2Cl_2$ at -80°C (all the steps of this procedure are performed at -80°C, when this is not the case, it will be specified). The reaction mixture turned from bright red to bright green within a few seconds and is stirred for 15 minutes. Afterwards, 60 mL of hexane are slowly added to favour the precipitate formation and the reaction is stirred for additionally 30 minutes. The colourless solution is decanted off and the resulting olive-green precipitate is dissolved in 10 mL of $CH_2Cl_2$ and 0.5 mL of pentane, then it is stored at -80°C for a few weeks. After that time, it is layered with 20 mL of pentane and stored at room temperature. After two days, **11** crystallized as metallic dark red blocks, suitable for X-Ray analysis.

Yield **11**: 10 mg (0.009 mmol, 4 %)

**$^1$H NMR** (400 MHz, $CD_2Cl_2$, 300K): δ [ppm] = 2.45 (s, 10H, $C_5(CH_3)_5$, -13.77 (br. s, 5H, $C_5(CH_3)_5$, $\omega_{1/2}$ = 170 Hz)[2]

Paramagnetic.

**ESI-MS** ($CH_2Cl_2$): cation mode: *m/z* = 688.85 (61.3%, [**11**$^+$])

**EA** calculated for $C_{30}H_{45}Cl_6Mo_3P_5 \cdot (C_7H_8)$ (g·mol$^{-1}$): C: 38.53, H:4.63; found [%]: C:38.53, H:4.39 (analysis obtained on a second sample, crystallized by toluene layered with pentane, which still contains traces of toluene)

**Synthesis of [(Cp*Mo)$_2$(μ,η$^4$:η$^4$-P$_4$)(μ-PCl$_2$)] (12)**

[(Cp*Mo)$_2$(μ,η$^6$:η$^6$-P$_6$)] (**1**) (100 mg, 0.154 mmol, 1 equiv.) and $PCl_5$ (96 mg, 0.463 mmol, 3 equiv.) are weighted together and dissolved in 20 mL of $CH_2Cl_2$. The reaction mixture turned from bright red to red/brown and to brown/green after 20 minutes. It is stirred at room temperature for a total of 35 minutes and then solvent is removed *in vacuo*. The resulting green precipitate is extracted with 10 mL of toluene and layered with 20 mL of pentane. After one week, **12** crystallized as metallic brown blocks, suited for X-Ray analysis.

Yield **12**: 8 mg (0.012 mmol, 10 %)

Paramagnetic.

**EI-MS** ($CH_2Cl_2$): cation mode: *m/z* = 617.90 (100%, [**12**$^+$] - $Cl_2$)

**EA** calculated for $C_{20}H_{30}Mo_2P_5Cl_2$ (688.15 g·mol$^{-1}$): C:34.91, H: 4.39; found [%]: C: 34.52, H: 3.73

## Selected NMR and EPR spectra

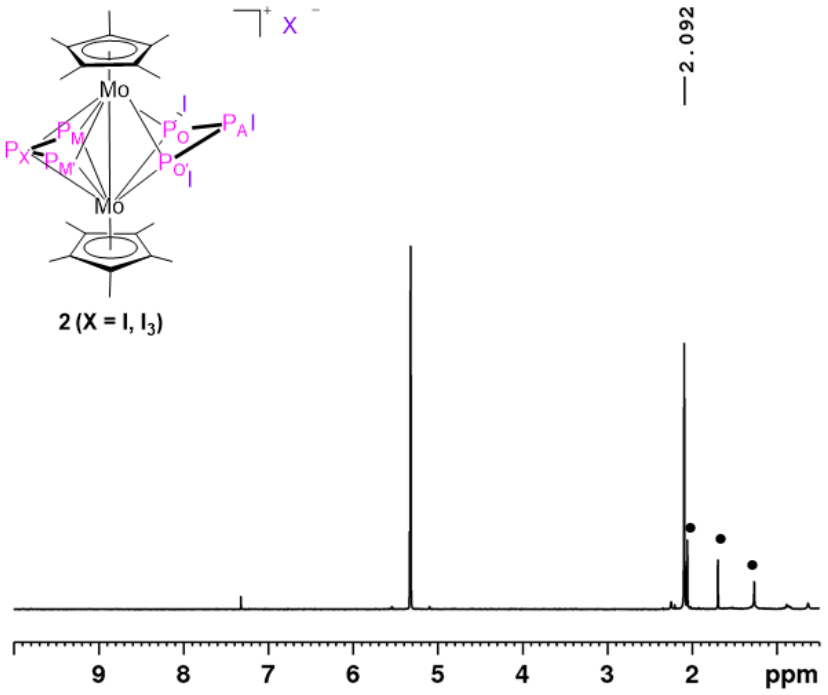


**Figure S 1.** $^1$H NMR spectrum of compound **2** ($CD_2Cl_2$, 300K), impurities are marked with ●.

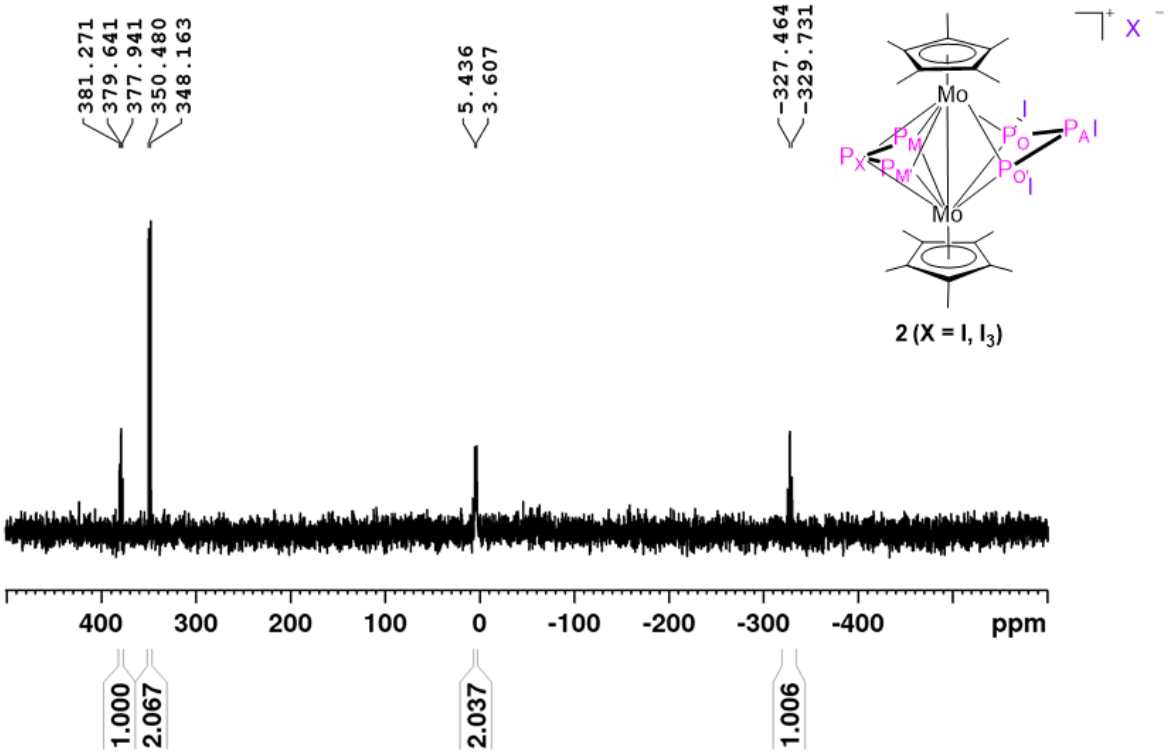


**Figure S 2.** $^{31}P\{^1H\}$ NMR spectrum of compound **2** ($C_6D_6$ capillary in $CH_2Cl_2$, 300 K).

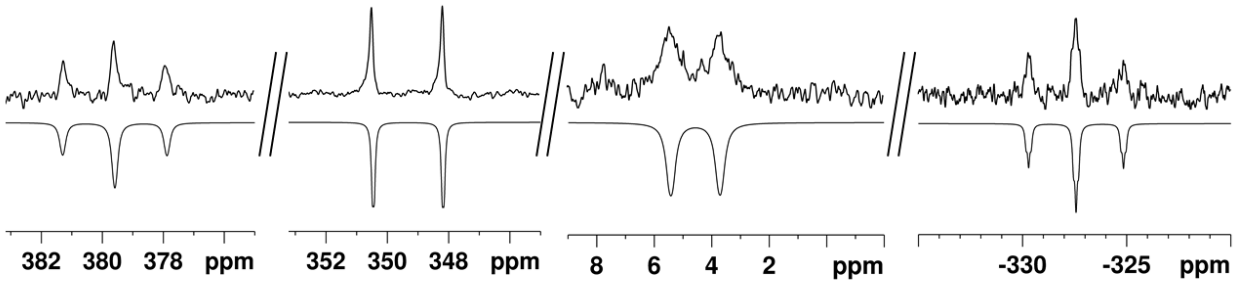


**Figure S 3.** Sections of the experimental (upwards) and simulated (downwards) $^{31}P\{^1H\}$ NMR spectrum of compound **2** (AMM'OO'X spin system).

**Table S 1.** Coupling constants of the AMM'OO'X spin system obtained from simulation.

| **δ (ppm)** | | **J (Hz)** | |
|---|---|---|---|
| **A** | 379.6 | $^1J_{AO}$ | 259.6 |
| | | $^1J_{AO'}$ | 283.1 |
| **MM'** | 349.3 | $^1J_{MX}$ | 364.7 |
| | | $^1J_{M'X}$ | 377.3 |
| **OO'** | 4.6 | $^2J_{AM}$ | 10.0 |
| | | $^2J_{AM'}$ | 11.9 |
| **X** | -327.4 | $^2J_{OX} = {}^2J_{O'X}$ | 20.0 |

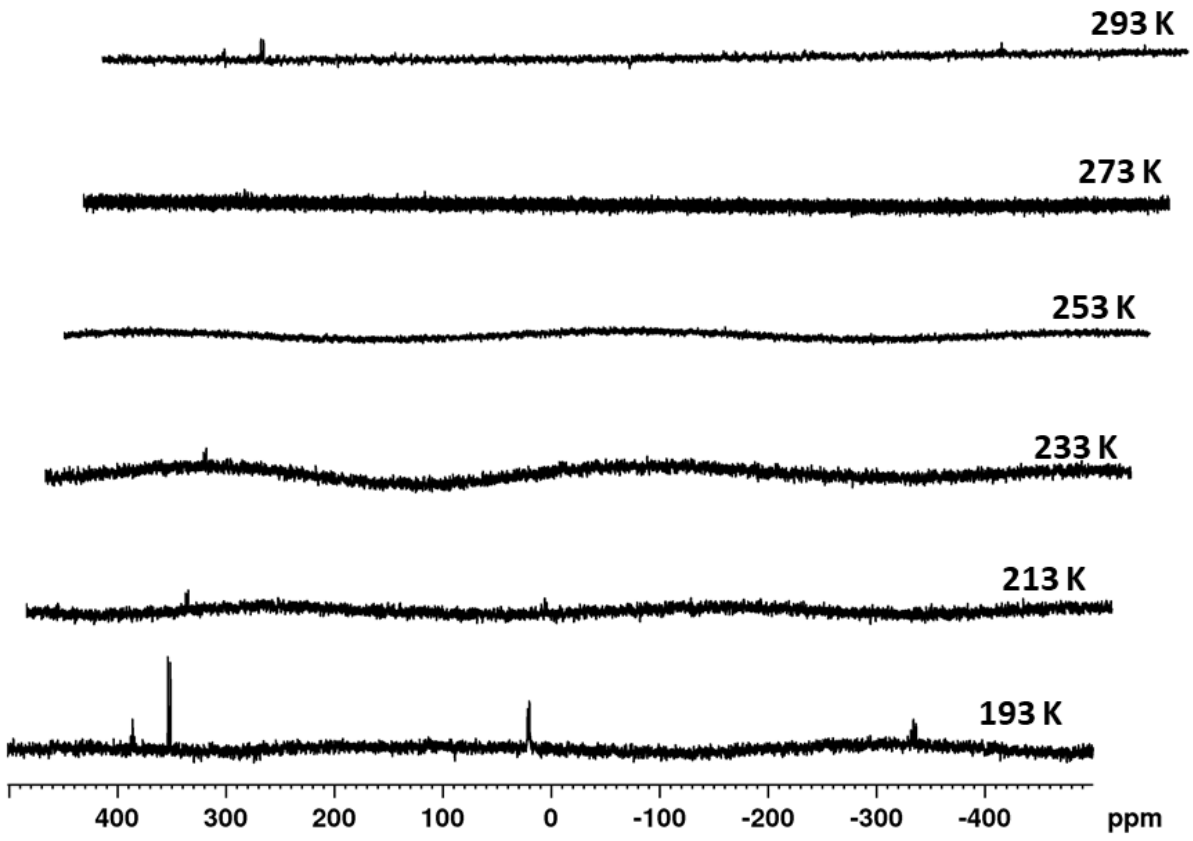


**Figure S 4.** VT-$^{31}$P{$^1$H} NMR spectra of the reaction solution of **1** (1 equiv.) with $I_2$ (6 equiv.) ($CD_2Cl_2$, from 193 K to 293 K).

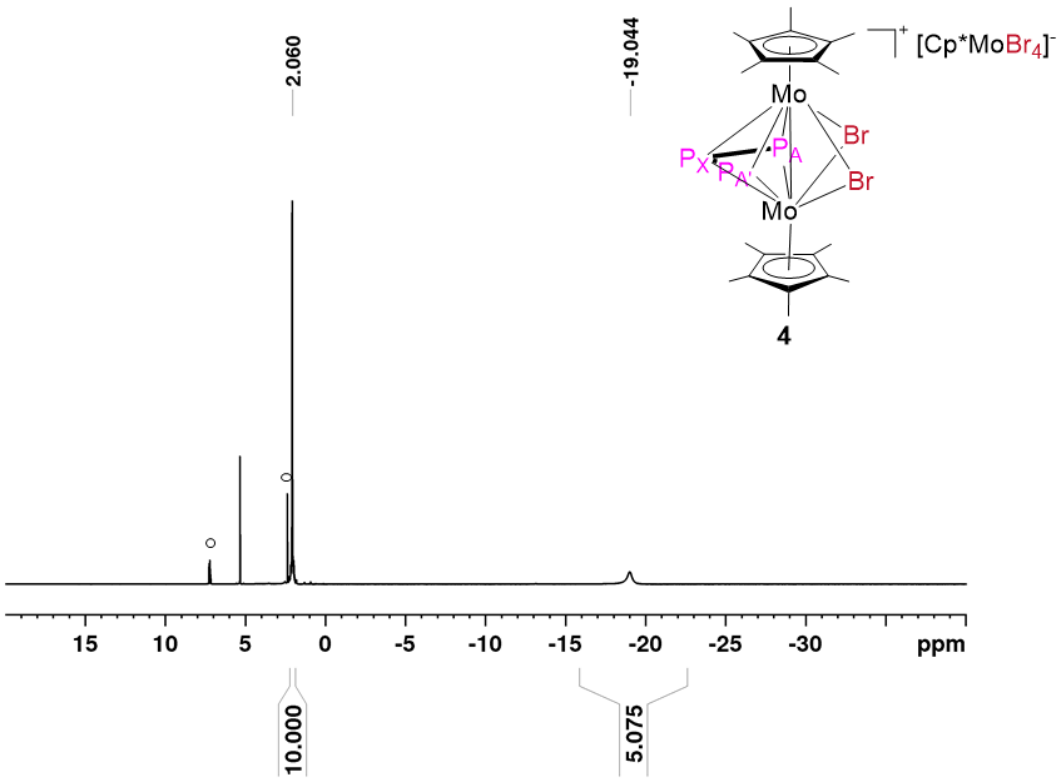


**Figure S 5.** $^1$H NMR spectrum of compound **4** ($CD_2Cl_2$, 300K), ° = residual toluene.

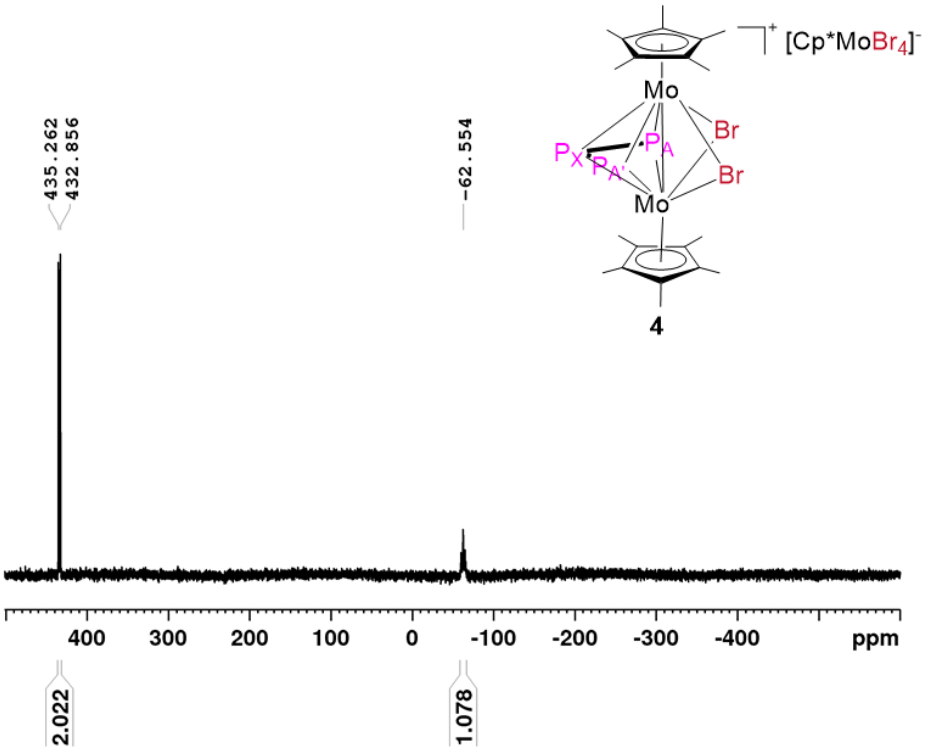


**Figure S 6.** $^{31}$P{$^1$H} NMR spectrum of compound **4** ($CD_2Cl_2$, 300K).

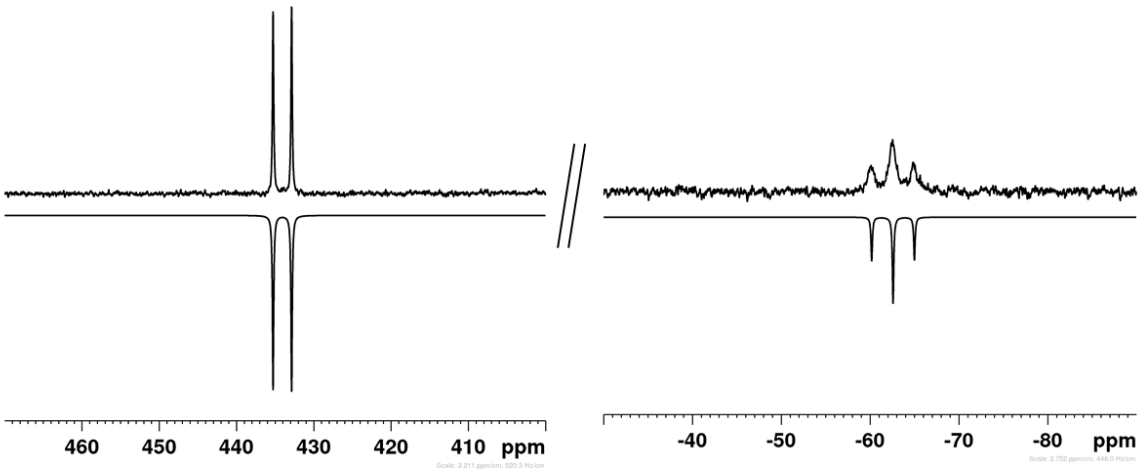


**Figure S 7.** Sections of the experimental (upwards) and simulated (downwards) $^{31}P\{^1H\}$ NMR spectrum of compound **4** ($A_2X$ spin system).

**Table S 2.** Coupling constants of the $A_2X$ spin system obtained from simulation.

| **δ (ppm)** | | **J (Hz)** | |
|---|---|---|---|
| **A** | 434.1 | $^1J_{AX}$ | 378.6 |
| | | $^1J_{A'X}$ | 391.6 |
| **X** | -62.6 | | |
| | | $^2J_{AA'}$ | 8.0 |

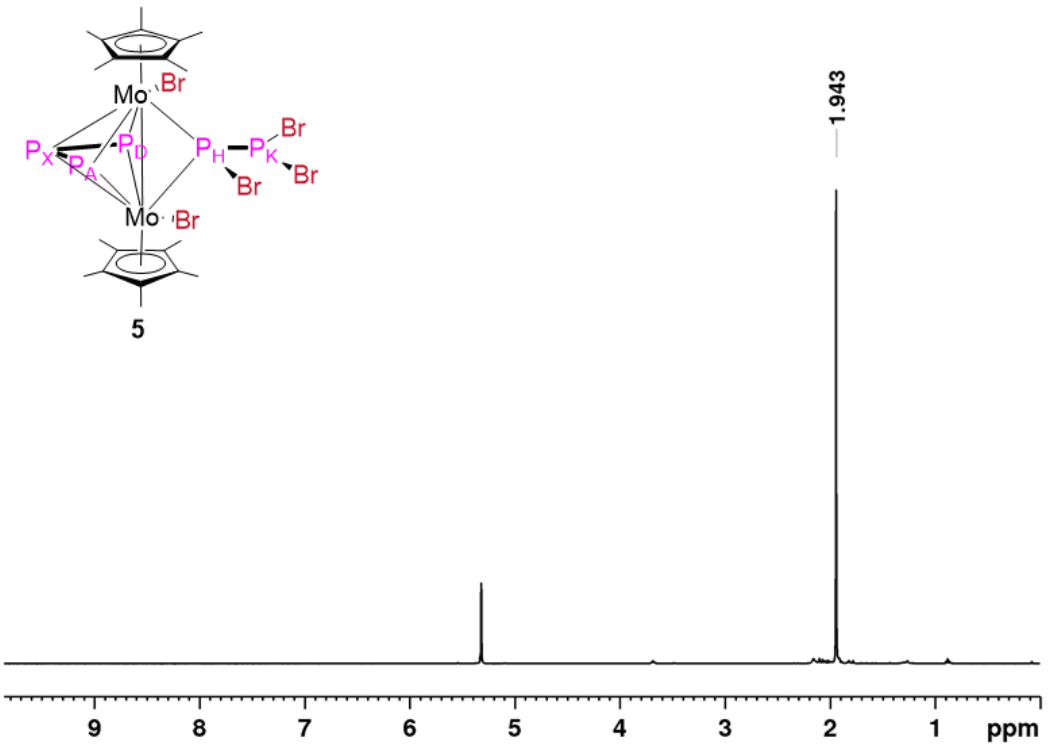


**Figure S 8.** $^1$H NMR spectrum of compound **5** ($CD_2Cl_2$, 300K).

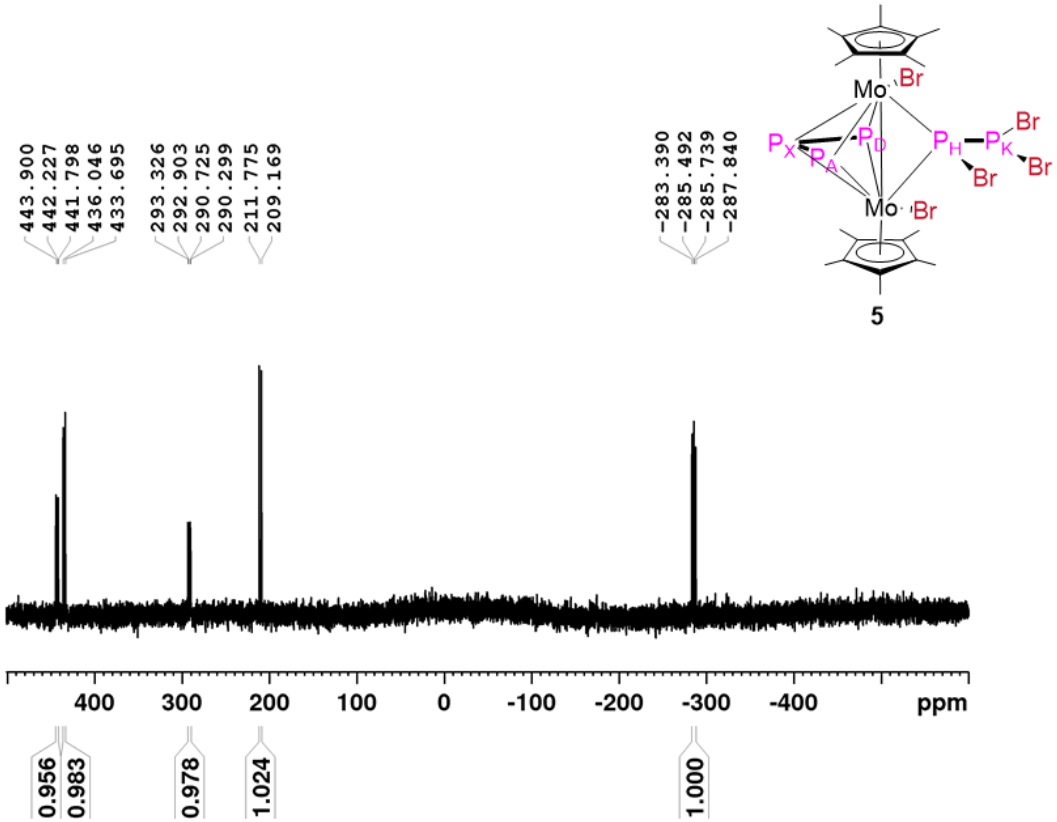


**Figure S 9.** $^{31}P\{^1H\}$ NMR spectrum of compound **5** ($CD_2Cl_2$, 300K).

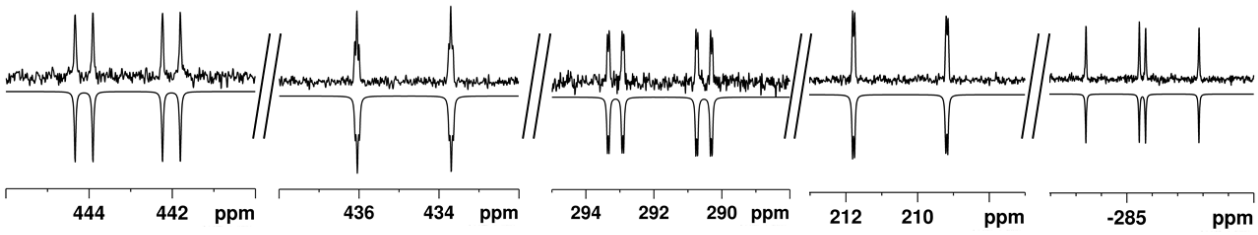


**Figure S 10.** Sections of the experimental (upwards) and simulated (downwards) $^{31}P\{^1H\}$ NMR spectrum of compound **5** (ADHKX spin system).

**Table S 3.** Coupling constants of the ADHKX spin system obtained from simulation.

| δ (ppm) | | J (Hz) | | | |
|---|---|---|---|---|---|
| **A** | 443.1 | $^1J_{AX}$ | 340.5 | $^2J_{AH}$ | 69.5 |
| **D** | 434.9 | $^1J_{DX}$ | 380.6 | $^2J_{DH}$ | 8.6 |
| **H** | 291.8 | | | | |
| **K** | 210.5 | $^1J_{HK}$ | 421.6 | $^2J_{DK}$ | 9.0 |
| **X** | -285.6 | | | | |

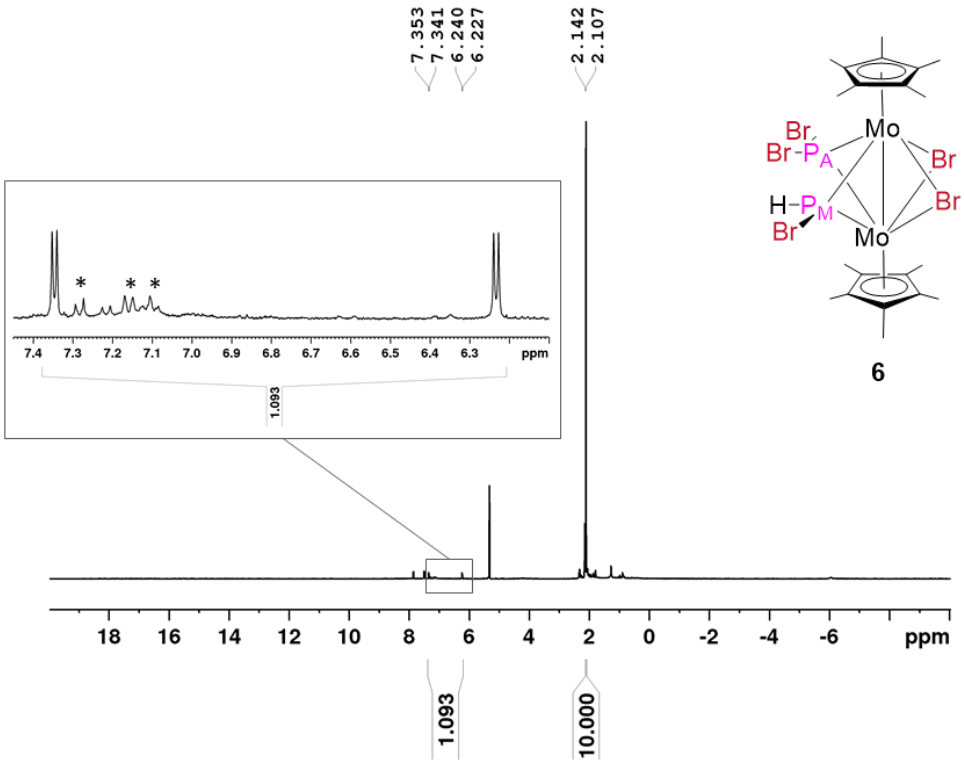


**Figure S 11.** $^1H$ NMR spectrum of compound **6** ($CD_2Cl_2$, 300K, $^1J_{PH}$ = 444 Hz, $^3J_{PH}$ = 5 Hz). Impurities are marked with *.

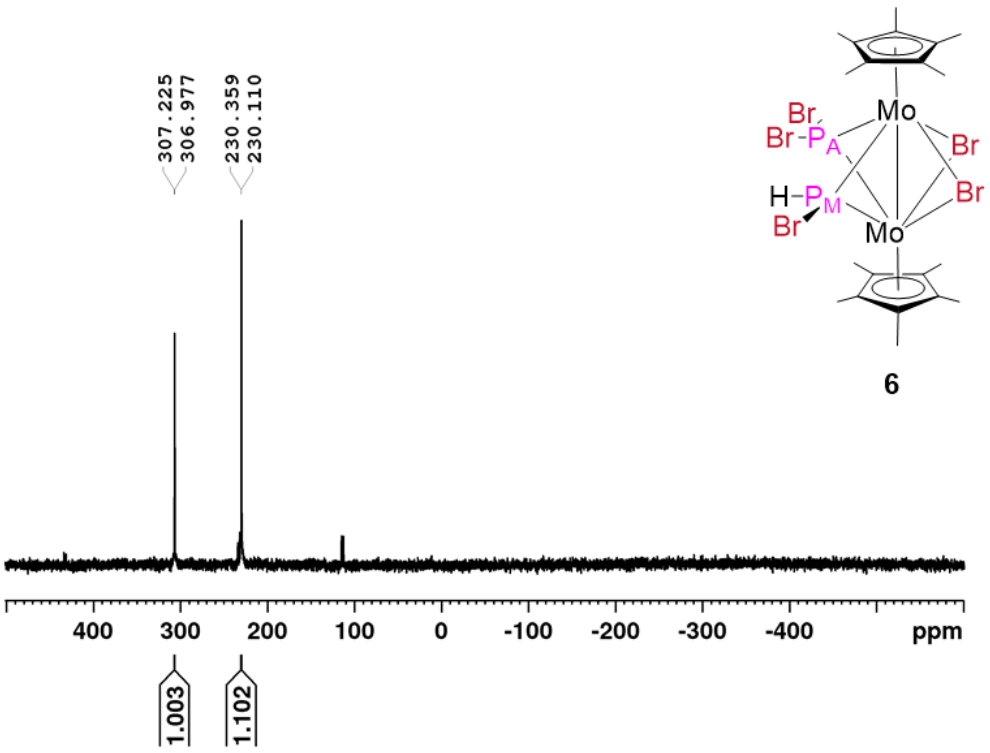


**Figure S 12.** $^{31}P\{^1H\}$ NMR spectrum of compound **6** ($CD_2Cl_2$, 300K, $^2J_{AM}$ = 38 Hz).

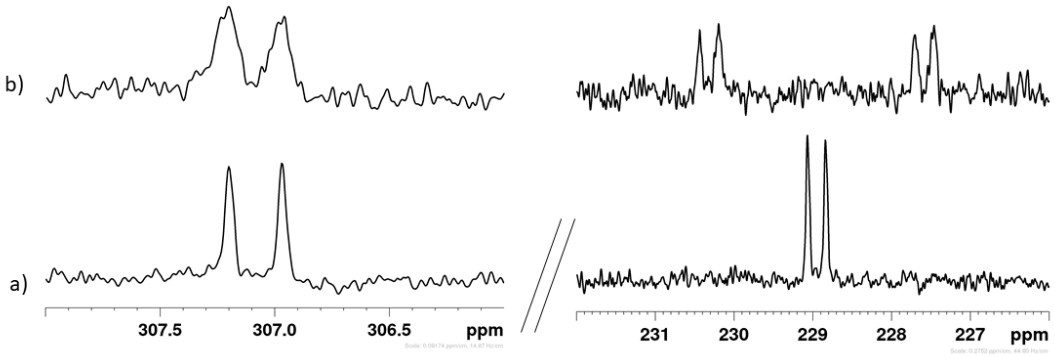


**Figure S 13.** a) Sections of $^{31}P\{^1H\}$ NMR spectrum of compound **6**; b) Sections of $^{31}P$ NMR spectrum of compound **6** ($CH_2Cl_2$ with $C_6D_6$ capillary, 300 K, $^2J_{AM}$ = 38 Hz, $^1J_{PH}$ = 444 Hz).

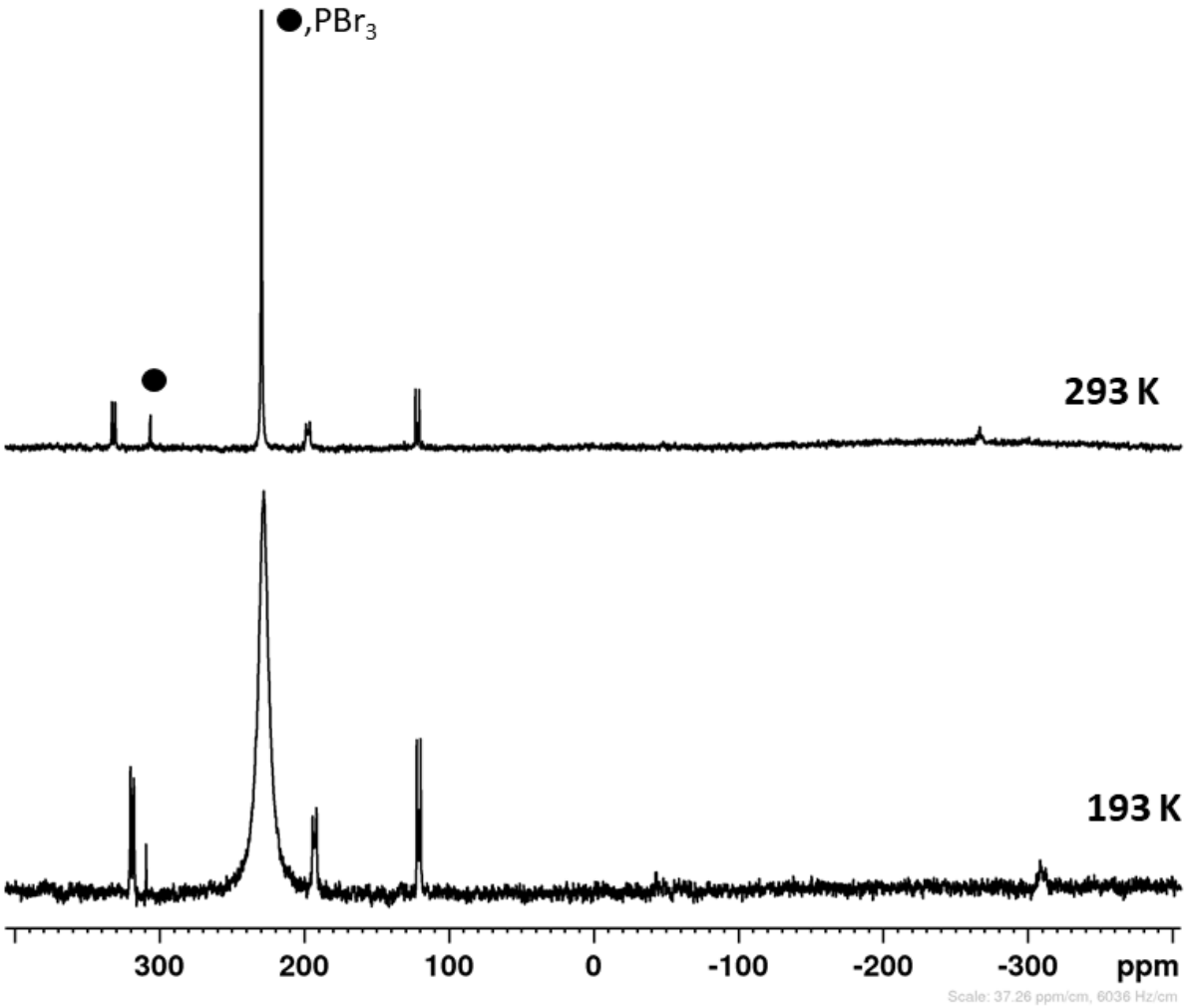


**Figure S 14.** VT-$^{31}$P{$^1$H} NMR spectra of the reaction solution of **1** (1 equiv.) with $PBr_5$ (6 equiv.) mixed together in the solid state ($CD_2Cl_2$, 193 K and 293 K). Signals of **6** are marked with the circles.

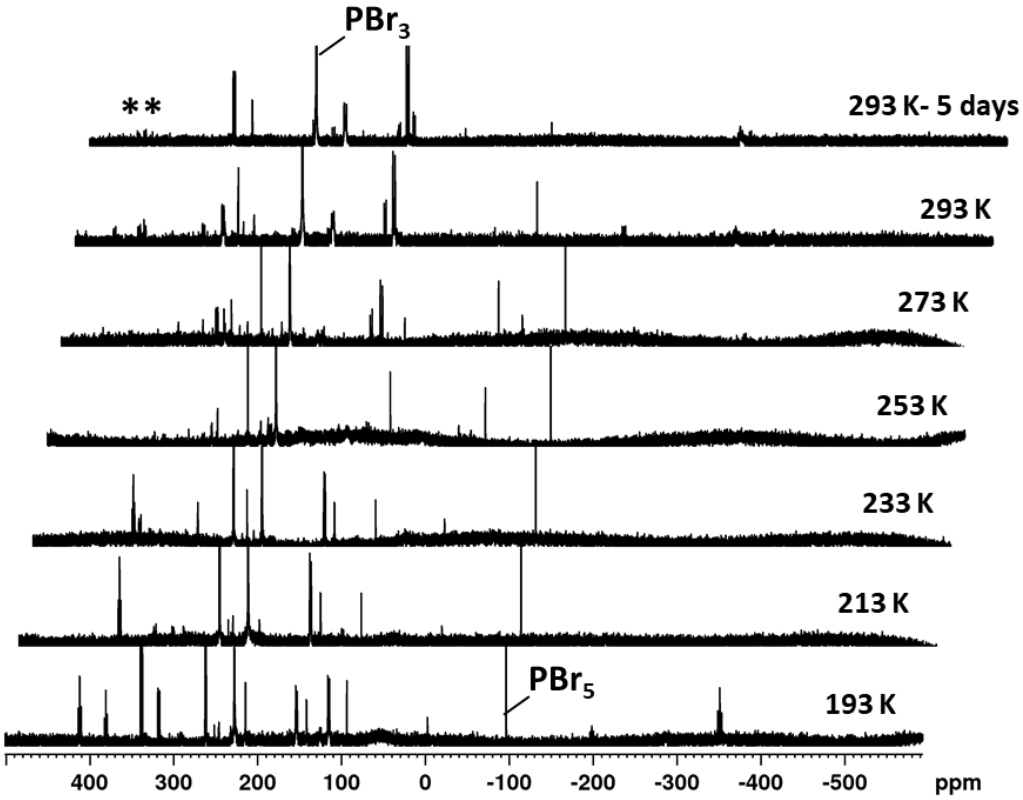


**Figure S 15.** VT-$^{31}$P{$^1$H} NMR spectra of the reaction between **1** (1 equiv.) and $PBr_5$ (6 equiv.) mixed as separated precooled solution ($CD_2Cl_2$, from 193 K to 293 K). Signals of **5** are (marked with *) are visible after five days.

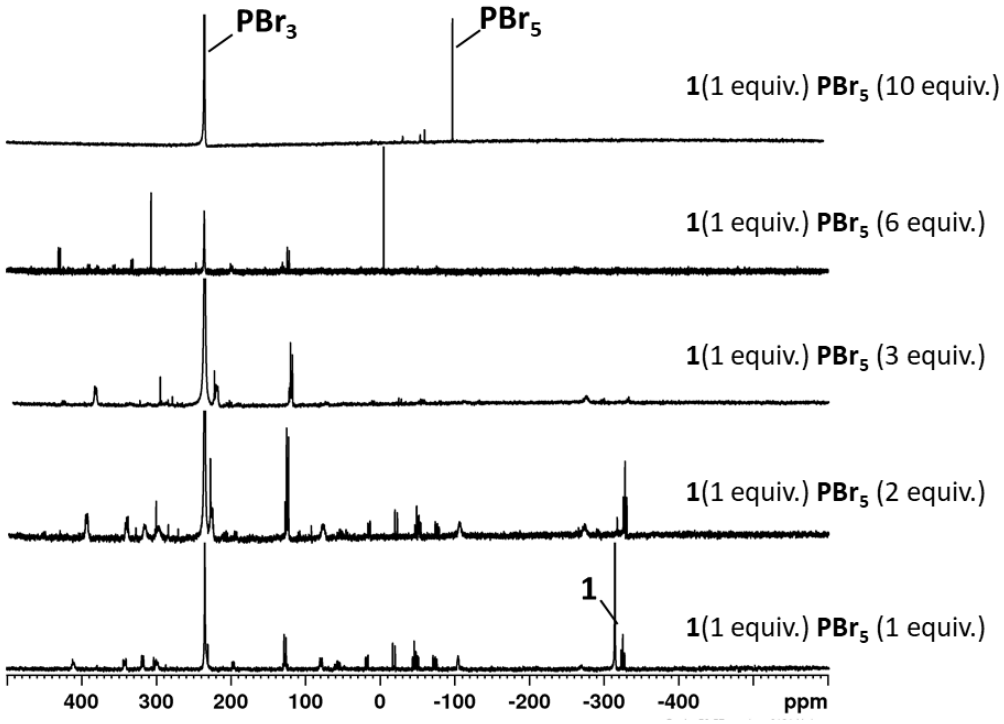


**Figure S 16.** $^{31}$P{$^1$H} NMR spectra of the reaction solution of **1** (1 equiv.) with increasing equiv. of $PBr_5$ ($CD_2Cl_2$, 300K).

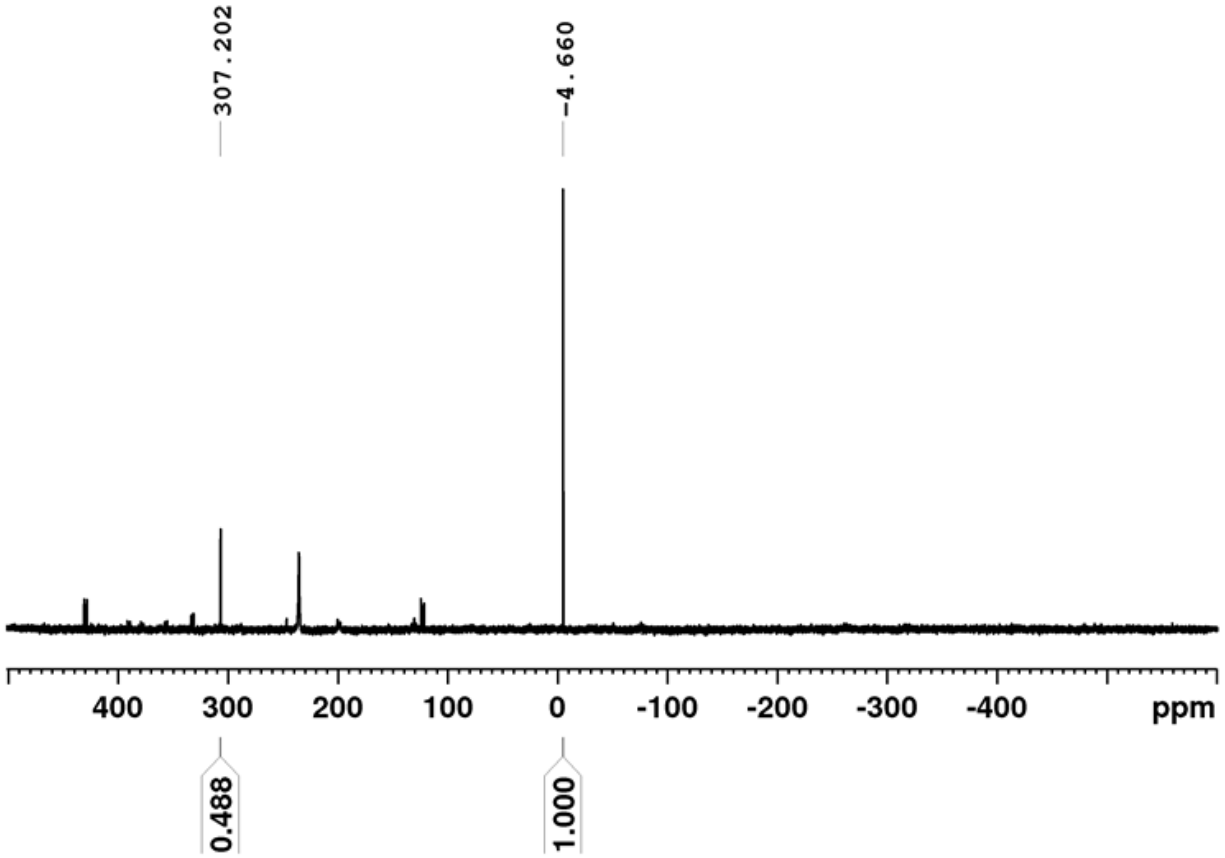


**Figure S 17.** $^{31}P\{^1H\}$ NMR spectrum of the reaction solution of **1** (1 equiv.) with $PBr_5$ (6 equiv.) ($CD_2Cl_2$, 300K, $PPh_3$ capillary as internal standard).

δ = -4.6 ppm = $PPh_3$ (Integration: 1.00)

δ = 307.2 ppm = **6** (Integration: 0.49)

mmol $PPh_3$ in the capillary = 0.016

mmol **6** in the NMR tube= (0.016*0.49) = 0.008

mmol **1** in the NMR tube =0.031

yield **3c** [%] = [0.008 mmol/(3*mmol **1**)]*100 = 9

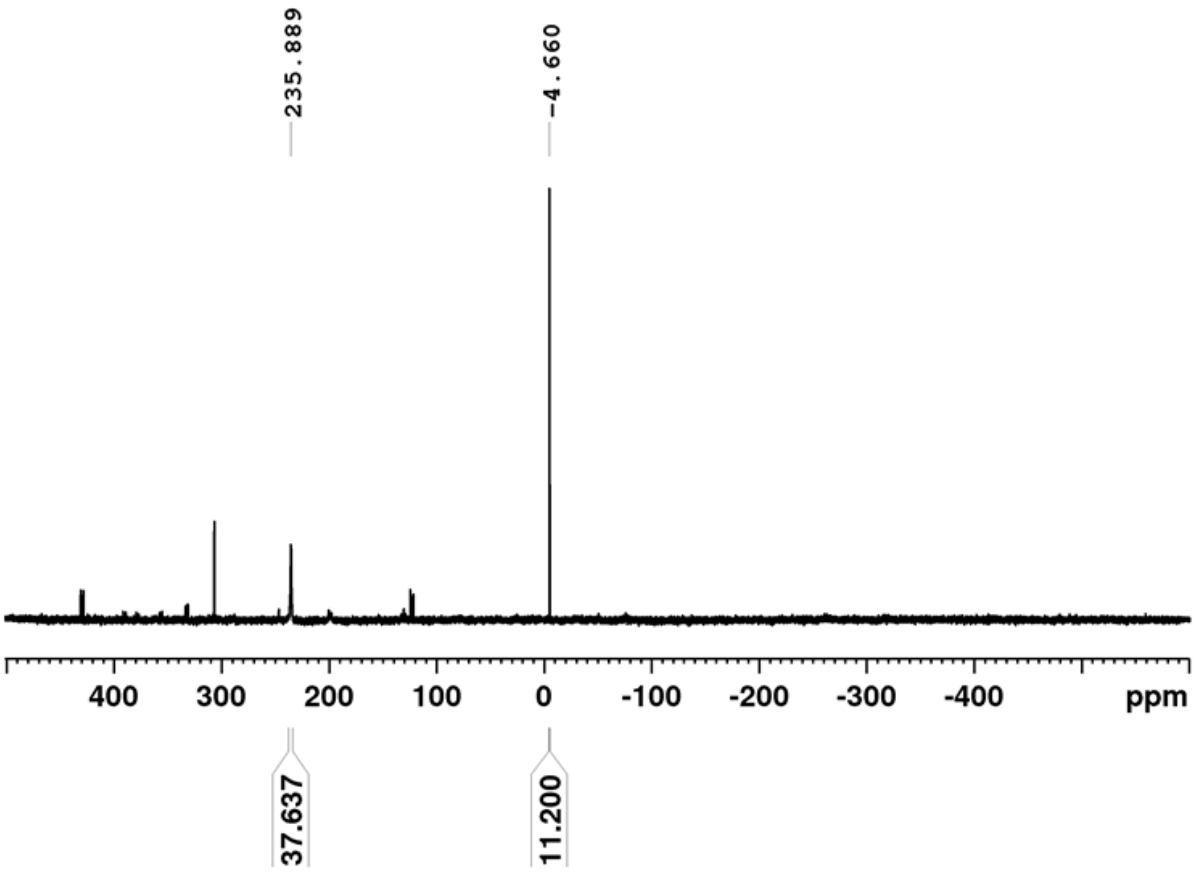


**Figure S 18.** $^{31}P\{^1H\}$ NMR spectrum of the reaction solution of **1** (1 equiv.) with $PBr_5$ (6 equiv.) ($CD_2Cl_2$, 300K, $PPh_3$ capillary as internal standard).

- δ = -4.6 ppm = $PPh_3$
- δ = 235.9 = $PBr_3$
- mmol $PPh_3$ in the capillary: 0.016
- mmol $PBr_5$ in the NMR tube: 0.179
- $\frac{PBr_5}{PPh_3} = \frac{0.179}{0.016}$ = 11.2
- Integration $PPh_3$ = 11.2
- Integration $PBr_3$ = 37.6
- 11.2 out of 37.6 (**30%**) equals the amount of $PBr_3$ coming from $PBr_5$
- (37.6–11.2) = 26.4 (**70%**) equals the amount of $PBr_3$ coming from **1**

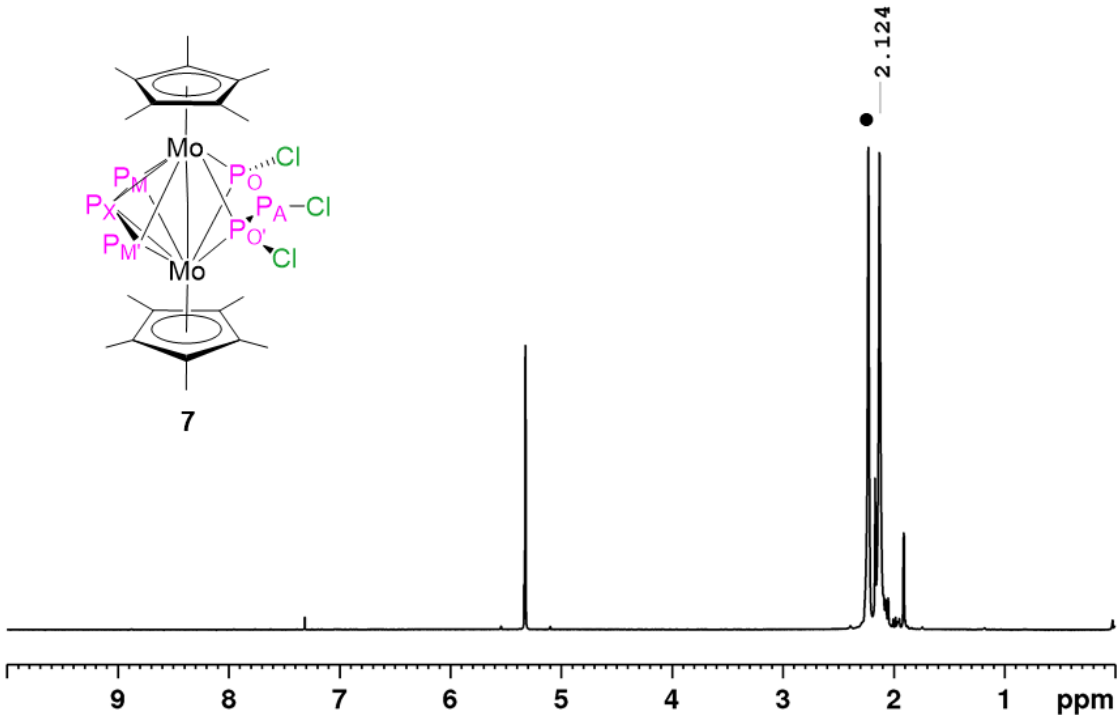


**Figure S 19.** $^1$H NMR spectrum of compound **7** ($CD_2Cl_2$, 193 K). The signal of compound **8** (●, δ = 2.22 ppm), which starts to form at that temperature, is already visible.

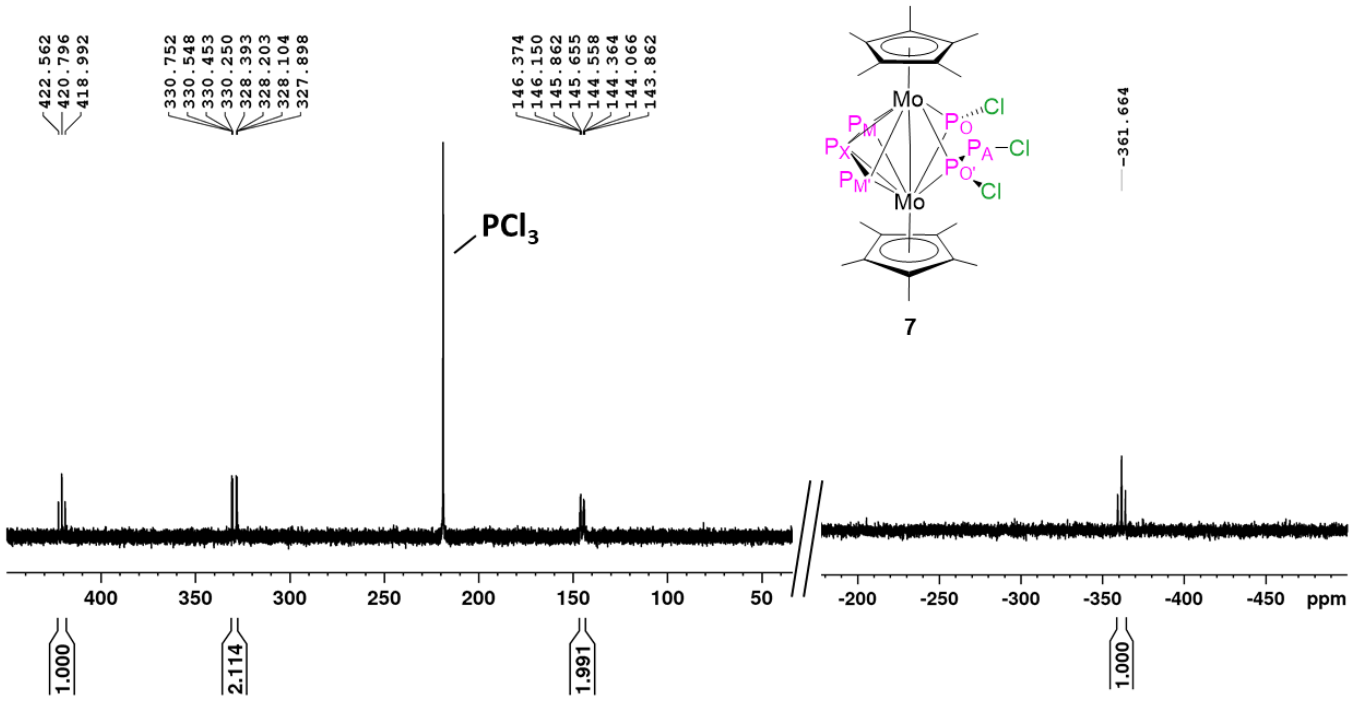


**Figure S 20.** $^{31}P\{^1H\}$ NMR spectrum of compound **7** ($CD_2Cl_2$, 193 K).

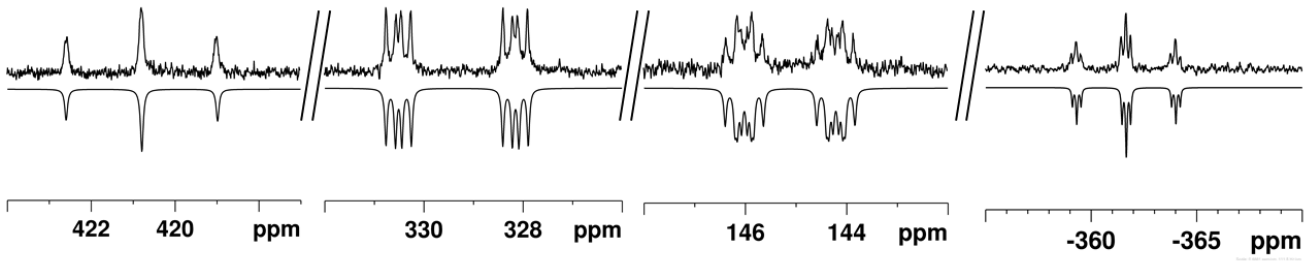


**Figure S 21.** Sections of the experimental (upwards) and simulated (downwards) $^{31}P\{^1H\}$ NMR spectrum of compound **7** (AMM'OO'X spin system).

**Table S 4.** Coupling constants of the AMM'OO'X spin system obtained from simulation.

| **δ (ppm)** | | **J (Hz)** | |
|---|---|---|---|
| **A** | 420.8 | $^1J_{AO} = {}^1J_{AO'}$ | 292.5 |
| | | $^1J_{MX} = {}^1J_{M'X}$ | 382.0 |
| **MM'** | 329.3 | $^2J_{MO} = {}^2J_{M'O'}$ | 52.0 |
| **OO'** | 145.1 | $^2J_{MO'} = {}^2J_{M'O}$ | 31.0 |
| **X** | -361.7 | $^2J_{OX} = {}^2J_{O'X}$ | 39.0 |

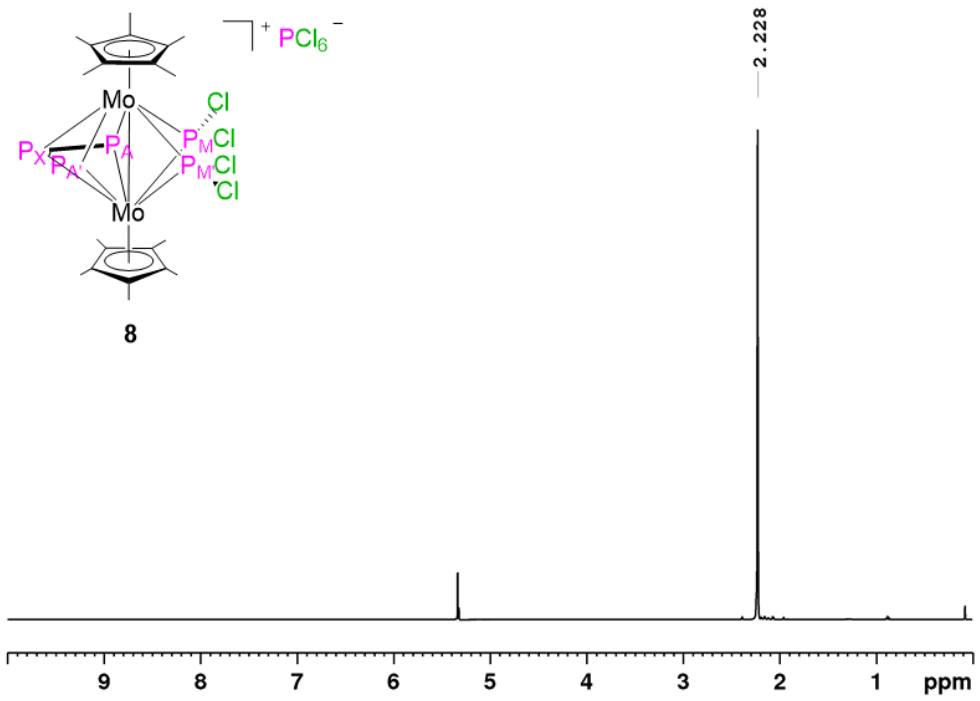


**Figure S 22.** $^1$H NMR spectrum of compound **8** ($CD_2Cl_2$, 233K).

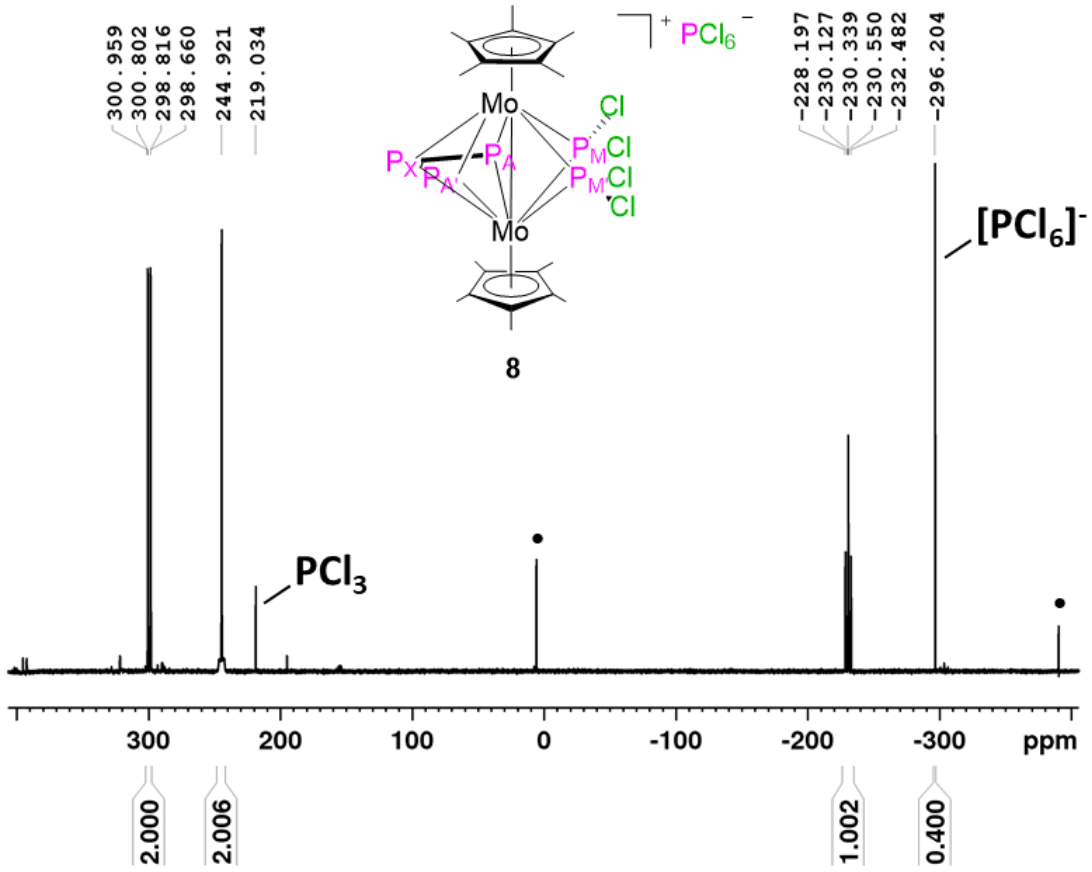


**Figure S 23.** $^{31}P\{^1H\}$ NMR spectrum of compound **8** ($CD_2Cl_2$, 233K). Impurities are marked with •.

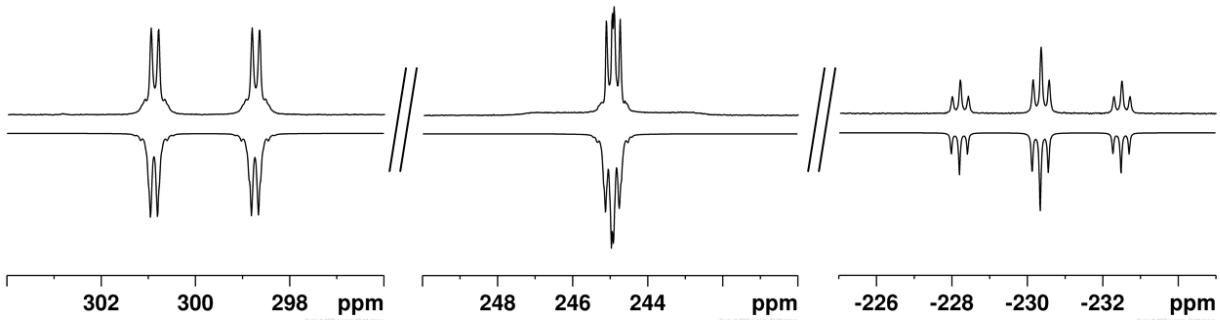


**Figure S 24.** Sections of the experimental (upwards) and simulated (downwards) $^{31}P\{^1H\}$ NMR spectrum of compound **8** (AA'MM'X spin system).

**Table S 5.** Coupling constants of the AA'MM'X spin system obtained from simulation.

| **δ(ppm)** | | **J (Hz)** | | | |
|---|---|---|---|---|---|
| **A** | 299.9 | $^1J_{AX}$ | 346.1 | $^2J_{A'M}$ | 1.7 |
| **A'** | 299.8 | $^1J_{A'X}$ | 348.0 | $^2J_{A'M'}$ | 30.6 |
| **M** | 245.0 | $^2J_{AA'}$ | 26.0 | $^2J_{MM'}$ | 29.0 |
| **M'** | 244.9 | $^2J_{AM}$ | 30.6 | $^2J_{MX}$ | 34.1 |
| **X** | -230.3 | $^2J_{AM'}$ | 2.2 | $^2J_{M'X}$ | 35.5 |

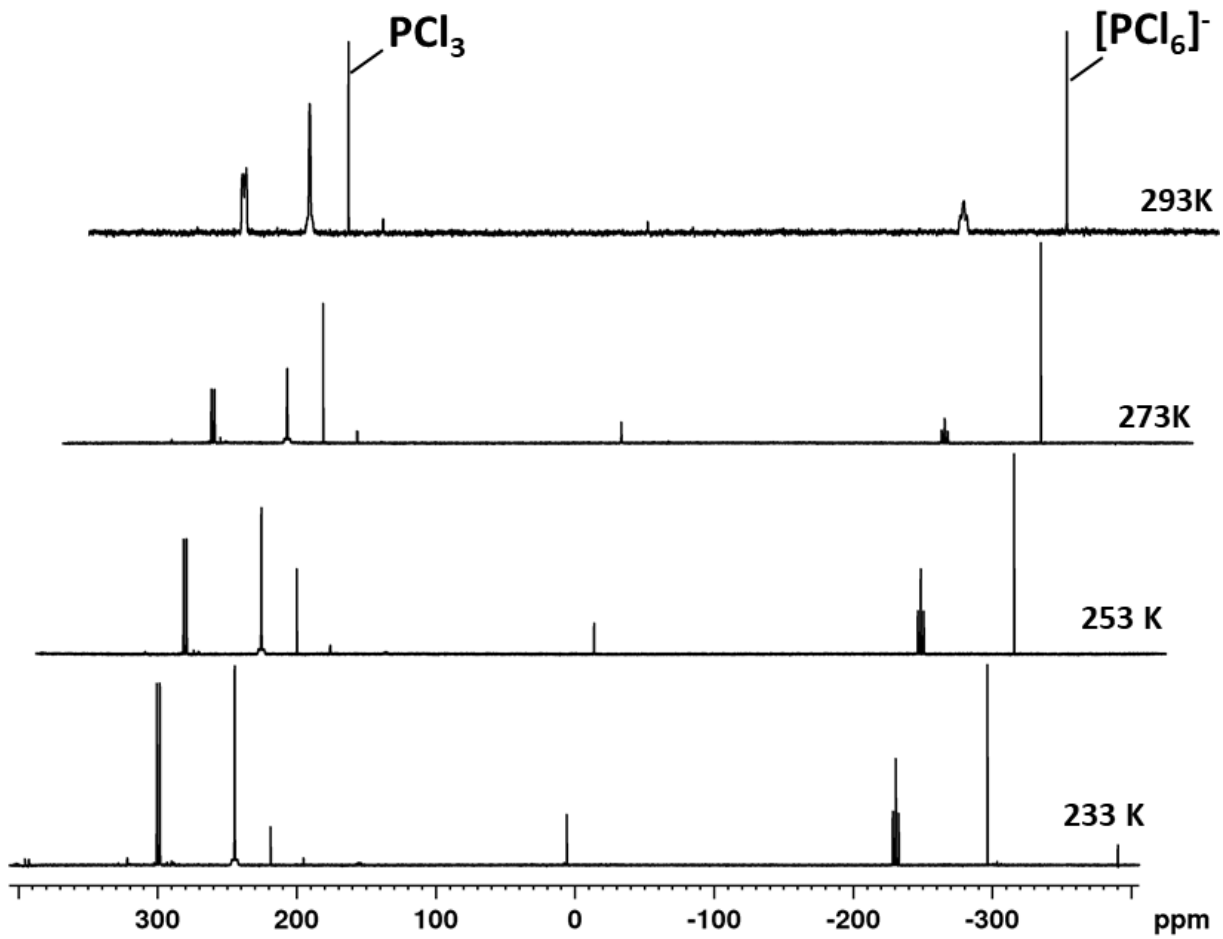


**Figure S 25.** VT-$^{31}$P{$^1$H} NMR spectra of compound **8** ($CD_2Cl_2$, from 233 K to 293 K).

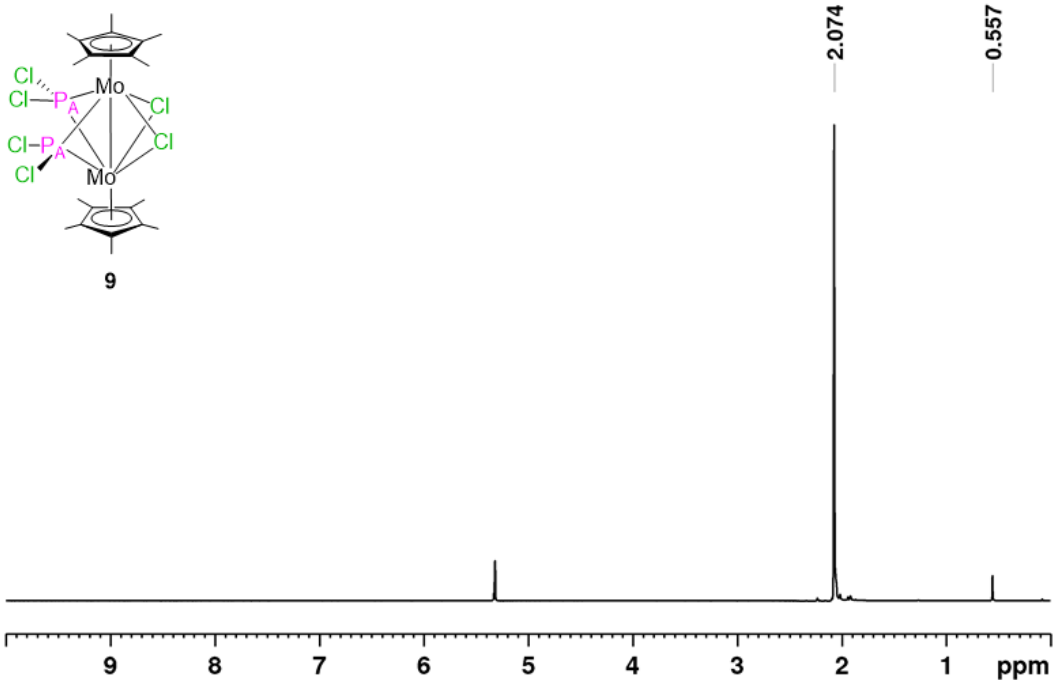


**Figure S 26.** $^1$H NMR spectrum of compound **9** ($CD_2Cl_2$, 300K) (traces of **1** are present at δ = 0.56 ppm).

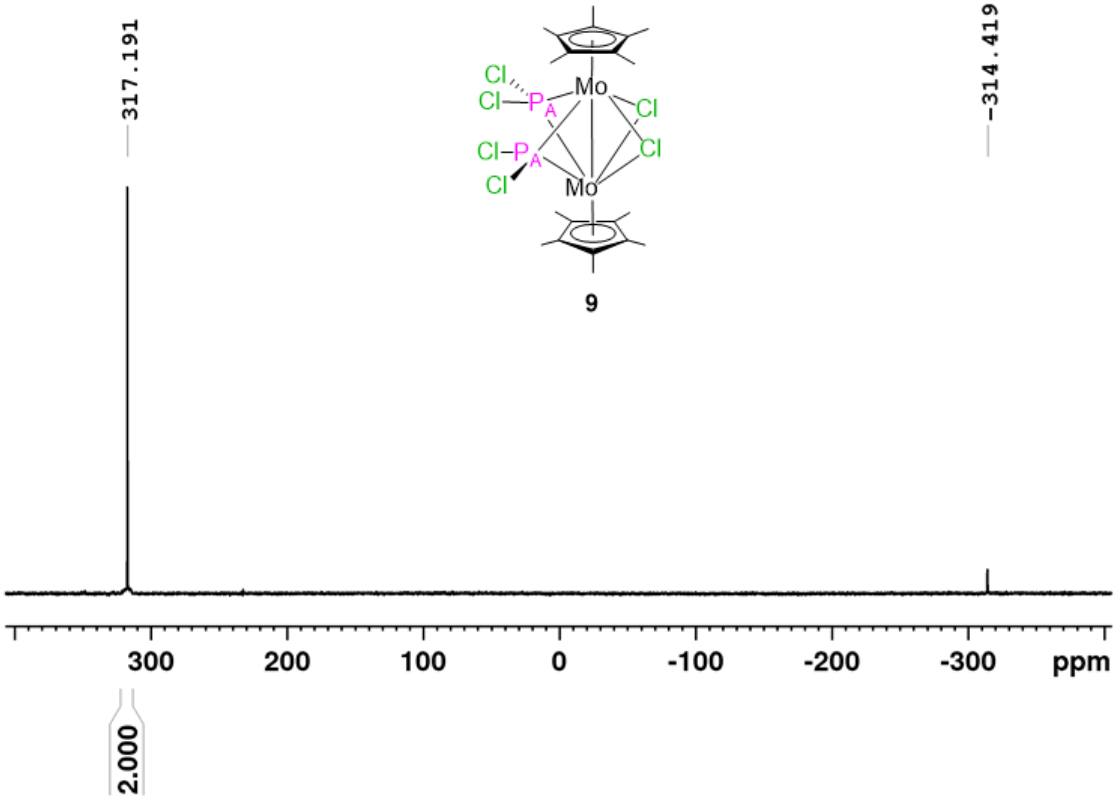


**Figure S 27.** $^{31}P\{^1H\}$ NMR spectrum of compound **9** ($CD_2Cl_2$, 300 K). Ttraces of **1** are present at δ = -314.4 ppm.

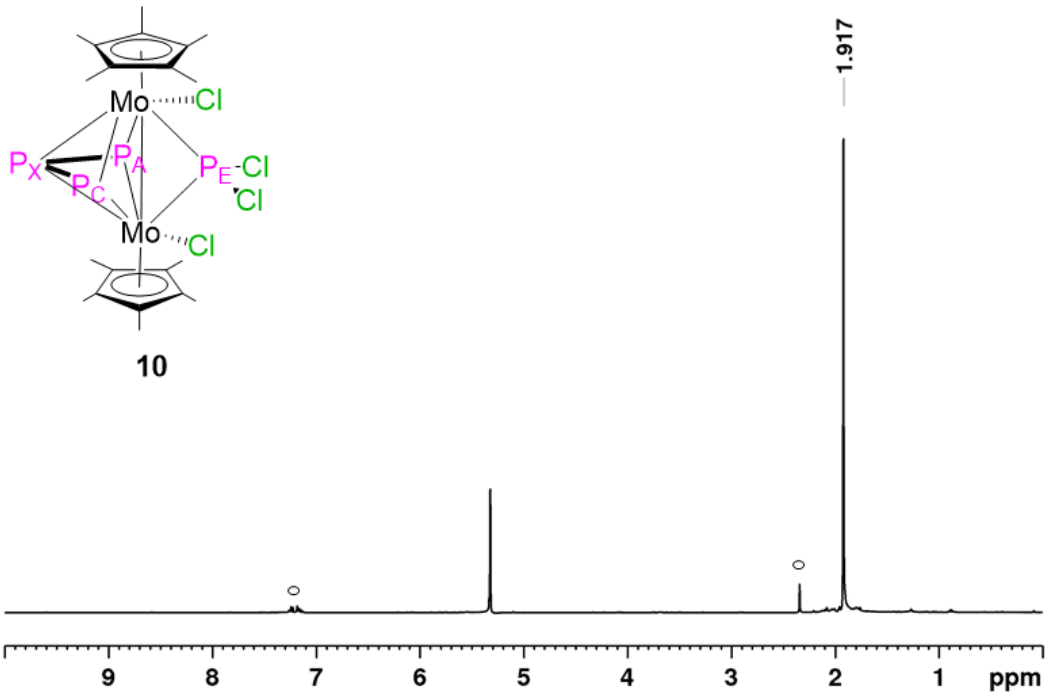


**Figure S 28.** $^1H$ NMR spectrum of compound **10** ($CD_2Cl_2$, 300K). ° = residual toluene.

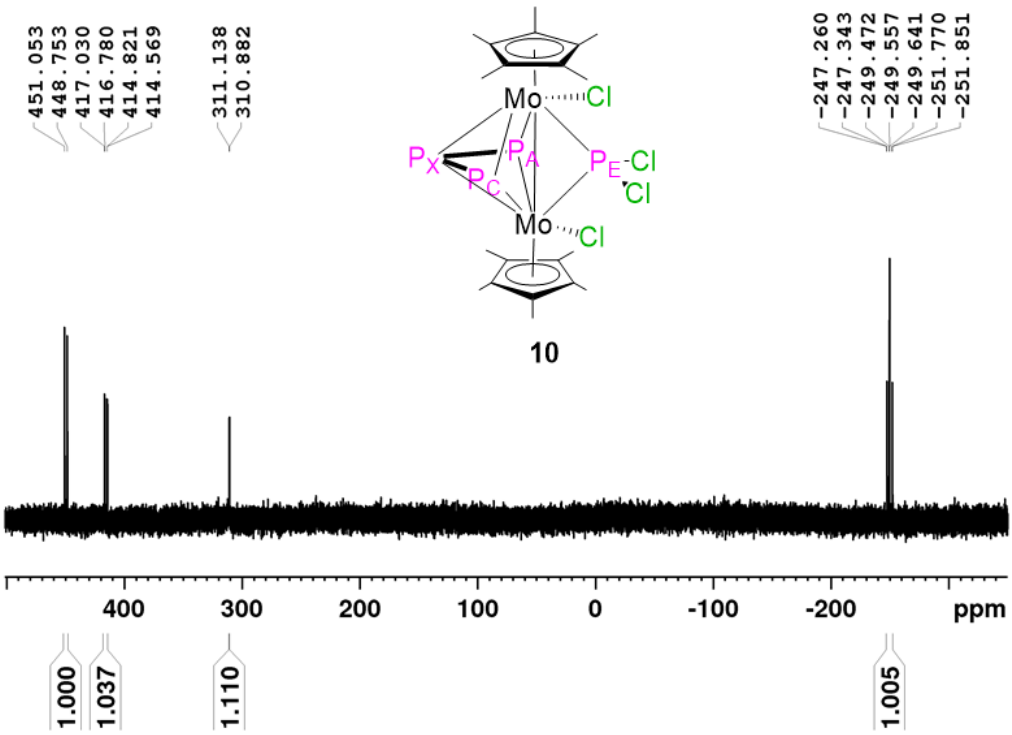


**Figure S 29.** $^{31}P\{^1H\}$ NMR spectrum of compound **10** ($CD_2Cl_2$, 300 K).

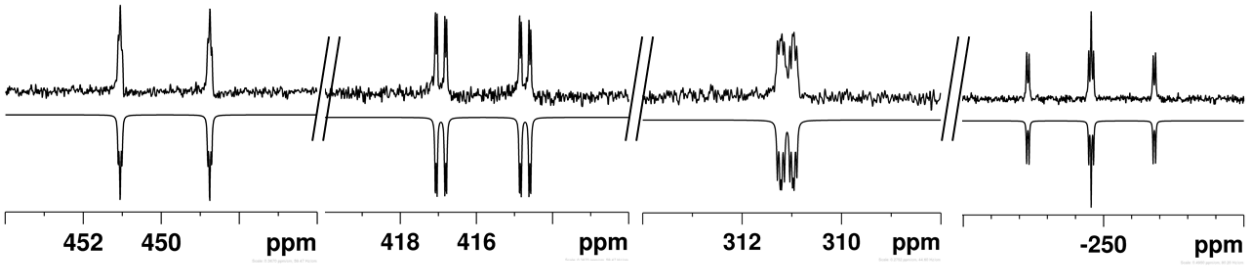


**Figure S 30.** Sections of the experimental (upwards) and simulated (downwards) $^{31}P\{^1H\}$ NMR spectrum of compound **10** (ACEX spin system).

**Table S 6.** Coupling constant of the ACEX spin system obtained from simulation.

| **δ (ppm)** | | **J (Hz)** | | | |
|---|---|---|---|---|---|
| **A** | 449.9 | $^1J_{AX}$ | 372.3 | $^2J_{AE}$ | 8.9 |
| **C** | 415.8 | $^1J_{CX}$ | 358.4 | $^2J_{CE}$ | 40.6 |
| **E** | 311.1 | | | | |
| **X** | -249.6 | $^2J_{AC}$ | 7.5 | $^2J_{EX}$ | 14.0 |

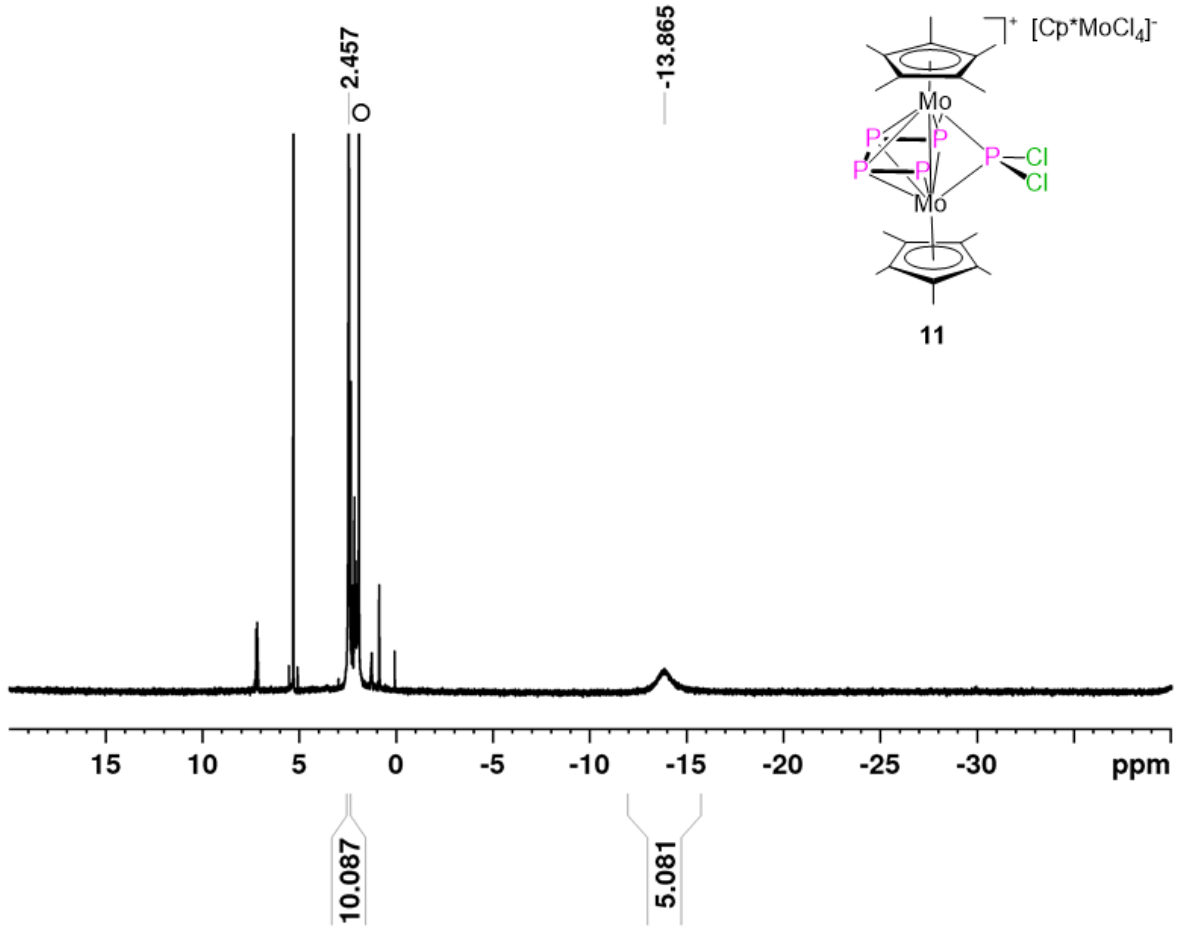


**Figure S 31.** $^1$H NMR spectrum of compound **11** ($CD_2Cl_2$, 300K). ○ = traces of compound **10**.

4. SI Halogenation of the Hexaphosphabenzene Complex [(Cp*Mo)$_2$(μ,η$^6$:η$^6$-P$_6$)] – Snapshots on the Reaction Progress

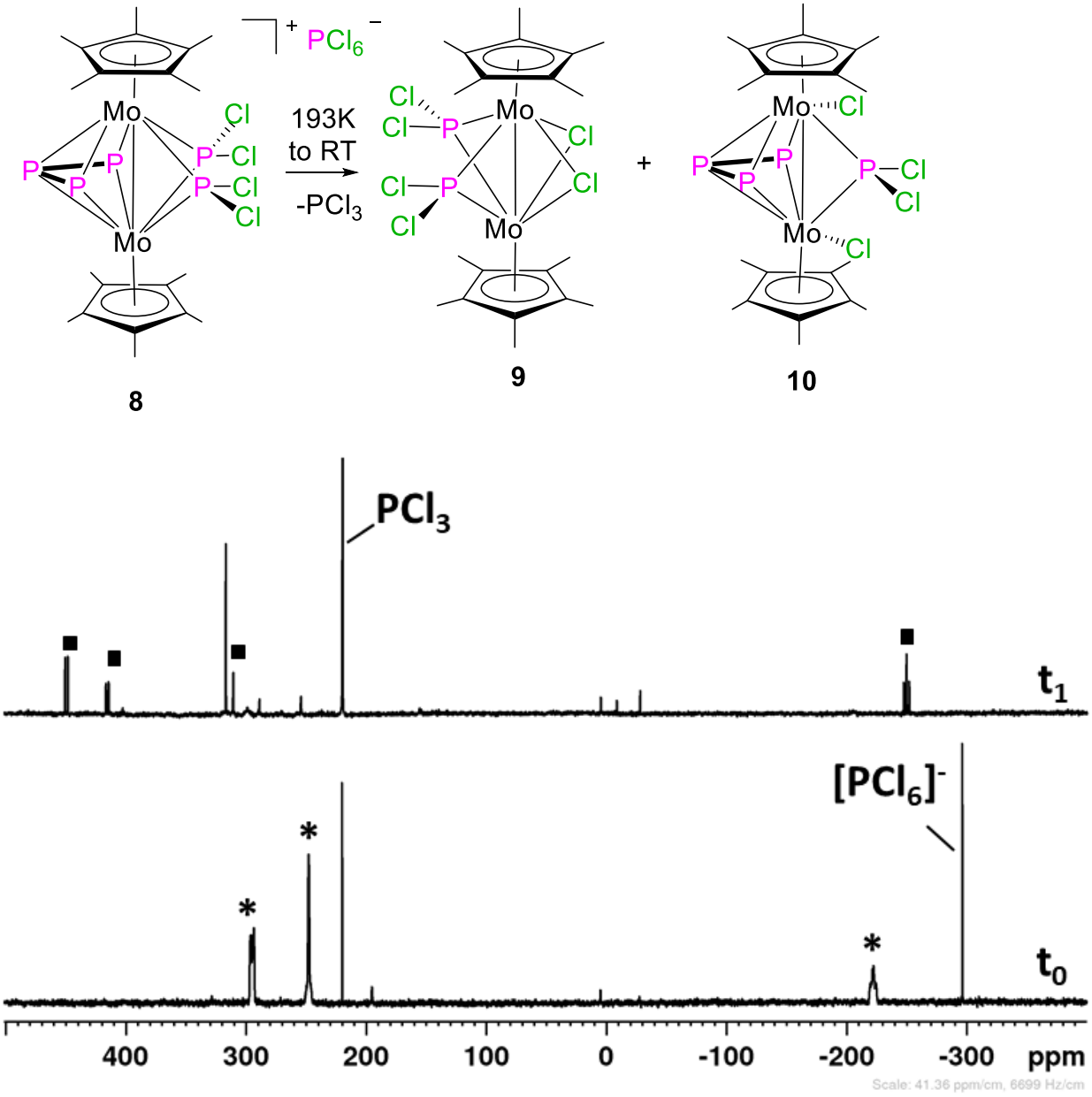


**Figure S 32.** Time-dependent $^{31}P\{^1H\}$ NMR spectra of compound **8** (*) at $t_0$ =twenty minutes, $t_1$ = seven hours ($CD_2Cl_2$, 300 K). Whereas, after twenty minutes only signals of **8** are visible (*), after seven hours in the $^{31}P\{^1H\}$ NMR spectrum of **8** is possible to observe its decomposition into **9** (●) and **10** (■).

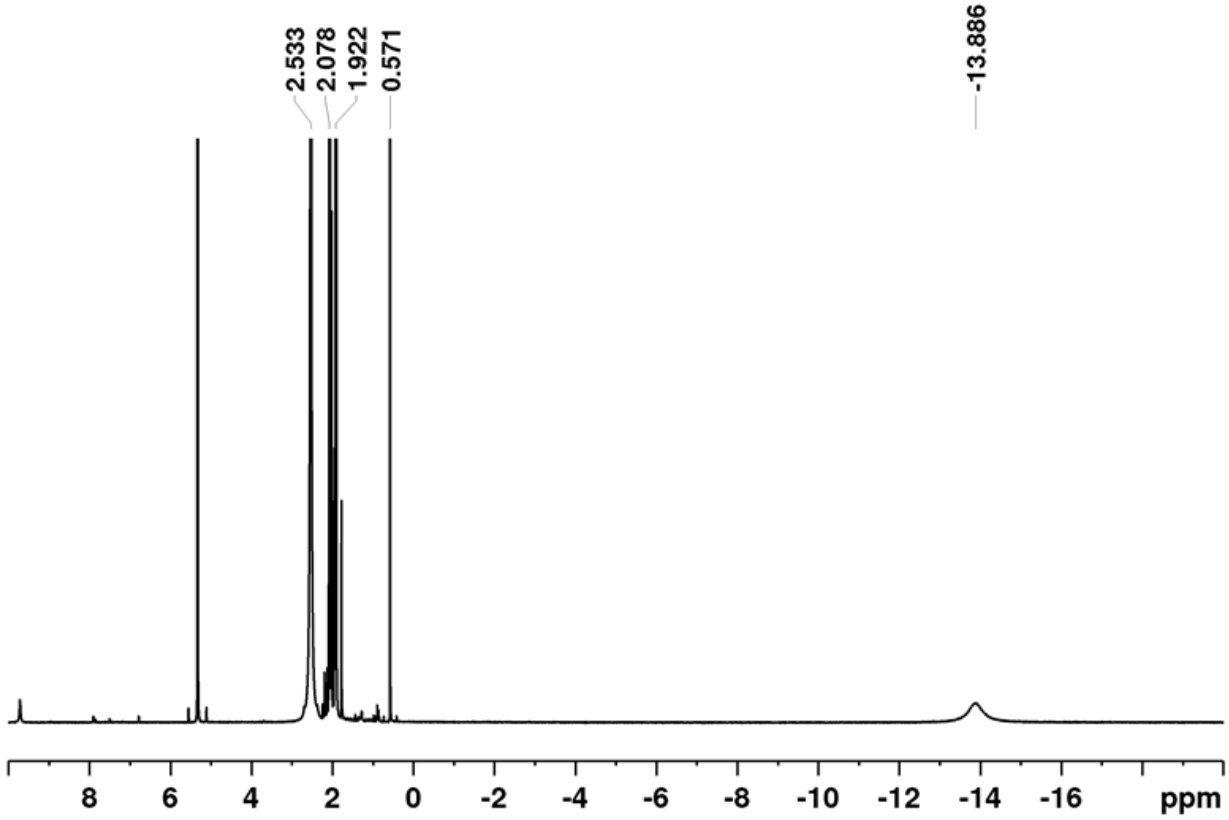


**Figure S 33.** $^1$H NMR spectrum of compound **8** after fifteen days. Together with the signals of **9** (δ =2.07 ppm), **10** (δ = 1.92 ppm), and **1** (δ = 0.57 ppm), is possible to see the signal of **11** (δ =2.53 ppm) together with the one for his counterion [Cp*MoCl$_4$]$^-$ (δ = -13.88 ppm ) resulted from the decomposition of **8** ($CD_2Cl_2$, 300 K).

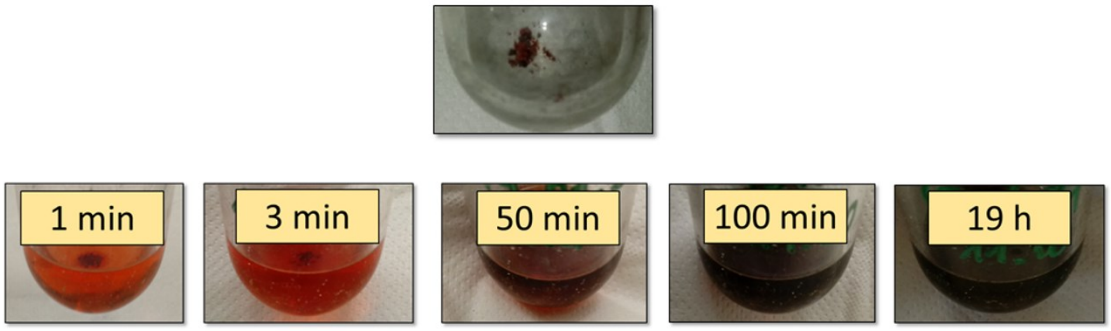


**Figure S 34** Decomposition of crystals of **8** in solution at T = 293 K during time visible by the color changing.

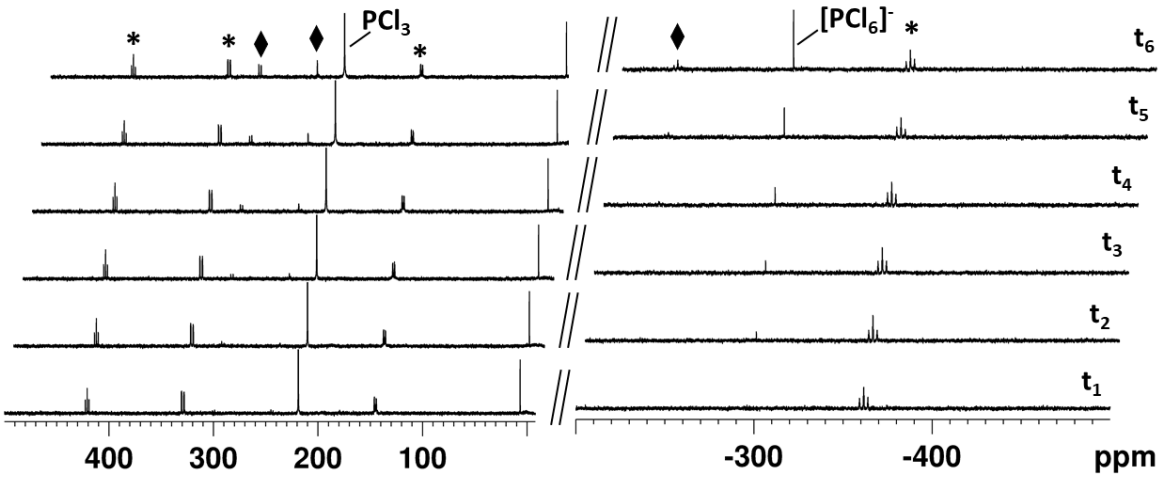


**Figure S 35.** Time-dependent $^{31}P\{^1H\}$ NMR spectra of the reaction between **1** and $PCl_5$ at 193 K. Signals of **7** are marked with stars (*) while signals of **8** are marked with squares (♦) ($CD_2Cl_2$, 300 K).

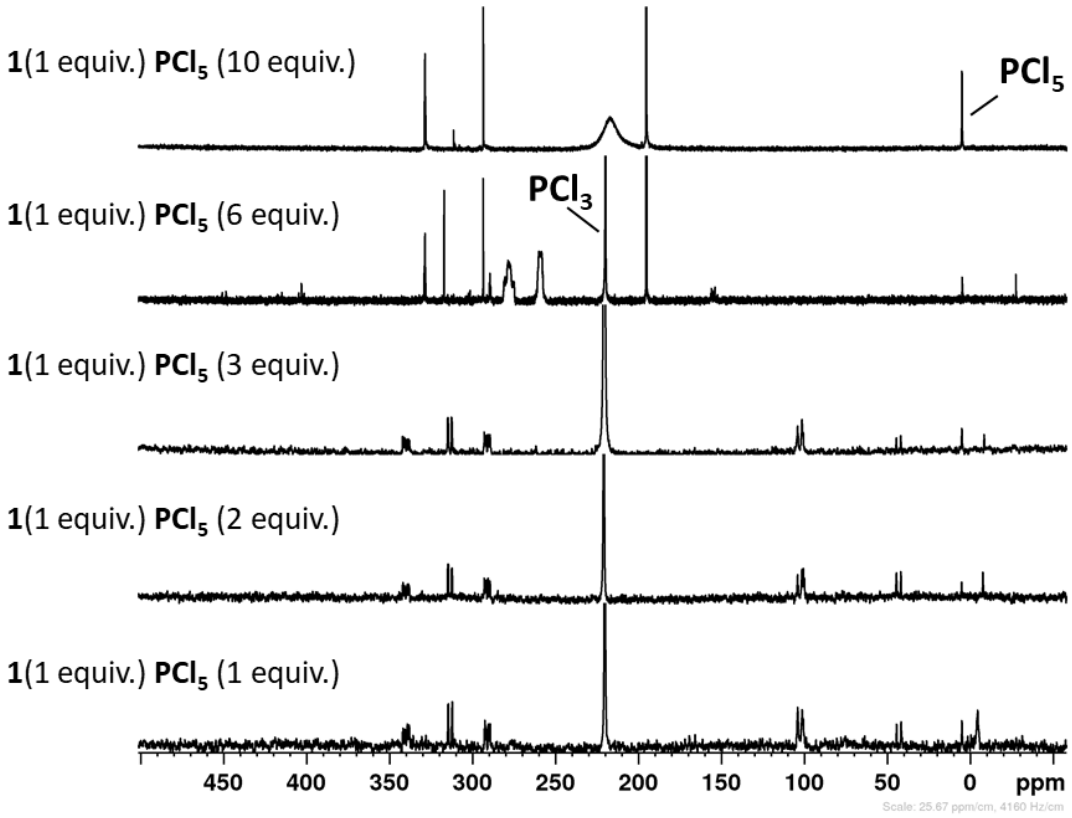


**Figure S 36.** $^{31}P\{^1H\}$ NMR spectra of the reaction of **1** (1 equiv.) with increasing equiv. of $PCl_5$ ($CD_2Cl_2$, 300K).

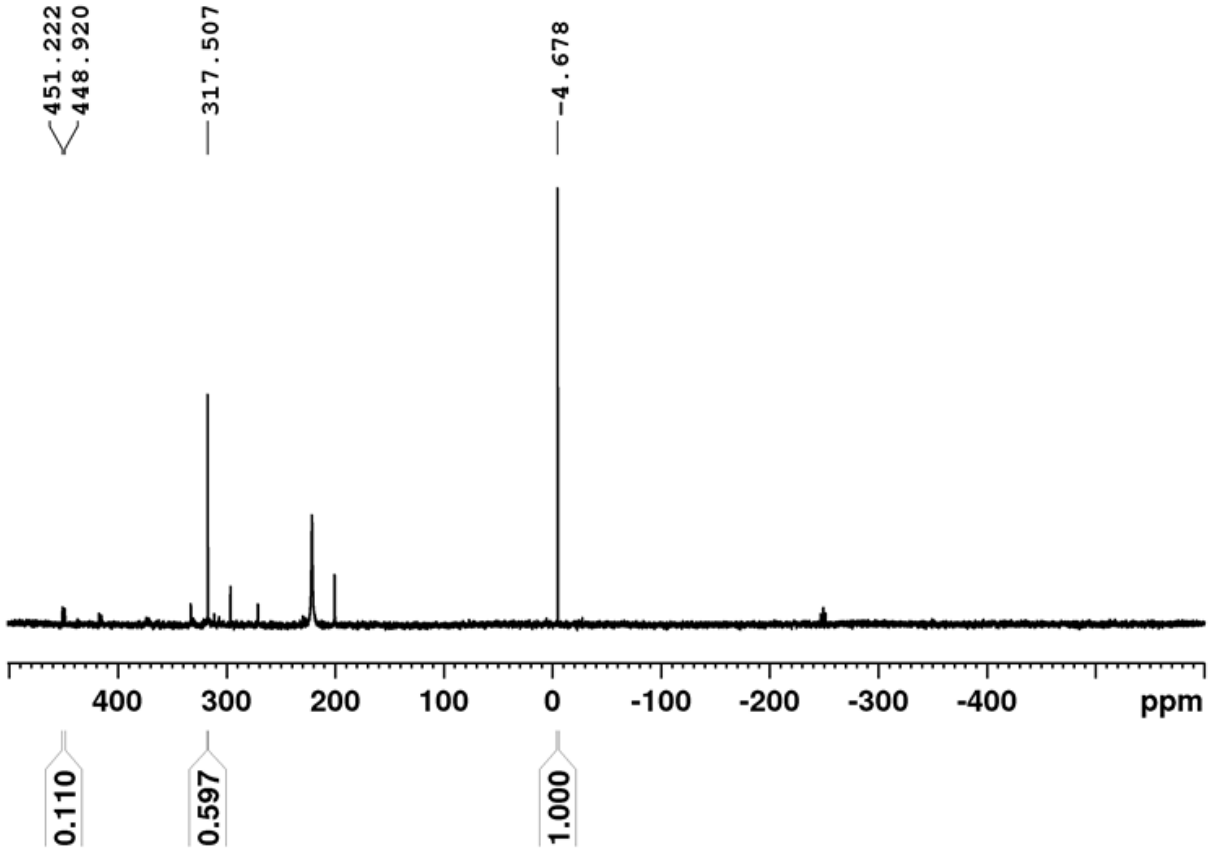


**Figure S 37.** $^{31}P\{^1H\}$ NMR spectrum of the reaction solution of **1** (1 equiv.) with $PCl_5$ (6 equiv.) ($CD_2Cl_2$, 300K, $PPh_3$ capillary as internal standard).

δ = -4.6 ppm = $PPh_3$ (Integration: 1.00)

δ = 317.5 ppm = **9** (2 P atoms for this signal, Integration: 0.60)

δ = 450.0 ppm = **10** (1 P atom for this signal, Integration = 0.11)

mmol $PPh_3$ in the capillary = 0.010

mmol **9** in the NMR tube= (0.010*0.60/2) = 0.003

mmol **1** in the NMR tube = 0.031

yield **9** [%] = [0.003 mmol/(3*mmol **1**)]*100 = 3

mmol **10** in the NMR tube= (0.010*0.11) = 0.001

yield **10** [%] = [0.001 mmol/(5/6*mmol **1**)]*100 = 4

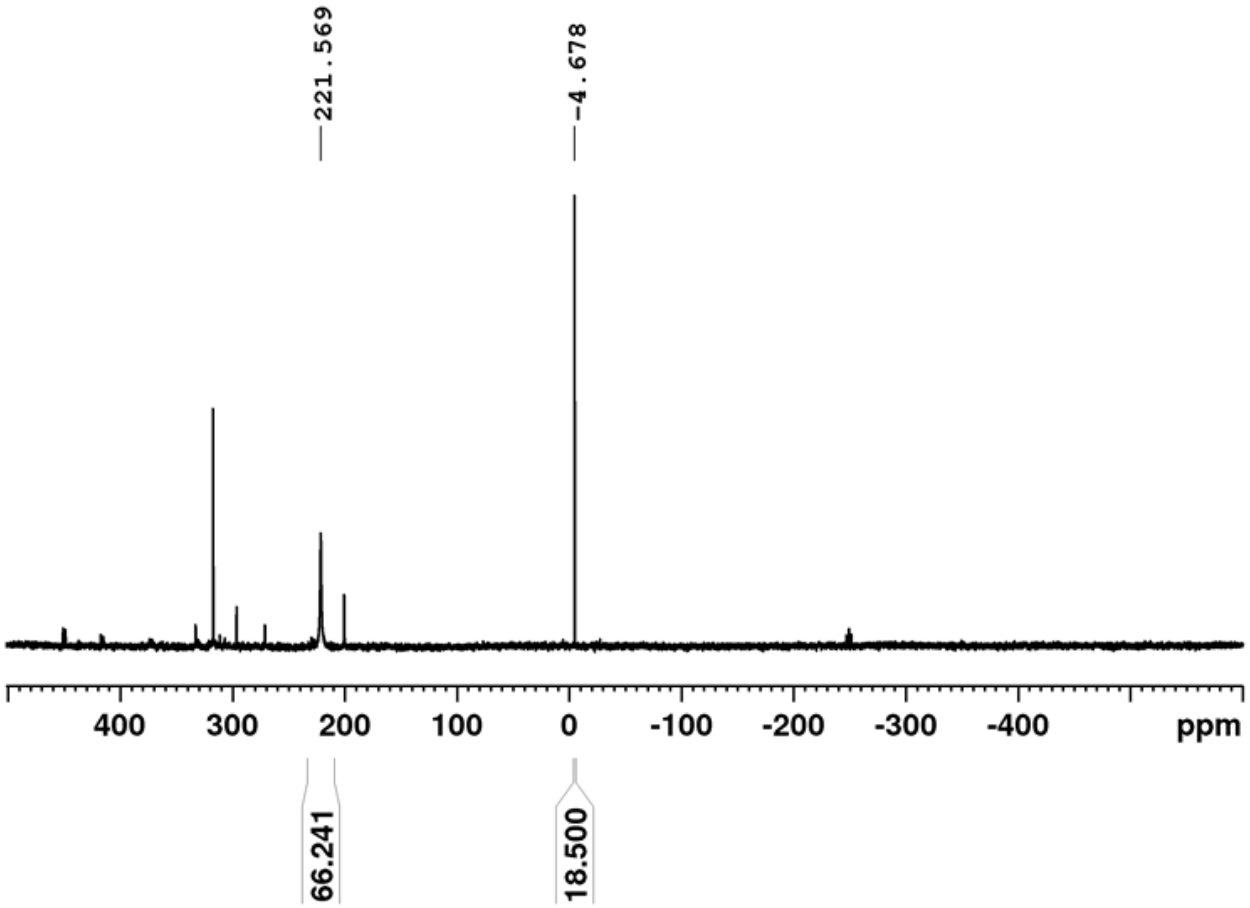


**Figure S 38.** $^{31}P\{^1H\}$ NMR spectrum of the reaction solution of **1** (1 equiv.) with $PCl_5$ (6 equiv.) ($CD_2Cl_2$, 300K, $PPh_3$ capillary as internal standard.

- δ = -4.6 ppm = $PPh_3$
- δ = 221.6 = $PCl_3$
- mmol $PPh_3$ in the capillary: 0.010
- mmol $PCl_5$ in the NMR tube: 0.185
- $\frac{PBr_5}{PPh_3} = \frac{0.185}{0.010} = 18.5$
- Integration $PPh_3$ = 18.5
- Integration $PCl_3$ = 66.2
- 18.5 out of 66.2 (**28%**) equals the amount of $PCl_3$ coming from $PCl_5$
- (66.2–18.5) = 47.74 (**72%**) equals the amount of $PCl_3$ coming from **1**

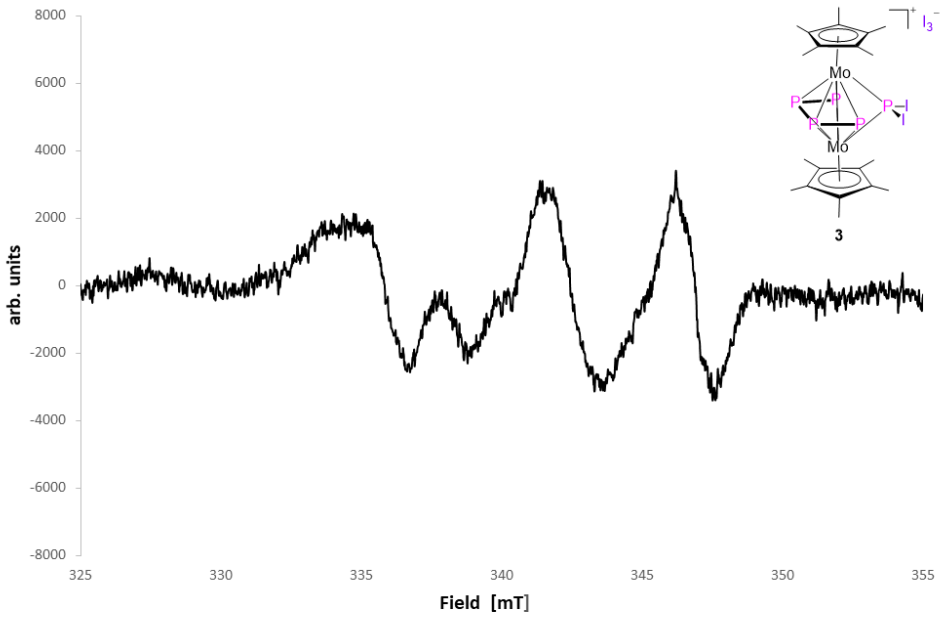


**Figure S39.** EPR spectrum of **3** in solution ($CH_2Cl_2$, 300K).

**Crystallographic details**

Suitable crystals were selected and mounted on a GV50 diffractometer equipped with a Titan$^{S2}$ CCD detector (**2-I$_3$**), on a SuperNova Dualflex diffractometer equipped with an Atlas$^{S2}$ CCD detector (**9**, **8, 6**, **3**), on a SuperNova Dualflex diffractometer equipped with Titan$^{S2}$ CCD detector (**10**) on a XtaLAB SynergyR DW diffractometer equipped with an HyPix-Arc 150 detector (**4**) or on a Gemini Ultra diffractometer equipped with an Atlas$^{S2}$ CCD detector (**12**, **11**, **5**) The crystals were kept at a steady T = 123(1) K or respectively at 100 K (**3**) during data collection. Data collection and reduction were performed with **CrysAlisPro** [Version 1.171.39.46 (**12**, **9**), Version 1.171.40.53 (**5**), Version 1.171.41.89a (**6**), Version 1.171.41.90a (**2-I$_3$**, **11**, **8**, **4**, **3**, **10**)].[3] For the compounds **2-I$_3$**, **9**, **6**, **4**, **3** and **10** a numerical absorption correction based on a gaussian integration over a multifaceted crystal model and an empirical absorption correction using spherical harmonics as implemented in SCALE3 ABSPACK was applied. For the compounds **12**, **11**, **5** and **8** an analytical numeric absorption correction using a multifaceted crystal model based on expressions derived by R.C. Clark & J.S. Reid. (Clark, R. C. & Reid, J. S. (1995). Acta Cryst. A51, 887-897) and an empirical absorption correction using spherical harmonics, as implemented in SCALE3 ABSPACK scaling algorithm, was applied. Using **Olex2**,[4] the structures were solved with **ShelXT**[5] and a least-square refinement on F2 was carried out with **ShelXL**[6] for all structures. All non-hydrogen atoms were refined anisotropically. Hydrogen atoms at the carbon atoms were located in idealized positions and refined isotropically according to the riding model.

Figures were created with Olex2.

CCDC-2155218 (**2-I$_3$**), CCDC-2155219 (**3**), CCDC-2155220 (**4**), CCDC-2155221 (**5**), CCDC-2155222 (**6**), CCDC-2155223 (**8**), CCDC-2155224 (**9**), CCDC-2155225 (**10**) and CCDC-2155226 (**11**), CCDC-2155227 (**12**) contain the supplementary crystallographic data for this paper. These data can be obtained free of charge at www.ccdc.cam.ac.uk/conts/retrieving.html (or from the Cambridge Crystallographic Data Centre, 12 Union Road, Cambridge CB2 1EZ, UK; Fax: + 44-1223-336-033; e-mail: deposit@ccdc.cam.ac.uk).

**Table S 7.** Crystallographic data for the compounds **2-I$_3$**, **3**, **4**, **5** and **6**.

| **Compound** | **2-I$_3$ · CH$_2$Cl$_2$** | **3** | **4 · 0.65 C$_7$H$_8$** | **5** | **6** |
|---|---|---|---|---|---|
| Data set (internal naming) | **AG94** | **AG505** | **AG493_a** | **AG382** | **AG489** |
| CCDC-number | 2155218 | 2155219 | 2155220 | 2155221 | 2155222 |
| Formula | $C_{21}H_{32}Cl_2I_6Mo_2P_6$ | $C_{20}H_{30}I_5Mo_2P_5$ | $Br_6C_{34.55}H_{50.2}Mo_3P_3$ | $C_{20}H_{30}Br_5Mo_2P_5$ | $C_{20}H_{31}Br_5Mo_2P_2$ |
| $D_{calc.}$/ g cm$^{-3}$ | 2.540 | 2.592 | 2.070 | 2.268 | 2.299 |
| Formula Weight | 1494.46 | 1251.67 | 1325.73 | 1016.72 | 924.82 |
| Colour | clear orange | metallic dark black | metallic red | dark red | metallic dark red |
| Shape | plate | block | plate | needle | block-shaped |
| Size/mm$^3$ | 0.15×0.10×0.04 | 0.15×0.12×0.11 | 0.07×0.04×0.02 | 0.65×0.10×0.07 | 0.09×0.05×0.05 |
| $T$/K | 122.9(2) | 100.01(10) | 123.01(10) | 123(1) | 122.97(10) |
| Crystal System | monoclinic | monoclinic | triclinic | tetragonal | monoclinic |
| Space Group | $Cc$ | $P2_1/m$ | $P\bar{1}$ | $P4_1$ | $P2_1/c$ |
| $a$/Å | 25.9390(6) | 9.4298(2) | 8.5569(2) | 12.64210(10) | 16.6982(7) |
| $b$/Å | 10.27490(16) | 16.4935(5) | 15.6724(3) | 12.64210(10) | 10.5399(3) |
| $c$/Å | 16.7077(4) | 10.4322(3) | 15.9298(3) | 18.6267(3) | 17.1822(7) |
| $\alpha$/° | 90 | 90 | 89.837(2) | 90 | 90 |
| $\beta$/° | 118.661(3) | 98.786(2) | 87.576(2) | 90 | 117.908(5) |
| $\gamma$/° | 90 | 90 | 85.106(2) | 90 | 90 |
| V/Å$^3$ | 3907.36(16) | 1603.48(8) | 2126.61(8) | 2976.97(7) | 2672.3(2) |
| $Z$ | 4 | 2 | 2 | 4 | 4 |
| $Z'$ | 1 | 0.5 | 1 | 1 | 1 |
| Wavelength/Å | 1.54184 | 1.54184 | 1.54184 | 0.71073 | 0.71073 |
| Radiation type | Cu K$_\alpha$ | Cu K$_\alpha$ | Cu K$_\alpha$ | Mo K$_\alpha$ | Mo K$_\alpha$ |
| $\mu$/mm$^{-1}$ | 46.176 | 46.638 | 14.989 | 7.833 | 8.542 |
| $\Theta_{min}$/° | 3.884 | 4.288 | 2.776 | 3.404 | 3.307 |
| $\Theta_{max}$/° | 74.568 | 66.889 | 75.338 | 32.378 | 30.019 |
| Measured Refl's. | 10740 | 16173 | 39685 | 25794 | 24349 |
| Indep't Refl's | 6472 | 2916 | 8649 | 9461 | 6811 |
| Refl's I≥2 $\sigma$(I) | 6275 | 2840 | 7130 | 8689 | 6023 |
| $R_{int}$ | 0.0517 | 0.0503 | 0.0413 | 0.0278 | 0.0283 |
| Parameters | 344 | 173 | 489 | 299 | 297 |
| Restraints | 2 | 19 | 120 | 1 | 30 |
| Largest Peak | 1.868 | 1.590 | 0.784 | 0.557 | 0.863 |
| Deepest Hole | -1.361 | -0.943 | -1.424 | -0.541 | -0.558 |
| GooF | 1.031 | 1.071 | 1.068 | 1.112 | 1.089 |
| $wR_2$ (all data) | 0.1047 | 0.1026 | 0.0998 | 0.0618 | 0.0470 |
| $wR_2$ | 0.1039 | 0.1017 | 0.0953 | 0.0599 | 0.0454 |
| $R_1$ (all data) | 0.0419 | 0.0381 | 0.0490 | 0.0385 | 0.0336 |
| $R_1$ | 0.0410 | 0.0373 | 0.0385 | 0.0314 | 0.0259 |

**Table S 8.** Crystallographic data for the compounds **8**, **9**, **10**, **11** and **12**.

| **Compound** | **8** | **9** | **10 · $C_7H_8$** | **11** | **12** |
|---|---|---|---|---|---|
| Data set (internal naming) | **AG474** | **AG461** | **AG521_mP_abs** | **AG435** | **AG355** |
| CCDC-number | 2155223 | 2155224 | 2155225 | 2155226 | 2155227 |
| Formula | $C_{21}H_{32}Cl_{12}Mo_2P_6$ | $C_{20}H_{30}Cl_6Mo_2P_2$ | $C_{27}H_{38}Cl_4Mo_2P_4$ | $C_{30}H_{45}Cl_6Mo_3P_5$ | $C_{20}H_{30}Cl_2Mo_2P_5$ |
| $D_{calc.}$/ g cm$^{-3}$ | 1.914 | 1.884 | 1.734 | 1.811 | 1.775 |
| Formula Weight | 1087.56 | 736.96 | 820.13 | 1061.03 | 688.07 |
| Colour | clear red | dark red | clear light green | metallic dark red | metallic brown |
| Shape | block | prism | plate-shaped | block | block |
| Size/mm$^3$ | 0.29×0.12×0.10 | 0.14×0.12×0.07 | 0.11×0.07×0.02 | 0.18×0.15×0.09 | 0.17×0.06×0.05 |
| $T$/K | 122.97(10) | 123.00(10) | 123.00(10) | 123(1) | 123(1) |
| Crystal System | orthorhombic | orthorhombic | monoclinic | triclinic | monoclinic |
| Space Group | $P2_12_12_1$ | $Pbcm$ | $P2_1/m$ | $P\bar{1}$ | $P2_1/n$ |
| $a$/Å | 10.4401(2) | 12.2413(2) | 8.4515(2) | 11.8302(4) | 10.67280(10) |
| $b$/Å | 15.7340(4) | 14.3806(2) | 13.3207(3) | 11.8615(4) | 16.9896(2) |
| $c$/Å | 22.9821(5) | 14.7590(2) | 14.0173(3) | 14.8904(5) | 14.2719(2) |
| $\alpha$/° | 90 | 90 | 90 | 81.712(3) | 90 |
| $\beta$/° | 90 | 90 | 95.595(2) | 73.829(3) | 95.6630(10) |
| $\gamma$/° | 90 | 90 | 90 | 76.710(3) | 90 |
| V/Å$^3$ | 3775.14(15) | 2598.13(7) | 1570.55(6) | 1945.88(12) | 2575.25(5) |
| $Z$ | 4 | 4 | 2 | 2 | 4 |
| $Z'$ | 1 | 0.5 | 0.5 | 1 | 1 |
| Wavelength/Å | 0.71073 | 0.71073 | 1.54184 | 1.54184 | 1.54184 |
| Radiation type | Mo K$_\alpha$ | Mo K$_\alpha$ | Cu K$_\alpha$ | Cu K$_\alpha$ | Cu K$_\alpha$ |
| $\mu$/mm$^{-1}$ | 1.786 | 1.715 | 11.732 | 13.708 | 12.876 |
| $\Theta_{min}$/° | 3.242 | 3.286 | 4.590 | 3.843 | 4.057 |
| $\Theta_{max}$/° | 29.428 | 30.694 | 66.789 | 71.978 | 71.655 |
| Measured Refl's. | 41385 | 18220 | 9971 | 12827 | 14581 |
| Indep't Refl's | 9246 | 3756 | 2891 | 7321 | 4933 |
| Refl's I≥2 $\sigma$(I) | 8792 | 3477 | 2646 | 6930 | 4484 |
| $R_{int}$ | 0.0315 | 0.0188 | 0.0328 | 0.0197 | 0.0337 |
| Parameters | 389 | 151 | 193 | 412 | 327 |
| Restraints | 0 | 0 | 0 | 0 | 61 |
| Largest Peak | 1.824 | 0.457 | 2.633 | 0.517 | 0.828 |
| Deepest Hole | -0.945 | -0.384 | -0.714 | -0.632 | -0.448 |
| GooF | 1.103 | 1.065 | 1.056 | 1.074 | 1.108 |
| $wR_2$ (all data) | 0.1372 | 0.0404 | 0.0906 | 0.0543 | 0.0808 |
| $wR_2$ | 0.1351 | 0.0393 | 0.0884 | 0.0533 | 0.0787 |
| $R_1$ (all data) | 0.0534 | 0.0192 | 0.0378 | 0.0238 | 0.0363 |
| $R_1$ | 0.0502 | 0.0168 | 0.0343 | 0.0220 | 0.0320 |

**Compound 2-I$_3$:**

The asymmetric unit contains one molecule of [(Cp*Mo)$_2$(μ,η$^3$:η$^3$-P$_3$)(μ,η$^1$:η$^1$η$^1$η$^1$-P$_3$I$_3$)] $^+$, an $I_3^-$ anion and a $CH_2Cl_2$ solvent molecule.

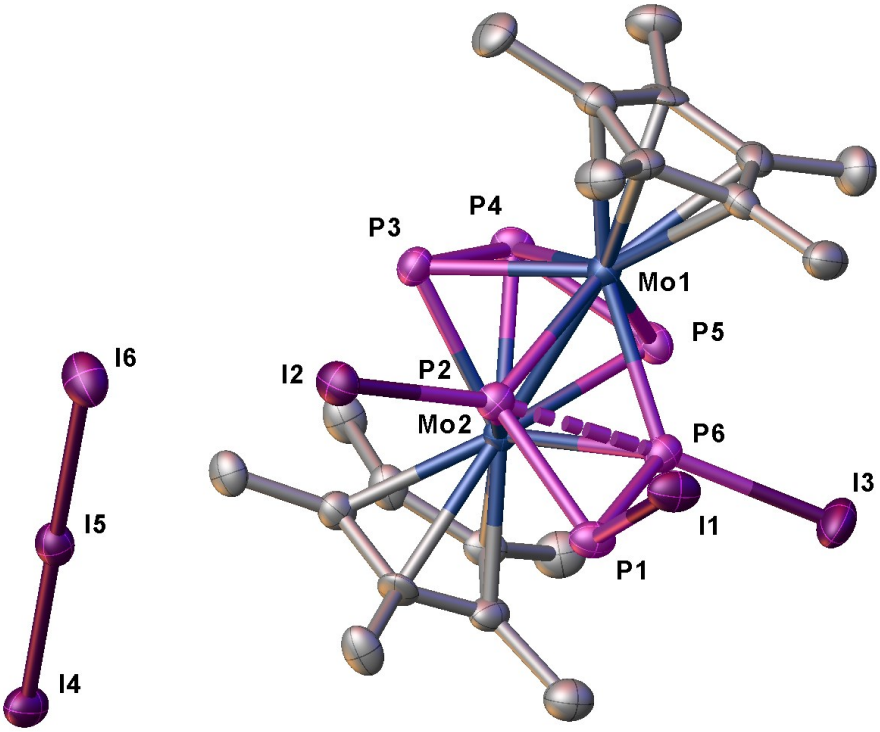


| Selected bond length [Å] | | Selected bond angles [°] | |
|---|---|---|---|
| P1–P2 | 2.216(5) | P1–P2–P6 | 56.42(15) |
| P2–P6 | 2.459(5) | P2–P6–P1 | 56.27(14) |
| P6–P1 | 2.220(5) | P6–P1–P2 | 67.31(15) |
| P3–P4 | 2.139(5) | P3–P4–P5 | 111.2(2) |
| P4–P5 | 2.138(6) | I1–P1–P2 | 106.58(18) |
| P2···P3 | 2.652(5) | I1–P1–P6 | 113.02(17) |
| P5···P6 | 2.665(5) | I2–P2–P1 | 110.69(16) |
| P1–I1 | 2.468(4) | I2–P2–P6 | 167.10(17) |
| P2–I2 | 2.443(3) | I3–P6–P1 | 112.37(17) |
| P6–I3 | 2.433(4) | I3–P6–P2 | 167.79(17) |
| I4–I5 | 2.9025(14) | I4–I5–I6 | 179.69(6) |
| I5–I6 | 2.9521(14) | P2-Mo1-Mo2 | 55.46(8) |
| Mo1-Mo2 | 2.7227(14) | P2-Mo1-P3 | 65.48(11) |

**Compound 3:**

The asymmetric unit contains half a molecule of [{Cp*Mo}$_2$(μ-PI$_2$)(μ,η$^{4:4}$-P$_4$)]$^+$and half of the anion $I_3^-$. Further, are two of the P atoms of the P$_4$ ligand disordered over two positions (0.58:0.42). The SADI and SIMU restraints were used during the refinement of the disordered ligand.

**Part 1** **Part 2** **Part 1 und 2**

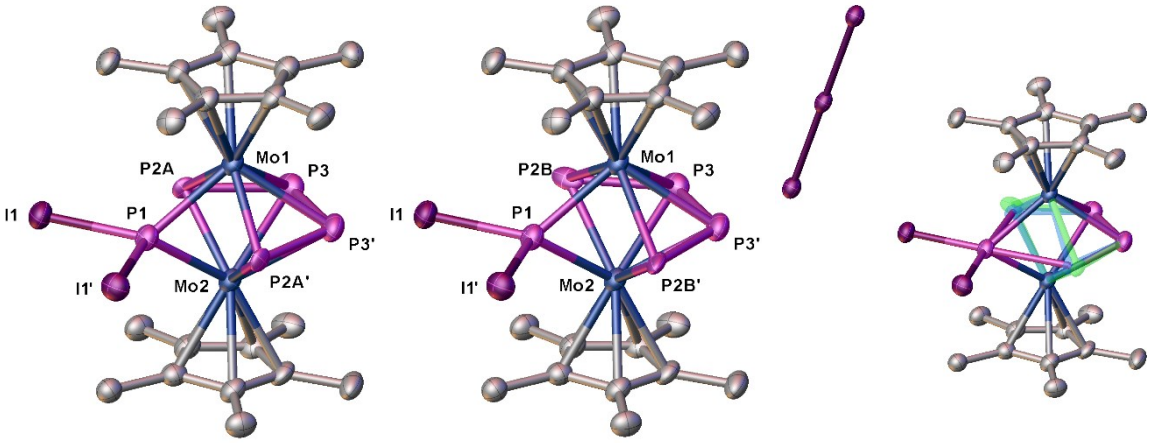


| Selected bond length [Å] | |
|---|---|
| P1–I1 | 2.4879(13) |
| P2A–P3 | 2.243(7) |
| P3–P3’ | 2.162(4) |
| Mo1–P1 | 2.404(2) |
| Mo2–P1 | 2.391(2) |
| Mo1–Mo2 | 2.74340(8) |
| P1···P2A | 2.596(11) |
| P1···P2A’ | 2.596(11) |

| Selected bond angles [°] | | | |
|---|---|---|---|
| I1–P1–I1’ | 99.65(7) | Mo1–P3–Mo2 | 64.97(4) |
| P2A–P3–P3’ | 111.9(3) | Mo1–P1–Mo2 | 69.79(6) |
| Mo1–P2A–Mo2 | 70.8(3) | I3–I2–I3’ | 180.0 |

**Compound 4:**

The asymmetric unit contains one molecule of [{Cp*Mo}$_2$(μ-Br)$_2$(μ,η$^{3:3}$-P$_3$)]$^+$, one molecule of [Cp*Mo(Br)$_4$]$^-$ and a partly occupied toluene. The content of solvent molecules per formula unit was estimated using a solvent mask. A total of 64 electrons were found in a volume of 292Å$^3$ in 1 void per unit cell. This is consistent with the presence of 0.65 toluene molecules per asymmetric unit, which account for 65 electrons per unit cell. Further, is the Cp* ligand of the [Cp*Mo(Br)$_4$]$^-$ molecule disordered over two positions (0.51:0.49). The SIMU restraint was used during the refinement of the disordered fragments.

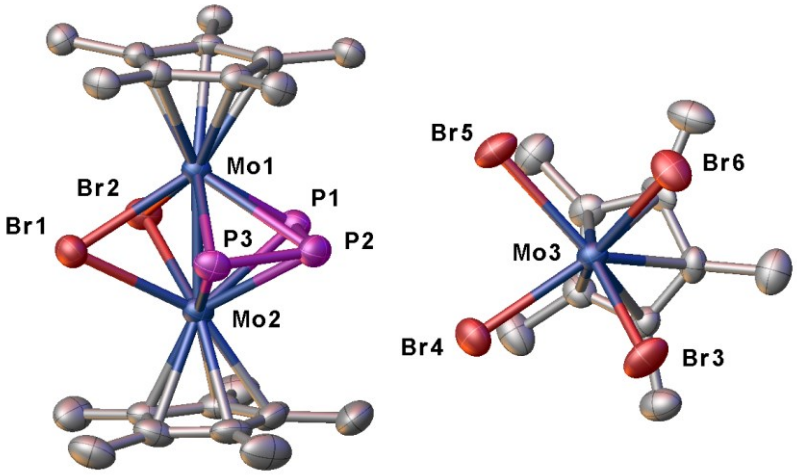


| Selected bond length [Å] | |
|---|---|
| P1–P2 | 2.126(2) |
| P2–P3 | 2.1182(19) |
| Mo1–Br1 | 2.6863(6) |
| Mo1–Br2 | 2.6906(6) |
| Mo2–Br1 | 2.6706(7) |
| Mo2–Br2 | 2.6962(7) |
| Mo1–Mo2 | 2.5791(6) |
| P1···P3 | 3.4827(19) |

| Selected bond angles [°] | | | |
|---|---|---|---|
| P1–P2–P3 | 110.30(8) | Mo1–P1–Mo2 | 64.21(3) |
| Mo1–Br1–Mo2 | 57.559(16) | Mo1–P2–Mo2 | 58.36(3) |
| Mo1–Br2–Mo2 | 57.210(16) | Mo1–P3–Mo2 | 64.08(3) |

**Compound 5:**

The asymmetric unit contains one molecule of [(Cp*MoBr)$_2$(μ,η$^3$:η$^3$-P$_3$)(μ,η$^1$:η$^1$-P$_2$Br$_3$)].

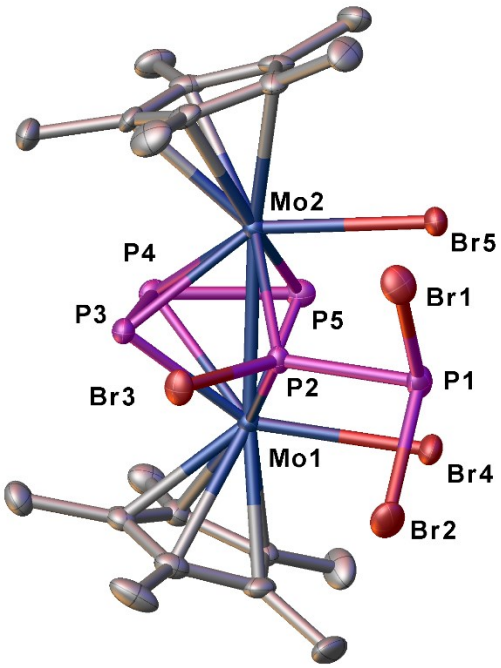


| Selected bond length [Å] | |
|---|---|
| P1–P2 | 2.260(2) |
| P1–Br1 | 2.2737(19) |
| P1–Br2 | 2.2829(18) |
| P2–Br3 | 2.2621(16) |
| P3–P4 | 2.174(2) |
| P4–P5 | 2.128(2) |
| P2···P5 | 3.715(2) |
| P2···P3 | 2.613(2) |
| Mo1-Mo2 | 2.9185(7) |

| Selected bond angles [°] | |
|---|---|
| Br1–P1–Br2 | 99.85(7) |
| Br1–P1–P2 | 96.57(7) |
| Br2–P1–P2 | 96.90(7) |
| P1–P2–Br3 | 103.69(7) |
| P3–P4–P5 | 107.51(8) |

**Compound 6:**

The asymmetric unit contains one molecule of [(Cp*Mo)$_2$(μ-PBr$_2$)(μ-PHBr)(μ-Br)$_2$]. The PBr$_2$ and PHBr ligand are disordered over two positions (0.99:0.01). The restraints DFIX, DANG and SIMU were used during the refinement of the disordered fragments.

**Part 1** **Part 2** **Part 1 und 2**

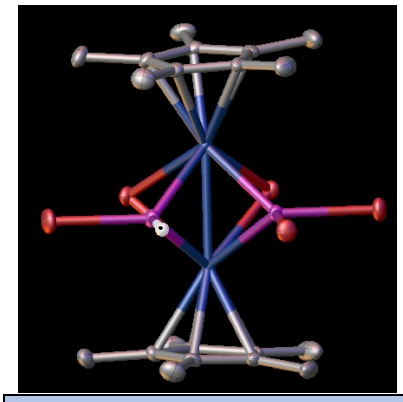
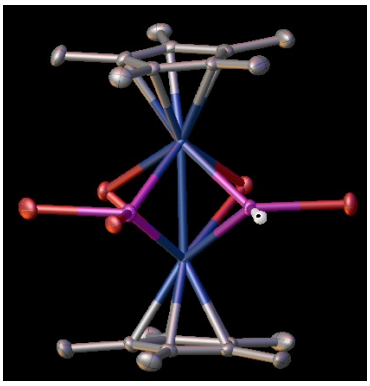
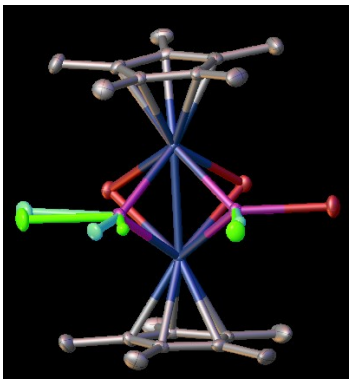

| Selected bond length [Å] | | | |
|---|---|---|---|
| P1–Br3 | 2.3089(7) | Mo2–Br2 | 2.6674(4) |
| P1–Br4A | 2.2522(7) | Mo1–P1 | 2.6763(4) |
| P2–Br5A | 2.2812(8) | Mo1–P2 | 2.3524(7) |
| Mo1–Br1 | 2.6683(4) | Mo2–P1 | 2.3595(8) |
| Mo1–Br2 | 2.6755(4) | Mo2–P2 | 2.3494(7) |
| P1···Br2 | 2.9954(10) | P1···P2 | 2.7618(9) |
| P2···Br1 | 3.0471(11) | Mo1-Mo2 | 2.7091(3) |

| Selected bond angles [°] | |
|---|---|
| Br3–P1–Br4A | 94.35(3) |
| Mo1–Br1–Mo2 | 61.025(9) |
| Mo1–Br2–Mo2 | 60.822(10) |
| Mo1–P1–Mo2 | 70.36(2) |
| Mo1–P2–Mo2 | 70.08(2) |

**Compound 8:**

The asymmetric unit contains one molecule of [{Cp*Mo}$_2$($\mu$-PCl$_2$)$_2$($\mu$,$\eta^{3:3}$-P$_3$)]$^+$, a $PCl_6^-$ anion and a $CH_2Cl_2$ solvent molecule. Additionally, one Mo atom is disordered over two positions (0.87:0.13).

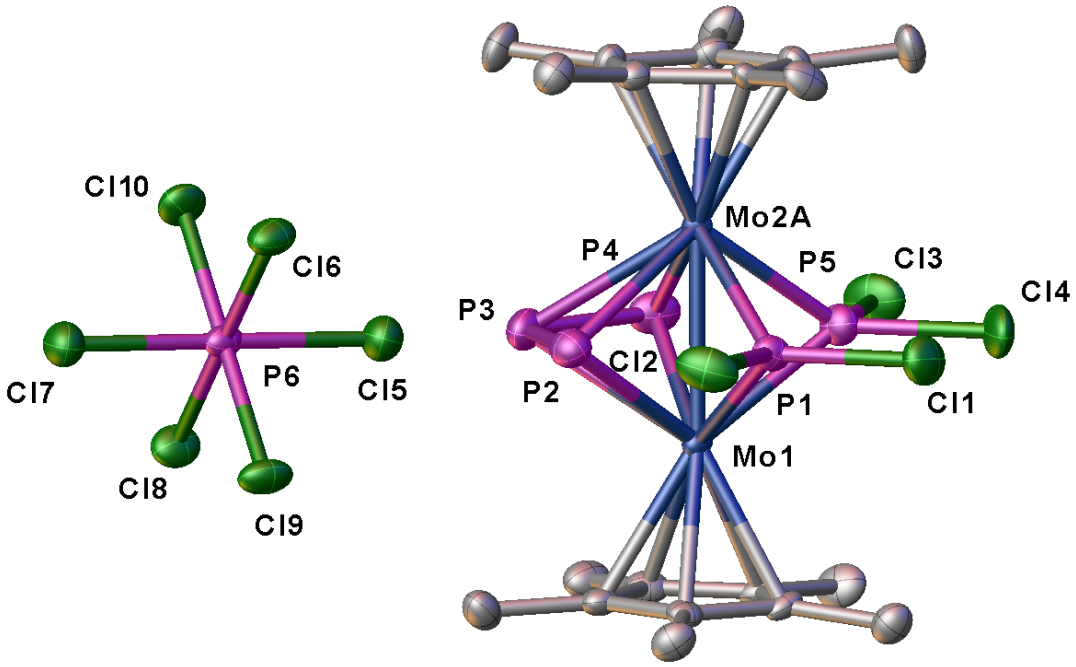


| Selected bond length [Å] | |
|---|---|
| P1–Cl1 | 2.039(3) |
| P1–Cl2 | 2.115(3) |
| P5–Cl3 | 2.071(3) |
| P5–Cl4 | 2.049(3) |
| P2–P3 | 2.105(4) |
| P3–P4 | 2.101(4) |
| Mo1–Mo2A | 2.728(2) |
| P2···P1 | 2.540(3) |
| P4···P5 | 2.554(4) |

| Selected bond angles [°] | |
|---|---|
| Cl1–P1–Cl2 | 91.12(14) |
| Cl3–P5–Cl4 | 91.64(16) |
| P2–P3–P4 | 114.48(15) |

**Compound 9:**

The asymmetric unit contains half a molecule of [(Cp*Mo)$_2$(μ-PCl$_2$)$_2$(μ-Cl)$_2$].

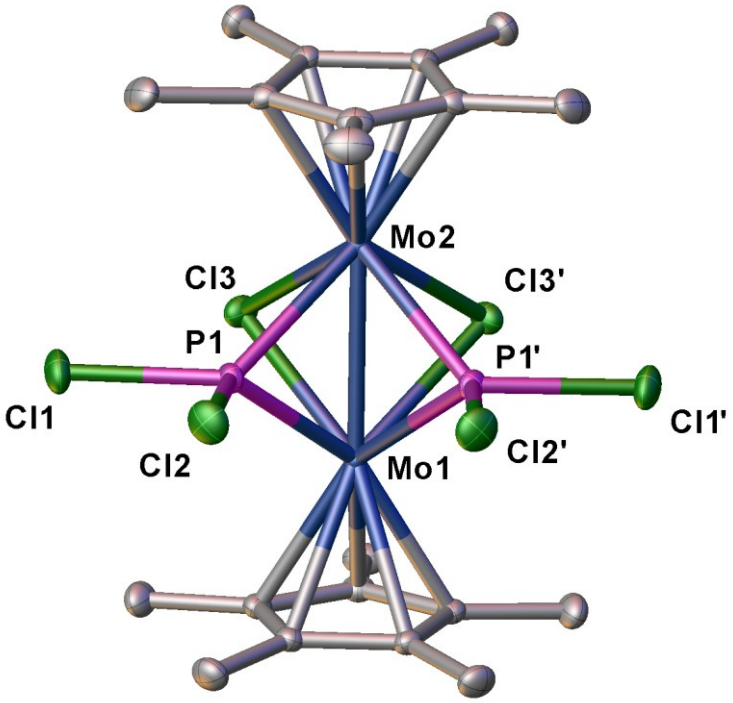


| Selected bond length [Å] | | Selected bond angles [°] | |
|---|---|---|---|
| P1–Cl1 | 2.1113(5) | Cl1–P1–Cl2 | 94.07(2) |
| P1–Cl2 | 2.0537(5) | Mo1–P1–Mo2 | 69.353(10) |
| Mo1–P1 | 2.3626(4) | Mo1–Cl3–Mo2 | 63.884(8) |
| Mo2–P1 | 2.3669(4) | Cl3–Mo1–Cl3’ | 70.765(16) |
| Mo1–Mo2 | 2.6908(2) | Cl3–Mo2–Cl3’ | 70.881(15) |
| Mo1–Cl3 | 2.5448(3) | P1–Mo1–P1’ | 75.537(17) |
| Mo2–Cl3 | 2.5412(3) | P1–Mo2–P1’ | 75.372(18) |
| P1···P1’ | 2.839(6) | P1-Mo1-Cl3 | 113.226(12) |
| Mo1-Mo2 | 2.6908(2) | Cl3-Mo1-Mo2 | 57.993(8) |

**Compound 10:**

The asymmetric unit contains half a molecule of [(Cp*MoCl)$_2$(μ,η$^3$:η$^3$-P$_3$)(μ-PCl$_2$)] and a molecule of toluene.

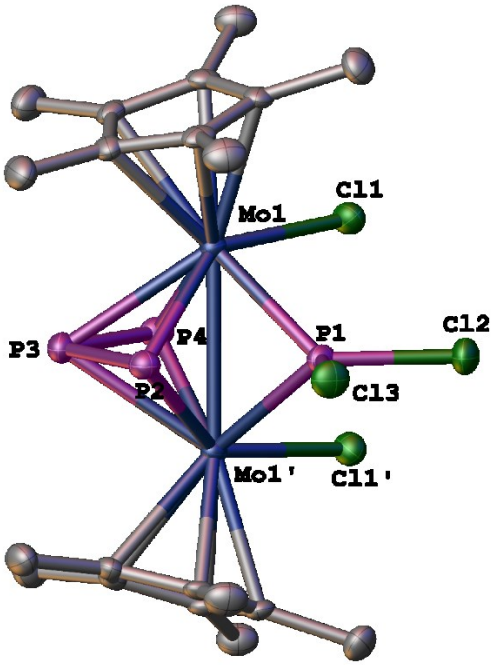


| Selected bond length [Å] | |
|---|---|
| Mo1-Mo1’ | 2.9195(6) |
| P2-P3 | 2.163(2) |
| P3–P4 | 2.123(2) |
| P1-Cl2 | 2.0653(18) |
| P1-Cl3 | 2.109(2) |
| Mo1-Cl1 | 2.4779(9) |
| P2···P1 | 2.5746(18) |
| P4···P1 | 3.727(2) |
| Mo1-Mo1’ | 2.9195(6) |

| Selected bond angles [°] | | | |
|---|---|---|---|
| P1-Mo1-Cl1 | 80.96(4) | Mo1–P3–Mo1’ | 68.04(3) |
| P2–P3–P4 | 107.78(8) | Mo1–P2–Mo1’ | 73.76(4) |
| Mo1–P1–Mo1’ | 75.21(4) | Cl2-P1-Cl3 | 93.70(8) |

**Compound 11:**

The asymmetric unit contains one molecule of [(Cp*Mo)$_2$(μ,η$^4$:η$^4$-P$_4$) (μ-PCl$_2$)]$^+$ and one molecule of [Cp*MoCl$_4$]$^-$.

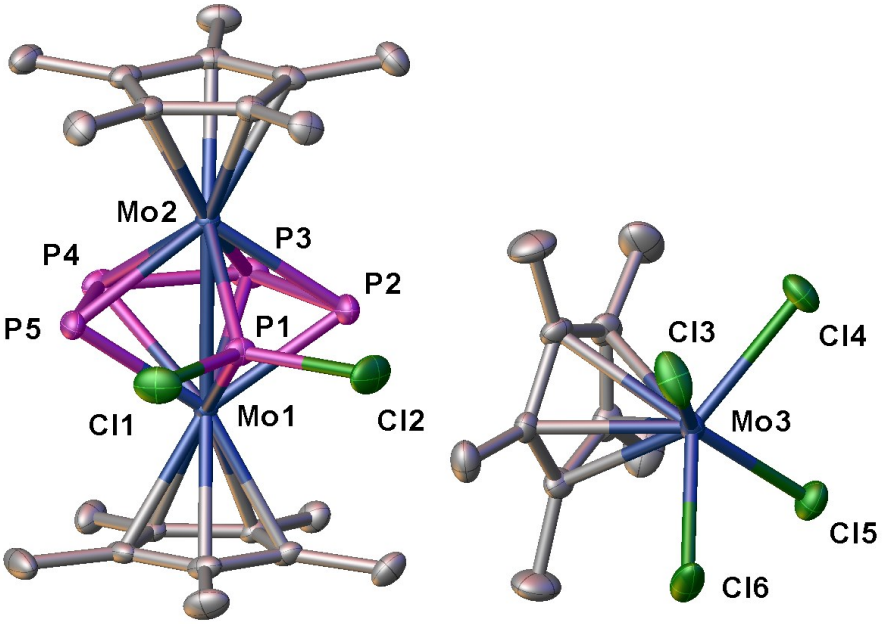


| Selected bond length [Å] | |
|---|---|
| P1–Cl1 | 2.0665(8) |
| P1–Cl1 | 2.0803(8) |
| P2–P3 | 2.2098(9) |
| P3–P4 | 2.1553(9) |
| P4–P5 | 2.1970(8) |
| P1···P2 | 2.6640(8) |
| P1···P5 | 2.6591(7) |
| Mo1-Mo2 | 2.7591(2) |

| Selected bond angles [°] | |
|---|---|
| Cl1–P1–Cl2 | 95.78(4) |
| P2–P3–P4 | 114.31(3) |
| P3–P4–P5 | 114.14(3) |

**Compound 12:**

The asymmetric unit contains one molecule of [(Cp*Mo)$_2$(μ,η$^4$:η$^4$-P$_4$)(μ-PCl$_2$)]. The middle deck is disordered over two positions with occupancies refined to 0.91 and 0.09. The restraints SADI and SIMU were used during the refinement of the disordered fragments.

**Part 1** **Part 2** **Part 1 und 2**

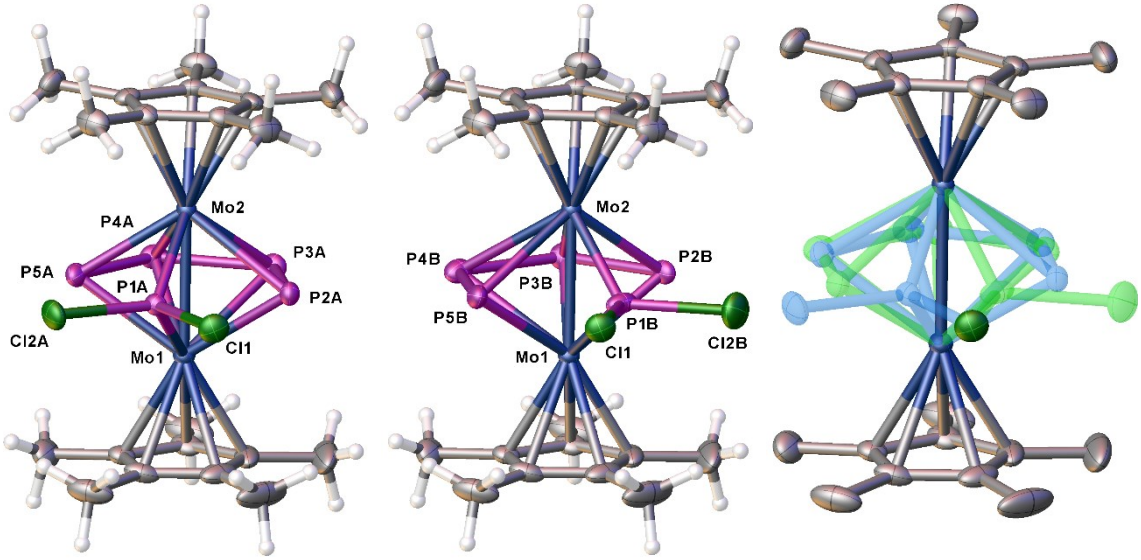


| Selected bond length [Å] | |
|---|---|
| P1A–Cl1 | 2.0945(15) |
| P1A–Cl2A | 2.1067(15) |
| P2A–P3A | 2.138(2) |
| P3A–P4A | 2.308(3) |
| P4A–P5A | 2.140(2) |
| P1A···P2A | 2.6806(15) |
| P1A···P5A | 2.694(2) |
| Mo1-Mo2 | 2.7577(5) |

| Selected bond angles [°] | |
|---|---|
| Cl1–P1A–Cl2A | 93.57(6) |
| P2A–P3A–P4A | 115.09(15) |
| P3A–P4A–P5A | 114.58(12) |

**Computational details**

The DFT calculations have been performed with the ORCA program.[20] The geometries have been optimised at the TPSSh[7]/def2-TZVP[8] level of theory starting from the X-ray coordinates. The dispersion effects have been incorporated by using the charge dependent atom-pairwise dispersion correction D4[9] as implemented in Orca. The solvation effects were incorporated via the CPCM model[10] using the dielectric constant of dichloromethane. For the geometry optimisations, the RIJCOSX[11] approximation has been used, followed by a single point calculation without the RIJCOX approximation. The NBO analysis has been performed with NBO6,[12] while the Interaction Region Indicator[13] (IRI) the Electron Localization Function (ELF)[14] and the Localized orbital locator (LOL)[15] were calculated with Multiwfn.[16]

**Table S 9.** Total energies of complexes **2-12** calculated at the D4-TPSSh(CPM)/def2-TZVP level of theory.

| Compound | Total energy (Hartree) |
|---|---|
| [(Cp*Mo)$_2$(μ,η$^3$:η$^3$-P$_3$)(μ,η$^1$:η$^1$:η$^1$-P$_3$I$_3$)]$^+$ (**2**) | -3858.615163657742 |
| [(Cp*Mo)$_2$(μ,η$^4$:η$^4$-P$_4$)(μ-PI$_2$)]$^+$ (**3**) – singlet spin state | -3219.542447874140 |
| [(Cp*Mo)$_2$(μ,η$^4$:η$^4$-P$_4$)(μ-PI$_2$)]$^+$ (**3**) – triplet spin state | -3219.503419774526 |
| [(Cp*Mo)$_2$(μ,η$^3$:η$^3$-P$_3$)(μ-Br)$_2$)]$^+$ (**4**) | -7089.619567989681 |
| [(Cp*MoBr)$_2$(μ,η$^3$:η$^3$-P$_3$)(μ,η$^1$:η$^1$-P(Br)PBr$_2$)]$^+$ (**5**) | -15494.912154220823 |
| [(Cp*Mo)$_2$(μ-Br)$_2$(μ-PBr$_2$)(μ-PHBr)] (**6**) | -14471.280442682093 |
| [(Cp*Mo)$_2$(μ,η$^3$:η$^3$-P$_3$)(μ,η$^1$:η$^1$:η$^1$-P$_3$Cl$_3$)]$^+$ (**7**) | -4346.430838269045 |
| [(Cp*Mo)$_2$(μ,η$^3$:η$^3$-P$_3$)(μ-PCl$_2$)$_2$]$^+$ (**8**) | -4465.265235764619 |
| [(Cp*Mo)$_2$(μ-PCl$_2$)$_2$(μ-Cl)$_2$] (**9**) | -4361.711040775027 |
| [(Cp*MoCl)$_2$(μ-PCl$_2$)] (**10**) | -4124.027482782973 |
| [(Cp*Mo)$_2$(μ,η$^4$:η$^4$-P$_4$)(μ-PCl$_2$)]$^+$ (**11**) – singlet spin state | -3544.754680973746 |
| [(Cp*Mo)$_2$(μ,η$^4$:η$^4$-P$_4$)(μ-PCl$_2$)]$^+$ (**11**) – triplet spin state | -3544.720554850667 |
| [(Cp*Mo)$_2$(μ,η$^4$:η$^4$-P$_4$)(μ-PCl$_2$)] (**12**) – doublet spin state | -3544.919441992913 |

## 4. SI Halogenation of the Hexaphosphabenzene Complex $[(Cp^*Mo)_2(\mu,\eta^6{:}\eta^6\text{-}P_6)]$ – Snapshots on the Reaction Progress

Cartesian coordinates od the optimizes geometry of $[(Cp^*Mo)_2(\mu,\eta^3{:}\eta^3\text{-}P_3)(\mu,\eta^1{:}\eta^1{:}\eta^1{:}\eta^1\text{-}P_3I_3)]^+$ (**2**) at the D4-TPSSh(CPCM)/def2-TZVP level of theory.

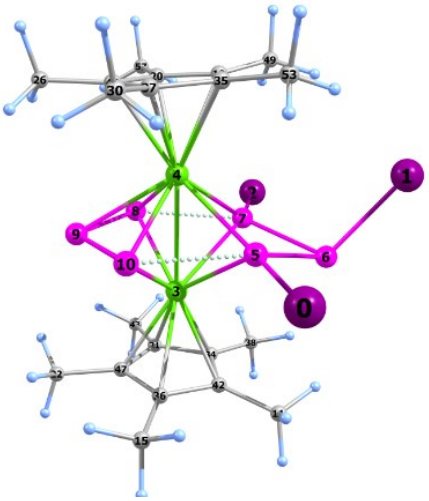

| Atom | x | y | z |
|---|---|---|---|
| I | 3.05730427541210 | 2.46937534685086 | 1.19129333843019 |
| I | 4.15821431275118 | 0.13684018530956 | -2.82167923350461 |
| I | 0.64518696249903 | -3.12598364619914 | -2.62477530466844 |
| Mo | 0.19899340404618 | -0.82493781811721 | 1.08279637489105 |
| Mo | -0.38974794555648 | 0.81666757058875 | -0.99555009790218 |
| P | 1.76797163957723 | 0.71238581385581 | 0.10133573703089 |
| P | 3.09022569216619 | -0.80602599052901 | -0.80240677289749 |
| P | 0.95036783976827 | -1.18521367187217 | -1.18488498557468 |
| P | -1.59234342252637 | -1.25337793599737 | -0.52447585160788 |
| P | -2.12191993082136 | 0.29663781047826 | 0.85236923618454 |
| P | -0.43152447276339 | 1.51787367207159 | 1.33905738109587 |
| C | 3.19852955527908 | -1.33366808063335 | 2.74707873603126 |
| H | 3.76650907884611 | -1.69172141074696 | 1.88886710071443 |
| H | 3.59925208183848 | -1.81958852849468 | 3.64261083763125 |
| H | 3.36465587113761 | -0.26116409902296 | 2.85025269465788 |
| C | 0.87656709695487 | 0.13679232753485 | 4.29062600808570 |
| H | 1.62986391566566 | 0.83513690076794 | 3.92404791119810 |
| H | 1.21184447940892 | -0.24065584617575 | 5.26217594905185 |
| H | -0.05304671747465 | 0.68512583460683 | 4.44205995009342 |
| C | -0.23691174550670 | 1.41304427437396 | -3.25194113758294 |
| C | -1.61261062642220 | 1.14294767233810 | -2.93949692366159 |
| C | -0.22326197691777 | -2.80869934372709 | 2.20923050994847 |
| C | -1.84057700532158 | -1.47041548165054 | 3.75639940139385 |
| H | -1.96314047157622 | -0.41683640828305 | 4.00861159091150 |
| H | -1.90601000022762 | -2.04798711255121 | 4.68425407323126 |
| H | -2.66906241278404 | -1.77336907817876 | 3.11591517601598 |
| C | -3.44968761375769 | 2.30203245942800 | -1.50939881670414 |
| H | -3.98995721117141 | 1.35563247822288 | -1.49060998630083 |
| H | -3.97977048405439 | 2.97747721372580 | -2.18886256481599 |
| H | -3.48023090651350 | 2.74152040507619 | -0.51218367746085 |
| C | -0.97436271295689 | 4.19802482497192 | -0.83464006124079 |
| H | -1.70412081259357 | 4.10360759894062 | -0.03008862290396 |
| H | -1.25874865130910 | 5.05772985620950 | -1.45022963382362 |
| H | -0.00076714146682 | 4.40735006638260 | -0.39062482981751 |
| C | 1.18247385103267 | -2.77210779339882 | 1.92638761449799 |
| C | 0.18075555574422 | 2.53506524834126 | -2.47780015052735 |
| C | 0.69085341618910 | -1.00455432523241 | 3.34352305803337 |
| C | -0.93452689726110 | 2.96842737846951 | -1.68352014865174 |
| C | 1.93708032199847 | -3.80660500387149 | 1.15713908648530 |
| H | 1.32346327720186 | -4.24652024395094 | 0.37135617236440 |
| H | 2.23987569070670 | -4.61081701083078 | 1.83571958496767 |
| H | 2.83903828789596 | -3.39489645597063 | 0.70304730996077 |
| C | 1.74565950738050 | -1.66037239759740 | 2.62419710704621 |
| C | -1.17290876470665 | -3.87935464855461 | 1.77742636098293 |
| H | -2.19629191749030 | -3.50609834073133 | 1.73224133349459 |
| H | -1.14554783927999 | -4.70698059811525 | 2.49334955587649 |
| H | -0.90755283251460 | -4.27322450718755 | 0.79620272497106 |
| C | -0.52003693940122 | -1.72996143563979 | 3.10586056981615 |
| C | -2.04818694196939 | 2.12368202337152 | -1.99412837343712 |
| C | 0.54222998895116 | 0.73363392916622 | -4.32850118320424 |
| H | 1.61353424376866 | 0.86060816758401 | -4.18718490372891 |
| H | 0.26976479435841 | 1.17183497006670 | -5.29435582828079 |
| H | 0.32281459868602 | -0.33350715390219 | -4.37395862234299 |
| C | 1.49708516961543 | 3.23650976093919 | -2.56283627078903 |
| H | 1.79708559419713 | 3.64598037431886 | -1.59777629255378 |
| H | 1.41751760196540 | 4.07069801184978 | -3.26726150709691 |
| H | 2.28327997635142 | 2.56965962221792 | -2.91295508140328 |
| C | -2.47850888000928 | 0.13176195030960 | -3.61798984396446 |
| H | -1.90116979854126 | -0.73837337262438 | -3.93131246196862 |
| H | -2.93279336335602 | 0.57626229359555 | -4.50967804937303 |
| H | -3.28267184514236 | -0.20730810217735 | -2.96432526730463 |

```
Mayer bond orders larger than 0.100000 for 2:
B(  0-I ,  5-P ) :   0.9775 B(  1-I ,  6-P ) :   1.0331 B(  2-I ,  7-P ) :   0.9743
B(  3-Mo,  4-Mo) :   0.7404 B(  3-Mo,  5-P ) :   0.7597 B(  3-Mo,  6-P ) :   0.1233
B(  3-Mo,  7-P ) :   0.7437 B(  3-Mo,  8-P ) :   0.8385 B(  3-Mo,  9-P ) :   0.6619
B(  3-Mo, 10-P ) :   0.9019 B(  3-Mo, 21-C ) :   0.3863 B(  3-Mo, 34-C ) :   0.4111
```

```
B(  3-Mo, 36-C ) :   0.3821 B(  3-Mo, 42-C ) :   0.4294 B(  3-Mo, 47-C ) :   0.4335
B(  4-Mo,  5-P ) :   0.7118 B(  4-Mo,  7-P ) :   0.7153 B(  4-Mo,  8-P ) :   0.9096
B(  4-Mo,  9-P ) :   0.6856 B(  4-Mo, 10-P ) :   0.8729 B(  4-Mo, 19-C ) :   0.4263
B(  4-Mo, 20-C ) :   0.3791 B(  4-Mo, 35-C ) :   0.4272 B(  4-Mo, 37-C ) :   0.3764
B(  4-Mo, 48-C ) :   0.4353 B(  5-P ,  6-P ) :   0.9045 B(  5-P , 10-P ) :   0.1616
B(  6-P ,  7-P ) :   0.9091 B(  7-P ,  8-P ) :   0.1767 B(  8-P ,  9-P ) :   0.8809
B(  8-P , 10-P ) :   0.1188 B(  9-P , 10-P ) :   0.8764 B( 11-C , 12-H ) :   0.9522
B( 11-C , 13-H ) :   0.9466 B( 11-C , 14-H ) :   0.9562 B( 11-C , 42-C ) :   1.0628

-------------------------   ----------------
Dispersion correction           -0.203305058
-------------------------   ----------------

-------------------------   --------------------
FINAL SINGLE POINT ENERGY     -3858.615163657742
-------------------------   --------------------
```

Cartesian coordinates od the optimizes geometry of [(Cp*Mo)$_2$(μ,η$^4$:η$^4$-P$_4$)(μ-PI$_2$)]$^+$ (**3**) in the singlet spin state, at the D4-TPSSh(CPCM)/def2-TZVP level of theory.

| Atom | x | y | z |
|---|---|---|---|
| Mo | 3.18034406468845 | 4.12333987092271 | 6.25601997569411 |
| Mo | 2.72540270081900 | 4.12334105418482 | 8.95056786650616 |
| P | 3.16193710592978 | 6.09777537889540 | 7.63594078466577 |
| P | 1.15633382181714 | 5.20730630963169 | 7.30002888894016 |
| P | 1.15673437655722 | 3.03895267957113 | 7.29922583013438 |
| P | 3.16242998061944 | 2.14896148485364 | 7.63624663938331 |
| P | 4.86350025619783 | 4.12372434351917 | 7.93256433035959 |
| I | 6.42301947786353 | 6.02944630340334 | 8.26083299515471 |
| I | 6.42372688550330 | 2.21860354092643 | 8.26115647311942 |
| C | 3.19127392486130 | 6.70531051046637 | 11.15347975477951 |
| H | 4.23324810390157 | 6.84844260200060 | 10.86577628829965 |
| H | 3.08644615344365 | 6.98829923128253 | 12.20601838054436 |
| H | 2.57662249589337 | 7.38312536852891 | 10.56107170852227 |
| C | 1.42239831230021 | 4.84031696743355 | 10.74580233442359 |
| C | 5.63699743386753 | 2.52923816956019 | 4.49251686605157 |
| H | 5.99189439961816 | 2.31856143283994 | 3.47837103808788 |
| H | 5.41226084534610 | 1.57773068225180 | 4.97493698445973 |
| H | 6.44857088658109 | 3.00791093372945 | 5.03941489615485 |
| C | 2.65193180548817 | 1.54076926306026 | 4.09530654056256 |
| H | 3.27504734982571 | 0.87611874268309 | 4.69442791853358 |
| H | 2.73807387848533 | 1.23048400072400 | 3.04907829052259 |
| H | 1.61418898090767 | 1.40845341179229 | 4.40342056667889 |
| C | 4.43080029838707 | 3.40479355021591 | 4.42655148432299 |
| C | 2.76334793043682 | 5.28500469814398 | 10.96871242228061 |
| C | 3.08776817679103 | 2.96244008499691 | 4.23638306161953 |
| C | 0.21433174008705 | 5.71480931361362 | 10.65000879729002 |
| H | -0.57173396431334 | 5.24767297461629 | 10.05629395826796 |
| H | 0.45538737763234 | 6.68073905280602 | 10.20570024001730 |
| H | -0.18547247231016 | 5.89545856334531 | 11.65322718605279 |
| C | 3.59161848754757 | 4.12316653631579 | 11.11173310511673 |
| C | 2.25211024779053 | 4.12322364281929 | 4.12752186070395 |
| C | 3.19088031192253 | 1.54115979796371 | 11.15348578128769 |
| H | 4.23198524599206 | 1.39714049069732 | 10.86314096301474 |
| H | 3.08847583477672 | 1.25907559858766 | 12.20650743399011 |
| H | 2.57434447126964 | 0.86277834498496 | 10.56360129934813 |
| C | 1.42229336350700 | 3.40653067606491 | 10.74579407212857 |
| C | 5.63650625868449 | 5.71835529196669 | 4.49177321928118 |
| H | 5.98885536914879 | 5.93129711618166 | 3.47718844232492 |
| H | 5.41156586752925 | 6.66888815514976 | 4.97605512997686 |
| H | 6.45001552186052 | 5.23942315657828 | 5.03566246726755 |
| C | 2.65217969095385 | 6.70600080504847 | 4.09545825975403 |
| H | 3.27679581376981 | 7.36991817642964 | 4.69378883906231 |
| H | 2.73747503650798 | 7.01612907213485 | 3.04910109571116 |
| H | 1.61476911808813 | 6.83914573643666 | 4.40445049292754 |
| C | 4.43073160826517 | 4.84200658944223 | 4.42648002386638 |
| C | 2.76311350047341 | 2.96150134426467 | 10.96861340722871 |
| C | 3.08756823247451 | 5.28416331509254 | 4.23627686549902 |
| C | 0.21393515715873 | 2.53252069564623 | 10.65014513543232 |
| H | -0.57336376454523 | 3.00187151766715 | 10.05988055557517 |
| H | 0.45323555879605 | 1.56786420085456 | 10.20214100343494 |

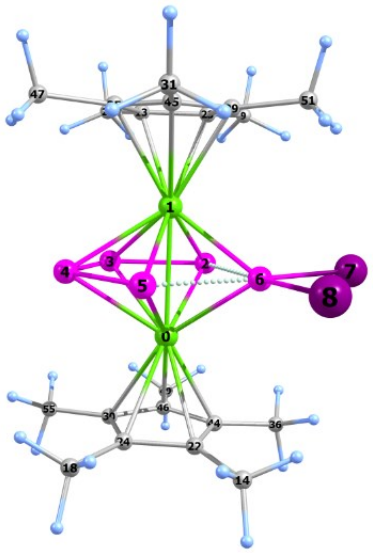

```
  H  -0.18368546835675      2.34884660193777     11.65367880315228
  C   5.03405592249309      4.12296901045063     11.49839626773964
  H   5.11588132826567      4.12381915879373     12.59015989856589
  H   5.54900658585608      3.23789865748482     11.12522025343785
  H   5.55007813286725      5.00674594956944     11.12361956943263
  C   0.78608348284851      4.12263959676999      3.83455998016957
  H   0.62650791380812      4.11916644899373      2.75171634226111
  H   0.29728209022719      3.24028135514505      4.24900506732116
  H   0.29806849779274      5.00804709452810      4.24324558755737


  Mayer bond orders larger than 0.100000 for 3 (singlet spin state)
B(  0-Mo,  1-Mo) :   0.7751 B(  0-Mo,  2-P ) :   0.9279 B(  0-Mo,  3-P ) :   0.6800
B(  0-Mo,  4-P ) :   0.6805 B(  0-Mo,  5-P ) :   0.9278 B(  0-Mo,  6-P ) :   0.7601
B(  0-Mo, 22-C ) :   0.4222 B(  0-Mo, 24-C ) :   0.3518 B(  0-Mo, 30-C ) :   0.4483
B(  0-Mo, 44-C ) :   0.4226 B(  0-Mo, 46-C ) :   0.3515 B(  1-Mo,  2-P ) :   0.9057
B(  1-Mo,  3-P ) :   0.6988 B(  1-Mo,  4-P ) :   0.6983 B(  1-Mo,  5-P ) :   0.9058
B(  1-Mo,  6-P ) :   0.6930 B(  1-Mo, 13-C ) :   0.4009 B(  1-Mo, 23-C ) :   0.3985
B(  1-Mo, 29-C ) :   0.4156 B(  1-Mo, 35-C ) :   0.4009 B(  1-Mo, 45-C ) :   0.3986
B(  2-P ,  3-P ) :   0.7379 B(  2-P ,  6-P ) :   0.1658 B(  2-P ,  7-I ) :   0.1114
B(  3-P ,  4-P ) :   0.8643 B(  4-P ,  5-P ) :   0.7379 B(  5-P ,  6-P ) :   0.1657
B(  5-P ,  8-I ) :   0.1113 B(  6-P ,  7-I ) :   0.9321 B(  6-P ,  8-I ) :   0.9319


-------------------------   ----------------
Dispersion correction           -0.180619340
-------------------------   ----------------


-------------------------   --------------------
FINAL SINGLE POINT ENERGY     -3219.542447874140
-------------------------   --------------------
```

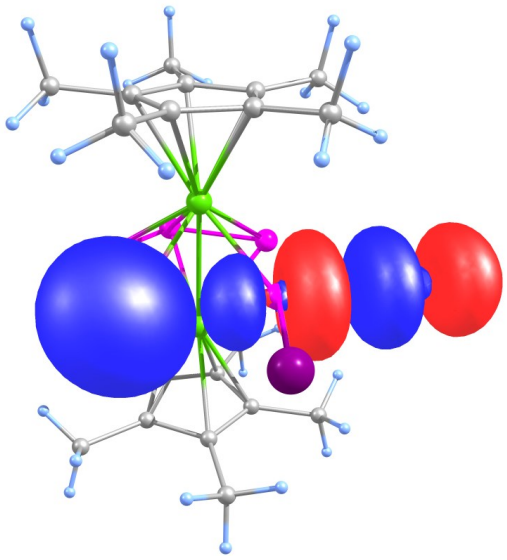

**Figure S 40.** Natural bonding orbitals in **3** (lone pair P3 and σ* P-I; superimposed) showing the Lp(P3) → σ*(P-I) delocalization resulting in a P···P bonding interaction and weakening of the P-I bond.

## 4. SI Halogenation of the Hexaphosphabenzene Complex $[(Cp^*Mo)_2(\mu,\eta^6{:}\eta^6\text{-}P_6)]$ – Snapshots on the Reaction Progress

Cartesian coordinates od the optimizes geometry of $[(Cp^*Mo)_2(\mu,\eta^3{:}\eta^3\text{-}P_3)(\mu\text{-}Br)_2)]^+$ (**4**) at the D4-TPSSh(CPCM)/def2-TZVP level of theory.

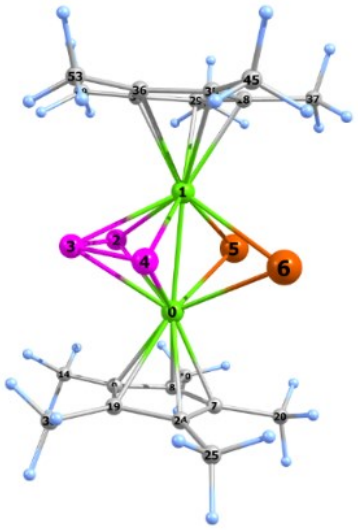

| Atom | x | y | z |
|---|---|---|---|
| Mo | 0.58482676804870 | 0.49368164559114 | -1.03388950978103 |
| Mo | -0.56194859792598 | -0.53069779078510 | 1.02970870510579 |
| P | 1.42251927059420 | 0.84238214571976 | 1.21470074606679 |
| P | -0.29355003358854 | 2.04626653315407 | 0.85220542878142 |
| P | -1.68495143726353 | 1.04788339628730 | -0.41305031499714 |
| Br | 1.63467522052073 | -1.74312188231253 | 0.03506158091389 |
| Br | -1.14108699712070 | -1.55777514046717 | -1.39756114440616 |
| C | 1.46093944311350 | 0.32217005507100 | -3.15260361663166 |
| C | 2.50901982418767 | 0.84588721617657 | -2.32883198251156 |
| C | 2.08813600977080 | 2.10769719149413 | -1.82091121900511 |
| C | 3.83646288735890 | 0.21122697136731 | -2.07380781182449 |
| H | 4.17575371400567 | 0.39246385651715 | -1.05329640166591 |
| H | 4.57654416200709 | 0.64360130137879 | -2.75488142658577 |
| H | 3.80711864303894 | -0.86413383581460 | -2.24650204366193 |
| C | 2.90835650394420 | 3.04057584708650 | -0.99294501120338 |
| H | 2.28116166259051 | 3.65444270584741 | -0.34488531428098 |
| H | 3.47205630655158 | 3.71142654750762 | -1.64917593854965 |
| H | 3.62074914020143 | 2.49803758661204 | -0.37113017216602 |
| C | -1.45904710462071 | -2.31536174951384 | 2.16352587227596 |
| C | 0.78980043845706 | 2.39411817277363 | -2.36768308538679 |
| C | 1.51792444632985 | -0.94727870677963 | -3.94398200837353 |
| H | 2.04351830834353 | -1.73297473862573 | -3.40051808119701 |
| H | 2.05146472257117 | -0.77168196191687 | -4.88317835963398 |
| H | 0.51874511778912 | -1.30840085509925 | -4.18639008722038 |
| C | 0.40173353587820 | 1.29714008458247 | -3.19149896957716 |
| C | -0.83402448770925 | 1.21600891466729 | -4.02667153444390 |
| H | -1.16124585173003 | 0.18423079497450 | -4.15560686308789 |
| H | -0.63276294734122 | 1.63272604188792 | -5.01873686093873 |
| H | -1.65072855726419 | 1.78322977958177 | -3.58005020674954 |
| C | -0.44159459131222 | -1.76679358957977 | 3.01105091032489 |
| C | 0.04974654360062 | 3.68047796723589 | -2.20775341022402 |
| H | -1.02304141153141 | 3.54602371101637 | -2.34704554102203 |
| H | 0.40437259779787 | 4.39388798317999 | -2.95836892815896 |
| H | 0.21967509588696 | 4.12207878540826 | -1.22480292248689 |
| C | -0.81943915145988 | -0.43756788929556 | 3.35463439851026 |
| C | -2.49572516889349 | -1.32723507535700 | 2.02221008985495 |
| C | -2.09506729642219 | -0.16775683779467 | 2.74799170147171 |
| C | -1.49783246770716 | -3.71635426670611 | 1.63956787920787 |
| H | -2.12772991938402 | -3.79194522653661 | 0.75381843189158 |
| H | -1.90793081526740 | -4.38338866603030 | 2.40416770445018 |
| H | -0.50001149922624 | -4.07289145477984 | 1.38178816591702 |
| C | 0.78142810517198 | -2.47822420744154 | 3.48805925914073 |
| H | 1.10522624567131 | -3.23797002213240 | 2.77736745481871 |
| H | 0.56048293559180 | -2.97878687258822 | 4.43663378789767 |
| H | 1.60526550784395 | -1.78447400696885 | 3.65671701224946 |
| C | -3.79934184662447 | -1.51763637879086 | 1.31849440230114 |
| H | -4.19595663235728 | -0.56926085797707 | 0.95517599368898 |
| H | -4.52775231836241 | -1.94882468590918 | 2.01277200457999 |
| H | -3.70020339169511 | -2.19653833485586 | 0.47163705440523 |
| C | -0.10105080843107 | 0.46810132549169 | 4.29863673674344 |
| H | 0.96805451086454 | 0.25659601226107 | 4.31877437435657 |
| H | -0.49611097065945 | 0.32382135441641 | 5.30930366715016 |
| H | -0.23982116431779 | 1.51642213886063 | 4.03044265650687 |
| C | -2.90803113360465 | 1.06758031726789 | 2.95395436126611 |
| H | -2.27373028248798 | 1.93719565067685 | 3.13046368821541 |
| H | -3.54957221080689 | 0.93770606297454 | 3.83127567065373 |
| H | -3.54776857261664 | 1.27503693699052 | 2.09566902702504 |

| | |
|---|---|
| Dispersion correction | -0.152926303 |
| FINAL SINGLE POINT ENERGY | -7089.619567989681 |

Mayer bond orders larger than 0.100000 for **4**.

B( 0-Mo, 1-Mo) : 0.8737 B( 0-Mo, 2-P ) : 0.9434 B( 0-Mo, 3-P ) : 0.6854

```
B(  0-Mo,  4-P ) :   0.9588 B(  0-Mo,  5-Br) :   0.6749 B(  0-Mo,  6-Br) :   0.6648
B(  0-Mo,  7-C ) :   0.5169 B(  0-Mo,  8-C ) :   0.3367 B(  0-Mo,  9-C ) :   0.3913
B(  0-Mo, 19-C ) :   0.4631 B(  0-Mo, 24-C ) :   0.3211 B(  1-Mo,  2-P ) :   0.9532
B(  1-Mo,  3-P ) :   0.6826 B(  1-Mo,  4-P ) :   0.9483 B(  1-Mo,  5-Br) :   0.6716
B(  1-Mo,  6-Br) :   0.6816 B(  1-Mo, 18-C ) :   0.5184 B(  1-Mo, 29-C ) :   0.3316
B(  1-Mo, 34-C ) :   0.3983 B(  1-Mo, 35-C ) :   0.3152 B(  1-Mo, 36-C ) :   0.4600
B(  2-P ,  3-P ) :   0.8991 B(  2-P ,  4-P ) :   0.1179 B(  3-P ,  4-P ) :   0.9018
B(  7-C ,  8-C ) :   1.0683 B(  7-C , 20-C ) :   1.0483 B(  7-C , 24-C ) :   0.9839
```

Cartesian coordinates od the optimizes geometry of [(Cp*MoBr)$_2$(μ,η$^3$:η$^3$-P$_3$)(μ,η$^1$:η$^1$-P(Br)PBr$_2$)]$^+$ (**5**) at the D4-TPSSh(CPCM)/def2-TZVP level of theory.

| Atom | x | y | z |
|---|---|---|---|
| Mo | 0.99340901328238 | -1.03852729085328 | -0.10971302311304 |
| Mo | -1.05123198630758 | 0.98387716218962 | 0.19264998424470 |
| P | 0.85878425999223 | 1.06288647522866 | -1.25901950582520 |
| P | 0.49701013646225 | 1.07733295032764 | -3.50243495890386 |
| P | -1.35819143180557 | -1.42358316665346 | 0.36942832077316 |
| P | -0.33154209819917 | -0.62624473061096 | 2.04470137702163 |
| P | 1.07050251638773 | 0.88639112142324 | 1.31999547258944 |
| Br | 2.48647936299255 | 2.62912026732112 | -0.93915778702669 |
| Br | 0.23310668173012 | 3.35683072421245 | -3.69054467638279 |
| Br | 2.69729722581492 | 0.90847850189690 | -4.13561944301851 |
| Br | 0.29578503199669 | -1.75386187116388 | -2.56551381331926 |
| Br | -2.15946103507514 | 0.60775802481503 | -2.18998382923621 |
| C | 3.00892612280945 | -2.12783776231467 | -0.77198675291291 |
| C | 2.09252754680863 | -3.16437561962659 | -0.35940994510723 |
| C | 3.30509354984635 | -1.33492904630411 | 0.36595535357124 |
| C | -1.31720913186446 | 3.24389301870640 | 0.90017963197826 |
| C | -3.21143962659197 | 1.96527085253519 | 0.53359345188852 |
| C | -2.69835593003752 | 1.60506753106227 | 1.79853379525516 |
| C | 2.73499748359370 | -1.45135324642409 | 2.89459789778173 |
| H | 2.95383355214132 | -0.38721110433315 | 2.99626771068107 |
| H | 3.58200742845299 | -2.00911092005901 | 3.30771850909011 |
| H | 1.85550856320395 | -1.68417760875578 | 3.49577638897349 |
| C | -1.51212551925143 | 2.38442954360910 | 2.02701045723308 |
| C | -0.26824074075503 | 4.29828743077468 | 0.78448927982735 |
| H | 0.65532695233378 | 3.99501619980527 | 1.27828300704989 |
| H | -0.62137434964916 | 5.21921951459050 | 1.26067186935844 |
| H | -0.03918426683111 | 4.51879001157813 | -0.25747349733308 |
| C | 0.97919287744918 | -3.89123436836007 | 1.86903869829578 |
| H | 0.47413117786155 | -3.34194526065507 | 2.66535533564859 |
| H | 1.62511929090953 | -4.64106803369828 | 2.33787113748797 |
| H | 0.22387157323060 | -4.41267662128854 | 1.28096637633855 |
| C | -4.52128037797848 | 1.51998469952765 | -0.02600813801504 |
| H | -4.56298545005721 | 1.66531167167449 | -1.10396498059472 |
| H | -5.32057997740648 | 2.11338702071205 | 0.43173855755588 |
| H | -4.71516586003430 | 0.46907922753329 | 0.19211257931313 |
| C | 4.32459730557917 | -0.24936255961386 | 0.45218496840517 |
| H | 4.49260886291120 | 0.21992843396498 | -0.51558897733976 |
| H | 5.27339999211808 | -0.67342069994931 | 0.79839535388571 |
| H | 4.02455289071636 | 0.52473891920908 | 1.15964722001359 |
| C | -3.35030163733471 | 0.69060952246968 | 2.78284036710818 |
| H | -3.90485291732933 | -0.10248164472181 | 2.28075606837087 |
| H | -4.05379928906643 | 1.26171608799459 | 3.39812840997670 |
| H | -2.62084308379349 | 0.23105679606422 | 3.45151987956684 |
| C | 1.79883101224259 | -2.98345741583732 | 1.01100281216921 |
| C | -2.35317618143995 | 2.98377887632098 | -0.02890601572123 |
| C | 3.69004426067052 | -2.05393803485136 | -2.09678445219639 |
| H | 2.98477170498679 | -2.20939694903919 | -2.91348727512335 |
| H | 4.45940174223543 | -2.83134725710197 | -2.15451658258175 |
| H | 4.16977883926489 | -1.08722672994920 | -2.24008423497781 |
| C | 2.55137585390703 | -1.84770306121490 | 1.46742260751745 |
| C | -0.78780795747948 | 2.48354255945332 | 3.32790303756307 |
| H | -0.71264308933716 | 1.51565652704822 | 3.82703217020251 |
| H | -1.33940966577689 | 3.15947795074479 | 3.98962454765709 |
| H | 0.21803615309282 | 2.88332390736291 | 3.19977599671575 |
| C | 1.67967348318054 | -4.34139814072164 | -1.17746012582435 |
| H | 0.63877525925826 | -4.61387453484194 | -0.99928697318987 |

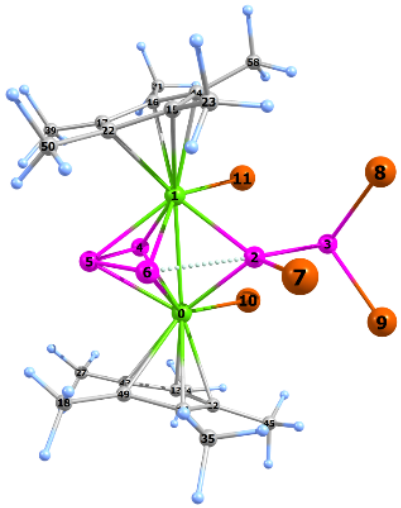

```
  H    2.30515494970453     -5.19583064703856     -0.89543761355202
  H    1.81396525015304     -4.15455276007379     -2.24084996299522
  C   -2.64843059838357      3.78877223409968     -1.24890279725865
  H   -1.74619733017319      4.24720341233936     -1.65026792640409
  H   -3.35149472646222      4.58641708674868     -0.98504132784662
  H   -3.09845364890012      3.17919282271152     -2.03112401530975

-------------------------   ----------------
Dispersion correction           -0.206600581
-------------------------   ----------------

-------------------------   --------------------
FINAL SINGLE POINT ENERGY    -15494.912154220823
-------------------------   --------------------


  Mayer bond orders larger than 0.100000 for 5.
B(  0-Mo,  1-Mo) :   0.5891 B(  0-Mo,  2-P ) :   0.8398 B(  0-Mo,  4-P ) :   0.9691
B(  0-Mo,  5-P ) :   0.6767 B(  0-Mo,  6-P ) :   0.9011 B(  0-Mo, 10-Br) :   0.8743
B(  0-Mo, 12-C ) :   0.4492 B(  0-Mo, 13-C ) :   0.3791 B(  0-Mo, 14-C ) :   0.2761
B(  0-Mo, 43-C ) :   0.3204 B(  0-Mo, 49-C ) :   0.5027 B(  1-Mo,  2-P ) :   0.8196
B(  1-Mo,  4-P ) :   0.9656 B(  1-Mo,  5-P ) :   0.6951 B(  1-Mo,  6-P ) :   0.8836
B(  1-Mo, 11-Br) :   0.8670 B(  1-Mo, 15-C ) :   0.2651 B(  1-Mo, 16-C ) :   0.3656
B(  1-Mo, 17-C ) :   0.3481 B(  1-Mo, 22-C ) :   0.4900 B(  1-Mo, 44-C ) :   0.4587
B(  2-P ,  3-P ) :   0.8476 B(  2-P ,  6-P ) :   0.1695 B(  2-P ,  7-Br) :   0.8876
B(  3-P ,  8-Br) :   0.9695 B(  3-P ,  9-Br) :   0.9756 B(  3-P , 10-Br) :   0.1740
B(  3-P , 11-Br) :   0.1700 B(  4-P ,  5-P ) :   0.9248 B(  5-P ,  6-P ) :   0.7803
B( 12-C , 13-C ) :   0.9568 B( 12-C , 14-C ) :   1.0776 B( 12-C , 45-C ) :   1.0264
```

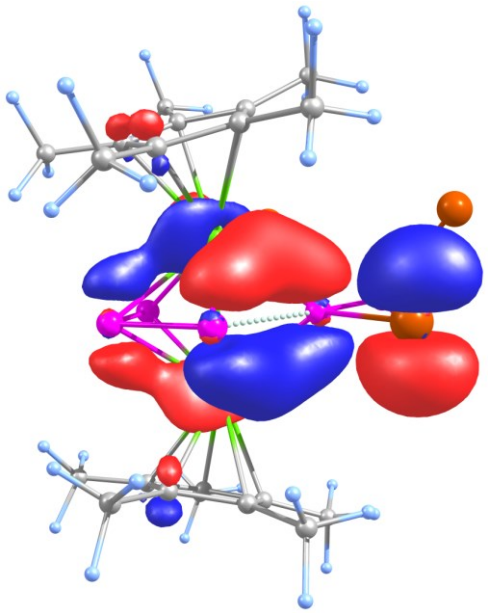

**Figure S 41.** The molecular orbital (MO: HOMO-6) representing the P···P interaction. Loewdin population: 26% Mo, 12% P2, 5% P5, 12% P6, 22% Br7.

## 4. SI Halogenation of the Hexaphosphabenzene Complex $[(Cp^*Mo)_2(\mu,\eta^6{:}\eta^6\text{-}P_6)]$ – Snapshots on the Reaction Progress

Cartesian coordinates od the optimizes geometry of $[(Cp^*Mo)_2(\mu\text{-}Br)_2(\mu\text{-}PBr_2)(\mu\text{-}PHBr)]$ (**6**), at the D4-TPSSh(CPCM)/def2-TZVP level of theory.

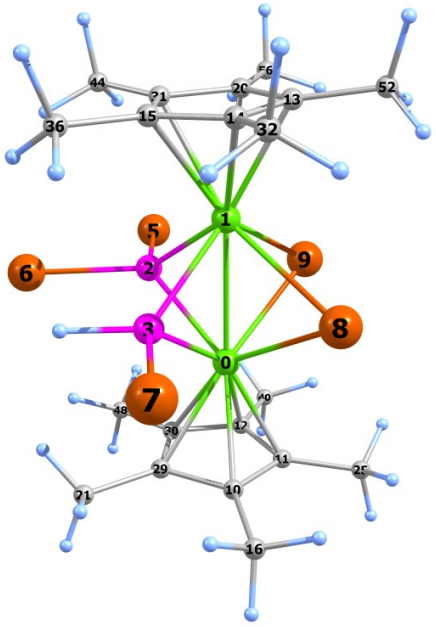

| Atom | x | y | z |
|---|---|---|---|
| Mo | 8.484968000 | 7.323383000 | 7.844388000 |
| Mo | 8.891815000 | 4.658102000 | 7.570915000 |
| P | 7.485079000 | 5.654614000 | 9.153149000 |
| P | 7.236451000 | 5.900610000 | 6.434550000 |
| H | 5.861535000 | 5.675194000 | 6.584940000 |
| Br | 7.789117000 | 5.477200000 | 11.445888000 |
| Br | 5.246164000 | 5.291448000 | 9.236817000 |
| Br | 7.082112000 | 6.068137000 | 4.135633000 |
| Br | 10.212891000 | 6.397565000 | 6.005554000 |
| Br | 10.474797000 | 6.118195000 | 9.166991000 |
| C | 8.110372000 | 9.307241000 | 6.844370000 |
| C | 9.197150000 | 9.469708000 | 7.782507000 |
| C | 8.666806000 | 9.259338000 | 9.098185000 |
| C | 10.201993000 | 2.870970000 | 7.134792000 |
| C | 9.116140000 | 2.891078000 | 6.184241000 |
| C | 7.893429000 | 2.687350000 | 6.908013000 |
| C | 8.166502000 | 9.565004000 | 5.372989000 |
| H | 9.165361000 | 9.379879000 | 4.977600000 |
| H | 7.903871000 | 10.607613000 | 5.163224000 |
| H | 7.470080000 | 8.923756000 | 4.833807000 |
| C | 9.633829000 | 2.655287000 | 8.435007000 |
| C | 5.540841000 | 8.856980000 | 7.056413000 |
| H | 5.551651000 | 8.560132000 | 6.007259000 |
| H | 5.015264000 | 9.814577000 | 7.133741000 |
| H | 4.971157000 | 8.114590000 | 7.616367000 |
| C | 10.595685000 | 9.897188000 | 7.463255000 |
| H | 11.312156000 | 9.444040000 | 8.149369000 |
| H | 10.689861000 | 10.984968000 | 7.549148000 |
| H | 10.873799000 | 9.611780000 | 6.448586000 |
| C | 6.927116000 | 8.994359000 | 7.597637000 |
| C | 7.275175000 | 8.977978000 | 8.981745000 |
| C | 8.219946000 | 2.530265000 | 8.288528000 |
| C | 9.269810000 | 2.944220000 | 4.699047000 |
| H | 8.355968000 | 3.291648000 | 4.219227000 |
| H | 9.503418000 | 1.944838000 | 4.315768000 |
| H | 10.079227000 | 3.613266000 | 4.406606000 |
| C | 6.528934000 | 2.537681000 | 6.314028000 |
| H | 5.763127000 | 2.928862000 | 6.984976000 |
| H | 6.311712000 | 1.479891000 | 6.131357000 |
| H | 6.451862000 | 3.066458000 | 5.363741000 |
| C | 9.414358000 | 9.383072000 | 10.386248000 |
| H | 9.057319000 | 8.659903000 | 11.119961000 |
| H | 9.270542000 | 10.386455000 | 10.800944000 |
| H | 10.483354000 | 9.226697000 | 10.242682000 |
| C | 7.265323000 | 2.168971000 | 9.377276000 |
| H | 7.562021000 | 2.603621000 | 10.332134000 |
| H | 7.248342000 | 1.080092000 | 9.493805000 |
| H | 6.253691000 | 2.499523000 | 9.146514000 |
| C | 6.325015000 | 8.814818000 | 10.120188000 |
| H | 5.464886000 | 8.208825000 | 9.838178000 |
| H | 5.957789000 | 9.799986000 | 10.427514000 |
| H | 6.807603000 | 8.351606000 | 10.980567000 |
| C | 11.657740000 | 2.922821000 | 6.793960000 |
| H | 11.841810000 | 3.583716000 | 5.946631000 |
| H | 12.016959000 | 1.923630000 | 6.524421000 |
| H | 12.249052000 | 3.280160000 | 7.637388000 |
| C | 10.381363000 | 2.515295000 | 9.722854000 |
| H | 11.345070000 | 3.022030000 | 9.679455000 |
| H | 10.563629000 | 1.456838000 | 9.937400000 |
| H | 9.812110000 | 2.935945000 | 10.552484000 |

| | |
|---|---|
| Dispersion correction | -0.173759119 |

| | |
|---|---|
| FINAL SINGLE POINT ENERGY | -14471.280442682093 |

```
-------------------------   --------------------


  Mayer bond orders larger than 0.100000
B(  0-Mo,  1-Mo) :   0.8348 B(  0-Mo,  2-P ) :   0.8869 B(  0-Mo,  3-P ) :   0.9467
B(  0-Mo,  8-Br) :   0.6802 B(  0-Mo,  9-Br) :   0.6652 B(  0-Mo, 10-C ) :   0.4026
B(  0-Mo, 11-C ) :   0.4589 B(  0-Mo, 12-C ) :   0.4150 B(  0-Mo, 29-C ) :   0.4639
B(  0-Mo, 30-C ) :   0.3493 B(  1-Mo,  2-P ) :   0.8871 B(  1-Mo,  3-P ) :   0.9428
B(  1-Mo,  8-Br) :   0.6704 B(  1-Mo,  9-Br) :   0.6593 B(  1-Mo, 13-C ) :   0.4584
B(  1-Mo, 14-C ) :   0.4017 B(  1-Mo, 15-C ) :   0.4525 B(  1-Mo, 20-C ) :   0.4136
B(  1-Mo, 31-C ) :   0.3588 B(  2-P ,  5-Br) :   0.8144 B(  2-P ,  6-Br) :   0.9005
B(  2-P , 30-C ) :   0.1033 B(  2-P , 31-C ) :   0.1035 B(  3-P ,  4-H ) :   0.8869
B(  3-P ,  7-Br) :   0.8439 B(  3-P ,  8-Br) :  -0.1024 B( 10-C , 11-C ) :   1.0214


********************************** NBO 6.0 **********************************

   (Occupancy)   Bond orbital / Coefficients / Hybrids

129. (1.67423) BD ( 1)Mo  1-Mo  2
               ( 44.93%)   0.6703*Mo  1 s( 14.14%)p 0.06(  0.87%)d 6.00( 84.82%)
               ( 55.07%)   0.7421*Mo  2 s(  7.51%)p 0.01(  0.09%)d12.30( 92.39%)
130. (1.74464) BD ( 1)Mo  1- P  3
               ( 33.36%)   0.5776*Mo  1 s( 16.75%)p 0.13(  2.26%)d 4.81( 80.58%)
               ( 66.64%)   0.8163* P  3 s( 37.51%)p 1.65( 62.01%)d 0.01(  0.45%)
131. (1.77019) BD ( 1)Mo  1- P  4
               ( 35.81%)   0.5984*Mo  1 s( 26.91%)p 0.04(  0.97%)d 2.67( 71.92%)
               ( 64.19%)   0.8012* P  4 s( 32.69%)p 2.04( 66.76%)d 0.02(  0.53%)
132. (1.68282) BD ( 1)Mo  1-Br  9
               ( 18.73%)   0.4328*Mo  1 s( 24.28%)p 0.06(  1.42%)d 3.04( 73.89%)
               ( 81.27%)   0.9015*Br  9 s( 24.70%)p 3.04( 75.07%)d 0.01(  0.22%)
133. (1.67643) BD ( 1)Mo  1-Br 10
               ( 19.56%)   0.4423*Mo  1 s( 15.92%)p 0.10(  1.60%)d 5.15( 82.02%)
               ( 80.44%)   0.8969*Br 10 s( 25.37%)p 2.93( 74.38%)d 0.01(  0.23%)
134. (1.86548) BD ( 1)Mo  2- P  3
               ( 41.25%)   0.6422*Mo  2 s( 10.19%)p 0.01(  0.09%)d 8.80( 89.69%)
               ( 58.75%)   0.7665* P  3 s( 37.74%)p 1.64( 61.78%)d 0.01(  0.45%)
135. (1.85878) BD ( 1)Mo  2- P  4
               ( 42.12%)   0.6490*Mo  2 s( 12.68%)p 0.00(  0.06%)d 6.88( 87.23%)
               ( 57.88%)   0.7608* P  4 s( 32.03%)p 2.10( 67.40%)d 0.02(  0.54%)
136. (1.96268) BD ( 1) P  3-Br  6
               ( 35.56%)   0.5963* P  3 s( 11.41%)p 7.63( 87.10%)d 0.12(  1.43%)
               ( 64.44%)   0.8027*Br  6 s( 13.36%)p 6.46( 86.28%)d 0.03(  0.34%)
137. (1.96382) BD ( 1) P  3-Br  7
               ( 36.13%)   0.6011* P  3 s( 13.14%)p 6.49( 85.25%)d 0.12(  1.54%)
               ( 63.87%)   0.7992*Br  7 s( 14.08%)p 6.07( 85.48%)d 0.03(  0.42%)
138. (1.97172) BD ( 1) P  4- H  5
               ( 51.84%)   0.7200* P  4 s( 24.95%)p 2.97( 74.21%)d 0.03(  0.82%)
               ( 48.16%)   0.6940* H  5 s( 99.56%)p 0.00(  0.44%)
139. (1.97243) BD ( 1) P  4-Br  8
               ( 34.33%)   0.5859* P  4 s( 10.15%)p 8.71( 88.45%)d 0.13(  1.32%)
               ( 65.67%)   0.8104*Br  8 s( 13.55%)p 6.35( 86.13%)d 0.02(  0.29%)
```

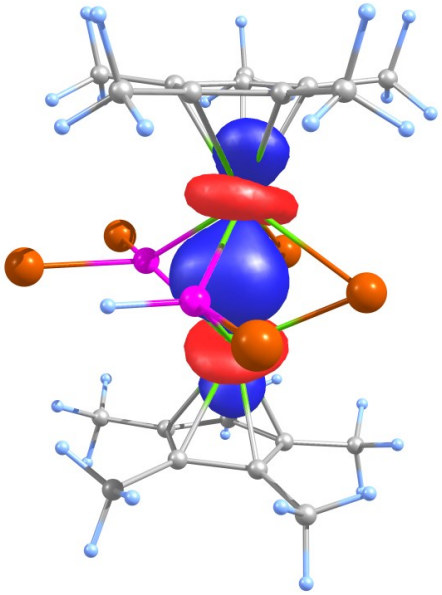

**Figure S 42.** Isosurface of the NBO 129 representing the Mo-Mo bond.

Cartesian coordinates od the optimizes geometry of [(Cp*Mo)$_2$(μ,η$^3$:η$^3$-P$_3$)(μ,η$^2$:η$^2$-P$_3$Cl$_3$)]$^+$ (**7**) at the D4-TPSSh(CPCM)/def2-TZVP level of theory.

| Atom | x | y | z |
|---|---|---|---|
| Cl | 2.97830239895243 | 2.30530188804612 | 0.88052969128923 |
| Cl | 4.07686030557535 | 0.23721775662234 | -2.70814260610696 |
| Cl | 0.98890341068367 | -2.78448867379110 | -2.49664070513224 |
| Mo | 0.39522572354052 | -0.76800370360703 | 0.92314080809766 |
| Mo | -0.20437120048559 | 0.86720292336522 | -1.16544818463051 |
| P | 1.92086251739892 | 0.80363552464661 | -0.03857140656222 |
| P | 3.29292913425247 | -0.64118579045272 | -0.98228732785669 |
| P | 1.16588673667576 | -1.10514303094459 | -1.32660536209187 |
| P | -1.37746031422692 | -1.22973686487738 | -0.70273119062859 |
| P | -1.95623346753471 | 0.30720646940705 | 0.66309647744727 |
| P | -0.30051111155172 | 1.56107318987852 | 1.17505336484970 |
| C | 3.41456437944546 | -1.26510032505077 | 2.54728234441155 |
| H | 3.97371922628961 | -1.62058874429524 | 1.68242685685748 |
| H | 3.82747615565382 | -1.75217277935548 | 3.43656150288850 |
| H | 3.57856699808247 | -0.19255127479798 | 2.65071778046185 |
| C | 1.10417077998440 | 0.18740454437375 | 4.12717929925482 |
| H | 1.85763807988498 | 0.88515380095357 | 3.76076155916670 |
| H | 1.44237939799788 | -0.19504607951422 | 5.09574449880802 |
| H | 0.17638449689929 | 0.73695598532402 | 4.28427818478255 |
| C | -0.02357236005988 | 1.44702619837424 | -3.42189754105333 |
| C | -1.40614057307284 | 1.20090807512198 | -3.12036832031546 |
| C | -0.00621280618048 | -2.75681445838437 | 2.04992731630180 |
| C | -1.61191623213335 | -1.42695660899201 | 3.61655725607760 |
| H | -1.73689551640771 | -0.37385302066126 | 3.86921383510380 |
| H | -1.66456315598217 | -2.00441528423934 | 4.54525598428411 |
| H | -2.44542154695079 | -1.73457182896255 | 2.98491636103671 |
| C | -3.23538578591474 | 2.39601197898982 | -1.70774690866775 |
| H | -3.79381694630081 | 1.46018021444609 | -1.69866834225724 |
| H | -3.74704173582964 | 3.08573200574617 | -2.38692939859743 |
| H | -3.26517846825679 | 2.83029499516123 | -0.70821106565523 |
| C | -0.73797767531182 | 4.25757528473664 | -1.02650470364478 |
| H | -1.47683995652789 | 4.17958956123357 | -0.22858511007629 |
| H | -1.00260347362304 | 5.11795243213661 | -1.64983356926284 |
| H | 0.23415750568243 | 4.45388198514969 | -0.57364062492207 |
| C | 1.39468372150365 | -2.71217504391070 | 1.74896832163203 |
| C | 0.40537916382451 | 2.56751959957549 | -2.65127731578388 |
| C | 0.91274851420572 | -0.95125308954540 | 3.17778438809114 |
| C | -0.70982600684340 | 3.02278868753865 | -1.86862273013963 |

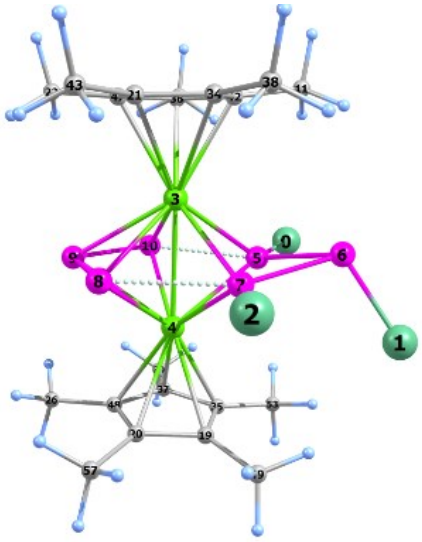

| | | | |
|---|---|---|---|
| C | 2.14726879792047 | -3.73856155443598 | 0.96573778293272 |
| H | 1.52221524230175 | -4.19272754338138 | 0.19759432319841 |
| H | 2.48062527706369 | -4.53346808850148 | 1.64075613491462 |
| H | 3.03118759687194 | -3.31457670617726 | 0.48798865333893 |
| C | 1.96087206663297 | -1.59776358308658 | 2.44134819162739 |
| C | -0.95870956893797 | -3.82956395163585 | 1.62935638249825 |
| H | -1.98166477370789 | -3.45512590908131 | 1.58224224617615 |
| H | -0.93166014608789 | -4.64973726326739 | 2.35372235434450 |
| H | -0.69628804311122 | -4.23350923055992 | 0.65163340180224 |
| C | -0.29710257278728 | -1.68081938486188 | 2.95240734618562 |
| C | -1.83369838356584 | 2.19397121659143 | -2.18328729194056 |
| C | 0.76495648495126 | 0.74487513772791 | -4.47833627439602 |
| H | 1.83514885359483 | 0.83320215092859 | -4.30246052893618 |
| H | 0.53946957262788 | 1.19813159467848 | -5.44925566490318 |
| H | 0.50750150754022 | -0.31265130843944 | -4.53696606207921 |
| C | 1.73071081096527 | 3.25348615142121 | -2.74129564654300 |
| H | 2.03057118367000 | 3.67800644890154 | -1.78310547145973 |
| H | 1.66088757021093 | 4.07511257835508 | -3.46130303236867 |
| H | 2.51116058439145 | 2.57390425298681 | -3.07799890390204 |
| C | -2.28698199088926 | 0.20231919108100 | -3.79882693120064 |
| H | -1.72062101481596 | -0.66907731320951 | -4.12728375520517 |
| H | -2.74826021117989 | 0.66021527252513 | -4.68004768823747 |
| H | -3.08660425899854 | -0.13679837200439 | -3.13949842030447 |

| | |
|---|---|
| Dispersion correction | -0.190514852 |
| FINAL SINGLE POINT ENERGY | -4346.430838269045 |

Mayer bond orders larger than 0.100000 for **7**.

| | | | | | |
|---|---|---|---|---|---|
| B( 0-Cl, 5-P ) : | 0.9381 | B( 1-Cl, 6-P ) : | 1.0112 | B( 2-Cl, 7-P ) : | 0.9358 |
| **B( 3-Mo, 4-Mo) :** | **0.7530** | B( 3-Mo, 5-P ) : | 0.7759 | B( 3-Mo, 6-P ) : | 0.1398 |
| B( 3-Mo, 7-P ) : | 0.7611 | B( 3-Mo, 8-P ) : | 0.8394 | B( 3-Mo, 9-P ) : | 0.6519 |
| B( 3-Mo, 10-P ) : | 0.8883 | B( 3-Mo, 21-C ) : | 0.3846 | B( 3-Mo, 34-C ) : | 0.4015 |
| B( 3-Mo, 36-C ) : | 0.3821 | B( 3-Mo, 42-C ) : | 0.4376 | B( 3-Mo, 47-C ) : | 0.4389 |
| B( 4-Mo, 5-P ) : | 0.7420 | B( 4-Mo, 7-P ) : | 0.7394 | B( 4-Mo, 8-P ) : | 0.8877 |
| B( 4-Mo, 9-P ) : | 0.6669 | B( 4-Mo, 10-P ) : | 0.8707 | B( 4-Mo, 19-C ) : | 0.4238 |
| B( 4-Mo, 20-C ) : | 0.3834 | B( 4-Mo, 35-C ) : | 0.4201 | B( 4-Mo, 37-C ) : | 0.3804 |
| B( 4-Mo, 48-C ) : | 0.4392 | B( 5-P , 6-P ) : | 0.9195 | **B( 5-P , 10-P ) :** | **0.1837** |
| B( 6-P , 7-P ) : | 0.9257 | **B( 7-P , 8-P ) :** | **0.1992** | B( 8-P , 9-P ) : | 0.8991 |
| B( 8-P , 10-P ) : | 0.1216 | B( 9-P , 10-P ) : | 0.8912 | B( 11-C , 12-H ) : | 0.9510 |

Cartesian coordinates od the optimizes geometry of [(Cp*Mo)$_2$(*μ*,*η*$^3$:*η*$^3$-P$_3$)(*μ*-PCl$_2$)$_2$]$^+$ (**8**) at the D4-TPSSh(CPCM)/def2-TZVP level of theory.

| Atom | x | y | z |
|---|---|---|---|
| Mo | -0.84718563787480 | -0.20903741898002 | 1.05166799325840 |
| Mo | 0.81848413192839 | 0.28728206642290 | -1.02993456197227 |
| P | -0.24313494376925 | 1.99611335905987 | 0.28164495314797 |
| P | 1.52798668074388 | 0.04976325008827 | 1.26340332012887 |
| P | 0.60290512830419 | -1.94913938382752 | 0.04473424820387 |
| P | -1.04445016723705 | -1.50843197229315 | -1.20360159169561 |
| P | -1.65832975284070 | 0.51273931035989 | -1.17888994202357 |
| Cl | -1.72630949993290 | 3.29702708629428 | -0.47745850132404 |
| Cl | 0.69678563741629 | 3.56737157423112 | 1.25534281040446 |
| Cl | 2.54987094363352 | 1.37573634156234 | 2.48242517796243 |
| Cl | 2.73287543428700 | -1.56065832963033 | 1.91590680496018 |
| C | 2.85073547639331 | -0.10039595836406 | -2.07298369071676 |
| C | 2.70176219944091 | 1.31478892687390 | -1.87234839403599 |
| C | -0.12539515972689 | -0.47507222635651 | 4.41578251350746 |
| H | 0.67810655829660 | -1.18991056275806 | 4.24007472521984 |
| H | -0.59513037777322 | -0.72637768110232 | 5.37233497030645 |
| H | 0.30769682190176 | 0.52038268072613 | 4.50450023299491 |
| C | -2.69841804294502 | -1.36829356594736 | 1.82481561504488 |
| C | -1.95215715985799 | 1.94481719266377 | 3.45486817912029 |

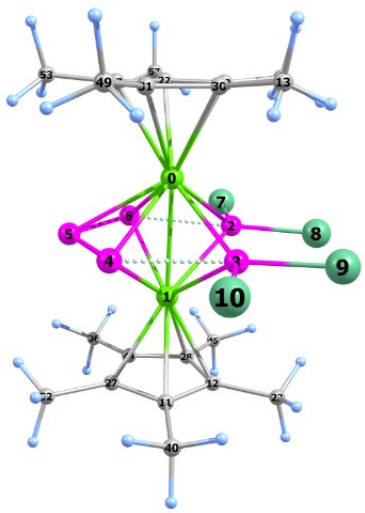

| | | | |
|---|---|---|---|
| H | -0.93935271774423 | 2.23428563472126 | 3.73427256937290 |
| H | -2.58036425818133 | 2.01014698588325 | 4.34873212502012 |
| H | -2.32861158181301 | 2.66344280425597 | 2.72726139790005 |
| C | -2.95158919653206 | 0.03366474105966 | 1.98030349190088 |
| C | 3.62327406919496 | 2.19743352854259 | -1.09348161554315 |
| H | 3.08337453832264 | 3.00920146945778 | -0.60633359035861 |
| H | 4.36058122896995 | 2.64092861289773 | -1.77015742597660 |
| H | 4.15954144611567 | 1.63475737645324 | -0.33041811281126 |
| C | 1.82017397563851 | -0.52940513301114 | -2.96565214264497 |
| C | 1.59252760094471 | 1.75706082248859 | -2.66443236085178 |
| C | -1.99494340698353 | 0.55005955788899 | 2.91862993521769 |
| C | -1.16061816621977 | -0.53239460610276 | 3.34140106012048 |
| C | -1.58465437318971 | -1.71757622091657 | 2.65734750459229 |
| C | 1.65279835780689 | -1.91166738261211 | -3.50830027171677 |
| H | 1.95148627787395 | -2.66462040334406 | -2.77857793048241 |
| H | 2.28303111161160 | -2.03305881613894 | -4.39478722916010 |
| H | 0.62082124150767 | -2.10466807714108 | -3.80272271319445 |
| C | -0.06682375697724 | 0.64273643037430 | -4.33217402325548 |
| H | -0.60680074316393 | -0.30418587752436 | -4.35552732161579 |
| H | 0.35400437670880 | 0.81730852015936 | -5.32758830381226 |
| H | -0.77944966160543 | 1.44041000824684 | -4.12313628826161 |
| C | 3.96232052244006 | -0.94765279630400 | -1.54742651749421 |
| H | 4.31607331066141 | -0.59363499683483 | -0.57987232332742 |
| H | 4.80312840609506 | -0.90980197632054 | -2.24734052299870 |
| H | 3.65468550132086 | -1.98808034726068 | -1.44384967452215 |
| C | 1.03948913209655 | 0.61914212354319 | -3.32893020962494 |
| C | 1.15878107028624 | 3.17422191535662 | -2.84921907121526 |
| H | 0.09184757727926 | 3.24375048812504 | -3.05978068946329 |
| H | 1.69829442190018 | 3.60495197659879 | -3.69870806826479 |
| H | 1.38130128913965 | 3.77834604546138 | -1.97013974143503 |
| C | -1.06375574892245 | -3.09865779157821 | 2.89624079765516 |
| H | -1.19546444533817 | -3.73199158149961 | 2.01908538999424 |
| H | -1.61245395174020 | -3.55424266835205 | 3.72663136818297 |
| H | -0.00553959680679 | -3.08664900170317 | 3.15771685604664 |
| C | -3.52645305209529 | -2.32488036938046 | 1.03015634970858 |
| H | -4.00384227809277 | -1.83271050436694 | 0.18291577304108 |
| H | -4.31418507850701 | -2.73608407008599 | 1.66969083697743 |
| H | -2.92992860210224 | -3.15877434045810 | 0.65902933893130 |
| C | -4.10200048435559 | 0.78606312563066 | 1.39336175913030 |
| H | -3.85446986914184 | 1.83544638356895 | 1.23469830286565 |
| H | -4.95295531892737 | 0.73679398558259 | 2.08004846803248 |
| H | -4.41297743786271 | 0.35732973561566 | 0.44104796084901 |

| | |
|---|---|
| Dispersion correction | -0.189602993 |

| | |
|---|---|
| FINAL SINGLE POINT ENERGY | -4465.265235764619 |

Mayer bond orders larger than 0.100000 for **8**.

| | | | | | |
|---|---|---|---|---|---|
| **B( 0-Mo, 1-Mo) : 0.8098** | B( 0-Mo, 2-P ) : 0.7650 | B( 0-Mo, 3-P ) : 0.7480 |
| B( 0-Mo, 4-P ) : 0.7998 | B( 0-Mo, 5-P ) : 0.6577 | B( 0-Mo, 6-P ) : 0.8368 |
| B( 0-Mo, 17-C ) : 0.4096 | B( 0-Mo, 22-C ) : 0.4347 | B( 0-Mo, 29-C ) : 0.4236 |
| B( 0-Mo, 30-C ) : 0.3948 | B( 0-Mo, 31-C ) : 0.4345 | B( 1-Mo, 2-P ) : 0.7890 |
| B( 1-Mo, 3-P ) : 0.8085 | B( 1-Mo, 4-P ) : 0.8050 | B( 1-Mo, 5-P ) : 0.6409 |
| B( 1-Mo, 6-P ) : 0.7673 | B( 1-Mo, 11-C ) : 0.3972 | B( 1-Mo, 12-C ) : 0.4589 |
| B( 1-Mo, 27-C ) : 0.4302 | B( 1-Mo, 28-C ) : 0.3784 | B( 1-Mo, 44-C ) : 0.4132 |
| **B( 2-P , 6-P ) : 0.2425** | **B( 2-P , 7-Cl) : 0.9054** | **B( 2-P , 8-Cl) : 0.9447** |
| **B( 3-P , 4-P ) : 0.2396** | B( 3-P , 9-Cl) : 0.9429 | B( 3-P , 10-Cl) : 0.9053 |
| B( 4-P , 5-P ) : 0.9223 | B( 4-P , 6-P ) : 0.1137 | B( 5-P , 6-P ) : 0.9194 |

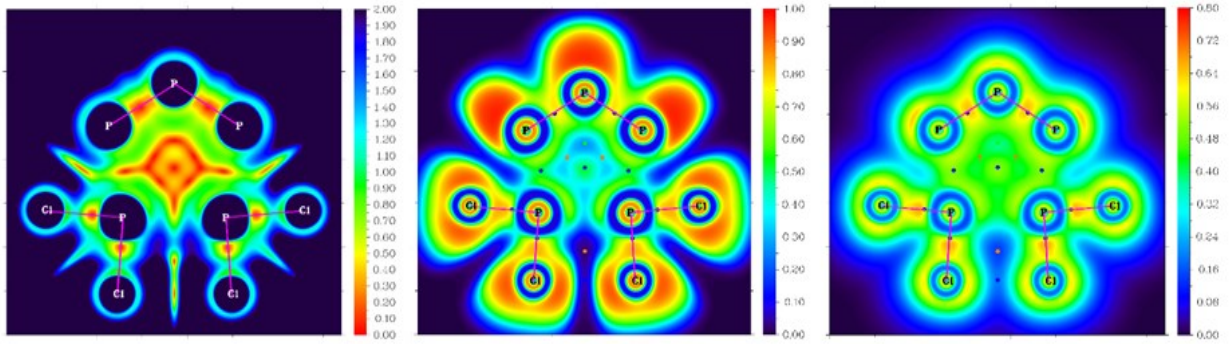

**Figure S 43 Left.** Interaction Region Indicator (IRI) plot in the plane defined by the phosphorus atoms indicating the regions with notable chemical bond interaction (orange) and areas where weak interactions occur (green) (IRI < 1.0). The regions with IRI > 1.0 are not significant for bonding (either large gradient of electron density or negligible electron density). **Middle**: Electron Localization Function (ELF) plot. Blue dots represent (3,-1) critical points. **Right**: Localized orbital locator (LOL) plot.

Cartesian coordinates od the optimizes geometry of [(Cp*Mo)$_2$($\mu$-PCl$_2$)$_2$($\mu$-Cl)$_2$] (**9**) at the D4-TPSSh(CPCM)/def2-TZVP level of theory.

| Atom | x | y | z |
|---|---|---|---|
| Mo | 7.78574794304539 | 6.40075543521442 | 3.68962355342938 |
| Mo | 9.70215441606676 | 8.28807802735410 | 3.68760514659751 |
| P | 9.66171989661661 | 6.40402651168774 | 2.26117809572626 |
| P | 9.64652642783569 | 6.42343685852445 | 5.13888452527897 |
| Cl | 9.39952267429482 | 6.56554896822971 | 0.15366061533678 |
| Cl | 11.13174618394131 | 4.95784351130212 | 2.08846163406482 |
| Cl | 11.11625342950403 | 4.98211074636181 | 5.34661121089455 |
| Cl | 9.36468681463593 | 6.61697314518972 | 7.24131797095704 |
| Cl | 7.63039114321831 | 8.47798500145141 | 5.15027767246244 |
| Cl | 7.64604585374883 | 8.45981966646165 | 2.20103479124670 |
| C | 11.36778940341449 | 9.31503766660552 | 4.84958989035699 |
| C | 7.14499437304205 | 4.27375392974370 | 2.97571491729061 |
| C | 6.20229839851647 | 5.25236058100712 | 2.52847143673836 |
| C | 11.77203823746952 | 9.06844094195512 | 6.26774454407756 |
| H | 10.93996221711800 | 9.22583208698762 | 6.95377333691715 |
| H | 12.57750065078265 | 9.75592234382613 | 6.54763382386120 |
| H | 12.13463309652986 | 8.04986203417436 | 6.40486869361916 |
| C | 10.50193203012245 | 10.36437273106462 | 4.40042746409821 |
| H | 3.52460222732853 | 6.33274099413205 | 3.68239906920788 |
| H | 4.53150792837394 | 7.49917011231036 | 2.81227503053375 |
| H | 4.52278370875621 | 7.48797867508604 | 4.57723120268314 |
| C | 5.82152556482094 | 5.51415897111636 | 1.10624027137828 |
| H | 5.46724464696264 | 6.53625470503746 | 0.97181115297292 |
| H | 5.01528948401789 | 4.83565895755126 | 0.80775398053839 |
| H | 6.66509948150044 | 5.35415750880597 | 0.43545324859173 |
| C | 9.75303577799547 | 11.30477951536560 | 5.28690295988624 |
| H | 10.39384875525216 | 12.15358939563598 | 5.54808191052297 |
| H | 9.45000891953481 | 10.81656052051321 | 6.21358887168190 |
| H | 8.86176685751939 | 11.69357074335778 | 4.79413772287403 |
| C | 7.90297884212772 | 3.33310277350071 | 2.09913381305903 |
| H | 8.84841900917717 | 3.03897091872617 | 2.55365855258577 |
| H | 8.11209072603066 | 3.77791016737501 | 1.12614289229175 |
| H | 7.30791927659191 | 2.42807897236538 | 1.93620479854304 |
| C | 11.36198861215769 | 9.31547222746864 | 2.52453958143668 |
| C | 11.91455367398043 | 8.66395137075484 | 3.68589748438779 |
| C | 5.60977263640151 | 5.86512572465912 | 3.69003954849421 |
| C | 7.14782315844623 | 4.27464375053494 | 4.40116050235245 |
| C | 6.20598939525795 | 5.25383073817870 | 4.85108452792106 |
| C | 11.75886723334546 | 9.07077747499386 | 1.10390151749468 |

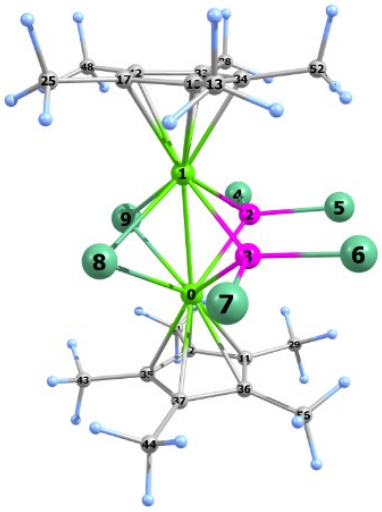

```
  H  10.92053774962297      9.21995606339510      0.42360242340514
  H  12.55641720127882      9.76451618540148      0.81693867121721
  H  12.12871585818942      8.05498591457353      0.96598369006355
  C  10.49803095531101     10.36495955761847      2.97905661465682
  C   4.48789691437508      6.85414865174776      3.69053518742683
  C   5.82762161648746      5.51425825425599      6.27421675901412
  H   5.47083238975789      6.53539041188161      6.40934514752466
  H   5.02435047008282      4.83336518635875      6.57517695936188
  H   6.67356846086435      5.35766035328112      6.94278061711911
  C   9.74714806752616     11.30851443505265      2.09753018891976
  H  10.38943686346256     12.15505968586507      1.83263688203192
  H   9.43605691657113     10.82224405390618      1.17249305319605
  H   8.86068362559469     11.70059164671413      2.59628580122920
  C  13.03885165854494      7.68134485557221      3.68353770101017
  H  13.99424911636895      8.21782307885884      3.69669036364835
  H  13.00156523419772      7.03165053058777      4.55699177809847
  H  13.01429035726479      7.05202900965149      2.79489677782968
  C   7.90803059232084      3.33360034072450      5.27540320364777
  H   8.85350203151401      3.04130621457371      4.81955908176828
  H   8.11781704099069      3.77722349864181      6.24876139207200
  H   7.31453777419038      2.42742766672618      5.43775974436722


-------------------------   ----------------
Dispersion correction           -0.171753125
-------------------------   ----------------

-------------------------   --------------------
FINAL SINGLE POINT ENERGY     -4361.711040775027
-------------------------   --------------------
  Mayer bond orders larger than 0.100000 for 9.
B(  0-Mo,  1-Mo) :   0.8251 B(  0-Mo,  2-P ) :   0.8637 B(  0-Mo,  3-P ) :   0.8645
B(  0-Mo,  8-Cl) :   0.6507 B(  0-Mo,  9-Cl) :   0.6479 B(  0-Mo, 11-C ) :   0.3826
B(  0-Mo, 12-C ) :   0.4442 B(  0-Mo, 35-C ) :   0.4533 B(  0-Mo, 36-C ) :   0.3898
B(  0-Mo, 37-C ) :   0.4438 B(  1-Mo,  2-P ) :   0.9232 B(  1-Mo,  3-P ) :   0.9206
B(  1-Mo,  8-Cl) :   0.6174 B(  1-Mo,  9-Cl) :   0.6204 B(  1-Mo, 10-C ) :   0.4211
B(  1-Mo, 17-C ) :   0.4200 B(  1-Mo, 33-C ) :   0.4262 B(  1-Mo, 34-C ) :   0.4628
B(  1-Mo, 42-C ) :   0.4185 B(  2-P ,  4-Cl) :   0.8668 B(  2-P ,  5-Cl) :   0.9498
B(  3-P ,  6-Cl) :   0.9505 B(  3-P ,  7-Cl) :   0.8669 B( 10-C , 13-C ) :   1.0276
```

Cartesian coordinates od the optimizes geometry of [(Cp*MoCl)$_2$(*μ*-PCl$_2$)] (**10**) at the D4-TPSSh(CPCM)/def2-TZVP level of theory.

| Atom | x | y | z |
|---|---|---|---|
| Mo | 0.01821161692121 | -1.44112055621263 | 0.01390764714639 |
| Mo | 0.01665760284964 | 1.44195177859544 | 0.01827360318940 |
| P | -1.25968102753282 | -0.00253329004173 | 1.42864407654935 |
| P | 1.29066307371747 | -0.00107877909185 | 1.48508601720033 |
| P | 2.08389656554007 | 0.00219923980689 | -0.53706004185955 |
| P | 0.45189269185941 | 0.00404564929350 | -1.89066209376953 |
| Cl | -3.33631734175345 | -0.00362645703005 | 1.61147980701450 |
| Cl | -0.92767802956073 | -0.00773466795404 | 3.52296070409945 |
| Cl | -2.17701043357969 | 1.63324802617743 | -1.10971578153600 |
| Cl | -2.17648071368954 | -1.63391463472536 | -1.11156269948904 |
| C | 0.58399609918828 | -3.21840165583115 | 1.46911858447591 |
| C | 1.29217449269422 | -3.30846146435011 | -0.74228394294906 |
| C | 1.69389142766778 | -2.98667075671459 | 0.59944291502931 |
| C | -0.51170518524356 | -3.64974935138731 | 0.67251282328527 |
| C | -0.05322792785852 | -3.73920616270557 | -0.69120492121250 |
| C | -0.81116464737129 | -4.32614797320015 | -1.83212515302300 |
| H | -1.88234282292189 | -4.31241857883450 | -1.64449742027664 |
| H | -0.49187279789097 | -5.36627199888244 | -1.96480105234768 |
| H | -0.61436689268792 | -3.79140279802775 | -2.76142609238537 |
| C | -1.85719427759164 | -4.07607292957838 | 1.16031895229892 |
| H | -2.03755181576650 | -3.72273717542467 | 2.17568787494454 |
| H | -1.93015223813904 | -5.16833968498021 | 1.15901712667603 |
| H | -2.64044445507393 | -3.67984043055006 | 0.51230364535456 |
| C | 0.63003967496295 | -3.13965954259576 | 2.95783418721678 |
| H | 1.27843085691004 | -2.32970351362027 | 3.29441238814224 |
| H | 1.02874184028453 | -4.07837446128662 | 3.35703746410050 |
| H | -0.35944686341195 | -2.98162553070822 | 3.38317323417587 |

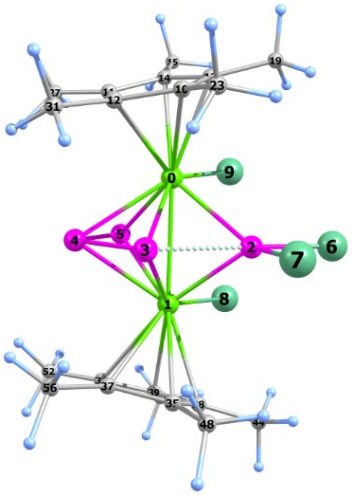

| | | | |
|---|---|---|---|
| C | 2.18332508923887 | -3.32825424788335 | -1.94092665842365 |
| H | 1.61115136822572 | -3.19483429720249 | -2.85890961028464 |
| H | 2.70680304027996 | -4.28817436672960 | -2.00149257482764 |
| H | 2.93722171347203 | -2.54081916311575 | -1.88957398645721 |
| C | 3.09361824990206 | -2.72019746122901 | 1.04449038301903 |
| H | 3.69345494832399 | -2.28111996496381 | 0.24686890680385 |
| H | 3.55936864022034 | -3.66683022583966 | 1.33834048814428 |
| H | 3.12569362525638 | -2.05240927691593 | 1.90722256579803 |
| C | 0.55971807274193 | 3.22470677240707 | 1.47711945719267 |
| C | 1.30754406437337 | 3.30421806883989 | -0.72151318812304 |
| C | 1.68459499697013 | 2.98677160382148 | 0.62846760450582 |
| C | -0.51998433607958 | 3.65556472521007 | 0.65962198548875 |
| C | -0.03842404075796 | 3.73490676362635 | -0.69720970013908 |
| C | -0.77748655908237 | 4.31348520548801 | -1.85494225417322 |
| H | -1.85192089846404 | 4.29518244696999 | -1.68721896140374 |
| H | -0.46108532762143 | 5.35449990351533 | -1.98727999433147 |
| H | -0.56094058203082 | 3.77498200536502 | -2.77774352291241 |
| C | -1.87033391859181 | 4.09281103489954 | 1.12291800570128 |
| H | -2.06577746621364 | 3.75398096833858 | 2.14045245749939 |
| H | -1.93788895450427 | 5.18532275217947 | 1.10570895572560 |
| H | -2.64621798723162 | 3.69167238483676 | 0.46915948823416 |
| C | 0.57819962270952 | 3.14677272767747 | 2.96641898778476 |
| H | 1.21753805134643 | 2.33443499842445 | 3.31443564440839 |
| H | 0.97314240742847 | 4.08396497893822 | 3.37290733789733 |
| H | -0.41965270620710 | 2.99268779215730 | 3.37336119850104 |
| C | 2.21958893018365 | 3.31810739127310 | -1.90430617537797 |
| H | 1.66515804472499 | 3.16996372379060 | -2.83093527064138 |
| H | 2.73594141432174 | 4.28182405835210 | -1.96584489152868 |
| H | 2.97906223811806 | 2.53786850149531 | -1.83086998551073 |
| C | 3.07593581021704 | 2.72019217155052 | 1.09913660107879 |
| H | 3.68558936303663 | 2.26520750176280 | 0.31797053986451 |
| H | 3.54228075089354 | 3.66910758584659 | 1.38463888416394 |
| H | 3.09082386227754 | 2.06645063697379 | 1.97285543027216 |

| | |
|---|---|
| Dispersion correction | -0.180469935 |

| | |
|---|---|
| FINAL SINGLE POINT ENERGY | -4124.027482782973 |

Mayer bond orders larger than 0.100000 for **10**.

| | | | | | |
|---|---|---|---|---|---|
| B( 0-Mo, 1-Mo) : | 0.6234 | B( 0-Mo, 2-P ) : | 0.8602 | B( 0-Mo, 3-P ) : | 0.8457 |
| B( 0-Mo, 4-P ) : | 0.6660 | B( 0-Mo, 5-P ) : | 0.9575 | B( 0-Mo, 9-Cl) : | 0.9910 |
| B( 0-Mo, 10-C ) : | 0.2989 | B( 0-Mo, 11-C ) : | 0.3207 | B( 0-Mo, 12-C ) : | 0.4923 |
| B( 0-Mo, 13-C ) : | 0.4408 | B( 0-Mo, 14-C ) : | 0.3795 | B( 1-Mo, 2-P ) : | 0.8585 |
| B( 1-Mo, 3-P ) : | 0.8425 | B( 1-Mo, 4-P ) : | 0.6657 | B( 1-Mo, 5-P ) : | 0.9596 |
| B( 1-Mo, 8-Cl) : | 0.9898 | B( 1-Mo, 35-C ) : | 0.2963 | B( 1-Mo, 36-C ) : | 0.3253 |
| B( 1-Mo, 37-C ) : | 0.4910 | B( 1-Mo, 38-C ) : | 0.4432 | B( 1-Mo, 39-C ) : | 0.3760 |
| **B( 2-P , 3-P ) :** | **0.2196** | B( 2-P , 6-Cl) : | 0.8880 | B( 2-P , 7-Cl) : | 0.8641 |
| **B( 3-P , 4-P ) :** | **0.8107** | **B( 4-P , 5-P ) :** | **0.9296** | B( 10-C , 12-C ) : | 1.0212 |

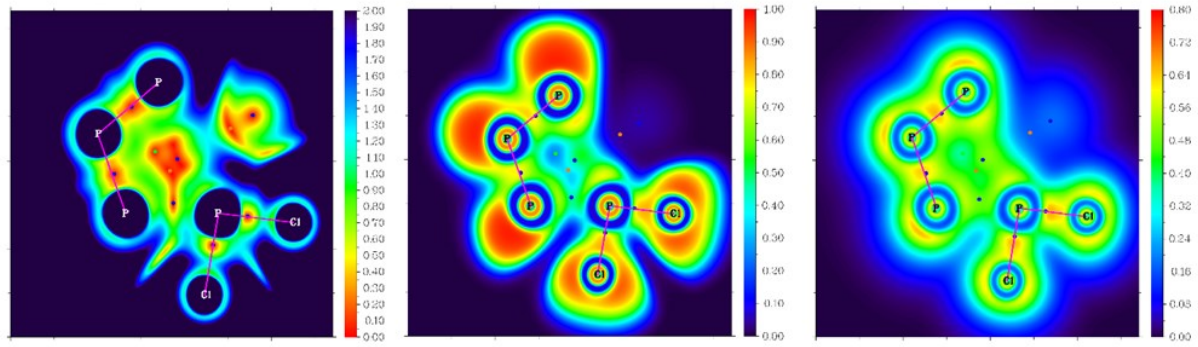

**Figure S 44 Left.** Interaction Region Indicator (IRI) plot in the plane defined by the phosphorus atoms indicating the regions with notable chemical bond interaction (orange) and areas where weak interactions

occur (green) (IRI < 1.0). The regions with IRI > 1.0 are not significant for bonding (either large gradient of electron density or negligible electron density). **Middle**: Electron Localization Function (ELF) plot. Blue dots represent (3,-1) critical points. **Right**: Localized orbital locator (LOL) plot.

Cartesian coordinates of the optimizes geometry of [(Cp*Mo)$_2$(μ,η$^4$:η$^4$-P$_4$)(μ-PCl$_2$)]$^+$ (**11**) in the singlet spin state, at the D4-TPSSh(CPCM)/def2-TZVP level of theory.

| Atom | x | y | z |
|---|---|---|---|
| Mo | 1.06011650652889 | 0.87883038411900 | -0.10419080872797 |
| Mo | -1.07802834244014 | -0.83729011030598 | -0.02529178184825 |
| P | -0.92646778593583 | 1.09871464522997 | -1.36380497074935 |
| P | -0.90272740561428 | 1.18914963339566 | 1.26088307667879 |
| P | 0.42741524237626 | -0.42489424583597 | 1.97891119585389 |
| P | 1.30618428779289 | -1.59696411761292 | 0.39239528480198 |
| P | 0.70847013001135 | -0.94304714860619 | -1.63845528686334 |
| Cl | -2.26669910209641 | 2.67790385566173 | -1.16595329849410 |
| Cl | -0.93693854362011 | 1.03043040676429 | -3.44913395781115 |
| C | -3.34552671737886 | -1.12691104247521 | 0.40900152007118 |
| C | 1.88635052366063 | 3.01082115392173 | -0.52315099892426 |
| C | -2.62501722771687 | -2.03130126082179 | 1.24698590450176 |
| C | -2.22814828350429 | -2.63722473735613 | -0.95637620999173 |
| C | -2.67636802359886 | -2.06460830360736 | 2.74004662480939 |
| H | -2.83653005227791 | -1.06933618032849 | 3.15510954311472 |
| H | -1.76018335184584 | -2.47537891905643 | 3.16480226393326 |
| H | -3.50797992452188 | -2.70003032985358 | 3.06101057223419 |
| C | 2.56284138267239 | 2.09161375445628 | -1.39788357221152 |
| C | 3.31909372358467 | 1.19158897242780 | -0.58950454888462 |
| C | -3.09968563391245 | -1.50211209202414 | -0.95513581311884 |
| C | 1.07745840211147 | 4.19291065651805 | -0.94602006935153 |
| H | 0.61451646163008 | 4.03376462213822 | -1.91966405385995 |
| H | 1.73059595228565 | 5.06847704455566 | -1.02056648178829 |
| H | 0.29352573323266 | 4.41893771994870 | -0.22335860250970 |
| C | -1.92940264815969 | -2.96138134927133 | 0.40536683139356 |
| C | -1.13461245242092 | -4.13802681598042 | 0.87375430356805 |
| H | -0.40160041899957 | -4.44555683505882 | 0.12795511158183 |
| H | -1.80808311505701 | -4.98208026770847 | 1.05465980217013 |
| H | -0.61034034105374 | -3.92287607878935 | 1.80559965453316 |
| C | 3.10314246532627 | 1.54186335082963 | 0.78424705292132 |
| C | 2.22622482545535 | 2.67443425165938 | 0.82174919096296 |
| C | -3.76039303551576 | -0.91269426698076 | -2.15874024395329 |
| H | -4.66907434179733 | -1.48053529807102 | -2.38316426615511 |
| H | -3.11285944053403 | -0.95759617537314 | -3.03365340507333 |
| H | -4.04677414011485 | 0.12530937452813 | -1.99084679932201 |
| C | 4.23172343162608 | 0.12253566588836 | -1.09646398908356 |
| H | 4.37582926594517 | -0.66263872772718 | -0.35419361321850 |
| H | 5.21007700432822 | 0.55492202170565 | -1.32929074859497 |
| H | 3.84243152015021 | -0.33340406988145 | -2.00745844021950 |
| C | -4.29171497908774 | -0.06549408942096 | 0.87030817985064 |
| H | -5.29035748260533 | -0.49608558003168 | 0.99700204124699 |
| H | -4.36285642370570 | 0.74467900241919 | 0.14494603797132 |
| H | -3.98293902232823 | 0.35638796438741 | 1.82664504636804 |
| C | -1.80728995888913 | -3.41731326278448 | -2.15917725919694 |
| H | -1.79202119914030 | -2.79029277830923 | -3.05048547940482 |
| H | -2.51452307693676 | -4.23488439737642 | -2.33217069792848 |
| H | -0.81640391837593 | -3.85284186170728 | -2.02699547845341 |
| C | 2.58140650956615 | 2.14821773409878 | -2.89051706598378 |
| H | 2.76611537175881 | 1.16440663932109 | -3.32192281644164 |
| H | 3.38295565460841 | 2.81728961786585 | -3.21947181802215 |
| H | 1.64259422524862 | 2.52954549746955 | -3.29036326727676 |
| C | 3.77638226464182 | 0.92329299009868 | 1.96708530058011 |
| H | 3.14977726059671 | 0.98023138943273 | 2.85760943631673 |
| H | 4.70679115820534 | 1.46044463801113 | 2.17700985883250 |
| H | 4.02578350752400 | -0.12247847530147 | 1.78581660102657 |
| C | 1.82492033249158 | 3.42618300309152 | 2.04839641041883 |
| H | 0.85057463710579 | 3.89922683285390 | 1.92462488619376 |
| H | 2.55906235381042 | 4.21186914484913 | 2.25335654121376 |
| H | 1.78268625490988 | 2.77194685001043 | 2.91962757031351 |

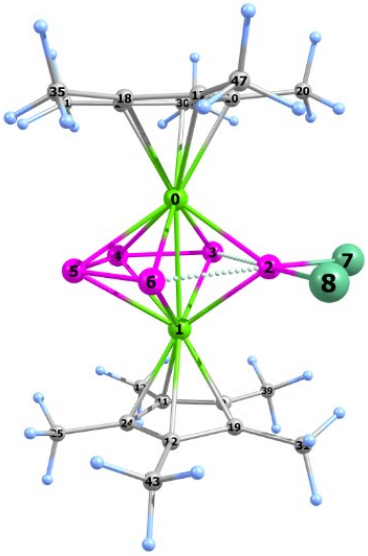

```
-------------------------   ----------------
Dispersion correction           -0.171126328
-------------------------   ----------------

-------------------------   --------------------
FINAL SINGLE POINT ENERGY     -3544.754680973746
-------------------------   --------------------


  Mayer bond orders larger than 0.100000
B(  0-Mo,  1-Mo) :   0.7958 B(  0-Mo,  2-P ) :   0.7901 B(  0-Mo,  3-P ) :   0.9147
B(  0-Mo,  4-P ) :   0.6604 B(  0-Mo,  5-P ) :   0.6631 B(  0-Mo,  6-P ) :   0.9595
B(  0-Mo, 10-C ) :   0.4207 B(  0-Mo, 17-C ) :   0.4103 B(  0-Mo, 18-C ) :   0.3727
B(  0-Mo, 29-C ) :   0.4457 B(  0-Mo, 30-C ) :   0.3549 B(  1-Mo,  2-P ) :   0.7751
B(  1-Mo,  3-P ) :   0.9468 B(  1-Mo,  4-P ) :   0.6758 B(  1-Mo,  5-P ) :   0.6764
B(  1-Mo,  6-P ) :   0.8998 B(  1-Mo,  9-C ) :   0.4040 B(  1-Mo, 11-C ) :   0.3938
B(  1-Mo, 12-C ) :   0.3774 B(  1-Mo, 19-C ) :   0.4189 B(  1-Mo, 24-C ) :   0.4199
B(  2-P ,  3-P ) :   0.1831 B(  2-P ,  6-P ) :   0.1801 B(  2-P ,  7-Cl) :   0.9390
B(  2-P ,  8-Cl) :   0.9320 B(  3-P ,  4-P ) :   0.7664 B(  3-P ,  5-P ) :   0.1002
B(  4-P ,  5-P ) :   0.8921 B(  4-P ,  6-P ) :   0.1004 B(  5-P ,  6-P ) :   0.7596
```

Cartesian coordinates od the optimizes geometry of [(Cp*Mo)$_2$(μ,η$^4$:η$^4$-P$_4$)(μ-PCl$_2$)] (**12**) in the doublet spin state, at the D4-TPSSh(CPCM)/def2-TZVP level of theory.

| Atom | x | y | z |
|---|---|---|---|
| Mo | -1.35177169292308 | 0.28853779803485 | -0.05654088303344 |
| Mo | 1.33220297571124 | -0.24026541946400 | 0.03381457508477 |
| P | 0.36192476984515 | 1.90371956909363 | 0.07134883169536 |
| P | -0.05566269705745 | 0.14427543746835 | 2.03569268613971 |
| P | -0.39041364706791 | -1.73257015467707 | 1.05681318510231 |
| P | -0.29295372203063 | -1.64237470230079 | -1.25065618705661 |
| P | 0.10987865178129 | 0.30391980151885 | -2.04475247589906 |
| Cl | 0.76469805083013 | 3.36750653738278 | -1.40747788096671 |
| Cl | 0.60204299967123 | 3.26259279699658 | 1.68289471923641 |
| C | 3.28632434969375 | -0.35843284783547 | 1.29021091177046 |
| C | -3.16201586637525 | 1.51967869350236 | 0.68276451491513 |
| C | -3.41040406894913 | 0.15399607273746 | 1.02018728637913 |
| C | -3.11038964027547 | 1.61984261164928 | -0.74922504109035 |
| C | -3.82948981102246 | -2.04829842744780 | -0.31935157273563 |
| H | -3.33361391512060 | -2.49096906493304 | -1.18420222531144 |
| H | -4.90895622199197 | -2.18880900611978 | -0.43981869162619 |
| H | -3.51227849205145 | -2.59682035018553 | 0.56826913464913 |
| C | -3.60320344458769 | -0.37120552826393 | 2.40636574535154 |
| H | -3.33661697086419 | -1.42694496432804 | 2.47275775328940 |
| H | -4.65007128997865 | -0.26316259492235 | 2.70986043954385 |
| H | -2.98777902861586 | 0.17813497529288 | 3.12006624722378 |
| C | -3.07760331529063 | 2.65617180343713 | 1.65022019277182 |
| H | -2.60971576205806 | 2.34323253443151 | 2.58427276368158 |
| H | -4.08094912018011 | 3.03050546851101 | 1.88088570418511 |
| H | -2.49448810653309 | 3.48075292292572 | 1.24121127194644 |
| C | 3.51284963452877 | 0.54360784181677 | 0.20268293113692 |
| C | 3.03152471078209 | -1.65525001131338 | 0.74306358244092 |
| C | -3.50782913588553 | -0.59294388676072 | -0.19793683301302 |
| C | -3.32836766643718 | 0.31593195508655 | -1.28873150571468 |
| C | -2.95644415215452 | 2.87882772765092 | -1.54054782562606 |
| H | -2.41020193423488 | 3.63508362764893 | -0.97744992099096 |
| H | -3.94108782046613 | 3.28763988693371 | -1.79240273467138 |
| H | -2.41751293895379 | 2.69525852837034 | -2.47051386892435 |
| C | -3.42959219881817 | -0.02053861966871 | -2.74090756108536 |
| H | -2.79406935645404 | 0.63232356159958 | -3.34002584532843 |
| H | -4.46227469463363 | 0.10387603783222 | -3.08412997115742 |
| H | -3.13104955205440 | -1.05243641518838 | -2.93088725898266 |
| C | 3.10055594344462 | -1.55403878242288 | -0.68559227056017 |
| C | 3.91093551358871 | 1.97946862406813 | 0.34038439009061 |
| H | 3.66058756126284 | 2.54803369450497 | -0.55499011723471 |
| H | 4.99203640429205 | 2.05310726428282 | 0.50034423913079 |
| H | 3.41409407361198 | 2.44821029804280 | 1.18988003681799 |
| C | 3.39798346804659 | -0.19420457775880 | -1.02041825624338 |

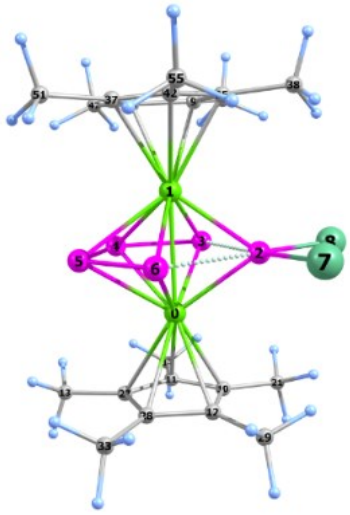

```
  C   3.42064468017992     -0.03347779064811      2.74355790655203
  H   3.16346237284018      1.00733165640289      2.94272732220963
  H   4.45359184420060     -0.19857365496915      3.06980201926270
  H   2.77183822097742     -0.66500197728058      3.35096683836333
  C   2.85817469970879     -2.91565107325582      1.52923451771135
  H   2.35859501459147     -2.72379692431221      2.47962334298787
  H   3.83639491147299     -3.35887785642335      1.74571930649421
  H   2.26981532957294     -3.64930179267071      0.97783567312883
  C   3.00932464649012     -2.69137961567630     -1.65270732577032
  H   2.39058477488926     -3.49742817249215     -1.25769481659783
  H   4.00759277091599     -3.09641302400890     -1.85154096165036
  H   2.58207721208415     -2.36933419108372     -2.60327556948390
  C   3.65733377400776      0.32193952617752     -2.40076764130469
  H   3.06401447420696     -0.21950701432214     -3.13810360056200
  H   4.71455597538396      0.19440368325764     -2.65872693391807
  H   3.41171645445298      1.38144750407565     -2.48128229275396


-------------------------   ----------------
Dispersion correction           -0.174361729
-------------------------   ----------------

-------------------------   --------------------
FINAL SINGLE POINT ENERGY     -3544.919441992913
-------------------------   --------------------

  Mayer bond orders larger than 0.100000
B(  0-Mo,  1-Mo) :   0.7736 B(  0-Mo,  2-P ) :   0.7876 B(  0-Mo,  3-P ) :   0.8829
B(  0-Mo,  4-P ) :   0.7238 B(  0-Mo,  5-P ) :   0.7156 B(  0-Mo,  6-P ) :   0.8734
B(  0-Mo, 10-C ) :   0.4042 B(  0-Mo, 11-C ) :   0.3519 B(  0-Mo, 12-C ) :   0.3996
B(  0-Mo, 27-C ) :   0.4104 B(  0-Mo, 28-C ) :   0.3496 B(  1-Mo,  2-P ) :   0.7578
B(  1-Mo,  3-P ) :   0.8414 B(  1-Mo,  4-P ) :   0.7424 B(  1-Mo,  5-P ) :   0.7406
B(  1-Mo,  6-P ) :   0.8416 B(  1-Mo,  9-C ) :   0.4018 B(  1-Mo, 25-C ) :   0.3646
B(  1-Mo, 26-C ) :   0.3765 B(  1-Mo, 37-C ) :   0.3815 B(  1-Mo, 42-C ) :   0.4084
B(  2-P ,  3-P ) :   0.1692 B(  2-P ,  6-P ) :   0.1739 B(  2-P ,  7-Cl) :   0.8443
B(  2-P ,  8-Cl) :   0.8453 B(  3-P ,  4-P ) :   0.9473 B(  4-P ,  5-P ) :   0.6074
B(  5-P ,  6-P ) :   0.9550 B(  9-C , 25-C ) :   1.0927 B(  9-C , 26-C ) :   1.0784


-----------------------------------------
LOEWDIN ATOMIC CHARGES AND SPIN POPULATIONS
-----------------------------------------
   0 Mo:   -0.569052    0.250729
   1 Mo:   -0.558986    0.239273
   2 P :    0.025557   -0.012392
   3 P :    0.200570    0.157446
   4 P :    0.206747    0.093578
   5 P :    0.205543    0.092060
   6 P :    0.196109    0.153330
   7 Cl:    0.051756    0.003087
   8 Cl:    0.051362    0.003023
```

## References


[1] O.J. Scherer, H. Sitzmann, G. Wolmershäuser, *Journal of Organometallic Chemistry*, **1984**, *268*, C9-C12
[2] H.B. Kraatz, R.Poli, Journal of Organometallic Chemistry, 1994, 475, 167-175
[3] CrysAlisPro Software System, Rigaku Oxford Diffraction (**2018-2020**).
[4] O. V. Dolomanov, L. J. Bourhis, R. J. Gildea, J. A. K. Howard, H. Puschmann, *J. Appl. Cryst*. **2009**, 42, 339–341.
[5] G. M. Sheldrick, *Acta Cryst.* **2015**, A71, 3-8.
[6] G. M. Sheldrick, *Acta Cryst.* **2015**, *C71*, 3-8.
[7] TPSSh: J. Tao, J. P. Perdew, V. N. Staroverov, G. E. Scuseria, *Phys. Rev. Lett.* **2003**, *91*, 146401; V. N. Staroverov, G. E. Scuseria, J. Tao, J. P. Perdew, *J. Chem. Phys.* **2003**, *119*, 12129-12137; Erratum: *J. Chem. Phys.* **2004**, *121*, 11507-11507.
[8] a) F. Weigend and R. Ahlrichs, *Phys. Chem. Chem. Phys.,* **2005**, *7*, 3297–3305; b) F. Weigend, M. Häser, H. Patzelt and R. Ahlrichs, *Chem. Phys. Lett.,* **1998**, *294*, 143–152.
[9] a) E. Caldeweyher, S. Ehlert, A. Hansen, H. Neugebauer, S. Spicher, C. Bannwarth, S. Grimme, *J. Chem. Phys.* **2019**, *150*, 154122; b) E. Caldeweyher, C. Bannwarth, S. Grimme, J. Chem. Phys. **2017**, *147*, 034112.
[10] J. Tomasi, B. Mennucci, R. Cammi, *Chem. Rev.* **2005**, *105*, 2999-3094.
[11] F. Neese, F. Wennmohs, A. Hansen and U. Becker, *Chem. Phys.,* 2009, **356**, 98–109.
[12] NBO 6.0. E. D. Glendening, J. K. Badenhoop, A. E. Reed, J. E. Carpenter, J. A. Bohmann, C. M. Morales, C. R. Landis, F. Weinhold (Theoretical Chemistry Institute, University of Wisconsin, Madison, WI, 2013); http://nbo6.chem.wisc.edu/
[13] T. Lu, Q. Chen, *Chemistry–Methods* **2021**, *1*, 231-239.
[14] a) C. F.-W. LU Tian, *Acta Phys. -Chim. Sin.* **2011**, *27*, 2786-2792; b) A. Savin, O. Jepsen, J. Flad, O. K. Andersen, H. Preuss, H. G. von Schnering, *Angew. Chem. Int. Ed. Engl.* **1992**, *31*, 187-188; c) A. D. Becke, K. E. Edgecombe, *J. Chem. Phys.* **1990**, *92*, 5397-5403.
[15] H. Jacobsen, *Can. J. Chem.* **2008**, *86*, 695-702.
[16] T. Lu, F. Chen, *J. Comput. Chem.* **2012**, *33*, 580-592.

5. Halogenation and nucleophilic quenching of pnictogen-containing cations. Two routes to E-X bond formation (E = As, P; X = F, Cl, Br, I)

**Authors**

Anna Garbagnati, Martin Piesch, Michael Seidl, Gábor Balázs, Manfred Scheer.

**Author contribution**

A. Garbagnati prepared the manuscript and performed the synthesis and characterization of the herein presented compounds. M. Piesch performed the synthesis of the starting materials. M.Seidl did the refinement of the solid-state structures. G. Balázs performed all DFT calculations, contributed to the corresponding parts in the manuscript and the Supporting Information. M. Scheer supervised the research. The manuscript was revised by all the authors.

**Acknowledgement**

This work was comprehensively supported by Deutsche Forschungsgemeinschaft (DFG) within the project Sche384/36-2. We thank Matthias Ackermann and Sabrina Dinauer for the EPR measurements.

5. Halogenation and nucleophilic quenching of pnictogen-containing cations. Two routes to E-X bond formation (E = As, P; X = F, Cl, Br, I)

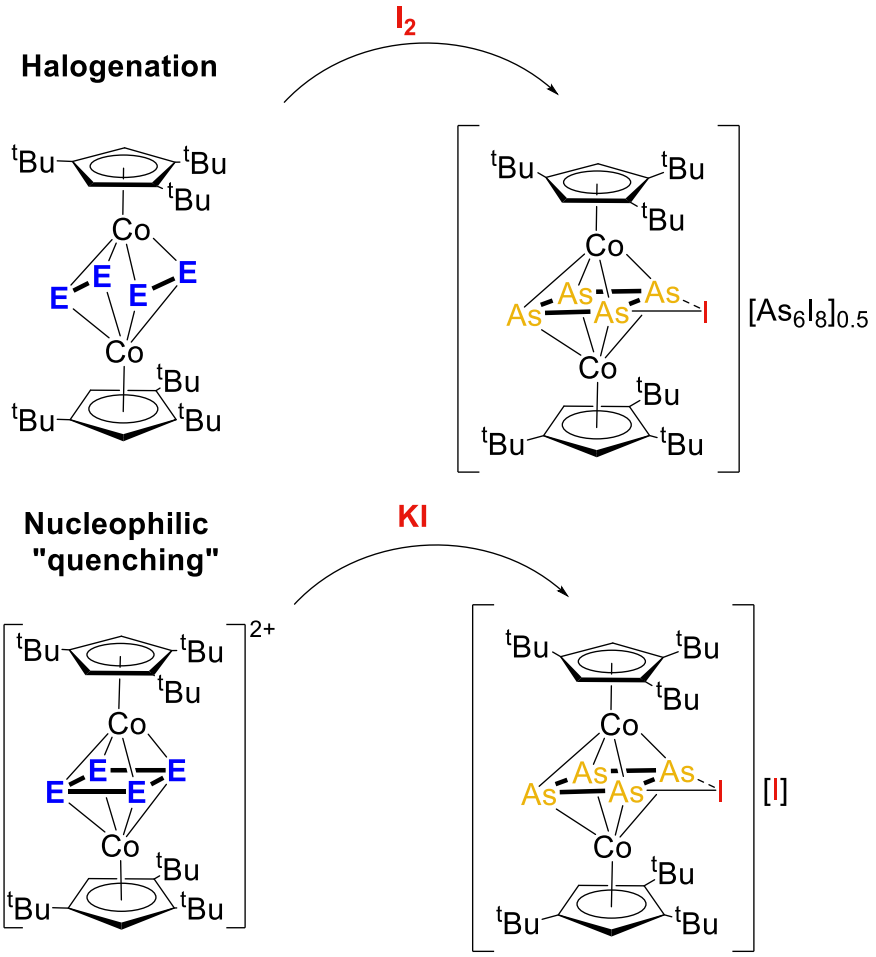

# 5 Halogenation and nucleophilic quenching of pnictogen-containing cations. Two routes to E-X bond formation (E = As, P; X = F, Cl, Br, I)

***Abstract:*** The oxidation of $[(Cp'''Co)_2(\mu,\eta^2:\eta^2\text{-}E_2)_2]$ (E = As (**1**), P (**2**); Cp''' = 1,2,4-tri(tert-butyl)cyclopentadienyl) with halogens or halogen sources ($I_2$, $PBr_5$, $PCl_5$) was investigated. For the arsenic derivative, the ionic compounds $[(Cp'''Co)_2(\mu,\eta^4:\eta^4\text{-}As_4X)][Y]$ (X = I, Y = $[As_6I_8]_{0.5}$ (**3a**), Y = $[Co_2Cl_{6-n}I_n]_{0.5}$ (n = 0, 2, 4) (**3b**); X = Br, Y = $[Co_2Br_6]_{0.5}$ (**4**); X = Cl, Y = $[Co_2Cl_6]_{0.5}$ (**5**)) were isolated. The oxidation of the phosphorus analogue **2** with bromine and chlorine sources yielded the complexes $[(Cp'''Co)_2(\mu\text{-}PBr_2)_2(\mu\text{-}Br)][Co_2Br_6]_{0.5}$ (**6a**) $[(Cp'''Co)_2(\mu\text{-}PCl_2)_2(\mu\text{-}Cl)][Co_2Cl_6]_{0.5}$ (**6b**) and the neutral species $[(Cp'''Co)_2(\mu\text{-}PCl_2)(\mu\text{-}PCl)(\mu,\eta^1:\eta^1\text{-}P_2Cl_3]$ (**7**), respectively. The quenching of the dications $[(Cp'''Co)_2(\mu,\eta^4:\eta^4\text{-}E_4)][TEF]_2$ (TEF = $[Al\{OC(CF_3)_3\}_4]^-$, E = As (**8**), P (**9**)) with KI resulted in in the formation of $[(Cp'''Co)_2(\mu,\eta^4:\eta^4\text{-}As_4I)][I]$ (**10**), representing the homolog of **3**, and in the neutral complex $[(Cp'''Co)(Cp'''CoI_2)(\mu,\eta^4:\eta^1\text{-}P_4)]$ (**11**), respectively. The use of $[(CH_3)_4N]F$ instead of KI leads to the formation of $[(Cp'''Co)_2(\mu\text{-}PF_2)(\mu,\eta^2:\eta^1:\eta^1\text{-}P_3F_2)]$ (**12**) and **2**, revealing a synthetic access to polyphosphorus compounds bearing P-F groups and avoiding the use of very strong and difficult to control fluorinating reagents such as $XeF_2$ or $PF_5$.

## 5.1 Introduction

White phosphorus is the most reactive allotrope of the element and the starting material to produce useful organophosphorus compounds.[1] The current used industrial processes starts from the chlorination of $P_4$ into $PCl_3$, or $POCl_3$ which are in turn converted in useful organophosphorus compounds.[1,2a,b] This process requires a lot of energy,[3] involve toxic, corrosive and pyrophoric reagents and produces large amounts of waste.[1] A promising alternative is the functionalization of polyphosphorus compounds obtained from a transition metal mediated conversion of $P_4$ to result in metal complexes with $P_4$ ligands (TM-$P_4$).[4,5,6] The main goal of this research area is the development of an effective catalytic cycle that converts white phosphorus into the desired organophosphorus compounds. One possibility would be the halogenation of TM-$P_n$ compounds, but only a

few examples are known so far, like [RuCp*($PCy_3$)(μ,$\eta^2$:$\eta^4$-$P_4X_2$)RuCp*] (X = Cl, Br; Scheme 1 **A**)[3] obtained from the ruthenium mediated halogenation of white phosphorus. The halogenation of polyphosphorus compounds could also be used for the synthesis of new halogen-containing polyphosphorus compounds, which could be used for further derivatization/functionalization. Recent studies from our group targeted the halogenation of polypnictogen complexes containing different $P_n$ units such as a $P_2$ containing dimetalla-tetrahedranes,[7] a *cyclo*-$P_5$-end-deck[8] and a *cyclo*-$P_6$-triple decker complex,[9] which resulted in neutral or cationic halogenated species (Scheme 1 **B**-**E**). Regarding the differences that emerged from these results, the question arose as to what would happen when the TM-$P_n$ compound combines the features of triple-decker complexes and separated $E_n$ units?

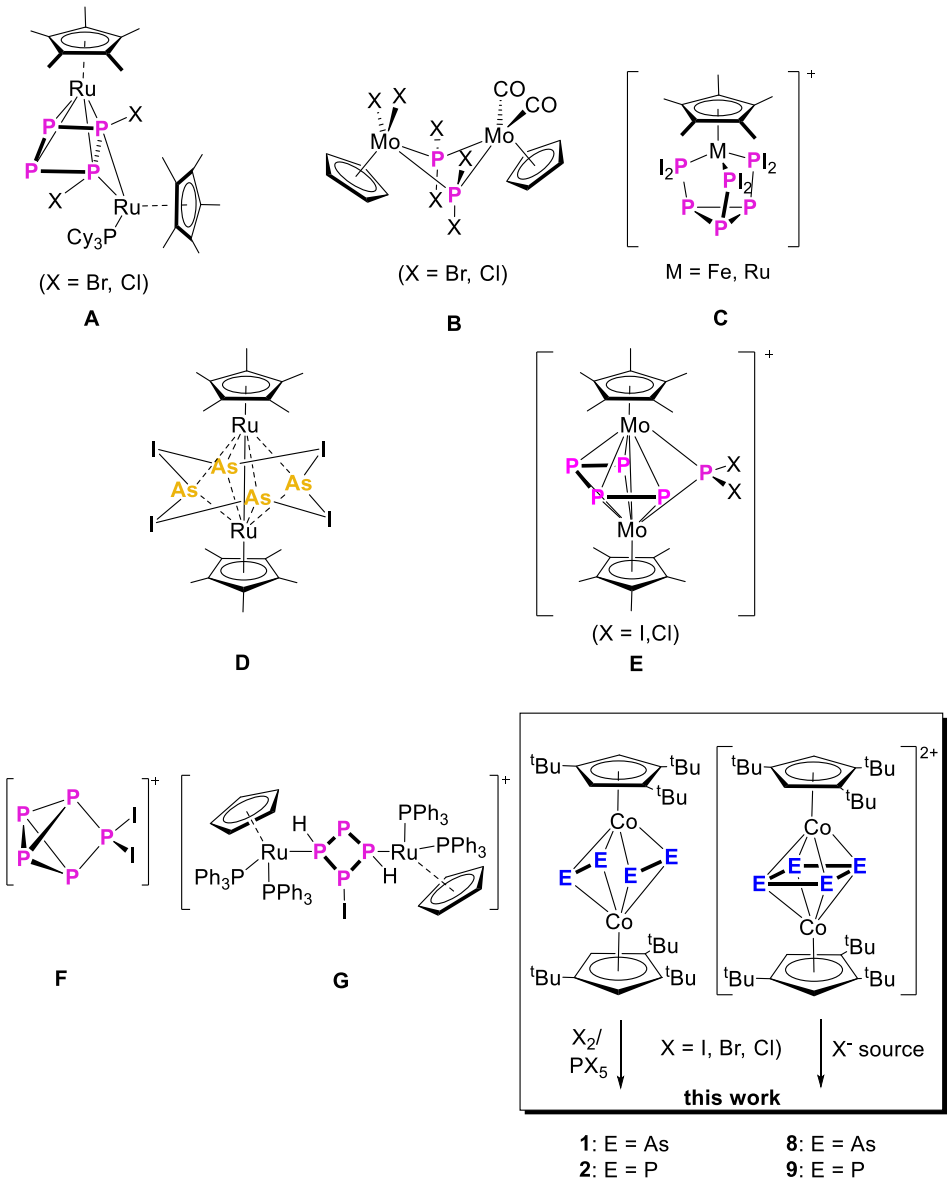


**Scheme 1.** Selected examples of halogenated polypnictogen complexes.

Therefore, the redox active compounds $[(Cp'''Co)_2(\mu,\eta^2:\eta^2\text{-}E_2)_2]$ (E = As (**1**), P (**2**); Cp''' = 1,2,4-tri(*tert*-butyl)cyclopentadienyl)[10] came into the focus of research. A former investigation on these complexes showed that they exhibit a unique redox chemistry, different from the usual behaviour observed for triple-decker complexes such as $[(CpMo)_2(\mu,\eta^6:\eta^6\text{-}P_6)]$[11] or for heterobimetallic triple-decker complexes.[12] The oxidation and reduction of **1** and **2** both leads to the formation of novel E-E bonds, revealing a way to the corresponding dications $[(Cp'''Co)_2(\mu,\eta^4:\eta^4\text{-}E_4)][TEF]_2$ ( E = As (**8**), P (**9**)) in good yields.[13] Since there have some successful examples of halogenation of cationic species been reported, like $[P_5I_2]^+$ (Scheme 1 **F**), which resulted from the iodination of $[Ag(\eta^2\text{-}P_4)_2]^+$,[14] and $[\{CpRu(PPh_3)_2\}_2(\mu,\eta^1:\eta^1\text{-}P_4H_2I)]^+$ (Scheme 1 **G**),[15] we were interested in the comparison of the halogenation of the neutral compounds **1** and **2** together with the well accessible corresponding cationic species **8** and **9**. Moreover, the cationic compounds offers the possibility to "quench" the Lewis acidity of the cations with nucleophilic halides which would enlarge the group of halogen sources to milder and non-hazardous reagents like KI or $[(CH_3)_4N]F$ (TMAF). This approach would represent a new method to synthesize compounds containing the E-X bond, representing a milder alternative to the halogenation of polypnictogen compounds. Especially for fluorination reactions our former results showed that the use of $XeF_2$, even at low temperature, leads to complete decomposition of polyphosphorus complexes to get $PF_6^-$ species. In this respect, a novel approach to fluorine containing pnictogen complexes would be of benefit.

Herein we present the reactivity of the polypnictogen compounds **1** and **2** towards halogen and halogen sources ($I_2$, $PBr_5$, $PCl_5$), leading to the formation of the new cationic and neutral species containing E-X bonds. Furthermore, we present a new, alternative way for the synthesis of functionalized TM-$P_n$ compounds by nucleophilic quenching of cationic polypnictogen species **8** and **9** by the salts KI and $[(CH_3)_4N]F$ and a novel approach to fluorine containing derivatives.

## 5.2 Results and discussion

The reaction of **1** with an excess (4 equiv.) of halogen or halogen sources ($I_2$; $PX_5$, X = Br, Cl) leads to the isolation of the isostructural compounds $[(Cp'''Co)_2(\mu,\eta^4:\eta^4\text{-}As_4X)][Y]$ (X = I, Y = $[As_6I_8]_{0.5}$ (**3a**); X = Br, Y = $[Co_2Br_6]_{0.5}$ (**4**); X = Cl, Y = $[Co_2Cl_6]_{0.5}$ (**5**); Scheme 2). The rather low yields are probably due to the harsh reaction conditions which lead to fragmentations of the starting material in several species that could not be all identified (cf. SI). The cation of complexes **3a**, **4** and **5** contains a strongly distorted *cyclo*-$As_4$ ligand with an *exocyclic* halide attached to one of the As-As edges. For all the reactions, two new As-

As bonds are formed and new triple-decker complexes with unprecedented cyclic $As_4X$ units as middle decks are obtained. Few examples of complexes bearing different arsenic halides are reported in the literature, such as $AsX_3$ (X = Cl, Br, I)[16a,b] or the more peculiar ligand $As_4I_4$ in $[(Cp^*Ru)_2(\mu,\eta^4{:}\eta^4\text{-}As_4I_4)]$,[8] which represents a tetramer of {AsI} fragments.[17a,b] However no example of a polyarsenic sub-halides as ligands exists. Crystals suitable for X-ray structure analysis were obtained from solutions in $CH_2Cl_2$ layered with *n*-pentane at room temperature (**3a**, **3b**, **4** and **5**). From the reaction solution of **1** with iodine, among **3a**, a few crystals of the same cation but with $[Co_2Cl_{6-n}I_n]_{0.5}$ (n = 0, 2, 4) as counterion were isolated (**3b**). The solid-state structure of the anion in **3a** ($[As_6I_8]^{2-}$, Figure 1) was already found in salts with different counterions[8,18a,b] and therefore will not be further discussed (cf. SI for further details). The solid-state structures reveal triple-decker sandwich complexes with a planar cyclic $As_4$ unit with an additional side-on bond to a halogen atom X (X = I, Br, Cl) as a ligand coordinating in a $\eta^4{:}\eta^4$ fashion to two {Cp'''Co} fragments.

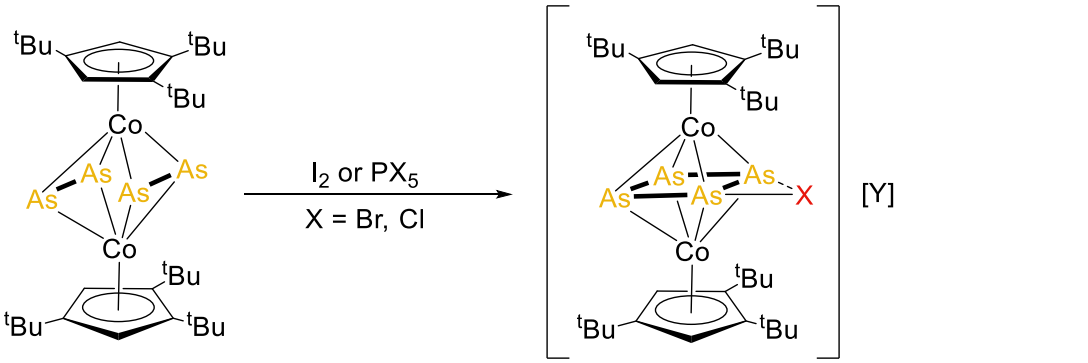


**1**

**3a**: X = I, Y = $[As_6I_8]_{0.5}$ (3%)
**3b**: X = I, Y = $[Co_2Cl_{6-n}I_n]_{0.5}$ (n = 0, 2, 4; <1%)
**4**: X = Br, Y = $[Co_2Br_6]_{0.5}$ (33%)
**5**: X = Cl, Y = $[Co_2Cl_6]_{0.5}$ (16%)

**Scheme 2** Reaction of **1** with $X_2$ (X =I) or $PX_5$ (X = Br, Cl). Isolated yields are given in parenthesis.

The $As_4$ unit in **3a**, **4** and **5** possess a trapezoidal shape (Figure 1). One of the As-As bond is shortened (As3-As4: 2.330(8) Å in **3a**, As2-As3: 2.337(5) Å in **4**, As2: As3: 2.342(5) Å in **5**), two are in the range of a normal As-As single bond[19] and the side-on one coordinated to the halogen atom is elongated (As4-As1A: 2.699(3) Å in **3a**, As1: As2: 2.702(19) Å in **4**, As1-As2: 2.737(8) Å in **5**). The As-X bond lengths are elongated compared to their respective single bonds (As1A-I1: 2.837 Å, As1-Br1: 2.656(3) Å, As1A-Cl1: 2.447(12) Å; lit.: As-I: 2.54 Å, As-Br: 2.35 Å, As-Cl: 2.20 Å).[19] DFT calculations, which have been performed with the ORCA program,[20] and whose geometries have been optimised at the TPSSh[21]/def2-TZVP[22] level of theory starting from the X-ray structure

coordinates, reproduce well the geometric parameters of the cations in **3**, **4** and **5**. The calculations show that, although two As-As distances are rather long, they can be considered as bonding interactions, being built up by delocalised multi-centred interactions (c.f. SI). The intrinsic bonding orbitals representing the bonding within the $As_4I$ unit in **3** are depicted in Figure 2. The description of the bonding in **3** is in agreement with the calculated Mayer bond orders (BOs), which show a BO of 0.53 for each As2A-As3 and As1A-As2A bond (labelling according to Fig. 1). The BOs corresponding to the As1A-I1 and As2A-I1 bonds are 0.48 and 0.44, respectively.

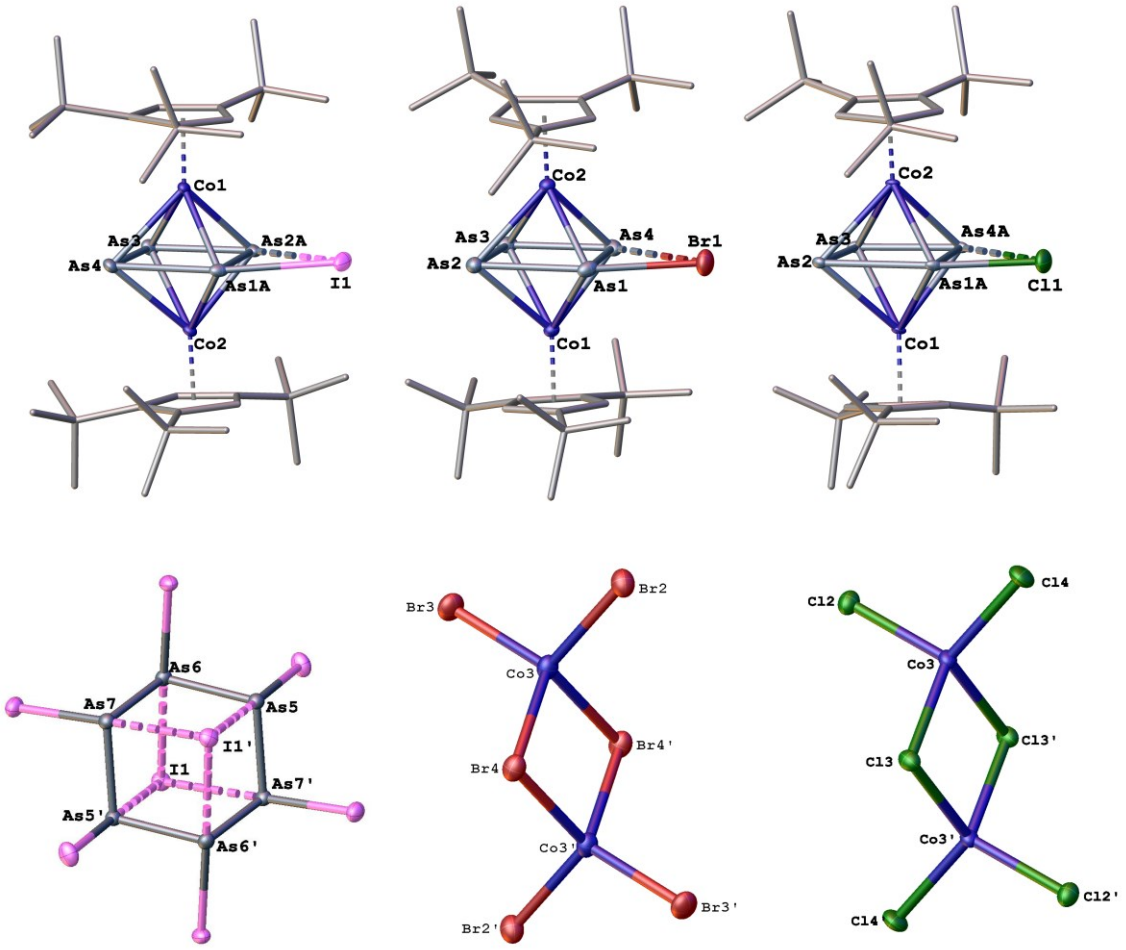


**Figure 1.** Molecular structure of **3a** (left), **4** (middle) and **5** (right) with thermal ellipsoids at 50% probability level. In case of disorder only the major parts are depicted. Hydrogen atoms and the solvent molecules are omitted for clarity.

The analysis of Intrinsic Bonding Orbitals (IBOs) and BOs in the cation of **5** shows a similar bonding situation like in **3**, with the exception that the Cl atom is bonded to only one arsenic atom (BO 0.61) and there is only a weak interaction with the second As (BO

0.16; for details see SI). This is also confirmed by the Electron Localisation Function and Interaction Region Indicator (cf. SI). The dianions of **4** and **5**, with the formula $[Co_2X_6]^{2-}$ (X = Br, Cl), suggest that part of the starting material get completely converted during the oxidation process, resulting in the halogenation of the metal atoms. Their solid-state structures were already described in products with different counterions.[23a,b]

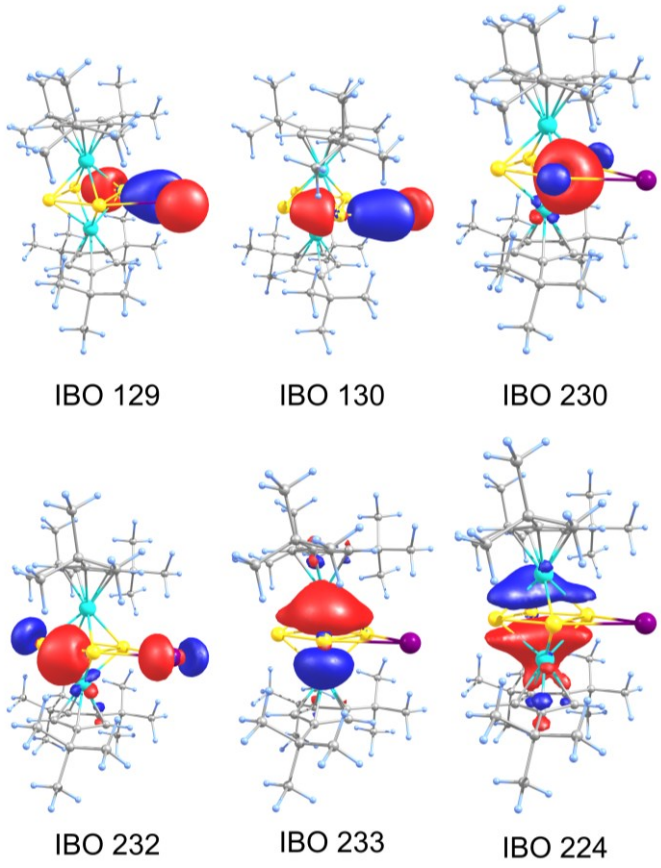


**Figure 2.** Selected intrinsic bonding orbitals representing the bonding within the $As_4I$ unit in the cation of **3** at the D4-TPSSh(CPCM)/def2-TZVP level of theory.

The $^1$H NMR spectrum of **3a** ($CD_2Cl_2$) shows three sharp singlets for the magnetically equivalent Cp''' ligands at δ = 4.67, 1.49 and 1.46 ppm (integral ratio: 2:18:9). However, in the $^1$H NMR spectrum of the reaction solution, three additional singlets corresponding to the side product [Cp'''$CoI_2$] were observed, which was isolated and fully characterized as the main product of the iodination of the P analogue compound **2** (*vide infra* and SI). The ratio between [Cp'''$CoI_2$] and **3a** is approximately 1.5:1, which could partly explain the low yield of isolated **3a**. The $^1$H NMR spectrum of **4** ($CD_2Cl_2$) shows three broad signals for the Cp''' ligands centred at δ = 4.28, 0.93 and 0.81 ppm with an integral ratio of 2:9:18. In the case of **5**, there are two broad singlets centred at δ = 0.83 and 0.71 ppm (integral

ratio: 18:9) corresponding to the $^{t}$Bu groups of the Cp''' ligand, and a very broad signal at 4.04 ppm ($\omega_{1/2}$ = 312 Hz) which is assigned to the H atoms bonded directly to the Cp ring. The broadening of the signals does not indicates a dynamic process in solution, contrarily to what observed for the dicationic species $[(Cp'''Co)_2(\mu,\eta^4{:}\eta^4\text{-}P_4)][TEF]_2$ (**9**).[13]

This is supported by the fact that by lowering the temperature to -80°C of the solution of the dissolved crystals, the signals do not get sharper in the $^{31}P\{^1H\}$ NMR spectrum. The broadening of the signals in **4** and **5** might be caused by the contact-interaction shift of the paramagnetic anion $[Co_2X_6]^{2-}$ (X = Br, Cl) with the cation. The same phenomenon was described for another salt of the $[Co_2Cl_6]^{2-}$ anion[24] and this might explain why it is not observed with **3a** (where the anion is diamagnetic).The signals of the $^{t}$Bu groups in **4** and **5** are upfield-shifted by approximately 0.5 ppm compared to the starting material, while for the iodine derivative they are in line with the latter.[10]

Even if the cations formed by the two-electron oxidation of **1** or by the halogenation of the sandwich complex are not comparable, there are some similarities. In both cases triple-decker complexes with a *cyclo*-$As_4$ or *cyclo*-$As_4X$ ligand are observed as the result of the formation of two new As-As bonds. The main differences are the more reactive reagents used in the reactions when a halogen is the oxidating agent, what results in the partial decomposition of the starting material under formation of the corresponding anions. While the oxidation with silver salts leads to the same results for the As (**1**) and the P containing (**2**) derivatives, the halogenation of $[(Cp'''Co)_2(\mu,\eta^2{:}\eta^2\text{-}P_2)_2]$ (**2**) (*vide infra*) gave different species compared to **1**. Interestingly, a recent investigation concerning the iodination of $[Cp^*M(\eta^5\text{-}E_5)]$ ($Cp^* = C_5Me_5$; M = Fe, Ru; E = As, P) showed likewise a different behaviour between the As and P derivatives.[8] The halogenation of **2** leads to different compounds with every used halogenating agent, in contrary to what was observed for the halogenation of the heavier analogue **1**, which led to analogues species. As mentioned above, when the reaction between **2** and $I_2$ is carried out under the same conditions as for **1** (4 equiv. of $I_2$), the only product detected by $^1H$ NMR spectroscopy of the reaction solution is $[Cp'''CoI_2]$ (cf. SI for further details). The $^{31}P\{^1H\}$ NMR spectrum of the reaction solution at room temperature was silent but a few crystals of $P_2I_4$ could be isolated.[25] The variable temperature $^{31}P\{^1H\}$ NMR spectrum of the reaction solution showed two broad singlets centred at δ = 348.9 and 183.4 ppm (integral ratio: 1:1) indicating the formation of a diamagnetic compound which is only stable between 213 and 233 K, and that could not be isolated, despite numerous attempts.

Similar reaction products were observed for the reaction of **2** with $PBr_5$ (4 equiv.) at room temperature with a silent $^{31}P\{^1H\}$ NMR spectrum of the crude reaction mixture. This

time, the variable temperature NMR spectra of the reaction solution showed many different signals, indicating that the low temperature is not a way to better control the reaction outcome (cf. SI). Nevertheless, when **2** was reacted with $Br_2$ (4 equiv.) at -50°C, $[(Cp'''Co)_2(\mu\text{-}PBr_2)_2(\mu\text{-}Br)][Co_2Br_6]_{0.5}$ (**6a**) could be isolated (Scheme 3).

Surprisingly, a different reaction behaviour was observed when the chlorine source $PCl_5$ was used instead. While the VT $^{31}P\{^1H\}$ NMR spectra of the crude reaction mixture showed a similar multi-signal situation as for $PBr_5$ (cf. SI), the reaction between **2** and $PCl_5$ (4 equiv.) at room temperature leads to the isolation of the ionic complex $[(Cp'''Co)_2(\mu\text{-}PCl_2)_2(\mu\text{-}Cl)][Co_2Cl_6]_{0.5}$ (**6b**), which represents an analogue of **6a**, and to the neutral species $[(Cp'''Co)_2(\mu\text{-}PCl_2)(\mu\text{-}PCl)(\mu,\eta^1{:}\eta^1\text{-}P_2Cl_3]$ (**7**) (Scheme 3). **7** can be isolated after extraction with *n*-hexane.

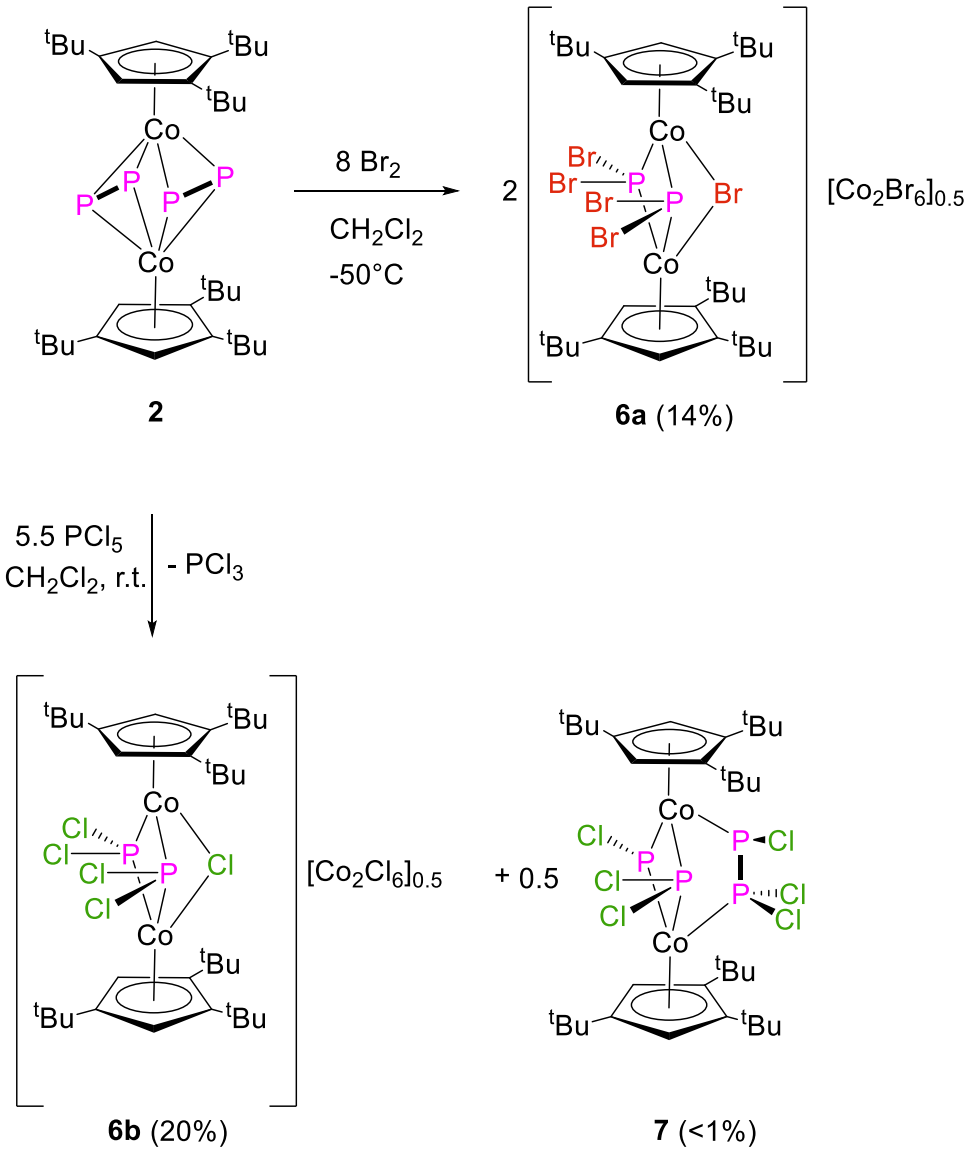


**Scheme 3.** Reaction of **2** with $Br_2$ and $PCl_5$. Isolated yields are given in parenthesis.

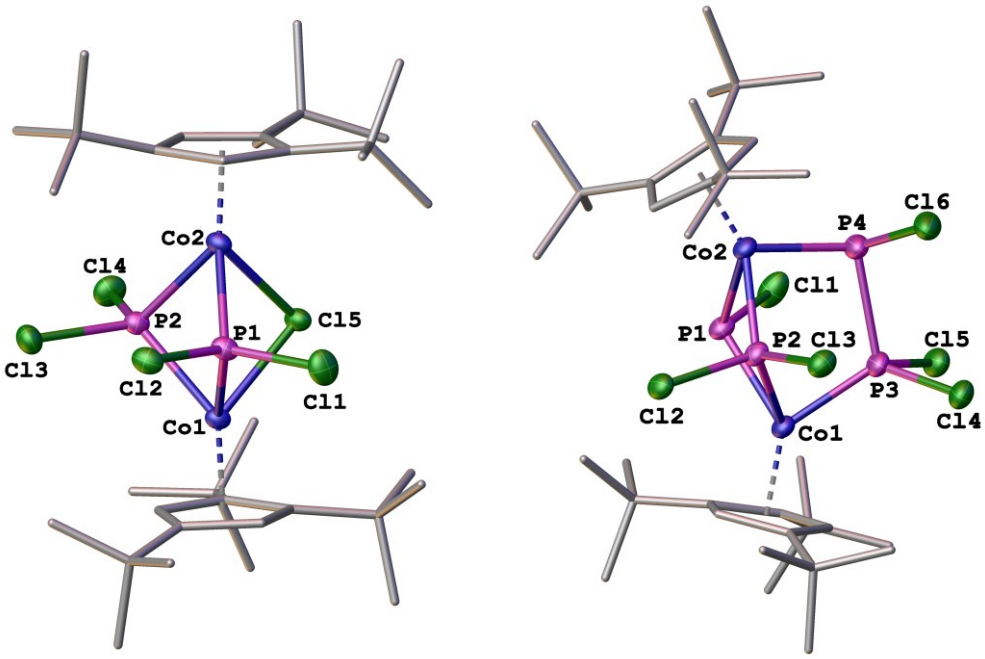


**Figure 3.** Molecular structure of the cation of **6b** (left) and of the neutral compound **7** (right) with thermal ellipsoids at 50% probability level. Due to the presence of disorder for compound **7**, only the major part is depicted. Hydrogen atoms and the solvent molecules are omitted for clarity.

The structures of **6a**,**b** and **7** in the solid state (Figure 3 and SI) show dinuclear complexes bearing halogen-containing phosphorus ligands. For the monocations in **6a**,**b** the two {Cp'''Co} fragments are connected by two bridging $PX_2$ units and an additional X ion (**6a**: X = Br; **6b**: X = Cl). The distance between P1 and P2 (**6a**: 2.696(17) Å, **6b**: 2.688(9) Å) is clearly too long to be considered as a bond. This is supported by DFT calculations (cf. SI), which show a bond order of 0.10 for the P1-P2 bond. The neutral compound **7** bears a {PCl} and a $\{PCl_2\}$ bridging ligand, with a distance comparable to the one in **6** (P1-P2: 2.608(3) Å: BO: 0.11) and a $\{P_2Cl_3\}$ bridging ligand, coordinating in a $\mu,\eta^1:\eta^1$ fashion to the two metal fragments. The P3-P4 bond length (2.240(3) Å) in the latter is in the range of a P-P single bond, which is in line with the results of DFT calculations (BO: 0.95).[19] The ligand $\{P_2Cl_3\}$ was so far only reported in the bimetallic complex $[\{Cp^*Mo(CO)_3\}_2(\mu\text{-}P_2Cl_3)][AlCl_4]$.[26] Compound **7** is extremely sensitive to moisture and air, probably due to the presence of a free lone pair on the P1 and P4 atoms (cf. SI). This might be the reason why, despite numerous attempts, compound **7** always co-crystalizes with the oxidized compound $[(Cp'''Co)_2(\mu\text{-}PCl_2)(\mu\text{-}PCl)(\mu,\eta^1:\eta^1\text{-}P_2OCl_3)]$ in an approximate ratio of 89:11 (cf. SI).

The $^{1}$H NMR spectra of **6a**,**b** ($CD_2Cl_2$) show the characteristic signals for the magnetically equivalent Cp''' ligands with the integral ratio of 2:18:9, centered at δ = 4.70, 1.21 and 1.02 ppm (**6a**) and at δ = 4.82, 1.07 and 0.79 ppm (**6b**). The $^{31}$P{$^{1}$H} NMR spectra show each one singlet at δ = 135.2 ppm (**6a**) and at δ = 176.2 ppm (**6b**) for the two equivalent P atoms. In the $^{31}$P{$^{1}$H} NMR spectrum of **6a** there are two additional doublets, centered at δ = 139.2 and at 30.9 ppm, with a $^{2}J_{PP}$ coupling constant of 21 Hz which may be assigned to an unidentified side-product (approximate ratio **6a**: side-product: 70:30) with two non-equivalent P atoms (cf. SI). The $^{31}$P{$^{1}$H} NMR spectrum of **7** shows an AMNX spin system with four resonances centered at δ = 211.6, 160.5, 147.4 and −22.4 ppm (integral ratio: 1:1:1:1). The signals of the two P atoms connected with a single bond resonates at δ = 160.5 ($P^M$) and at δ = 147.4 ($P^N$) ($^{1}J_{PMPN}$ = 358 Hz). The other two resonances belong to the bridging P atoms and for the upfield shifted one ($P^X$) a $^{2}J_{PMPX}$ coupling of 238 Hz is detected, due to the coupling with $P^M$ (cf. SI for further details).[27] Since the signal of $PX_3$ (X = Cl, Br) is always detected when using $PX_5$ (X = Cl, Br) as a regent, the question arose as which part of it comes from the halogenation of **2**. The $^{31}$P NMR spectroscopic investigation shows that only roughly 5% of $PCl_3$ and 9% of $PBr_3$ comes from $PCl_5$ and $PBr_5$ respectively, while the remaining > 90% results from the halogenation of **2**. The same investigation with $Br_2$ instead of $PBr_5$ showed that **2** is also partly transferred to $PBr_3$ (cf. SI).

Since the halogenation of **1** revealed a synthetic way to obtain the halogenated monocationic species **3**-**5** but with rather low yields and the halogenation of **2** showed some difficulties in the detection and isolation of the resulting species due to the moderate selectivity of the reaction, especially with iodine, the question arose as if it would be possible to find an alternative and milder way to form new P-X bonds, including the possibility to have access to fluorinated species. Therefore, the idea of quenching the cationic species $[(Cp'''Co)_2(\mu,\eta^4{:}\eta^4\text{-}E_4)][TEF]_2$[13] (E = As (**8**), P (**9**)) with weak nucleophiles, such as $X^-$ (X = I, F) arose.

The reaction of **8** with KI (2 equiv.) results in the formation of $[(Cp'''Co)_2(\mu,\eta^4{:}\eta^4\text{-}As_4I)][I]$ (**10**), which contains the same cation as **3a**, but $I^-$ instead of $[As_6I_8]^{2-}{}_{0.5}$ anion in slightly higher yields (**3a**: 3%, **10**: 9%) (Scheme 4). The solid-state structure of the cation in **10** (cf. SI) reveals the same strongly distorted *cyclo*-$As_4$ middle deck with an iodine attached to one As-As edge like in **3a**,**b**. The As-As bond lengths are comparable to the one observed in **3a** (bond lengths in **10**: As1-As2: 2.620(4) Å, As2-As3: 2.443(4) Å, 2.395(4) Å, As4-As1: 2.592(4) Å). The As1-I1 distance of 3.095 Å is elongated compared to the one in **3a** and to an As-I single bond.[19] The ESI mass spectrum of freshly dissolved crystals of **10** reveals

the molecular ion peak at *m/z* = 1010.9. The electronic structure of the cation in **10** is the same as for the cation in **3a**, therefore it will not be further discussed.

When the phosphorus analogue **9** was reacted under the same conditions with KI (2 equiv.), the iodide attacked the Co atom of only one of the two metal fragments, resulting in compound **11**, [(Cp'''Co)(Cp'''$CoI_2$)(μ,$\eta^4$:$\eta^1$-$P_4$)] (Scheme 4). The structure in the solid-state (Figure 4) reveals a sandwich complex with a square planar *cyclo*-$P_4$ ligand as middle-deck, coordinating in a $\eta^4$ fashion to the {Cp'''Co} fragment and in a $\eta^1$ mode to a new formed {Cp'''$CoI_2$} unit. The P-P bond lengths in the $P_4$ unit vary from 2.130(3) Å to 2.183(3) Å, being all in the range of a shortened P-P single bond[19] and are similar to those observed for the sandwich complex [Cp'''Co($\eta^4$-$P_4$)].[28] The sum of the internal P-P-P bond angles is close to 360° for both compounds. With the same procedure, **9** was reacted with the nucleophilic fluorinating agent tetramethylammonium fluoride ([$(CH_3)_4$N]F) to overcome the use of stronger fluorine sources such as $XeF_2$ or $PF_5$ in the reaction with $E_n$ ligand complexes.[29] The reaction of **9** with [$(CH_3)_4$N]F (2 equiv.) leads to compound [$(Cp'''Co)_2$(μ-$PF_2$)(μ,$\eta^2$:$\eta^1$:$\eta^1$-$P_3F_2$)] (**12**, Scheme 4) and to the neutral complex [$(Cp'''Co)_2$(μ,$\eta^2$:$\eta^2$-$P_2$)$_2$] (**2**). It could therefore formally be described as a disproportionation of **9** into **12** and **2**.[30] Compound **12** could also be obtained when the monocation [$(Cp'''Co)_2$(μ,$\eta^4$:$\eta^4$-$P_4$)][$BF_4$][13] (1 equiv.) was reacted with [$(CH_3)_4$N][F] (1 equiv.) under the same conditions (cf. SI). The solid state structure of **12** (Figure 4) reveals a cage-like complex with two {Cp'''Co} fragments connected via a bridging {$PF_2$} unit and a {$P_3F_2$} chain-like ligand. The $P_3$ ligand contains a P-P bond length in the range of a normal single bond (P3-P4: 2.202(12) Å) and a shortened one (P2-P3: 2.126(12) Å), being in the range of a P=P double bond, but it is better described as a vinyl like moiety. While the difluorophosphine ligand ($PF_2$) is widely known for both organic[31a,b] and inorganic compounds,[32a,b,c] the $P_3F_2$ unit was only reported so far in $Me_3SiR_2P_3F_2$ (R = $^t$Bu).[33] Therefore **12** represents the first complex bearing such a $P_3F_2$ ligand coordinated to a transition metal.

The $^1$H NMR spectrum of **10** ($CD_2Cl_2$) is comparable with the one observed for the analogue **3a**, the different anion is responsible for a small shift of the characteristic signals of the magnetically equivalent Cp''' ligands. Three sharp singlets, with an integral ratio of 2:18:9, are centred at δ = 4.79, 1.35 and 1.15 ppm. Compound **11** decomposes in solution at room temperature as proven by the $^{31}$P{$^1$H} NMR spectrum of the crystals dissolved in $CH_2Cl_2$, which shows only two resonances centred at −46.9 and −520.7 ppm, corresponding to **2** and $P_4$, respectively.[34] To check if the structure of **11** could be stable in solution at lower temperature, crystals of **11** were dissolved in $CD_2Cl_2$ at 193 K and a

variable temperature $^{31}P\{^{1}H\}$ NMR spectroscopic investigation was performed. The $^{31}P\{1H\}$ NMR spectrum at 193 K shows three multiplets centered at δ = 155.4, 129.3 and 42.3 (integral ratio: 2:1:1), corresponding to an $A_2BM$ spin system. At 213 K the spectrum shows two multiplets at δ = 158.6 and 44.1 ppm (integral ratio: 2:2), corresponding to an $A_2M_2$ spin system, which disappear at 253 K. Although these spectra may indicate a dynamic process in solution of the *cyclo*-$P_4$ ligand, the low yield of **11** and the resulting low resolution of the spectrum don't allow us to make any educated guess about the stability of **11** in solution at low temperature, nor to prove it.

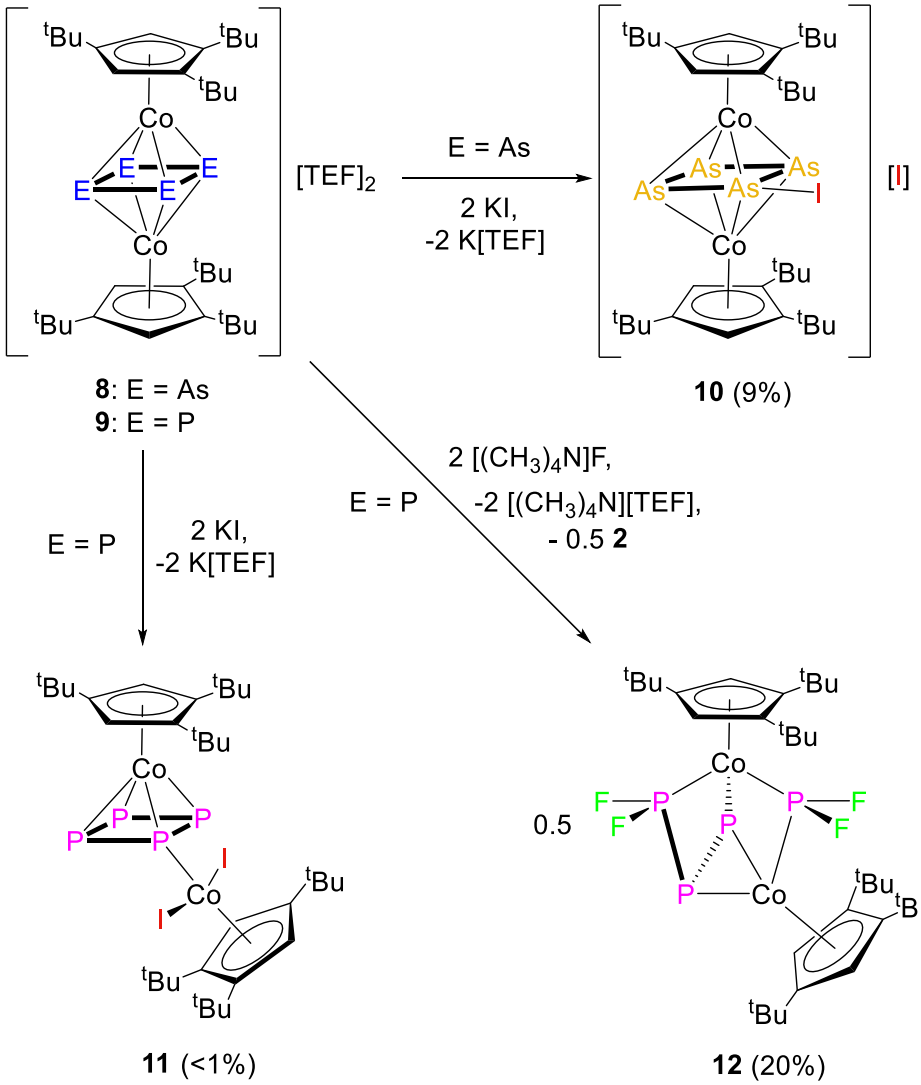


**Scheme 4.** Reaction of **8** and **9** with KI and ([$(CH_3)_4$N]F). Isolated yields are given in parenthesis.

The $^{1}H$ NMR spectrum, obtained from crystals of **12** ($CD_2Cl_2$) shows six signals for the two magnetically non-equivalent Cp''' ligands, together with the signals of the Cp''' from **2** which co-crystallizes with **12**.[35] The $^{31}P\{^{1}H\}$ NMR spectrum shows an AMXZ spin system with four signals at δ = 303.3, 218.9, 46.0 and −51.4 ppm. The signal of the P atom from

the bridging $PF_2$ ligand ($P^A$) resonates at 303.3 ppm and shows a large coupling constant to the F atoms ($^1J_{PF}$ = 1213 Hz and 1269 Hz ).

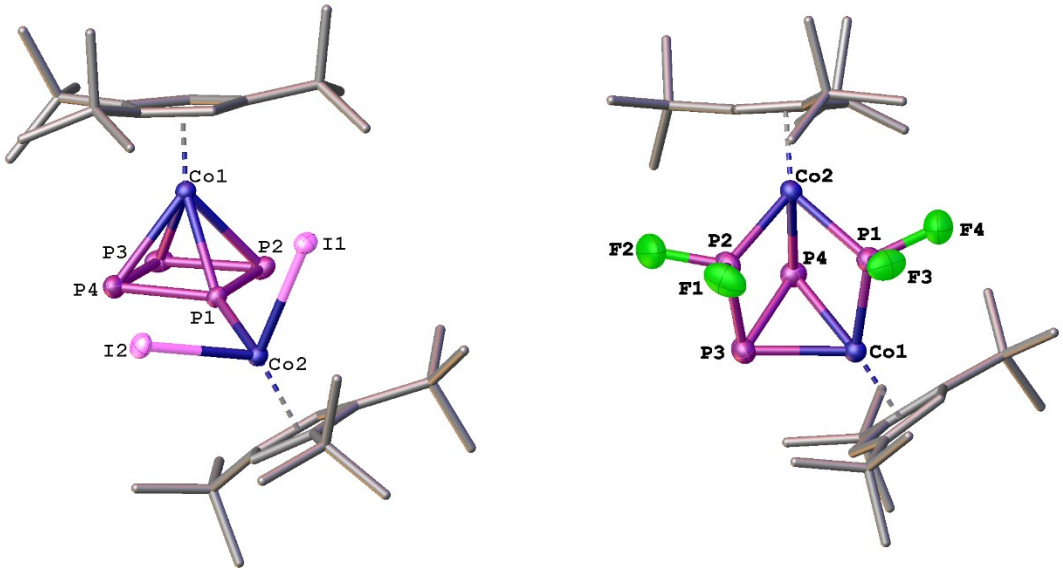


**Figure 4.** Molecular structure of **11** (left) and **12** (right) in the solid state with thermal ellipsoids at 50% probability level. In case of disorder only the major parts are depicted. The hydrogen atoms and the solvent molecules are omitted for clarity.

The other three resonances belong to the $P_3F_2$-chain ligand. The difluorinated P atom ($P^M$) resonates at 218.9 ppm ($^1J_{PF}$ =1322 Hz and 1367 Hz). The signal at −51.4 ppm partly overlaps with the signal of compound **2**, which co-crystallized with **12**. The $^{19}F\{^1H\}$ NMR spectrum of **12** shows an AMNX spin system, with four signals centred at δ = 13.2, −13.0, −17.4 and −34.9 ppm, corresponding to the four non-equivalent fluorine atoms (cf. SI for additional coupling constants). The $^{31}P/^{19}F$ NMR chemical shifts and coupling constants of compound **12** were calculated by iterative simulation of the experimental spectra.

## 5.3 Conclusions

In summary, we showed that $[(Cp'''Co)_2(\mu,\eta^2{:}\eta^2\text{-}As_2)_2]$ (**1**) can easily be oxidized by halogens to get the monocationic species **3**-**5** which reveal the formation of two new As-As single bonds to form a so far unprecedented cyclic $As_4X$ ligand (X = I, Br, Cl). An alternative route to the same cationic complexes was obtained by reacting the dication $[(Cp'''Co)_2(\mu,\eta^4{:}\eta^4\text{-}As_4)][TEF]_2$ (**8**) with KI. The quenching of this dication with a weak nucleophile such as the $I^-$ resulted in the analogue compound **10**, in higher yield. The use of this milder nucleophile resulted in the more selective halogenation “limited” to the $As_4$

middle-deck, contrarily to the formation of the anion $[As_6I_8]^{2-}$, obtained when the stronger elemental iodine was used. In the case of the P analogue complexes (**2** and **9**), the reaction of the neutral compound (**2**) towards halogens and halogen sources led to a different outcome from the complexes obtained by the quenching of the dicationic species (**9**) by a weak nucleophile. Nevertheless, it was possible to obtain new polyphosphorus compounds bearing P-X bonds. Moreover, by this method and the use of a mild fluoride source, such as $[(CH_3)_4N][F]$, novel P-F bonds are formed in a controlled way, as observed for compound **12**, $[(Cp'''Co)_2(\mu\text{-}PF_2)(\mu,\eta^2\text{:}\eta^1\text{-}P_3F_2)]$, which contains a novel and so far unprecedented $P_3F_2$-chain ligand. This result opens the possibility of synthesis of new polypnictogen compounds bearing P-X bonds with milder reagents and less harsh reaction conditions, enabling the formation of P-F bonds avoiding the hazardous and harsh reacting $XeF_2$ or $PF_5$ reagents.

## 5.4 References


[1] D. E. C., Corbridge, *Phosphorus: Chemistry, Biochemistry and Technology*, 6th Edition, CRC Press, Boca Raton, FL, **2013**.
[2] Halogenation of $P_4$: a) D. Wyllie, M. Ritchie, E. B. Ludlom *J. Chem. Soc*. **1940**, 583-587; b) B.W. Tattershall, N.L. Kendall *Polyhedron* **1994**, *13*, 1517-1521.
[3] M. Bispinghoff, Z. Benkő, H. Grützmacher, F. Delgado Calvo, M. Caporali, M. Peruzzini, *Dalton Trans.* **2019**, *48*, 3593-3600.
[4] M. Caporali, L. Gonsalvi, A. Rossin, M. Peruzzini, *Chem. Rev.* **2010**, *110*, 4178-4235.
[5] B. M. Cossairt, N. A. Piro, C. C. Cummins, *Chem. Rev.* **2010**, *110*, 4164-4177.
[6] C M. Hoidn, D. J. Scott; R. Wolf. *Chem. Eur. J.* **2021**, *27*, 1886-1902.
[7] A. Garbagnati, M. Seidl, G. Balázs, M. Scheer, *Inorg. Chem*. **2021**, *60*, 5163-5171.
[8] H. Brake, E. Peresypkina, A. V. Virovets, M. Piesch, W. Kremer, L. Zimmermann, Ch. Klimas, M. Scheer, *Angew. Chem. Int. Ed.* **2020**, *59*, 16241-16246.
[9] Cf. Chapter 4.
[10] compound **1**: C. Graβl, M. Bodensteiner, M. Zabel, M. Scheer, *Chem. Sci.* **2015**, *6*, 1379-1382; compound **2**: F. Dielmann, M. Sierka, A. V. Virovets, M. Scheer, *Angew. Chem. Int. Ed.* **2010**, *49*, 6860-6864.
[11] M. Fleischmann, F. Dielmann, G. Balázs, M. Scheer, *Chem. Eur. J*. **2016**, *22*, 15248-15251.
[12] M. Piesch, S. Reichl, C. Riesinger, M. Seidl, G. Balázs, M. Scheer, *Chem. Eur. J.* **2021**, *27*, 9129-9140.
[13] M Piesch, C. Graβl, M. Scheer, *Angew. Chem. Int. Ed*. **2020**, *59*, 7154-7160.
[14] I. Krossing, *J. Chem. Soc. Dalton Trans*. **2002**, 500-512.
[15] P. Barbaro, C. Bazzicalupi, M. Peruzzini, S. Seniori Costantini, P. Stoppioni, *Angew. Chem. Int. Ed.* **2012**, *51*, 8628-8631.
[16] a) N. J. Hill, W. Levason, G. Reid, *J. Chem. Soc. Dalton Trans*. **2002**, 1188-1192; b) N. J. Hill, W. Levason, G. Reid, *Inorg. Chem.* **2002**, *41*, 2070-2076.
[17] a) A. Strube, G. Huttner, L. Zsolnai, W. Imhof, *J. Organomet. Chem.* **1990**, *399*, 281-290; b) I. Y. Ilyin, S. N. Konchenko, N. A. Pushkarevsky, *J. Cluster Sci*. **2015**, *26*, 257-268.
[18] a) C. A. Ghilardi, S. Midollini, S. Moneti, A. Orlandini, *J. Chem. Soc. Chem. Commun.* **1988**, 1241-1242; b) B. D. Ellis, C. L. B. Macdonald, *Inorg. Chem*. **2004**, *43*, 5981-5986.
[19] P. Pykkö, M. Atsumi, *Chem. Eur. J*. **2009**, *15*, 12770-12779.
[20] a) ORCA - *An Ab Initio, DFT and Semiempirical electronic structure package*, Version 4.2.1; b) F. Neese, *WIREs Comput Mol Sci.*, **2012**, *2*, 73–78; b) F. Neese, *WIREs Comput Mol Sci.*, **2017**, *8*, e1327.
[21] J. Tao, J. P. Perdew, V. N. Staroverov, G. E. Scuseria, *Phys. Rev. Lett.* **2003**, *91*, 146401; V. N. Staroverov, G. E. Scuseria, J. Tao, J. P. Perdew, *J. Chem. Phys.* **2003**, *119*, 12129-12137; Erratum: *J. Chem. Phys.* **2004**, *121*, 11507-11507.
[22] a) F. Weigend and R. Ahlrichs, *Phys. Chem. Chem. Phys.*, **2005**, *7*, 3297–3305; b) F. Weigend, M. Häser, H. Patzelt and R. Ahlrichs, *Chem. Phys. Lett.*, **1998**, *294*, 143–152.
[23] a) K.A. Smart, A. Vanbergen, J. Lednik, C. Y. Tang, H. B. Mansaray, I. Siewert, S. Aldrige, *J. Organometal. Chem.* **2013**, *741*,33-39; b) W. Harrison, J. Trotter, *J. Chem. Soc. Dalton Trans.*, **1973**, 61-64.

[24] F. Baumann, E. Dormann, Y. Ehleiter, W. Kaim, J. Karcher, M. Kelemen, R. Krammer, D. Saurenz, D. Stalke, C. Wachter, G. Wolmershauser, H. Sitzmann, *J. Organometal. Chem.* **1999**, *587*, 267-277.
[25] The value of the unit cell parameters is similar to the one of the reported X-ray structure of $P_2I_4$. Cf. Y. C. Leung, J. Waser, *J. Phys. Chem.* **1956**, *60*, 539-543.
[26] R. A. Rajagopalan, A. Jayaraman, B. T. Sterenberg, *J. Organomet. Chem.* **2014**, *761*, 84-92.
[27] Although crystals of **7** could be obtained several times, the characterization of this compound was rather problematic. When the $^{31}P\{^1H\}$ NMR spectrum of the dark brown crystals was recorded ($CD_2Cl_2$), a very complex spectrum was obtained, showing that probably other compounds co-crystallize with **7**. The hexane solution used to extract **7** was filtered over silanized silica gel and this afforded a clean $^{31}P\{^1H\}$ NMR spectrum showing an AMNX spin system. This spectrum is too complex for compound **7** and, probably belongs to a different compound that could not be crystallized (compound $\mathbf{7_{silica}}$). When the same hexane solution was filtered over celite, the $^{31}P\{^1H\}$ NMR spectrum of the solution shows among some other signals, signals for $\mathbf{7_{silica}}$ and **7**. By comparing both spectra, and with the help of a COSY $^{31}P$-$^{31}P$ NMR experiment the signals corresponding to **7** could be unequivocally attributed (cf. SI for detailed spectra).
[28] F. Dielmann, A. Timoshkin, M. Piesch, G.Balázs, M. Scheer *Angew. Chem. Int. Ed*. **2017**, *56*, 1671-1675
[29] $XeF_2$ has proved not to be the ideal fluorine source for such purposes. The use of $XeF_2$ requires to work in the dark, with Teflon or plastic vessels and all our previous attempts of fluorination of **1** with $XeF_2$ resulted in its complete decomposition as well. (There is no direct evidence for the formation of $AsF_6^-$ as the final product of the decomposition but many signals are detected in the $^1$H-NMR spectra of the reaction solution, while the one of **1** disappears. Unfortunately, no crystals could be isolated).
[30] The attempt to isolate the heavier As analogue of **12**, by reacting **8** (1 equiv.) with TMAF (2 equiv.) resulted in the isolation of a few crystals of the neutral species **1**. This may suggest that the quenching of **8** with TMAF also proceed as a disproportionation but no crystals of the fluorinated As-derivative could be isolated yet.
[31] a) H. Kanter, K. Dimroth, *Angew. Chem. Int. Ed. Engl*. **1972**, *11*, 1090-1091; b) D. Bornemann, C. R. Pitts, L. Wettstein, F, Brüning, S. Küng, L. Guan, N. Trapp, H. Grützmacher, A. Togni, *Angew. Chem. Int. Ed*. **2020**, *59*, 22790-22795.
[32] a) S. Kahlal, W. Wang, L. Scoles, K. A. Udachin, J. Saillard, A. J. Carty, *Organometallics*, **2001**, *20*, 4469-4475; b) C. M. Hoidn, J. Leitl, C. G. P. Ziegler, I. G. Shenderovich, R. Wolf, *Eur. J. Inorg. Chem*. **2019**, 1567-1574; c) A. M. A. Boshaala, S. J. Simpson, J. Autschbach, S. Zheng, *Inorg. Chem*. **2008**, *47*, 9279-9292.
[33] G. Fritz, M. Jarmer, E. Matern, *Z. Anorg. Allg. Chem.* **1990**, *589*, 23-38
[34] The ESI mass spectrum of a solution of the crystals of **11** showed a peak at *m/z* = 708.3 which could be assigned to **2**. Our hypothesis is that, in solution at room temperature **11** decomposes to **2**, $P_4$ and $[(Cp'''Co)_2(I)_2]$ but the last compound could not be detected e.g. by ESI mass spectrometry.
[35] In the $^1$H NMR spectrum there are three additional signals that of a Cp''' ligand of a compound that could not be identified so far.

## 5.5 Supporting information

### General procedures

All manipulations were carried out under an inert atmosphere of dried nitrogen using standard Schlenk and glove box techniques. Solvents were dried using a MB SPS-800 device of the company MBRAUN. Deuterated solvents were freshly distilled under nitrogen from $CaH_2$ ($CD_2Cl_2$) and from Na/K alloy ($C_6D_6$).

NMR spectra were recorded on a Bruker Advance III 400 MHz NMR spectrometer. If not differently mentioned, chemical shifts were measured at room temperature and given in ppm; they are referenced to TMS for $^1H$ and 85% $H_3PO_4$ for $^{31}P$ as external standard. LIFDI-MS spectra (LIFDI = liquid injection field desorption ionization) were measured on a JEOL AccuTOF GCX. ESI-MS spectra (ESI = Electrospray ionization) were measured on an Agilent Q-TOF 6540 UHD. Elemental Analysis (CHN) was determined using a Vario micro cube instrument.

Compounds $[(Cp'''Co)_2(\mu,\eta^2:\eta^2\text{-}E_2)_2]$ (E = As (**1**), P (**2**)) were synthesized according to literature procedure,[1] as well as compounds $[(Cp'''Co)_2(\mu,\eta^4:\eta^4\text{-}E_4)][TEF]_2$ ( E = As (**8**), P (**9**))[2].

Phosphorous (V) chloride ($PCl_5$) and Tetramethylammonium fluoride anhydrous $(CH_3)_4NF$) were purchased from abcr, Phosphorous (V) bromide (95%) ($PBr_5$) from Alfa Aesar, Bromine ($Br_2$) and 18-crown-6 ($(C_2H_4O)_6$) from ACROS Organics, Iodine ($I_2$) and Potassium iodide (KI) from Sigma-Aldrich and they were all used as received without any further purifications.

**Synthesis of $[(Cp'''Co)_2(\mu,\eta^4\text{-}As_4X)][Y]$ (X = I, Y = $[As_6I_8]_{0.5}$) (3a) (X = I, Y = $[Co_2Cl_{6-n}I_n]_{0.5}$ (n = 0, 2, 4)) (3b)**

$[(Cp'''Co)_2(\mu,\eta^2:\eta^2\text{-}As_2)_2]$ (**1**) (100 mg, 0.112 mmol, 1 equiv.) is dissolved in 15 mL of $CH_2Cl_2$. To this solution, a solution of $I_2$ (60 mg, 0.452 mmol, 4 equiv.) in 15 mL of $CH_2Cl_2$ is added. A change in colour from mint green to dark brown/green is immediately observed. The solution is stirred for one hour and fifteen minutes, then the solvent is removed *in vacuo*. The resulting brown precipitate is redissolved in 20 mL of toluene, filtered over celite, layered with 40 mL of pentane. After a few days at room temperature, brown prisms shaped crystals of $[(Cp'''Co)_2(\mu,\eta^4:\eta^4\text{-}As_4I)][\ As_6I_8]_{0.5}$ (**3a**) were isolated. When toluene is replaced by $CH_2Cl_2$ as solvent of crystallization, together with **3a**, also a few crystals of $[(Cp'''Co)_2(\mu,\eta^4:\eta^4\text{-}As_4I)][Co_2Cl_{6-n}I_n]_{0.5}$ (n = 0, 2, 4) (**3b**) could be isolated.

Yield **3a**: 10 mg (3%)

Yield **3b**: a few crystals.

**$^1$H NMR 3a** (400 MHz, $CD_2Cl_2$, 300K): δ [ppm] = 4.68 (s, 2H, $C_5H_2{}^tBu_3$), 1.49 (s, 18H, -$(C_4H_9)_2$), 1.46 (s, 9H, -$(C_4H_9)$).

**ESI-MS** ($CH_2Cl_2$): **3a**: cation mode: *m/z* = 1010.92 (58%, **M$^+$**), 809.09 (100%, **M$^+$**- AsI); anion mode: *m/z* = 1084.05 (18%, $[As_6I_8]^{2-}$-3I), 126.91 (100%, $I^-$). **3b:** *m/z* = 1010.92 (100%, **M$^+$**), 809.09 (61%, **M$^+$**- AsI); anion mode: *m/z* = 439.65 (7%, $[CoI_3]^-$), 347.71(1%, $[CoI_2Cl]^-$), 126.91 (100%, $I^-$).

**EA** calculated for $[C_{34}H_{58}Co_2As_4I][As_6I_8]_{0.5}$ (1743.69 g·mol$^{-1}$): C: 23.42, H: 3.35; found [%]: C: 23.62, H: 2.96.

**Synthesis of $[(Cp'''Co)_2(\mu,\eta^4{:}\eta^4\text{-}As_4Br)][(Co_2Br_6)_{0.5}]$ (4)**

$[(Cp'''Co)_2(\mu,\eta^2{:}\eta^2\text{-}As_2)_2]$ (**1**) (100 mg, 0.112 mmol, 1 equiv.) and $PBr_5$ (193 mg, 0.448 mmol, 4 equiv.) are dissolved together in 25 mL of $CH_2Cl_2$. The resulting dark green solution is stirred for two hours and then the solvent is removed under reduced pressure. The formed brown oily precipitate is washed with pentane (5 mL), extracted with 15 mL of toluene and layered with 30 mL of pentane. After a few days at -30°C too bad diffracting crystals were isolated and recrystallized from $CH_2Cl_2$/pentane leading to green plates of $[(Cp'''Co)_2(\mu,\eta^4{:}\eta^4\text{-}As_4Br)][Co_2Br_6]_{0.5}$ (**4**) suitable for X-ray analysis.
Yield **4**: 47 mg (33%)

**$^1$H NMR** (400 MHz, $CD_2Cl_2$, 300K): δ [ppm] = 4.28 (br. s, $\omega_{1/2}$ = 60 Hz, 2H, $C_5H_2{}^tBu_3$), 0.93 (s, 9H, -$(C_4H_9)$), 0.81 (s, 18H, -$(C_4H_9)_2$).

**ESI-MS** ($CH_2Cl_2$): cation mode: *m/z* = 962.93 (29%, **M$^+$**), 809.09 (100%, **M$^+$**- AsBr); anion mode: *m/z* = 297.69 (100%, $[CoBr_3]^-$).

**EA** calculated for $[C_{34}H_{58}Co_2As_4Br][Co_2Br_6]_{0.5}\cdots(CH_2Cl_2)$ (1347.86 g·mol$^{-1}$): C: 31.19, H: 4.49; found [%]: C:31.07, H: 4.35.

**Synthesis of $[(Cp'''Co)_2(\mu,\eta^4{:}\eta^4\text{-}As_4Cl)][(Co_2Cl_6)_{0.5}]$ (5)**

$[(Cp'''Co)_2(\mu,\eta^2{:}\eta^2\text{-}As_2)_2]$ (**1**) (100 mg, 0.112 mmol, 1 equiv.) and $PCl_5$ (93 mg, 0.448 mmol, 4 equiv.) are dissolved together in 25 mL of $CH_2Cl_2$. The resulting dark green/brown solution is stirred for three hours at room temperature and afterwards the solvent is removed *in vacuo* to eliminate the formed $PCl_3$. The residue is redissolved in 10 mL of $CH_2Cl_2$ and precipitated by the addition of 25 mL of cold hexane. The resulting precipitate is dissolved in 15 mL of $CH_2Cl_2$ and layered with 30 mL of hexane affording green blocks crystals of $[(Cp'''Co)_2(\mu,\eta^4{:}\eta^4\text{-}As_4Cl)][(Co_2Cl_6)_{0.5}]$ (**5**), suitable for X-ray analysis.

Yield **5**: 19 mg (16%)

**$^1$H NMR** (400 MHz, $CD_2Cl_2$, 300K): δ [ppm] = 4.02 (s, $\omega_{1/2}$ = 312 Hz, 2H, $C_5H_2{}^tBu_3$), 0.83 (s, 18H, -$(C_4H_9)_2$), 0.71 (s, 9H, -$(C_4H_9)$).

**ESI-MS** ($CH_2Cl_2$): cation mode: *m/z* = 922.01 (1%, **M$^+$**), 809.09 (100%, **M$^+$**- AsCl); anion mode: *m/z* = 163.84 (100%, $[CoCl_3]^-$).

**EA** calculated for $[C_{34}H_{58}Co_2As_4Cl][Co_2Cl_6]_{0.5}\cdots(CH_2Cl_2)_3$ (1339.92 g·mol$^{-1}$): C: 33.17, H: 4.81; found [%]: C: 33.75, H: 4.87.

**$[(Cp'''Co)_2(\mu\text{-}PBr_2)_2(\mu\text{-}Br)][(Co_2Br_6)_{0.5}]$ (6a)**

$[(Cp'''Co)_2(\mu,\eta^2{:}\eta^2\text{-}P_2)_2]$ (**2**) (100 mg, 0.141 mmol, 1 equiv.) is dissolved in 15 mL of $CH_2Cl_2$ and cool to -50°C. To this solution, a solution of $Br_2$ in $CH_2Cl_2$ (dilution 1:100) (2.9 mL, 90 mg, 0.565 mmol, 4 equiv.) is added dropwise. The colour changes immediately from dark grey to brown/red and it turns red wine after five minutes. The solution is stirred at -50°C for one hour and a half, then the solvent is removed *in vacuo*, allowing the temperature to rise until -35°C. The residue is washed with 10 mL of toluene, redissolved in 10 mL of $CH_2Cl_2$ and precipitated by the addition of 25 mL of hexane ( T = -50°C).The resulting purple precipitate is redissolved in 10 mL of $CH_2Cl_2$ and layered with 20 mL of hexane. After a few days at -30°C purple blocks crystals of $[(Cp'''Co)_2(\mu\text{-}PBr_2)_2(\mu\text{-}Br)][Co_2Br_6]_{0.5}$ (**6a**) could be isolated.
Yield **6a**: 25 mg (14%)

**$^1$H NMR** (400 MHz, $CD_2Cl_2$, 300K): δ [ppm] = 4.70 (s, 2H, $C_5H_2{}^tBu_3$), 1.21 (s, 18H, -$(C_4H_9)_2$), 1.02 (s, 9H, -$(C_4H_9)$).

**$^{31}$P{$^1$H} NMR** (162 MHz, $CD_2Cl_2$, 300K). δ [ppm] = 135.2 (s).

**EI-MS** ($CH_2Cl_2$, sample at 203 K): cation mode: *m/z* = 1044.85 (100%, **M$^+$**), 887.01 (14%, **M$^+$**-2Br) 727.23 (15%, **M$^+$**-4Br); anion mode: *m/z* =299.68 (100%$[CoBr_3]^-$).

**EA** The compound in the solid state decomposes at room temperature, therefore it was not possible to obtain a correct elemental analysis.

**$[(Cp'''Co)_2(\mu\text{-}PCl_2)_2(\mu\text{-}Cl)][Co_2Cl_6]_{0.5}$ (6b)**

$[(Cp'''Co)_2(\mu,\eta^2{:}\eta^2\text{-}P_2)_2]$ (**2**) (100 mg, 0.141 mmol, 1 equiv.) is dissolved in 15 mL of $CH_2Cl_2$. To this solution, a solution of $PCl_5$ (118 mg, 0.565 mmol, 4 equiv.) in 20 mL of $CH_2Cl_2$ is added. A change in colour from dark grey to dark brown/red is observed. The solution is stirred for one hour and a half and then the solvent is removed *in vacuo*. The residue is

washed with 10 mL of hexane and the resulting purple precipitate is dissolved in 15 mL of $CH_2Cl_2$, layered with 30 mL of toluene and stored at room temperature. After a few days of $[(Cp'''Co)_2(\mu\text{-}PCl_2)_2(\mu\text{-}Cl)][Co_2Cl_6]_{0.5}$ (**6b**) could be isolated as purple block crystals, suitable for X-ray analysis.
Yield **6b**: 16 mg (20%)

**$^1$H NMR** (400 MHz, $CD_2Cl_2$, 300K): δ [ppm] = 4.82 (s, 2H, $C_5H_2{}^tBu_3$), 1.07 (s, 18H, -$(C_4H_9)_2$), 0.80 (s, 9H, -$(C_4H_9)$).

**$^{31}$P{$^1$H} NMR** (162 MHz, $CD_2Cl_2$, 300K): δ [ppm] = 176.15 (s).

**ESI-MS** ($CH_2Cl_2$): cation mode: *m/z* = 823.11 (100%, **M$^+$**); anion mode: *m/z* = 163.84 (100%, $[CoCl_3]^-$).

**EA** calculated for $[C_{34}H_{58}Co_2P_2Cl_5][Co_2Cl_6]_{0.5}$ (989.20 g·mol$^{-1}$): C: 41.28, H: 5.91, found [%]: C: 41.23, H: 5.47.

**$[(Cp'''Co)_2(\mu\text{-}PCl_2)(\mu\text{-}PCl)(\mu,\eta^1\text{:}\eta^1\text{-}P_2Cl_3]$ (7)**

$[(Cp'''Co)_2(\mu,\eta^2\text{:}\eta^2\text{-}P_2)_2]$ (**2**) (200 mg, 0.282 mmol, 1 equiv.) is dissolved in 25 mL of $CH_2Cl_2$. To this solution, a solution of $PCl_5$ (236 mg, 1.130 mmol, 4 equiv.) in 25 mL of $CH_2Cl_2$ is added. A change in colour from dark grey to dark brown/red is observed. The solution is stirred for one hour and a half and then the solvent is removed *in vacuo*. The residue is extracted with 10 mL of hexane and stored at room temperature in a double Schlenk for the slow diffusion. Crystals of $[(Cp'''Co)_2(\mu\text{-}PCl_2)(\mu\text{-}PCl)(\mu,\eta^1\text{:}\eta^1\text{-}P_2Cl_3]$ (**7**), suitable for X-ray analysis were isolated after two days in the shape of dark brown rods.
Yield **7**: a few crystals.

**$^1$H NMR** (400 MHz, $CD_2Cl_2$, 300K): δ [ppm] = Since crystals of **7** could not be separated from the other products extracted from the hexane fraction, a safe $^1$H NMR attribution could not be performed, contrarily to the $^{31}$P NMR signals that could be safely assigned with the exclusion of the signals attributed to other products (**$7_{silica}$**) and in combination with a $^{31}$P-$^{31}$P COSY 2D NMR.

**$^{31}$P{$^1$H} NMR** (162 MHz, $CD_2Cl_2$, 300K): AMNX spin system. δ [ppm]: $\delta_A$ = 211.6 (1P, br. m), 160.5 (1P, br. ddd), 147.4 (1P, br. dm), -22.4 (1P, br. dd). For coupling constants see TableS1.

**EA** Due to the very low yield of the reaction it was not possible to make an elemental analysis.

**[(Cp'''Co)$_2$(μ,η$^4$:η$^4$-As$_4$I)][I] (10)**

[(Cp'''Co)$_2$(μ,η$^4$:η$^4$-As$_4$)][TEF]$_2$ (**8**) (125 mg, 0.04 mmol, 1 equiv.) is dissolved in 15 mL of $CH_2Cl_2$. Separately, KI (15 mg, 0.089 mmol, 2 equiv.) and 18-crown-6 (23 mg, 0.089 mmol, 2 equiv.) are suspended in $CH_2Cl_2$ and left in the ultrasonic bath for two hours to dissolve completely. Afterwards, this solution is added to **8** leading to an immediate colour change from dark green to dark red. The solution is stirred for thirty minutes, filtered with a cannula and then the solvent is removed under reduced pressure. The resulting brown precipitate is washed with 10 mL of pentane, dissolved in 15 mL of toluene and layered with 30 mL of pentane. Crystals of [(Cp'''Co)$_2$(μ,η$^4$:η$^4$-As$_4$I)][I] (**10**) could be isolated after one week as black plates.

Yield **10**: 5 mg (9%)

**$^1$H NMR** (400 MHz, $CD_2Cl_2$, 300K): δ [ppm] = 4.79 (s, 2H, $C_5H_2{}^tBu_3$), 1.35 (s, 18H, -($C_4H_9$)$_2$), 1.15 (s, 9H, -($C_4H_9$)).

**ESI-MS** ($CH_2Cl_2$): cation mode: *m/z* = 1010.91 (53%, **M$^+$**), 809.09 (100%, **M$^+$**- AsI).

**EA** Due to the high sensitivity of this compound, it was not possible to get an exact elemental analysis, contrarily to the analogue **3a**.

**[(Cp'''Co)(Cp'''CoI$_2$)(μ,η$^4$:η$^1$-P$_4$)] (11)**

[(Cp'''Co)$_2$(μ,η$^4$:η$^4$-P$_4$)][TEF]$_2$ (**9**) (100 mg, 0.038 mmol, 1 equiv.) is dissolved in 15 mL of $CH_2Cl_2$. Separately, KI (13 mg, 0.076 mmol, 2 equiv.) and 18-crown-6 (20 mg, 0.076 mmol, 2 equiv.) are suspended in $CH_2Cl_2$ and left in the sonic bath for two hours to dissolve completely. Afterwards, this solution is added to **9** and within a few minutes, despite no visible colour change, the formation of a precipitate could be observed. The solution is stirred for one hour at room temperature and then the solvent is removed *in vacuo*. The product is extracted with 10 mL of pentane, filtered with a cannula and stored at room temperature in a double Schlenk for the slow diffusion. Crystals of [(Cp'''Co)(Cp'''CoI$_2$)(μ,η$^4$:η$^1$-P$_4$)] (**11**) could be isolated after one week in the shape of black plates.

Yield **11**: a few crystals

The following attribution comes from signals detected in the VT $^1$H and $^{31}$P{$^1$H} NMR investigations (193-300 K) performed on the crystals (dissolved in $CD_2Cl_2$ at 193 K). To be noted is that when $^{31}$P{$^1$H} NMR spectrum of the solution obtained by dissolving the crystals of **11** is recorded at room temperature, only signals of decomposition products are

detected (such as the neutral specie **2** at δ = -46.9 ppm and $P_4$ at δ = -520.7 ppm, cf. figures in the Selected NMR section).

**$^1$H NMR** Due to the presence of many different signals for decomposition products, a safe attribution of **11** could not be performed.

**$^{31}$P{$^1$H} NMR** (162 MHz, $CD_2Cl_2$, 193K, from VT $^{31}$P{$^1$H} NMR of the solution of crystals of **11**, prepared at 193K) δ [ppm] = 155.4 (m, 2P), 129.3 (m, 1P), 42.3 (m, 1P).

**$^{31}$P{$^1$H} NMR** (162 MHz, $CD_2Cl_2$, 213K, from VT $^{31}$P{$^1$H} NMR of the solution of crystals of **11**, prepared at 193K) δ [ppm] = 158.6 (m, 2P), 44.1 (m, 2P).

**ES-MS** ($CH_2Cl_2$): *m/z* = 123.89 (9%, **$P_4^+$**), 708.26 (<1%, **$2^+$**). Only decomposition products could be detected.

**EA** Due to the very low yield of the reaction it was not possible to make an elemental analysis.

**[(Cp’’’Co)$_2$(μ,PF$_2$)(μ,η$^2$:η$^1$-P$_3$F$_2$)] (12)**

[(Cp’’’Co)$_2$(μ,η$^4$:η$^4$-P$_4$)][TEF]$_2$ (**9**) (100 mg, 0.038 mmol, 1 equiv.) and $(CH_3)_4NF$ (7 mg, 0.073 mmol, 2 equiv.) are dissolved in 25 mL of $CH_2Cl_2$. No visible colour change is observed, the solution is stirred at room temperature for three days. The brown/red solution is filtered with a cannula, then the solvent is removed *in vacuo*. The precipitate is washed with hexane ( 3 x 10 mL) and the resulting orange solution is filtered, dried again *in vacuo* and the product is extracted with $CH_3CN$ and stored at -30°C. After a few days, the extremely air sensitive compound [(Cp’’’Co)$_2$(μ-PF$_2$)(μ,η$^2$:η1: η$^1$-P$_3$F$_2$)] (**12**) could be isolated as orange plate crystals suitable for X-ray analysis.
Yield **12**: 6 mg (20%)

**$^1$H NMR** (400 MHz, $CD_2Cl_2$, 300K): δ [ppm] =Due to the present of some impurities, it is not possible to make a safe assignment to the signals of the Cp’’’ ligand (cf. $^1$H NMR spectrum below).

**$^{31}$P{$^1$H} NMR** (162 MHz, $CD_2Cl_2$, 300K): AMXZ spin system. δ [ppm]: $\delta_A$ = 303.3 (1P, dd), $\delta_M$ = 218.9 (1P, ddd), $\delta_X$ = 46.0 (1P, dm), $\delta_Z$ = -51.4 (1P, dm). For coupling constants see Table S3.

**$^{19}$F{$^1$H} NMR** (377 MHz, $CD_2Cl_2$, 300K): δ [ppm] = AMNX spin system. δ [ppm]: $\delta_A$ = 13.2 (1F, dm), $\delta_M$ = -13.0 (1F, dm), $\delta_N$ = -17.4 (1F, dm), $\delta_X$ =-34.9 (1F, dm). For coupling constants see Table S4.

**LIFDI-MS** ($CH_3CN$): 677.24 (100%, $\mathbf{M^+}$-$PF_4$).

**EI-MS** ($CH_3CN$): cation mode: *m/z* 677.24 (76%, $\mathbf{M^+}$-$PF_4$).

**EA** calculated for $C_{34}H_{58}Co_2P_4F_4$ (784.58 g·mol$^{-1}$): C: 52.05, H: 7.45; found [%]: C: 53.67, H: 8.06.

**[(Cp'''$CoI_2$)]**

[(Cp'''Co)$_2$(μ,η$^2$:η$^2$-$P_2$)$_2$] (**2**) (100 mg, 0.141 mmol, 1 equiv.) is dissolved in 15 mL of $CH_2Cl_2$. To this solution, a solution of $I_2$ (143 mg, 0.565 mmol, 4 equiv.) in 20 mL of $CH_2Cl_2$ is added. A change in colour from dark grey to dark brown is observed. The solution is stirred for four hours and a half and then the solvent is removed *in vacuo*. The residue is washed with 10 mL of hexane, 10 mL of toluene and the resulting black precipitate is dissolved in 15 mL of $CH_2Cl_2$, layered with 30 mL of pentane and stored at room temperature. After a few days, dark block crystals of [(Cp'''$CoI_2$)] are obtained.

Yield [Cp'''$CoI_2$]:30 mg (75%)

**$^1$H NMR** (400 MHz, $CD_2Cl_2$, 300K): δ [ppm] = 6.02 (s, 2H, $C_5H_2{}^tBu_3$), 1.72 (s, 18H, -($C_4H_9$)$_2$), 1.34 (s, 9H, -($C_4H_9$)).

**LIFDI-MS** ($CH_2Cl_2$): cation mode: *m/z* = 545.96 (100%, [$\mathbf{M^+}$])

**EA** calculated for [$C_{17}H_{29}CoI_2$] (546.15 g·mol$^{-1}$): C: 37.39, H: 5.35; found [%]: C: 37.42, H: 5.46.

## Selected NMR spectra

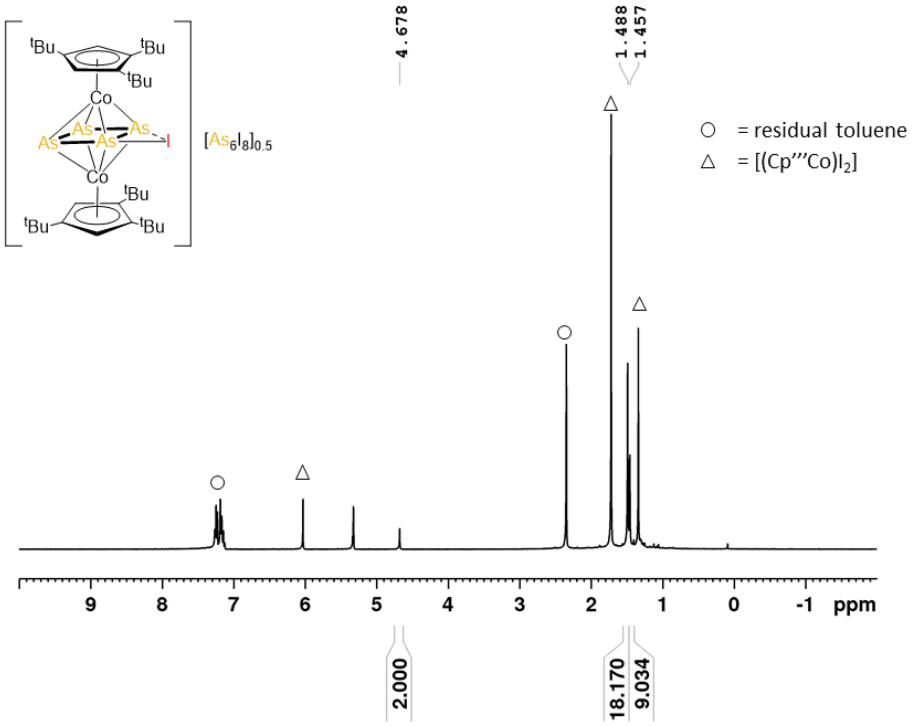


**Figure S 1** $^{1}$H NMR spectrum of compound **3a** ($CD_2Cl_2$, 300K). Residual toluene = ○, [Cp'''$CoI_2$] = Δ.

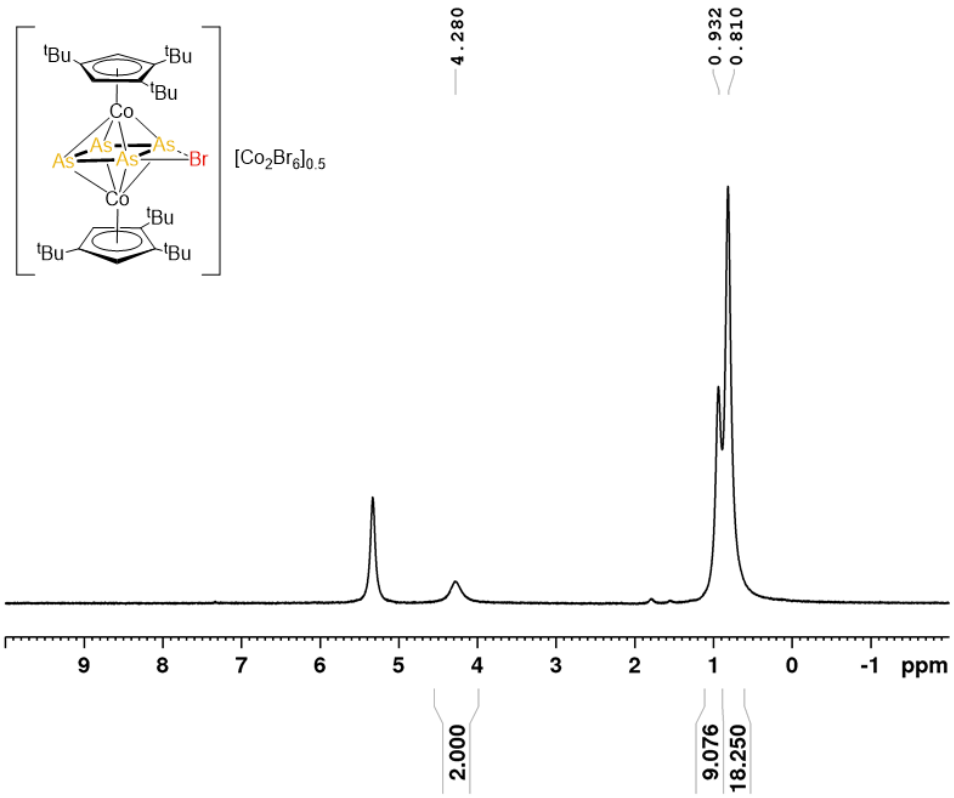


**Figure S 2** $^{1}$H NMR spectrum of compound **4** ($CD_2Cl_2$, 300K).

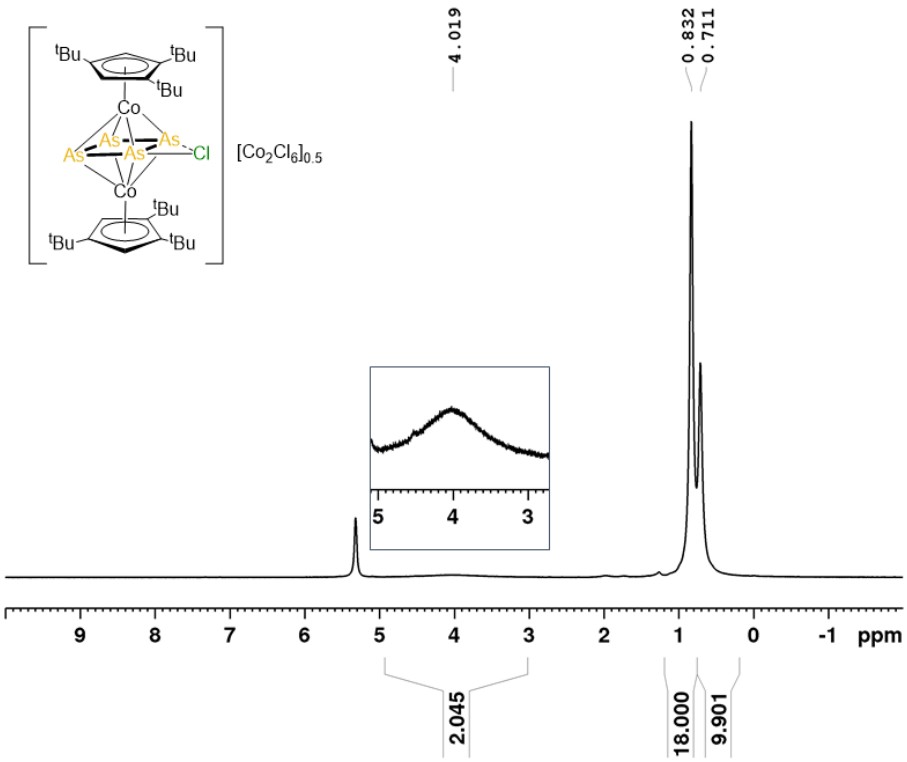


**Figure S 3** $^{1}$H NMR spectrum of compound **5** ($CD_2Cl_2$, 300K).

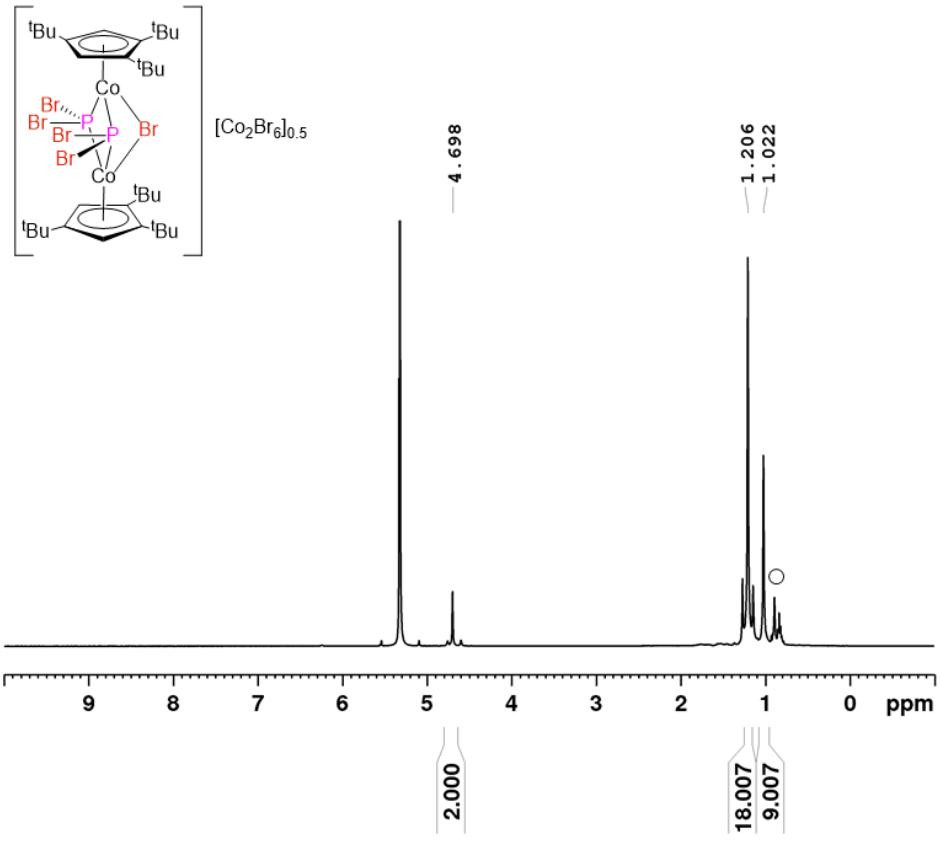


**Figure S 4** $^{1}$H NMR spectrum of compound **6a** ($CD_2Cl_2$, 233K). Residual pentane is marked with ○.

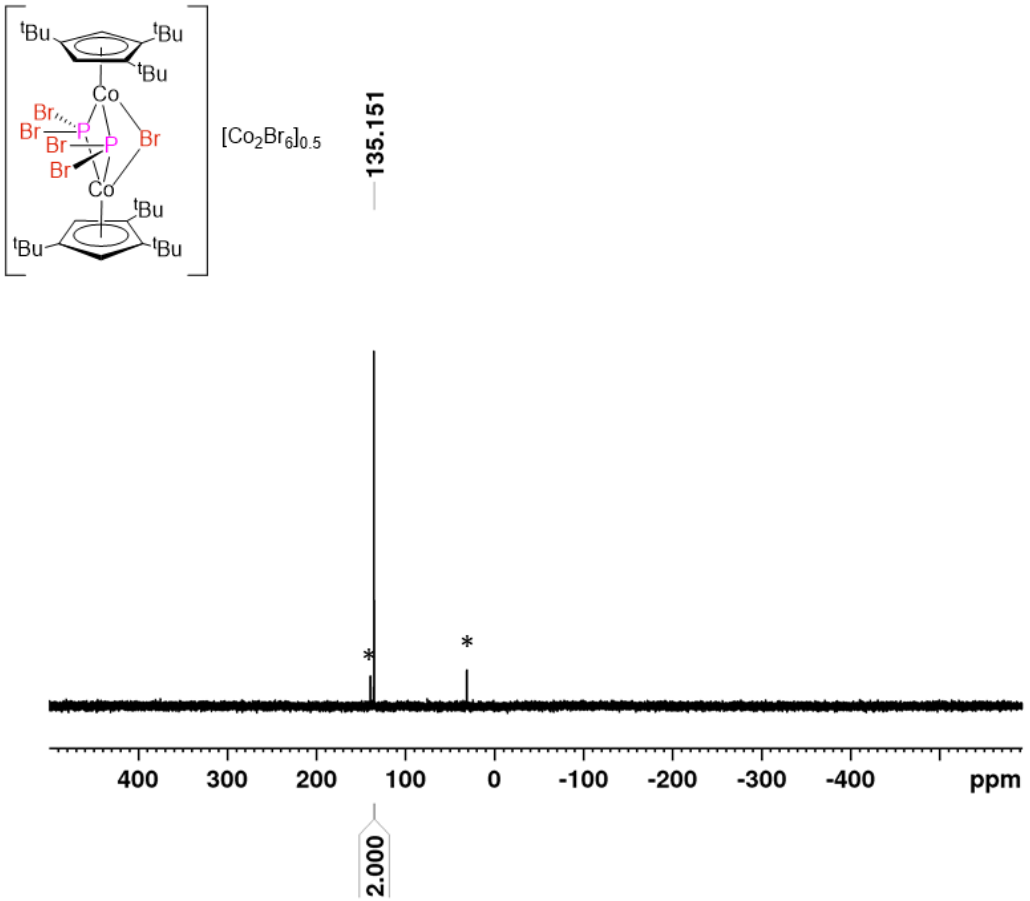


**Figure S 5** $^{31}P\{^{1}H\}$ NMR spectrum of compound **6a** ($CD_2Cl_2$, 233K). Unidentified impurities are marked with *.

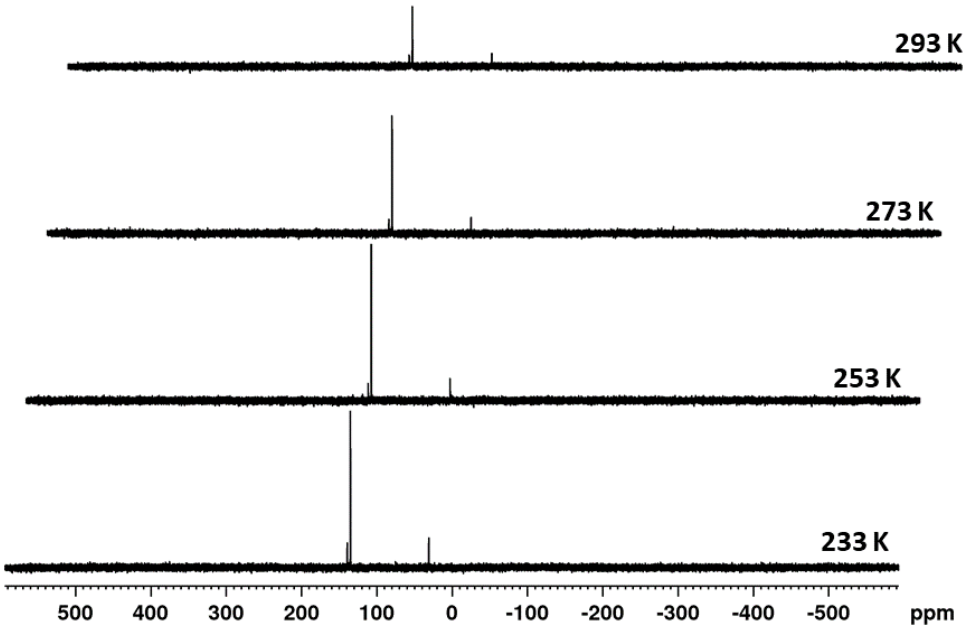


**Figure S 6** VT $^{31}P\{^{1}H\}$ NMR spectra of crystals of compound **6a** ($CD_2Cl_2$, 233-293K).

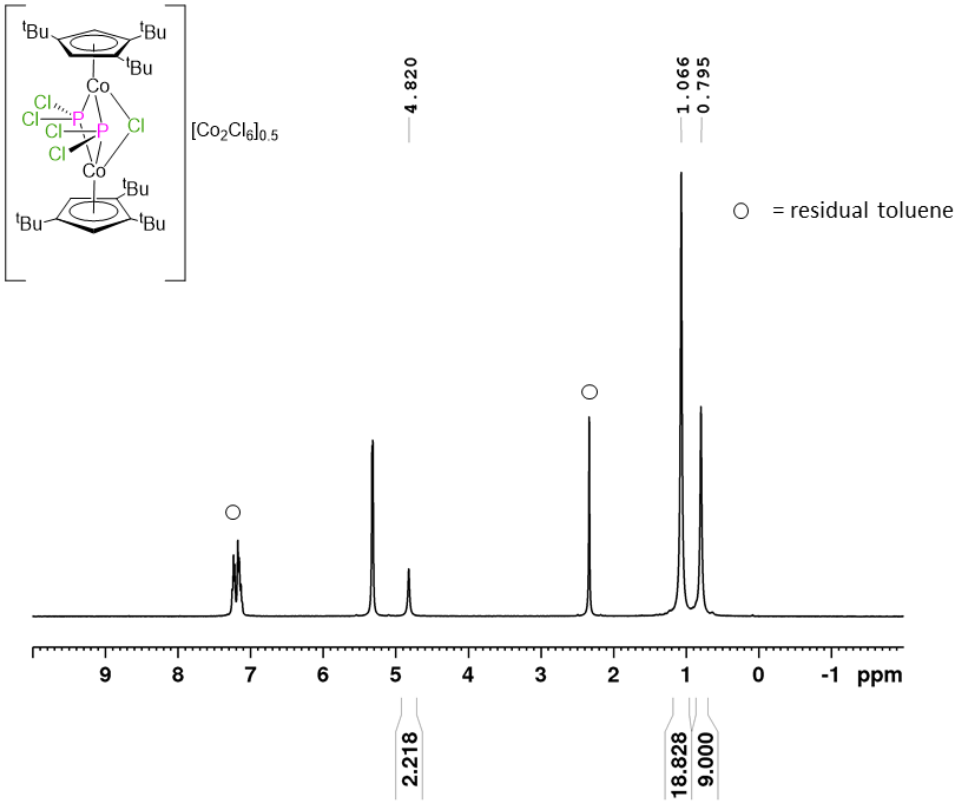


**Figure S 7** $^{1}H$ NMR spectrum of compound **6b** ($CD_2Cl_2$, 300K). Residual toluene is marked with ○.

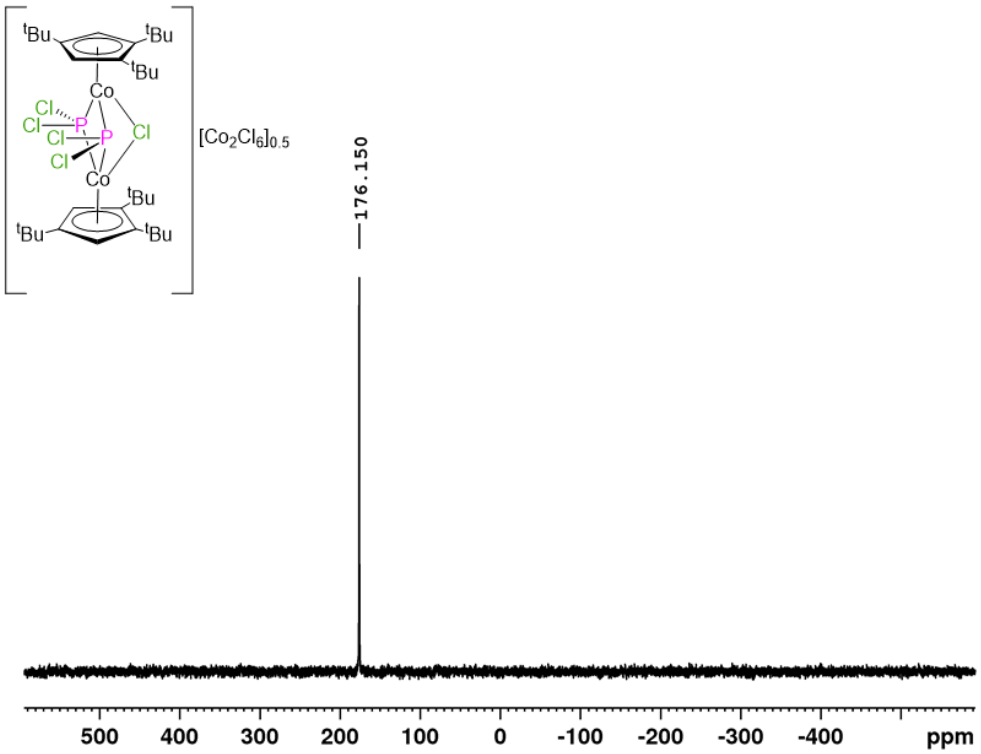


**Figure S 8** $^{31}P\{^{1}H\}$ NMR spectrum of compound **6b** ($CD_2Cl_2$, 300K).

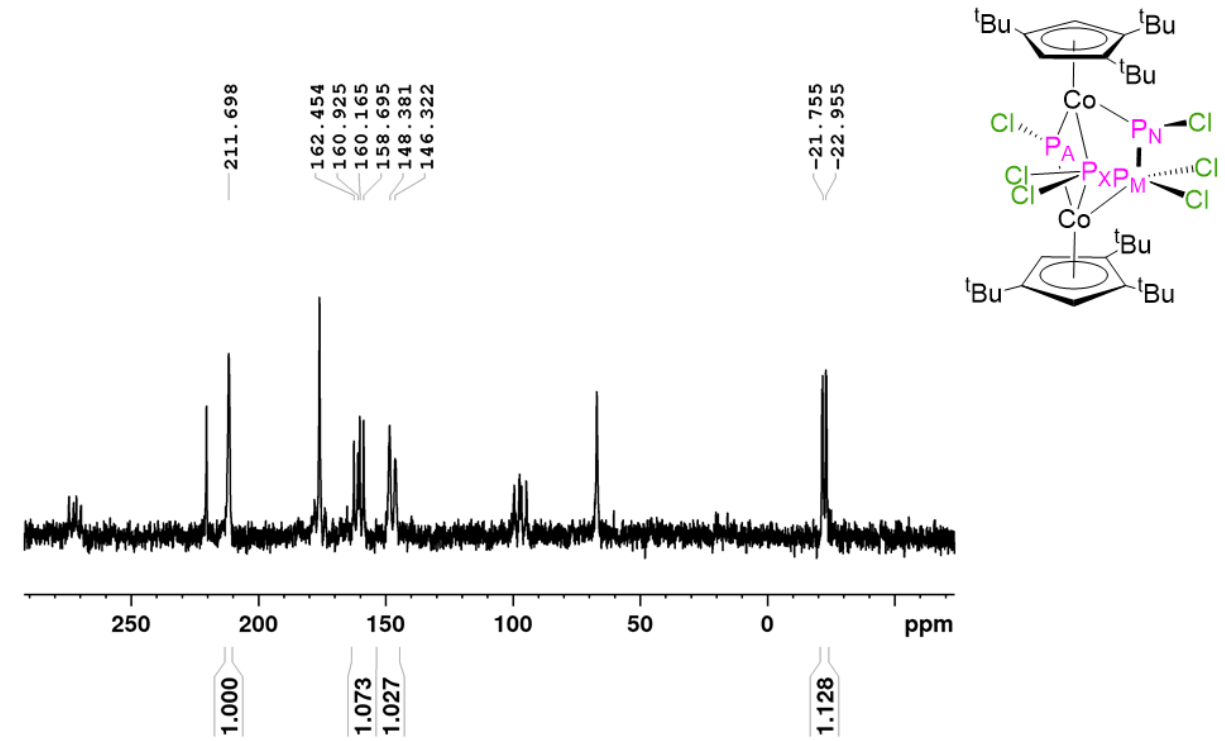


**Figure S 9** $^{31}P\{^{1}H\}$ NMR spectrum of the hexane fraction from which compound **7** is extracted. The signals of compound **7** are the one with the picks and the integrals marked. (AMNX spin system).

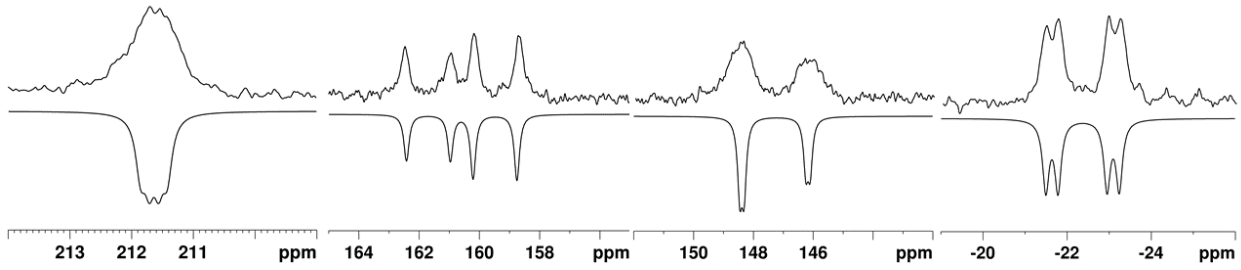


**Figure S 10** Sections of the experimental (upwards) and simulated (downwards) $^{31}P\{^{1}H\}$ NMR spectrum of compound **7** (AMNX spin system) ($CD_2Cl_2$, 300K).

**Table S 1** Coupling constants of the AMNX spin system obtained from simulation.

| **δ (ppm)** | | **J (Hz)** | | | |
|---|---|---|---|---|---|
| **A** | 211.6 | $^{1}J_{MN}$ | 358 | $^{2}J_{AN}$ | 23 |
| **M** | 160.5 | $^{2}J_{MX}$ | 238 | | |
| **N** | 147.4 | | | $^{2}J_{AM}$ | 5 |
| **X** | -22.4 | $^{2}J_{AX}$ | 47 | | |

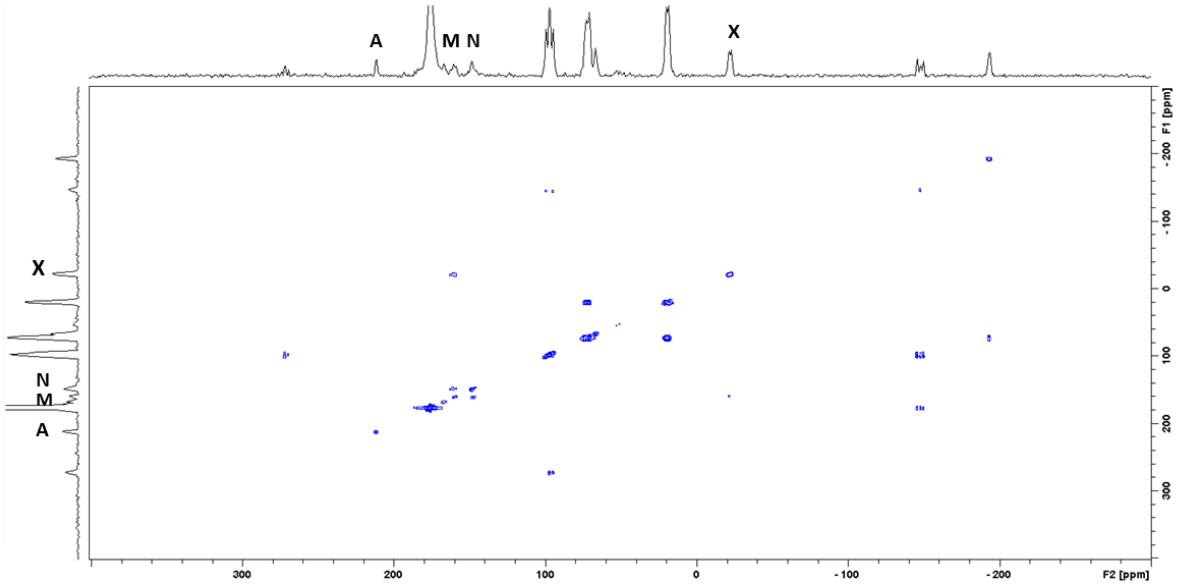


**Figure S 11** $^{31}P$-$^{31}P$ COSY 2D NMR of the hexane fraction from which compound **7** is extracted ($CD_2Cl_2$, 300K).

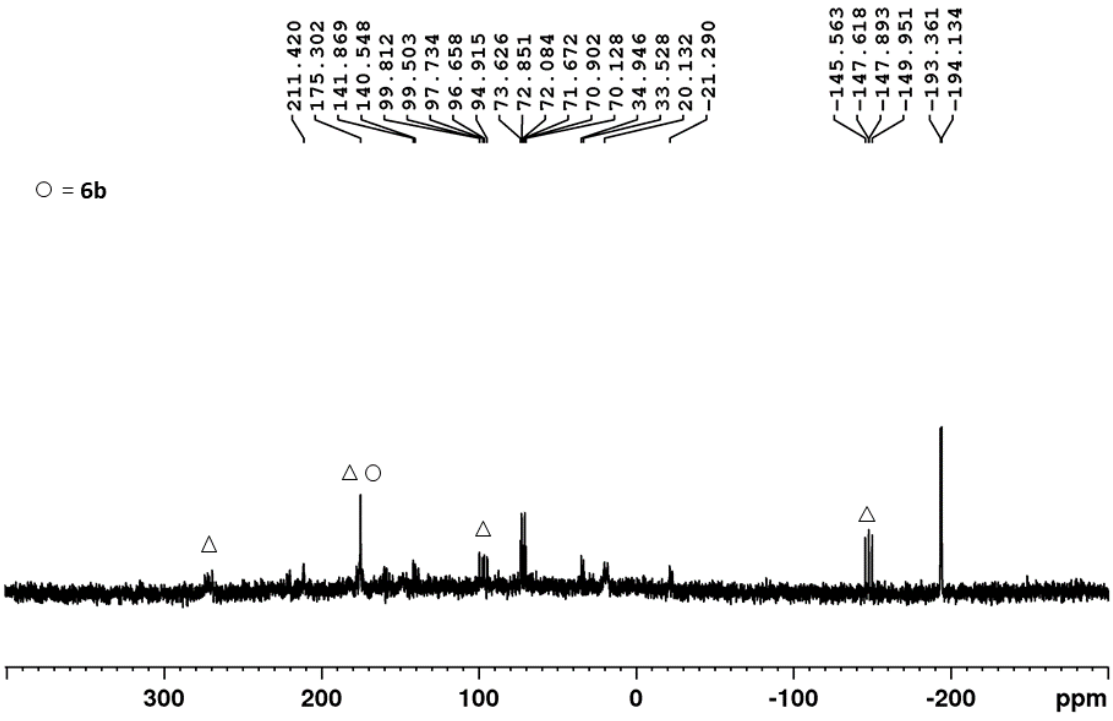


**Figure S 12** $^{31}P\{^{1}H\}$ NMR spectrum of hexane fraction from which compound **7** is extracted. The signals marked with Δ belongs to the compound $\mathbf{7}_{silica}$ (AMNX spin system, see next figure). Traces of **6b** are present (marked with ○). ($CD_2Cl_2$, 300K).

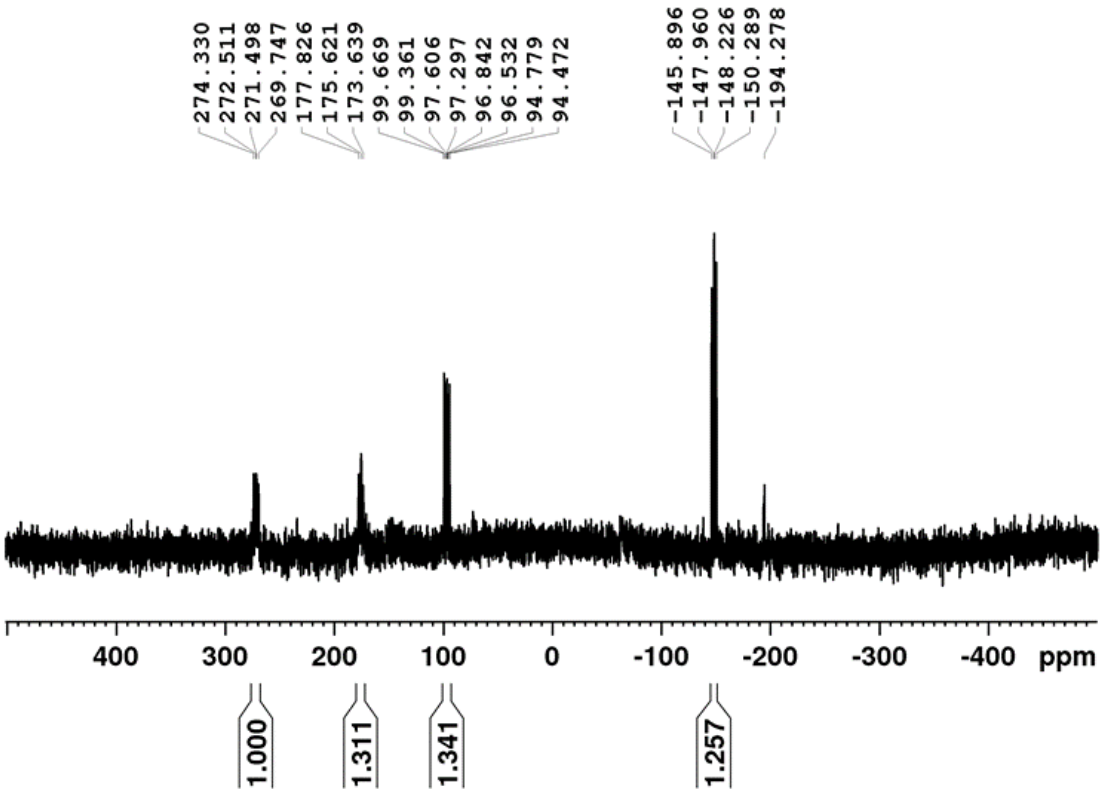


**Figure S 13** Simulated $^{31}P\{^{1}H\}$ NMR spectrum of the compound $\mathbf{7}_{silica}$ (AMNX spin system) ($CD_2Cl_2$, 300 K).

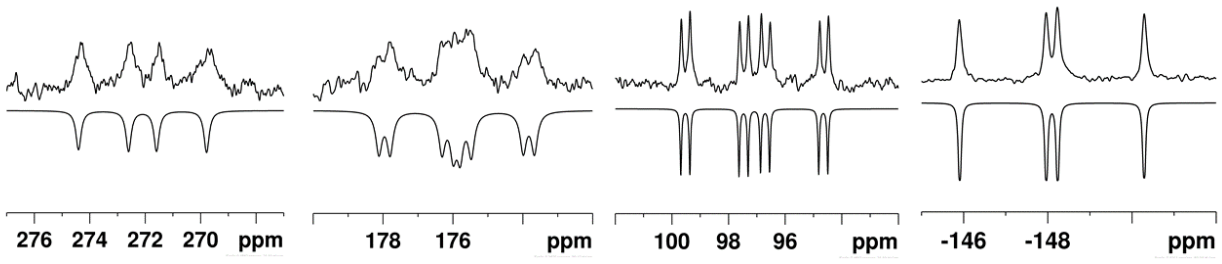


**Figure S 14** Sections of the experimental (upwards) and simulated (downwards) $^{31}P\{^{1}H\}$ NMR spectrum of compound $\mathbf{7}_{\mathbf{silica}}$ (AMNX spin system) ($CD_2Cl_2$, 300K).

**Table S 2** Coupling constants of the AMNX spin system obtained from simulation.

| **δ (ppm)** | | **J (Hz)** | | | |
|---|---|---|---|---|---|
| **A** | 272.08 | $^{1}J_{AM}$ | 292.7 | $^{2}J_{MN}$ | 51.8 |
| **M** | 175.90 | $^{1}J_{AN}$ | 456.2 | $^{1}J_{MX}$ | 376.9 |
| **N** | 97.10 | | | | |
| **X** | -148.09 | $^{2}J_{AX}$ | 6.0 | $^{1}J_{NX}$ | 333.05 |

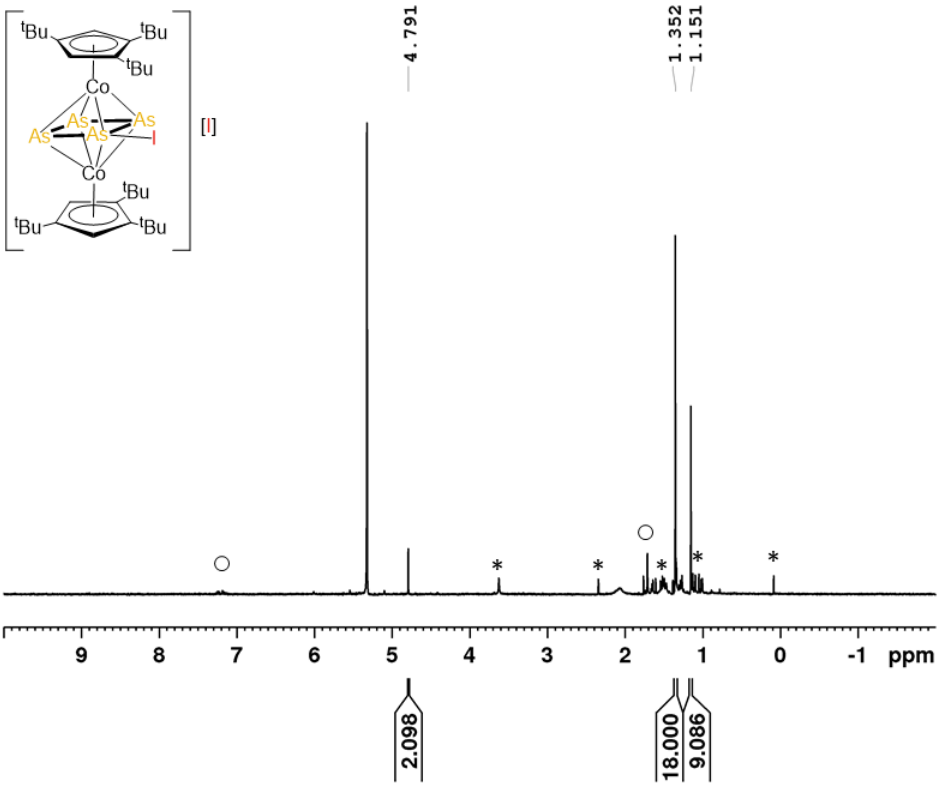


**Figure S 15** $^{1}H$ NMR spectrum of compound **10** ($CD_2Cl_2$, 300K). Residual toluene is marked with ○ and impurities are marked with *.

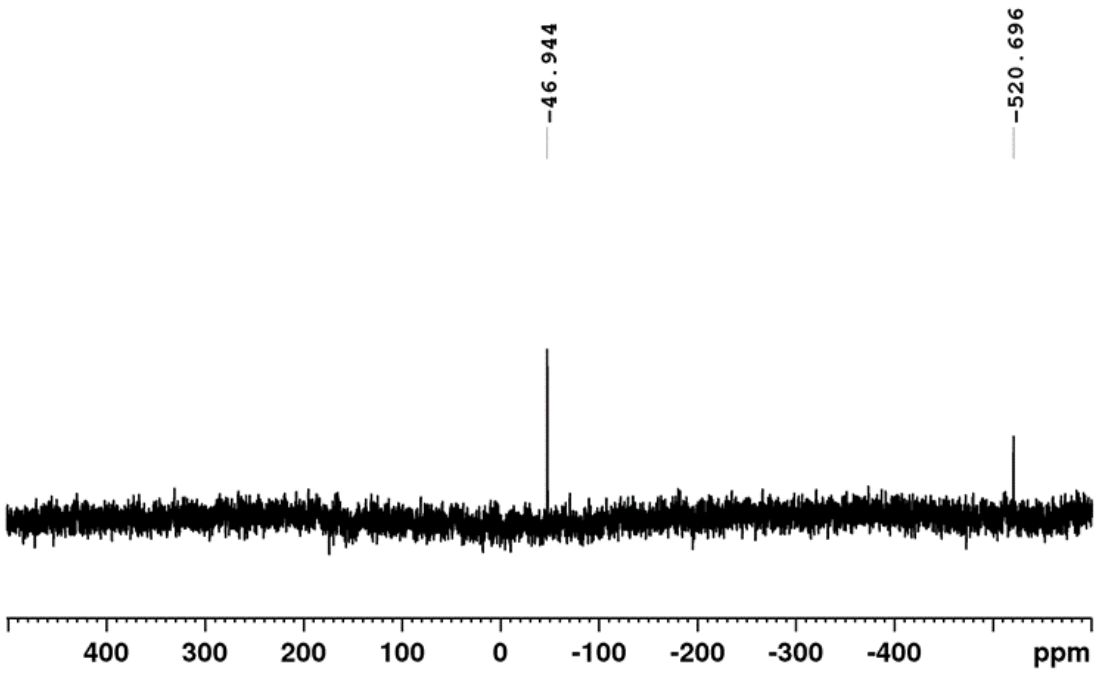


**Figure S 16** $^{31}P\{^{1}H\}$ NMR spectrum of the crystals of compound **11** ($CD_2Cl_2$, 300K). The signals at -46.9 belongs to **2** while the one at -520.7 ppm belongs to $P_4$.

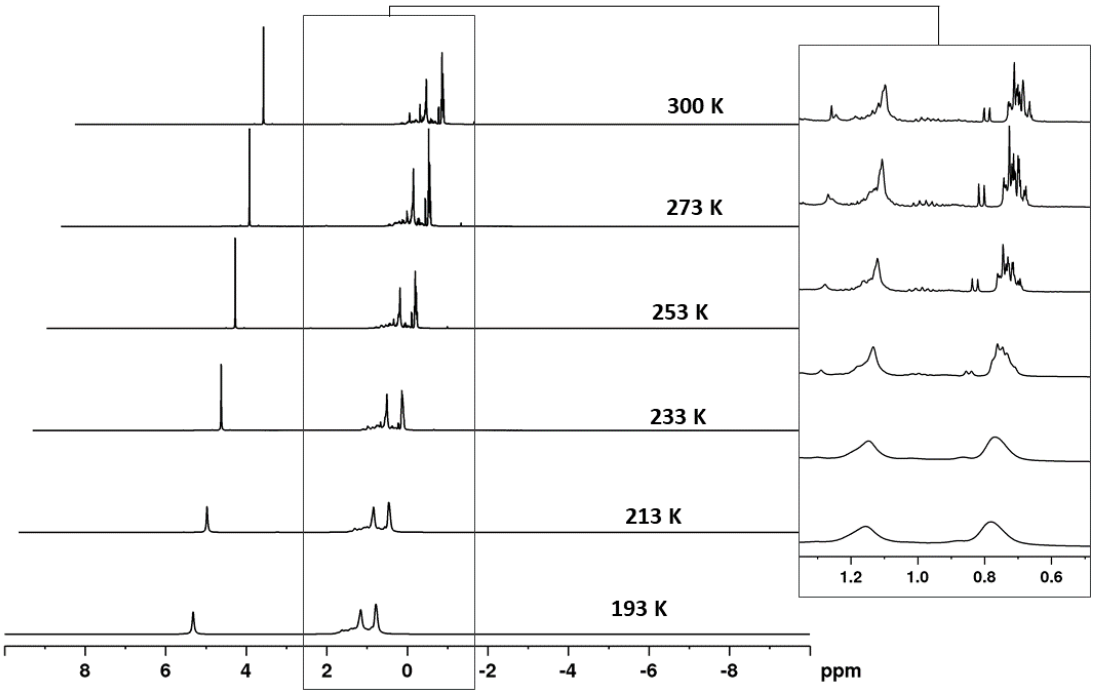


**Figure S 17** VT $^{1}H$ NMR spectra of crystals of compound **11**. (it shows a very complex mixture of decomposition products). ($CD_2Cl_2$, 193-300K).

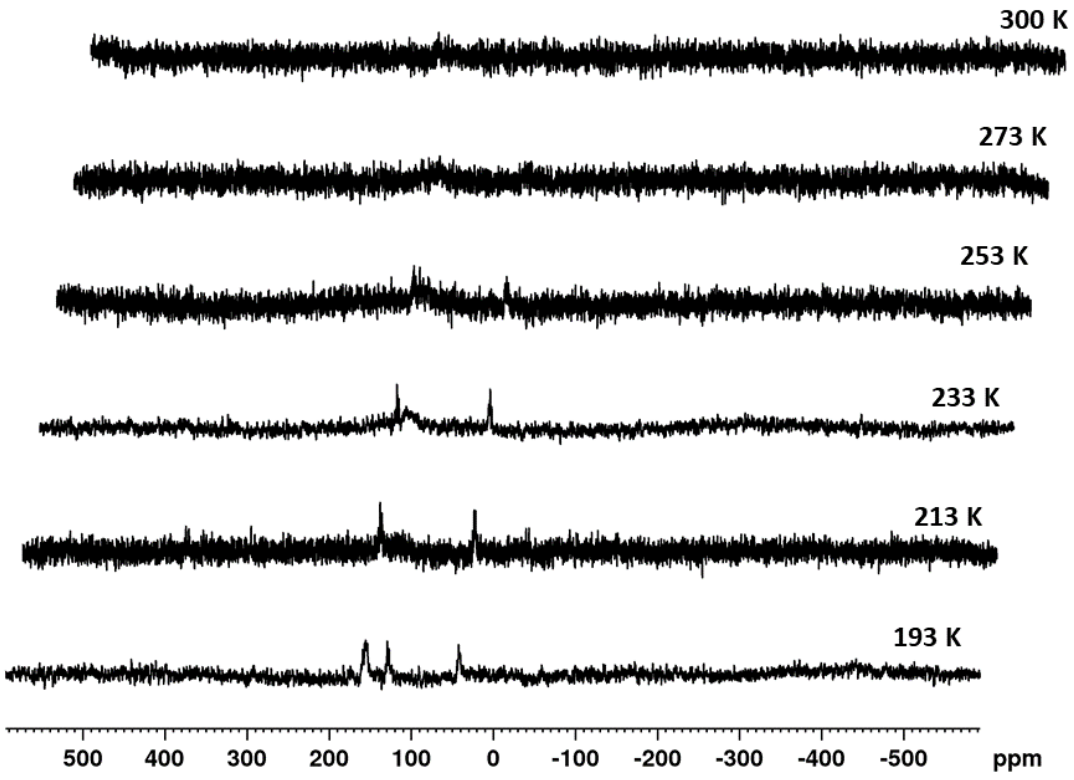


**Figure S 18** VT $^{31}P\{^{1}H\}$ NMR spectra of crystals of compound **11**. ($CD_2Cl_2$, 193-300K). (cf. figure below for spectra at T = 193 K and T = 213 K).

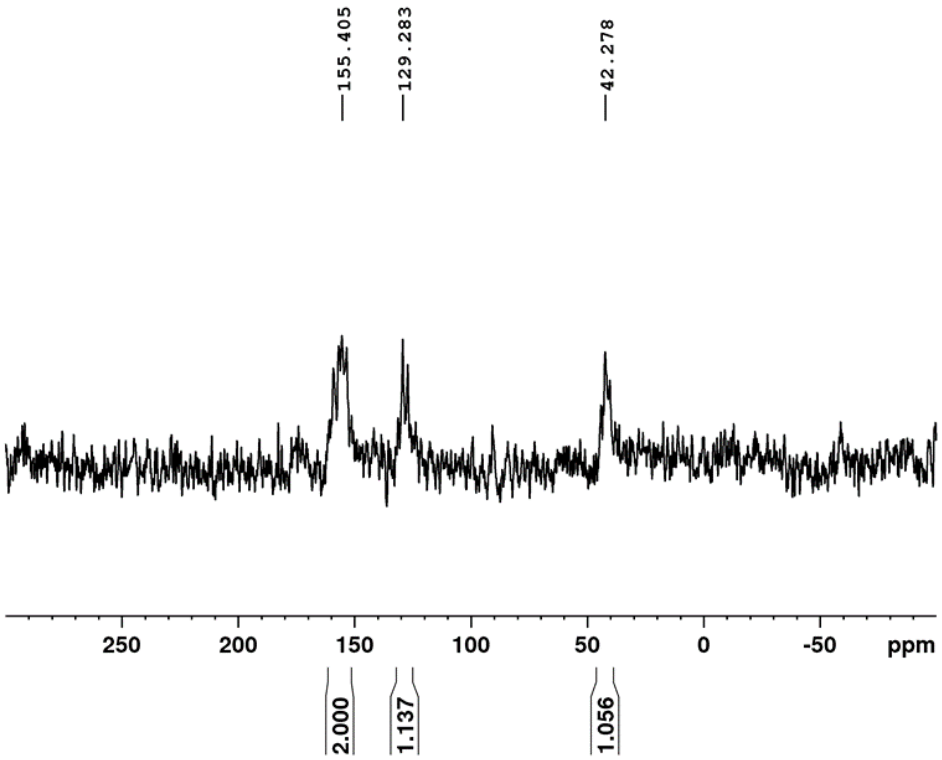


**Figure S 19** $^{31}P\{^{1}H\}$ NMR spectrum of crystals of compound **11**. ($CD_2Cl_2$, 193 K).

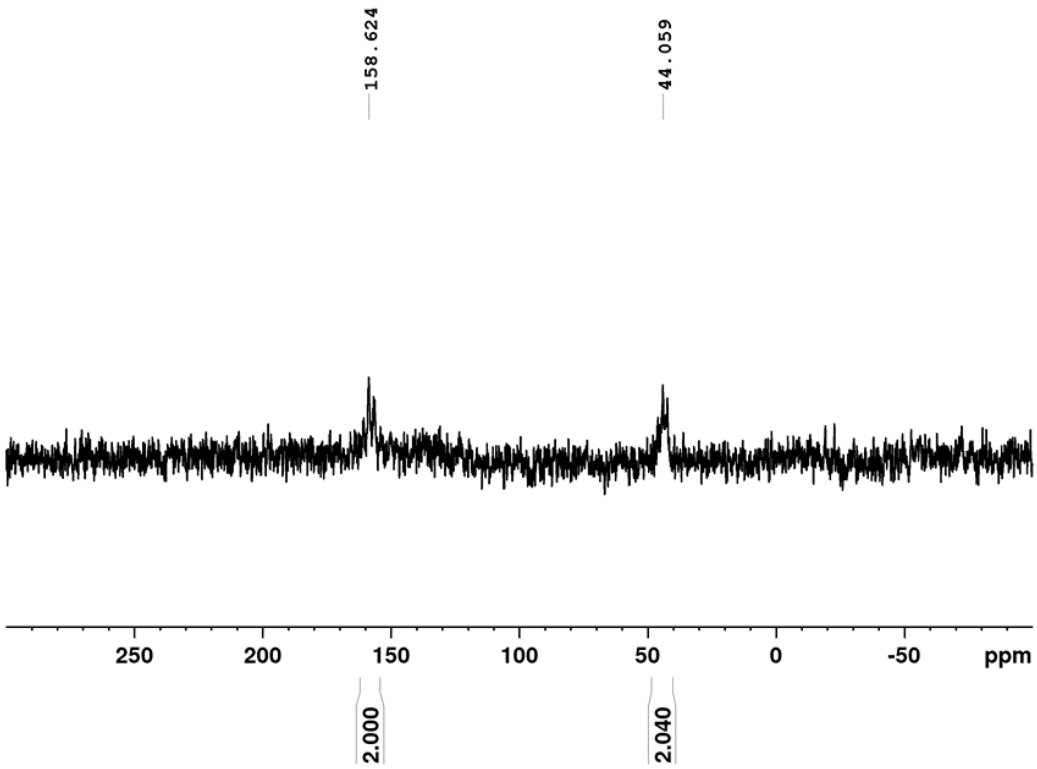


**Figure S 20** $^{31}P\{^{1}H\}$ NMR spectrum of crystals of compound **11**. ($CD_2Cl_2$, 213 K).

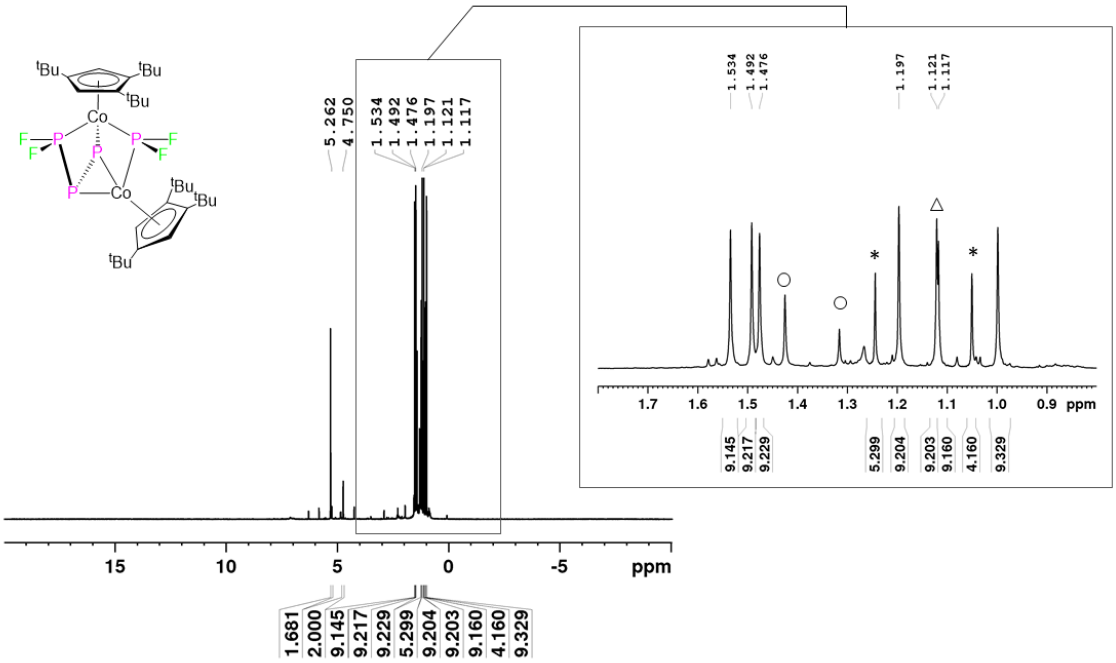


**Figure S 21** $^{1}$H NMR spectrum of compound **12** ($CD_2Cl_2$, 300K). The signals of the t*Bu* groups of compound **2** (that co-crystallizes with **12**) are marked with ○ while impurities are marked with *. There is an additional signals that integrates nine protons that could not be assigned (it should be one of the two singlets marked with Δ, but this cannot be unequivocally assigned).

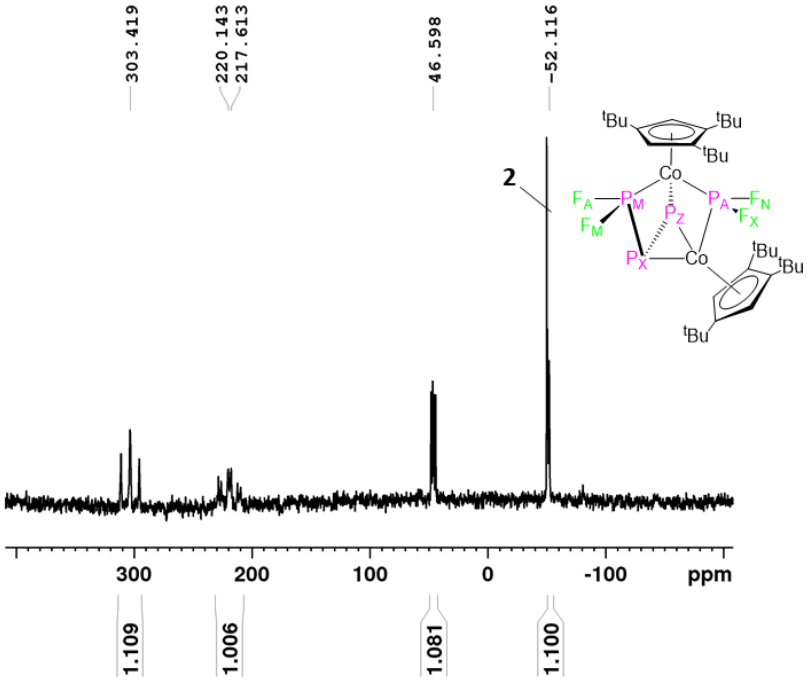


**Figure S 22** $^{31}P\{^{1}H\}$ NMR spectrum of compound **12** ($CD_2Cl_2$, 300K). The signal of the compound of co-crystallization (**2**) is indicated.

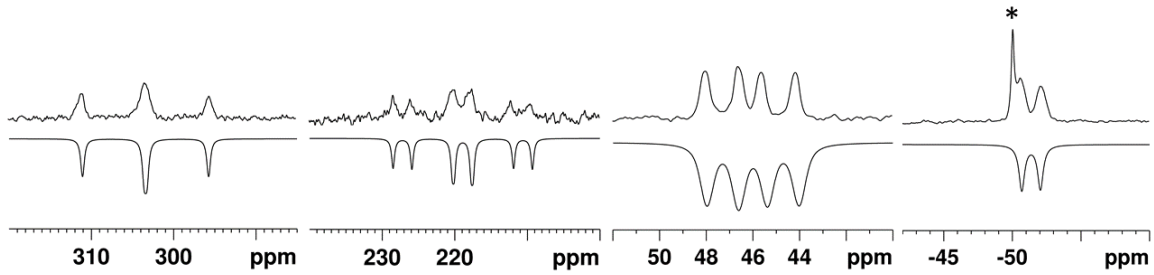


**Figure S 23** Sections of the experimental (upwards) and simulated (downwards) $^{31}P\{^{1}H\}$ NMR spectrum of compound **12** (AMXZ spin system; only P atoms considered for the nomenclature of the spin system) The signal of **2**, which co-crystallizes, is marked with *.

**Table S 3** Coupling constants of the AMXZ spin system obtained from simulation.

| δ (ppm) | | J (Hz) | | | |
|---|---|---|---|---|---|
| **A** | 303.3 | $^{1}J_{MX}$ | 420 | $^{1}J_{PA_FN}$ | 1213.0 |
| **M** | 218.9 | $^{1}J_{XZ}$ | 220 | $^{1}J_{PA_FX}$ | 1269.0 |
| **X** | 46.0 | | | $^{1}J_{PM_FA}$ | 1321.6 |
| **Z** | -51.4 | $^{2}J_{AX}$ | 20 | $^{1}J_{PM_FN}$ | 1367.0 |

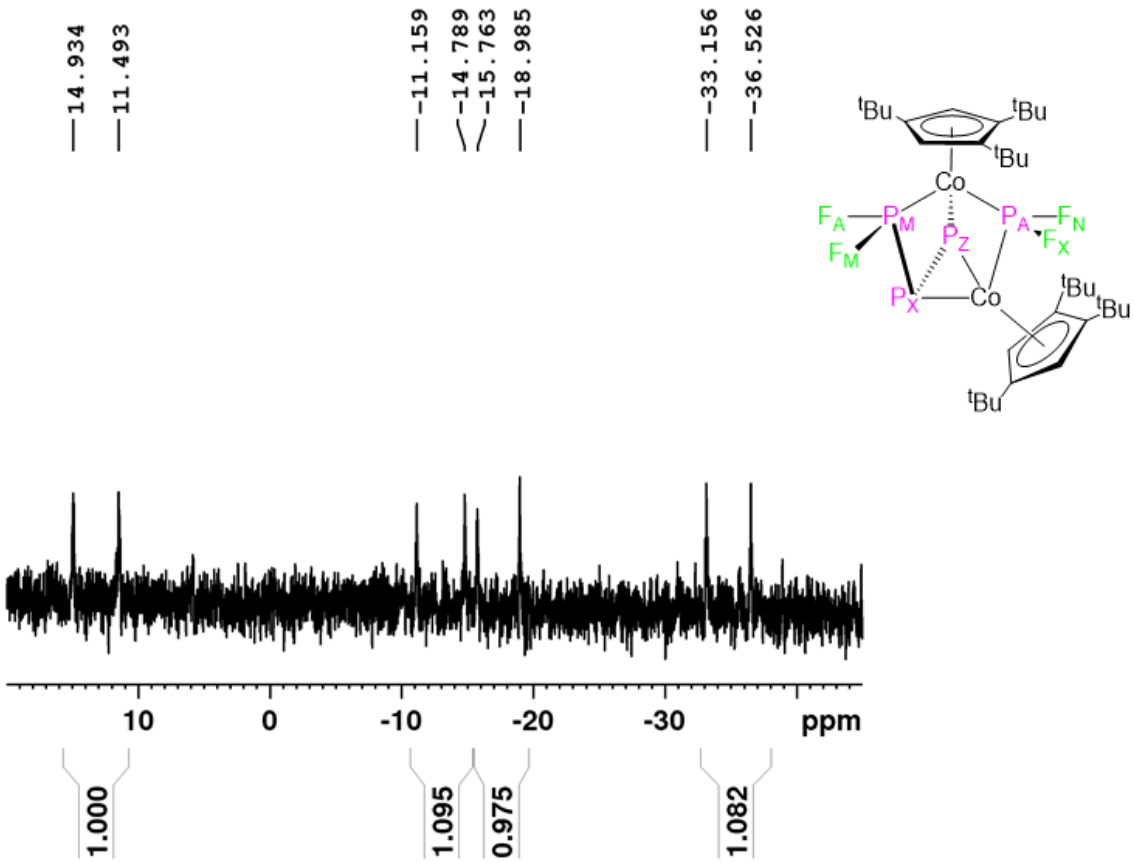


**Figure S 24** $^{19}F\{^{1}H\}$ NMR spectrum of compound **12** ($CD_2Cl_2$, 300K).

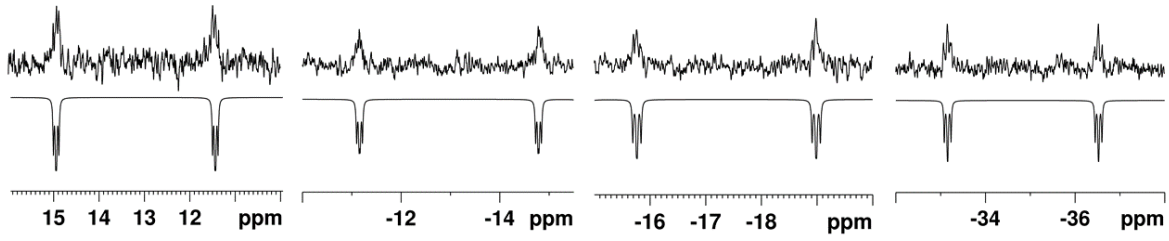


**Figure S 25** Sections of the experimental (upwards) and simulated (downwards) $^{19}F$ NMR spectrum of compound **12**. (AMNX spin system, only F atoms considered for the nomenclature of the spin system).

**Table S 4** Coupling constants of the AMNX spin system obtained from simulation.

| δ (ppm) | | J (Hz) | | | | | |
|---|---|---|---|---|---|---|---|
| **A** | 13.2 | $^{1}J_{P}^{A}{}_{F}^{N}$ | 1213.0 | $^{2}J_{P}^{X}{}_{F}^{A}$ | 18.6 | $^{1}J_{F}^{A}{}_{F}^{M}$ | 26.5 |
| **M** | -13.0 | $^{1}J_{P}^{A}{}_{F}^{X}$ | 1269.0 | $^{2}J_{P}^{X}{}_{F}^{M}$ | 17.9 | | |
| **N** | -17.4 | $^{1}J_{P}^{M}{}_{F}^{A}$ | 1321.6 | $^{2}J_{P}^{Z}{}_{F}^{N}$ | 24.5 | $^{1}J_{F}^{N}{}_{F}^{X}$ | 31.30 |
| **X** | -34.9 | $^{1}J_{P}^{M}{}_{F}^{M}$ | 1367.0 | $^{2}J_{P}^{Z}{}_{F}^{X}$ | 25.5 | | |

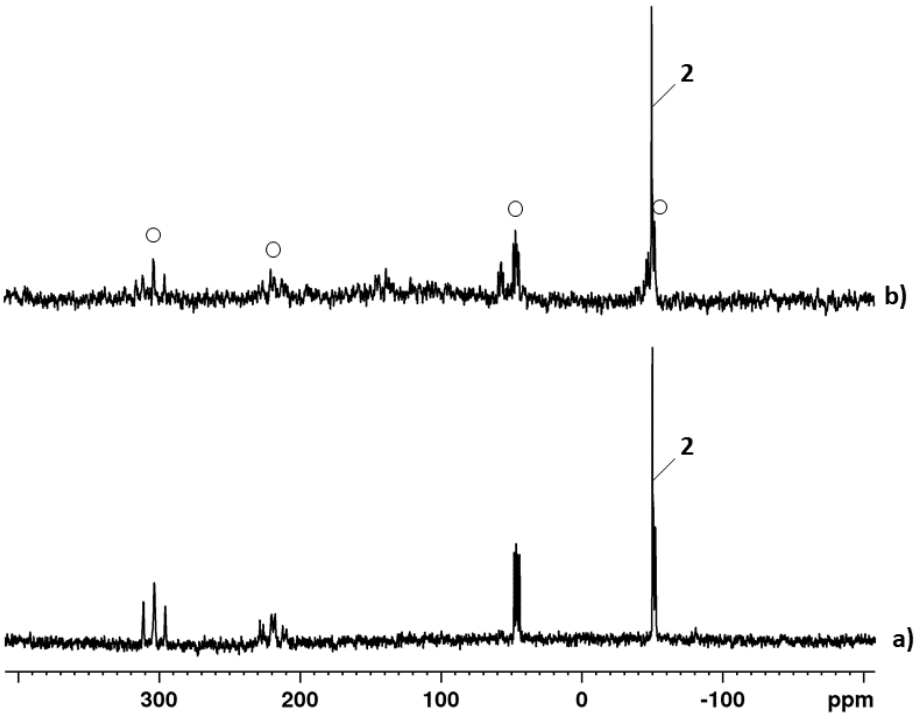


**Figure S 26 a)** $^{31}P\{^{1}H\}$ NMR spectrum of compound **12** obtained from the reaction between $[(Cp'''Co)_2(\mu,\eta^4{:}\eta^4\text{-}P_4)][TEF]_2$ (**9**) (1 equiv.) and TMAF (2 equiv.) The signal of **2** is present because it co-crystallizes with **12**. **b)** $^{31}P\{^{1}H\}$ NMR spectrum of the crude solution from the reaction between $[(Cp'''Co)_2(\mu,\eta^4{:}\eta^4\text{-}P_4)][BF_4]$ (1 equiv.) and TMAF (1 equiv.) The signals of **12** are marked with ○. ($CD_2Cl_2$, 233K).

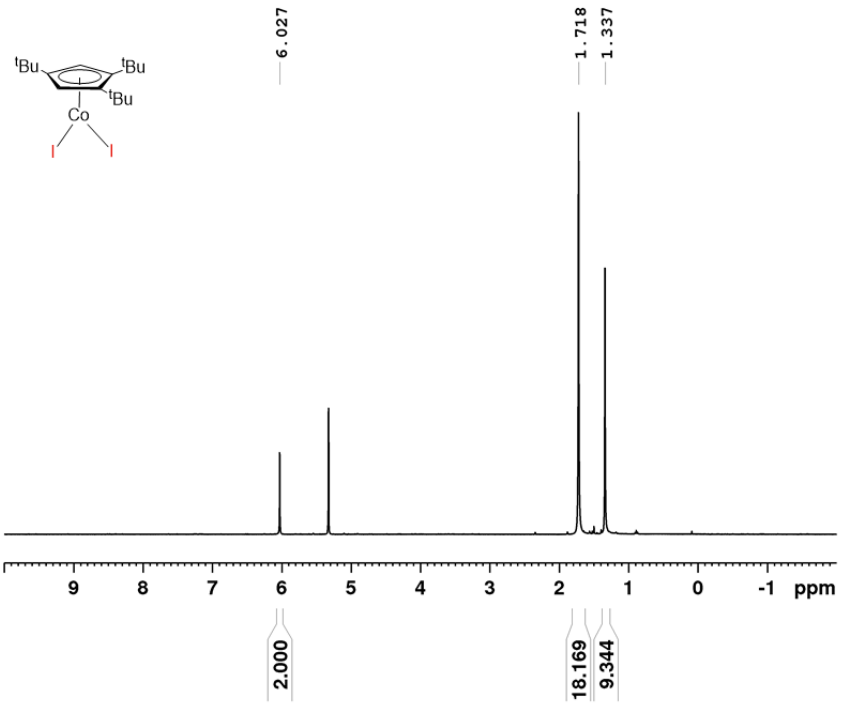


**Figure S 27** $^{1}$H NMR spectrum of [Cp'''$CoI_2$] ($CD_2Cl_2$, 300K).

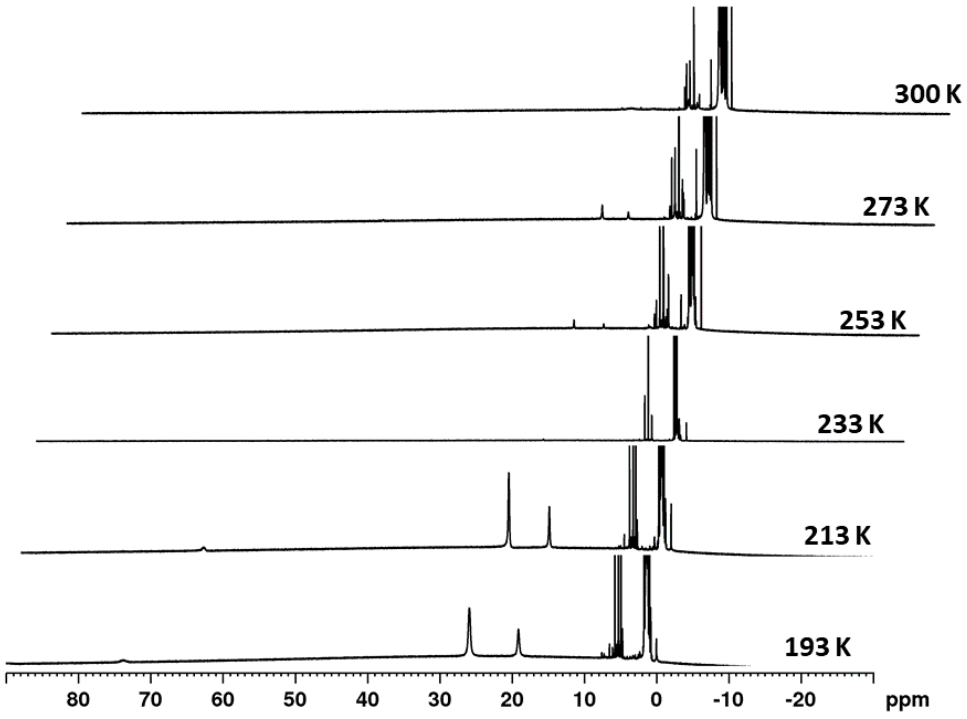


**Figure S 28** VT $^{1}$H NMR spectra of the reaction solution of **1** (1 equiv.) with $PCl_5$ (4 equiv.) ($CD_2Cl_2$, 193-300K).

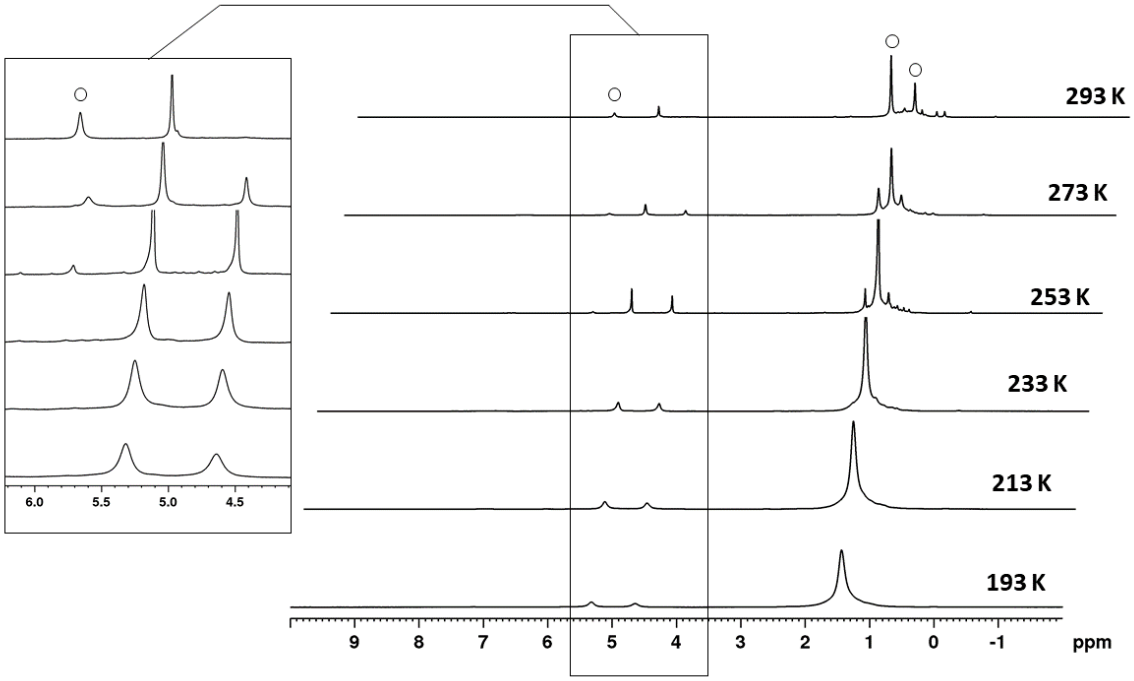


**Figure S 29** VT $^{1}H$ NMR spectra of the reaction solution of **2** (1 equiv.) with $I_2$ (4 equiv.) ($CD_2Cl_2$, 193-300K). The signals of [(Cp'''Co)$I_2$] are marked with ○.

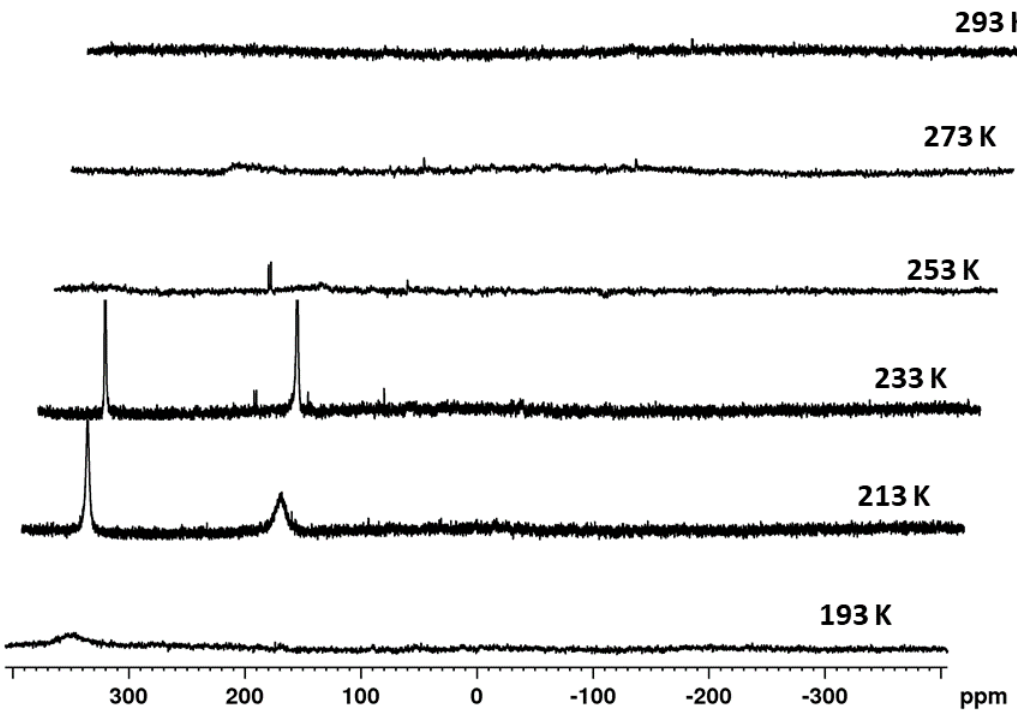


**Figure S 30** VT $^{31}P\{^{1}H\}$ NMR spectra of the reaction solution of **2** (1 equiv.) with $I_2$ (4 equiv.) ($CD_2Cl_2$, 193-300K).

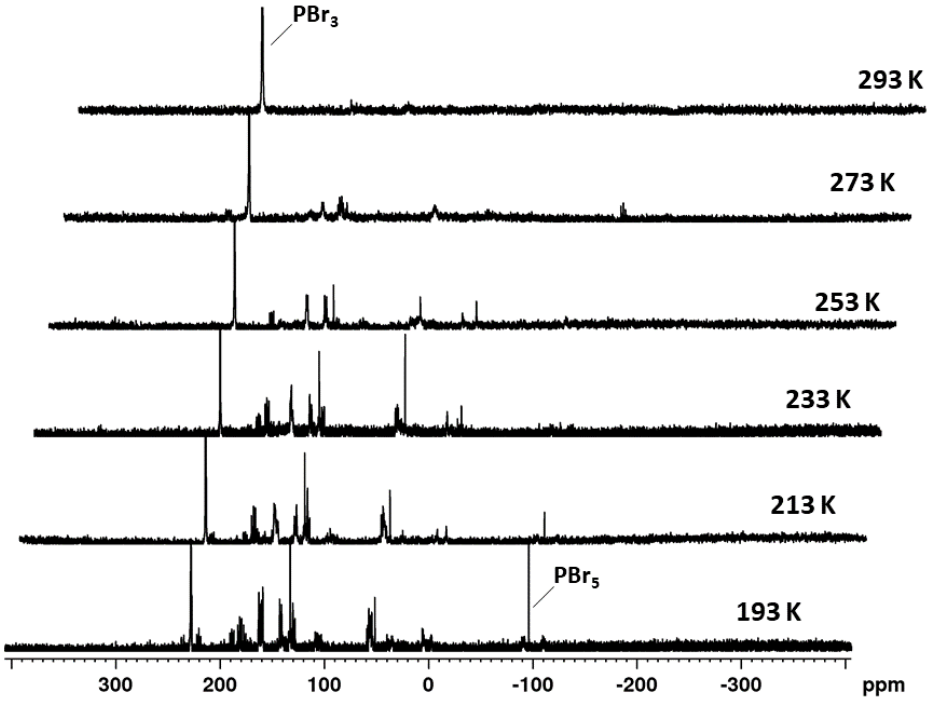


**Figure S 31** VT $^{31}P\{^{1}H\}$ NMR spectra of the reaction solution of **2** (1 equiv.) with $PBr_5$ (4 equiv.) ($CD_2Cl_2$, 193-300K).

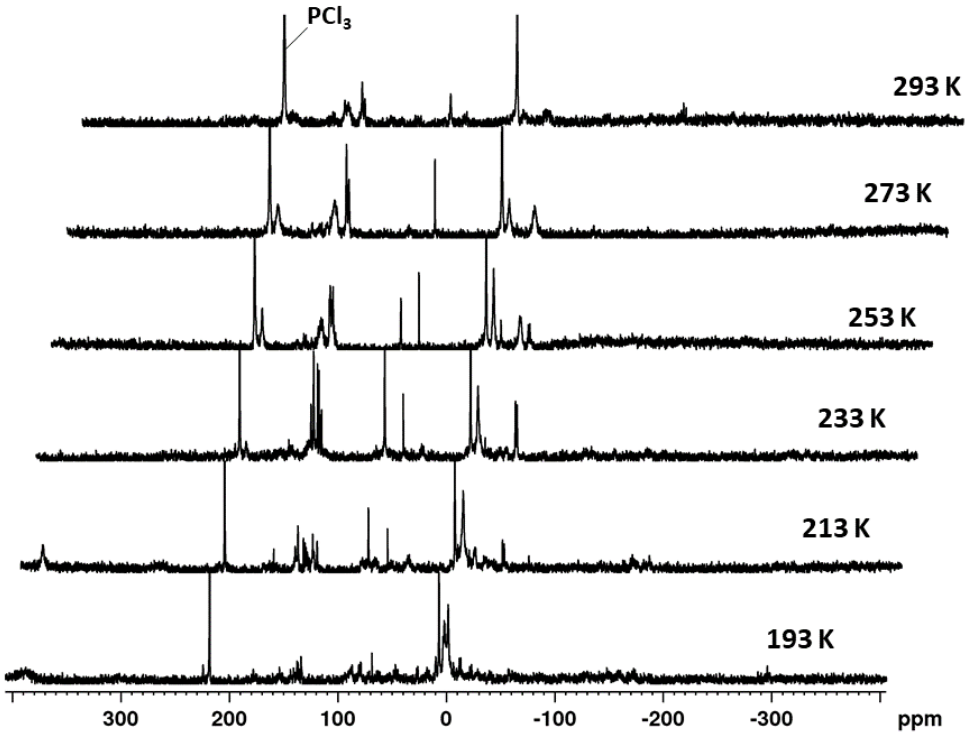


**Figure S 32** VT $^{31}P\{^{1}H\}$ NMR spectra of the reaction solution of **2** (1 equiv.) with $PCl_5$ (4 equiv.) ($CD_2Cl_2$, 193-300K).

**Crystallographic details**

Suitable crystals were selected and mounted on a GV50 diffractometer equipped with a Titan$^{S2}$ CCD detector (**4**, **6b**), on a SuperNova Dualflex diffractometer equipped with an Atlas$^{S2}$ CCD detector (**3b**, **10**, **[Cp'''$CoI_2$]**), on a XtaLAB Synergy R DW diffractometer equipped with an HyPix-Arc 150 detector (**6a**, **7**, **11**, **12**) or on a Gemini Ultra diffractometer equipped with an Atlas$^{S2}$ CCD detector (**3a**, **5**). The crystals were kept at a steady T = 123 K(**3a**, **4**, **5**, **6a**, **6b**, **11**, **12**, **[Cp'''$CoI_2$]**) or respectively at 100 K (**7**, **11**) or at 90 K (**3b**) during data collection. Data collection and reduction were performed with **CrysAlisPro** [Version 171.41.76a (**3a**), Version 1.171.39.46 (**3b**, **4**, **5**, **6b**, **10**), Version 171.41.89a (**11**, **[Cp'''$CoI_2$]**), Version 171.41.90a (**6a**, **7**), Version 171.41.93a (**12**).[3]

For the compound **3a**, an analytical absorption correction, an analytical numeric absorption correction using a multifaceted crystal model based on expressions derived by R.C. Clark & J.S. Reid. (Clark, R. C. & Reid, J. S. (1995). Acta Cryst. A51, 887-897) and an empirical absorption correction using spherical harmonics, implemented in SCALE3 ABSPACK, scaling algorithm were applied. For the compounds **3b**, **4**, **5**, **6b**, **7**, **10**, **11**, **12**, **[Cp'''$CoI_2$]** a gaussian absorption correction, a numerical absorption correction based on gaussian integration over a multifaceted crystal model and an empirical absorption correction using spherical harmonics, implemented in SCALE3 ABSPACK scaling algorithm, were performed. For compound **6a**, a gaussian absorption correction, a numerical absorption correction based on gaussian integration over a multifaceted crystal model, a spherical absorption correction using equivalent radius and absorption coefficient and an empirical absorption correction using spherical harmonics, implemented in SCALE3 ABSPACK scaling algorithm, were performed.

Using **Olex2**, [4] the structures were solved with **ShelXT** [5] and a least-square refinement on F2 was carried out with **ShelXL**[6] for all structures. All non-hydrogen atoms were refined anisotropically. Hydrogen atoms at the carbon atoms were located in idealized positions and refined isotropically according to the riding model.

Figures were created with Olex2.

The SADI (**3a**, **4, 5**, **6a**, **12**) and SIMU (**3a**, **3b**, **4**, **6a**, **7**, **12**) restraints were used during the refinement of the disordered atoms/ligands.

**Table S 5** Crystallographic data for the compounds **3a**, **3b**, **4** and **5**.

| Compound | 3a · 3 $CH_2Cl_2$ | 3b · $CH_2Cl_2$ | 4 · $CH_2Cl_2$ | 5 · $CH_2Cl_2$ |
|---|---|---|---|---|
| Data set (internal naming) | AG362 | AG466 | AG396 | AG410 |
| CCDC-number | - | - | - | - |
| Formula | $As_{14}C_{72}Cl_8Co_4H_{124}I_{10}$ | $C_{70}H_{120}As_8Cl_{8.3}Co_6I_{3.7}$ | $C_{70}H_{120}As_8Br_8Cl_4Co_6$ | $C_{70}H_{120}As_8Cl_{12}Co_6$ |
| $D_{calc.}$/ g cm$^{-3}$ | 2.191 | 1.909 | 1.937 | 1.730 |
| $\mu$/mm$^{-1}$ | 31.697 | 5.362 | 16.808 | 15.311 |
| Formula Weight | 3826.90 | 2678.36 | 2695.67 | 2339.99 |
| Colour | dark black | metallic dark black | green | metallic dark green |
| Shape | rhombohedral-shaped | prism-shaped | plate-shaped | block-shaped |
| Size/mm$^3$ | 0.19×0.08×0.02 | 0.19×0.07×0.02 | 0.11×0.07×0.04 | 0.46×0.08×0.04 |
| $T$/K | 123.15 | 90(1) | 123(1) | 123(1) |
| Crystal System | triclinic | triclinic | triclinic | triclinic |
| Space Group | *P*-1 | *P*-1 | *P*-1 | *P*-1 |
| $a$/Å | 13.1982(5) | 9.05180(10) | 9.0985(3) | 8.9430(3) |
| $b$/Å | 13.4528(6) | 14.2713(3) | 14.1448(5) | 14.0898(3) |
| $c$/Å | 17.7865(6) | 19.3342(3) | 19.3617(8) | 19.2216(6) |
| $\alpha$/° | 83.710(3) | 70.704(2) | 68.981(3) | 68.985(2) |
| $\beta$/° | 85.228(3) | 83.9170(10) | 88.579(3) | 89.683(2) |
| $\gamma$/° | 67.626(4) | 82.0440(10) | 83.588(3) | 83.855(2) |
| V/Å$^3$ | 2899.8(2) | 2329.76(7) | 2311.12(15) | 2246.52(12) |
| $Z$ | 1 | 1 | 1 | 1 |
| $Z'$ | 0.5 | 0.5 | 0.5 | 0.5 |
| Wavelength/Å | 1.54184 | 0.71073 | 1.54184 | 1.54184 |
| Radiation type | Cu$K_\alpha$ | Mo$K_\alpha$ | Cu $K_\alpha$ | Cu$K_\alpha$ |
| $\Theta_{min}$/° | 3.566 | 3.294 | 2.445 | 3.382 |
| $\Theta_{max}$/° | 71.816 | 30.634 | 74.181 | 71.657 |
| Measured Refl's. | 18299 | 23982 | 17418 | 23730 |
| Indep't Refl's | 10834 | 12561 | 8866 | 8483 |
| Refl's I≥2 $\sigma$(I) | 9791 | 10843 | 8349 | 8005 |
| $R_{int}$ | 0.0307 | 0.0567 | 0.0326 | 0.0489 |
| Parameters | 559 | 476 | 486 | 459 |
| Restraints | 74 | 6 | 73 | 20 |
| Largest Peak | 0.896 | 0.922 | 0.988 | 1.266 |
| Deepest Hole | -1.109 | -0.997 | -1.655 | -1.361 |
| GooF | 1.022 | 1.051 | 1.016 | 1.076 |
| $wR_2$ (all data) | 0.0752 | 0.0894 | 0.0830 | 0.1164 |
| $wR_2$ | 0.0727 | 0.0837 | 0.0811 | 0.1136 |
| $R_1$ (all data) | 0.0359 | 0.0451 | 0.0338 | 0.0445 |
| $R_1$ | 0.0312 | 0.0378 | 0.0318 | 0.0423 |

**Table S 6** Crystallographic data for the compounds **6a**, **6b** and **7**.

| Compound | 6a · 3 $CH_2Cl_2$ | 6b | 7 |
|---|---|---|---|
| Data set (internal naming) | AG569_B | AG379 | AG492 |
| CCDC-number | - | - | - |
| Formula | $C_{73.66}H_{127.32}Br_{15.36}Cl_{11.32}Co_6P_4$ | $C_{72.6}Cl_{25.2}Co_6H_{125.2}P_4$ | $C_{34}H_{58}Cl_6Co_2O_{0.11}P_4$ |
| $D_{calc.}$/ g cm$^{-3}$ | 1.863 | 1.474 | 1.424 |
| $\mu$/mm$^{-1}$ | 16.639 | 13.778 | 11.049 |
| Formula Weight | 3119.16 | 2368.92 | 923.00 |
| Colour | metallic dark brown | violet | dark brown |
| Shape | block-shaped | block-shaped | rod |
| Size/mm$^3$ | 0.23×0.10×0.04 | 0.14×0.10×0.05 | 0.39×0.09×0.08 |
| $T$/K | 123.00(10) | 123.1(1) | 100.00(10) |
| Crystal System | triclinic | triclinic | monoclinic |
| Space Group | $P$-1 | $P$-1 | $P2_1/c$ |
| $a$/Å | 13.7872(3) | 13.5056(4) | 14.2046(10) |
| $b$/Å | 13.8332(2) | 13.8000(3) | 19.6684(12) |
| $c$/Å | 15.6974(2) | 15.3692(4) | 16.3343(13) |
| $\alpha$/° | 74.4910(10) | 74.595(2) | 90 |
| $\beta$/° | 81.7430(10) | 83.168(2) | 109.408(8) |
| $\gamma$/° | 75.170(2) | 75.498(2) | 90 |
| V/Å$^3$ | 2779.63(9) | 2669.35(13) | 4304.2(6) |
| $Z$ | 1 | 1 | 4 |
| $Z'$ | 0.5 | 0.5 | 1 |
| Wavelength/Å | 1.54184 | 1.54184 | 1.54184 |
| Radiation type | Cu K$\alpha$ | Cu K$\alpha$ | Cu K$\alpha$ |
| $\Theta_{min}$/° | 2.931 | 3.385 | 3.299 |
| $\Theta_{max}$/° | 73.266 | 74.265 | 73.638 |
| Measured Refl's. | 10818 | 39741 | 8159 |
| Indep't Refl's | 10818 | 10594 | 8159 |
| Refl's I≥2 $\sigma$(I) | 9528 | 8724 | 7090 |
| $R_{int}$ | . | 0.0589 | . |
| Parameters | 623 | 442 | 474 |
| Restraints | 137 | 0 | 24 |
| Largest Peak | 1.399 | 0.450 | 1.365 |
| Deepest Hole | -0.931 | -0.389 | -2.239 |
| GooF | 1.059 | 1.044 | 1.043 |
| $wR_2$ (all data) | 0.1416 | 0.0971 | 0.1978 |
| $wR_2$ | 0.1373 | 0.0925 | 0.1908 |
| $R_1$ (all data) | 0.0568 | 0.0475 | 0.1005 |
| $R_1$ | 0.0499 | 0.0369 | 0.0896 |

**Table S 7** Crystallographic data for the compounds **10**, **11**, **12** and **[Cp'''CoI$_2$]**.

| Compound | 10 | 11 | 12 · $CH_3CN$ | [Cp'''$CoI_2$] |
|---|---|---|---|---|
| Data set (internal naming) | AG490 | AG491 | AG559 | AG511 |
| CCDC-number | - | - | - | - |
| Formula | $C_{34}H_{58}As_4Co_2I_2$ | $C_{34}H_{58}Co_2I_2P_4$ | $C_{36}H_{60.88}Co_2F_{3.76}NP_4$ | $C_{17}H_{29}CoI_2$ |
| $D_{calc.}$/ g cm$^{-3}$ | 1.868 | 1.630 | 1.377 | 1.867 |
| $\mu$/mm$^{-1}$ | 5.614 | 20.687 | 8.452 | 4.053 |
| Formula Weight | 1138.14 | 962.34 | 820.91 | 546.13 |
| Colour | black | dark black | orange | metallic dark brown |
| Shape | plate-shaped | plate-shaped | plate-shaped | block-shaped |
| Size/mm$^3$ | 0.35×0.08×0.04 | 0.10×0.06×0.05 | 0.15×0.11×0.05 | 0.50×0.11×0.03 |
| $T$/K | 123.0(1) | 100.1(1) | 123.01(10) | 123(1) |
| Crystal System | monoclinic | monoclinic | triclinic | orthorhombic |
| Flack Parameter | - | -0.014(3) | - | - |
| Hooft Parameter | - | -0.016(2) | - | - |
| Space Group | $P2_1/n$ | $P2_1$ | $P$-1 | $Pbca$ |
| $a$/Å | 13.5149(3) | 10.40860(10) | 8.6733(2) | 12.3736(2) |
| $b$/Å | 19.5096(3) | 14.8585(2) | 10.3049(2) | 16.9475(3) |
| $c$/Å | 15.6818(3) | 13.4579(2) | 24.4247(6) | 18.5284(3) |
| $\alpha$/° | 90 | 90 | 97.168(2) | 90 |
| $\beta$/° | 101.874(2) | 109.597(2) | 92.847(2) | 90 |
| $\gamma$/° | 90 | 90 | 113.188(2) | 90 |
| V/Å$^3$ | 4046.35(14) | 1960.79(5) | 1979.27(8) | 3885.43(11) |
| $Z$ | 4 | 2 | 2 | 8 |
| $Z'$ | 1 | 1 | 1 | 1 |
| Wavelength/Å | 0.71073 | 1.54184 | 1.54184 | 0.71073 |
| Radiation type | Mo$K_\alpha$ | Cu$K_\alpha$ | Cu $K_\alpha$ | Mo$K_\alpha$ |
| $\Theta_{min}$/° | 3.253 | 3.486 | 3.669 | 3.506 |
| $\Theta_{max}$/° | 29.471 | 73.328 | 73.056 | 29.469 |
| Measured Refl's. | 62546 | 19339 | 26585 | 75263 |
| Indep't Refl's | 10089 | 7450 | 7601 | 5138 |
| Refl's I≥2 $\sigma$(I) | 8518 | 7004 | 6773 | 4765 |
| $R_{int}$ | 0.0294 | 0.0348 | 0.0358 | 0.0247 |
| Parameters | 397 | 397 | 654 | 190 |
| Restraints | 0 | 1 | 471 | 0 |
| Largest Peak | 0.583 | 0.677 | 0.584 | 0.816 |
| Deepest Hole | -0.733 | -1.126 | -0.539 | -0.721 |
| GooF | 1.078 | 1.120 | 1.063 | 1.093 |
| $wR_2$ (all data) | 0.0505 | 0.0710 | 0.1335 | 0.0345 |
| $wR_2$ | 0.0472 | 0.0704 | 0.1309 | 0.0334 |
| $R_1$ (all data) | 0.0362 | 0.0317 | 0.0513 | 0.0194 |
| $R_1$ | 0.0253 | 0.0292 | 0.0465 | 0.0165 |

**Compound 3a:**

The asymmetric unit contains one molecule of $[(Cp'''Co)_2(\mu,\eta^4{:}\eta^4\text{-}As_4I)]^+$, half of the dianion $[As_6I_8]^-$ and two $CH_2Cl_2$ solvent molecules. Further, two of the As atoms of the $As_4$ ligand are disordered over two positions (0.81:0.19). Additionally, one Cl atom of one $CH_2Cl_2$ molecule is disordered over two positions (0.58:0.22), while the second $CH_2Cl_2$ molecule is fully disordered (0.7:0.1).

**Part 1** **Part 2** **Part 1 and 2**

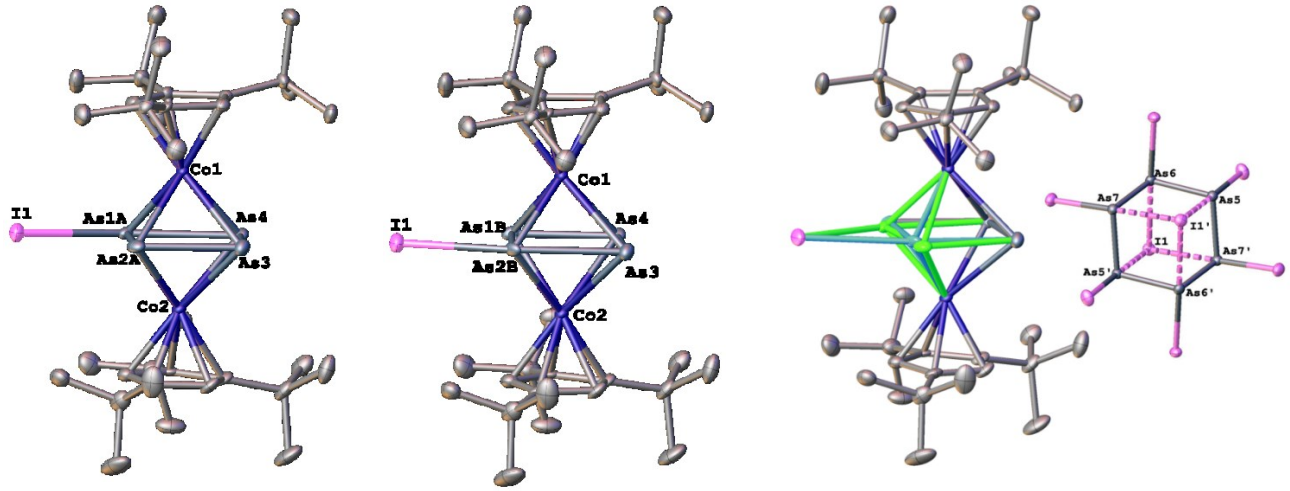


| Selected bond length [Å] | | Selected bond angles [°] | |
|---|---|---|---|
| As1A–As2A | 2.501(5) | As1A-As2A-As3 | 91.87 (16) |
| As2A–As3 | 2.512(4) | As2A-As3-As4 | 92.48(9) |
| As3–As4 | 2.330(8) | As3-As4-As1A | 91.17(6) |
| As4–As1A | 2.699(3) | As4-As1A-As2A | 84.49(14) |
| As1A-I1 | 2.837(3) | As4-As1A-I1 | 156.83(12) |
| As2A-I1 | 3.165(4) | As3-As2A-I1 | 150.48(14) |

**Compound 3b:**

The asymmetric unit contains one molecule of $[(Cp'''Co)_2(\mu,\eta^4:\eta^4\text{-}As_4I)]^+$, half of the dianion $[Co_2Cl_{6.3}I_{1.7}]^-$ and a $CH_2Cl_2$ solvent molecule. Further, two of the As atoms of the $As_4$ ligand are disordered over two positions (0.98:0.02). Additionally, the two bridging halogen atoms of the anion are occupied by Cl or I (0.92:0.08), as well as two of the terminal halogens (Cl :I = 0.23:0.77).

**Part 1**

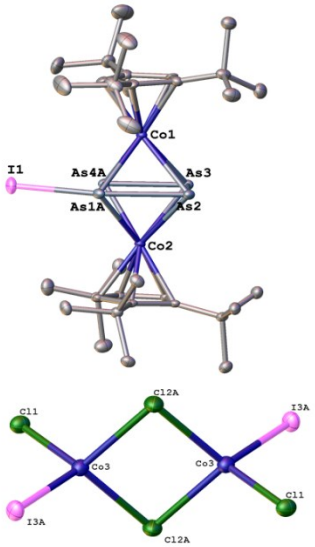


**Part 2**

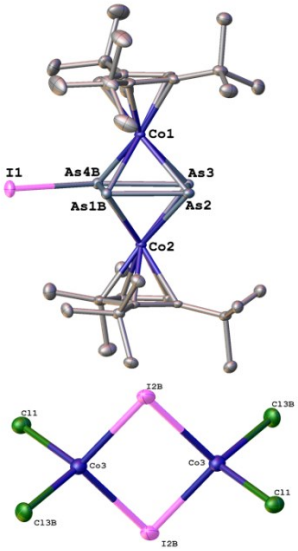


**Part 1 and 2**

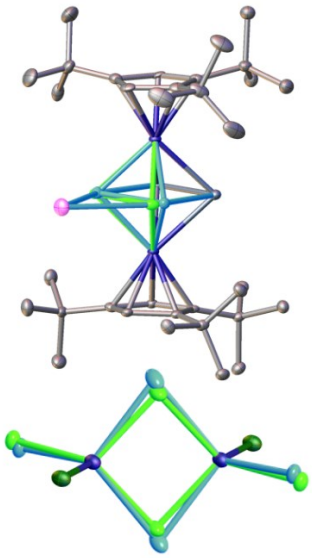

| Selected bond length [Å] | | Selected bond angles [°] | |
|---|---|---|---|
| As1A–As2 | 2.708(5) | As1A-As2-As3 | 91.696(17) |
| As2–As3 | 2.329(5) | As2-As3-As4A | 91.85(2) |
| As3–As4A | 2.498(7) | As3-As4A-As1A | 92.97(2) |
| As4A–As1A | 2.499(9) | As4A-As1A-As2 | 83.49(2) |
| As1A-I1 | 2.836(4) | As4A-As1A-I1 | 71.763(18) |
| As4A-I1 | 3.139(6) | As2-As1A-I1 | 155.21(2) |

**Compound 4:**

The asymmetric unit contains one molecule of $[(Cp'''Co)_2(\mu,\eta^4:\eta^4\text{-}As_4Br)]^+$, half of the dianion $[Co_2Br_6]^-$ and a $CH_2Cl_2$ solvent molecule. Further, two of the As atoms of the $As_4$ ligand are disordered over two positions (0.91:0.09). Additionally, the $CH_2Cl_2$ molecule is fully disordered (0.66:0.34).

**Part 1** **Part 2** **Part 1 and 2**

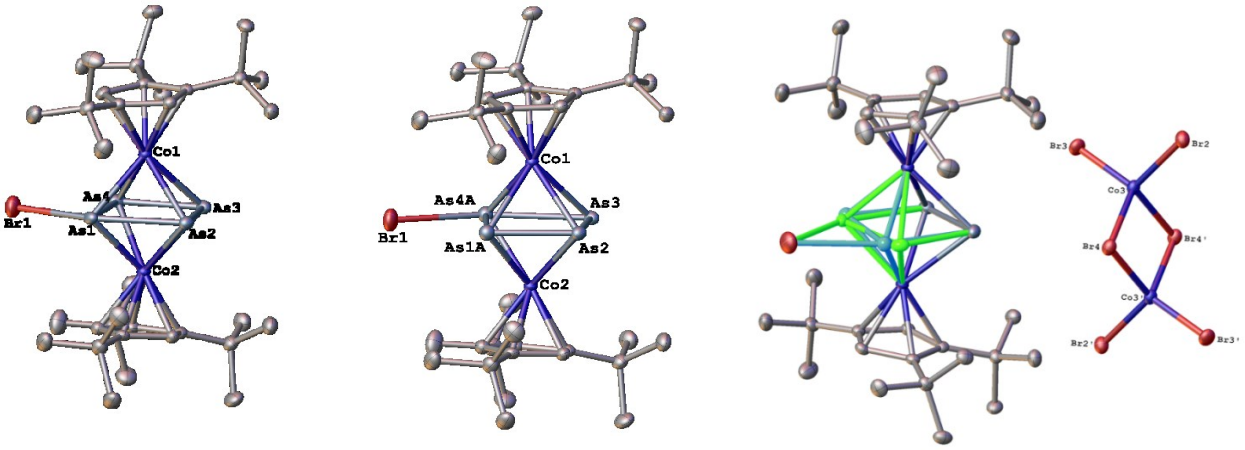


| Selected bond length [Å] | | Selected bond angles [°] | |
|---|---|---|---|
| As1–As2 | 2.702(19) | As1-As2-As3 | 90.40(4) |
| As2–As3 | 2.337(5) | As2-As3-As4 | 93.03(5) |
| As3–As4 | 2.466(19) | As3-As4-As1 | 92.46(5) |
| As4–As1 | 2.497(7) | As4-As1-As2 | 84.11(5) |
| As1-Br1 | 2.656(3) | As4-As1-Br1 | 71.87(11) |
| As4-Br1 | 3.027(2) | As2-As1-Br1 | 1.100(2) |

**Compound 5:**

The asymmetric unit contains one molecule of $[(Cp'''Co)_2(\mu,\eta^4{:}\eta^4\text{-}As_4Cl)]^+$, half of the dianion $[Co_2Cl_6]^-$ and a $CH_2Cl_2$ solvent molecule. Further, two of the As atoms of the $As_4$ ligand are disordered over two positions (0.95:0.05).

**Part 1**

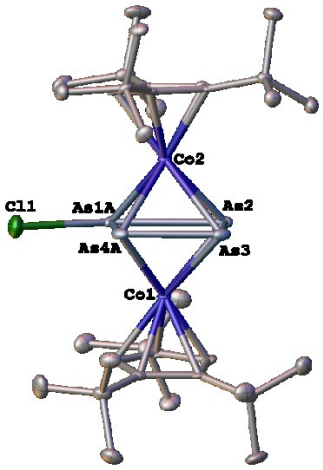


**Part 2**

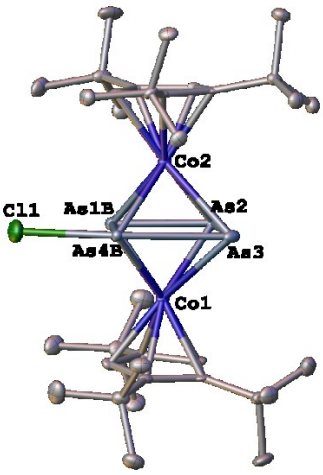


**Part 1 and 2**

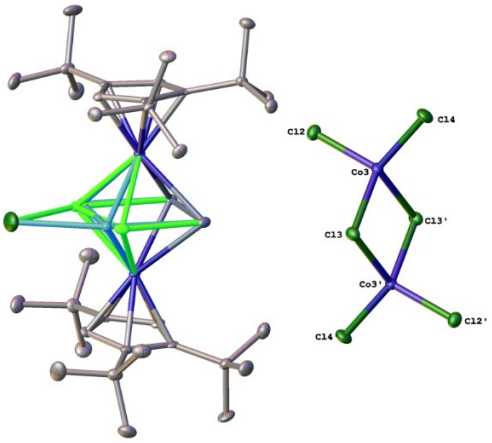


| Selected bond length [Å] | | Selected bond angles [°] | |
|---|---|---|---|
| As1A–As2 | 2.737(8) | As1A-As2-As3 | 90.51(2) |
| As2–As3 | 2.342(5) | As2-As3-As4A | 92.90(2) |
| As3–As4A | 2.432(8) | As3-As4A-As1A | 94.15(2) |
| As4A–As1A | 2.508(9) | As4A-As1A-As2 | 82.43(2) |
| As1A-Cl1 | 2.447(12) | As4A-As1A-Cl1 | 74.07(4) |
| As4A···Cl1 | 2.985(15) | As2-As1A-Cl1 | 156.50(4) |

**Compound 6a:**

The asymmetric unit contains one molecule of $[(Cp'''Co)_2(\mu\text{-}PBr_2)_2(\mu\text{-}Br)]^+$, half of the dianion $[Co_2Br_6]^-$ and four $CH_2Cl_2$ solvent molecules. The four Br atoms attached to the P atoms were only partly occupied and a free refinement resulted in an occupation of 0.92. Therefore, compound **6a** co-crystallizes with a second species (occupancy 0.08), which could not be fully identified, since it was, due to the low occupancy, not possible to determine if the positions of the phosphorus atoms P1 and P2 are partly occupied with Cl atoms or not. The anion is fully occupied. Additionally, two $CH_2Cl_2$ molecules are disordered. Since the measured crystal was twinned, a HKLF5 refinement was applied (twin law: 0.2156 -0.3119 0.8761 -0.1162 0.9045 0.2634 -1.1063 0.2288 0.4370; BASF 0.12).

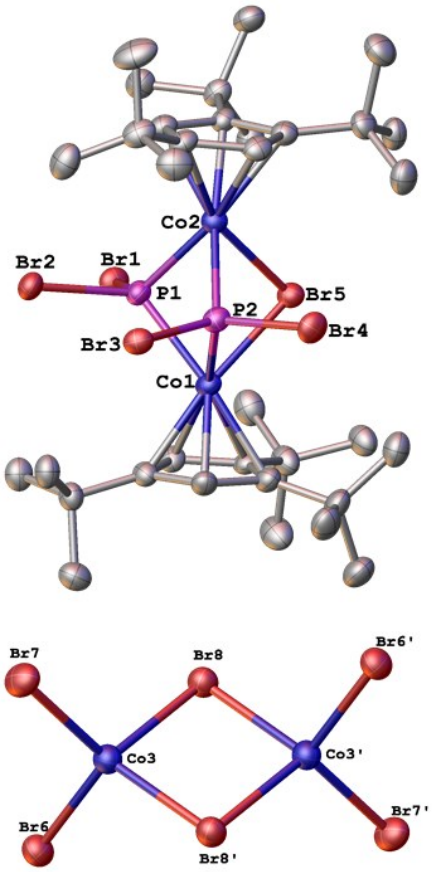


| Selected bond length [Å] | | Selected bond angles [°] | |
|---|---|---|---|
| P1···P2 | 2.696(17) | Co1-P1-Co2 | 91.51(5) |
| Co1···Co2 | 3.210(14) | Co1-P2-Co2 | 92.25(5) |
| Co1-Br5 | 2.430(10) | Co1-Br5-Co2 | 82.68(3) |
| Co2-Br5 | 2.430(9) | Br1-P1-Br2 | 97.84(5) |

**Compound 6b:**

The asymmetric unit contains one molecule of $[(Cp'''Co)_2(\mu\text{-}PCl_2)_2(\mu\text{-}Cl)]^+$ and half of the dianion $[Co_2Cl_6]^-$.

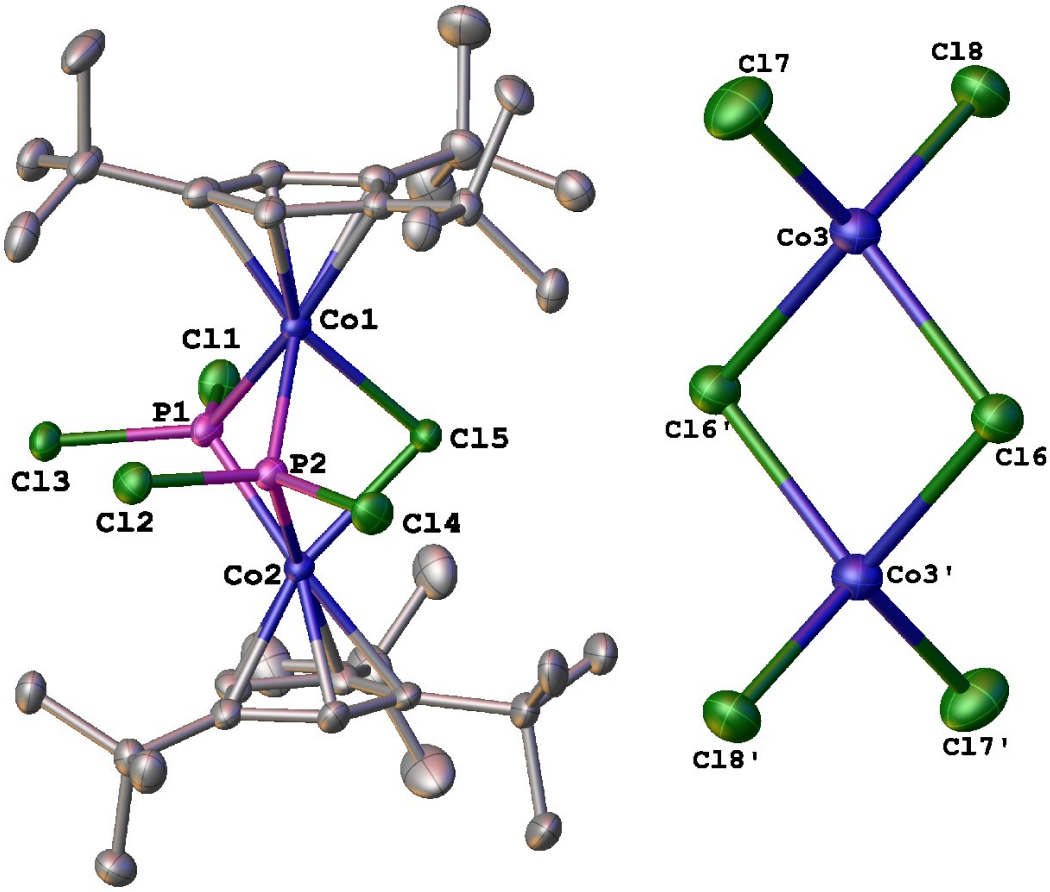


| Selected bond length [Å] | | Selected bond angles [°] | |
|---|---|---|---|
| P1···P2 | 2.688(9) | Co1-P1-Co2 | 90.89(3) |
| Co1···Co2 | 3.134(6) | Co1-P2-Co2 | 89.73(3) |
| Co1-Cl5 | 2.312(7) | Co1-Cl5-Co2 | 85.38(2) |
| Co2-Cl5 | 2.310(7) | Cl1-P1-Cl3 | 98.79(4) |

**Compound 7:**

The asymmetric unit contains one molecule of $[(Cp'''Co)_2(\mu\text{-}PCl_2)(\mu\text{-}PCl)(\mu,\eta^1{:}\eta^1\text{-}P_2Cl_3]$. Additionally, one oxygen atom with 11% occupancy is attached to P4 (Part 1: Part 2 =0.89: 0.11). Three methyl groups of one *tert*-butyl group are disordered over two positions (0.55:0.45).

**Part 1** **Part 2** **Part 1 and 2**

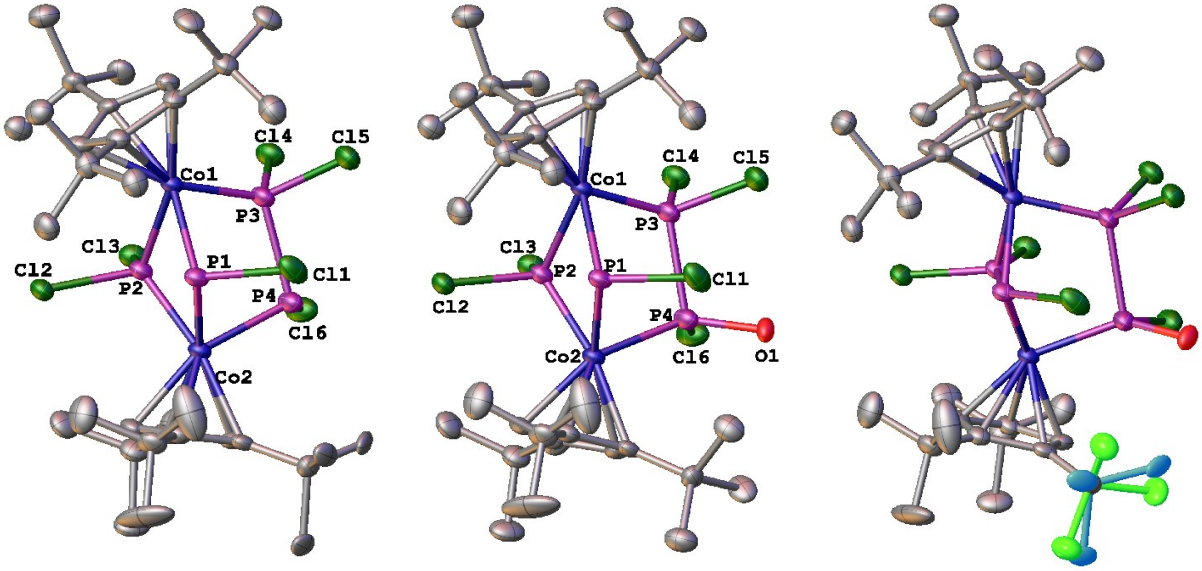


| Selected bond length [Å] | | Selected bond angles [°] | |
|---|---|---|---|
| P1···P2 | 2.608(3) | Co1-P1-Co2 | 99.36(9) |
| P3-P4 | 2.240(3) | Co1-P2-Co2 | 107.73(10) |
| Co1-P1 | 2.319(2) | Co1-P3-P4 | 112.07(10) |
| Co2-P1 | 2.271(2) | Co2-P4-P3 | 101.58(10) |

**Compound 10:**

The asymmetric unit contains one molecule of $[(Cp'''Co)_2(\mu,\eta^4{:}\eta^4\text{-}As_4I)]^+$ and one of the anion $I^-$.

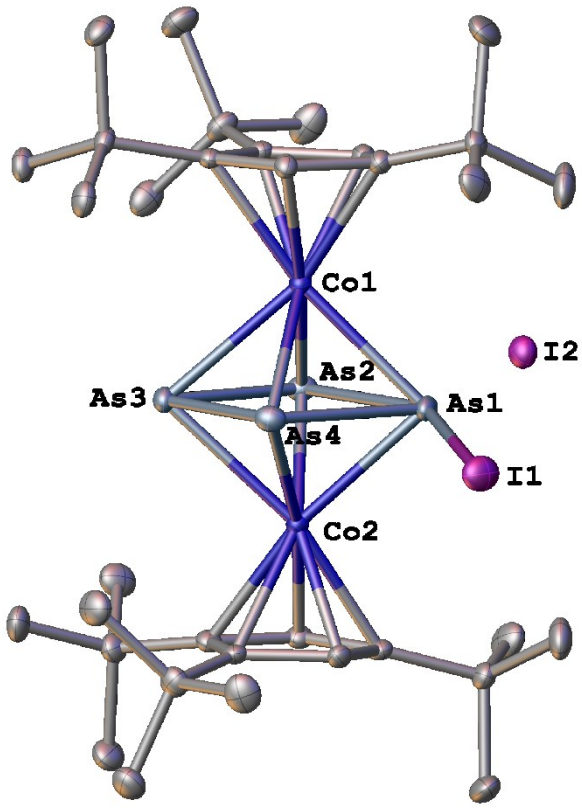


| Selected bond length [Å] | | Selected bond angles [°] | |
|---|---|---|---|
| As1–As2 | 2.620(4) | As1-As2-As3 | 90.623(12) |
| As2–As3 | 2.443(4) | As2-As3-As4 | 92.651(13) |
| As3–As4 | 2.395(4) | As3-As4-As1 | 92.379(12) |
| As4–As1 | 2.592(4) | As4-As1-As2 | 84.347(12) |
| As1-I1 | 3.095(3) | As4-As1-I1 | 69.737(10) |
| As4-I1 | 3.278(5) | As3-As4-I1 | 152.873(16) |

**Compound 11:**

The asymmetric unit contains one molecule of [(Cp'''Co)(Cp'''$CoI_2$)(μ,$\eta^4$:$\eta^1$-$P_4$)].

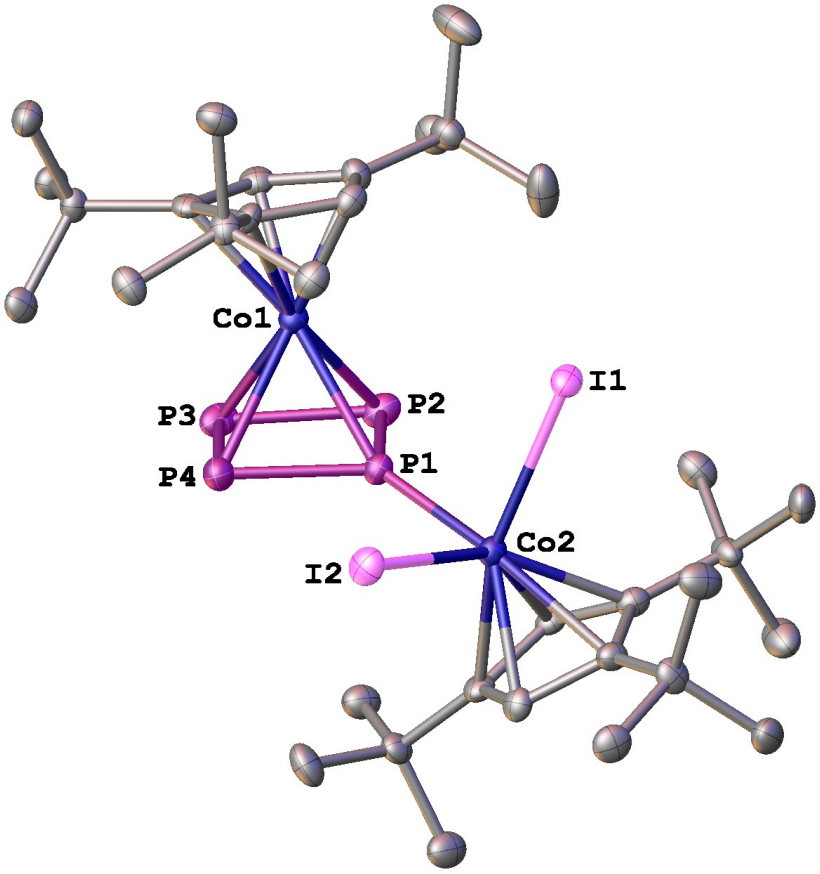


| Selected bond length [Å] | | Selected bond angles [°] | |
|---|---|---|---|
| P1–P2 | 2.140(2) | P1-P2-P3 | 86.35(9) |
| P2–P3 | 2.167(3) | P2-P3-P4 | 92.54(10) |
| P3–P4 | 2.183(3) | P3-P4-P1 | 86.21(9) |
| P4–P1 | 2.130(2) | P4-P1-P2 | 94.82(10) |

**Compound 12:**

The asymmetric unit contains one molecule of $[(Cp'''Co)_2(\mu\text{-}PF_2)(\mu,\eta^2{:}\eta1{:}\eta^1\text{-}P_3F_2)]$ and one $CH_3CN$ solvent molecule. Compound **12** co-crystallizes with the neutral specie $[(Cp'''Co)_2(\mu,\eta^2{:}\eta^2\text{-}P_2)_2]$ (**2**) (0.94:0.06).

**Part 1** **Part 2** **Part 1 and 2**

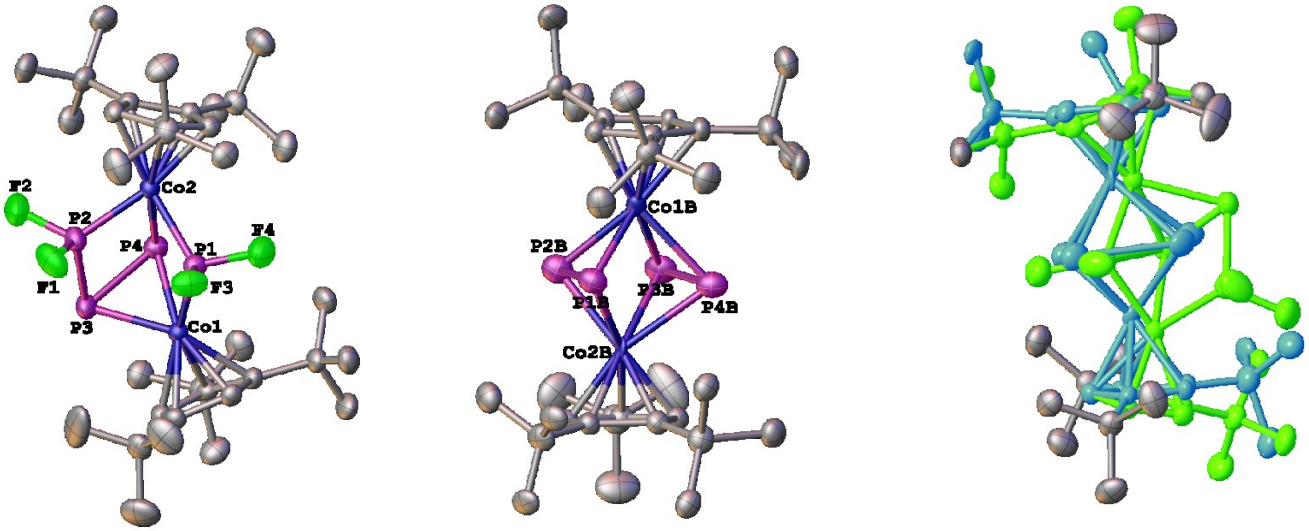


| Selected bond length [Å] | | Selected bond angles [°] | |
|---|---|---|---|
| P1···P2 | 2.878(14) | P2-P3-P4 | 78.84(4) |
| P2–P3 | 2.126(12) | F1-P2-F2 | 94.59(16) |
| P3–P4 | 2.202(12) | F3-P1-F4 | 91.87(14) |
| P4···P1 | 2.625(12) | Co1-P1-Co2 | 111.68(5) |

**[Cp'''$CoI_2$]:**

The asymmetric unit contains one molecule of [Cp'''$CoI_2$].

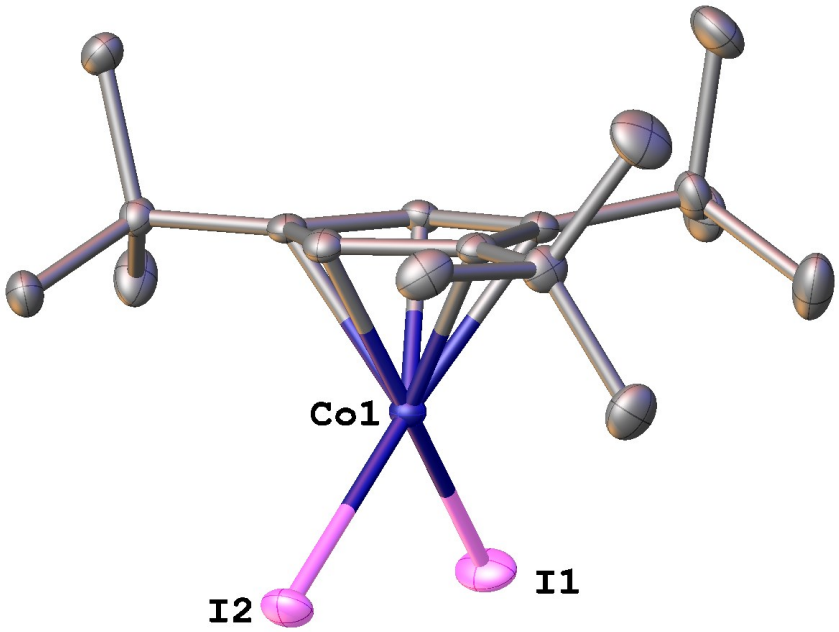


| Selected bond length [Å] | | Selected bond angles [°] | |
|---|---|---|---|
| Co1-I1 | 2.494(2) | I1-Co1-I2 | 95.667(8) |
| Co1-I2 | 2.504(2) | | |

## Computational details

The DFT calculations have been performed with the ORCA program.[7] The geometries have been optimised at the TPSSh[8]/def2-TZVP[9] level of theory starting from the X-ray coordinates. The dispersion effects have been incorporated by using the charge dependent atom-pairwise dispersion correction D4[10] as implemented in Orca. The solvation effects were incorporated via the CPCM model[11] using the dielectric constant of dichloromethane. For the geometry optimisations, the RIJCOSX[12] approximation has been used, followed by a single point calculation without the RIJCOX approximation. The NBO analysis has been performed with NBO6,[13] while the Interaction Region Indicator[14] (IRI) the Electron Localization Function (ELF)[15] and the Localized orbital locator (LOL)[16] were calculated with Multiwfn.[17]

**Table S 8** Total energies of the cation of complexes **3**, **5**, **6b**, and of the neutral **7** and **12** calculated at the D4-TPSSh(CPM)/def2-TZVP level of theory.

| Compound | Total energy (Hartree) |
|---|---|
| $[(Cp'''Co)_2(\mu,\eta^4{:}\eta^4\text{-}As_4I)]^+$ (**3**$^+$) | -13338.071104323799 |
| $[(Cp'''Co)_2(\mu,\eta^4{:}\eta^4\text{-}As_4Cl)]^+$ (**5**$^+$) | -13500.670516336872 |
| $[(Cp'''Co)_2(\mu\text{-}PCl_2)_2(\mu\text{-}Cl)]^+$ (**6b**$^+$) | -7081.029431665776 |
| $[(Cp'''Co)_2(\mu,\eta^1{:}\eta^1\text{-}PCl_2PCl)(\mu\text{-}PCl_2)(\mu\text{-}PCl]$ (**7**) | -8224.266470529861 |
| $[(Cp'''Co)_2(\mu\text{-}PF_2)(\mu,\eta^2{:}\eta^1{:}\eta^1\text{-}P_3F_2)]$ (**12**) | -5862.411580281280 |

Cartesian coordinates od the optimizes geometry of $[(Cp'''Co)_2(\mu,\eta^4{:}\eta^4\text{-}As_4I)]^+$ (**3**$^+$) at the D4-TPSSh(CPCM)/def2-TZVP level of theory.

| Atom | x | y | z |
|---|---|---|---|
| Co | 9.118461000 | 7.777764000 | 4.104358000 |
| Co | 11.059849000 | 10.404878000 | 4.089977000 |
| As | 11.230053000 | 8.239275000 | 3.124204000 |
| As | 9.249589000 | 9.702493000 | 2.733189000 |
| As | 8.973921000 | 9.921559000 | 5.282073000 |
| As | 10.822237000 | 8.556739000 | 5.672265000 |
| I | 10.606301000 | 8.642868000 | 0.269987000 |
| C | 12.267303000 | 11.516863000 | 2.908095000 |
| H | 12.473432000 | 11.262535000 | 1.881822000 |
| C | 12.362383000 | 11.581329000 | 5.222104000 |
| C | 11.237329000 | 12.332194000 | 4.750598000 |
| H | 10.531280000 | 12.837937000 | 5.387749000 |
| C | 9.077165000 | 5.714832000 | 4.035450000 |
| C | 8.377034000 | 6.309585000 | 2.929739000 |
| H | 8.655048000 | 6.196148000 | 1.895337000 |
| C | 11.181830000 | 12.333915000 | 3.332744000 |
| C | 11.469050000 | 11.826511000 | 7.574284000 |
| H | 10.878730000 | 12.708556000 | 7.325020000 |
| H | 11.781836000 | 11.928983000 | 8.615500000 |
| H | 10.829855000 | 10.943925000 | 7.497172000 |
| C | 7.344322000 | 7.042175000 | 4.805012000 |
| H | 6.671499000 | 7.565098000 | 5.463985000 |
| C | 12.730569000 | 11.684683000 | 6.701323000 |
| C | 8.440254000 | 5.788295000 | 6.718087000 |
| C | 8.401635000 | 6.180658000 | 5.242022000 |
| C | 14.368926000 | 8.887759000 | 4.524367000 |
| H | 14.063197000 | 8.910846000 | 5.564814000 |
| H | 15.390200000 | 8.502104000 | 4.473980000 |
| H | 13.725713000 | 8.178799000 | 3.996491000 |
| C | 14.320418000 | 10.260633000 | 3.833253000 |
| C | 10.272198000 | 13.188730000 | 2.483616000 |
| C | 13.021217000 | 11.040602000 | 4.036273000 |
| C | 7.291352000 | 7.106053000 | 3.388010000 |
| C | 11.523870000 | 5.001513000 | 4.481685000 |
| H | 12.017385000 | 5.840991000 | 3.984523000 |
| H | 12.179022000 | 4.132378000 | 4.385375000 |
| H | 11.429456000 | 5.241847000 | 5.534451000 |
| C | 13.548194000 | 10.536048000 | 7.295067000 |
| H | 13.008181000 | 9.588701000 | 7.233173000 |
| H | 13.719856000 | 10.751112000 | 8.352328000 |
| H | 14.521005000 | 10.418696000 | 6.823841000 |
| C | 8.021018000 | 6.969622000 | 7.612616000 |
| H | 8.721256000 | 7.802877000 | 7.522344000 |
| H | 8.028932000 | 6.633821000 | 8.651672000 |
| H | 7.016822000 | 7.333813000 | 7.393618000 |
| C | 8.828342000 | 13.189385000 | 3.002269000 |
| H | 8.352348000 | 12.216258000 | 2.858341000 |
| H | 8.246514000 | 13.930525000 | 2.449955000 |
| H | 8.779263000 | 13.443385000 | 4.063361000 |
| C | 13.533437000 | 13.002968000 | 6.825201000 |
| H | 14.443785000 | 12.980469000 | 6.225436000 |
| H | 13.812061000 | 13.155709000 | 7.871109000 |
| H | 12.927492000 | 13.851917000 | 6.500288000 |

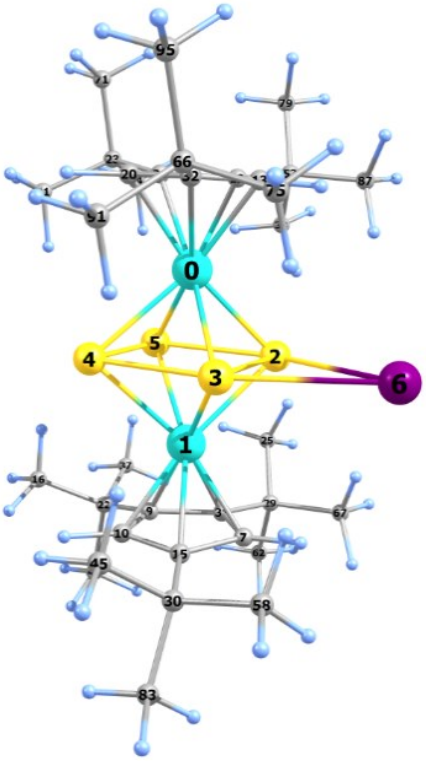

| | | | |
|---|---|---|---|
| C | 10.185270000 | 4.692315000 | 3.791948000 |
| C | 9.767790000 | 5.270613000 | 7.272763000 |
| H | 10.108775000 | 4.363702000 | 6.779202000 |
| H | 9.624639000 | 5.034063000 | 8.329677000 |
| H | 10.551028000 | 6.029072000 | 7.206693000 |
| C | 10.311694000 | 12.761131000 | 1.014489000 |
| H | 11.320166000 | 12.850357000 | 0.603949000 |
| H | 9.651695000 | 13.405793000 | 0.430468000 |
| H | 9.979671000 | 11.728042000 | 0.883725000 |
| C | 15.493404000 | 11.143209000 | 4.311121000 |
| H | 15.493946000 | 11.290246000 | 5.389814000 |
| H | 15.458310000 | 12.123577000 | 3.830229000 |
| H | 16.433002000 | 10.658226000 | 4.036249000 |
| C | 6.189432000 | 7.730397000 | 2.569713000 |
| C | 14.542821000 | 9.997643000 | 2.333500000 |
| H | 15.456570000 | 9.411805000 | 2.213954000 |
| H | 14.660385000 | 10.925864000 | 1.770200000 |
| H | 13.720353000 | 9.422658000 | 1.898451000 |
| C | 7.366998000 | 4.681721000 | 6.857060000 |
| H | 6.386413000 | 5.057508000 | 6.555981000 |
| H | 7.311216000 | 4.364110000 | 7.901348000 |
| H | 7.606604000 | 3.812368000 | 6.243078000 |
| C | 6.594251000 | 7.890765000 | 1.102072000 |
| H | 7.459759000 | 8.547622000 | 0.989142000 |
| H | 5.764216000 | 8.327815000 | 0.542857000 |
| H | 6.838294000 | 6.926926000 | 0.649765000 |
| C | 9.657327000 | 3.308498000 | 4.228702000 |
| H | 9.519174000 | 3.235891000 | 5.306438000 |
| H | 10.376522000 | 2.543210000 | 3.927846000 |
| H | 8.702174000 | 3.092411000 | 3.744285000 |
| C | 10.827062000 | 14.627801000 | 2.602200000 |
| H | 10.760993000 | 14.985852000 | 3.632398000 |
| H | 10.238788000 | 15.293370000 | 1.966151000 |
| H | 11.870209000 | 14.673411000 | 2.280555000 |
| C | 10.488610000 | 4.600520000 | 2.286171000 |
| H | 9.625956000 | 4.248688000 | 1.716447000 |
| H | 11.303195000 | 3.888696000 | 2.137944000 |
| H | 10.809626000 | 5.563923000 | 1.879827000 |
| C | 5.742371000 | 9.077687000 | 3.149594000 |
| H | 5.464975000 | 8.994240000 | 4.202502000 |
| H | 4.872570000 | 9.441790000 | 2.598420000 |
| H | 6.533512000 | 9.826983000 | 3.061789000 |
| C | 5.009323000 | 6.732976000 | 2.653350000 |
| H | 5.303444000 | 5.753169000 | 2.269979000 |
| H | 4.177660000 | 7.106558000 | 2.051109000 |
| H | 4.667784000 | 6.615317000 | 3.684297000 |

| | |
|---|---|
| Dispersion correction | -0.244407638 |
| FINAL SINGLE POINT ENERGY | -13338.071104323799 |

Mayer bond orders larger than 0.100000
B( 0-Co, 1-Co) : 0.1399 B( 0-Co, 2-As) : 0.5001 B( 0-Co, 3-As) : 0.5063

```
B(  0-Co,  4-As) :   0.5069 B(  0-Co,  5-As) :   0.5098 B(  0-Co, 12-C ) :
0.3156
B(  0-Co, 13-C ) :   0.6305 B(  0-Co, 20-C ) :   0.5851 B(  0-Co, 24-C ) :
0.3802
B(  0-Co, 32-C ) :   0.2782 B(  1-Co,  2-As) :   0.4990 B(  1-Co,  3-As) :
0.5137
B(  1-Co,  4-As) :   0.5064 B(  1-Co,  5-As) :   0.5111 B(  1-Co,  7-C ) :
0.6310
B(  1-Co,  9-C ) :   0.3688 B(  1-Co, 10-C ) :   0.5957 B(  1-Co, 15-C ) :
0.2758
B(  1-Co, 31-C ) :   0.3200 B(  2-As,  3-As) :   0.7845 B(  2-As,  5-As) :
0.5306
B(  2-As,  6-I ) :   0.4842 B(  2-As, 12-C ) :  -0.1107 B(  2-As, 31-C ) :  -
0.1161
B(  3-As,  4-As) :   0.5286 B(  3-As,  6-I ) :   0.4431 B(  4-As,  5-As) :
1.0257
B(  4-As, 10-C ) :   0.1510 B(  4-As, 20-C ) :   0.1468 B(  7-C ,  8-H ) :
0.9604


-------------------------   ----------------
Intrinsic Bonding Orbitals
-------------------------   ----------------

MO 130:   6I  -   0.554034  and   3As -   0.318301
MO 129:   6I  -   0.562220  and   2As -   0.314789
MO 128:   5As -   0.452924  and   4As -   0.451000
MO 127:   2As -   0.041583  and   1Co -   0.832768
MO 126:   2As -   0.042417  and   0Co -   0.832374
MO 125:   1Co -   0.939005  and   0Co -   0.000526
MO 124:   1Co -   0.000615  and   0Co -   0.939121
More delocalized orbitals:
MO 234:  0Co- 0.100 2As- 0.089 5As- 0.389 6I - 0.207
MO 233:  0Co- 0.142 2As- 0.101 3As- 0.521
MO 232:  1Co- 0.186 3As- 0.087 4As- 0.384 6I - 0.207
MO 230:  1Co- 0.184 2As- 0.393 3As- 0.376
MO 228:  0Co- 0.554 2As- 0.093 4As- 0.083 12C - 0.081
MO 224:  1Co- 0.097 2As- 0.108 4As- 0.112 5As- 0.480
```

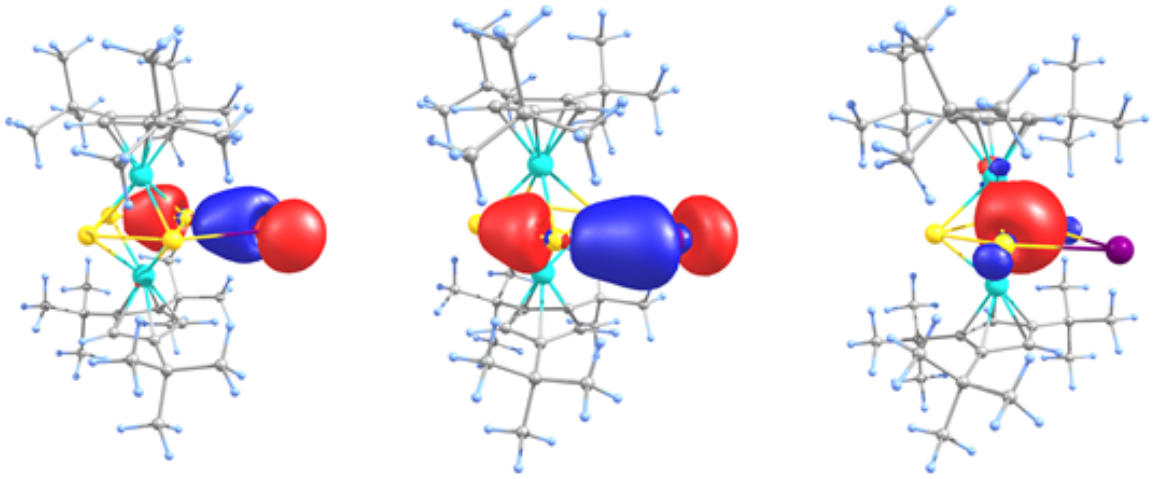

**Figure S 33** Intrinsic bonding orbital representing the As-I bond (IBO 129; left and IBO 130 middle) and the As2-As3 bond (IBO 230; right).

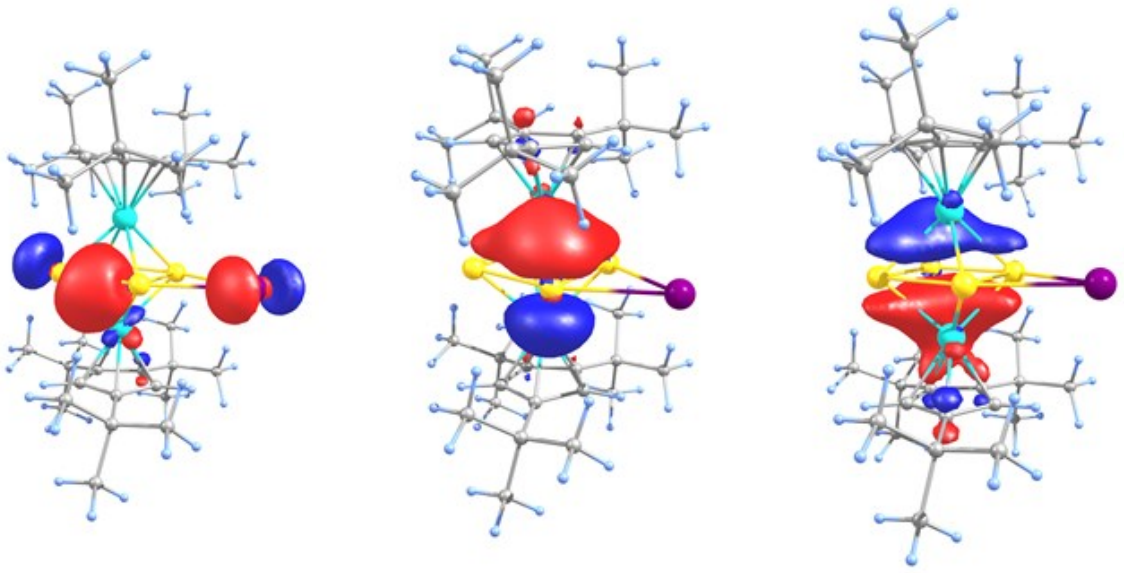

**Figure S 34** Selected Intrinsic bonding orbital representing the As-As bonding (IBO 232; left IBO 233 middle and IBO 224; right).

```
-----------------------------------------------
LOEWDIN REDUCED ORBITAL POPULATIONS PER MO (IBO)
-----------------------------------------------
                    126       127       128       129       130       131
                  -0.73128  -0.71707  -0.71690  -0.71158  -0.68982  -0.68955
                   2.00000   2.00000   2.00000   2.00000   2.00000   2.00000
                  --------  --------  --------  --------  --------  --------
 2 As pz             0.1       0.1       0.4      23.9       0.3       0.0
 3 As pz             0.2       0.4       0.4       0.1      20.8       0.0
 4 As s              0.0       0.0       2.9       0.0       0.7       0.0
 4 As pz             0.3       0.1       5.4       0.1       5.9       0.0
 4 As px             0.3       1.1      21.1       0.0       0.0       0.0
 4 As py             2.2       0.8       9.2       0.0       0.0       0.0
```

| | | | | | | |
|---|---|---|---|---|---|---|
| 5 As px | 0.6 | 0.2 | 21.8 | 0.4 | 0.0 | 0.0 |
| 5 As py | 0.5 | 1.0 | 13.2 | 0.2 | 0.0 | 0.0 |
| 6 I pz | 0.0 | 0.0 | 1.7 | 33.6 | 14.3 | 0.0 |
| 6 I px | 0.2 | 0.2 | 0.1 | 13.6 | 25.0 | 1.3 |
| 6 I py | 0.0 | 0.2 | 0.1 | 5.9 | 13.3 | 2.2 |

```
NBO
141. (1.73678) BD ( 1)As  3- I  7
               ( 22.98%)   0.4793*As  3 s(  0.03%)p99.99( 98.32%)d60.77(  1.63%)
               ( 77.02%)   0.8776* I  7 s(  8.45%)p10.82( 91.43%)d 0.01(  0.11%)
```

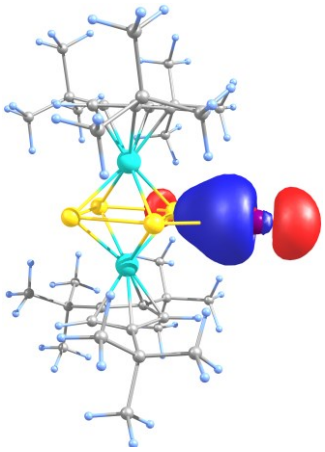

**Figure S 35** Natural Bond Orbital (NBO 141) representing the As-I bond.

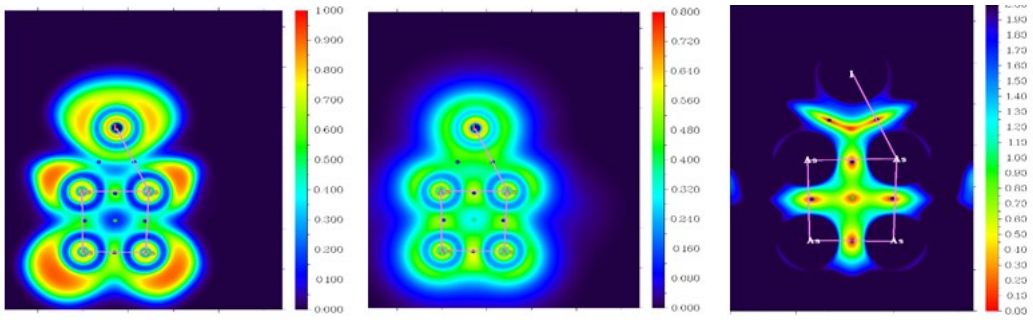

**Figure S 36** Electron Localization Function (ELF; left), Localized Orbital Locator (LOL; middle) and Interaction Region Indicator (IRI; right) in the plain defined by As3, As4, I7. Blue dots represent (3,-1) critical points and green dot (3,+1) critical point. IRI < 1.0 indicates regions with notable chemical bond interaction (orange) and areas where weak interactions occur (green). The regions with IRI > 1.0 are not significant for bonding (either large gradient of electron density or negligible electron density).

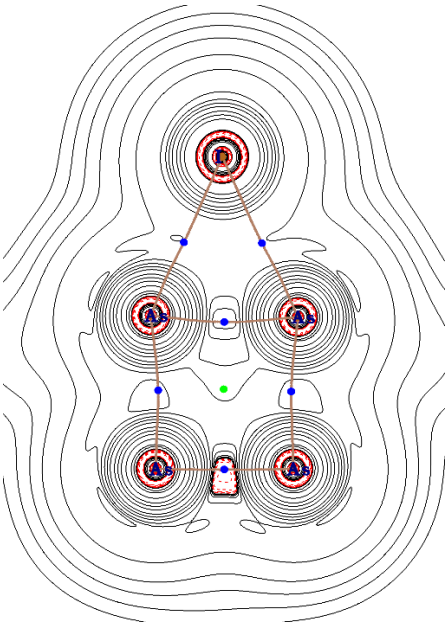

**Figure S 37** Contour line plot of the Laplacian of the electron density in the plane defined by the atoms As6, As5 and I7. Negative contour lines in red. Blue dots represent (3,-1) critical points and green dot (3,+1) critical point.

Cartesian coordinates od the optimizes geometry of $[(Cp'''Co)_2(\mu,\eta^4:\eta^4\text{-}As_4Cl)]^+$ (**5**) at the D4-TPSSh(CPCM)/def2-TZVP level of theory.

| Atom | x | y | z |
|---|---|---|---|
| Co | 5.751811000 | 13.307585000 | 12.368474000 |
| Co | 4.368689000 | 11.224263000 | 14.454394000 |
| As | 5.105988000 | 13.478068000 | 14.648315000 |
| As | 6.626149000 | 11.650572000 | 13.835924000 |
| As | 4.595015000 | 11.236829000 | 12.077822000 |
| As | 3.362839000 | 13.000338000 | 13.015947000 |
| Cl | 7.762881000 | 12.787497000 | 15.679937000 |
| C | 5.463851000 | 14.880577000 | 11.088528000 |
| H | 4.516798000 | 15.356931000 | 10.896248000 |
| C | 7.246765000 | 13.413990000 | 10.963887000 |
| C | 7.446847000 | 14.356235000 | 12.035401000 |
| H | 8.285676000 | 14.343947000 | 12.710676000 |
| C | 5.970122000 | 13.757663000 | 10.351314000 |
| C | 4.732227000 | 10.168815000 | 16.136860000 |
| H | 5.665454000 | 10.216458000 | 16.671891000 |
| C | 6.371929000 | 15.282969000 | 12.101286000 |
| C | 5.243321000 | 13.351238000 | 9.068255000 |
| C | 3.111731000 | 9.572994000 | 14.591336000 |
| C | 4.456359000 | 9.257473000 | 15.056322000 |
| C | 3.616776000 | 11.013377000 | 16.386443000 |
| C | 8.337575000 | 12.412900000 | 10.593615000 |
| C | 1.142717000 | 9.933435000 | 13.044320000 |
| H | 0.581459000 | 10.487726000 | 13.796858000 |
| H | 0.418928000 | 9.403130000 | 12.421752000 |
| H | 1.674363000 | 10.645077000 | 12.408697000 |
| C | 5.463852000 | 11.926744000 | 8.552272000 |
| H | 5.113289000 | 11.181858000 | 9.269470000 |
| H | 6.501471000 | 11.717676000 | 8.302488000 |
| H | 4.877635000 | 11.804798000 | 7.638533000 |

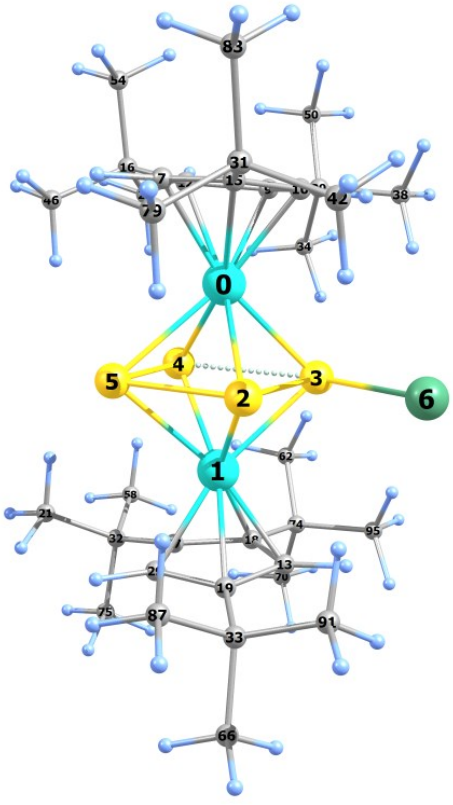

| | | | |
|---|---|---|---|
| C | 2.649362000 | 10.657119000 | 15.412840000 |
| H | 1.692081000 | 11.138509000 | 15.301811000 |
| C | 6.282669000 | 16.533866000 | 12.940908000 |
| C | 2.109393000 | 8.899291000 | 13.651473000 |
| C | 3.422106000 | 11.953759000 | 17.549923000 |
| C | 7.884588000 | 10.945192000 | 10.598327000 |
| H | 8.682192000 | 10.324422000 | 10.182804000 |
| H | 6.981275000 | 10.766620000 | 10.026137000 |
| H | 7.709807000 | 10.612547000 | 11.625578000 |
| C | 9.505950000 | 12.510660000 | 11.590437000 |
| H | 9.184549000 | 12.293702000 | 12.612778000 |
| H | 9.977710000 | 13.495190000 | 11.571123000 |
| H | 10.259344000 | 11.769675000 | 11.315800000 |
| C | 7.194734000 | 16.449870000 | 14.168990000 |
| H | 6.928200000 | 15.609285000 | 14.814166000 |
| H | 7.105706000 | 17.368991000 | 14.752242000 |
| H | 8.240981000 | 16.337172000 | 13.875236000 |
| C | 3.721722000 | 13.526377000 | 9.226768000 |
| H | 3.242386000 | 13.253439000 | 8.284471000 |
| H | 3.434884000 | 14.552909000 | 9.456133000 |
| H | 3.326489000 | 12.870886000 | 10.005661000 |
| C | 8.896211000 | 12.803806000 | 9.208309000 |
| H | 9.760737000 | 12.174577000 | 8.984556000 |
| H | 9.221004000 | 13.846949000 | 9.205335000 |
| H | 8.166523000 | 12.670326000 | 8.411648000 |
| C | 5.727571000 | 14.352127000 | 7.993532000 |
| H | 6.801402000 | 14.265964000 | 7.821158000 |
| H | 5.506829000 | 15.379394000 | 8.293051000 |
| H | 5.209102000 | 14.145953000 | 7.053869000 |
| C | 2.674119000 | 8.100048000 | 12.474224000 |
| H | 3.243658000 | 8.738194000 | 11.795159000 |
| H | 1.832769000 | 7.688038000 | 11.912076000 |
| H | 3.299487000 | 7.265777000 | 12.782004000 |
| C | 5.917553000 | 8.166546000 | 13.235526000 |
| H | 6.522429000 | 7.276626000 | 13.045108000 |
| H | 6.552955000 | 9.039251000 | 13.056931000 |
| H | 5.103485000 | 8.184057000 | 12.518446000 |
| C | 2.681213000 | 11.125010000 | 18.624365000 |
| H | 1.712700000 | 10.780328000 | 18.253836000 |
| H | 2.515286000 | 11.744092000 | 19.509347000 |
| H | 3.270551000 | 10.252866000 | 18.916183000 |
| C | 4.803668000 | 6.791472000 | 15.044505000 |
| H | 5.532718000 | 5.998508000 | 14.862967000 |
| H | 3.920889000 | 6.580521000 | 14.444451000 |
| H | 4.516076000 | 6.761424000 | 16.098063000 |
| C | 5.447088000 | 8.151291000 | 14.698199000 |
| C | 1.281036000 | 7.953740000 | 14.552839000 |
| H | 1.905409000 | 7.188132000 | 15.015288000 |
| H | 0.518821000 | 7.459089000 | 13.945546000 |
| H | 0.781279000 | 8.515888000 | 15.345097000 |
| C | 4.838761000 | 16.830039000 | 13.365909000 |
| H | 4.168824000 | 16.883585000 | 12.505327000 |
| H | 4.800891000 | 17.791427000 | 13.883131000 |
| H | 4.460327000 | 16.066732000 | 14.049931000 |
| C | 6.774205000 | 17.681861000 | 12.029575000 |
| H | 7.797291000 | 17.501158000 | 11.691256000 |
| H | 6.752285000 | 18.620546000 | 12.588672000 |
| H | 6.131814000 | 17.786144000 | 11.152160000 |

```
C        2.556062000     13.159595000     17.166536000
H        3.064684000     13.799032000     16.441213000
H        2.351978000     13.758539000     18.056759000
H        1.598920000     12.851707000     16.740121000
C        4.762435000     12.424506000     18.123774000
H        5.365014000     11.582010000     18.470057000
H        4.580731000     13.080372000     18.978022000
H        5.344879000     12.980069000     17.385649000
C        6.712269000      8.274530000     15.565170000
H        6.487966000      8.166062000     16.628450000
H        7.220778000      9.229222000     15.405741000
H        7.404876000      7.478827000     15.284158000

-------------------------   ----------------
Dispersion correction           -0.240469423
FINAL SINGLE POINT ENERGY    -13500.670516336872
-------------------------   --------------------

Mayer bond orders larger than 0.100000
B(  0-Co,  1-Co) :   0.1292 B(  0-Co,  2-As) :   0.4946 B(  0-Co,  3-As) :
0.5666
B(  0-Co,  4-As) :   0.5902 B(  0-Co,  5-As) :   0.4654 B(  0-Co,  7-C ) :
0.5854
B(  0-Co,  9-C ) :   0.3216 B(  0-Co, 10-C ) :   0.6234 B(  0-Co, 12-C ) :
0.3598
B(  0-Co, 15-C ) :   0.2805 B(  1-Co,  2-As) :   0.4997 B(  1-Co,  3-As) :
0.5623
B(  1-Co,  4-As) :   0.5900 B(  1-Co,  5-As) :   0.4714 B(  1-Co, 13-C ) :
0.6165
B(  1-Co, 17-C ) :   0.3513 B(  1-Co, 18-C ) :   0.3192 B(  1-Co, 19-C ) :
0.2873
B(  1-Co, 29-C ) :   0.5851 B(  2-As,  3-As) :   0.7106 B(  2-As,  5-As) :
0.7645
B(  2-As,  6-Cl) :   0.1644 B(  3-As,  4-As) :   0.3914 B(  3-As,  6-Cl) :
0.6056
B(  3-As,  9-C ) :  -0.1167 B(  3-As, 18-C ) :  -0.1097 B(  4-As,  5-As) :
0.9726
B(  5-As,  7-C ) :   0.1314 B(  5-As, 29-C ) :   0.1298 B(  7-C ,  8-H ) :
1.0282


********************************** NBO 6.0 **********************************

    (Occupancy)   Bond orbital / Coefficients / Hybrids
 ------------------ Lewis ------------------------------------------------------

136. (1.69841) BD ( 1)As  3-As  6
               ( 47.40%)   0.6885*As  3 s( 10.27%)p 8.58( 88.05%)d 0.16(  1.67%)
               ( 52.60%)   0.7253*As  6 s( 10.65%)p 8.22( 87.58%)d 0.16(  1.75%)
137. (1.93743) BD ( 1)As  4-Cl  7
               ( 22.33%)   0.4725*As  4 s(  1.25%)p77.63( 97.38%)d 1.03(  1.30%)
               ( 77.67%)   0.8813*Cl  7 s( 14.80%)p 5.74( 84.98%)d 0.01(  0.21%)
138. (1.78161) BD ( 1)As  5-As  6
               ( 47.62%)   0.6901*As  5 s(  6.35%)p14.49( 91.97%)d 0.26(  1.65%)
               ( 52.38%)   0.7237*As  6 s( 10.92%)p 8.00( 87.36%)d 0.16(  1.70%)


-------------------------------------------------------------------------------
```

LOCALIZED MOLECULAR ORBITAL COMPOSITIONS (IBO)

---

**MO 127:** 6Cl - 0.800988 and 3As - 0.164317
MO 126: 5As - 0.443267 and 4As - 0.433383
MO 230: 0Co- 0.097 1Co- 0.096 2As- 0.430 5As- 0.178
MO 229: 2As- 0.371 5As- 0.422
**MO 227:** 0Co- 0.105 1Co- 0.107 2As- 0.360 3As- 0.407
MO 226: 0Co- 0.187 1Co- 0.182 3As- 0.495
**MO 224:** 0Co- 0.107 1Co- 0.105 3As- 0.163 4As- 0.421
MO 223: 0Co- 0.111 1Co- 0.105 4As- 0.482 5As- 0.188

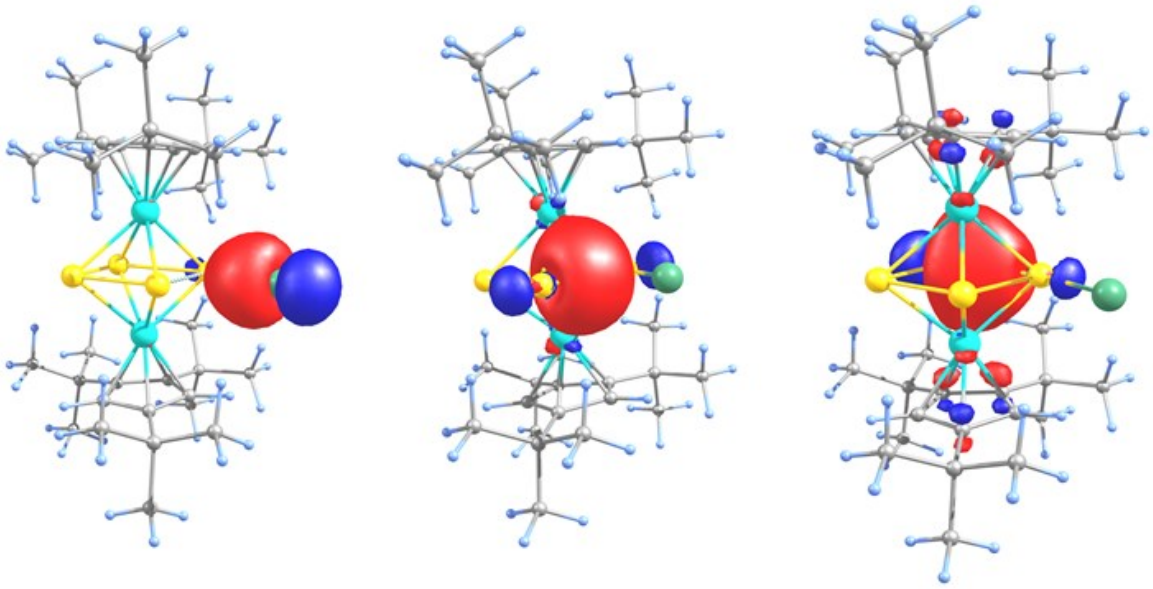

**Figure S 38** Intrinsic bonding orbital representing the As-Cl bond (IBO 127; left), As2-As3 bond (IBO 227; middle) and As3-As4 bond (IBO 224, right).

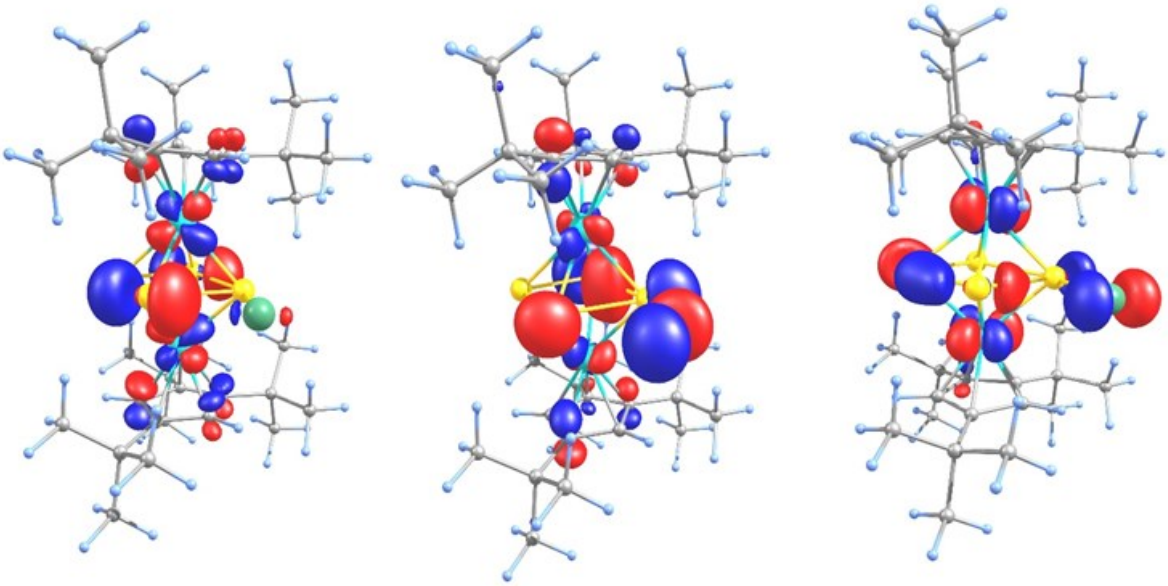

**Figure S 39** Frontier molecular orbitals at the D4-TPSSh(CPCM)/def2-TZVP level of theory. Left: LUMO (Loewdin reduced orbital populations: 17% Co0, 19% Co1, 13%As2, 3% As3, 12 %As4, 8% As5, 2% Cl6), middle: HOMO (7% Co0, 7% Co1, 8%As2, 14% As3, 19 %As4, 3% As5, 13% Cl6) and right: HOMO-1 (13% Co0, 26% Co1, 7%As2, 6% As3, 3 %As4, 10% As5, 9% Cl6.

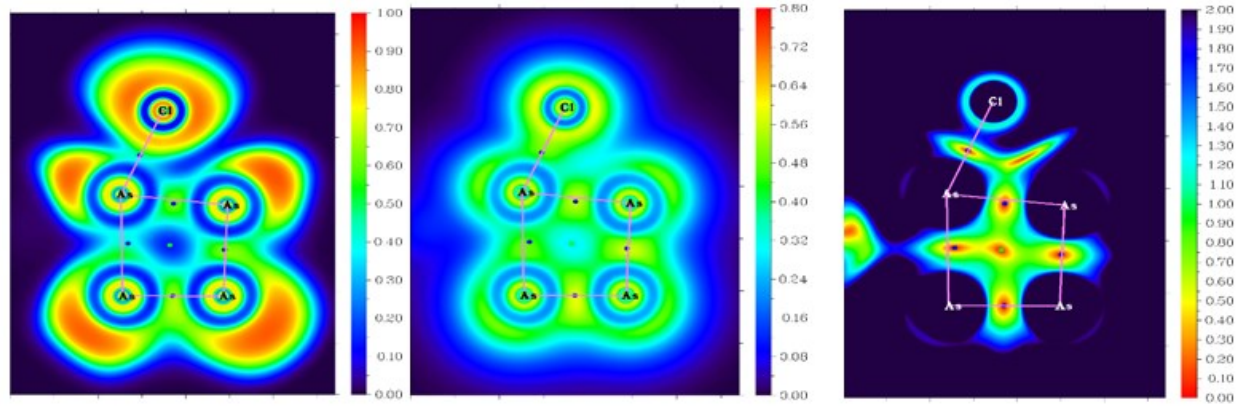


**Figure S 40** Electron Localization Function (ELF; left), Localized Orbital Locator (LOL; middle) and Interaction Region Indicator (IRI; right) in the plain defined by As6, As5, Cl7. Blue dots represent (3,-1) critical points and green dot (3,+1) critical point. IRI < 1.0 indicates regions with notable chemical bond interaction (orange) and areas where weak interactions occur (green). The regions with IRI > 1.0 are not significant for bonding (either large gradient of electron density or negligible electron density)

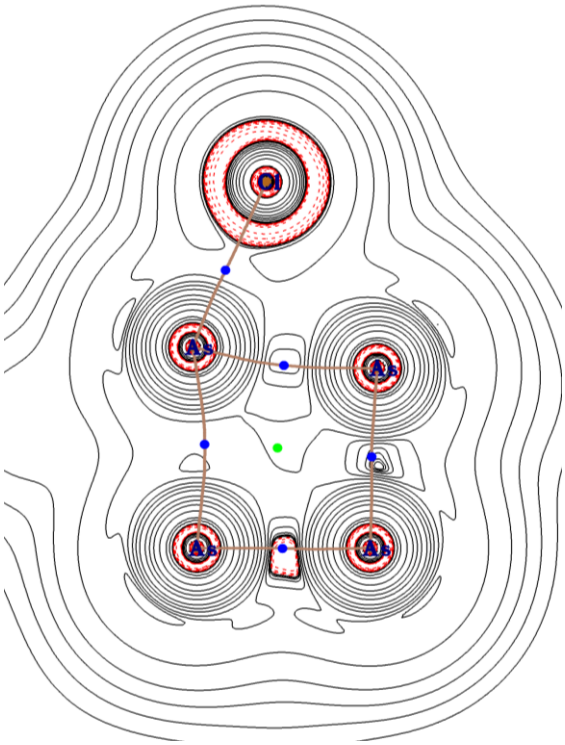


**Figure S 41** Contour line plot of the Laplacian of the electron density in the plane defined by the atoms As6, As5 and Cl7. Negative contour lines in red. Blue dots represent (3,-1) critical points and green dot (3,+1) critical point.

Cartesian coordinates od the optimizes geometry of $[(Cp'''Co)_2(\mu\text{-}PCl_2)_2(\mu\text{-}Cl)]^+$ (**6b**) at the D4-TPSSh(CPCM)/def2-TZVP level of theory.

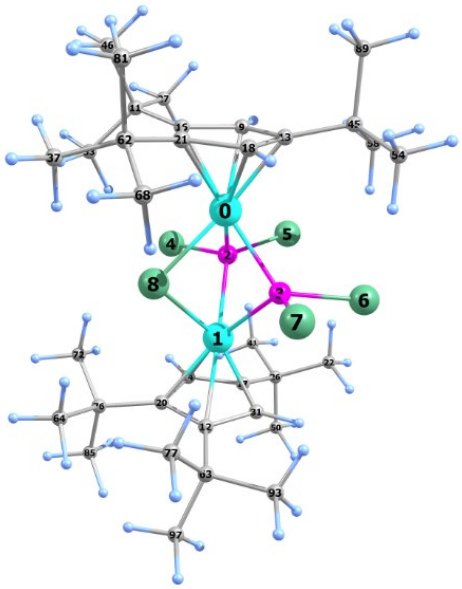

| Atom | x | y | z |
|---|---|---|---|
| Co | 11.075636000 | 5.138990000 | 4.038822000 |
| Co | 7.948714000 | 5.355275000 | 3.874255000 |
| P | 9.569592000 | 6.524739000 | 4.836460000 |
| P | 9.587826000 | 5.403138000 | 2.417023000 |
| Cl | 9.237823000 | 6.681624000 | 6.865647000 |
| Cl | 9.977333000 | 8.495977000 | 4.437582000 |
| Cl | 9.521115000 | 7.039267000 | 1.183504000 |
| Cl | 9.771795000 | 3.928203000 | 0.993642000 |
| Cl | 9.372795000 | 3.725057000 | 4.655854000 |
| C | 12.819294000 | 6.017331000 | 4.583968000 |
| H | 12.875818000 | 7.003729000 | 5.012081000 |
| C | 12.848258000 | 4.818144000 | 6.859828000 |
| C | 6.203351000 | 4.418838000 | 3.163743000 |
| C | 12.872517000 | 5.744797000 | 3.189165000 |
| C | 6.281560000 | 5.833485000 | 4.995063000 |
| H | 6.301002000 | 6.194008000 | 6.008498000 |
| C | 12.693329000 | 4.804627000 | 5.338534000 |
| C | 6.335571000 | 6.667070000 | 3.840859000 |
| C | 12.715332000 | 4.332858000 | 3.070579000 |
| H | 12.683579000 | 3.800413000 | 2.135930000 |
| C | 6.156527000 | 4.467333000 | 4.623908000 |
| C | 12.645845000 | 3.724598000 | 4.353806000 |
| C | 6.825764000 | 8.849951000 | 2.660210000 |
| H | 7.905465000 | 8.800933000 | 2.784379000 |
| H | 6.530134000 | 9.901183000 | 2.629724000 |
| H | 6.568317000 | 8.401454000 | 1.698250000 |
| C | 6.093534000 | 8.154744000 | 3.811154000 |
| C | 12.991832000 | 6.271153000 | 7.350886000 |
| H | 13.870072000 | 6.757525000 | 6.920543000 |
| H | 13.115061000 | 6.260979000 | 8.435710000 |
| H | 12.108515000 | 6.870111000 | 7.120260000 |
| C | 6.330943000 | 5.779879000 | 2.729826000 |
| H | 6.398809000 | 6.093466000 | 1.701681000 |
| C | 11.676641000 | 4.194441000 | 7.632291000 |
| H | 10.749470000 | 4.717717000 | 7.409486000 |
| H | 11.873945000 | 4.292166000 | 8.702963000 |
| H | 11.530926000 | 3.142767000 | 7.413654000 |
| C | 12.084963000 | 1.548695000 | 5.684966000 |
| H | 12.643009000 | 1.796377000 | 6.585094000 |
| H | 12.141033000 | 0.465229000 | 5.558552000 |
| H | 11.037560000 | 1.816533000 | 5.829425000 |
| C | 6.421219000 | 8.809274000 | 5.157067000 |
| H | 5.813961000 | 8.384067000 | 5.959151000 |
| H | 6.196883000 | 9.876802000 | 5.102254000 |
| H | 7.471745000 | 8.697841000 | 5.423513000 |
| C | 13.347271000 | 6.681939000 | 2.107357000 |
| C | 14.169808000 | 4.105614000 | 7.211475000 |
| H | 14.133296000 | 3.037189000 | 7.004468000 |
| H | 14.368969000 | 4.236140000 | 8.278230000 |
| H | 15.002953000 | 4.537782000 | 6.651952000 |
| C | 4.567834000 | 8.285639000 | 3.576165000 |
| H | 4.284292000 | 7.880543000 | 2.602121000 |
| H | 4.294114000 | 9.343320000 | 3.607767000 |

```
H        4.004152000      7.760318000      4.350479000
C       13.007027000      6.167315000      0.705254000
H       13.453713000      5.187217000      0.524250000
H       13.409764000      6.858939000     -0.037694000
H       11.932154000      6.093014000      0.546464000
C       12.839996000      8.113111000      2.301866000
H       11.760346000      8.175090000      2.178223000
H       13.309057000      8.762380000      1.559279000
H       13.098012000      8.497046000      3.291043000
C       12.673050000      2.199526000      4.430911000
C        5.929335000      3.304857000      2.154508000
C        6.203409000      1.985418000      5.441863000
H        7.257400000      1.838912000      5.202256000
H        5.593589000      1.575921000      4.639611000
H        5.981138000      1.409127000      6.342585000
C       11.951549000      1.580513000      3.216923000
H       10.904073000      1.884002000      3.177611000
H       11.992428000      0.493633000      3.311450000
H       12.426796000      1.842253000      2.271409000
C        6.646610000      3.833865000      7.017749000
H        6.341510000      4.802355000      7.414092000
H        7.724558000      3.848255000      6.851977000
H        6.426165000      3.086163000      7.782060000
C        5.884323000      3.452886000      5.732529000
C        6.904614000      2.119707000      2.218173000
H        7.928011000      2.457150000      2.064463000
H        6.653812000      1.419779000      1.417187000
H        6.861858000      1.581285000      3.157778000
C       14.171050000      1.817378000      4.333101000
H       14.598498000      2.163406000      3.389514000
H       14.260091000      0.728938000      4.378002000
H       14.751039000      2.243573000      5.151830000
C        4.368543000      3.582252000      6.025899000
H        4.109211000      2.905732000      6.844091000
H        3.765469000      3.317314000      5.156410000
H        4.116184000      4.601854000      6.325613000
C       14.889245000      6.680742000      2.259438000
H       15.187262000      7.053667000      3.242152000
H       15.321677000      7.331406000      1.495474000
H       15.294627000      5.674920000      2.127057000
C        6.002437000      3.868878000      0.723971000
H        5.259627000      4.652418000      0.558279000
H        5.792159000      3.059252000      0.022359000
H        6.992009000      4.266135000      0.490424000
C        4.477483000      2.826864000      2.361434000
H        4.328737000      2.350510000      3.329108000
H        4.229924000      2.097796000      1.585888000
H        3.781027000      3.664972000      2.278230000


-------------------------   ----------------
Dispersion correction           -0.241830702
FINAL SINGLE POINT ENERGY     -7081.029431665776
-------------------------   --------------------

  Mayer bond orders larger than 0.100000
B(  0-Co,  2-P ) :   0.7913 B(  0-Co,  3-P ) :   0.7424 B(  0-Co,  8-Cl) :
0.6101
```

```
B(  0-Co,  9-C ) :   0.6087 B(  0-Co, 13-C ) :   0.3744 B(  0-Co, 16-C ) :
0.3613
B(  0-Co, 18-C ) :   0.5345 B(  0-Co, 21-C ) :   0.3900 B(  1-Co,  2-P ) :
0.7437
B(  1-Co,  3-P ) :   0.7877 B(  1-Co,  8-Cl) :   0.6139 B(  1-Co, 12-C ) :
0.3604
B(  1-Co, 14-C ) :   0.5315 B(  1-Co, 17-C ) :   0.3677 B(  1-Co, 20-C ) :
0.3928
B(  1-Co, 31-C ) :   0.6123 B(  2-P ,  3-P ) :   0.1012 B(  2-P ,  4-Cl) :
1.0047
B(  2-P ,  5-Cl) :   1.0221 B(  3-P ,  6-Cl) :   1.0247 B(  3-P ,  7-Cl) :
1.0068
```

Cartesian coordinates od the optimizes geometry of [(Cp'''Co)$_2$(μ,η$^1$:η$^1$-PCl$_2$PCl)(μ-PCl$_2$)(μ-PCl] (**7**) at the D4-TPSSh(CPCM)/def2-TZVP level of theory.

| Atom | x | y | z |
|---|---|---|---|
| Co | 8.971475000 | 8.216747000 | 3.304059000 |
| Co | 12.435245000 | 8.381415000 | 3.724348000 |
| P | 10.540535000 | 9.415381000 | 4.082648000 |
| P | 10.706979000 | 6.870242000 | 3.740571000 |
| P | 9.791603000 | 8.361924000 | 1.281415000 |
| P | 11.955605000 | 8.685716000 | 1.701109000 |
| Cl | 10.268501000 | 9.744596000 | 6.151300000 |
| Cl | 10.545866000 | 11.442035000 | 3.524167000 |
| Cl | 10.831091000 | 5.453524000 | 2.100151000 |
| Cl | 12.589956000 | 10.479282000 | 0.885497000 |
| Cl | 12.808754000 | 7.503630000 | 0.219484000 |
| Cl | 9.338322000 | 10.202984000 | 0.326665000 |
| C | 7.492807000 | 8.380900000 | 4.744945000 |
| H | 7.683778000 | 8.739152000 | 5.740449000 |
| C | 13.336624000 | 8.662030000 | 5.567548000 |
| H | 12.807824000 | 8.973710000 | 6.450543000 |
| C | 14.293167000 | 11.007018000 | 4.891910000 |
| C | 14.479234000 | 8.723584000 | 3.629154000 |
| H | 14.989982000 | 9.081332000 | 2.750677000 |
| C | 16.106172000 | 5.638809000 | 4.162964000 |
| H | 16.794279000 | 5.008528000 | 3.592954000 |
| H | 15.633401000 | 5.015134000 | 4.918878000 |
| H | 16.688905000 | 6.414843000 | 4.665999000 |
| C | 7.535854000 | 7.007649000 | 4.357683000 |
| C | 15.910909000 | 6.908089000 | 2.066950000 |
| H | 15.284818000 | 7.420032000 | 1.335722000 |
| H | 16.460363000 | 6.120985000 | 1.545247000 |
| H | 16.640134000 | 7.617467000 | 2.466037000 |
| C | 14.377761000 | 6.152686000 | 7.220151000 |
| H | 14.141492000 | 5.429126000 | 8.005349000 |
| H | 14.528819000 | 7.129344000 | 7.687046000 |
| H | 15.311273000 | 5.850781000 | 6.746250000 |
| C | 7.263588000 | 6.976763000 | 2.931724000 |
| C | 7.043521000 | 8.345990000 | 2.538221000 |
| H | 6.790892000 | 8.656419000 | 1.536607000 |
| C | 5.096026000 | 10.510535000 | 3.886120000 |
| H | 4.658723000 | 10.050966000 | 2.996336000 |
| H | 4.656178000 | 11.503143000 | 4.017835000 |

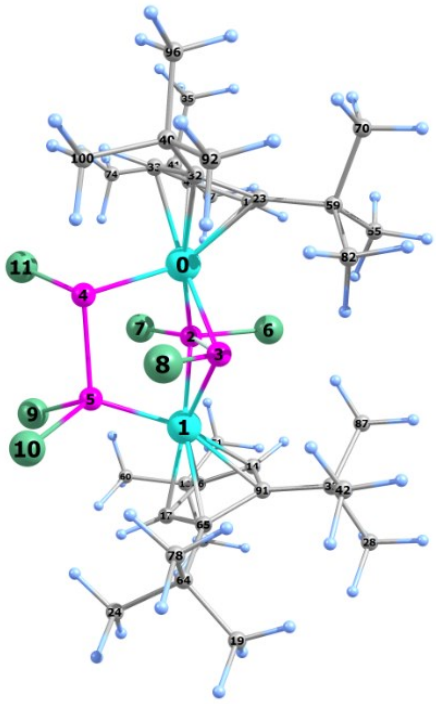

| | | | |
|---|---|---|---|
| H | 4.834351000 | 9.899490000 | 4.753647000 |
| C | 13.204610000 | 6.211077000 | 6.215272000 |
| C | 6.847900000 | 5.879609000 | 1.943545000 |
| C | 6.630194000 | 10.637682000 | 3.744739000 |
| C | 12.945726000 | 4.812396000 | 5.648251000 |
| H | 13.838726000 | 4.361141000 | 5.221329000 |
| H | 12.160797000 | 4.833601000 | 4.889463000 |
| H | 12.610043000 | 4.167221000 | 6.464071000 |
| C | 7.135870000 | 9.215230000 | 3.650437000 |
| C | 7.164705000 | 11.354505000 | 4.989078000 |
| H | 6.729231000 | 12.355965000 | 5.039866000 |
| H | 8.248799000 | 11.455043000 | 4.962201000 |
| H | 6.887870000 | 10.824286000 | 5.903348000 |
| C | 13.361533000 | 11.654942000 | 5.919399000 |
| H | 13.695887000 | 12.678049000 | 6.109959000 |
| H | 13.378099000 | 11.115849000 | 6.869335000 |
| H | 12.334155000 | 11.692953000 | 5.559645000 |
| C | 7.935022000 | 6.562063000 | 6.803982000 |
| H | 8.882505000 | 7.103857000 | 6.766260000 |
| H | 8.029406000 | 5.764421000 | 7.544592000 |
| H | 7.153692000 | 7.244227000 | 7.146022000 |
| C | 7.595769000 | 5.927132000 | 5.442370000 |
| C | 14.310909000 | 11.840113000 | 3.608475000 |
| H | 13.307976000 | 11.948575000 | 3.198451000 |
| H | 14.948431000 | 11.388061000 | 2.845500000 |
| H | 14.706306000 | 12.834860000 | 3.831422000 |
| C | 15.082103000 | 6.258612000 | 3.190362000 |
| C | 14.294450000 | 7.331280000 | 3.950497000 |
| C | 15.722611000 | 10.976907000 | 5.484326000 |
| H | 16.030293000 | 11.993351000 | 5.745902000 |
| H | 16.435764000 | 10.572328000 | 4.762045000 |
| H | 15.759657000 | 10.361536000 | 6.386848000 |
| C | 6.168733000 | 5.351635000 | 5.570798000 |
| H | 5.446174000 | 6.154469000 | 5.739243000 |
| H | 6.132351000 | 4.670554000 | 6.425568000 |
| H | 5.862068000 | 4.797498000 | 4.684472000 |
| C | 6.945076000 | 11.456689000 | 2.491580000 |
| H | 6.559519000 | 10.972398000 | 1.591768000 |
| H | 8.018499000 | 11.592193000 | 2.370857000 |
| H | 6.473837000 | 12.440160000 | 2.572851000 |
| C | 14.240088000 | 5.150748000 | 2.548460000 |
| H | 13.601163000 | 5.556065000 | 1.768038000 |
| H | 13.605793000 | 4.635000000 | 3.262263000 |
| H | 14.915376000 | 4.417956000 | 2.096551000 |
| C | 8.614724000 | 4.794042000 | 5.242005000 |
| H | 8.636893000 | 4.400343000 | 4.232489000 |
| H | 8.366013000 | 3.977272000 | 5.925804000 |
| H | 9.618433000 | 5.143568000 | 5.484048000 |
| C | 13.951751000 | 9.553314000 | 4.644592000 |
| C | 11.948764000 | 6.603246000 | 7.014379000 |
| H | 11.718605000 | 5.799256000 | 7.716916000 |
| H | 11.092019000 | 6.734923000 | 6.352900000 |
| H | 12.087837000 | 7.516425000 | 7.593776000 |
| C | 13.559310000 | 7.299993000 | 5.200888000 |
| C | 7.285617000 | 4.444360000 | 2.244003000 |
| H | 6.894091000 | 4.069374000 | 3.187671000 |
| H | 8.371431000 | 4.351572000 | 2.240104000 |
| H | 6.892496000 | 3.802290000 | 1.451157000 |

```
C         5.301454000      5.917027000      1.925520000
H         4.929455000      5.163020000      1.226125000
H         4.938544000      6.895492000      1.601829000
H         4.885459000      5.704380000      2.912290000
C         7.345386000      6.182304000      0.519526000
H         6.891428000      5.461929000     -0.166258000
H         8.429171000      6.079579000      0.458157000
H         7.071397000      7.180772000      0.175180000


-------------------------   ----------------
Dispersion correction           -0.281975723
FINAL SINGLE POINT ENERGY     -8224.266470529861
-------------------------   --------------------

Mayer bond orders larger than 0.100000
B(  0-Co,  2-P ) :   0.8698 B(  0-Co,  3-P ) :   0.8316 B(  0-Co,  4-P ) :
0.9264
B(  0-Co, 12-C ) :   0.5339 B(  0-Co, 23-C ) :   0.3136 B(  0-Co, 32-C ) :
0.2891
B(  0-Co, 33-C ) :   0.5690 B(  0-Co, 46-C ) :   0.2671 B(  1-Co,  2-P ) :
0.7786
B(  1-Co,  3-P ) :   0.8022 B(  1-Co,  5-P ) :   0.9388 B(  1-Co, 14-C ) :
0.5107
B(  1-Co, 17-C ) :   0.5599 B(  1-Co, 65-C ) :   0.3280 B(  1-Co, 86-C ) :
0.2867
B(  1-Co, 91-C ) :   0.3317 B(  2-P ,  3-P ) :   0.1114 B(  2-P ,  6-Cl) :
0.9421
B(  2-P ,  7-Cl) :   0.9390 B(  3-P ,  4-P ) :   0.1330 B(  3-P ,  5-P ) :
0.1431
B(  3-P ,  8-Cl) :   0.7962 B(  4-P ,  5-P ) :   0.9542 B(  4-P , 11-Cl) :
0.9298
B(  4-P , 32-C ) :  -0.1421 B(  4-P , 33-C ) :   0.1118 B(  5-P ,  9-Cl) :
1.0152
B(  5-P , 10-Cl) :   0.9731 B( 12-C , 13-H ) :   0.9846 B( 12-C , 23-C ) :
1.0559


********************************** NBO 6.0 *********************************

    (Occupancy)   Bond orbital / Coefficients / Hybrids
 ------------------ Lewis ------------------------------------------------------
110. (1.92869) LP ( 1) P  4            s( 75.49%)p 0.32( 24.46%)d 0.00(  0.05%)
111. (1.92349) LP ( 1) P  5            s( 70.86%)p 0.41( 29.02%)d 0.00(  0.11%)
140. (1.89113) BD ( 1) P  5- P  6
               ( 42.39%)   0.6511* P  5 s( 10.49%)p 8.42( 88.29%)d 0.11(  1.21%)
               ( 57.61%)   0.7590* P  6 s(  5.79%)p16.12( 93.35%)d 0.15(  0.85%)
```

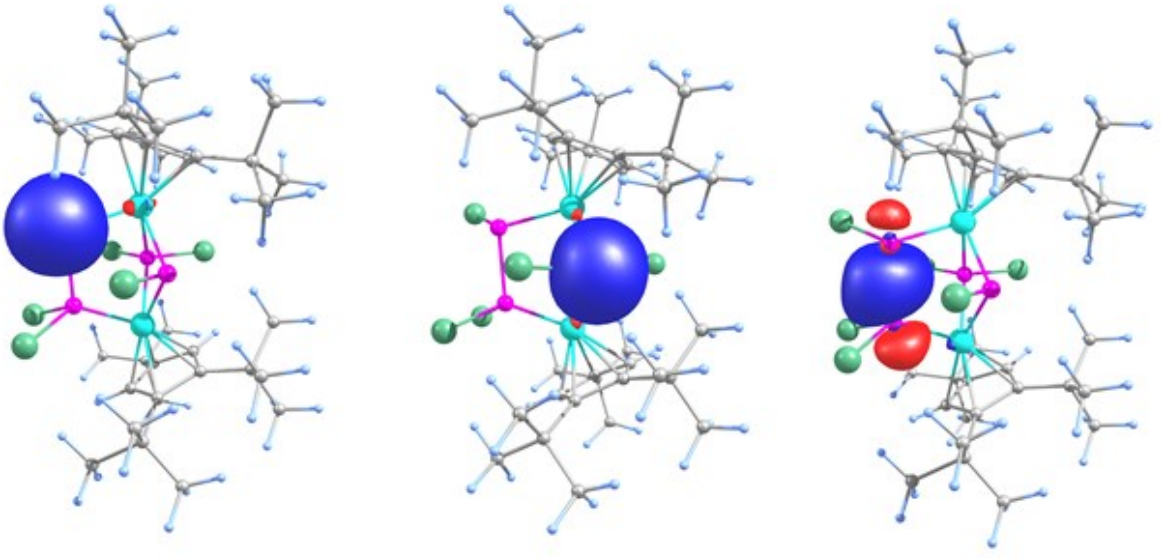

**Figure S 42** Natural bond orbitals representing the phosphorus lone pairs and P-P bond (NBOs 110, 111 and 140).

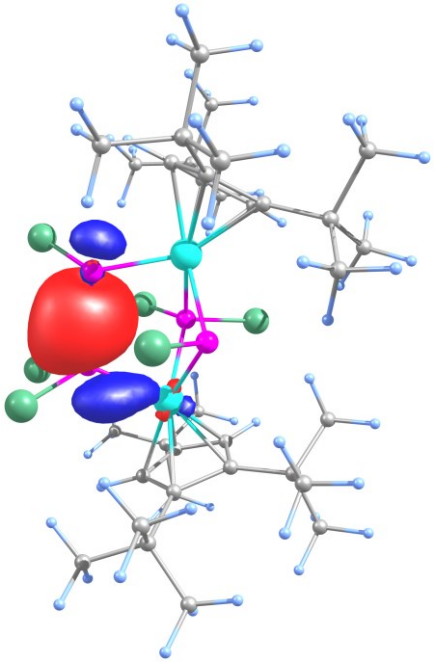

**Figure S 43** Intrinsic bond orbital representing the P-P bond (IBO 133: 5P - 0.577600 and 4P - 0.393823).

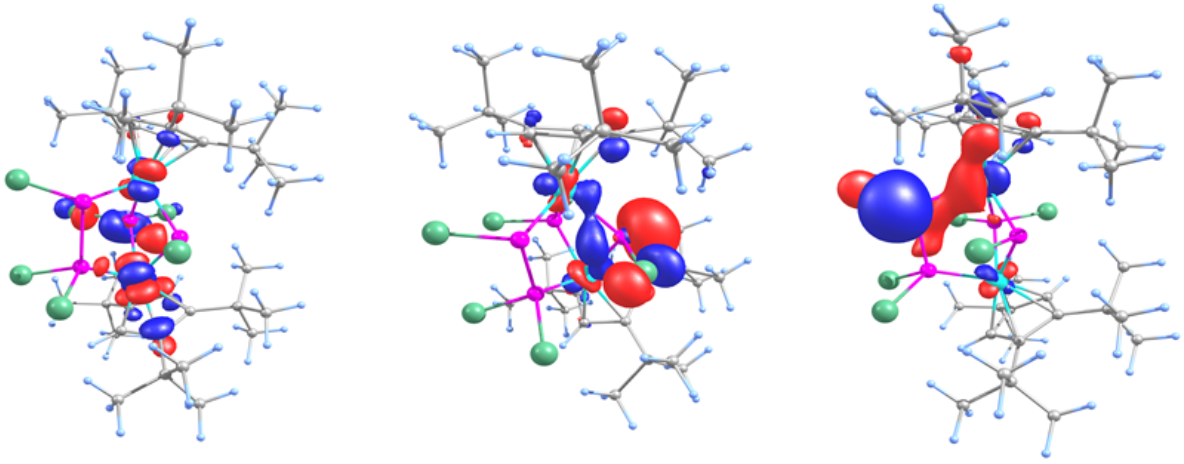

**Figure S 44** Frontier molecular orbitals in **7** (Left: LUMO (−2.7827 eV); Middle: HOMO (−5.0862 eV) and Right HOMO-1 (−5.4577 eV).

Cartesian coordinates od the optimizes geometry of [(Cp'''Co)$_2$(μ-PF$_2$)(μ,η$^2$:η$^1$:η$^1$-P$_3$F$_2$)] (**12**) at the D4-TPSSh(CPCM)/def2-TZVP level of theory.

| Atom | x | y | z |
|---|---|---|---|
| Co | 0.114242000 | 5.355016000 | 4.312474000 |
| Co | 1.656231000 | 4.744719000 | 7.386407000 |
| P | 1.661563000 | 4.344206000 | 5.290408000 |
| P | 0.501726000 | 6.454239000 | 6.274204000 |
| P | -1.373596000 | 5.308881000 | 5.990622000 |
| P | -0.301082000 | 4.046804000 | 7.298820000 |
| F | 1.806817000 | 2.763368000 | 4.918789000 |
| F | 3.115931000 | 4.683558000 | 4.663805000 |
| F | -0.594058000 | 2.492601000 | 7.022687000 |
| F | -1.112387000 | 4.067785000 | 8.684369000 |
| C | -0.785632000 | 4.477437000 | 2.667481000 |
| C | 3.680911000 | 4.775276000 | 7.768525000 |
| H | 4.444605000 | 4.801209000 | 7.011003000 |
| C | 3.086639000 | 5.934566000 | 8.367688000 |
| C | 0.544820000 | 4.878546000 | 2.389160000 |
| H | 1.335241000 | 4.209999000 | 2.094228000 |
| C | 0.698253000 | 6.303907000 | 2.543547000 |
| C | -0.594978000 | 6.807987000 | 2.969151000 |
| C | 2.111652000 | 5.450336000 | 9.333706000 |
| C | -1.467169000 | 5.674064000 | 3.026695000 |
| H | -2.504795000 | 5.717080000 | 3.314466000 |
| C | 3.122024000 | 3.588354000 | 8.311365000 |
| C | 3.588738000 | 2.166086000 | 8.106107000 |
| C | 2.149985000 | 4.021917000 | 9.253570000 |
| H | 1.525974000 | 3.361758000 | 9.833518000 |
| C | -1.408884000 | 3.117525000 | 2.457390000 |
| C | 3.685189000 | 7.308054000 | 8.058416000 |
| C | 4.523448000 | 2.066707000 | 6.896832000 |
| H | 4.019214000 | 2.375294000 | 5.980207000 |

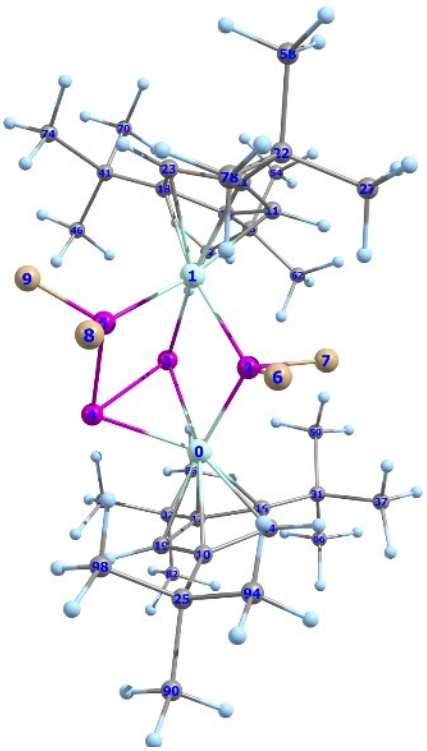

| | | | |
|---|---|---|---|
| H | 4.856316000 | 1.032822000 | 6.773265000 |
| H | 5.411098000 | 2.689913000 | 7.033287000 |
| C | 1.978369000 | 7.000949000 | 2.076065000 |
| C | -1.174606000 | 8.203920000 | 3.202270000 |
| C | -2.310540000 | 8.143252000 | 4.240723000 |
| H | -2.719403000 | 9.147955000 | 4.374647000 |
| H | -1.935383000 | 7.799865000 | 5.208495000 |
| H | -3.130237000 | 7.492543000 | 3.934630000 |
| C | 2.940361000 | 5.971444000 | 1.454844000 |
| H | 3.833992000 | 6.495762000 | 1.106881000 |
| H | 2.490130000 | 5.464883000 | 0.597189000 |
| H | 3.252930000 | 5.222212000 | 2.183950000 |
| C | 1.285781000 | 6.157237000 | 10.411236000 |
| C | 2.771424000 | 8.522922000 | 8.250356000 |
| H | 2.458543000 | 8.670950000 | 9.280866000 |
| H | 1.883692000 | 8.443960000 | 7.620059000 |
| H | 3.325163000 | 9.415183000 | 7.945943000 |
| C | 0.191449000 | 7.071847000 | 9.841551000 |
| H | -0.324735000 | 7.574654000 | 10.665174000 |
| H | -0.540740000 | 6.480856000 | 9.289219000 |
| H | 0.582685000 | 7.830020000 | 9.169464000 |
| C | 2.756485000 | 7.692132000 | 3.203116000 |
| H | 3.171326000 | 6.938260000 | 3.869298000 |
| H | 2.140848000 | 8.363205000 | 3.794643000 |
| H | 3.584985000 | 8.265432000 | 2.775990000 |
| C | 4.932933000 | 7.457019000 | 8.956899000 |
| H | 5.432157000 | 8.404260000 | 8.734418000 |
| H | 5.638682000 | 6.643058000 | 8.773163000 |
| H | 4.670289000 | 7.448240000 | 10.015808000 |
| C | 4.365634000 | 1.770992000 | 9.379691000 |
| H | 5.203591000 | 2.451233000 | 9.552603000 |
| H | 4.759906000 | 0.756050000 | 9.276539000 |
| H | 3.711942000 | 1.799770000 | 10.255282000 |
| C | 4.139112000 | 7.357348000 | 6.590462000 |
| H | 3.287760000 | 7.199997000 | 5.928298000 |
| H | 4.902885000 | 6.614855000 | 6.357580000 |
| H | 4.561503000 | 8.342910000 | 6.379701000 |
| C | 1.632934000 | 7.997214000 | 0.952750000 |
| H | 2.558555000 | 8.391548000 | 0.524198000 |
| H | 1.044745000 | 8.841185000 | 1.306772000 |
| H | 1.072071000 | 7.499270000 | 0.157397000 |
| C | 2.225975000 | 6.935786000 | 11.351982000 |
| H | 2.753994000 | 7.745631000 | 10.854579000 |
| H | 2.968895000 | 6.261022000 | 11.786024000 |
| H | 1.637623000 | 7.366731000 | 12.167014000 |
| C | 0.583670000 | 5.121170000 | 11.308198000 |
| H | 0.021982000 | 5.656949000 | 12.077613000 |
| H | 1.307750000 | 4.473638000 | 11.809681000 |
| H | -0.117760000 | 4.501122000 | 10.750473000 |
| C | 2.404195000 | 1.207750000 | 7.930490000 |
| H | 1.716525000 | 1.268429000 | 8.777831000 |
| H | 2.772832000 | 0.179915000 | 7.867539000 |
| H | 1.850019000 | 1.436640000 | 7.020930000 |
| C | -1.790483000 | 8.679885000 | 1.869432000 |
| H | -2.560584000 | 7.978949000 | 1.536894000 |
| H | -1.041123000 | 8.760958000 | 1.081524000 |
| H | -2.255487000 | 9.660662000 | 2.005820000 |
| C | -0.187006000 | 9.246086000 | 3.734560000 |

```
H       -0.733200000     10.169235000      3.946540000
H        0.603424000      9.488865000      3.028360000
H        0.266428000      8.896789000      4.665344000
C       -2.307023000      3.226318000      1.207727000
H       -2.766000000      2.258133000      0.988092000
H       -1.722003000      3.538339000      0.338429000
H       -3.104767000      3.957060000      1.363737000
C       -0.334715000      2.053817000      2.211707000
H        0.338369000      1.972967000      3.066897000
H        0.258395000      2.284002000      1.322617000
H       -0.812244000      1.083242000      2.052762000
C       -2.259796000      2.706053000      3.665285000
H       -1.627472000      2.567730000      4.544026000
H       -2.779196000      1.766747000      3.453612000
H       -3.010172000      3.464472000      3.901317000

-------------------------   ----------------
Dispersion correction           -0.236145457
FINAL SINGLE POINT ENERGY     -5862.411580281280
-------------------------   --------------------


  Mayer bond orders larger than 0.100000
B(  0-Co,  1-Co) :   0.1012 B(  0-Co,  2-P ) :   1.0008 B(  0-Co,  3-P ) :
0.6002
B(  0-Co,  4-P ) :   0.7173 B(  0-Co, 10-C ) :   0.3335 B(  0-Co, 14-C ) :
0.5600
B(  0-Co, 16-C ) :   0.3167 B(  0-Co, 17-C ) :   0.3472 B(  0-Co, 19-C ) :
0.5143
B(  1-Co,  2-P ) :   0.9188 B(  1-Co,  3-P ) :   0.7816 B(  1-Co,  5-P ) :
1.0318
B(  1-Co, 11-C ) :   0.4166 B(  1-Co, 13-C ) :   0.3483 B(  1-Co, 18-C ) :
0.3437
B(  1-Co, 21-C ) :   0.3575 B(  1-Co, 23-C ) :   0.5168 B(  2-P ,  3-P ) :
0.1739
B(  2-P ,  5-P ) :   0.1186 B(  2-P ,  6-F ) :   0.8817 B(  2-P ,  7-F ) :
0.8923
B(  3-P ,  4-P ) :   0.9995 B(  3-P ,  5-P ) :   0.1895 B(  4-P ,  5-P ) :
1.1232
B(  4-P , 19-C ) :   0.2013 B(  5-P ,  8-F ) :   0.9768 B(  5-P ,  9-F ) :
0.9588


********************************** NBO 6.0 **********************************

    (Occupancy)   Bond orbital / Coefficients / Hybrids
 ------------------ Lewis ------------------------------------------------------

 83. (1.95592) LP ( 1) P  4           s( 74.24%)p 0.35( 25.70%)d 0.00(  0.06%)
 84. (1.94337) LP ( 1) P  5           s( 68.47%)p 0.46( 31.38%)d 0.00(  0.15%)
109. (1.91366) BD ( 1) P  4- P  5
               ( 47.25%)   0.6874* P  4 s(  8.87%)p10.14( 89.98%)d 0.13(  1.14%)
               ( 52.75%)   0.7263* P  5 s( 11.87%)p 7.28( 86.43%)d 0.14(  1.68%)
110. (1.97132) BD ( 1) P  5- P  6
               ( 46.83%)   0.6843* P  5 s( 11.00%)p 7.94( 87.35%)d 0.15(  1.61%)
               ( 53.17%)   0.7292* P  6 s( 36.00%)p 1.74( 62.63%)d 0.04(  1.35%)
```

## References


[1] Compound **1**) C. Graβl, M. Bodensteiner, M. Zabel, M. Scheer, *Chem. Sci.* **2015**, *6*, 1379-1382; Compound **2**) F. Dielmann, M. Sierka, A. V. Virovets, M. Scheer, *Angew. Chem. Int. Ed.* **2010**, *49*, 6860-6864.

[2] M Piesch, C. Graβl, M. Scheer, *Angew. Chem. Int. Ed*. **2020**, *59*, 7154-7160.

[3] CrysAlisPro Software System, Rigaku Oxford Diffraction (**2018-2020**).

[4] O. V. Dolomanov, L. J. Bourhis, R. J. Gildea, J. A. K. Howard, H. Puschmann, *J. Appl. Cryst*. **2009**, 42, 339–341.

[5] G. M. Sheldrick, *Acta Cryst.* **2015**, A71, 3-8.

[6] G. M. Sheldrick, *Acta Cryst.* **2015**, *C71*, 3-8.

[7] a) ORCA - *An Ab Initio, DFT and Semiempirical electronic structure package*, Version 4.2.1; b) F. Neese, *WIREs Comput Mol Sci.*, **2012**, *2*, 73–78; b) F. Neese, *WIREs Comput Mol Sci.*, **2017**, *8*, e1327.

[8] J. Tao, J. P. Perdew, V. N. Staroverov, G. E. Scuseria, *Phys. Rev. Lett.* **2003**, *91*, 146401; V. N. Staroverov, G. E. Scuseria, J. Tao, J. P. Perdew, *J. Chem. Phys.* **2003**, *119*, 12129-12137; Erratum: *J. Chem. Phys.* **2004**, *121*, 11507-11507.

[9] a) F. Weigend and R. Ahlrichs, *Phys. Chem. Chem. Phys.,* **2005**, *7*, 3297–3305; b) F. Weigend, M. Häser, H. Patzelt and R. Ahlrichs, *Chem. Phys. Lett.,* **1998**, *294*, 143–152.

[10] a) E. Caldeweyher, S. Ehlert, A. Hansen, H. Neugebauer, S. Spicher, C. Bannwarth, S. Grimme, *J. Chem. Phys.* **2019**, *150*, 154122; b) E. Caldeweyher, C. Bannwarth, S. Grimme, J. Chem. Phys. **2017**, *147*, 034112.

[11] J. Tomasi, B. Mennucci, R. Cammi, *Chem. Rev.* **2005**, *105*, 2999-3094.

[12] F. Neese, F. Wennmohs, A. Hansen and U. Becker, *Chem. Phys.,* 2009, **356**, 98–109.

[13] NBO 6.0. E. D. Glendening, J. K. Badenhoop, A. E. Reed, J. E. Carpenter, J. A. Bohmann, C. M. Morales, C. R. Landis, F. Weinhold (Theoretical Chemistry Institute, University of Wisconsin, Madison, WI, 2013); http://nbo6.chem.wisc.edu/

[14] T. Lu, Q. Chen, *Chemistry–Methods* **2021**, *1*, 231-239.

[15] a) C. F.-W. LU Tian, *Acta Phys. -Chim. Sin.* **2011**, *27*, 2786-2792; b) A. Savin, O. Jepsen, J. Flad, O. K. Andersen, H. Preuss, H. G. von Schnering, *Angew. Chem. Int. Ed. Engl.* **1992**, *31*, 187-188; c) A. D. Becke, K. E. Edgecombe, *J. Chem. Phys.* **1990**, *92*, 5397-5403.

[16] H. Jacobsen, *Can. J. Chem.* **2008**, *86*, 695-702.

[17] T. Lu, F. Chen, *J. Comput. Chem.* **2012**, *33*, 580-592.

## 6. Halogenation of heterobimetallic triple-decker complexes containing $P_5$ and $As_5$ middle deck

### Authors

Anna Garbagnati, Michael Seidl, Martin Piesch, Gábor Balázs, Manfred Scheer.

### Author contribution

A. Garbagnati prepared the manuscript and performed the synthesis and characterization of the herein presented compounds. M. Seidl did the refinement of all the solid-state structures. M. Piesch performed the synthesis of the starting materials, G. Balázs performed all DFT calculations, contributed to the corresponding parts in the manuscript and the Supporting Information and revised the manuscript. M. Scheer supervised the research and revised the manuscript.

### Acknowledgement

This work was comprehensively supported by Deutsche Forschungsgemeinschaft (DFG) within the project Sche384/36-2.

6. Halogenation of heterobimetallic triple-decker complexes containing $P_5$ and $As_5$ middle deck

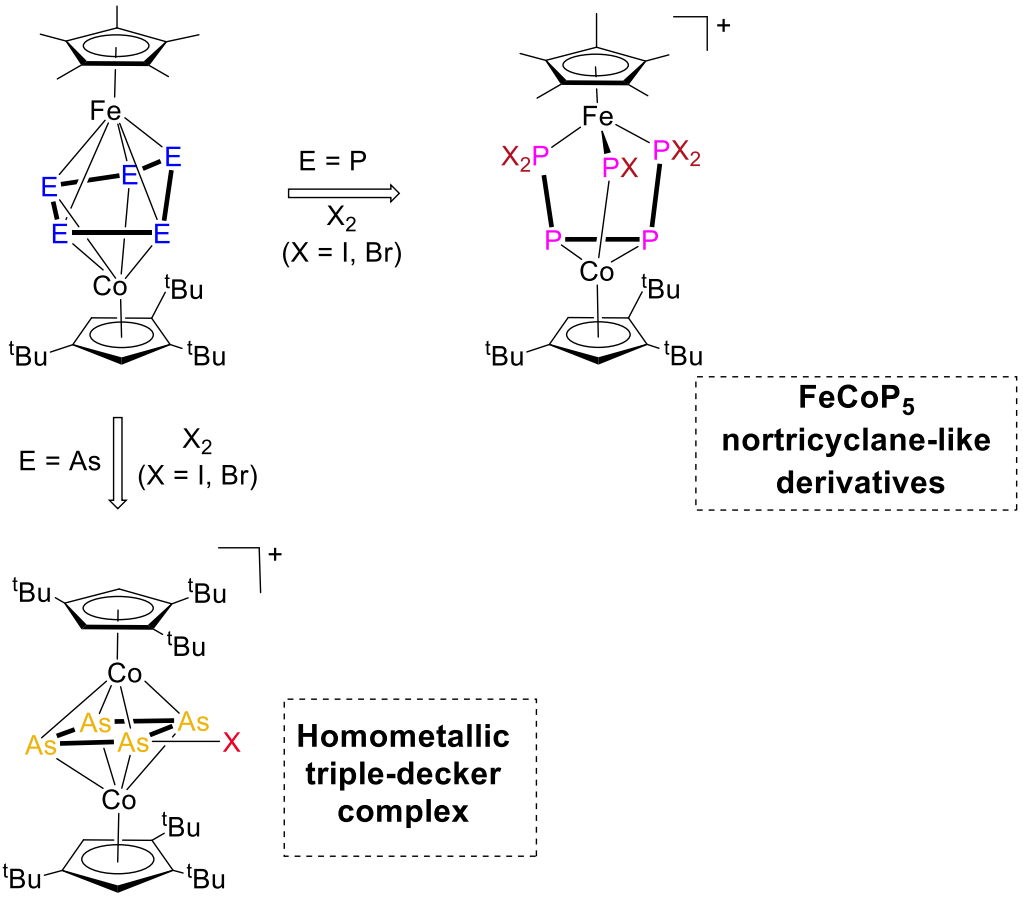

# 6 Halogenation of heterobimetallic triple-decker complexes containing $P_5$ and $As_5$ middle deck

***Abstract:*** *The halogenation of the heterobimetallic triple-decker complexes [(Cp*Fe)(Cp'''Co)(μ,η⁵:η⁴-E₅)] (E = P (**1**), As (**6**), Cp* = η⁵-C₅Me₅, Cp''' = 1,2,4-tri(tert-butyl)cyclopentadienyl) was investigated. Compound **1** has been oxidised to the isostructural ionic compounds [(Cp*Fe)(Cp'''Co)(μ-PX)(μ,η²:η¹:η¹-P₄X₄)][Y] (X = I, Y = [I₃] (**2**), X = Br, Y = [FeBr₄] (**3**)) and to the neutral species [(Cp*Fe)(Cp'''Co)(μ-PCl₂)(μ,η²:η¹:η¹-P₄Cl₄)] (**4**) and [(Cp*Fe)(Cp'''Co)(μ-PCl₂)₂(μ,η¹:η¹-P₂Cl₃)] (**5**). Compounds **2**, **3** and **4** possess a heterobimetallic nortricyclane-like $FeCoP_5$ core. The oxidation of the heavier homologue **6** with bromine and iodine afforded the homometallic complexes [(Cp'''Co)₂(μ,η⁴:η⁴-As₄X)][FeX₄] (X = I (**7**) and X = Br (**9**)). With iodine as halogenating agent, the trinuclear monocation bearing an $As_6$ prism as ligand [(Cp*Fe)(Cp'''Co)₂(μ₃,η⁴:η⁴:η⁴-As₆)][FeI₄] (**8**) was additionally isolated. When $PCl_5$ was used as oxidizing agent, the initially folded $As_5$ ligand planarised resulting in the dicationic species [(Cp*Fe)(Cp'''Co)(μ,η⁵:η⁵-As₅)][FeCl₄]₂ (**10**).*

## 6.1 Introduction

The direct conversion of white phosphorus by coordination to main group elements is an active research area. The final goal is to react the activated $P_4$-species with organic substrates to obtain widely used organophosphorus compounds, while avoiding the production of stoichiometric amounts of waste.[1] In order to serve this purpose, a deep understanding of the nature of the P-M bonds, and therefore of the reactivity of $P_4$ towards the metal centres, is required. One way to search for new insights into this topic is by studying the redox chemistry of polyphosphorus ($P_n$)-ligand complexes. Several investigations have been conducted in this field, showing that the oxidation of polyphosphorus compounds can lead to P-P bond formation,[2] dimerisation reactions[3,4] or rearrangement processes.[5] To expand these studies, investigations of the reactivity of these complexes towards halogens and halogen sources were carried out. Formally, in a broad sense, the halogenation process can be seen as an oxidation using harsher conditions, which is why it represents an additional tool for the synthesis of new polyphosphorus compounds. After the success achieved in the halogenation of free[6,7] (including theoretical investigations[8]) and coordinated[9,10] white phosphorus, our group focused on investigating the halogenation of several $E_n$-ligand complexes (E = P, As). The halogenation of the tetrahedrane complex [{$CpMo(CO)_2$}₂(μ,η²:η²-$P_2$)], which is the isolobal analogue of $P_4$ (**A**, Scheme 1), showed that $I_2$, $Br_2$ and chlorine sources (*e.g.* $PCl_5$) are all

suitable oxidizing reagents for the synthesis of new derivatives bearing P-X and $PX_2$ ligands (X = I, Br, Cl).[11] The iodination of the *cyclo*-$P_5$ analogue of ferrocene and ruthenocene [Cp*M($\eta^5$-$E_5$)] (M = Fe, Ru; E = P, As) (**B**, Scheme 1) revealed that these sandwich complexes are suitable starting materials for the synthesis of a variety of complexes with new $E_nX_m$ ligands, exploiting the differences in the reactivity of P- and As-based *cyclo*-$E_5$ ligands.[12] The reaction of the *cyclo*-$P_5$ derivatives towards $I_2$ led to the formation of $[Cp^*M(P_6I_6)]^+$ (M = Fe, Ru), bearing the tripodal *cyclo*-$P_3(PI_2)_3$ ligand. In contrast, the iodination of the *cyclo*-$As_5$ analogues resulted in several different complexes containing $As_5$, $As_4I_4$ and $As_8I_6$ ligands.[12]

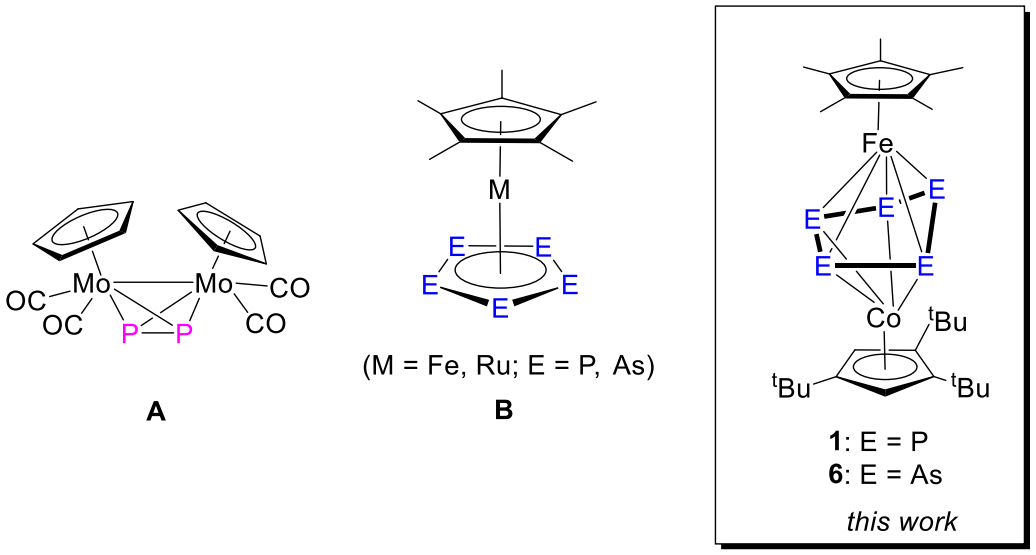


**Scheme 6.** Selected examples of $E_n$ complexes investigated in halogenation reactions.

The redox properties of the triple-decker complexes $[(Cp'''Co)_2(\mu,\eta^2:\eta^2\text{-}E_2)_2]$ (E = P, As)[13] and $[(Cp^*Mo)_2(\mu,\eta^6:\eta^6\text{-}P_6)]$[14] under classic oxidation conditions (*e.g.* with Ag[FAl], [FAl] = $[FAl\{OC_6F_{10}(C_6F_5)\}_3]$ as oxidizing agent) were previously investigated, showing diverse structural changes (*e.g.* rearrangement of the $E_n$ unit). Intrigued by these results, our group decided on extending the scope of these studies to heterobimetallic triple-decker complexes. Therefore, the redox behaviour of the compounds $[(Cp^*Fe)(Cp'''Co)(\mu,\eta^5:\eta^4\text{-}E_5)]$ (E = P (**1**),[15] As (**6**),[16] Cp* = $\eta^5$-$C_5Me_5$, Cp''' = 1,2,4-tri(*tert*-butyl)cyclopentadienyl) was investigated, showing that they can be reversibly oxidised twice and reduced once, with the reduction of **6** is accompanied by the fragmentation of the $As_5$ ligand.[17] Encouraged by this, we decided to compare the reactivity of this type of complexes, *i.e.* [(Cp*Fe)(Cp'''Co)(μ,$\eta^5$:$\eta^4$-$E_5$)] (E = P (**1**), As (**6**)), by means of halogenation reactions. In particular, we exploited the outcome of such reactions with the previously reported oxidations, emphasizing the occurring structural changes and the possible impact of the

involved pnictogen atom. Herein, we present the reactivity of **1** and **6** towards halogens and halogen sources and illustrate the different behaviours of **1** and **6**.

## 6.2 Results and discussions

The reaction of **1** with an excess (4 equiv.) of halogen ($I_2$, $Br_2$) leads to the isostructural compounds [(Cp*Fe)(Cp'''Co)($\mu$-PX)($\mu$,$\eta^2$:$\eta^1$:$\eta^1$-$P_4X_4$)][Y] (X = I, Y = [$I_3$] (**2**, 26%), X = Br, Y = [$FeBr_4$] (**3**, 24%) containing a dimetalla-nortricyclane-type core (Scheme 2).

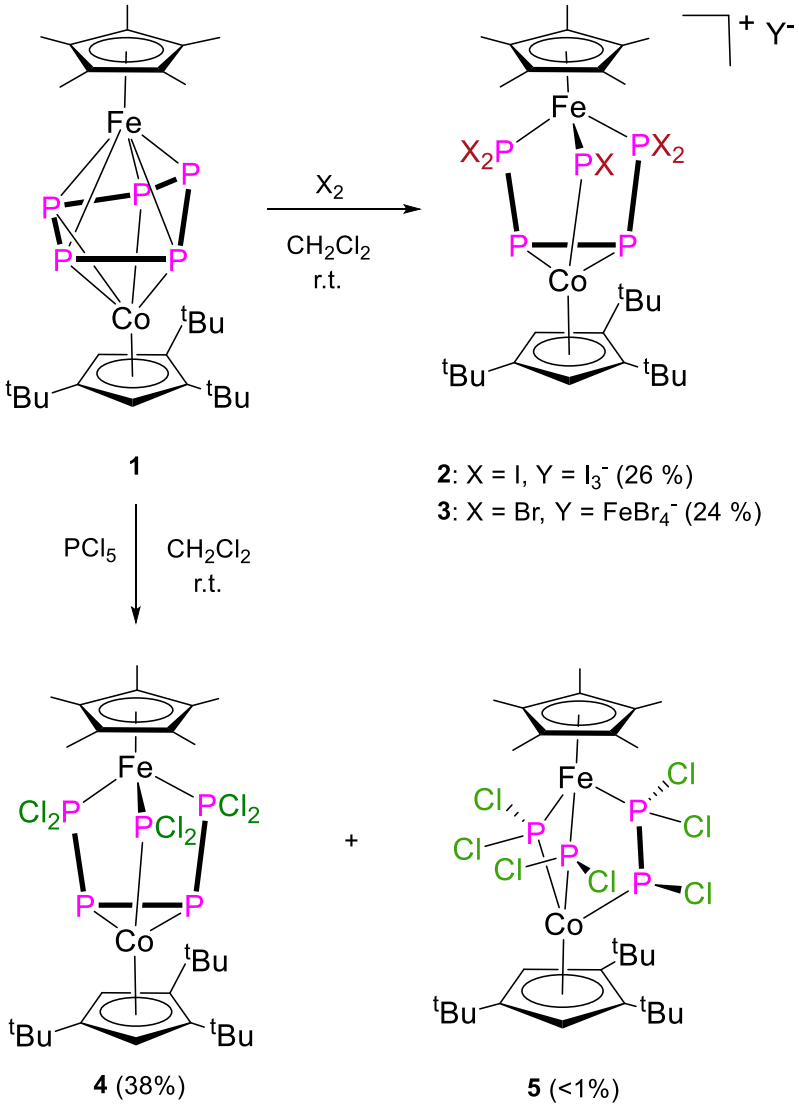


**Scheme 7.** Reaction of **1** with $X_2$ (X = I, Br) or $PCl_5$. Isolated yields are given in parenthesis.

When $PCl_5$ was used as halogen source (4 equiv.), the reaction afforded the neutral species [(Cp*Fe)(Cp'''Co)($\mu$-$PCl_2$)($\mu$,$\eta^2$:$\eta^1$:$\eta^1$-$P_4Cl_4$)] (**4**, 38%) as major product and a few crystals of the compound [(Cp*Fe)(Cp'''Co)($\mu$-$PCl_2$)$_2$($\mu$,$\eta^1$:$\eta^1$-$P_2Cl_3$)] (**5**) (Scheme 2). **4** represents the neutral analogue of **2** and **3**, in which the bridging PX unit (X = I, Br) is replaced by a $PCl_2$-bridging ligand. The presented formation of the neutral species **4** vs.

the ionic species *i.e.* the cations in **2** and **3** is probably due to the steric repulsion between the bulky Cp''' substituent and the large Br or I substituents on the bridging P atom. The formation of the anions $FeX_4^-$ (X = I, Br) and of **5** indicates a partial decomposition of **1** which explains the rather low yields. The molecular structure of **2**, **3** and **4** (Figure 1) each reveals a heterobimetallic dinuclear complex.

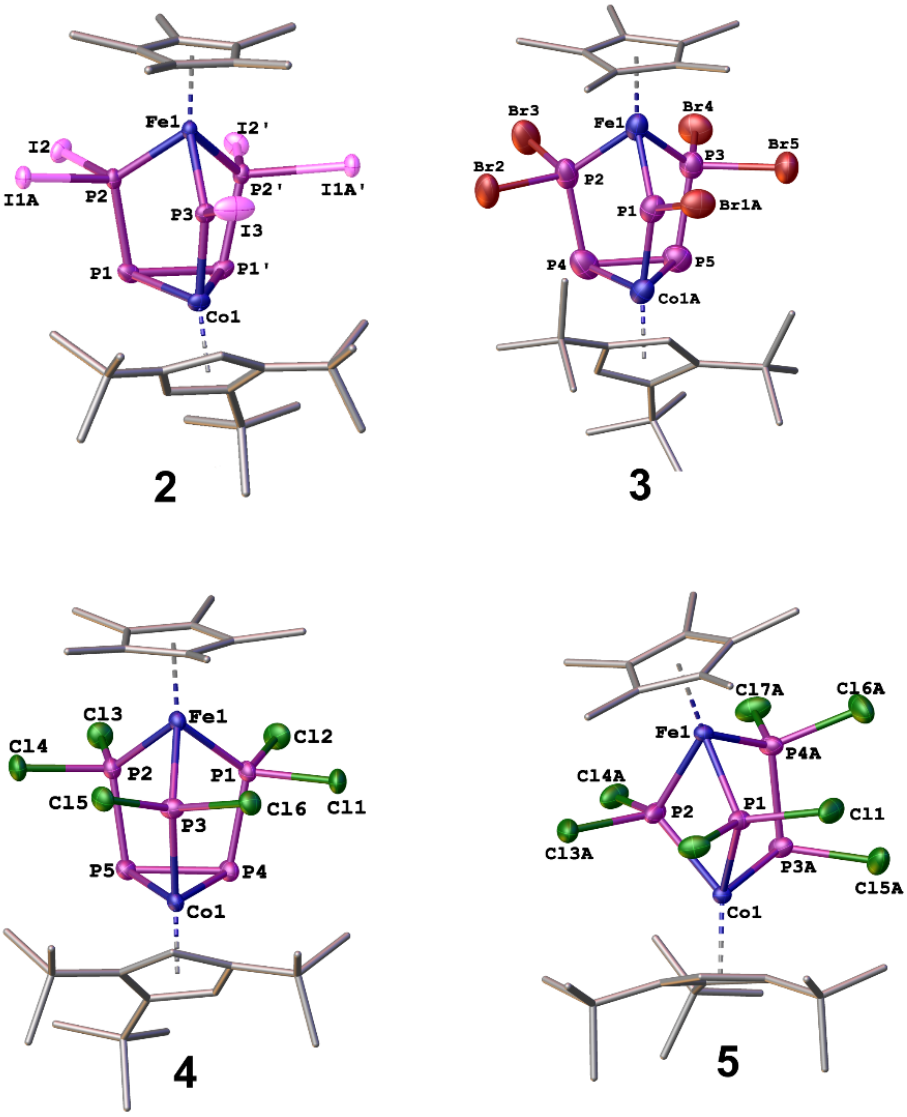


**Figure 4.** Molecular structure of **4** and **5** and of the cations in **2** and **3** with thermal ellipsoids at 50% probability level. In case of disorder, only major parts are depicted. Hydrogen atoms and the solvent molecules are omitted for clarity.

They all bear a $P_4X_4$ ligand (X = I, Br, Cl) coordinated in an $\eta^2$:$\eta^1$:$\eta^1$ fashion to the two {$Cp^RM$} fragments (R = $C_5Me_5$, M = Fe; R = $C_5H_2{}^tBu_3$, M = Co) and a bridging $PX_n$ ligand (n = 1, X = I, Br; n = 2, X = Cl) with the resulting $FeCoP_5$ core resembling the nortricyclane structure of $P_7^{3-}$.[18] A similar result was observed by the iodination of [Cp*M($\eta^5$-$P_5$)] (M =

Fe, Ru) with the formation of the monometallo-nortricyclane derivatives, bearing an $MP_6$ core.[12] For all the compounds, the P-P bond lengths of the basal triangle are in the range between a single and a double bond[19] (**2**: P1-P1' 2.161(3) Å, **3**: P4-P5 2.150(3) Å, **4**: P4-P5 2.168(14) Å). The other P-P distances are slightly longer and are all in the range of a normal single bond[19] (**2**: P1-P2 = P1'-P2' 2.209(18) Å, **3**: P2-P4 2.203(3) Å, P3-P5 2.206(2) Å, **4**: P1-P4 2.192(15), P2-P5 2.190(15) Å). These values are in line with the ones observed for the cations $[Cp^*M(P_6I_6)]^+$ (M = Fe, Ru)[12] and for the $P_7$ ligand in the compound $[P_7\{FeCp(CO)_2\}_3]$.[20] Compound **4** is extremely sensitive to moisture and air which might explain why it always co-crystallises with the oxidised compound $[(Cp^*Fe)(Cp'''Co)(\mu\text{-}PO)(\mu,\eta^2\text{:}\eta^1\text{:}\eta^1\text{-}P_4Cl_4)]$ (cf. SI).[21] The solid-state structure of **5** shows a dinuclear complex with two bridging $PCl_2$ units and a bridging $P_2Cl_3$ ligand coordinating in an $\eta^1\text{:}\eta^1$ fashion to the two metal centers. The P-P distance between the two $PCl_2$ units is too long to be considered as a bond (P1···P2: 2.529(14) Å). The rather unusual $P_2Cl_3$ ligand in an $\eta^1\text{:}\eta^1$ coordination mode was found in $[\{Cp^*Mo(CO)_3\}_2(\mu\text{-}P_2Cl_3)][AlCl_4]$.[22]

The $^1H$ NMR spectra of **2**, **4** and **5** ($CD_2Cl_2$) each show the expected signals for the Cp''' ligand and one singlet with the correct integral ratio for the Cp* ligand.[23] In the $^1H$ NMR spectrum of **3**, the signals are broadened due to the contact interaction shift of the paramagnetic anion $FeBr_4^-$ with the cation, as already observed by Baumann *et. al* for $[(Cp^RCo)_2(\mu\text{-}Cl)_3]_2[Co_2Cl_6]$ containing the paramagnetic anion $[Co_2Cl_6]^{2-}$.[24] The magnetic properties of the tetrahaloferrate(III) ions $FeX_4^-$ (X = Br, Cl) were elucidated and investigated in several publications proving their paramagnetic nature.[25,26,27]

The $^{31}P\{^1H\}$ NMR spectra of **2**, **3** and **4** are similar to each other and therefore will be discussed together. The $^{31}P\{^1H\}$ NMR spectra of **2** at room temperature shows five resonances with an integral ratio of 1:1:1:1:1, displaying an AMNPQ spin system, while for **4** a AMM'OO' spin system is detected (cf. Figure 2, and SI). For compound **3**, three broad resonances with basically no fine structure and a slightly sharper singlet at 710 ppm were observed. Due to the broadness of the signals and the poor solubility of **3** (hindering variable temperature NMR studies), the $^{31}P\{^1H\}$ NMR spectrum of **3** could not be simulated, and the assignment of the signals is based on the similarity to **2** and **4**. The resonance signal of the metal-bridging P atom ($P^A$) in **2** and **3** is considerably downfield-shifted compared to the P atoms of the $PX_2$ groups as well as in other compounds (cf. Table 1).[11,28] This downfield shift is in line with the phosphinidene-like nature of the PX unit (*vide infra*). In the $^{31}P\{^1H\}$ NMR spectrum of **3**, there is an additional singlet at 719.8 ppm (with an approximate ratio of 0.70:1 to the signal of the metal bridging P atom) which

can be attributed to the compound [(Cp*Fe)(Cp'''Co)(μ-PCl)(μ,η²:η¹:η¹-$P_4Br_4$)][$FeBr_4$] (**3-Cl**), resulted by the presence of one Cl atom, originating from the solvent used $CH_2Cl_2$ (cf. SI).

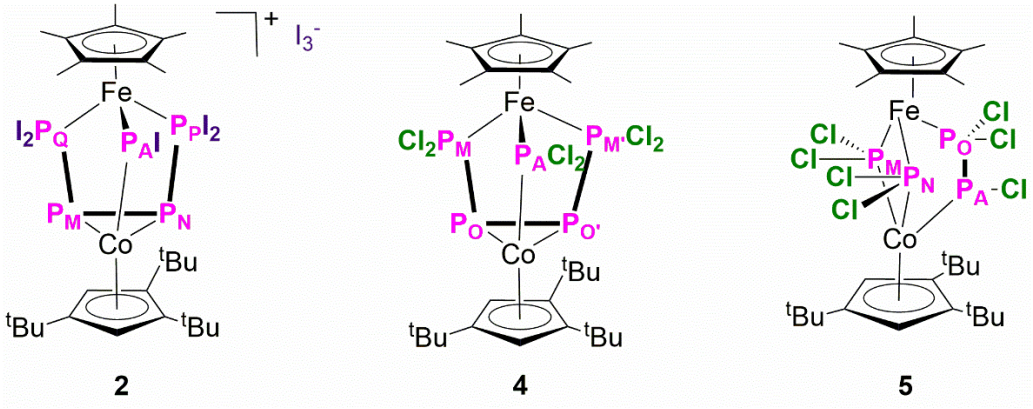


**Figure 5**. Compounds **2**, **4** and **5** with the P atoms labelled according to the corresponding spin systems in the NMR spectra.

**Table 2.** $^{31}P\{^1H\}$ NMR chemical shifts and coupling constants for **2**, **4** and **5** obtained from simulation.

| **2** | | | **4** | | | **5** | |
|---|---|---|---|---|---|---|---|
| **δ[ppm]** | | **J (Hz)** | **δ[ppm]** | | **J (Hz)** | **δ[ppm]** | **J (Hz)** |
| $P^A$ | 690.5 | $^1J_{NQ}$ 310<br>$^1J_{PQ}$ 125 | $P^A$ | 647.3 | $^1J_{M'O'}$ 260<br>$^1J_{OO'}$ 150 | $P^A$ 375.4 | $^1J_{AO}$ 327<br>$^2J_{AN}$ 151 |
| $P^M$ | 237.2 | $^1J_{MP}$ 294<br>$^2J_{AM}$ 10 | $P^M$ | 269.1 | $^2J_{AM}$ 30<br>$^2J_{AM'}$ 30 | $P^M$ 236.6 | $^2J_{AM}$ 91<br>$^2J_{MO}$ 20 |
| $P^N$ | 228.1 | $^2J_{AN}$ 10<br>$^2J_{AP}$ 65 | $P^{M'}$ | 269.1 | $^2J_{AO}$ 10<br>$^2J_{AO'}$ 25 | $P^N$ 224.8 | $^2J_{MN}$ 15 |
| $P^P$ | 116.7 | $^2J_{AQ}$ 35 | $P^O$ | 123.7 | $^2J_{MM'}$ 110<br>$^1J_{MO}$ 340 | $P^O$ 221.0 | $^2J_{NO}$ 30 |
| $P^Q$ | 104.0 | $^2J_{MN}$ 380<br>$^2J_{MQ}$ 15<br>$^2J_{NP}$ 10 | $P^{O'}$ | 123.7 | $^2J_{MO'}$ 50<br>$^2J_{M'O}$ 50 | | |

The $^{31}P\{^1H\}$ NMR spectrum of **5** ($CD_2Cl_2$) shows an AMNO spin system with four resonances in a 1:1:1:1 integral ratio, centred at δ = 375.4, 236.6, 224.8, 221.0 ppm (Table 1). The signals of the two P atoms connected by a single bond (P3A and P4A in Figure 1) resonate at δ = 375.4 ($P^A$) and at δ = 221.0 ppm ($P^O$) and show a $^1J_{P^AP^O}$ coupling of 327 Hz. The other two resonances belong to the bridging P atoms $P^M$ and $P^N$ (P2 and P1, respectively, considering the labelling in Figure 1). A rather large $J_{P^AP^N}$ coupling constant of 151 Hz was detected, which is probably due to through-space coupling of those nuclei (the lone pair of $P^A$ points towards $P^N$; P3A and P2, respectively, for labelling see Figure 1). The $^{31}P\{^1H\}$ NMR chemical shifts and coupling constants of compounds **2**, **4** and **5** were determined by iterative simulation of the experimental spectra.

In order to determine the electronic structures of **3**-**5**, DFT calculations were performed. The geometric parameters are well reproduced for all compounds. For **3**, the lowest unoccupied molecular orbital (LUMO) is mainly centred on the P atom of the PBr ligand (empty orbital of almost pure p(P) character with only small contributions from the metals and Br (Figure 3). This is characteristic of the phosphinidene-like nature of the PX unit and is in accordance with the downfield resonance detected in the $^{31}P\{^{1}H\}$ NMR spectrum (708.89 ppm). In comparison, for the phosphinidene complex $ClP\{W(CO)_5\}$, a $^{31}P$ chemical shift of 868 ppm was reported.[29] The electron-deficient nature of the PBr unit is also substantiated by the Loewdin atomic charge distribution, which shows a positive charge accumulation on the PBr ligand (0.75), while the $PBr_2$ units are less positively charged (0.36 and 0.42; cf. SI). The NBO analysis confirms the phosphinidene-like character of the P atom in the PBr ligand as well. A Natural Bond Orbital of pure p character, localised on that P atom and having a low population, was detected which basically corresponds to the LUMO orbital (cf. SI). Additionally, the P1 atom has an $sp^{1.3}$ hybridisation in the Co-P1 bond (labelling according to Figure 1), while the atoms P4 and P5 have an almost pure p orbital contribution (hybridisation $sp^{10.3}$) in the corresponding Co-P bonds. The hybridisation of the P atoms in all three Fe-P bonds is sp and they are all very similar. The Mayer bond order (BO) of the P4-P5 bond is slightly higher (1.05) compared to the BOs of the P2-P4 and P3-P5 bonds (0.94 and 0.97, respectively). While the Fe-P BOs are very similar and vary between 0.94 and 1.03, the BOs for the Co-P4 and Co-P5 bonds are considerably lower compared to the Co-P1 BO (*i.e.* 0.64, 0.66 vs. 1.10). The HOMO of **4**, which mainly represents the Co-P5/P5 bonding (labelling according to Figure 1), is similar to that of **3**, but the LUMO represents a complex combination of metal d orbitals and P-Cl antibonding combinations (cf. SI). In **5**, the BOs for all Fe-P bonds are similar (varying from 0.88 to 1.05), while the BO for the Co1-P3A bond is slightly lower compared to the other two bonds (0.75 and 0.85, 0.90, respectively). This is in line with the different natures of the corresponding Co-P bonds. According to the NBO analysis, the hybridisation of the P atoms in all three Fe-P bonds is roughly sp. The hybridisation of the P atoms in the Co-P bonds are different. While the P3A atom is $sp^6$-hybridised, the other two P atoms are roughly $sp^2$. The lone pair on P3A is of high s character ($sp^{0.45}$).

6. Halogenation of heterobimetallic triple-decker complexes containing $P_5$ and $As_5$ middle deck

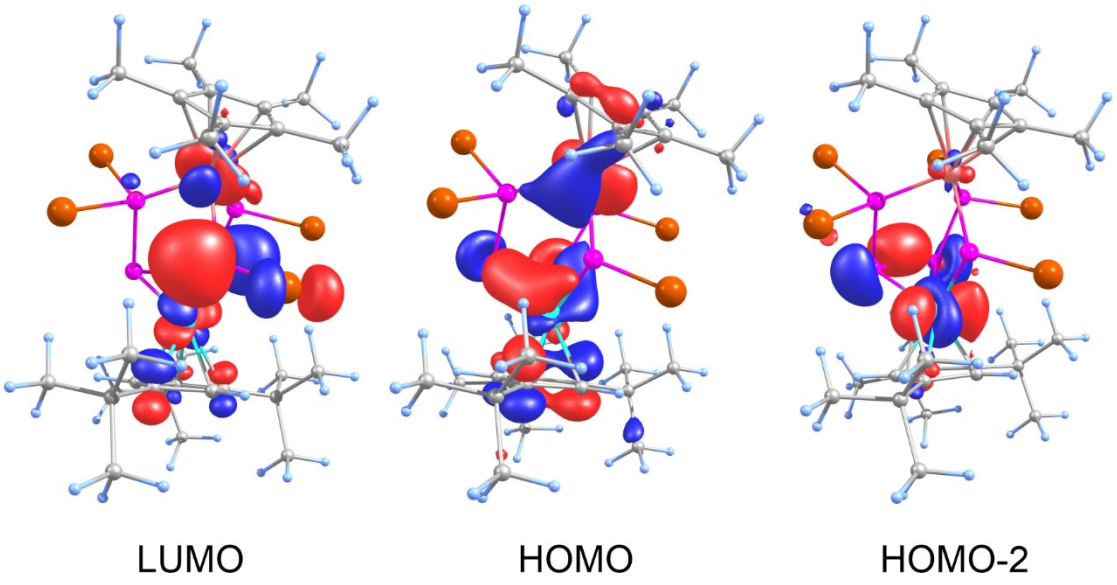


**Figure 6.** Selected molecular orbitals in **3**, calculated at the TPSSh/def2-TZVP level of theory.

After investigating the reactivity of the P-containing complex **1**, the question arose as to what would be the difference when the heavier homologue [(Cp*Fe)(Cp'''Co)($\mu$,$\eta^5$:$\eta^4$-$As_5$)] (**6**) was used instead. **1** and **6** show a similar behaviour towards classic oxidation, they both can be oxidised twice, with the initially folded *cyclo*-$E_5$ ligand that planarizes, in a way that strongly depends on the oxidation state. While the oxidation of **1** and **6** leads to isostructural compounds, independent of the pnictogen atom, this is not the case for the reduction. Two isostructural monoanions are initially formed, but only the phosphorus analogue is stable, while the arsenic-containing species is fragmented into an $As_6$ and an $As_3$ ligand complex.[17] Hence, following the procedure applied in the synthesis of **2** and **3**, **6** was reacted with an excess (4 equiv.) of halogen ($I_2$, $Br_2$), affording, as the only isolable compounds, the isostructural complexes [(Cp'''Co)$_2$($\mu$,$\eta^4$:$\eta^4$-$As_4X$)][$FeX_4$] (X = I, **7**; X = Br, **9**) and [(Cp*Fe)(Cp'''Co)$_2$($\mu_3$,$\eta^4$:$\eta^4$:$\eta^4$-$As_6$)][$FeI_4$] (**8**) in very low yields (Scheme 3). These results are in stark contrast to the reactivity of **1** towards halogens.

## 6. Halogenation of heterobimetallic triple-decker complexes containing $P_5$ and $As_5$ middle deck

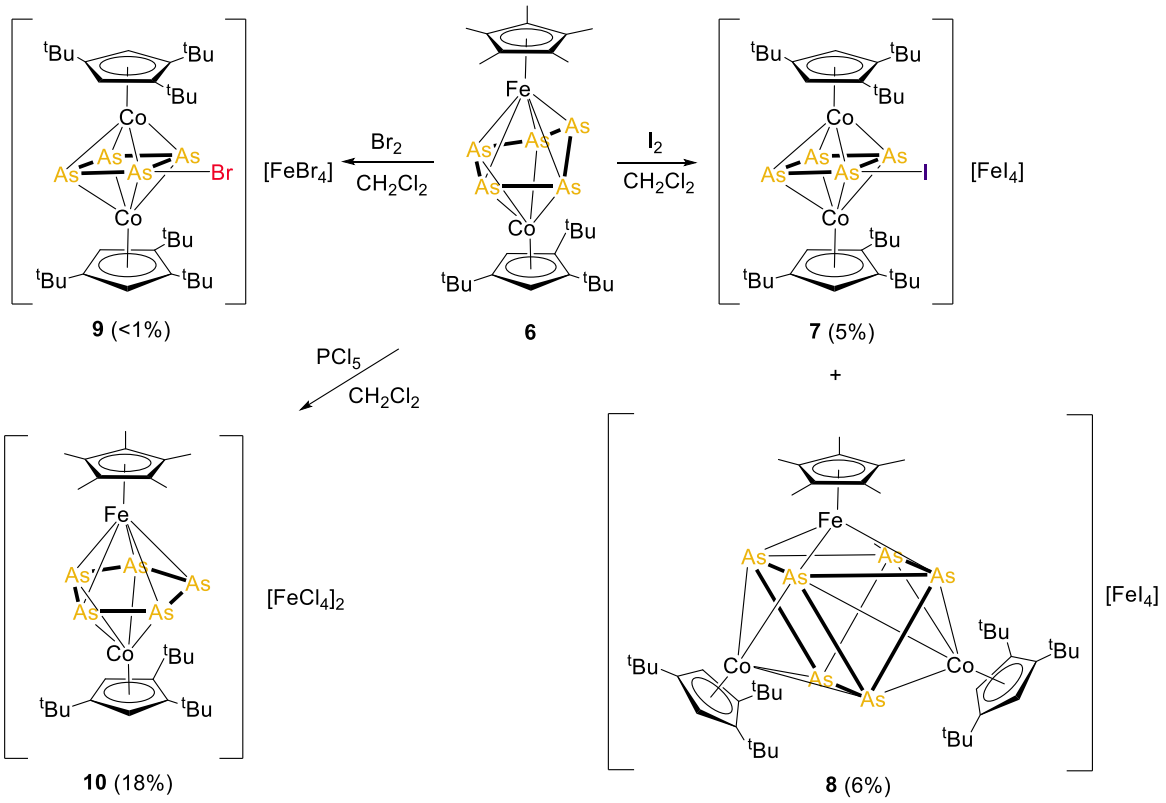


**Scheme 8.** Reaction of **6** with $X_2$ (X = I, Br) or $PCl_5$. Isolated yields are given in parenthesis.

The formation of a homometallic compound with a *cyclo*-$As_4$ ligand, *i.e.* **7** and **9**, indicates that the oxidation with $I_2$ and $Br_2$ leads to the partial degradation of the starting material. In the case of iodine, before the precipitate obtained by the removal of the solvent *in vacuo* is dissolved in $CH_2Cl_2$ to isolate **7**, the additional extraction with toluene allows the isolation of crystals of $[(Cp^*Fe)(Cp'''Co)_2(\mu_3,\eta^4{:}\eta^4{:}\eta^4\text{-}As_6)][FeI_4]$ (**8**), bearing a prismatic $As_6$-ligand which is the result of fragmentation and re-aggregation processes. When **6** is reacted with an excess of $PCl_5$ (4 equiv.), crystals of $[(Cp^*Fe)(Cp'''Co)(\mu,\eta^5{:}\eta^5\text{-}As_5)][FeCl_4]_2$ (**10**, Scheme 3) were isolated. The dication of **10** is identical with the one afforded *via* the two-electron oxidation of **6**,[17] with the previously folded *cyclo*-$As_5$ ligand being planar now (*vide infra* for comparison of structural parameters). The solid-state structures of **7** and **9** (Figure 4) reveal bimetallic triple-decker sandwich complexes, with the monocation bearing a planar cyclic $As_4X$ unit (X = I, Br) as a ligand coordinating in an $\eta^4{:}\eta^4$ fashion to two {Cp'''Co} fragments. The $As_4$ unit has a trapezoidal shape (Figure 4) with the sum of the internal angles being close to 360° for both compounds.

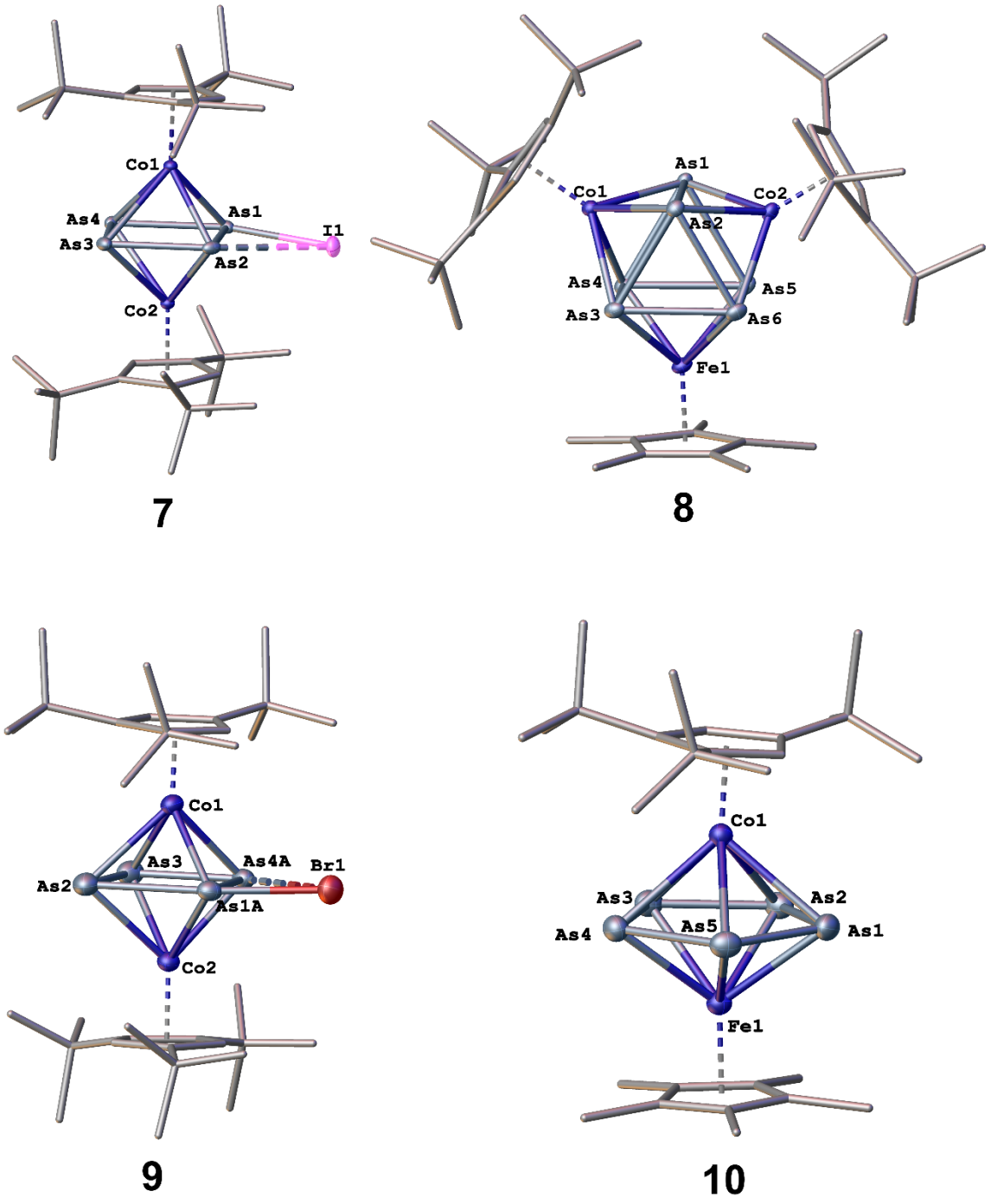


**Figure 7.** Molecular structures of the cations of **7**, **8**, **9** and **10** with thermal ellipsoids at 50% probability level. In case of disorder, only the mayor parts are depicted. Hydrogen atoms and the anions are omitted for clarity.

One of the As-As bond is shortened (As3-As4: 2.315(17) Å in **7**, As2-As3: 2.329(11) Å in **9**), two are in the range of a normal As-As single bond[19] and one is elongated (As1-As4: 2.707(18) Å in **7**, As1A-As2: 2.764(4) Å in **9**) but still representing a bond. The same is true for the As-X bonds which are longer compared to ordinary As-X single bonds (As1-I1: 2.794(4) Å in **7**, As1A-Br1: 2.520(4) Å in **9**; lit.: As-I: 2.54 Å, As-Br: 2.35 Å).[19] The solid-state structure of **8** shows a heterotrimetallic complex with an $As_6$ prism, with two of the

quadrangular faces being capped by a {Cp'''Co} fragment and one by a {Cp*Fe} fragment (Figure 4). The structure of the cation resembles the one of the neutral homometallic species $[(Cp^{BIG}Fe)_3(\mu_3,\eta^4:\eta^4:\eta^4\text{-}As_6)]$ ($Cp^{BIG}$ = $C_5(4\text{-}n\text{Bu}C_6H_4)_5$) with very similar As-As bond lengths and distances.[30]

The As-As bond lengths in the triangular faces are shorter (As-$As_{av}$: 2.56 Å) while the distances between the triangles are longer (As-$As_{av}$: 2.79 Å, with the longest being: As1···As2: 2.843 Å) and in both cases larger than the sum of their covalent radii (2.42 Å)[19] but still below the sum of their van der Waals radii ($\sum_{vdW}$ = 3.76 Å).[31] A heterometallic complex related to **8** comprising a prismatically shaped $As_6$ ligand *i.e.* $[(Cp^*Fe)_2(Cp^RCo)(\mu_3,\eta^2:\eta^2:\eta^2\text{-}As_3)_2]$ (R = Cp*,[32] Cp'''[16]) has already been reported. The $As_6$ core of this compound is better described as being formed by two $As_3$ subunits connected to each other *via* two shorter and one longer As-As contacts (As-As: 2.935(12) Å) that are too long to be considered as a bond. The structure of **10** in the solid state is depicted in Figure 4 and reveals a triple-decker complex with a planar *cyclo*-$As_5$ ligand as middle deck. An analogous dication with very similar bond lengths (As-$As_{av}$: 2.34 Å) was obtained by the two-electron oxidation of **6** with Ag[FAl].[17] The As-As distances of the $As_5$ ligand in **10** are in the range of 2.349(11) Å and 2.359(11) Å and therefore in between single and double bonds.[19] For all these compounds (**7**-**10**), the anion is always $FeX_4^-$ in a tetrahedral configuration (X = I, Br, Cl). Since there are several examples known of solid-state structures of salts of this species, the crystal structure of this anion will not be further discussed.

The $^1$H NMR spectra of the isostructural compounds **7** and **9** ($CD_2Cl_2$) each show the characteristic three singlets for the two magnetically equivalent Cp''' ligands (integral ratio: 2:18:9). For the trimetallic compound **8**, the $^1$H NMR spectrum in $CD_2Cl_2$ shows four singlets (integral ratio: 4:18:36:15) for the two magnetically equivalent Cp''' ligands (the first three values) and for the Cp* ligand, respectively. The main difference between the $^1$H NMR spectra of **7**, **8** and **9** is that the signals of the latter are significantly broadened which, as previously mentioned for **3**, might be explained by the contact interaction shift with the paramagnetic counterion $FeX_4^-$ (X = Br, Cl, *vide supra*).[25-27] Similarly, the same contact interaction shift-induced broadening of the signals is observed in the $^1$H NMR spectrum of **10** ($CD_2Cl_2$) where the dication is associated with two molecules of $FeCl_4^-$ as counterions. The resulting signals in the $^1$H NMR spectrum are too broad to allow for interpretation and overlap. In contrast, a $^1$H NMR spectrum with sharper signals was observed for an analogous cation, but this difference could be explained by the fact that its corresponding anion was the diamagnetic $[FAl\{OC_6F_{10}(C_6F_5)\}_3]^-$.[17] Despite there

having been reported some examples of salts of $FeI_4^-$ being antiferromagnetic,[33,34] in the case of **7** and **8**, the anion does not seem to affect the $^1H$ NMR spectrum of the cation.

## 6.3 Conclusions

The reactivity of the heterobimetallic triple-decker complexes **1** and **6** towards halogens and halogen sources was investigated. It was shown that the outcome of the reaction differs depending on the pnictogen atom of the used starting complex, in contrast to what was observed for the one- or two-electron oxidation when using classic oxidizing reagents. The *cyclo*-$P_5$ ligand of **1** undergoes fragmentation and rearrangements which resulted, with all of the halogenating reagents, in the dimetalla-nortricyclane-like derivatives **2**, **3** and **4** characterised by an $FeCoP_5$ core. With $I_2$ or $Br_2$, the resulting compounds **2** and **3** are ionic bearing a bridging PX ligand (X = I, Br), while, when the chlorine is the used halogen, the isolated complex **4** is neutral, the PX unit is replaced by a $PCl_2$ unit and an additional heterobimetallic compound (**5**) with four chlorinated P atoms is accessible, as the result of the partial conversion of **1**. For the arsenic homologue **6**, the obtained products differ depending on the halogen used. With $I_2$ and $Br_2$, a fragmentation of the $As_5$ ligand afforded the two analogous homometallic complexes **7** and **9** showing cyclo-$As_4X$ units (X = I, Br) as middle decks. With $I_2$, the additional complex **8** bearing the prismatically shaped $As_6$ ligand was isolated. By chlorination, the middle deck was planarised, resulting in compound **10** whose cationic part, formed by a triple-decker complex bearing a planar *cyclo*-$As_5$ ligand as middle-deck, identical to that of one of the products obtained by the two-electron oxidation of **6**. The one- or two-electron oxidation of **1** and **6** leads only to changes in the geometry resulting in compounds that can be isolated in high yields. In contrast, the harsher conditions related to the oxidation of **1** and **6** by halogens lead not only to changes in the geometry but more often to the fragmentation of the $E_5$ middle-deck (E = P, As), resulting in the isolation of compounds with a halogenated $E_nX_m$ ligand in lower yields that might be useful for the further functionalisation of the pnictogen atom. It may thus be concluded that the halogenation of the heterobimetallic triple-decker complexes **1** and **6** is a complementary tool to the “classic” one- or two-electron oxidation for the synthesis of a large variety of new $E_n$-ligand complexes.

## 6.4 References

[1] C. M. Hoidn, D. J. Scott, R. Wolf, Chem. Eur. J. 27 (2021) 1886-1902.
[2] M. Piesch, C. Graβl, M. Scheer, Angew. Chem. Int. Ed. 59 (2020) 7154-7160.
[3] L. Dütsch, M. Fleischmann, S. Welsch, G. Balázs, M. Scheer, Angew. Chem. Int. Ed. 57 (2018) 3256-3261.
[4] M. V. Butovskiy, G. Balázs, M. Bodensteiner, E. V. Peresypkina, A. V. Virovets, J. Sutter, M. Scheer, Angew. Chem. Int. Ed. 52 (2013) 2972 –2976.

[5] M. Piesch, Reactivity of En ligand complexes - Synthesis, redox chemistry and subsequent reactions. PhD thesis. University of Regensburg. 2021
[6] B.W. Tattershall, N.L. Kendall, Polyhedron, 13 (1994) 1517-1521.
[7] M. Bispinghoff, Z. Benkő, H. Grützmacher, F. Delgado Calvo, M. Caporali, M. Peruzzini, Dalton Trans. 48 (2019) 3593-3600.
[8] C. Mealli, A. Ienco, M. Peruzzini, G. Manca, Dalton Trans. 47 (2018) 394 - 408.
[9] I. Krossing, J. Chem. Soc. Dalton Trans. (2002) 505-512.
[10] P. Barbaro, C. Bazzicalupi, M. Peruzzini, S. Seniori Costantini, P. Stoppioni, Angew. Chem. Int. Ed 51 (2012) 8628-8631.
[11] A. Garbagnati, M. Seidl, G. Balázs, M. Scheer, Inorg. Chem. 60 (2021) 5163-5171.
[12] H. Brake, E. Peresypkina, A. V. Virovets, M. Piesch, W. Kremer, L. Zimmermann, Ch. Klimas, M. Scheer, Angew. Chem. Int. Ed. 59 (2020) 16241-16246.
[13] M. Piesch, Ch. Graßl, M. Scheer, Angew. Chem. Int. Ed. 59 (2020) 7154-7160.
[14] M. Fleischmann, F. Dielmann, G. Balázs, M. Scheer, Chem. Eur. J. 22 (2016) 15248-15251.
[15] M. Piesch, F. Dielmann, S. Reichl, M. Scheer, Chem. Eur. J. 26 (2020) 1518-1524.
[16] M. Piesch, M. Scheer, Organometallics 39 (2020) 4247-4252.
[17] M. Piesch, S. Reichl, C. Riesinger, M. Seidl, G. Balázs, M. Scheer, Chem. Eur. J. 27 (2021) 9129-9140.
[18] W. Dahlmann, H. G. Von Schnering, Z. Naturwissensch. 59 (1972) 420.
[19] P. Pykkö, M. Atsumi, Chem. Eur. J. 15 (2009) 12770-12779.
[20] R. Ahlrichs, D. Fenske, K. Fromm, H. Krautscheid, U. Krautscheid, O. Treutler, Chem. Eur. J. (1996) 238-244.
[21] The identity of [(Cp*Fe)(Cp'''Co)(*μ*-PO)(*μ*,*η*2:*η*1:*η*1-P4Cl4)] is based on the X-ray diffraction data obtained from single crystals of **4**, which show an approximate ratio of 59:41, respectively (c.f. SI). All attempts to isolate and fully characterize [(Cp*Fe)(Cp'''Co)(*μ*-PO)(*μ*,*η*2:*η*1:*η*1-P4Cl4)] failed.
[22] R. A. Rajagopalan, A. Jayaraman, B. T. Sterenberg, J. Organomet. Chem.761 (2014) 84-92.
[23] In the1H NMR spectra of **2** and **4**, two signals in an integral ratio 9:18 for the *t*Bu groups of the Cp''' ligand are detected, while for **5**, three signals in a 9:9:9 ratio are detected for the Cp''' ligand, indicating that the three *t*Bu groups are not equivalent.
[24] F. Baumann, E. Dormann, Y. Ehleiter, W. Kaim, J. Karcher, M. Kelemen, R. Krammer, D. Saurenz, D. Stalke, C. Wachter, G. Wolmershäuser, H. Sitzmann, J. Organometal. Chem. 587 (1999) 267-277.
[25] O. Roubeau, M. Evangelistia, E. Natividad, Chem. Commun. 48 (2012) 7604-7606.
[26] M. Döbbelin, V. Jovanovski, I. Llarena, L. J. Claros Marfil, G. Cabañero, J. Rodriguez, D. Mecerreyes, Polym. Chem. 2 (2011) 1275-1278.
[27] M. Takenaka, T. Kawakami, A.Ito, K. Kinoshita, Y. Kitagawa, S. Yamanaka, K. Yamaguchi, M. Okumura, Polyhedron 30 (2011) 3284-3291.
[28] C. Riesinger, M. Seidl, G. Balázs, M. Scheer, Chem. Sci. 12 (2021) 13037-13048.
[29] U. Vogel, G. Stößer, M. Scheer, Angew. Chem. Int. Ed. 40 (2001) 1443-1445.
[30] S. Heinl, A. Y. Timoshkin, J. Müller, M. Scheer, Chemm. Commun. 54 (2018) 2244-2247.
[31] S. Alvarez, Dalton Trans. 42 (2013) 8617-8636.
[32] G. Friedrich, O. J. Scherer, G. Wolmershäuser Z. Anorg. Allg. Chem. 622 (1996) 1478-1486.
[33] J. M. Friedt, D. Petridis, J. P. Sanchez, Phys. Rev. B 19 (1979) 360-364.
[34] A. A. Pasynskii, I. L. Eremenko, E. E. Stomakhina, S. E. Nefedov, O. G. Ellert, J. Organomet. Chem. 406 (1990) 383-390.

## 6.5 Supporting information

### General procedure

All manipulations were carried out under an inert atmosphere of dried nitrogen using standard Schlenk and glove box techniques. Solvents were dried using a MB SPS-800 device of the company MBRAUN. Deuterated solvents were freshly distilled under nitrogen from $CaH_2$ ($CD_2Cl_2$) and from Na/K alloy ($C_6D_6$).

NMR spectra were recorded on a Bruker Avance III 400 MHz NMR spectrometer. If not differently mentioned, chemical shifts were measured at room temperature and given in ppm; they are referenced to TMS for $^1H$ and 85% $H_3PO_4$ for $^{31}P$ as external standard. LIFDI-MS spectra (LIFDI = liquid injection field desorption ionization) were measured on a JEOL AccuTOF GCX. ESI-MS spectra (ESI = Electrospray ionization) were measured on an Agilent Q-TOF 6540 UHD. Elemental Analysis (CHN) was determined using a Vario micro cube instrument.

Compounds [(Cp*Fe)(Cp'''Co)($\mu$,$\eta^5$:$\eta^4$-$E_5$)] (E = P (**1**), As (**6**)) were synthesized according to literature procedure[1].

Phosphorous (V) chloride ($PCl_5$) was purchased from ABCR, Phosphorous (V) bromide (95%) ($PBr_5$) from Alfa Aesar, Bromine ($Br_2$) from ACROS Organics, Iodine ($I_2$) from Sigma-Aldrich and they were all used as received without any further purifications.

### Synthesis of [(Cp*Fe)(Cp'''Co)($\mu$-PI)($\mu$,$\eta^2$:$\eta^1$:$\eta^1$-$P_4I_4$)][$I_3$] (2)

[(Cp*Fe)(Cp'''Co)($\mu$,$\eta^5$:$\eta^4$-$P_5$)] (50 mg, 0.078 mmol, 1 equiv.) is dissolved in 15 mL of $CH_2Cl_2$. To this solution, a solution of $I_2$ (80 mg, 0.315 mmol, 4 equiv.) in 15 mL of $CH_2Cl_2$ is added. A change in colour from wine red to green/brown is observed immediately. By the end of the addition, the solution appears completely brown. The solution is stirred for one hour and a half, then the solvent is removed *in vacuo*. The resulting brown precipitate is washed with 10 mL of pentane, 10 mL of toluene and then redissolved in 15 mL of $CH_2Cl_2$. The solution is layered with 30 mL of toluene and [(Cp*Fe)(Cp'''Co)($\mu$-PI)($\mu$,$\eta^2$:$\eta^1$:$\eta^1$-$P_4I_4$)][$I_3$] (**2**) crystallizes as black blocks within a few days.

Yield **2**: 35 mg (26%)

**$^1$H NMR (**400 MHz, $CD_2Cl_2$, 300K): δ [ppm] = 2.39 (s, 2H, $C_5H_2{}^tBu_3$), 1.75 (s, 15H, $C_5Me_5$), 1.61 (s, 9H, -($C_4H_9$)), 1.55 (s, 18H, -($C_4H_9$)$_2$).

**$^{31}$P{$^1$H} NMR** (162 MHz, $CD_2Cl_2$, 300K). AMNPQ spin system, δ [ppm] = 690.5 (m, 1P), 237.2 (m, 1P), 228.1 (m, 1P), 116.7 (m, 1P), 104.0 (m, 1P). For coupling constants see Table S1.

**ESI-MS** ($CH_2Cl_2$): cation mode: *m/z* = 1272.61 (100%, **M$^+$**); anion mode: *m/z* =380.72 (100%, [$I_3$]$^-$).

**EA** calculated for $[C_{27}H_{44}CoFeP_5I_5][I_3]$ (1653.52 g·mol$^{-1}$): C: 19.61, H: 2.68, found [%]: C: 19.42, H: 2.65.

**Synthesis of [(Cp*Fe)(Cp'''Co)(*μ*-PBr)(*μ*,*η*$^2$:*η*$^1$-P$_4$Br$_4$)][FeBr$_4$] (3)**

[(Cp*Fe)(Cp'''Co)(*μ*,*η*$^5$:*η*$^4$-P$_5$)] (100 mg. 0.156 mmol, 4 equiv.) is dissolved in 25 mL of $CH_2Cl_2$. To this solution, a solution of $Br_2$ in $CH_2Cl_2$ (dilution 1:100) (3.2 mL, 102 mg, 0.624 mmol, 4 equiv.) is added dropwise. The colour changes immediately to dark brown. The reaction mixture is stirred for three hours at room temperature and then the solvent is removed under reduced pressure. The resulting precipitate is washed with 10 mL of pentane, dissolved in 10 mL of $CH_2Cl_2$ and reprecipitated by the addition of cold pentane. The resulting precipitate is dissolved in 15 mL of $CH_2Cl_2$ and layered with 30 mL of pentane. [(Cp*Fe)(Cp'''Co)(*μ*-PBr)(*μ*,*η*$^2$:*η*$^1$-P$_4$Br$_4$)][FeBr$_4$] (**3**) crystallizes as red plates within one week.

Yield **3**:55 mg (25%)

**$^1$H NMR** (400 MHz, $CD_2Cl_2$, 300K): δ [ppm] = 3.46 (br. s, 2H, $C_5H_2{}^tBu_3$), 1.64 (br. s, 18H, -($C_4H_9$)$_2$), 1.53 (br. s, 15H, $C_5Me_5$), 0.83 (br. s, 9H, -($C_4H_9$)).

**$^{31}$P{$^1$H} NMR** (162 MHz, $CD_2Cl_2$, 300K). AMNN'Q spin system, δ [ppm] = 710 (m, 1P), 212 (m, 1P), 202 (m, 2P), 173 (m, 1P).

**TOF-ESI-MS** ($CH_2Cl_2$): cation mode: *m/z* =1036.80 (100%, **M$^+$**), 992.87 (17%, $[C_{27}H_{44}CoFeP_5Br_4Cl]^+$); anion mode: *m/z* = 375.61(100%, $[FeBr_4]^-$).

**EA** calculated for $[C_{27}H_{44}CoFeP_5Br_5][FeBr_4]\cdots(C_5H_{12})$ (1485.41 g·mol$^{-1}$): C: 25.87, H: 3.80, found[%]: C: 25.31, H: 3.27.

**Synthesis of [(Cp*Fe)(Cp'''Co)(*μ*-PCl$_2$)(*μ*,*η*$^2$:*η*$^1$-P$_4$Cl$_4$)] (4)**

[(Cp*Fe)(Cp'''Co)(*μ*,*η*$^5$:*η*$^4$-P$_5$)] (50 mg, 0.078 mmol, 1 equiv.) is dissolved in 15 mL of $CH_2Cl_2$. To this solution, a solution of $PCl_5$ (67 mg, 0.315 mmol, 4 equiv.) in 20 mL of $CH_2Cl_2$ is added. The colour changed from wine red to dark red/ brown within a few minutes. The solution is stirred for two hours and a half and afterwards the solvent is removed *in vacuo*. The precipitate is washed with 10 mL of pentane, dissolved in 15 mL of toluene and layered with 30 mL of pentane. Red crystals of [(Cp*Fe)(Cp'''Co)(*μ*-PCl$_2$)(*μ*,*η*$^2$:*η*$^1$-P$_4$Cl$_4$)] (**4**) formed after a couple of weeks. Compound **4** is extremely sensitive to moisture and air which might explain why it always co-crystallizes with the oxidized compound [(Cp*Fe)(Cp'''Co)(μ-PO)(μ,*η*$^2$:*η*$^1$-P$_4$Cl$_4$)] (vide infra and crystallographic details)."

Yield **4**: 38% (calculated via $^{31}$P NMR).

**$^1$H NMR** (400 MHz, $CD_2Cl_2$, 300K): δ [ppm] = 5.00 (s, 2H, $C_5H_2{}^tBu_3$), 1.67 (s, 15H, $C_5Me_5$), 1.35 (s, 18H, -$(C_4H_9)_2$), 1.31 (s, 9H, -$(C_4H_9)$).

**$^{31}$P{$^1$H} NMR** (162 MHz, $CD_2Cl_2$, 300K). AMM'OO' spin system, δ [ppm] = 647.3 (m, 1P), 269.1 (m, 2P), 123.7 (m, 2P). For coupling constants see Table S2.

**ESI-MS** ($CH_2Cl_2$): cation mode: *m/z* = 795.95 (100%, **M$^+$O**-$Cl_2$).

Due to the high air instability of compound **4**, it was not possible to obtain a correct elemental analysis.

**Synthesis of [(Cp*Fe)(Cp'''Co)($\mu$-$PCl_2$)$_2$($\mu$,$\eta^1$:$\eta^1$-$P_2Cl_3$)] (5)**

[(Cp*Fe)(Cp'''Co)($\mu$,$\eta^5$:$\eta^4$-$P_5$)] (50 mg, 0.078 mmol, 1 equiv.) is dissolved in 15 mL of $CH_2Cl_2$. To this solution, a solution of $PCl_5$ (67 mg, 0.315 mmol, 4 equiv.) in 20 mL of $CH_2Cl_2$ is added. The colour changed from wine red to dark red/brown within a few minutes. The solution is stirred for two hours and a half and afterwards the solvent is removed *in vacuo*. Compound [(Cp*Fe)(Cp'''Co)($\mu$-$PCl_2$)$_2$($\mu$,$\eta^1$:$\eta^1$-$P_2Cl_3$)] (**5**) is extracted with pentane (10 mL) and recrystallized by slow evaporation.

Yield **5**: a few crystals.

**$^1$H NMR** (400 MHz, $CD_2Cl_2$, 300K): δ [ppm] = 4.70 (s, 4H, $C_5H_2{}^tBu_3$), 1.70 (s, 36H, -$(C_4H_9)_2$), 1.55 (s, 15H, $C_5Me_5$), 1.54 (s, 18H, -$(C_4H_9)_2$).

**$^{31}$P{$^1$H} NMR** (162 MHz, $CD_2Cl_2$, 300K). AMNO spin system, δ [ppm] = 375.4 (m, 1P), 236.6 (m, 1P), 224.8 (m, 1P), 221.0 (m, 1P). For coupling constants see Table S3.

**ESI-MS** ($CH_2Cl_2$): cation mode: *m/z* = 854.89 (2%, **M$^+$**), 818.92 (1%, **M$^+$**-Cl).

**EA** Due to the very low yield of compound **5**, it was not possible to perform the Elemental Analysis.

**Synthesis of [(Cp'''Co)$_2$($\mu$,$\eta^4$:$\eta^4$-$As_4I$)][$FeI_4$] (7)**

[(Cp*Fe)(Cp'''Co)($\mu$,$\eta^5$:$\eta^4$-$As_5$)] (100 mg, 117 mmol, 1 equiv.) is dissolved in 15 mL of $CH_2Cl_2$. To this solution, a solution of $I_2$ (119 mg, 0.467 mmol, 4 equiv.) is added. The colour of the reaction mixture changed from green to dark brown. The solution is stirred for one hour and a half, then the solvent is removed under reduced pressure. The resulting precipitate is washed with 10 mL of hexane, 10 mL of toluene and the remaining powder is redissolved in 15 mL of $CH_2Cl_2$. The latter solution is layered with 30 mL of hexane and crystals of [(Cp'''Co)$_2$($\mu$,$\eta^4$:$\eta^4$-$As_4I$)][$FeI_4$] (**7**) are formed within one week.

Yield **7**: 10 mg (5%)

**$^1$H NMR** (400 MHz, $CD_2Cl_2$, 300K): δ [ppm] = 4.71 (s, 2H, $C_5H_2{}^tBu_3$), 1.84 (s, 18H, -$(C_4H_9)_2$), 1.73 (s, 9H, -$(C_4H_9)$).

**ESI-MS** ($CH_2Cl_2$): cation mode: *m/z* = 1010.91 (100%, **M$^+$**); anion mode: *m/z* = 563.55 (100%, $[FeI_4]^-$).

Due to the high air instability of compound **7**, it was not possible to obtain a correct elemental analysis.

**Synthesis of [(Cp*Fe)(Cp'''Co)$_2$($\mu_3$,$\eta^4$:$\eta^4$-As$_6$)] (8)**

[(Cp*Fe)(Cp'''Co)($\mu$,$\eta^5$:$\eta^4$-As$_5$)] (100 mg, 117 mmol, 1 equiv.) is dissolved in 15 mL of $CH_2Cl_2$. To this solution, a solution of $I_2$ (119 mg, 0.467 mmol, 4 equiv.) is added. The colour of the reaction mixture changed from green to dark brown. The solution is stirred for one hour and a half, then the solvent is removed under reduced pressure. The resulting precipitate is washed with 10 mL of hexane, then [(Cp*Fe)(Cp'''Co)$_2$($\mu_3$,$\eta^4$:$\eta^4$:$\eta^4$-As$_6$)][FeI$_4$](**8**) is extracted with toluene. The layering of the toluene solution (15 mL) with 30 mL of hexane, afforded black needle-crystals, suited for X-ray structure analysis.

Yield **8**: 6 mg (6%)

**$^1$H NMR** (400 MHz, $CD_2Cl_2$, 300K): δ [ppm] = 3.68 (s, 4H, $C_5H_2{}^tBu_3$), 1.71 (s, 18 H, -($C_4H_9$)), 1.52 (s, 36H, -($C_4H_9$)$_2$), 1.33 (s, 15H, $C_5Me_5$).

**ESI-MS** ($CH_2Cl_2$): cation mode: *m/z* = 1224. 90 (17%, **M$^+$**); anion mode: *m/z* = 563.55 (1%, [FeI$_4$]$^-$), 126.91 (54%, I$^-$).

Due to the high air instability of compound **8**, it was not possible to obtain a correct elemental analysis.

**Synthesis of [(Cp'''Co)$_2$($\mu$,$\eta^4$:$\eta^4$-As$_4$Br)][FeBr$_4$] (9)**

[(Cp*Fe)(Cp'''Co)($\mu$,$\eta^5$:$\eta^4$-As$_5$)] (100 mg, 117 mmol, 1 equiv.) is dissolved in 15 mL of $CH_2Cl_2$. To this solution, a solution of $Br_2$ in $CH_2Cl_2$ (dilution 1:100) (2.4 mL, 75 mg, 0.467 mmol, 4 equiv.) is added dropwise. The colour of the reaction mixture turned immediately dark brown then it is stirred for two hours and a half, then the solvent is removed *in vacuo*. The residue is washed with 10 mL of hexane, 10 mL of toluene and then redissolved in 15 mL of $CH_2Cl_2$ and layered with 30 mL of hexane. Crystals of [(Cp'''Co)$_2$($\mu$,$\eta^4$:$\eta^4$-As$_4$Br)][FeBr$_4$] (**9**) formed within one week.

Yield **9**: a few crystals.

**$^1$H NMR** (400 MHz, $CD_2Cl_2$, 300K): δ [ppm] =4.78 (br. s, $\omega_{1/2}$ = 155Hz, 2H, $C_5H_2{}^tBu_3$), 1.80 (br. s, $\omega_{1/2}$ = 44 Hz, 18 H, -($C_4H_9$)$_2$), 1.56 (br. s, $\omega_{1/2}$ = 35 Hz, 9H, -($C_4H_9$)).

**ESI-MS** ($CH_2Cl_2$): cation mode: *m/z* = 809.09 (43%, **M$^+$**-AsBr); anion mode: *m/z* = 375.61(100%, [FeBr$_4$]$^-$).

Due to the very low yield of compound **9**, it was not possible to perform the Elemental Analysis.

**Synthesis of [(Cp*Fe)(Cp'''Co)($\mu$,$\eta^5$:$\eta^5$-$As_5$)][$FeCl_4$]$_2$ (10)**

[(Cp*Fe)(Cp'''Co)($\mu$,$\eta^5$:$\eta^4$-$As_5$)] (100 mg, 117 mmol, 1 equiv.) is dissolved in 15 mL of $CH_2Cl_2$. To this solution, a solution $PCl_5$ (98 mg, 0.467 mmol, 4 equiv.) is added leading to an immediate colour change from green to dark brown. The solution is stirred for three hours and after that, the solvent is removed *in vacuo*. The precipitate is washed with 10 mL of hexane, 10 mL of toluene and redissolved in 15 mL of $CH_2Cl_2$. The layering of the latter with 30 mL of hexane afforded black crystals of [(Cp*Fe)(Cp'''Co)($\mu$,$\eta^5$:$\eta^5$-$As_5$)][$FeCl_4$]$_2$ (**10**).

Yield **10**: 13 mg (18%)

**$^1$H NMR** (400 MHz, $CD_2Cl_2$, 300K): δ [ppm] = 1.58 (br. s, $\omega_{1/2}$ = 64 Hz). Due to the broadening of the signal and additionally to the poor solubility of compound **10**, a proper attribution could not be performed.

**ESI-MS** ($CH_2Cl_2$): cation mode: *m/z* = 857.82 (26%, **M$^+$**); anion mode: *m/z* = 197.81 (100%, [$FeCl_4$]$^-$).

Due to the high air instability of compound **10**, it was not possible to obtain a correct elemental analysis.

## Selected NMR spectra

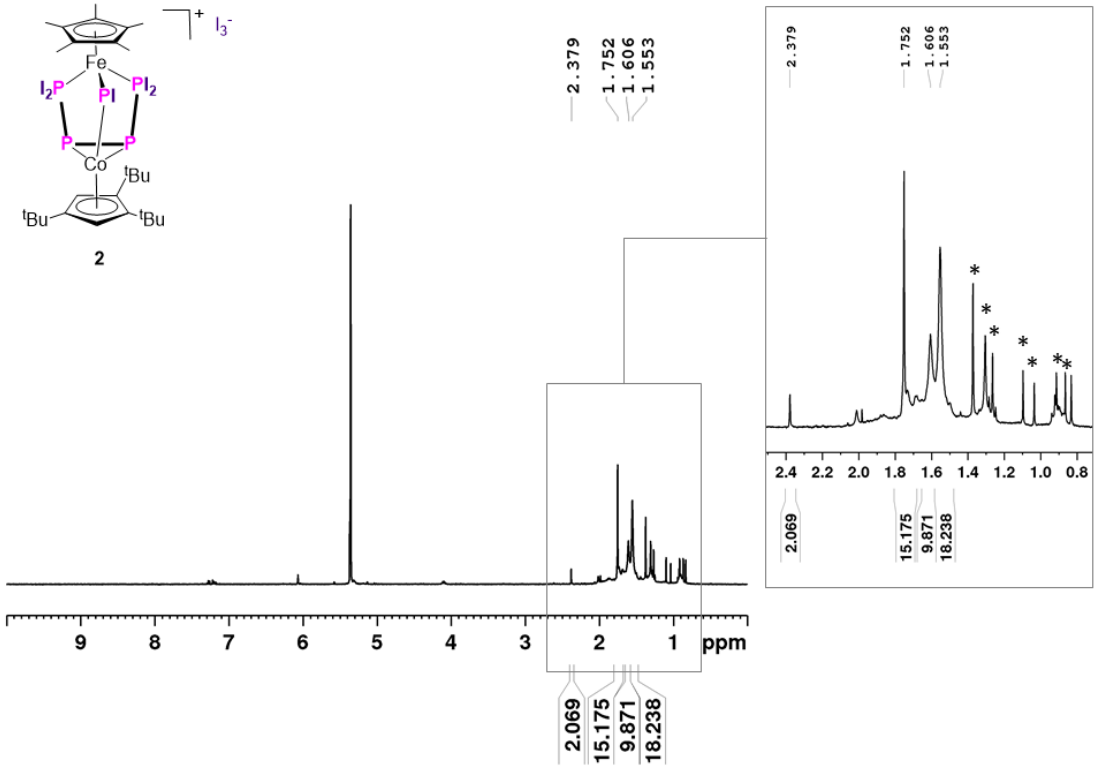


**Figure S36.** $^{1}H$ NMR spectrum of compound **2** ($CD_2Cl_2$, 300 K). Signals of **2** are the one with the picks picked, impurities are marked with *.

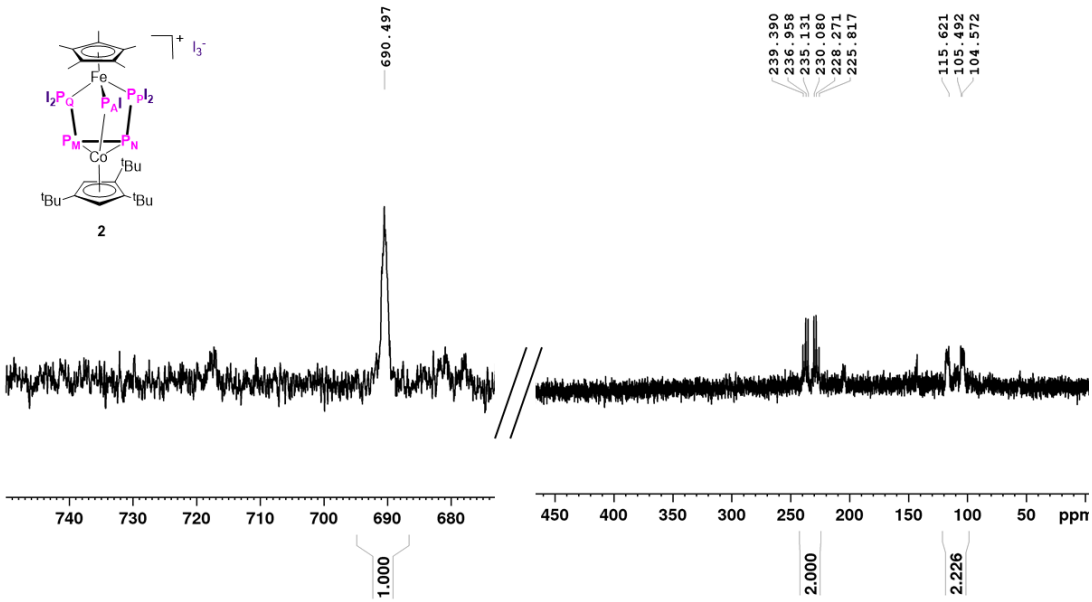


**Figure S37** $^{31}P\{^{1}H\}$ NMR spectrum of compound **2** ($CD_2Cl_2$, 300 K).

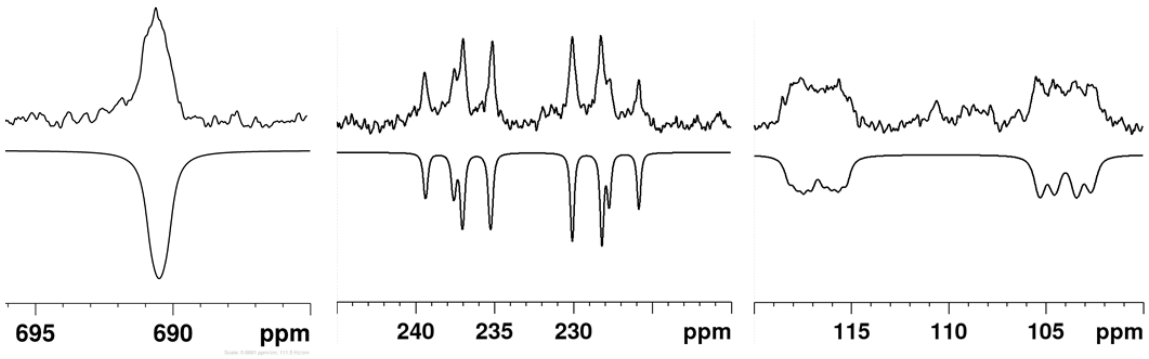


**Figure S38** Sections of the experimental (upwards) and simulated (downwards) $^{31}P\{^{1}H\}$ NMR spectrum of compound **2** (AMNPQ spin system) ($CD_2Cl_2$, 300K).

**Table S 19** Chemical shifts and coupling constants obtained from simulation.

| δ (ppm) | | J (Hz) | | | |
|---|---|---|---|---|---|
| **A** | 690.5 | $^{2}J_{AM}$ | 10 | $^{1}J_{MP}$ | 294 |
| **M** | 237.2 | $^{2}J_{AN}$ | 10 | $^{2}J_{MQ}$ | 15 |
| **N** | 228.1 | $^{2}J_{AP}$ | 65 | $^{2}J_{NP}$ | 10 |
| **P** | 116.7 | $^{2}J_{AQ}$ | 35 | $^{1}J_{NQ}$ | 310 |
| **Q** | 104.0 | $^{2}J_{MN}$ | 380 | $^{1}J_{PQ}$ | 125 |

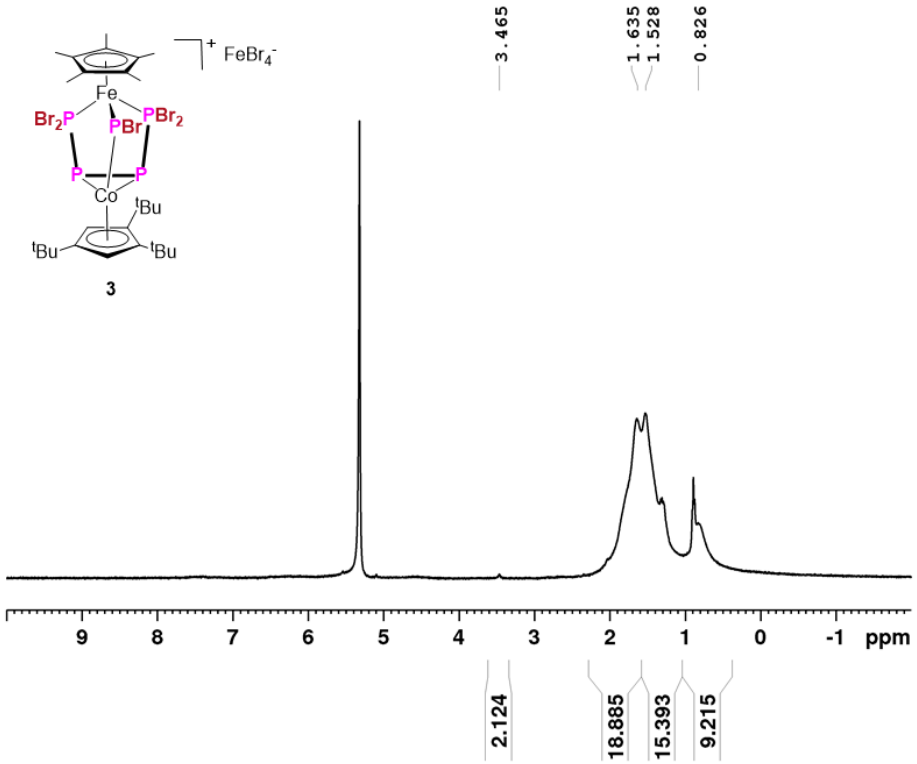


**Figure S 39** $^{1}H$ NMR spectrum of compound **3** ($CD_2Cl_2$, 300 K).

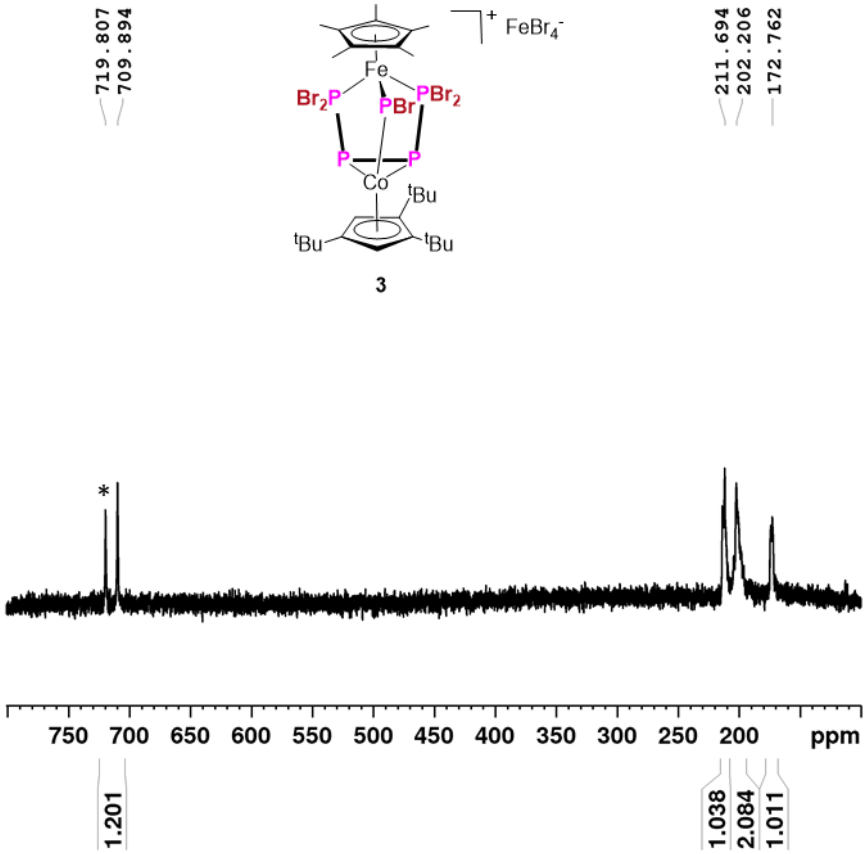


**Figure S40** $^{31}P\{^{1}H\}$ NMR spectrum of compound **3** ($CD_2Cl_2$, 300 K). The signal marked with * corresponds to an impurity, resulting probably from the partial chlorinated compound [(Cp*Fe)(Cp'''Co)($\mu$-PCl)($\mu$,$\eta^2$:$\eta^1$:$\eta^1$-$P_4Br_4$)][$FeBr_4$] (**3-Cl**) due to halogen exchange with the chlorinated solvent.

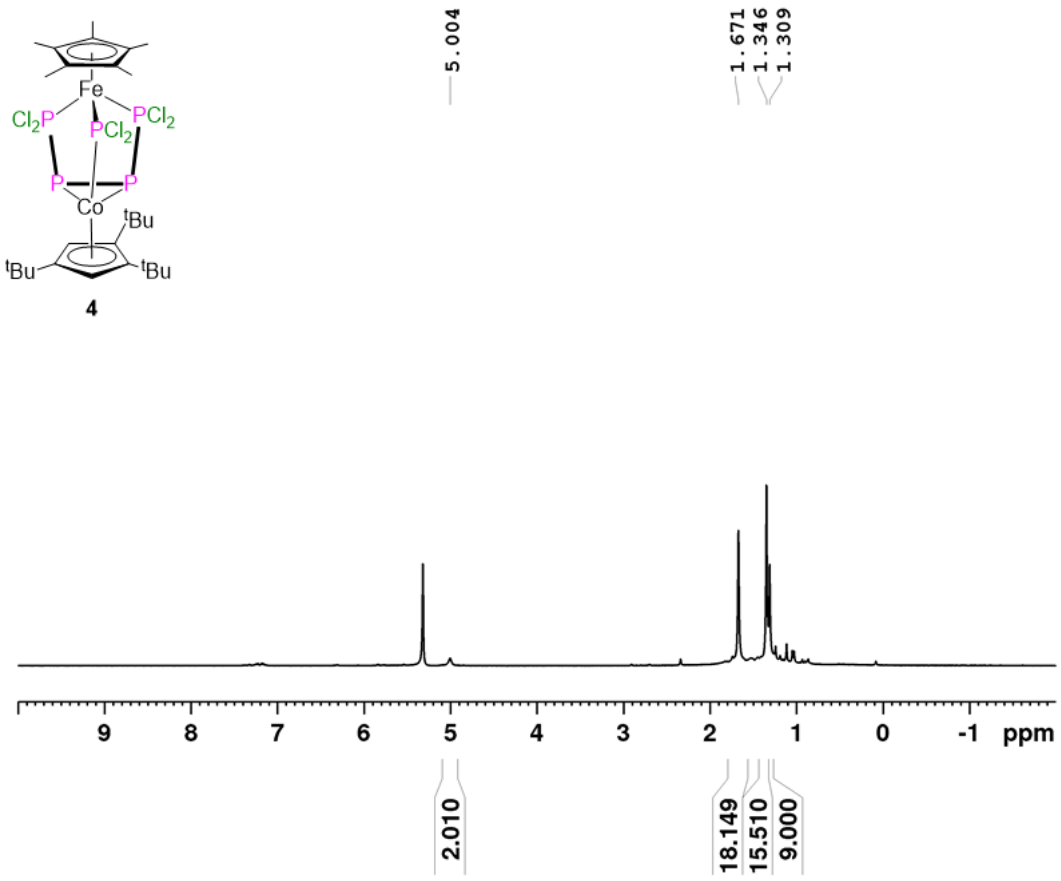


**Figure S41** $^{1}H$ NMR spectrum of compound **4** ($CD_2Cl_2$, 300 K).

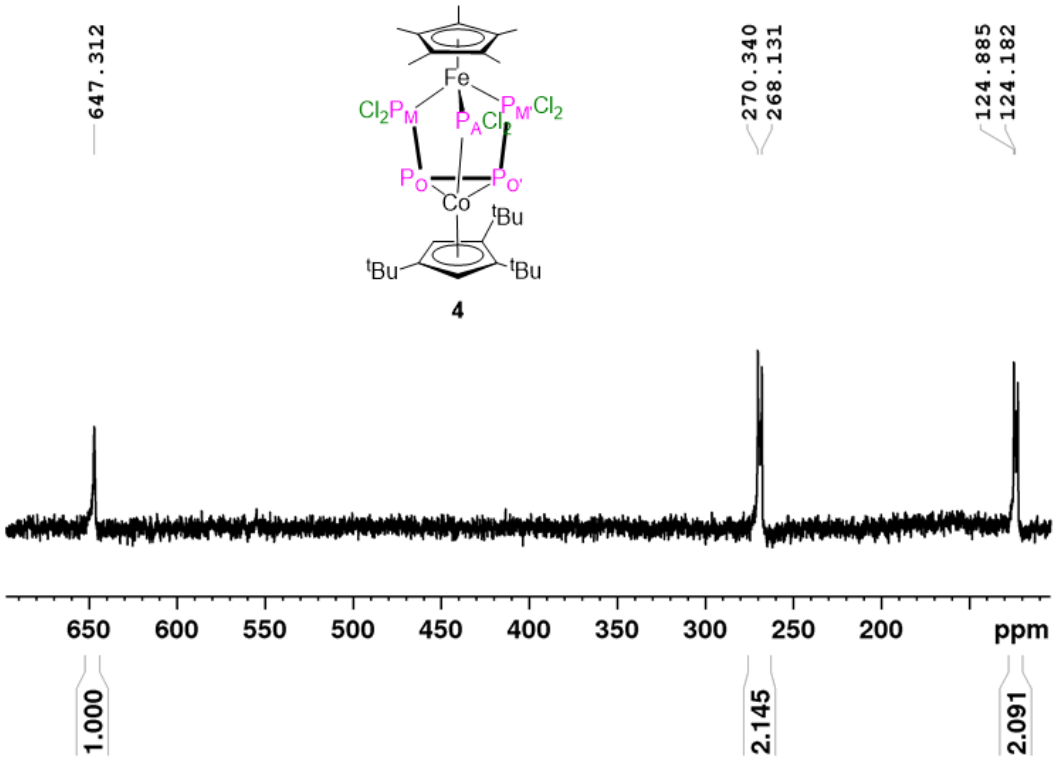


**Figure S42** $^{31}P\{^{1}H\}$ NMR spectrum of compound **4** ($CD_2Cl_2$, 300 K).

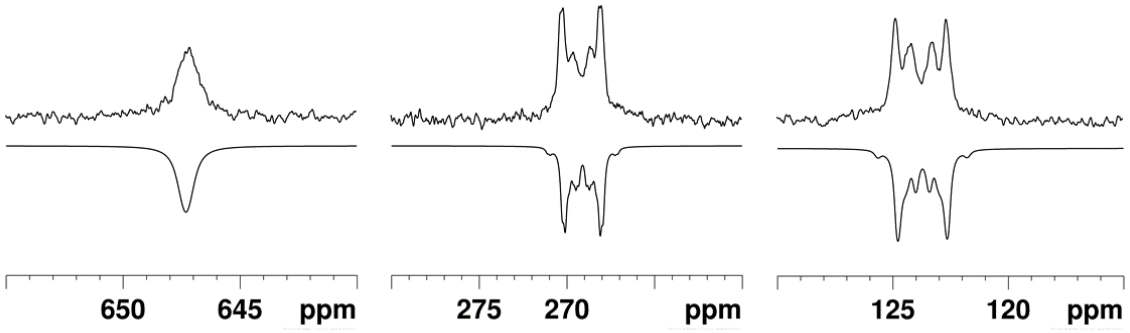


**Figure S 43** Sections of the experimental (upwards) and simulated (downwards) $^{31}P\{^1H\}$ NMR spectrum of compound **4** (AMM'OO' spin system) ($CD_2Cl_2$, 300K).

**Table S 20** chemical shifts and coupling constants obtained from simulation.

| **δ (ppm)** | | ***J* (Hz)** | | | |
|---|---|---|---|---|---|
| **A** | 647.3 | $^2J_{AM}$ | 30 | $^1J_{MO}$ | 340 |
| **M** | 269.1 | $^2J_{AM'}$ | 30 | $^2J_{MO'}$ | 50 |
| **M'** | 269.1 | $^2J_{AO}$ | 10 | $^2J_{M'O}$ | 50 |
| **O** | 123.7 | $^2J_{AO'}$ | 25 | $^1J_{M'O'}$ | 260 |
| **O'** | 123.7 | $^2J_{MM'}$ | 110 | $^1J_{OO'}$ | 150 |

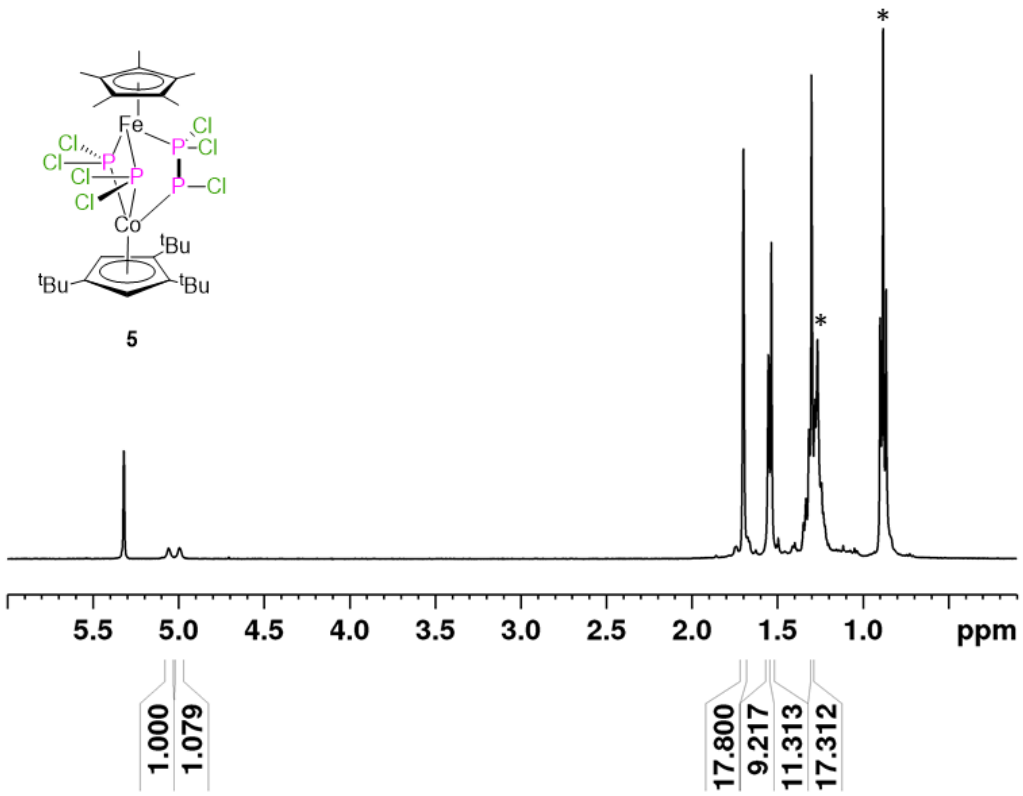


**Figure S 44** $^{1}H$ NMR spectrum of compound **5** ($CD_2Cl_2$, 300 K). Signals of pentane are marked with *.

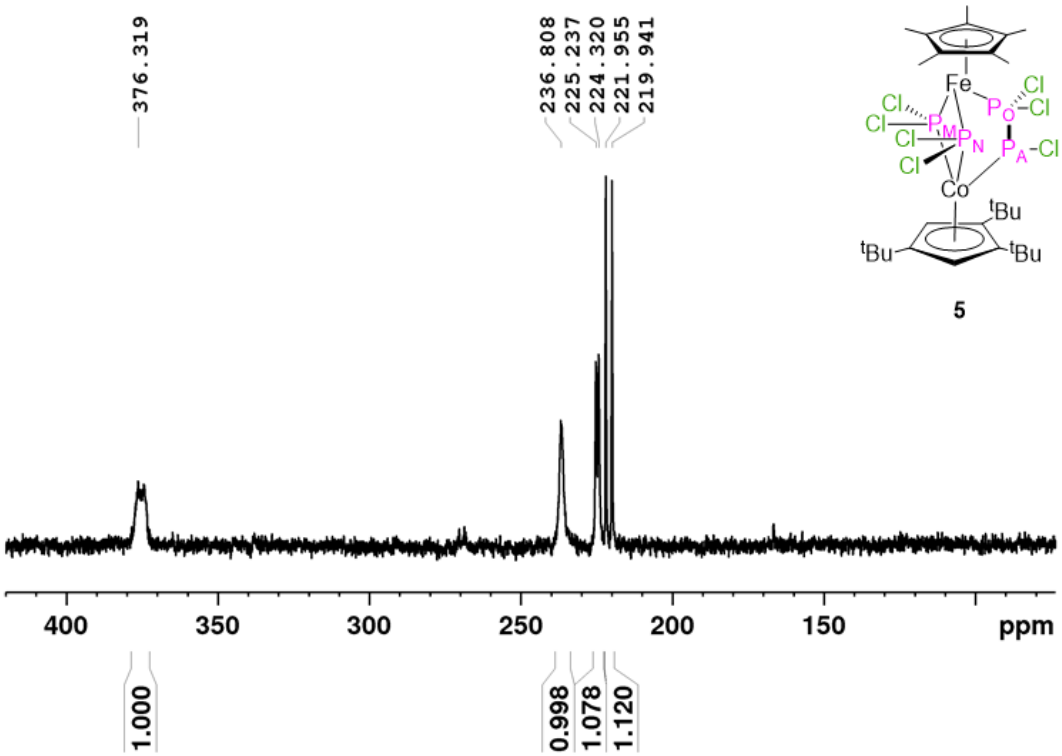


**Figure S 45** $^{31}P\{^{1}H\}$ NMR spectrum of compound **5** ($CD_2Cl_2$, 300 K).

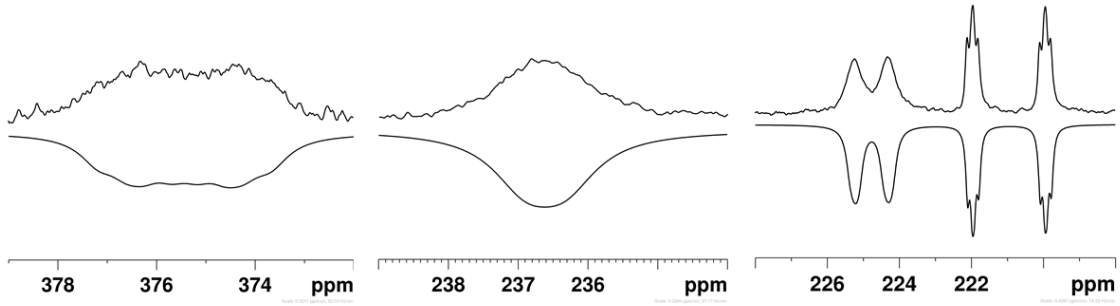


**Figure S 46** Sections of the experimental (upwards) and simulated (downwards) $^{31}P\{^{1}H\}$ NMR spectrum of compound **5** (AMNO spin system) ($CD_2Cl_2$, 300K).

**Table S 21** chemical shifts and coupling constants obtained from simulation.

| **δ (ppm)** | | ***J* (Hz)** | | | |
|---|---|---|---|---|---|
| **A** | 375.4 | $^{1}J_{AO}$ | 327 | $^{2}J_{MO}$ | 20 |
| **M** | 236.6 | $^{2}J_{AN}$ | 151 | $^{2}J_{MN}$ | 15 |
| **N** | 224.8 | $^{2}J_{AM}$ | 91 | $^{2}J_{NO}$ | 30 |
| **O** | 221.0 | | | | |

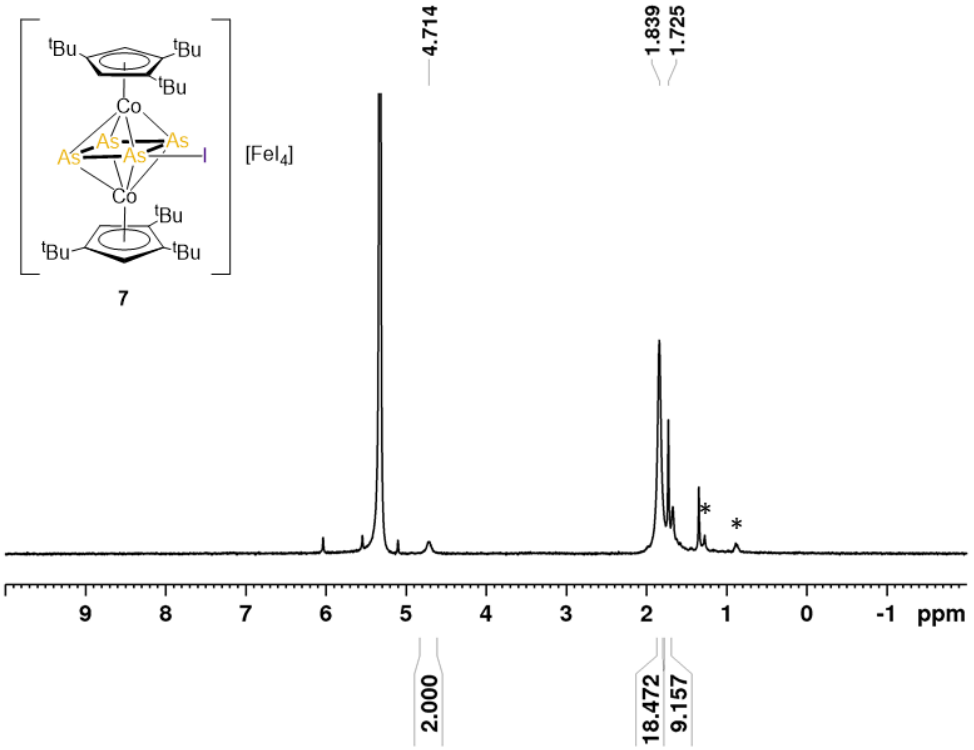


**Figure S 47** $^1$H NMR spectrum of compound **7** ($CD_2Cl_2$, 300 K). Traces of hexane are marked with *.

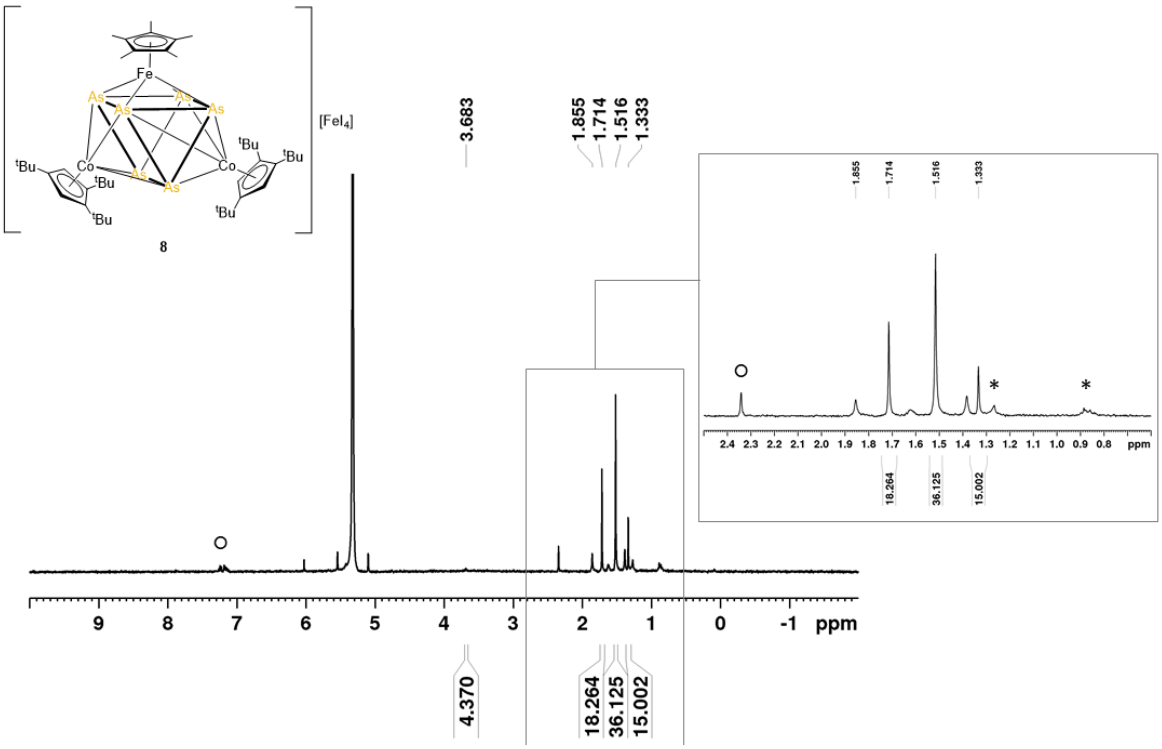


**Figure S 48** $^1$H NMR spectrum of compound **8** ($CD_2Cl_2$, 300 K). Traces of hexane are marked with *, traces of toluene are marked with ○. The signal of $C_5H_2{}^t Bu_3$ is almost below the noise background.

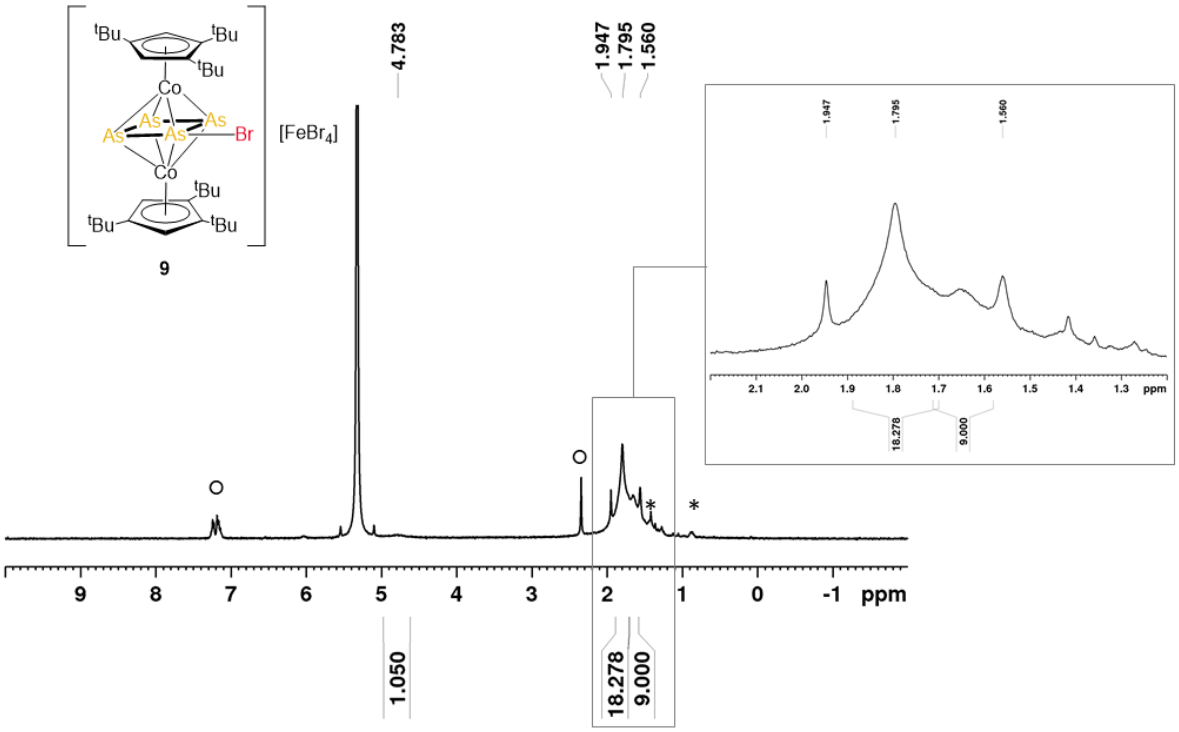


**Figure S 49** $^1$H NMR spectrum of compound **9** ($CD_2Cl_2$, 300 K). Traces of hexane are marked with *, traces of toluene are marked with ○. The signal of $C_5H_2{}^tBu_3$ is very broad and almost below the noise background. This might be the reason why the integration does not fit (1 H instead of 2).

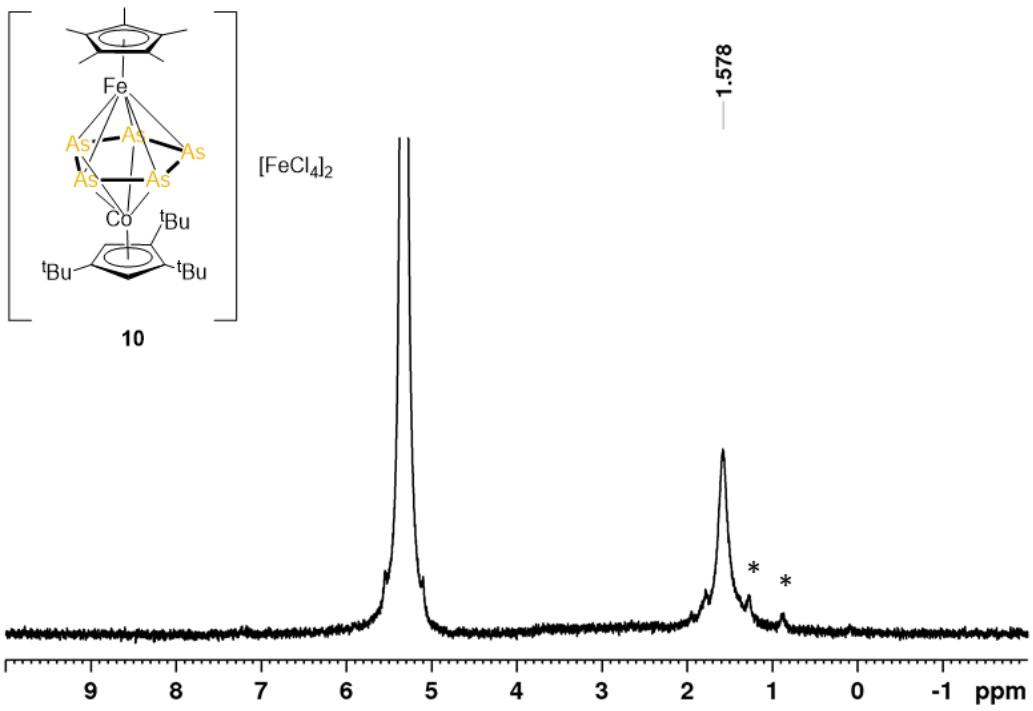


**Figure S 50** $^1$H NMR spectrum of compound **10** ($CD_2Cl_2$, 300 K). Traces of hexane are marked with *. Here the broadening of the signal is too big and does not allow a proper attribution.

**Crystallographic Details**

Suitable crystals were selected and mounted on a on a SuperNova Dualflex diffractometer equipped with an Atlas$^{S2}$ CCD detector (**2**, **5**), on a XtaLAB SynergyR DW diffractometer equipped with an HyPix-Arc 150 detector (**3**, **7**, **8**, **9**, **10**), on a Gemini Ultra diffractometer equipped with an Atlas$^{S2}$ CCD detector (**4**). The crystals were kept at a steady T = 123(1) K during data collection. Data collection and reduction were performed with **CrysAlisPro** [Version 1.171.41.90a (**2**, **3**, **4**, **7**, **9**, **10**), Version 1.171.41.76a (**5**), Version 1.171.41.93a (**8**)].[2] For the compounds **2**, **4**, **5**, **7**, **8**, **9** and **10** a gaussian absorption correction, a numerical absorption correction based on gaussian integration over a multifaceted crystal model and an empirical absorption correction using spherical harmonics as implemented in SCALE3 ABSPACK scaling algorithm were applied. For compound **3**, a spherical absorption correction using equivalent radius and absorption coefficient and an empirical absorption correction using spherical harmonics as implemented in SCALE3 ABSPACK scaling algorithm were performed. Using **Olex2**,[3] the structures were solved with **ShelXT**[4] and a least-square refinement on F2 was carried out with **ShelXL**[5] for all structures. All non-hydrogen atoms were refined anisotropically. Hydrogen atoms at the carbon atoms were located in idealized positions and refined isotropically according to the riding model. Figures were created with **Olex2**[3].

CCDC-2155229 (**2**·$\mathbf{CH_2Cl_2}$), CCDC-2155230 (**3**), CCDC-2155231 (**4**), CCDC-2155232 (**5**), CCDC-2155233 (**7**), CCDC-2155234 (**8**), CCDC-2155235 (**9**), and CCDC-2155236 (**10**) contain the supplementary crystallographic data for this paper. These data can be obtained free of charge at www.ccdc.cam.ac.uk/conts/retrieving.html (or from the Cambridge Crystallographic Data Centre, 12 Union Road, Cambridge CB2 1EZ, UK; Fax: + 44-1223-336-033; e-mail: deposit@ccdc.cam.ac.uk).

**Table S22** Crystallographic data for compounds **2**, **3**, **4** and **5**.

| Compound | 2···$CH_2Cl_2$ | 3 | 4 | 5 |
|---|---|---|---|---|
| Data set (internal naming) | AG394_tI_abs | AG496_aP_abs | AG350_mP_abs | AG432_mP_abs_gaus |
| CCDC-number | 2155229 | | 2155231 | 2155232 |
| Formula | $C_{27.3}H_{44.6}Cl_{0.6}CoFeI_8P_5$ | $C_{27}H_{44}Br_{8.87}Cl_{0.13}CoFe_2P_5$ | $C_{27}H_{44}Cl_{5.18}CoFeO_{0.41}P_5$ | $C_{27}H_{44}Cl_7CoFeP_4$ |
| $D_{calc.}$/ g cm$^{-3}$ | 2.284 | 2.154 | 1.590 | 1.577 |
| $\mu$/mm$^{-1}$ | 5.909 | 20.063 | 13.143 | 13.436 |
| Formula Weight | 1678.93 | 1410.59 | 828.44 | 855.43 |
| Colour | metallic dark black | red | clear dark red | dark brown |
| Shape | block-shaped | plate-shaped | prism-shaped | block |
| Size/mm$^3$ | 0.18×0.06×0.06 | 0.12×0.02×0.02 | 0.28×0.19×0.07 | 0.08×0.05×0.04 |
| $T$/K | 123.00(10) | 100.00(10) | 123(1) | 123.01(10) |
| Crystal System | tetragonal | triclinic | monoclinic | monoclinic |
| Space Group | $I4/m$ | $P\bar{1}$ | $P2_1/n$ | $P2_1/n$ |
| $a$/Å | 25.8946(3) | 9.4320(2) | 16.8853(3) | 13.7508(3) |
| $b$/Å | 25.8946(3) | 13.0176(2) | 9.2420(2) | 16.2228(3) |
| $c$/Å | 14.5656(3) | 18.6901(2) | 22.9159(5) | 16.1685(3) |
| $\alpha$/° | 90 | 108.306(2) | 90 | 90 |
| $\beta$/° | 90 | 92.9140(10) | 104.600(2) | 92.305(2) |
| $\gamma$/° | 90 | 91.0260(10) | 90 | 90 |
| V/Å$^3$ | 9766.7(3) | 2174.47(7) | 3460.64(13) | 3603.89(12) |
| $Z$ | 8 | 2 | 4 | 4 |
| $Z'$ | 0.5 | 1 | 1 | 1 |
| Wavelength/Å | 0.71073 | 1.54184 | 1.54184 | 1.54184 |
| Radiation type | Mo K$\alpha$ | Cu K$\alpha$ | Cu K$\alpha$ | Cu K$\alpha$ |
| $\Theta_{min}$/° | 3.010 | 2.494 | 3.743 | 3.861 |
| $\Theta_{max}$/° | 31.879 | 67.074 | 71.615 | 65.965 |
| Measured Refl's. | 22702 | 61328 | 12060 | 13349 |
| Indep't Refl's | 7950 | 7734 | 6468 | 6106 |
| Refl's I≥2 $\sigma$(I) | 6564 | 6347 | 6114 | 5656 |
| $R_{int}$ | 0.0339 | 0.0869 | 0.0324 | 0.0320 |
| Parameters | 299 | 600 | 480 | 438 |
| Restraints | 17 | 65 | 278 | 126 |
| Largest Peak | 2.357 | 1.290 | 2.075 | 0.915 |
| Deepest Hole | -2.335 | -1.130 | -0.568 | -0.802 |
| GooF | 1.113 | 1.149 | 1.127 | 1.053 |
| $wR_2$ (all data) | 0.1141 | 0.1728 | 0.1338 | 0.1155 |
| $wR_2$ | 0.1079 | 0.1678 | 0.1320 | 0.1127 |
| $R_1$ (all data) | 0.0591 | 0.0649 | 0.0579 | 0.0469 |
| $R_1$ | 0.0460 | 0.0559 | 0.0550 | 0.0436 |

**Table S23** Crystallographic data for compounds **7**, **8**, **9** and **10**.

| Compound | 7 | 8 | 9 | 10 |
|---|---|---|---|---|
| Data set (internal naming) | AG598_DCM | AG598_tol | AG599_tol | AG600 |
| CCDC-number | 2155233 | 2155234 | 2155235 | 2155236 |
| Formula | $C_{34}H_{58}As_{3.6}Co_2Fe_1I_{5.2}$ | $C_{44}H_{73}As_6Co_2Fe_2I_4$ | $As_4Br_5C_{40.3}Co_2FeH_{65.2}$ | $C_{27}H_{44}As_5Cl_8CoFe_3$ |
| $D_{calc.}$/ g cm$^{-3}$ | 2.273 | 2.124 | 1.961 | 1.961 |
| $\mu$/mm$^{-1}$ | 7.155 | 6.876 | 15.820 | 20.188 |
| Formula Weight | 1573.18 | 1791.78 | 1422.66 | 1253.30 |
| Colour | clear dark black | clear dark black | clear green | clear dark black |
| Shape | prism-shaped | needle-shaped | plate-shaped | prism-shaped |
| Size/mm$^3$ | 0.16×0.10×0.10 | 0.19×0.05×0.02 | 0.15×0.02×0.01 | 0.10×0.05×0.05 |
| $T$/K | 123.01(10) | 123.01(10) | 123.01(10) | 123.00(10) |
| Crystal System | monoclinic | orthorhombic | monoclinic | orthorhombic |
| Flack Parameter | - | 0.148(7) | - | -0.020(2) |
| Hooft Parameter | - | 0.025(5) | - | -0.0253(15) |
| Space Group | $P2_1/n$ | $Pca2_1$ | $P2_1/n$ | $P2_12_12_1$ |
| $a$/Å | 16.43130(10) | 19.7585(3) | 10.71500(10) | 10.36410(10) |
| $b$/Å | 14.71320(10) | 18.3668(2) | 26.0501(3) | 18.1754(2) |
| $c$/Å | 19.0699(2) | 15.4389(2) | 18.0248(2) | 22.5328(2) |
| $\alpha$/° | 90 | 90 | 90 | 90 |
| $\beta$/° | 94.2380(10) | 90 | 106.6700(10) | 90 |
| $\gamma$/° | 90 | 90 | 90 | 90 |
| V/Å$^3$ | 4597.68(6) | 5602.78(13) | 4819.76(9) | 4244.54(7) |
| $Z$ | 4 | 4 | 4 | 4 |
| $Z'$ | 1 | 1 | 1 | 1 |
| Wavelength/Å | 0.71073 | 0.71073 | 1.54184 | 1.54184 |
| Radiation type | Mo K$_\alpha$ | Mo K$_\alpha$ | Cu K$_\alpha$ | Cu K$_\alpha$ |
| $\Theta_{min}$/° | 2.100 | 2.008 | 3.070 | 3.124 |
| $\Theta_{max}$/° | 29.701 | 29.719 | 74.548 | 74.375 |
| Measured Refl's. | 43715 | 36306 | 70082 | 35339 |
| Indep't Refl's | 11382 | 12659 | 9655 | 8357 |
| Refl's I≥2 $\sigma$(I) | 10502 | 11775 | 8357 | 7778 |
| $R_{int}$ | 0.0206 | 0.0231 | 0.0380 | 0.0392 |
| Parameters | 478 | 643 | 497 | 411 |
| Restraints | 6 | 173 | 59 | 0 |
| Largest Peak | 1.054 | 0.785 | 1.960 | 0.777 |
| Deepest Hole | -0.910 | -0.714 | -2.498 | -0.990 |
| GooF | 1.218 | 1.031 | 1.060 | 1.079 |
| $wR_2$ (all data) | 0.0504 | 0.0420 | 0.1628 | 0.0958 |
| $wR_2$ | 0.0496 | 0.0410 | 0.1582 | 0.0943 |
| $R_1$ (all data) | 0.0278 | 0.0257 | 0.0647 | 0.0393 |
| $R_1$ | 0.0240 | 0.0213 | 0.0580 | 0.0359 |

## Compound 2

The asymmetric unit contains half of the molecule [(Cp*Fe)(Cp'''Co)(*μ*-PI)(*μ*,$\eta^2$:$\eta^1$:$\eta^1$-$P_4I_4$)]$^+$, an $I_3^-$ anion and a $CH_2Cl_2$ solvent molecule. Further, one I atom is disordered over two positions (0.50:0.50), as well as one of the *tert*-butyl group (0.50:0.50).

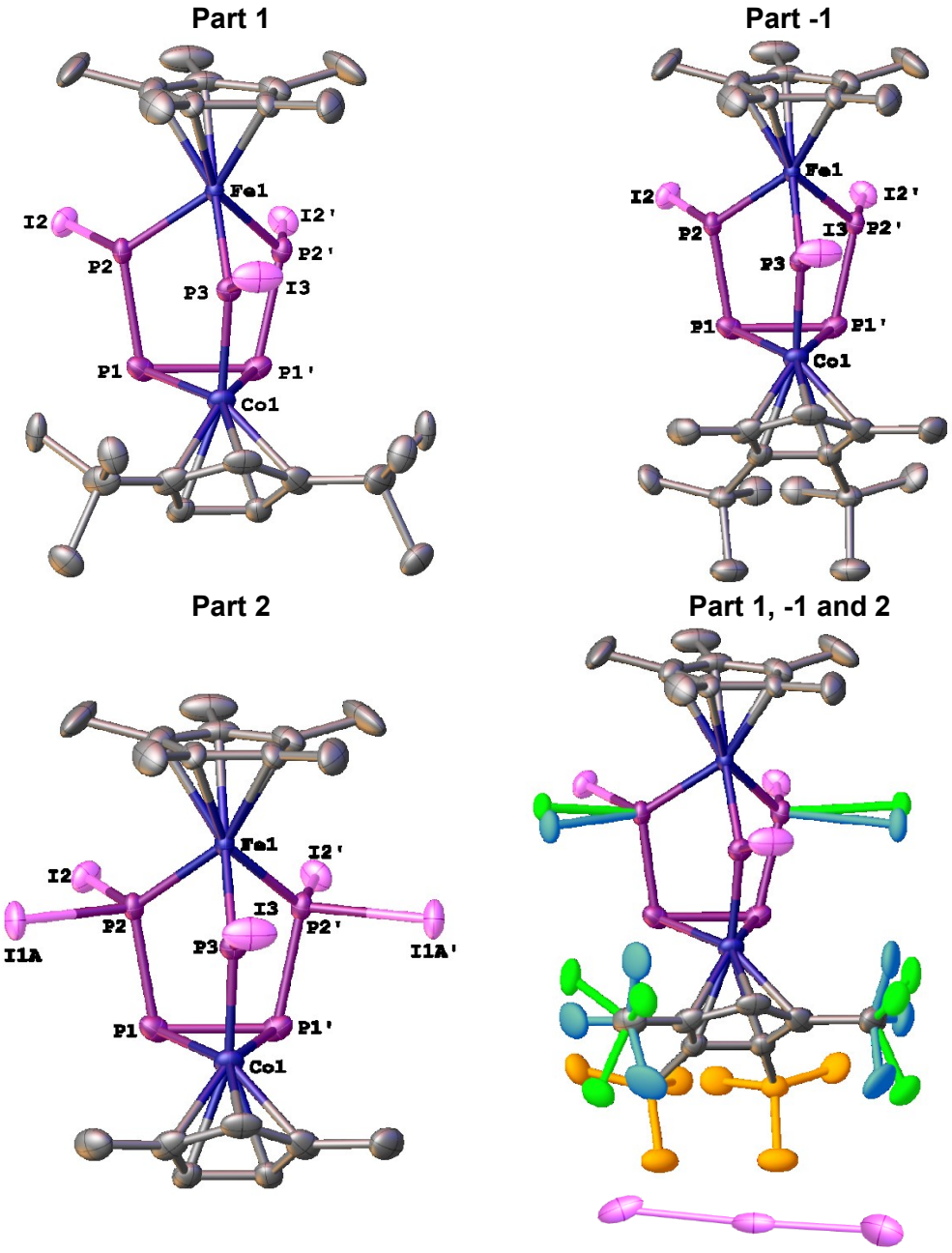


| Selected bond length [Å] | | Selected bond angles [°] | |
|---|---|---|---|
| **P1-P1'** | 2.161(3) | **P1-Co1-P1'** | 56.69(7) |
| **P1-P2** | 2.2086(18) | **P2-P1-P1'** | 100.70(5) |
| **P2···P2'** | 2.980(2) | **P2-Fe1-P2'** | 87.72(7) |

## Compound 3

The asymmetric unit contains one molecule of $[(Cp^*Fe)(Cp'''Co)(\mu\text{-PBr})(\mu,\eta^2{:}\eta^1{:}\eta^1\text{-}P_4Br_4)]^+$ and one of the $FeBr_4^-$ anion. The {Cp'''Co} fragment is disordered over two positions (0.72:0.28), as well as two Br atoms of the $FeBr_4^-$ anion (0.65:0.35). The Br atom at the P1 atom is disordered and additionally partly replaced with a Cl atom (0.66 (Br1a): 0.21 (Br1b):0.13 (Cl1c)).

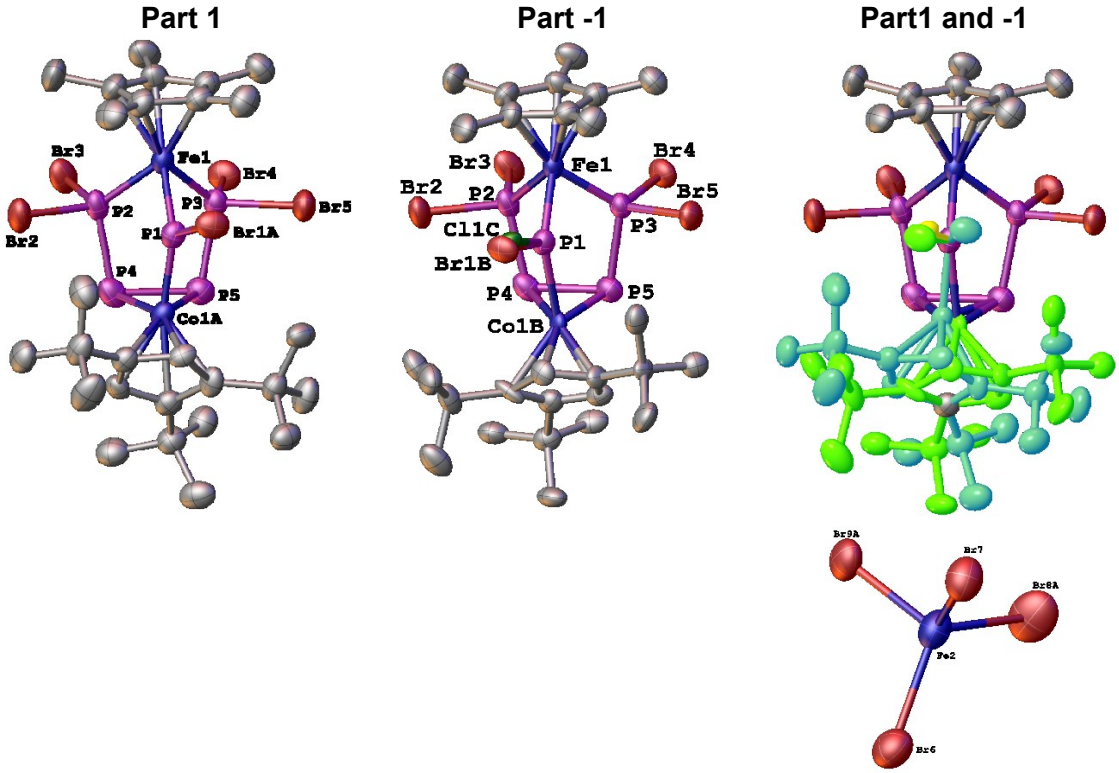


| Selected bond length [Å] | | Selected bond angles [°] | |
|---|---|---|---|
| **P4-P5** | 2.150(3) | **P4-Co1A-P5** | 55.80(14) |
| **P2-P4** | 2.203(3) | **P2-P4-P5** | 100.16(11) |
| **P3-P5** | 2.206(2) | **P3-P5-P4** | 100.06(10) |
| **P2···P3** | 2.924(2) | **P3-Fe1-P1** | 81.43(7) |

## Compound 4

The asymmetric unit contains one molecule of [(Cp*Fe)(Cp'''Co)($\mu$-$PCl_2$)($\mu$,$\eta^2$:$\eta^1$:$\eta^1$-$P_4Cl_4$)]. Additionally, one oxygen atom with 41% occupancy is attached to P3 (Part 1: Part 2 = 0.59:0.41). One of the *tert*-butyl group is disordered over two positions (0.67:0.33), as well as three methyl groups and three carbon atoms of the Cp* ligand (0.52:0.48).

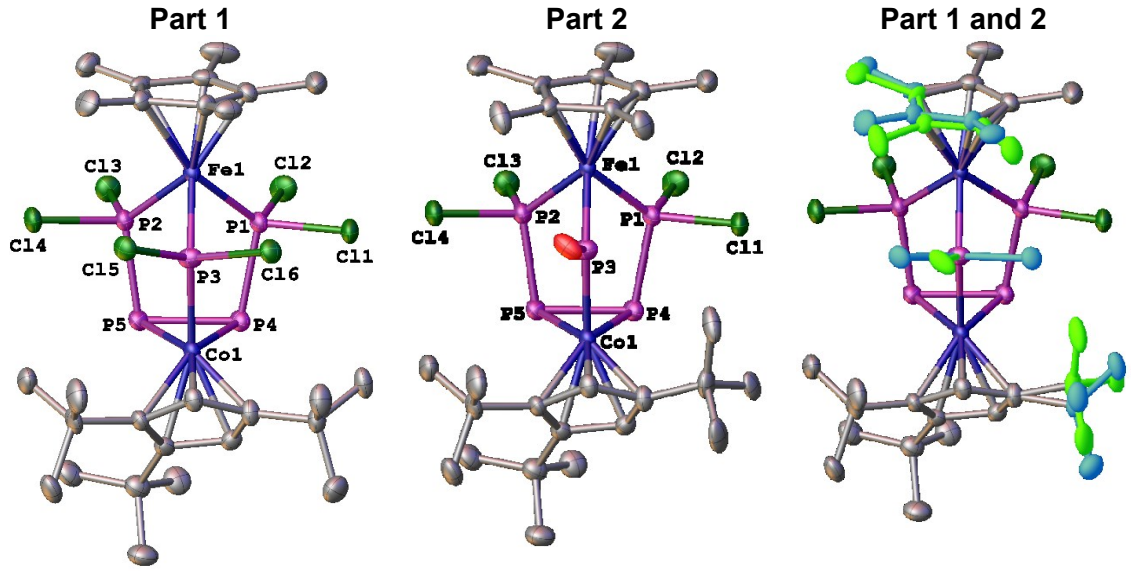


| Selected bond length [Å] | | Selected bond angles [°] | |
|---|---|---|---|
| **P1-P4** | 2.1921(15) | **P4-Co1-P5** | 57.37(4) |
| **P4-P5** | 2.1676(14) | **P1-P4-P5** | 99.90(6) |
| **P2-P5** | 2.1901(15) | **P2-P5-P4** | 98.60(6) |
| **P1···P2** | 2.8734(14) | **P1-Fe1-P2** | 86.02(5) |

## Compound 5

The asymmetric unit contains one molecule of [(Cp*Fe)(Cp'''Co)($\mu$-$PCl_2$)$_2$($\mu$,$\eta^1$:$\eta^1$-$P_2Cl_3$)]. The $P_2Cl_3$ ligand is disordered over two positions (0.13:0.87), as well as the two Cl atoms of one of the two $PCl_2$ bridging ligands (0.92:0.08).

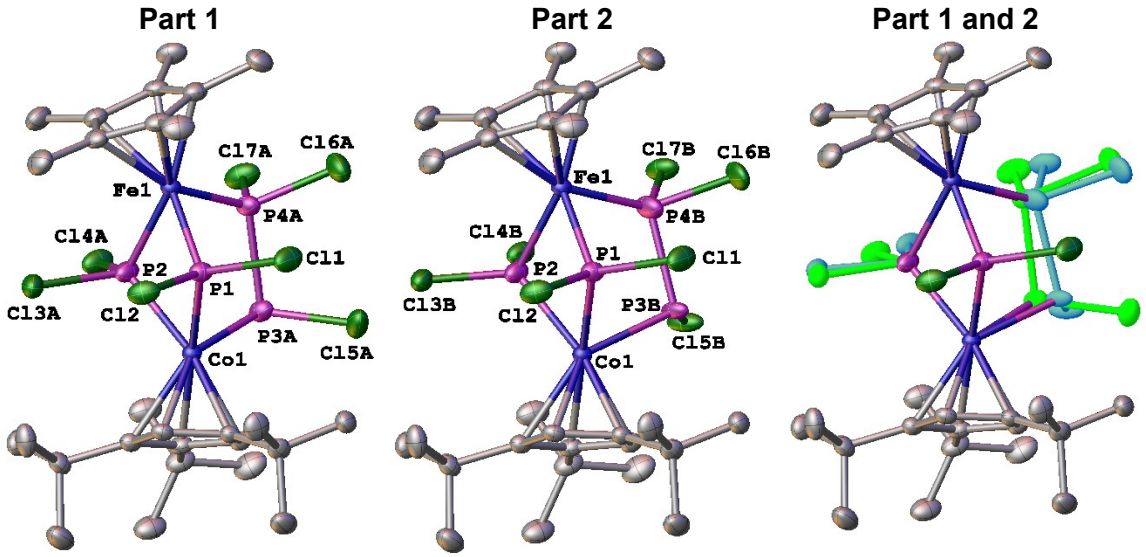


| Selected bond length [Å] | | Selected bond angles [°] | |
|---|---|---|---|
| **P3A-P4A** | 2.238(3) | **P4A-P3A-Co1** | 100.29(7) |
| **P1···P2** | 2.5285(14) | **Fe1-P1-Co1** | 105.79(4) |

## Compound 7

The asymmetric unit contains one molecule of [(Cp'''Co)$_2$($\mu$,$\eta^4$:$\eta^4$-As$_4$I)] and one of the $FeI_4^-$ anion. The four As atoms were only partly occupied and a free refinement resulted in an occupation of 0.90. Therefore, compound **7** co-crystallizes with a second species (occupancy 0.10), corresponding to [[(Cp'''Co)$_2$($\mu$-I)$_3$]. In the latter, two I atoms are further disorder over two positions (0.05:0.05).

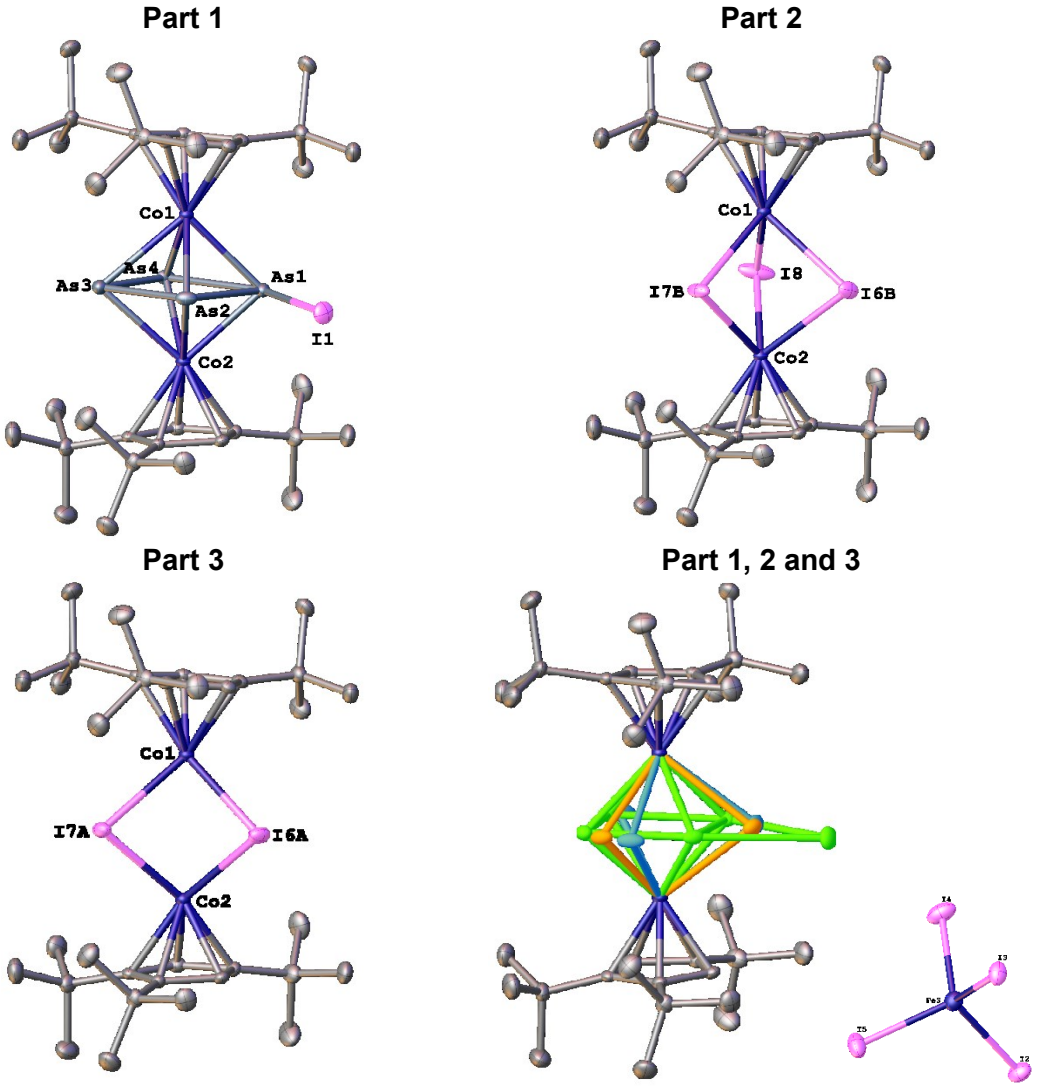


| Selected bond length [Å] | | Selected bond angles [°] | |
|---|---|---|---|
| **As1-As2** | 2.4914(5) | **As1-As2-As3** | 92.123(17) |
| **As2-As3** | 2.5351(5) | **As2-As3-As4** | 91.82(5) |
| **As3-As4** | 2.3154(17) | **As3-As4-As1** | 91.90(7) |
| **As4-As1** | 2.7066(18) | **As4-As1-As2** | 84.16(4) |
| **As1-I1** | 2.7937(4) | **As4-As1-I1** | 156.04(4) |
| **As2···I1** | 3.1190(5) | **As3-As2-I1** | 150.368(16) |

## Compound 8

The asymmetric unit contains one molecule of $[(Cp^*Fe)(Cp'''Co)_2(\mu_3,\eta^4{:}\ \eta^4{:}\ \eta^4\text{-}As_6)]^+$ and one of the $FeI_4^-$ anion. The Cp* ligand is disordered over two positions (0.51:0.49). It was refined as a two-component inversion twin.

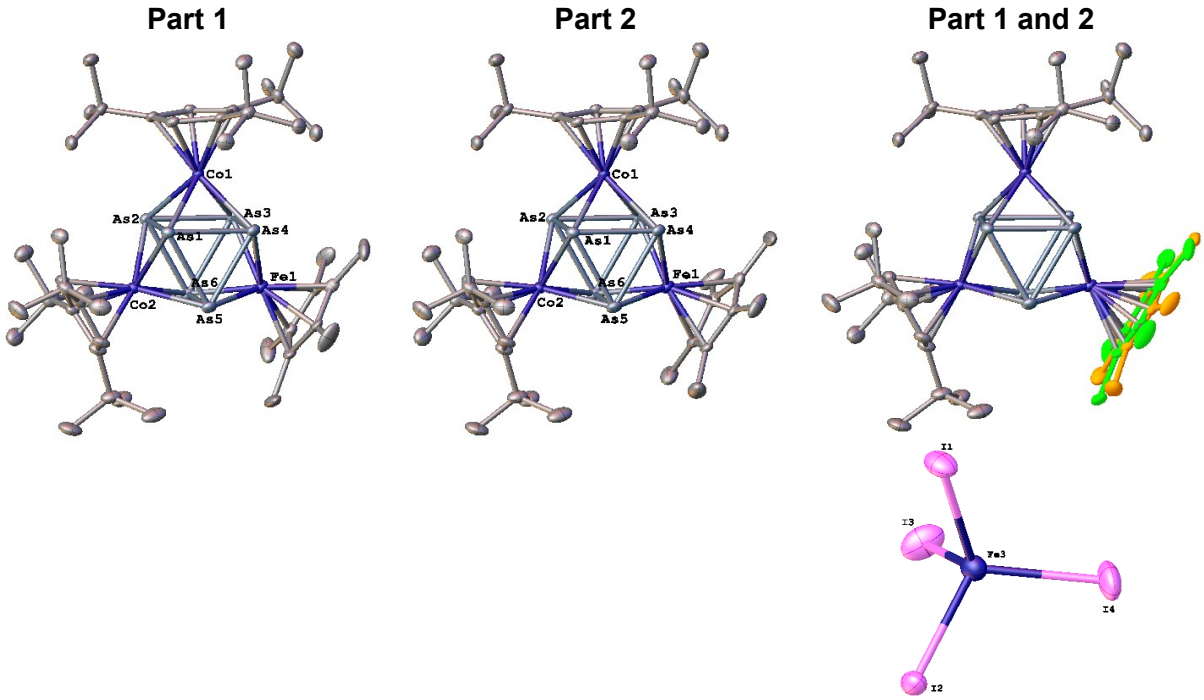


| Selected bond length [Å] | |
|---|---|
| **As1···As2** | 2.8432(6) |
| **As2-As3** | 2.5557(6) |
| **As3···As4** | 2.7339(6) |
| **As4-As5** | 2.5740(6) |
| **As5···As6** | 2.7339(6) |
| **As1-As4** | 2.5644(6) |
| **As1-As5** | 2.5528(6) |
| **As2-As6** | 2.5508(6) |
| **As3-As6** | 2.5704(6) |

| Selected bond angles [°] | |
|---|---|
| **As3-As2-As6** | 60.445(17) |
| **As4-As1-As5** | 60.397(17) |
| **As2-As3-As6** | 59.684(16) |
| **As1-As4-As5** | 59.577(16) |
| **As2-As6-As3** | 59.870(17) |
| **As1-As5-As4** | 60.026(16) |

## Compound 9

The asymmetric unit contains one molecule of $[(Cp'''Co)_2(\mu,\eta^4{:}\eta^4\text{-}As_4Br)]^+$ and one $FeBr_4^-$ anion. Two As atoms of the *cyclo*-$As_4Br$ ligand are disordered over two positions (0.53:0.47), as well as the whole $FeBr_4^-$ anion (0.88:0.12).

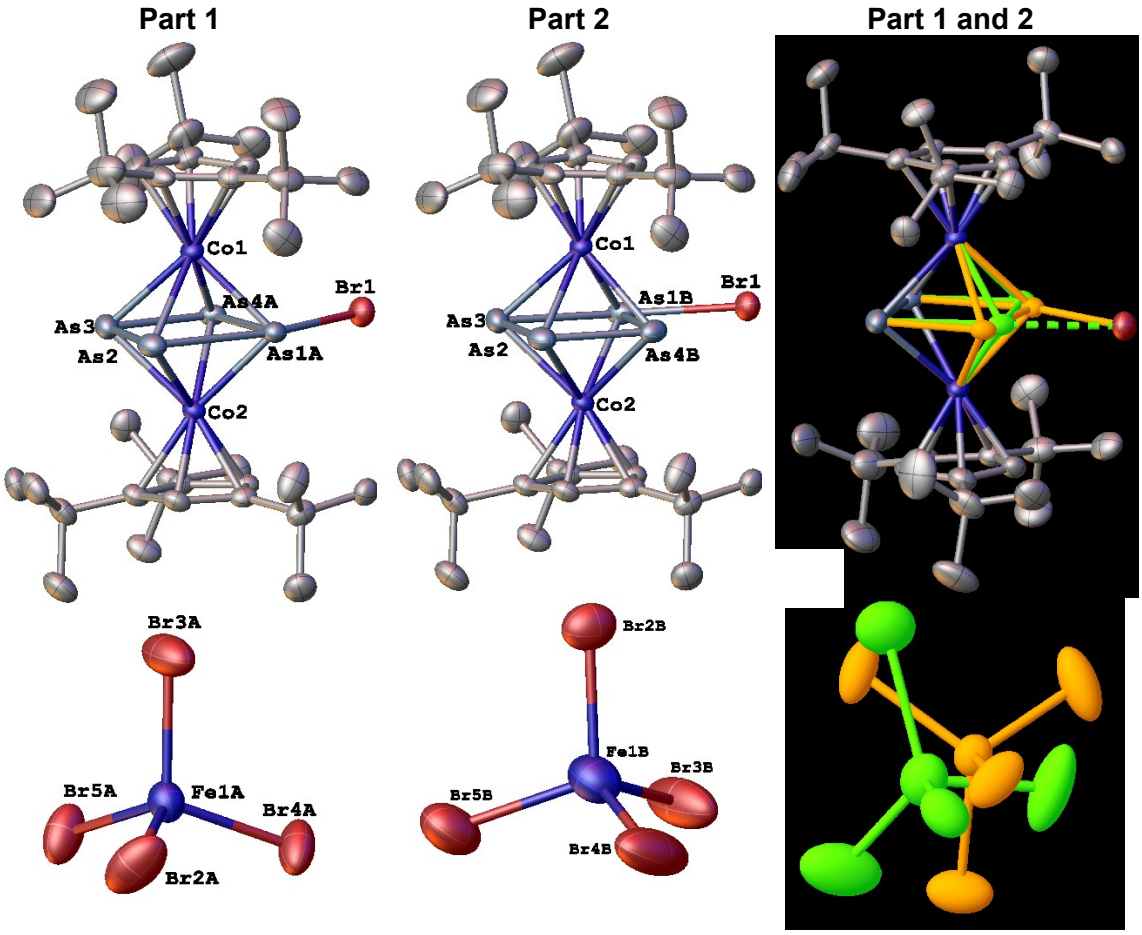


| Selected bond length [Å] | | Selected bond angles [°] | |
|---|---|---|---|
| **As1A-As2** | 2.764(4) | **As1A-As2-As3** | 87.78(9) |
| **As2-As3** | 2.3295(11) | **As2-As3-As4A** | 96.17(11) |
| **As3-As4A** | 2.465(4) | **As3-As4A-As1A** | 90.95(14) |
| **As4A-As1** | 2.507(7) | **As4A-As1A-As2** | 85.09(13) |
| **As1A-Br1** | 2.520(4) | **As4A-As1A-Br1** | 75.30(19) |
| **As4A···Br1** | 3.070(4) | **As3-As4A-Br1** | 143.50(2) |

## Compound 10

The asymmetric unit contains one molecule of $[(Cp^*Fe)(Cp'''Co)(\mu,\eta^5{:}\eta^5\text{-}As_5)]^{2+}$ and two molecules of the $FeCl_4^-$ anion.

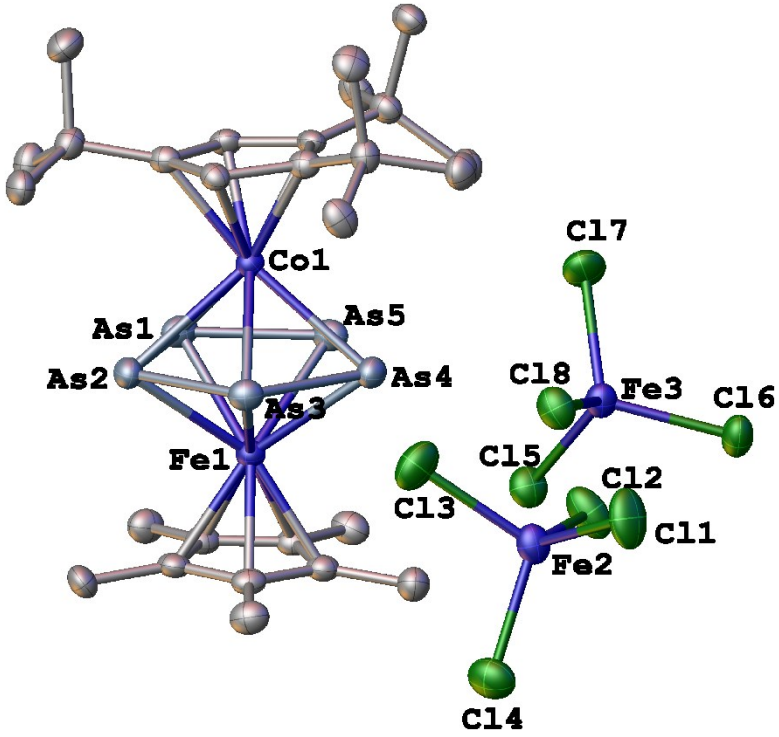


| Selected bond length [Å] | | Selected bond angles [°] | |
|---|---|---|---|
| **As1-As2** | 2.3595(11) | **As2-As1-As5** | 107.38(4) |
| **As2-As3** | 2.3491(10) | **As1-As2-As3** | 108.75(4) |
| **As3-As4** | 2.3586(10) | **As2-As3-As4** | 107.37(4) |
| **As4-As5** | 2.3565(10) | **As3-As4-As5** | 108.14(4) |
| **As5-As1** | 2.3486(11) | **As4-As5-As1** | 108.27(4) |

## DFT calculations

The DFT calculations have been performed with the ORCA program.[6] The geometries have been optimised at the TPSSh[7]/def2-TZVP[8] level of theory starting from the X-ray coordinates. The dispersion effects have been incorporated by using the charge dependent atom-pairwise dispersion correction D4[9] as implemented in Orca. The solvation effects were incorporated via the CPCM model[10] using the dielectric constant of dichloromethane. For the geometry optimisations, the RIJCOSX[11] approximation has been used, followed by a single point calculation without the RIJCOX approximation. The NBO analysis has been performed with NBO6.[12]

**Table S 24**. Total energies of complexes **2-12** calculated at the D4-TPSSh(CPM)/def2-TZVP level of theory.

| Compound | Total energy (Hartree) |
|---|---|
| [(Cp*Fe)(Cp'''Co)(μ-PI)(μ,η²:η¹:η¹-P₄I₄)]⁺ (cation in **2**) | -6897.847354334273 |
| [(Cp*Fe)(Cp'''Co)(μ-PBr)(μ,η²:η¹:η¹-P₄Br₄)]⁺ (cation in **3**) | -18280.106404458602 |
| [(Cp*Fe)(Cp'''Co)(μ-$PCl_2$)(μ,η²:η¹:η¹-$P_4Cl_4$)] (**4**) | -8171.336918689756 |
| [(Cp*Fe)(Cp'''Co)(μ-$PCl_2$)₂(μ,η¹:η¹-$P_2Cl_3$)] (**5**) | -8290.160876657630 |

Cartesian coordinates od the optimizes geometry of [(Cp*Fe)(Cp'''Co)(μ-PI)(μ,η²:η¹:η¹-P₄I₄)]⁺ (cation in **2**) at the D4-TPSSh(CPCM)/def2-TZVP level of theory.

| | | | |
|---|---|---|---|
| Fe | 8.871792000 | 12.810438000 | 9.350064000 |
| Co | 7.413951000 | 13.709625000 | 12.804856000 |
| P | 8.872121000 | 11.240566000 | 10.790618000 |
| P | 7.495826000 | 11.477100000 | 12.503990000 |
| P | 5.917984000 | 12.592792000 | 11.542759000 |
| P | 6.752685000 | 12.824880000 | 9.520168000 |
| P | 8.755678000 | 13.927629000 | 11.188355000 |
| I | 11.013257000 | 10.916549000 | 11.954183000 |
| I | 8.296839000 | 8.911062000 | 10.209109000 |
| I | 5.353433000 | 11.160487000 | 8.367585000 |
| I | 5.571472000 | 14.900963000 | 8.910513000 |
| I | 10.580122000 | 15.487339000 | 11.624463000 |
| C | 10.786630000 | 13.269052000 | 8.503600000 |
| C | 5.831693000 | 14.435323000 | 13.932778000 |
| C | 10.422664000 | 11.930567000 | 8.168069000 |
| C | 6.640157000 | 15.523594000 | 13.531181000 |
| C | 12.114339000 | 13.646659000 | 9.071926000 |
| H | 12.222802000 | 14.725129000 | 9.160333000 |
| H | 12.288450000 | 13.196733000 | 10.051131000 |
| H | 12.894331000 | 13.280455000 | 8.397151000 |
| C | 6.173307000 | 16.804449000 | 12.887010000 |
| C | 11.277077000 | 10.720801000 | 8.324097000 |
| H | 10.687206000 | 9.824741000 | 8.520926000 |
| H | 11.808219000 | 10.560726000 | 7.379132000 |
| H | 12.019367000 | 10.839699000 | 9.110466000 |
| C | 4.749888000 | 16.648132000 | 12.342552000 |
| H | 4.038610000 | 16.462028000 | 13.151088000 |
| H | 4.448731000 | 17.567182000 | 11.834820000 |
| H | 4.684980000 | 15.826300000 | 11.627442000 |
| C | 7.124545000 | 17.270039000 | 11.781821000 |
| H | 7.167395000 | 16.536657000 | 10.974138000 |
| H | 6.773199000 | 18.218436000 | 11.368128000 |
| H | 8.134987000 | 17.422053000 | 12.166734000 |
| C | 6.162352000 | 17.863916000 | 14.014490000 |
| H | 7.167739000 | 18.027058000 | 14.409970000 |

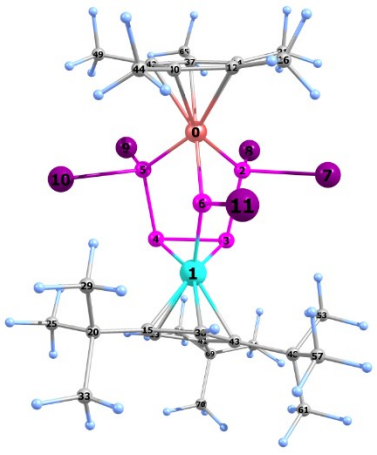

| | | | |
|---|---|---|---|
| H | 5.787461000 | 18.810778000 | 13.617564000 |
| H | 5.512501000 | 17.552006000 | 14.835436000 |
| C | 9.200623000 | 11.963800000 | 7.432551000 |
| C | 7.933607000 | 15.246635000 | 14.065104000 |
| H | 8.797964000 | 15.873399000 | 13.924649000 |
| C | 9.779091000 | 14.142681000 | 7.971194000 |
| C | 6.571684000 | 13.515508000 | 14.750910000 |
| C | 8.820587000 | 13.334409000 | 7.284258000 |
| C | 7.919455000 | 14.055989000 | 14.854287000 |
| C | 9.798065000 | 15.633484000 | 7.953357000 |
| H | 10.388138000 | 16.040052000 | 8.772592000 |
| H | 8.789384000 | 16.043836000 | 8.016432000 |
| H | 10.242897000 | 15.979163000 | 7.014425000 |
| C | 9.119479000 | 13.657274000 | 15.707234000 |
| C | 7.751794000 | 13.822739000 | 6.368497000 |
| H | 6.847254000 | 13.214757000 | 6.418561000 |
| H | 8.135575000 | 13.755415000 | 5.344578000 |
| H | 7.489181000 | 14.860425000 | 6.561621000 |
| C | 9.686314000 | 12.285060000 | 15.327607000 |
| H | 8.951801000 | 11.487565000 | 15.391343000 |
| H | 10.520507000 | 12.038800000 | 15.989884000 |
| H | 10.061008000 | 12.316993000 | 14.304579000 |
| C | 10.255022000 | 14.678954000 | 15.526748000 |
| H | 10.607213000 | 14.715837000 | 14.494540000 |
| H | 11.094987000 | 14.380310000 | 16.157442000 |
| H | 9.945993000 | 15.682572000 | 15.828943000 |
| C | 8.733236000 | 13.709184000 | 17.199180000 |
| H | 8.380968000 | 14.707610000 | 17.469910000 |
| H | 9.620254000 | 13.483881000 | 17.796687000 |
| H | 7.962338000 | 12.991564000 | 17.466690000 |
| C | 8.597655000 | 10.794795000 | 6.732448000 |
| H | 9.258698000 | 10.499362000 | 5.910722000 |
| H | 8.489227000 | 9.934282000 | 7.393749000 |
| H | 7.623998000 | 11.035063000 | 6.311102000 |
| C | 5.793544000 | 12.431987000 | 15.502986000 |
| C | 5.180973000 | 13.154790000 | 16.727445000 |
| H | 4.524240000 | 13.965966000 | 16.404829000 |
| H | 4.588320000 | 12.439872000 | 17.303880000 |
| H | 5.947556000 | 13.573551000 | 17.379437000 |
| C | 6.569973000 | 11.196765000 | 15.972208000 |
| H | 7.358017000 | 11.424680000 | 16.684620000 |
| H | 5.865349000 | 10.527274000 | 16.471036000 |
| H | 7.002572000 | 10.657625000 | 15.128090000 |
| C | 4.624374000 | 11.898769000 | 14.654379000 |
| H | 4.982002000 | 11.359485000 | 13.773977000 |
| H | 4.053989000 | 11.192443000 | 15.261355000 |
| H | 3.937747000 | 12.680555000 | 14.330693000 |
| H | 4.792502000 | 14.323426000 | 13.676306000 |

Cartesian coordinates od the optimizes geometry of [(Cp*Fe)(Cp'''Co)($\mu$-PBr)($\mu$,$\eta^2$:$\eta^1$:$\eta^1$-$P_4Br_4$)]$^+$ (cation in **3**) at the D4-TPSSh(CPCM)/def2-TZVP level of theory.

| | | | |
|---|---|---|---|
| Fe | 6.824609000 | 7.305947000 | 5.976741000 |
| Co | 7.056174000 | 9.212390000 | 2.689114000 |
| P | 6.129849000 | 6.264341000 | 4.275868000 |
| P | 6.796391000 | 6.999520000 | 2.314871000 |
| P | 8.750595000 | 7.739230000 | 2.845163000 |
| P | 8.718182000 | 7.356242000 | 5.010157000 |
| P | 6.414853000 | 8.922796000 | 4.662068000 |
| Br | 3.918952000 | 6.281315000 | 3.909165000 |
| Br | 6.568513000 | 4.079125000 | 4.027973000 |
| Br | 10.072430000 | 5.580815000 | 5.130656000 |
| Br | 10.144522000 | 8.967292000 | 5.645348000 |
| Br | 4.869094000 | 10.356985000 | 5.369859000 |
| C | 6.176169000 | 10.998142000 | 2.275350000 |
| H | 5.423704000 | 11.453221000 | 2.897167000 |
| C | 5.392351000 | 7.500705000 | 7.543032000 |
| C | 5.689100000 | 6.119451000 | 7.333430000 |
| C | 7.085789000 | 5.917500000 | 7.553302000 |
| C | 6.613220000 | 8.163066000 | 7.901866000 |
| C | 7.652912000 | 7.179258000 | 7.925022000 |

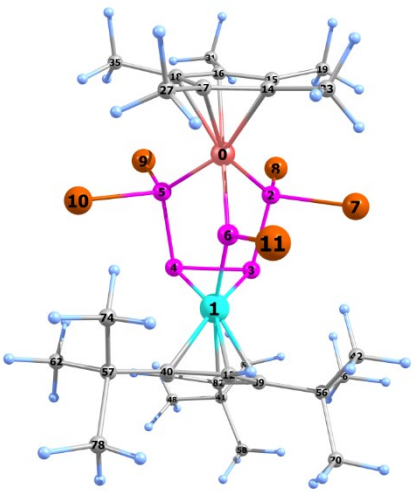

| | | | |
|---|---|---|---|
| C | 4.681898000 | 5.037184000 | 7.147827000 |
| H | 4.410191000 | 4.655936000 | 8.138456000 |
| H | 5.078485000 | 4.201499000 | 6.571879000 |
| H | 3.773977000 | 5.401506000 | 6.670951000 |
| C | 4.005795000 | 8.050734000 | 7.613342000 |
| H | 3.450981000 | 7.894171000 | 6.687234000 |
| H | 4.004353000 | 9.113349000 | 7.844202000 |
| H | 3.469222000 | 7.528207000 | 8.411515000 |
| C | 6.756765000 | 9.580095000 | 8.345000000 |
| H | 6.017569000 | 10.226568000 | 7.875733000 |
| H | 7.750771000 | 9.968296000 | 8.121478000 |
| H | 6.608099000 | 9.635035000 | 9.428581000 |
| C | 7.758209000 | 4.588324000 | 7.625509000 |
| H | 7.423449000 | 4.078221000 | 8.535005000 |
| H | 8.840698000 | 4.684921000 | 7.673052000 |
| H | 7.500994000 | 3.954347000 | 6.776996000 |
| C | 9.032645000 | 7.370266000 | 8.457380000 |
| H | 9.036990000 | 7.054002000 | 9.506036000 |
| H | 9.344153000 | 8.411775000 | 8.419385000 |
| H | 9.768182000 | 6.762844000 | 7.929522000 |
| C | 5.895613000 | 10.101152000 | 1.193267000 |
| C | 7.583264000 | 11.216804000 | 2.407547000 |
| C | 7.609376000 | 9.049137000 | -0.686132000 |
| C | 3.552043000 | 9.803974000 | 2.036645000 |
| H | 2.532407000 | 9.564471000 | 1.727208000 |
| H | 3.524353000 | 10.763825000 | 2.553152000 |
| H | 3.885040000 | 9.037743000 | 2.738030000 |
| C | 8.175829000 | 10.404172000 | 1.413693000 |
| H | 9.235993000 | 10.304694000 | 1.266372000 |
| C | 9.131977000 | 9.186805000 | -0.872154000 |
| H | 9.683922000 | 8.686779000 | -0.072290000 |
| H | 9.446668000 | 10.231686000 | -0.920398000 |
| H | 9.407054000 | 8.707726000 | -1.813969000 |
| C | 7.312746000 | 7.548453000 | -0.815393000 |
| H | 7.554657000 | 7.238643000 | -1.835651000 |
| H | 6.279906000 | 7.282681000 | -0.614628000 |
| H | 7.952480000 | 6.973913000 | -0.141386000 |
| C | 4.451082000 | 9.831462000 | 0.789391000 |
| C | 8.315838000 | 12.217342000 | 3.270155000 |
| C | 6.950224000 | 9.826092000 | -1.844437000 |
| H | 7.380334000 | 9.478073000 | -2.786800000 |
| H | 7.142908000 | 10.897596000 | -1.753372000 |
| H | 5.873883000 | 9.671652000 | -1.889553000 |
| C | 9.828928000 | 11.993354000 | 3.171355000 |
| H | 10.191027000 | 12.169055000 | 2.155644000 |
| H | 10.100661000 | 10.978325000 | 3.467879000 |
| H | 10.342600000 | 12.690978000 | 3.835799000 |
| C | 4.214638000 | 8.509208000 | 0.054937000 |
| H | 4.552481000 | 7.662339000 | 0.656454000 |
| H | 4.703801000 | 8.467942000 | -0.915165000 |
| H | 3.141709000 | 8.394448000 | -0.115609000 |
| C | 4.002134000 | 11.019565000 | -0.089933000 |
| H | 2.956493000 | 10.881192000 | -0.376492000 |
| H | 4.599095000 | 11.104423000 | -0.998139000 |
| H | 4.087478000 | 11.956014000 | 0.466684000 |
| C | 7.881574000 | 12.167214000 | 4.736340000 |
| H | 6.816148000 | 12.370029000 | 4.847010000 |
| H | 8.430729000 | 12.923145000 | 5.302335000 |
| H | 8.100580000 | 11.189760000 | 5.173500000 |
| C | 7.979050000 | 13.617379000 | 2.707667000 |
| H | 8.256669000 | 13.692477000 | 1.653728000 |
| H | 8.537291000 | 14.371968000 | 3.266949000 |
| H | 6.912494000 | 13.832556000 | 2.807676000 |
| C | 7.186786000 | 9.730831000 | 0.625150000 |

**Mayer bond orders larger than 0.100000**

B( 0-Fe, 1-Co) : 0.1202 B( 0-Fe, 2-P ) : 0.9429 B( 0-Fe, 3-P ) : 0.1017
B( 0-Fe, 5-P ) : 0.9589 B( 0-Fe, 6-P ) : 1.0268 B( 0-Fe, 14-C ) : 0.4713
B( 0-Fe, 15-C ) : 0.3777 B( 0-Fe, 16-C ) : 0.5191 B( 0-Fe, 17-C ) : 0.4304
B( 0-Fe, 18-C ) : 0.3994 B( 1-Co, 3-P ) : 0.6409 B( 1-Co, 4-P ) : 0.6613

```
B(  1-Co,  6-P ) :   1.0999 B(  1-Co, 12-C ) :   0.5853 B(  1-Co, 39-C ) :   0.2697
B(  1-Co, 40-C ) :   0.2815 B(  1-Co, 46-C ) :   0.5589 B(  1-Co, 82-C ) :   0.3455
B(  2-P ,  3-P ) :   0.9423 B(  2-P ,  6-P ) :   0.1693 B(  2-P ,  7-Br) :   1.0030
B(  2-P ,  8-Br) :   0.9822 B(  3-P ,  4-P ) :   1.0540 B(  3-P ,  6-P ) :   0.1106
B(  4-P ,  5-P ) :   0.9652 B(  4-P , 46-C ) :   0.1846 B(  4-P , 82-C ) :  -0.1160
B(  5-P ,  9-Br) :   0.9993 B(  5-P , 10-Br) :   1.0006 B(  6-P , 11-Br) :   0.9796


********************************** NBO 6.0 **********************************

166. (1.82412) BD ( 1)Fe  1- P  3
               ( 35.38%)   0.5948*Fe  1 s( 31.67%)p 0.00(  0.08%)d 2.16( 68.25%)
               ( 64.62%)   0.8038* P  3 s( 47.95%)p 1.08( 51.73%)d 0.01(  0.29%)
167. (1.83360) BD ( 1)Fe  1- P  6
               ( 34.18%)   0.5847*Fe  1 s( 31.88%)p 0.00(  0.09%)d 2.13( 68.03%)
               ( 65.82%)   0.8113* P  6 s( 48.32%)p 1.06( 51.40%)d 0.01(  0.26%)
168. (1.79693) BD ( 1)Fe  1- P  7
               ( 36.73%)   0.6061*Fe  1 s( 33.74%)p 0.00(  0.13%)d 1.96( 66.13%)
               ( 63.27%)   0.7954* P  7 s( 44.76%)p 1.23( 54.98%)d 0.01(  0.23%)
169. (1.65372) BD ( 1)Co  2- P  4
               ( 51.73%)   0.7192*Co  2 s( 27.37%)p 0.01(  0.27%)d 2.64( 72.36%)
               ( 48.27%)   0.6948* P  4 s(  8.44%)p10.71( 90.44%)d 0.13(  1.10%)
170. (1.71000) BD ( 1)Co  2- P  5
               ( 50.72%)   0.7122*Co  2 s( 24.68%)p 0.01(  0.27%)d 3.04( 75.05%)
               ( 49.28%)   0.7020* P  5 s(  8.72%)p10.33( 90.10%)d 0.13(  1.16%)
171. (1.85744) BD ( 1)Co  2- P  7
               ( 30.77%)   0.5547*Co  2 s( 43.38%)p 0.01(  0.25%)d 1.30( 56.37%)
               ( 69.23%)   0.8320* P  7 s( 42.71%)p 1.34( 57.02%)d 0.01(  0.25%)
172. (1.95337) BD ( 1) P  3- P  4
               ( 56.18%)   0.7496* P  3 s( 25.98%)p 2.82( 73.15%)d 0.03(  0.86%)
               ( 43.82%)   0.6619* P  4 s( 10.93%)p 8.01( 87.59%)d 0.13(  1.45%)
175. (1.91694) BD ( 1) P  4- P  5
               ( 50.03%)   0.7073* P  4 s( 11.73%)p 7.40( 86.79%)d 0.12(  1.46%)
               ( 49.97%)   0.7069* P  5 s( 12.33%)p 6.98( 86.02%)d 0.13(  1.63%)
176. (1.95214) BD ( 1) P  5- P  6
               ( 43.94%)   0.6629* P  5 s( 11.32%)p 7.69( 87.10%)d 0.14(  1.56%)
               ( 56.06%)   0.7487* P  6 s( 25.21%)p 2.93( 73.96%)d 0.03(  0.81%)
---------------- non-Lewis ----------------------------------------------------
 255. (0.86282) LV ( 1) P  7            s(  0.19%)p99.99( 99.73%)d 0.26(  0.05%)
```

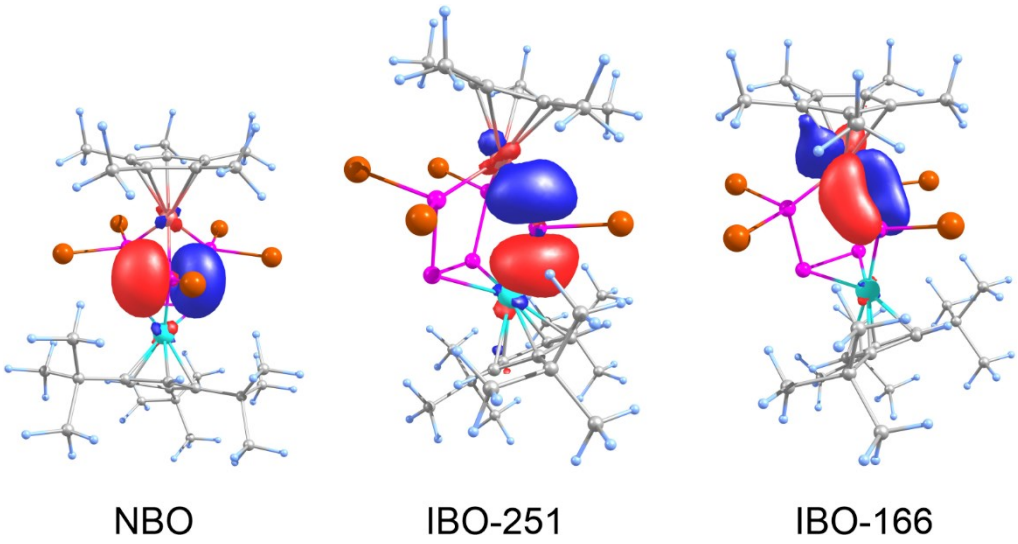


**Figure S 51**. Selected Natural Bonding Orbital, representing the empty p orbital of the PBr ligand (left; NBO 255) and Intrinsic Bonding Orbitals representing the BrPFeCo bonding (right and middle).

```
IBO 251:  0Fe- 0.191 1Co- 0.147 6P - 0.580
IBO 166:   6P  -   0.136772  and   0Fe -   0.727891
```

# 6. SI Halogenation of heterobimetallic triple-decker complexes containing $P_5$ and $As_5$ middle deck

Cartesian coordinates od the optimizes geometry of [(Cp*Fe)(Cp'''Co)($\mu$-$PCl_2$)($\mu$,$\eta^2$:$\eta^1$:$\eta^1$-$P_4Cl_4$)] (**4**) at the D4-TPSSh(CPCM)/def2-TZVP level of theory.

| | | | |
|---|---|---|---|
| Fe | 0.391823000 | 1.785753000 | 13.316156000 |
| Co | 1.776021000 | 3.152792000 | 9.959842000 |
| P | 1.890689000 | 3.252961000 | 13.449667000 |
| P | 2.274891000 | 4.490800000 | 11.681125000 |
| P | 0.260185000 | 4.514171000 | 10.865524000 |
| P | -0.735267000 | 3.294202000 | 12.383359000 |
| P | 1.194703000 | 1.515135000 | 11.279846000 |
| Cl | 3.832315000 | 2.688901000 | 13.952751000 |
| Cl | 1.703113000 | 4.762617000 | 14.891282000 |
| Cl | -1.553842000 | 4.833443000 | 13.546544000 |
| Cl | -2.484532000 | 2.813606000 | 11.355403000 |
| Cl | -0.113688000 | 0.206151000 | 10.248487000 |
| Cl | 2.808933000 | 0.145667000 | 11.388171000 |
| C | 3.133664000 | 4.172888000 | 8.793811000 |
| H | 3.730486000 | 5.003220000 | 9.132206000 |
| C | 1.069925000 | 0.281959000 | 14.655703000 |
| C | 1.397725000 | 2.951216000 | 7.882949000 |
| C | 1.845953000 | 4.301302000 | 8.180512000 |
| C | 3.540784000 | 2.816852000 | 8.861108000 |
| C | 2.441540000 | 2.076061000 | 8.343300000 |
| H | 2.404078000 | 1.000810000 | 8.281977000 |
| C | 1.380934000 | 5.701638000 | 7.765985000 |
| C | 0.349381000 | 1.297833000 | 15.374820000 |
| C | 0.209615000 | 2.428275000 | 7.073127000 |
| C | 1.920436000 | 6.763261000 | 8.745194000 |
| H | 1.578749000 | 6.582552000 | 9.767435000 |
| H | 1.547358000 | 7.742483000 | 8.436629000 |
| H | 3.009943000 | 6.813673000 | 8.744340000 |
| C | -1.137539000 | 2.668191000 | 7.772444000 |
| H | -1.170253000 | 2.130386000 | 8.718817000 |
| H | -1.948770000 | 2.302120000 | 7.135794000 |
| H | -1.313592000 | 3.720755000 | 7.980952000 |
| C | 0.207544000 | 3.053632000 | 5.663117000 |
| H | -0.044859000 | 4.111006000 | 5.659849000 |
| H | -0.536289000 | 2.535129000 | 5.052440000 |
| H | 1.182948000 | 2.931645000 | 5.185497000 |
| C | 2.431790000 | -0.233727000 | 14.984507000 |
| H | 2.983855000 | -0.503879000 | 14.084740000 |
| H | 2.337535000 | -1.132483000 | 15.604212000 |
| H | 3.014946000 | 0.496567000 | 15.542068000 |
| C | 2.043869000 | 5.978932000 | 6.395946000 |
| H | 3.131109000 | 5.901017000 | 6.475949000 |
| H | 1.792505000 | 6.993320000 | 6.073356000 |
| H | 1.707291000 | 5.280742000 | 5.630640000 |
| C | 0.844814000 | 2.017611000 | 16.584763000 |
| H | 1.918462000 | 2.201955000 | 16.541253000 |
| H | 0.647598000 | 1.395940000 | 17.465226000 |
| H | 0.337429000 | 2.970605000 | 16.725590000 |
| C | -0.130362000 | 5.933821000 | 7.655900000 |
| H | -0.608007000 | 5.296678000 | 6.917337000 |
| H | -0.296687000 | 6.969687000 | 7.347490000 |
| H | -0.623627000 | 5.782133000 | 8.616994000 |
| C | 0.358061000 | 0.914476000 | 6.836021000 |
| H | 1.265313000 | 0.692418000 | 6.267575000 |
| H | -0.497914000 | 0.568873000 | 6.251451000 |
| H | 0.379007000 | 0.351912000 | 7.767239000 |
| C | 4.950402000 | 2.358746000 | 9.180175000 |
| C | 5.317806000 | 2.651550000 | 10.639776000 |
| H | 6.353764000 | 2.354151000 | 10.829429000 |
| H | 4.667013000 | 2.105605000 | 11.319398000 |
| H | 5.219494000 | 3.717918000 | 10.858873000 |
| C | 5.901178000 | 3.158947000 | 8.263741000 |
| H | 5.855264000 | 4.228265000 | 8.482565000 |
| H | 5.648040000 | 3.009639000 | 7.210875000 |
| H | 6.929327000 | 2.822374000 | 8.422731000 |
| C | 5.133586000 | 0.869830000 | 8.867991000 |
| H | 6.154622000 | 0.570122000 | 9.119105000 |
| H | 4.972138000 | 0.672901000 | 7.804303000 |
| H | 4.447076000 | 0.249575000 | 9.441902000 |
| C | 0.404710000 | -1.600848000 | 13.007930000 |
| H | -0.255890000 | -1.713936000 | 12.151416000 |
| H | 0.195095000 | -2.418876000 | 13.707362000 |
| H | 1.435452000 | -1.701472000 | 12.673992000 |

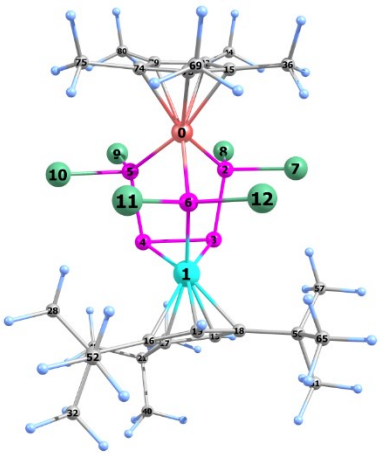

```
C         0.165869000     -0.320444000     13.734006000
C        -1.085303000      0.352281000     13.826298000
C        -2.344232000     -0.069535000     13.145611000
H        -3.096611000      0.716263000     13.171972000
H        -2.755099000     -0.945541000     13.659733000
H        -2.164733000     -0.342117000     12.105900000
C        -0.975909000      1.344491000     14.862109000
C        -2.111575000      2.127247000     15.432189000
H        -1.777108000      3.064389000     15.875061000
H        -2.590669000      1.533501000     16.218367000
H        -2.867201000      2.352791000     14.680069000
```

```
  Mayer bond orders larger than 0.100000
B(  0-Fe,  2-P ) :   1.0206 B(  0-Fe,  5-P ) :   1.0248 B(  0-Fe,  6-P ) :   0.8863
B(  0-Fe, 15-C ) :   0.5025 B(  0-Fe, 22-C ) :   0.3829 B(  0-Fe, 73-C ) :   0.3365
B(  0-Fe, 74-C ) :   0.4952 B(  0-Fe, 79-C ) :   0.3886 B(  1-Co,  3-P ) :   0.6853
B(  1-Co,  4-P ) :   0.6953 B(  1-Co,  6-P ) :   0.8651 B(  1-Co, 13-C ) :   0.5485
B(  1-Co, 16-C ) :   0.3414 B(  1-Co, 17-C ) :   0.3286 B(  1-Co, 18-C ) :   0.2918
B(  1-Co, 19-C ) :   0.5467 B(  2-P ,  3-P ) :   1.0022 B(  2-P ,  7-Cl) :   0.9820
B(  2-P ,  8-Cl) :   0.9530 B(  3-P ,  4-P ) :   1.0177 B(  3-P , 13-C ) :   0.1875
B(  4-P ,  5-P ) :   0.9985 B(  5-P ,  9-Cl) :   0.9592 B(  5-P , 10-Cl) :   0.9844
B(  6-P , 11-Cl) :   0.8816 B(  6-P , 12-Cl) :   0.8796 B( 13-C , 14-H ) :   1.0037
```

```
********************************** NBO 6.0 **********************************
133. (1.91949) BD ( 1)Fe  1- P  6
               ( 43.40%)   0.6588*Fe  1 s(  5.91%)p 0.01(  0.05%)d15.91( 94.04%)
               ( 56.60%)   0.7523* P  6 s( 49.04%)p 1.03( 50.70%)d 0.00(  0.23%)
134. (1.85664) BD ( 1)Co  2- P  4
               ( 56.57%)   0.7521*Co  2 s(  4.39%)p 0.03(  0.14%)d21.75( 95.47%)
               ( 43.43%)   0.6590* P  4 s(  9.85%)p 9.05( 89.18%)d 0.10(  0.95%)
135. (1.86022) BD ( 1)Co  2- P  5
               ( 56.89%)   0.7542*Co  2 s(  4.59%)p 0.03(  0.13%)d20.77( 95.28%)
               ( 43.11%)   0.6566* P  5 s(  9.93%)p 8.97( 89.14%)d 0.09(  0.90%)
136. (1.95611) BD ( 1) P  3- P  4
               ( 56.23%)   0.7499* P  3 s( 32.74%)p 2.03( 66.38%)d 0.03(  0.86%)
               ( 43.77%)   0.6616* P  4 s( 11.48%)p 7.58( 87.07%)d 0.12(  1.43%)
139. (1.90576) BD ( 1) P  4- P  5
               ( 50.12%)   0.7079* P  4 s( 12.08%)p 7.15( 86.44%)d 0.12(  1.46%)
               ( 49.88%)   0.7063* P  5 s( 11.59%)p 7.51( 87.01%)d 0.12(  1.38%)
140. (1.95524) BD ( 1) P  5- P  6
               ( 44.76%)   0.6690* P  5 s( 11.76%)p 7.39( 86.91%)d 0.11(  1.30%)
               ( 55.24%)   0.7433* P  6 s( 26.01%)p 2.81( 73.10%)d 0.03(  0.88%)
```

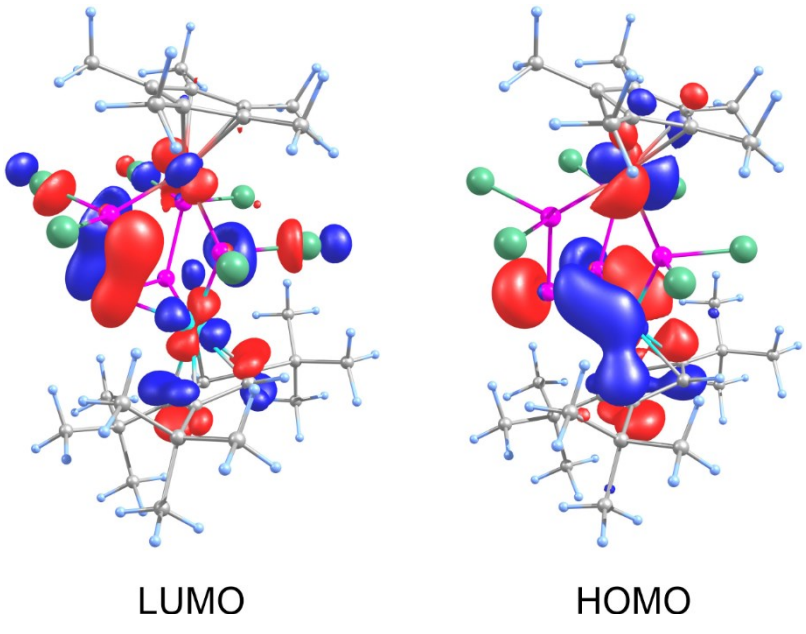


**Figure S 52.** Frontier Molecular Orbitals in [(Cp*Fe)(Cp'''Co)($\mu$-$PCl_2$)($\mu$,$\eta^2$:$\eta^1$:$\eta^1$-$P_4Cl_4$)] (**4**).

# 6. SI Halogenation of heterobimetallic triple-decker complexes containing $P_5$ and $As_5$ middle deck

Cartesian coordinates od the optimizes geometry of [(Cp*Fe)(Cp'''Co)($\mu$-$PCl_2$)$_2$($\mu$,$\eta^1$:$\eta^1$-$P_2Cl_3$)] (**5**) at the D4-TPSSh(CPCM)/def2-TZVP level of theory.

| | | | |
|---|---|---|---|
| Fe | 4.722295000 | 7.013495000 | 12.231814000 |
| Co | 7.427134000 | 4.850891000 | 11.844804000 |
| P | 6.877599000 | 6.938554000 | 12.440123000 |
| P | 5.499829000 | 5.427841000 | 10.980192000 |
| P | 4.661197000 | 5.560031000 | 13.745109000 |
| P | 6.499344000 | 4.284410000 | 13.772592000 |
| Cl | 7.617208000 | 7.616758000 | 14.300845000 |
| Cl | 7.812769000 | 8.430290000 | 11.316769000 |
| Cl | 5.872102000 | 6.034964000 | 8.993741000 |
| Cl | 4.105845000 | 3.924168000 | 10.521049000 |
| Cl | 3.011304000 | 4.314554000 | 13.905185000 |
| Cl | 4.691355000 | 6.121604000 | 15.772334000 |
| Cl | 5.626220000 | 2.371305000 | 13.661360000 |
| C | 9.373397000 | 4.069483000 | 12.360927000 |
| C | 3.376994000 | 8.388629000 | 13.126253000 |
| C | 8.459246000 | 3.040091000 | 11.962631000 |
| H | 8.163421000 | 2.212148000 | 12.582834000 |
| C | 8.040533000 | 3.214976000 | 10.621613000 |
| C | 9.521295000 | 4.933980000 | 11.199423000 |
| C | 4.306690000 | 8.709012000 | 11.034035000 |
| C | 8.646987000 | 4.427113000 | 10.194460000 |
| H | 8.523930000 | 4.860965000 | 9.217805000 |
| C | 4.385819000 | 9.092288000 | 12.413752000 |
| C | 3.243174000 | 7.760017000 | 10.907052000 |
| C | 10.555221000 | 5.981481000 | 10.797376000 |
| C | 10.117052000 | 3.951435000 | 13.699040000 |
| C | 2.669669000 | 7.555650000 | 12.190418000 |
| C | 6.514899000 | 1.198448000 | 10.476981000 |
| H | 6.999286000 | 0.731549000 | 11.337443000 |
| H | 6.192325000 | 0.401334000 | 9.801994000 |
| H | 5.635989000 | 1.735059000 | 10.828449000 |
| C | 7.476637000 | 2.127575000 | 9.732855000 |
| C | 10.957680000 | 6.972194000 | 11.893791000 |
| H | 10.094558000 | 7.473395000 | 12.329175000 |
| H | 11.610744000 | 7.733545000 | 11.460136000 |
| H | 11.514380000 | 6.481303000 | 12.690592000 |
| C | 2.698093000 | 7.217670000 | 9.628166000 |
| H | 3.428544000 | 7.276594000 | 8.823866000 |
| H | 1.823472000 | 7.809468000 | 9.336140000 |
| H | 2.377166000 | 6.180658000 | 9.731620000 |
| C | 5.006961000 | 9.367359000 | 9.890959000 |
| H | 5.795540000 | 10.032062000 | 10.237049000 |
| H | 4.281224000 | 9.966575000 | 9.330395000 |
| H | 5.443470000 | 8.643378000 | 9.203658000 |
| C | 2.989996000 | 8.638266000 | 14.545300000 |
| H | 2.483552000 | 7.781799000 | 14.988310000 |
| H | 2.300275000 | 9.489126000 | 14.580118000 |
| H | 3.854232000 | 8.882916000 | 15.161794000 |
| C | 11.622817000 | 3.736294000 | 13.456019000 |
| H | 11.798879000 | 2.956079000 | 12.711745000 |
| H | 12.085461000 | 3.420817000 | 14.395075000 |
| H | 12.122868000 | 4.648110000 | 13.134047000 |
| C | 9.913932000 | 5.148427000 | 14.634249000 |
| H | 10.158412000 | 6.095740000 | 14.162244000 |
| H | 10.553150000 | 5.024188000 | 15.513287000 |
| H | 8.877584000 | 5.195341000 | 14.968828000 |
| C | 9.629996000 | 2.704682000 | 14.461839000 |
| H | 8.560213000 | 2.749516000 | 14.680587000 |
| H | 10.160511000 | 2.657495000 | 15.415548000 |
| H | 9.840747000 | 1.783705000 | 13.913017000 |
| C | 6.819417000 | 2.668587000 | 8.460469000 |
| H | 5.918226000 | 3.236300000 | 8.681299000 |
| H | 6.545172000 | 1.827686000 | 7.818066000 |
| H | 7.503348000 | 3.309857000 | 7.899539000 |
| C | 10.088583000 | 6.742903000 | 9.538470000 |
| H | 10.148154000 | 6.100754000 | 8.657036000 |
| H | 10.755676000 | 7.591621000 | 9.373660000 |
| H | 9.071826000 | 7.116805000 | 9.624697000 |
| C | 8.722155000 | 1.305407000 | 9.314966000 |
| H | 9.436411000 | 1.927413000 | 8.769707000 |
| H | 8.410025000 | 0.484422000 | 8.663851000 |
| H | 9.224367000 | 0.883523000 | 10.188959000 |
| C | 5.251081000 | 10.165606000 | 12.985240000 |

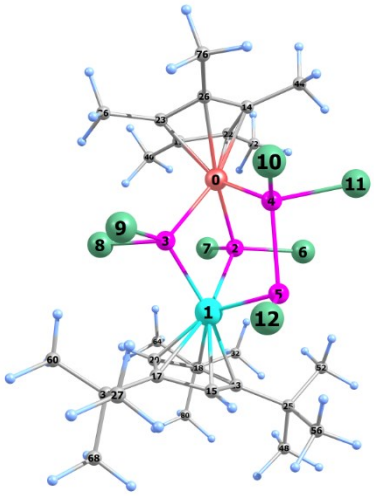

```
H         5.526432000      9.949888000     14.018041000
H         4.703473000     11.114480000     12.972272000
H         6.164483000     10.296963000     12.407958000
C         1.409953000      6.797812000     12.449737000
H         1.373890000      5.867057000     11.883116000
H         0.558192000      7.413311000     12.138471000
H         1.284342000      6.561055000     13.504789000
C        11.816869000      5.202819000     10.344906000
H        12.290418000      4.661050000     11.159897000
H        12.537647000      5.919997000      9.941745000
H        11.563840000      4.492287000      9.554594000
```

```
  Mayer bond orders larger than 0.100000
B(  0-Fe,  2-P ) :   0.9176 B(  0-Fe,  3-P ) :   0.8788 B(  0-Fe,  4-P ) :   1.0466
B(  0-Fe, 14-C ) :   0.4419 B(  0-Fe, 19-C ) :   0.5397 B(  0-Fe, 22-C ) :   0.3430
B(  0-Fe, 23-C ) :   0.3299 B(  0-Fe, 26-C ) :   0.4656 B(  1-Co,  2-P ) :   0.7548
B(  1-Co,  3-P ) :   0.8483 B(  1-Co,  5-P ) :   0.8992 B(  1-Co, 13-C ) :   0.3525
B(  1-Co, 15-C ) :   0.4954 B(  1-Co, 17-C ) :   0.3190 B(  1-Co, 18-C ) :   0.3148
B(  1-Co, 20-C ) :   0.5159 B(  2-P ,  3-P ) :   0.1098 B(  2-P ,  4-P ) :   0.1032
B(  2-P ,  6-Cl) :   0.9224 B(  2-P ,  7-Cl) :   0.9064 B(  3-P ,  4-P ) :   0.1024
B(  3-P ,  8-Cl) :   0.9202 B(  3-P ,  9-Cl) :   0.9343 B(  4-P ,  5-P ) :   0.9566
B(  4-P , 10-Cl) :   1.0183 B(  4-P , 11-Cl) :   0.9637 B(  5-P , 12-Cl) :   0.9638
```

```
********************************** NBO 6.0 *********************************

107. (1.93172) LP ( 1) P  6            s( 68.81%)p 0.45( 31.09%)d 0.00(  0.09%)
135. (1.81224) BD ( 1)Fe  1- P  3
               ( 36.01%)   0.6001*Fe  1 s( 30.94%)p 0.00(  0.10%)d 2.23( 68.96%)
               ( 63.99%)   0.8000* P  3 s( 42.12%)p 1.37( 57.53%)d 0.01(  0.34%)
136. (1.81005) BD ( 1)Fe  1- P  4
               ( 35.97%)   0.5997*Fe  1 s( 30.79%)p 0.00(  0.10%)d 2.24( 69.11%)
               ( 64.03%)   0.8002* P  4 s( 42.02%)p 1.37( 57.64%)d 0.01(  0.33%)
137. (1.85240) BD ( 1)Fe  1- P  5
               ( 32.31%)   0.5684*Fe  1 s( 34.92%)p 0.00(  0.07%)d 1.86( 65.01%)
               ( 67.69%)   0.8227* P  5 s( 48.90%)p 1.04( 50.84%)d 0.00(  0.24%)
138. (1.81172) BD ( 1)Co  2- P  3
               ( 34.84%)   0.5903*Co  2 s( 33.99%)p 0.01(  0.22%)d 1.94( 65.80%)
               ( 65.16%)   0.8072* P  3 s( 34.45%)p 1.89( 65.14%)d 0.01(  0.40%)
139. (1.83014) BD ( 1)Co  2- P  4
               ( 36.61%)   0.6051*Co  2 s( 33.70%)p 0.01(  0.20%)d 1.96( 66.10%)
               ( 63.39%)   0.7962* P  4 s( 34.78%)p 1.86( 64.72%)d 0.01(  0.49%)
140. (1.78266) BD ( 1)Co  2- P  6
               ( 46.27%)   0.6802*Co  2 s( 28.04%)p 0.01(  0.37%)d 2.55( 71.59%)
               ( 53.73%)   0.7330* P  6 s( 14.14%)p 6.02( 85.12%)d 0.05(  0.73%)
145. (1.95849) BD ( 1) P  5- P  6
               ( 55.58%)   0.7455* P  5 s( 24.68%)p 3.01( 74.38%)d 0.04(  0.92%)
               ( 44.42%)   0.6665* P  6 s( 10.80%)p 8.15( 88.05%)d 0.10(  1.13%)
```

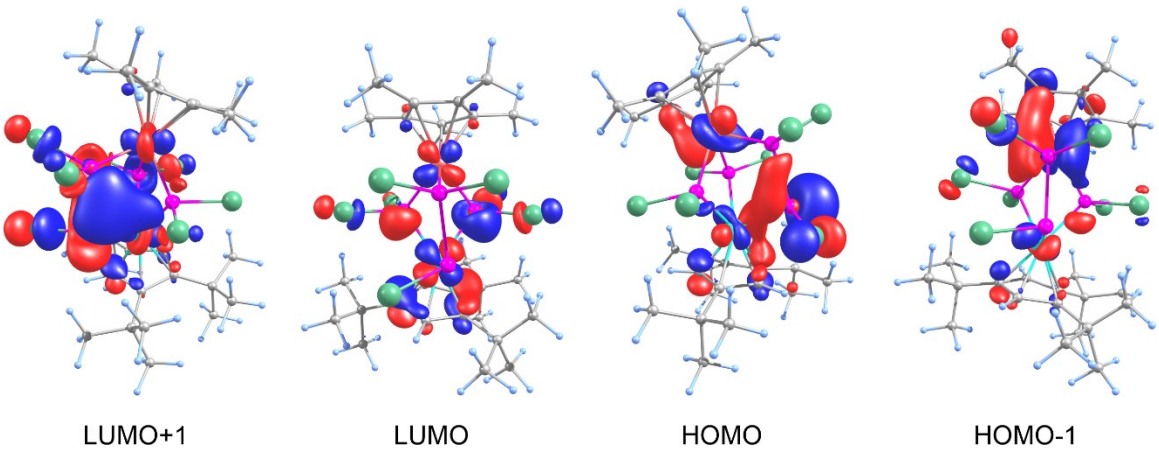


**Figure S 53.** Frontier Molecular Orbitals in [(Cp*Fe)(Cp'''Co)($\mu$-$PCl_2$)$_2$($\mu$,$\eta^1$:$\eta^1$-$P_2Cl_3$)] (**5**).

## Reference


[1] a) M. Piesch, F. Dielmann, S. Reichl, M. Scheer, Chem. Eur. J. 26 (2020) 1518-1524; b) M. Piesch, M. Scheer, Organometallics, 39 (2020) 4247–4252.
[2] CrysAlisPro Software System, Rigaku Oxford Diffraction (2018-2020).
[3] O. V. Dolomanov, L. J. Bourhis, R. J. Gildea, J. A. K. Howard, H. Puschmann, J. Appl. Cryst. 42 (2009) 339–341.
[4] G. M. Sheldrick, Acta Cryst. A71 (2015) 3-8.
[5] G. M. Sheldrick, Acta Cryst. C71 (2015) 3-8.
[6] a) ORCA - An Ab Initio, DFT and Semiempirical electronic structure package, Version 4.2.1; b) F. Neese, WIREs Comput Mol Sci. 2 (2012) 73–78; b) F. Neese, WIREs Comput. Mol. Sci. 8 (2017) e1327.
[7] TPSSh: J. Tao, J. P. Perdew, V. N. Staroverov, G. E. Scuseria, Phys. Rev. Lett. 91 (2003) 146401; V. N. Staroverov, G. E. Scuseria, J. Tao, J. P. Perdew, J. Chem. Phys. 119 (2003) 12129-12137; Erratum: J. Chem. Phys. 121 (2004) 11507-11507.
[8] a) F. Weigend and R. Ahlrichs, Phys. Chem. Chem. Phys. 7 (2005) 3297–3305; b) F. Weigend, M. Häser, H. Patzelt and R. Ahlrichs, Chem. Phys. Lett. 294 (1998) 143–152.
[9] a) E. Caldeweyher, S. Ehlert, A. Hansen, H. Neugebauer, S. Spicher, C. Bannwarth, S. Grimme, J. Chem. Phys. 150 (2019) 154122; b) E. Caldeweyher, C. Bannwarth, S. Grimme, J. Chem. Phys. 147 (2017) 034112.
[10] J. Tomasi, B. Mennucci, R. Cammi, Chem. Rev. 105 (2005) 2999-3094.
[11] F. Neese, F. Wennmohs, A. Hansen and U. Becker, Chem. Phys. 356 (2009) 98–109.
[12] NBO 6.0. E. D. Glendening, J. K. Badenhoop, A. E. Reed, J. E. Carpenter, J. A. Bohmann, C. M. Morales, C. R. Landis, F. Weinhold (Theoretical Chemistry Institute, University of Wisconsin, Madison, WI, 2013); http://nbo6.chem.wisc.edu/

# 7 Thesis treasury

## 7.1 Reactivity of [CpMo(CO)$_2$(η$^3$-P$_3$)] towards I$_2$

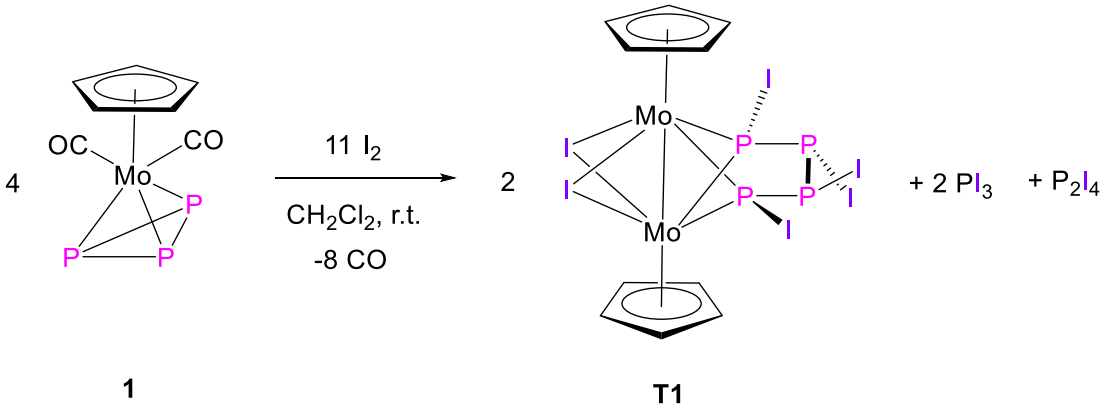


**1** **T1**

**Scheme 1.** Reaction of [CpMo(CO)$_2$(η$^3$-P$_3$)] (**1**) with I$_2$.

The addition of an excess of I$_2$ (3 equiv.) to a solution of [CpMo(CO)$_2$(η$^3$-P$_3$)][1] (**1**, Cp = C$_5$H$_5$) (1 equiv.) in CH$_2$Cl$_2$ at room temperature resulted in an immediate color change from bright yellow to dark brown. After work up, the compound [(CpMo)$_2$(μ-I)$_2$(μ-η$^1$:η$^1$:η$^1$-P$_4$I$_4$)] (**T1**) could be isolated in a crystalline yield of 7%. No signal could be detected in the $^{31}$P NMR spectrum of the solution of the crystals, but this could be partly explained by the low concentration of it, due in turn to the extremely low solubility of this compound in several solvents such as CH$_2$Cl$_2$, THF and CH$_3$CN. In the $^{31}$P NMR spectrum of the reaction solution at room temperature, no signal of **1** is observed, indicating its full conversion, and two singlets centered at δ = 179 and 107 ppm could be detected, corresponding to PI$_3$ and P$_2$I$_4$, respectively. An EPR spectrum of the CH$_2$Cl$_2$ solution of the crystals was recorded but this was silent as well.

The compound **T1** could be characterized by Elemental analysis and fragments could be detected via EI mass spectrometry (cf. SI). The EI-MS spectrum of the reaction solution (CH$_2$Cl$_2$) shows the molecular ion peak of the complex [(CpMo)$_2$(μ-I)$_4$][I$_3$], which was mentioned by Gordon *et. al.*[2] and which was already found as a side-product of the iodination of [{CpMo(CO)$_2$}$_2$(μ,η$^2$:η$^2$-P$_2$)].[3]

When the reaction was performed in the same conditions but with [Cp*Mo(CO)$_2$(η$^3$-P$_3$)] (**1A**, Cp* = C$_5$Me$_5$) as starting material, the $^{31}$P NMR spectrum of the reaction solution (CH$_2$Cl$_2$) at room temperature shows again the two signals for PI$_3$ and P$_2$I$_4$. No analogue of **T1** could be isolated but a few crystals of the paramagnetic complex [(Cp*Mo)$_2$(μ-I)$_4$][I$_3$] crystallizes instead. The latter compound has been already described by Gordon *et.al.*[2]

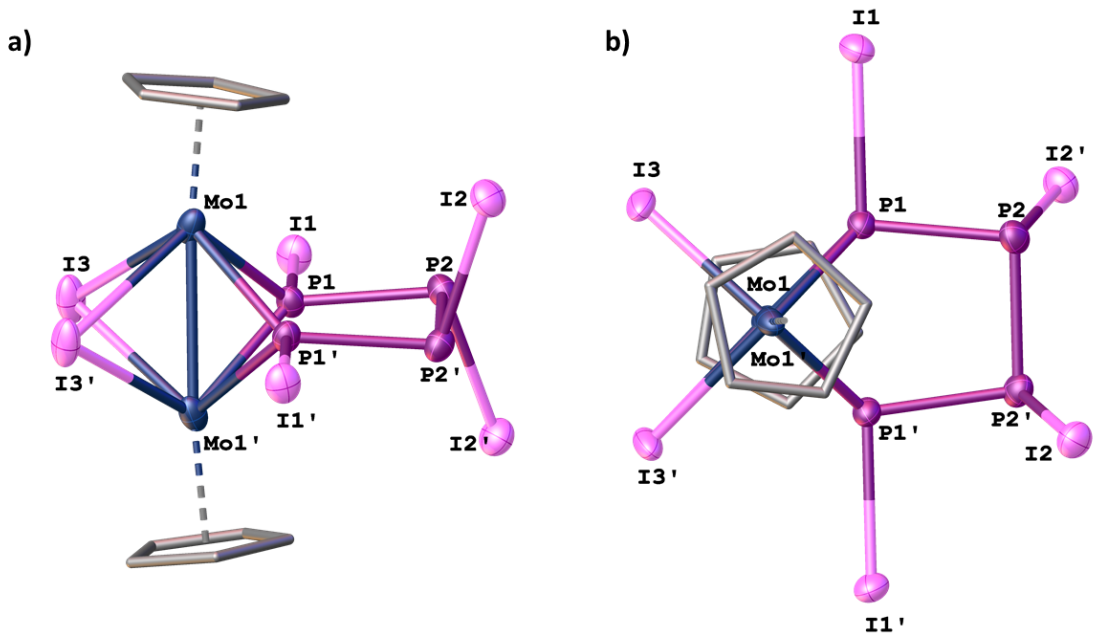


**Figure 1.** Molecular structure of **T2** with atomic displacement parameters at 50% probability level. Hydrogen atoms are omitted for clarity, side view (a) and top view (b).

The molecular structure of $[(CpMo)_2(\mu\text{-}I)_2(\mu\text{-}\eta^1\text{:}\eta^1\text{:}\eta^1\text{-}P_4I_4)]$ is a centrosymmetric dinuclear complex with an unprecedented bridging $P_4I_4$ chain ligand (Figure 1). The P1-P2 (= P1'-P2') (2.209(3) Å) and the P2-P2' (2.238(5) Å) distances lie all in the range of a P-P single bond (2.22 Å)[4] and therefore the ligand cannot be described as a tetraphosphabuta-1,3-diene like as it is in analogue *cisoid*-$P_4$ ligands found in the complexes $[(Cp^RFe)_2(\mu,\eta^4\text{:}\eta^4\text{-}P_4)]$ (R = $Cp^{BIG}$ [5],Cp''[6], $C_5H_3(SiMe_3)_2$)[7]; $Cp^{BIG}$ =($C_5$(4-$^n$Bu$C_6H_4)_5$), Cp'' = $C_5H_3{}^t$Bu$_2$). The Mo1-Mo1' bond length (2.7306(14) Å) is below the sum of their covalent radii (3.08 Å)[8] and the two Cp ligands are not coplanar, being tilted by 38°.

## 7.2 Reactivity of $[CpMo(CO)_2(\eta^3\text{-}P_3)]$ towards $PCl_5$ and $PBr_5$

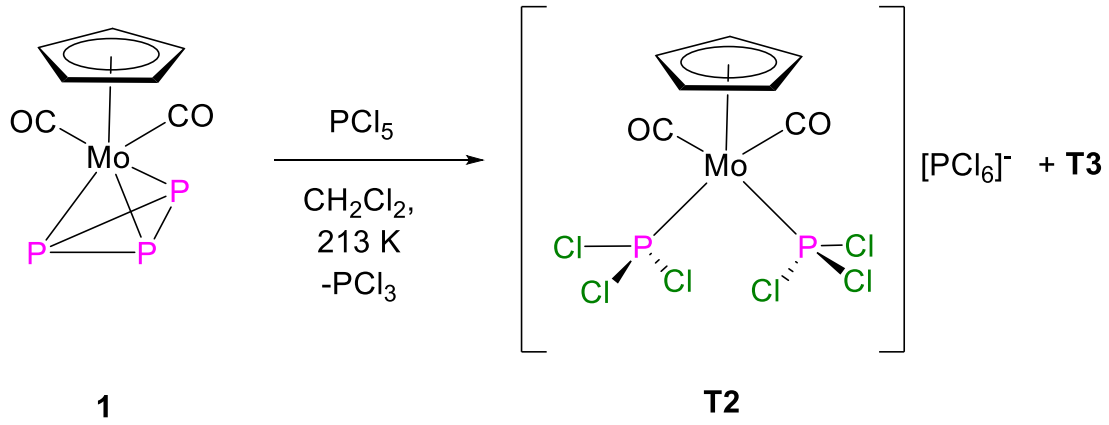


**Scheme 2.** Reaction of $[CpMo(CO)_2(\eta^3\text{-}P_3)]$ (**1**) with $PCl_5$.

When [CpMo(CO)$_2$($\eta^3$-P$_3$)] (**1**) (1 equiv.) is reacted with an excess of $PCl_5$ (3 equiv.) in $CH_2Cl_2$ at room temperature, an immediate color change of the solution from bright yellow to bright red is observed, which in turn switches to dark brown within one hour. The $^{31}$P NMR spectrum of the reaction solution at room temperature shows two singlets, centered at δ = 220 and -353 ppm, corresponding to $PCl_3$ and **1**, respectively. Although the NMR spectrum shows still the signals of **1**, the color change suggests a partial conversion of the starting material and indeed a few crystals in the shape of red blocks could be isolated. They were identified to be the complex [CpMoCl$_4$], originally described by Green *et. al*.[9] When the reaction was repeated al -60°C, a few orange block crystals of the complex [CpMo(CO)$_2$($PCl_3$)$_2$][$PCl_6$] (**T2**) were isolated. To have better insights of the reaction, a time-dependent $^{31}$P NMR investigation was performed at 213 K (Figure 2).

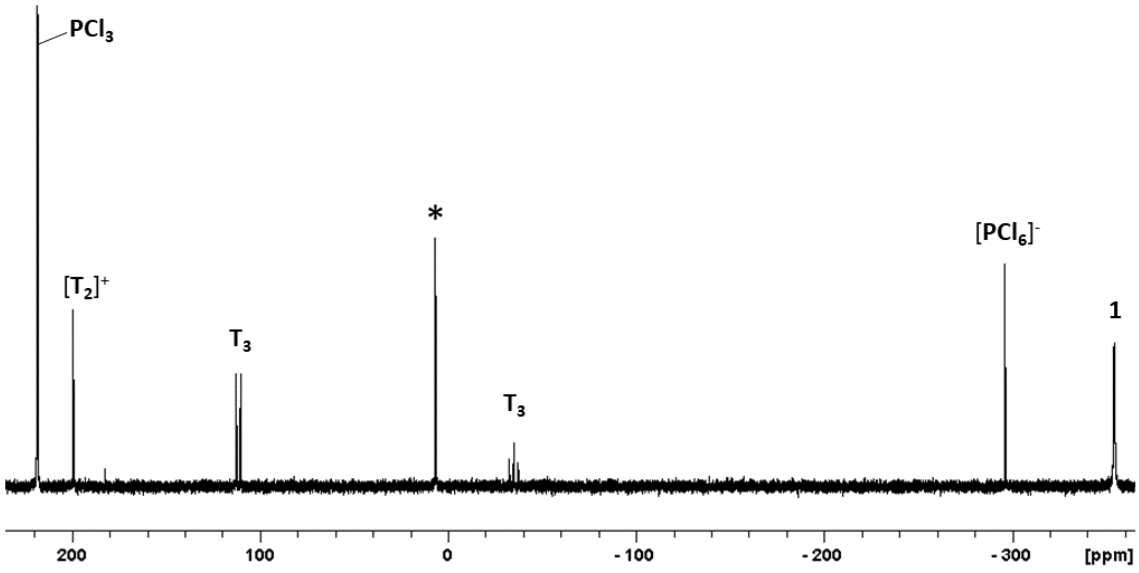


**Figure 2.** $^{31}$P{$^1$H} NMR spectrum of the solution of the reaction between **1** (1 equiv.) and $PCl_5$ (3 equiv.) ($CD_2Cl_2$, 213K). The signal marked with * belongs to an unknown specie.

After 15 minutes ($t_1$), together with the signals of **1** and $PCl_3$, five resonances could be detected, centered at δ = 199, 111, 6, -34 and - 296 ppm. The singlets at 199 and -296 ppm may be assigned to compound **T2** (to the cation [(CpMo)$_2$(CO)$_2$($PCl_3$)$_2$]$^+$ and the anion [$PCl_6$]$^-$, respectively). Among the remaining signals, the singlet at 6 ppm could not be assigned but the other two signals belonging to an $A_2M$ spin system, which suggests the formation of a compound with an allylic-$P_3$ unit (which will be denoted as **T3**). In compound **T3**, the central atom of the allylic-$P_3$ unit ($P^M$) is the one that resonates at -34 ppm (triplet) and it is coupled with the two other P atoms ($P^A$, doublet, δ = 111 ppm) with a $^1J_{PAM}$ of 392 Hz. The formation of an allylic-$P_3$ unit from the *cyclo*-$P_3$ unit of **1** may indicate the formation of an additional halogenated species that could not be isolated so far. Compounds **T2** and

**T3** are stable in solution at -60°C for at least four hours but once room temperature is reached their signals disappear, suggesting their thermal decomposition (cf.SI).

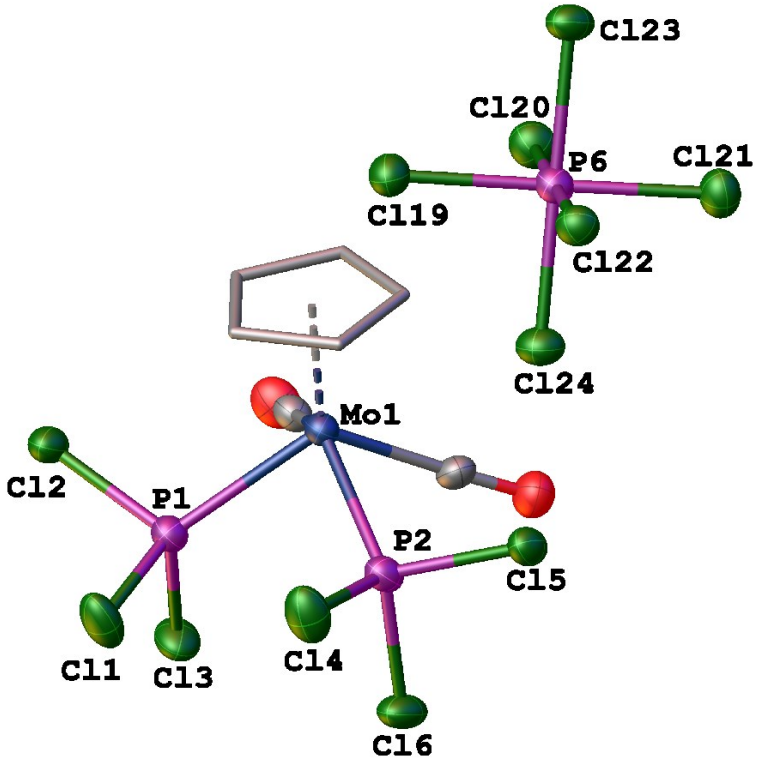


**Figure 3.** Molecular structure of **T2** with atomic displacement parameters at 50% probability level. Hydrogen atoms are omitted for clarity.

The solid state structure of **T2** reveals a mononuclear compound with two terminal $PCl_3$ ligands connected to the {$CpMo(CO)_2$} fragment. The P1···P2 distance of 3.315(4) Å is too long for a bond.

When **1** (1 equiv.) is reacted with an excess of $PBr_5$ (3 equiv.), the $^{31}P$ NMR spectrum of the reaction solution at 213 K shows, together with the signals of $PBr_3$ and **1** (δ = 229 and -353 ppm, respectively) two sets of signals that correspond to an $A_2M$ spin system, similarly to what was observed for compound **T3**. The central atom of this allylic-$P_3$ unit ($P^M$, triplet) resonates at δ = -37 ppm while the other two P atoms ($P^A$, doublet) resonates at δ = 105 ppm. The coupling constant between these nuclei is $^1J_{PAM}$ = 380 Hz. Additionally, there are many other signals that cannot be assigned which also exist at room temperature. Regardless of several attempts, no compound could be isolated from the reaction mixture so far (cf. SI for NMR details).

## 7.3 References


[1] O. J. Scherer, H. Sitzmann, G. Wolmershäuser, J. *Organomet. Chem.* **1984**, *268*, C9-C12.
[2] Gordon, J. C.; Lee, V. T.; Poli, R. *Inorg. Chem*. **1993**, *32*, 4460-4463.
[3] A. Garbagnati, M. Seidl, G. Balázs, M. Scheer, *Inorg. Chem*. **2021**, *60*, 5163–5171.
[4] P. Pyykkç, M. Atsumi, *Chem. Eur. J*. **2009**, *15*, 12770–12779.
[5] S. Heinl, G. Balázs, M. Scheer, *Phosphorus, Sulfur, Silicon Relat. Elem.* **2014**, *189*, 1-9.
[6] Scherer, O. J.; Schwarz, G.; Wolmershäuser, *G. Z. Anorg. Allg. Chem*. **1996**, *622*, 951-957.
[7] Miluykov, V. A.; Sinyashin, O. G.; Lonnecke, P.; Hey-Hawkins, E. Mendeleev *Commun*. **2003**, *13*, 212-213.
[8] S. Alvarez, *Dalton Trans.* **2013**, *42*, 8617–8636 .
[9] M. Cousins, M. L. H. Green, *J. Chem. Soc.* **1964**, *95*, *56*, 1567-1572.


## 7.4 Supporting Information

### General procedures

All manipulations were carried out under an inert atmosphere of dried nitrogen using standard Schlenk and glove box techniques. Solvents were dried using a MB SPS-800 device of the company MBRAUN. Deuterated solvents were freshly distilled under nitrogen from $CaH_2$ ($CD_2Cl_2$) and from Na/K alloy ($C_6D_6$).

NMR spectra were recorded on a Bruker Advance III 400 MHz NMR spectrometer. If not differently mentioned, the chemical shifts were measured at room temperature and given in ppm; they are referenced to TMS for $^1H$ and 85% $H_3PO_4$ for $^{31}P$ as external standard. EI-MS spectra were measured on a JEOL AccuTOF GCX. Elemental Analysis (CHN) was determined using a Vario micro cube instrument. The X-Band EPR measurements were carried out with a MiniScope MS400 device with a frequency of 9.44 GHz and a rectangular resonator TE102 of the company Magnettech GmbH.

The compound $[CpMo(CO)_2(\eta^3\text{-}P_3)]$ (**1**) was synthesized according to literature procedure.[1] Phosphorous (V) chloride was purchased from abcr, Phosphorous (V) bromide (95%) from Alfa Aesar, Iodine from Sigma-Aldrich and they all were used as received without any further purifications.

### Synthesis of $[(CpMo)_2(\mu\text{-}I)_2(\mu\text{-}\eta^1\text{:}\eta^1\text{:}\eta^1\text{-}P_4I_4)]$ (T1)

$[CpMo(CO)_2(\eta^3\text{-}P_3)]$ (**1**) (9 mg, 0.03 mmol, 1 equiv.) is dissolved in 10 mL of $CH_2Cl_2$. To this solution, a solution of $I_2$ (22 mg, 0.09 mmol, 3 equiv.) in 10 mL of $CH_2Cl_2$ is added. A change in colour from bright yellow to dark brown is immediately observed. The solution is stirred at room temperature overnight and then is filtered over celite and stored at room temperature. After few weeks, $[(CpMo)_2(\mu\text{-}I)_2(\mu\text{-}\eta^1\text{:}\eta^1\text{:}\eta^1\text{-}P_4I_4)]$ crystallizes as dark red blocks, suited for X-ray analysis.

**Yield T1**: 5 mg (7%)

**EI-MS** ($CH_2Cl_2$): cation mode: *m/z* = 769.71 (30%, [**T1**$^+$]- $P_2I_3$), 700.62 (25%, [**T1**$^+$]- 4I), 637.68 (72%, [**T1**$^+$]- $P_2I_4$), 508.76 (100%, [**T1**$^+$]- $P_2I_5$).

**EA** calculated for $C_{10}H_{10}Mo_2P_4I_6$ (1207.43 g·mol$^{-1}$): C: 9.95, H: 0.83, found [%]: C:10.53, H: 0.97.

**Synthesis of $[(CpMo)_2(CO)_2(PCl_3)_2][PCl_6]$ (T2)**

$[CpMo(CO)_2(\eta^3\text{-}P_3)]$ (**1**) (9 mg, 0.03 mmol, 1 equiv.) and $PCl_5$ ( 18 mg, 0.09 mmol, 3 equiv.) are cool down to -60°C and suspended together in 10 mL of hexane. 10 mL of $CH_2Cl_2$ are added slowly to allow the complete dissolution of $PCl_5$. The reaction solution is stirred at -60°C for five minutes and then is stored at -80°C. After a few days, crystals of $[(CpMo)_2(CO)_2(PCl_3)_2][PCl_6]$ (**T2**) are formed as orange blocks.

**Yield T2**: a few crystals

**$^1$H NMR**: Due to the very low yield of **T2**, a low temperature NMR spectrum of the solution of the isolated crystals could not be performed. Contrarily to the signals of the $^{31}$P NMR spectrum that could be safely assigned from the NMR spectrum of the reaction solution at 213 K, for the $^1$H-NMR spectrum this was not possible.

**$^{31}$P{$^1$H} NMR** (162 MHz, $CD_2Cl_2$, 213 K): δ [ppm] = 199.1 (s, 2P, $[CpMo(CO)_2(PCl_3)_2]^+$), -296.2 (s, 1P, $[PCl_6]^-$)

Due to the high temperature sensibility, no MS or EA could be performed.

## Selected NMR spectra

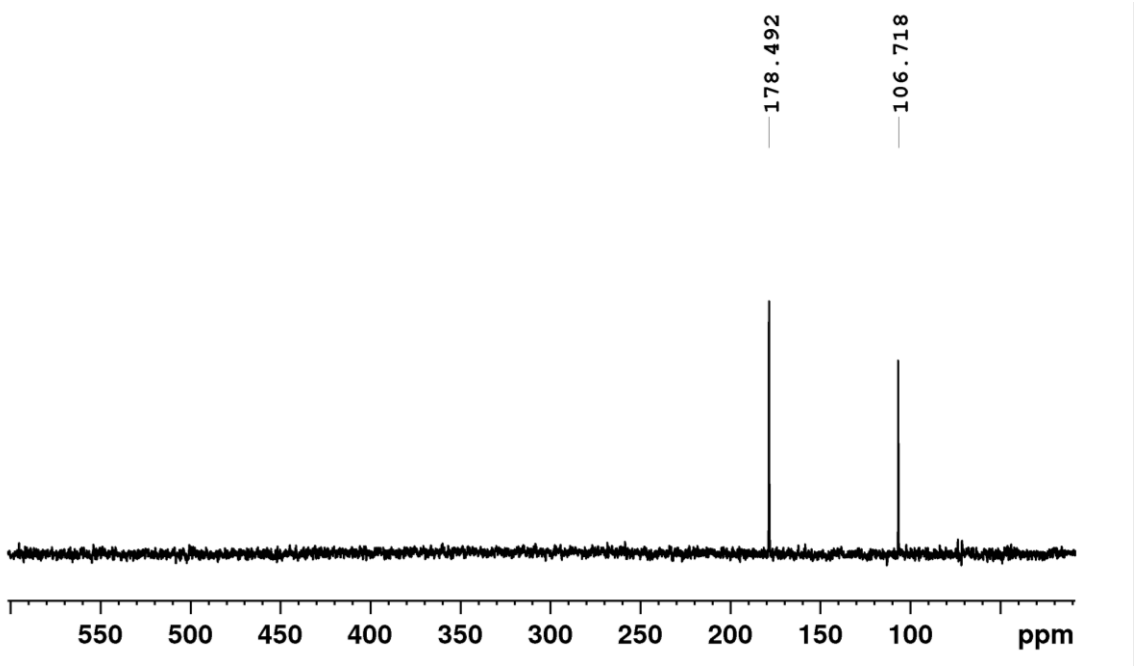


**Figure S 1.** $^{31}P\{^{1}H\}$ NMR spectrum of the solution of the reaction between **1** (1 equiv.) and $I_2$ (3 equiv.) ($C_6D_6$ capillary, 300 K). The signals at δ = 178.5 ppm corresponds to $PI_3$ while the one at δ = 106.7 belongs to $P_2I_4$. The exact same spectrum is obtained when **1A** is used instead of **1**.

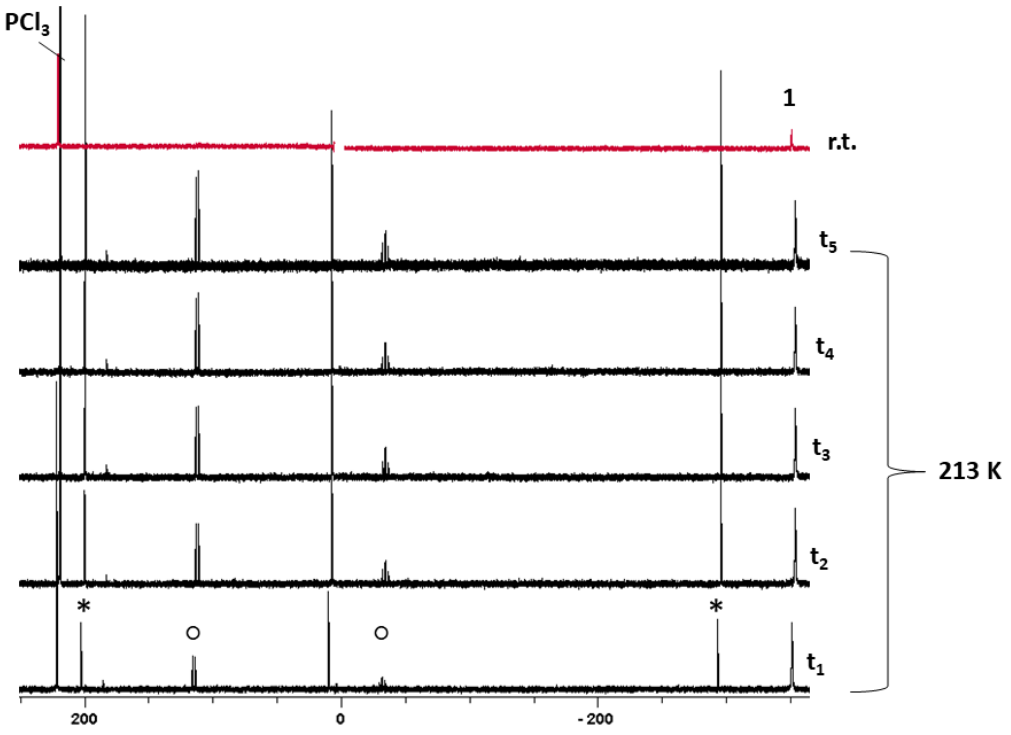


**Figure S 2.** Time dependent $^{31}P\{^{1}H\}$ NMR spectra of the reaction solution between **1** (1 equiv.) and $PCl_5$ (3 equiv.) ($CD_2Cl_2$, r.t and 213 K). Signals of **T2** are marked with *, while the signals of **T3** are marked with ○. ($t_1$ = 15 min, $t_2$ = 1 hour, $t_3$ = 2 hours, $t_4$ = 3 hours, $t_5$ = 4 hours).

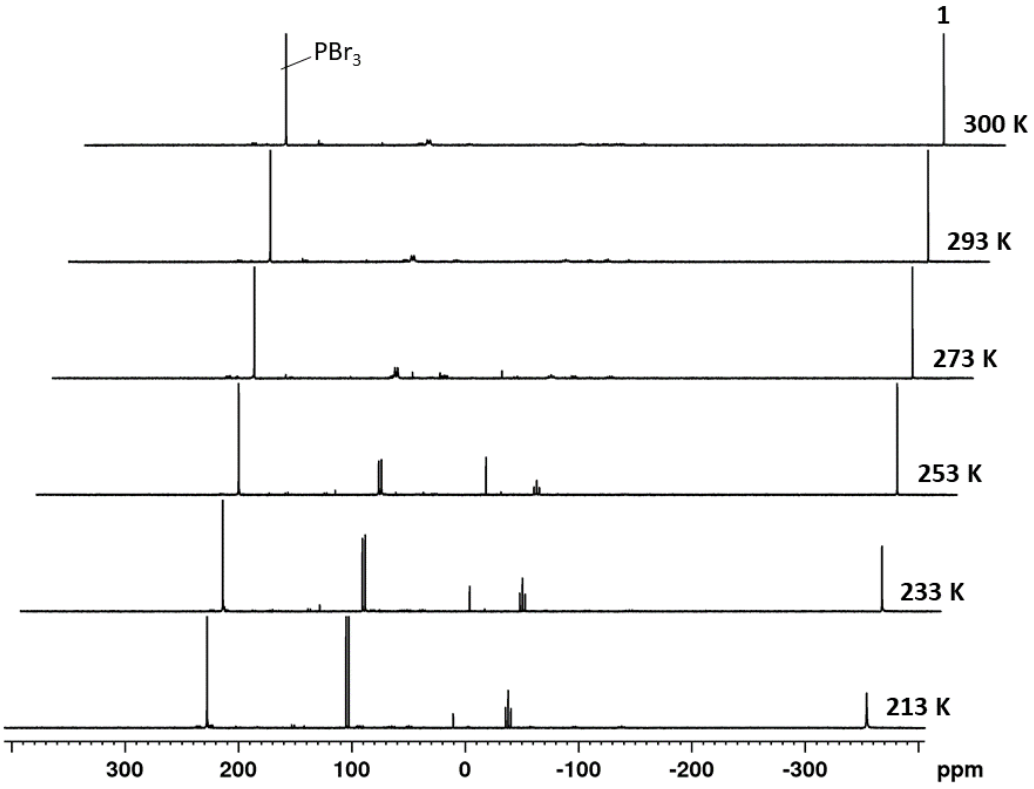


**Figure S 3** VT $^{31}P\{^{1}H\}$ NMR spectra of the solution of the reaction between **1** (1 equiv.) and $PBr_5$ (3 equiv.) ($CD_2Cl_2$, 213-300 K).

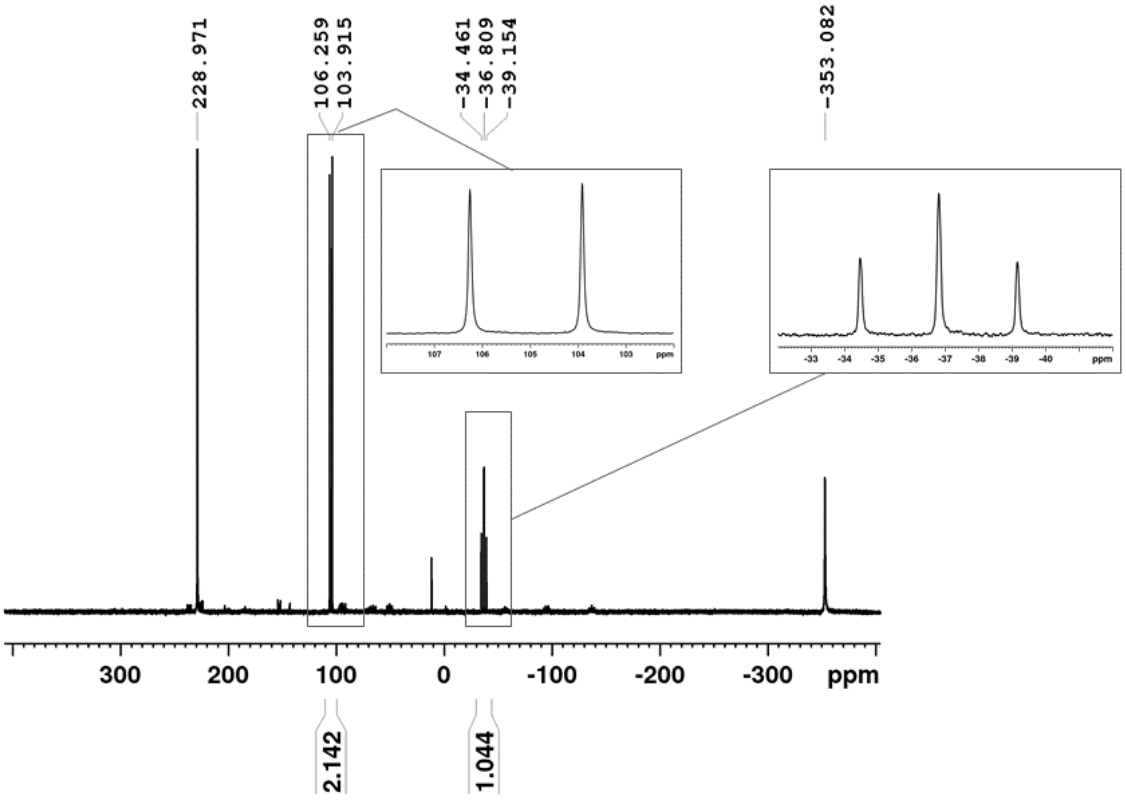


**Figure S 4.** $^{31}P\{^{1}H\}$ NMR spectrum of the solution of the reaction between **1** (1 equiv.) and $PBr_5$ (3 equiv.) ($CD_2Cl_2$, 213 K) with zoom of the signals from the $A_2M$ spin system.

**Crystallographic details**

The crystals were selected and mounted on a Rigaku (formerly Agilent Technologies) SuperNova diffractometer equipped with an Atlas detector (**T1**) and on a Supernova diffractometer equipped with a Titan$^{S2}$ detector (**T2**). All crystals were kept at a steady T = 123(1) K during data collection. Data collection and reduction were performed with **CrysAlispro** (Version 1. 171.40.14a (**T1**)[2], Version 1.171.39.37b (**T2**)[3]). For compound **T1** and **T2** an analytical absorption correction, an analytical numeric absorption correction using a multifaceted crystal model based on expressions derived by R.C. Clark & J.S. Reid using spherical harmonicas implemented in SCALE3 ABSPACK were applied. For compound **T2**, an additional spherical absorption correction using equivalent radius and absorption coefficient was used.

Using **Olex2**[4], all structures were solved by **ShelXT**[5] and a least square refinement on $F^2$ was carried out with **ShelXL**[6]. All non-hydrogens atoms were refined anisotropically. Hydrogen atom positions were calculated geometrically and refined using the riding model.

The images showing the compounds **T1**-**T2** were generated using **Olex2**.[4]

**Compound T1**: The asymmetric unit contains half molecule of the complex $[(CpMo)_2(\mu\text{-}I)_2(\mu\text{-}\eta^1\text{:}\eta^1\text{:}\eta^1\text{-}P_4I_4)]$ with the other half consisting of symmetry equivalent atoms.

**Compound T2**: The asymmetric unit contains two molecules of the complex $[(CpMo)_2(CO)_2(PCl_3)_2][PCl_6]$. Twin special details: Component 2 rotated by -179.9812° around [-0.42 0.00 0.91] (reciprocal) or [-0.00 0.00 1.00] (direct).

**Table S 1.** Crystallographic details of the compounds **T1** and **T2**.

| Compound | T1 | T2 |
|---|---|---|
| CCDC | - | - |
| Formula | $C_{10}H_{10}I_6Mo_2P_4$ | $C_{14}H_{10}Cl_{24}Mo_2O_4P_6$ |
| $D_{calc.}$/ g cm$^{-3}$ | 3.467 | 2.194 |
| $\mu$/mm$^{-1}$ | 74.324 | 14.875 |
| Formula Weight | 1207.34 | 1470.72 |
| Color | dark red | orange |
| Shape | block | block |
| Size/mm$^3$ | 0.18×0.10×0.02 | 0.17×0.06×0.04 |
| $T$/K | 123.01(10) | 123.00(10) |
| Crystal System | monoclinic | monoclinic |
| Flack Parameter | $C2/c$ | $P2/c$ |
| Hooft Parameter | 16.8481(6) | 24.4581(10) |
| Space Group | 9.5601(3) | 8.6372(2) |
| $a$/Å | 14.7403(5) | 23.4234(8) |
| $b$/Å | 90 | 90 |
| $c$/Å | 103.012(4) | 115.846(5) |
| $\alpha$/° | 90 | 90 |
| $\beta$/° | 2313.25(14) | 4453.2(3) |
| $\gamma$/° | 4 | 4 |
| V/Å$^3$ | 0.5 | 1 |
| $Z$ | 1.54184 | 1.39222 |
| $Z'$ | Cu K$_\alpha$ | Cu K\b |
| Wavelength/Å | 5.355 | 3.411 |
| Radiation type | 73.606 | 67.730 |
| $\Theta_{min}$/° | 6193 | 13539 |
| $\Theta_{max}$/° | 2242 | 13539 |
| Measured Refl's. | 2122 | 10157 |
| Ind't Refl's | 0.0424 | 0.0737 |
| Refl's with I > 2(I) | 100 | 452 |
| $R_{int}$ | 0 | 0 |
| Parameters | 2.600 | 0.991 |
| Restraints | -2.395 | -1.446 |
| Largest Peak | 1.090 | 1.071 |
| Deepest Hole | 0.1611 | 0.1673 |
| GooF | 0.1571 | 0.1517 |
| $wR_2$ (all data) | 0.0550 | 0.0779 |
| $wR_2$ | 0.0529 | 0.0569 |
| $R_1$ (all data) | $C_{10}H_{10}I_6Mo_2P_4$ | $C_{14}H_{10}Cl_{24}Mo_2O_4P_6$ |
| $R_1$ | 3.467 | 2.194 |

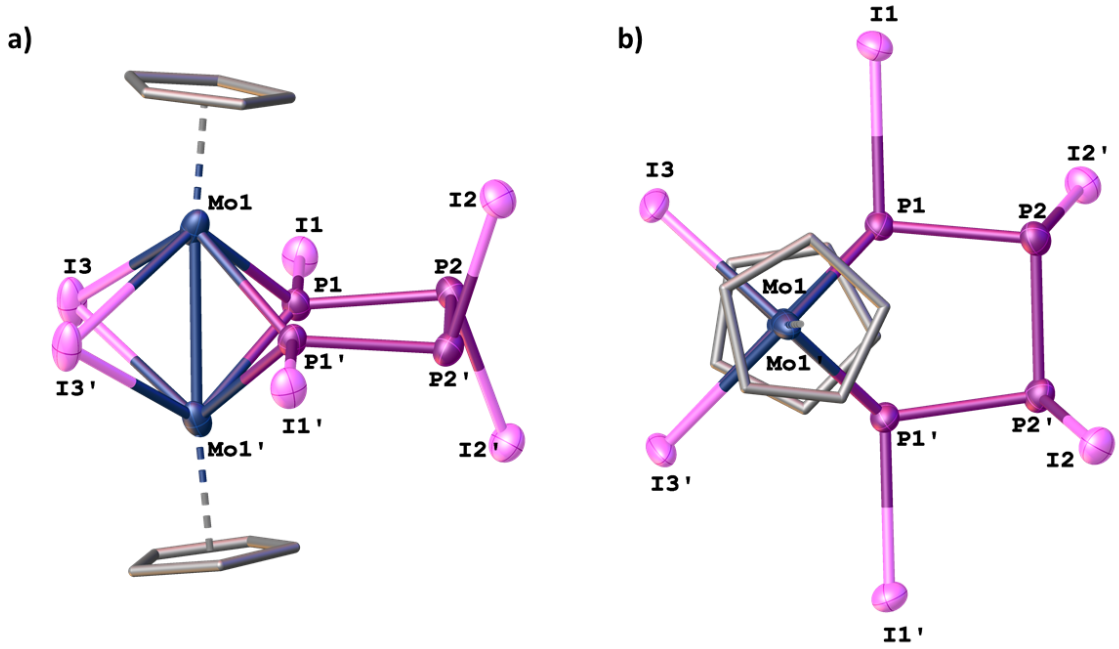


**Table S 2.** Selected bond lengths and angles of **T1**.

| **Selected bond length [Å]** | | **Selected bond angles [°]** | |
|---|---|---|---|
| **P1–P2** | 2.209(3) | **P1–P2–P2'** | 95.56(9) |
| **P2–P2'** | 2.238(5) | **P2–P2'–P1'** | 95.56(9) |
| **P1···P1'** | 2.701(5) | **P1-Mo1-P1'** | 69.54(10) |
| **Mo1-Mo1'** | 2.7306(14) | **I3-Mo1-P1** | 75.08(6) |

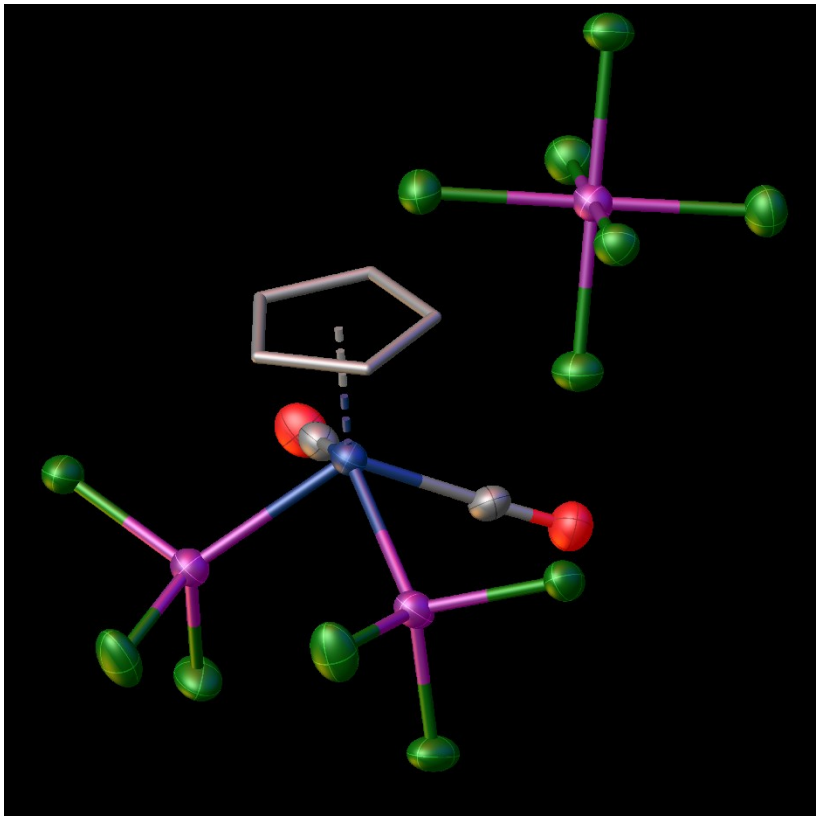

**Table S 3.** Selected bond lengths and angles of **T2**.

| Selected bond length [Å] | | Selected bond angles [°] | |
|---|---|---|---|
| **Mo1-P1** | 2.403(2) | **P1–Mo1–P2** | 86.57(8) |
| **Mo1-P2** | 2.433(2) | **Mo1-P2-Cl5** | 11.78(10) |
| **P1···P2** | 3.315(4) | **Cl22-P6-Cl23** | 89.23(14) |

## References


[1] O. J. Scherer, H. Sitzmann, G. Wolmershäuser, J. *Organomet. Chem.* **1984**, *268*, C9-C12.
[2] CrysAlisPro Software System, Rigaku Oxford Diffraction, **2018**.
[3] CrysAlisPro Software System, Rigaku Oxford Diffraction, **2017**.
[4] Dolomanov, O.V.; Bourhis, L.J.; Gildea, R.J.; Howard, J.A.K.; Puschmann, H. Olex2: A complete structure solution, refinement and analysis program. *J. Appl. Cryst.* **2009**, *42*, 339-341.
[5] Sheldrick, G.M. ShelXT-Integrated space-group and crystal-structure determination. *Acta Cryst.* **2015**, *A71*, 3-8.
[6] Sheldrick, G.M. Crystal structure refinement with ShelXL. *Acta Cryst.* **2015**, *C71*, 3-8.

# 8 Conclusion

The investigation of the redox chemistry of polypnictogen ligand complexes ($E_n$) has shown that the nature of the $E_n$ ligand affects the final product. [{CpMo(CO)$_2$}$_2$(μ,η$^2$:η$^2$-$E_2$)] (E = P (**A**), As, Sb, Bi) and [Cp*Fe(η$^5$-$P_5$)] form cationic radical species upon oxidation, that dimerize by the formation of a new E-E bond.[1],[2] When the $E_n$ ligand is part of a triple-decker complex, like in [(Cp*Mo)$_2$(μ,η$^6$:η$^6$-$P_6$)] (**B**), no dimerization occurs but only a bis-allylic distortion of the *cyclo*-$P_6$ ligand is observed.[3] When the compound that undergoes oxidation is a triple-decker complex which contains two separated $E_n$ units, like [(Cp'''Co)$_2$(μ,η$^2$:η$^2$-$E_2$)$_2$] (E = As (**C**), P(**D**)), the results are again different. Two new E-E bonds are formed after the withdrawal of one or two electrons leading to the formation of a *cyclo*-$E_4$ as middle deck.[4] When the substrate is an heterobimetallic triple-decker complex, like [(Cp*Fe)(Cp'''Co)(μ,η$^5$:η$^4$-$E_5$)] (E = P (**E**), As (**F**)), the oxidation leads to a planarization of the initially folded *cyclo*-$E_5$ ligand, whose folding is strongly dependent on the oxidation state.[5] After the successful investigation of the iodination of the pentaphosphametallocenes [Cp*M(η$^5$-$E_5$)] (M = Fe, Ru; E = P, As), which leads to fragmentation and rearrangement of the complex instead of dimerization,[6] it was clear that this harsher form of oxidation could be used as a complementary tool, for the synthesis of new polypnictogen complexes, with the one or two-electron withdrawal. The question arose as to what would happen when these compounds, whose redox properties have been elucidated, were reacted with halogens as a hint of classical oxidation. Within this thesis, a summary of the reactivity of the complexes **A**-**F** towards halogens ($I_2$, $Br_2$) and halogen sources ($PBr_5$, $PCl_5$) is presented. The reactivity is reported on the base of the $E_n$ ligand involved rather than of the halogen used because the first one resulted to be the variable that affects the results the most.

## 8.1 Halogenation of the diphosphorus complex [{CpMo(CO)$_2$}$_2$(μ,η$^2$:η$^2$-$P_2$)]

The first complex to be investigated was [{CpMo(CO)$_2$}$_2$(μ,η$^2$:η$^2$-$P_2$)] (**A**), a mimic of $P_4$ which represents an isolobal analogue in which two vertices are replaced by two {CpMo} fragments, to increase the stability of the starting material. The reactivity of **A** towards halogens is strongly dependent on the halogen used and on the stoichiometry of the reaction. In the case of $I_2$, the best reaction condition was achieved by reacting **A** with an excess of iodine, at room temperature. This afforded the isolation of the paramagnetic compound [(CpMo)$_4$(μ$_4$-P)(μ$_3$-PI)$_2$(μ-I)(I)$_3$(I$_3$)] (**2**, Scheme 1). DFT calculations indicated a triplet spin state for the latter, in line with the silent EPR spectra observed. The reaction

proceeds with the elimination of all CO groups from **A**, followed by aggregation of the formed species, under elimination of $PI_3$ and $P_2I_4$, respectively.

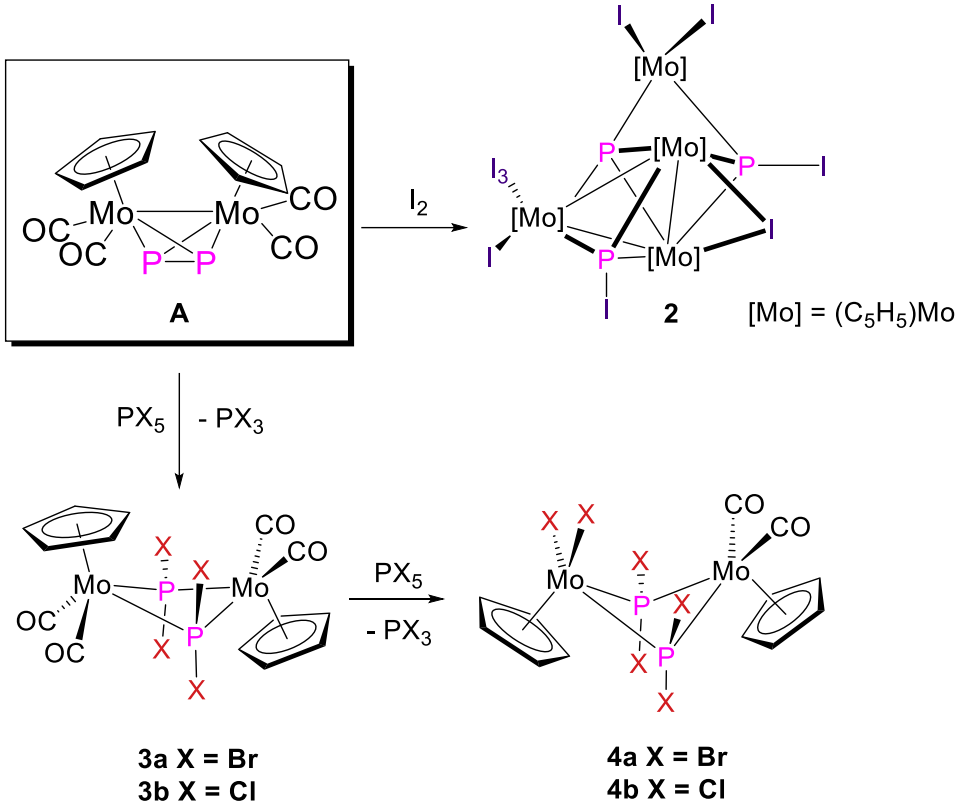


**Scheme 1.** Summary of the reactions of [{CpMo(CO)$_2$}$_2$(μ,η$^2$:η$^2$-P$_2$)] (**A**) with $I_2$ and $PX_5$ (X = Br, Cl).

The reaction of **A** towards $PBr_5$ (2 equiv.) proceeds with the halogenation of the P atoms, forming the bridging $PBr_2$ ligands of **3a** (Scheme 1), followed by the halogenation of one Mo atom, resulting in the final product **4a** (detected only after a week in the $^{31}$P NMR spectrum of the reaction solution, Scheme 1). When an excess of $PBr_5$ was used instead, **4a** could be directly obtained. The same products were obtained with $Br_2$, with some differences regarding the yield and the formation of side products. When $PCl_5$ was used instead, the analogue of **3a** and **4a**, **3b** and **4b**, respectively (Scheme 1), could be isolated, showing for **A** a very similar reactivity towards $Br_2$ and $Cl_2$ sources. The main difference concerned the isolation of **3b**, which was not achieved because it was always formed in a mixture with **4b**. The latter, on the other hand, could be isolated in almost quantitative yield when an excess of $PCl_5$ was used. With both $PBr_5$ and $PCl_5$, the decomposition of part of **A** in the form of $PX_3$ (not derived from $PX_5$ itself, X = Br, Cl,) was observed. The amount of the latter was however different depending on the halogen, allowing to explain the different yield of the final product **4a** and **4b** (54% *versus* 91%, respectively).

To summarize, the halogenation of **A** resulted to be different from its one electron oxidation, which leaded to its dimerization into [{CpMo(CO)$_2$}$_4$(μ,η$^2$:η$^2$:η$^2$:η$^2$-P$_4$)]$^{2+}$.[3] After

the successful iodination of the pentaphosphametallocenes,[6] this study allowed us to add $Br_2$ and $Cl_2$ sources like $PBr_5$ and $PCl_5$, respectively, to the list of oxidizing agents that can be used for the synthesis of new functionalized $E_n$ ligand complexes.

## 8.2 Halogenation of the triple-decker complex [(Cp*Mo)$_2$(μ,η$^6$:η$^6$-P$_6$)]

After having found that bromination and chlorination are potentially powerful tools for the synthesis of new polypnictogen complexes together with the iodination, the variable to change was now the $E_n$ ligand. Therefore, the halogenation of the triple-decker complex [(Cp*Mo)$_2$(μ,η$^6$:η$^6$-P$_6$)] (**B**), bearing a *cyclo*-P$_6$ ligand as middle deck, was investigated.

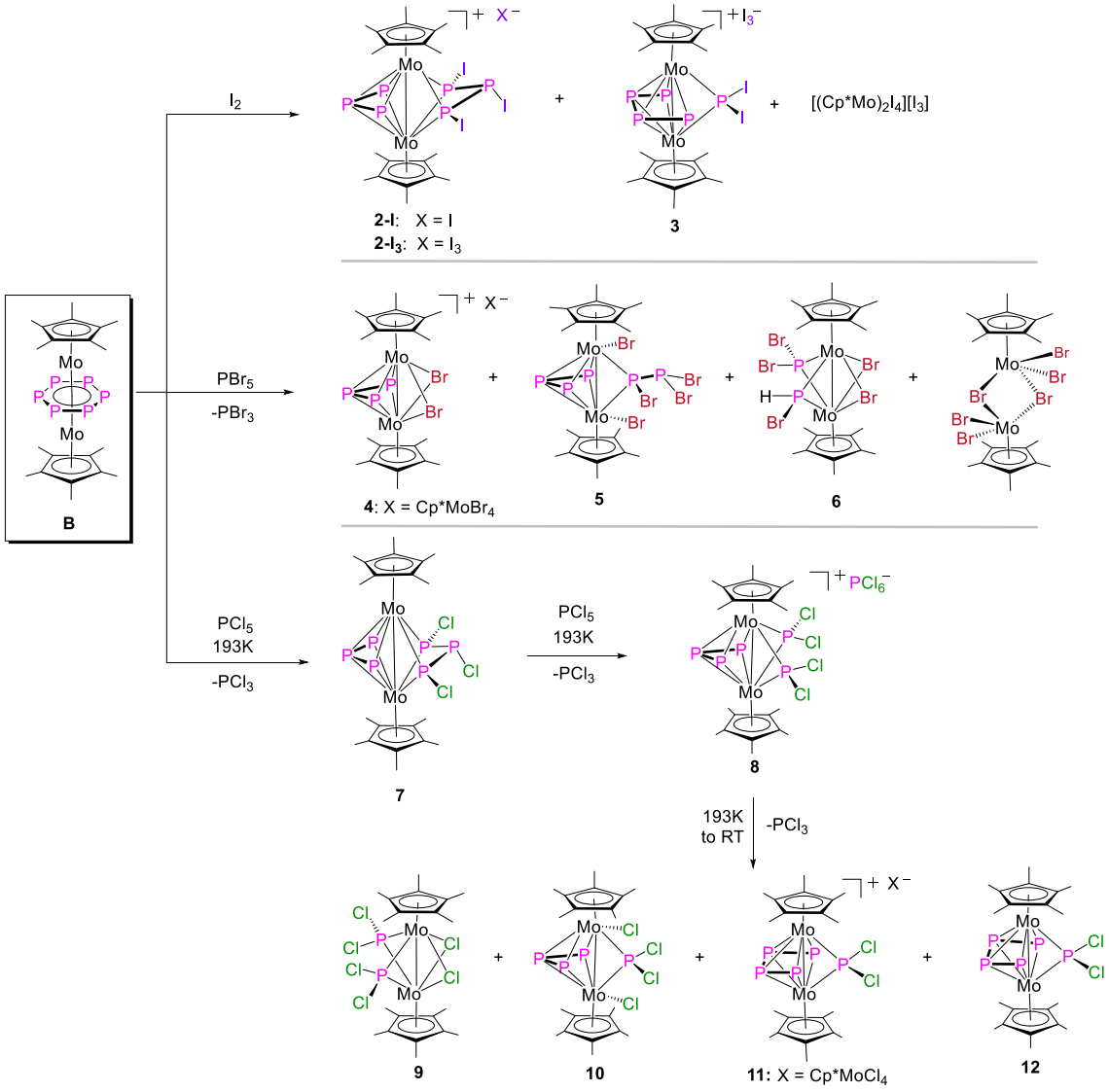


**Scheme 2.** Summary of the reactions of [(Cp*Mo)$_2$(μ,η$^6$:η$^6$-P$_6$)] (**B**) with $I_2$ and $PX_5$ (X = Br, Cl).

All the presented results (Scheme 2) were obtained by the same conditions, meaning with an excess (6 equiv.) of halogen or halogen source, with $CH_2Cl_2$ as solvent and, where not differently specified, at room temperature.

The reaction of **B** with $I_2$ afforded its full conversion into the ionic compounds $[(Cp^*Mo)_2(\mu,\eta^3{:}\eta^3\text{-}P_3)(\mu,\eta^1{:}\eta^1{:}\eta^1\text{-}P_3I_3)][I_3]$ (**2-I₃**, Scheme 2) and $[(Cp^*Mo)_2(\mu,\eta^4{:}\eta^4\text{-}P_4)(\mu\text{-}PI_2)][I_3]$ (**3**, Scheme 2) and in the paramagnetic complex $[(Cp^*Mo)_2(\mu\text{-}I)_4][I_3]$, which was only detected in the ESI-MS spectrum of the reaction solution. When $PBr_5$ was used instead, the reaction was started at lower temperature to have a better control. This way, compounds $[(Cp^*Mo)_2(\mu,\eta^3{:}\eta^3\text{-}P_3)(\mu\text{-}Br)_2][Cp^*MoBr_4]$ (**4**, Scheme 2), $[(Cp^*MoBr)_2(\mu,\eta^3{:}\eta^3\text{-}P_3)(\mu\text{-}P_2Br_3)]$ (**5**, Scheme 2) and $[(Cp^*Mo)_2(\mu\text{-}PBr_2)(\mu\text{-}PBr)(\mu\text{-}Br)_2]$ (**6**, Scheme 2) and the side product $[(Cp^*MoBr_2)_2(\mu\text{-}Br)_2]$ could be isolated. When **B** was reacted with $PCl_5$, the reduced selectivity of the reaction required to work at lower temperature. The $^{31}P$ NMR investigation at -80°C revealed a spin system of the type AMM'OO'X, which could be assigned to **7**, based on its similarity to **2**. Attempts to crystallize it leaded to the isolation of $[(Cp^*Mo)_2(\mu,\eta^3{:}\eta^3\text{-}P_3)(\mu\text{-}PCl_2)_2][PCl_6]$ (**8**, Scheme 2) instead (74% yield). The latter is also instable at room temperature and further $^{31}P$ NMR investigation showed its complete decomposition and formation of the diamagnetic complexes **9** and **10** (Scheme 2), which then could be isolated, and their molecular structure elucidated. These two compounds could also be obtained by performing the reaction of **B** with $PCl_5$ directly at room temperature. The $^{31}P$ NMR spectrum of the reaction solution shows the signals of **9** and **10**, among others that could not be assigned. The attempts to isolate these other products afforded the isolation of the paramagnetic compound **11** instead (Scheme 2), which was afterwards proved to be an additional product resulting from the decomposition of **8**. When **B** was reacted with three equivalents of $PCl_5$, the analogue of **11** *i.e.* $[(Cp^*Mo)_2(\mu,\eta^4{:}\eta^4\text{-}P_4)(\mu\text{-}PCl_2)]$ (**12**, Scheme 2), could be isolated. The latter is also paramagnetic but EPR silent, probably due to its triplet spin state.

To conclude, the halogenation of **B** shows a way to synthesize a plethora of complexes bearing different $P_n$ units. The final products are phosphorus free complexes of the type $[Cp^*MoX_n]$ as well as $PX_3$. Contrarily to the halogenation of **A**, we could not observe similarities in the reactivity of the $E_n$ ligand towards $PBr_5$ and $PCl_5$, with the reactivity with the latter needing a lower temperature to isolate some of the products. The only product that could be compared with the one obtained by the one electron oxidation of **B** is **2-I₃**, with P-P bond lengths and distances similar to the one of the bis-allylic distorted *cyclo*-$P_6$.

## 8.3 Halogenation of the triple-decker complexes with two separated $E_2$ units $[(Cp'''Co)_2(\mu,\eta^2{:}\eta^2\text{-}E_2)_2]$ (E = P, As)

After observing the different reactivity from the tetrahedrane complex **A** to the triple-decker complex **B**, the question arose as to how compounds having a high steric protection of two separated $E_n$ ligands in a triple-decker moiety will react towards halogens or halogen

sources. Therefore, the halogenation of the complexes $[(Cp'''Co)_2(\mu,\eta^2:\eta^2\text{-}E_2)_2]$ (E = As (**C**), P(**D**)) was investigated.

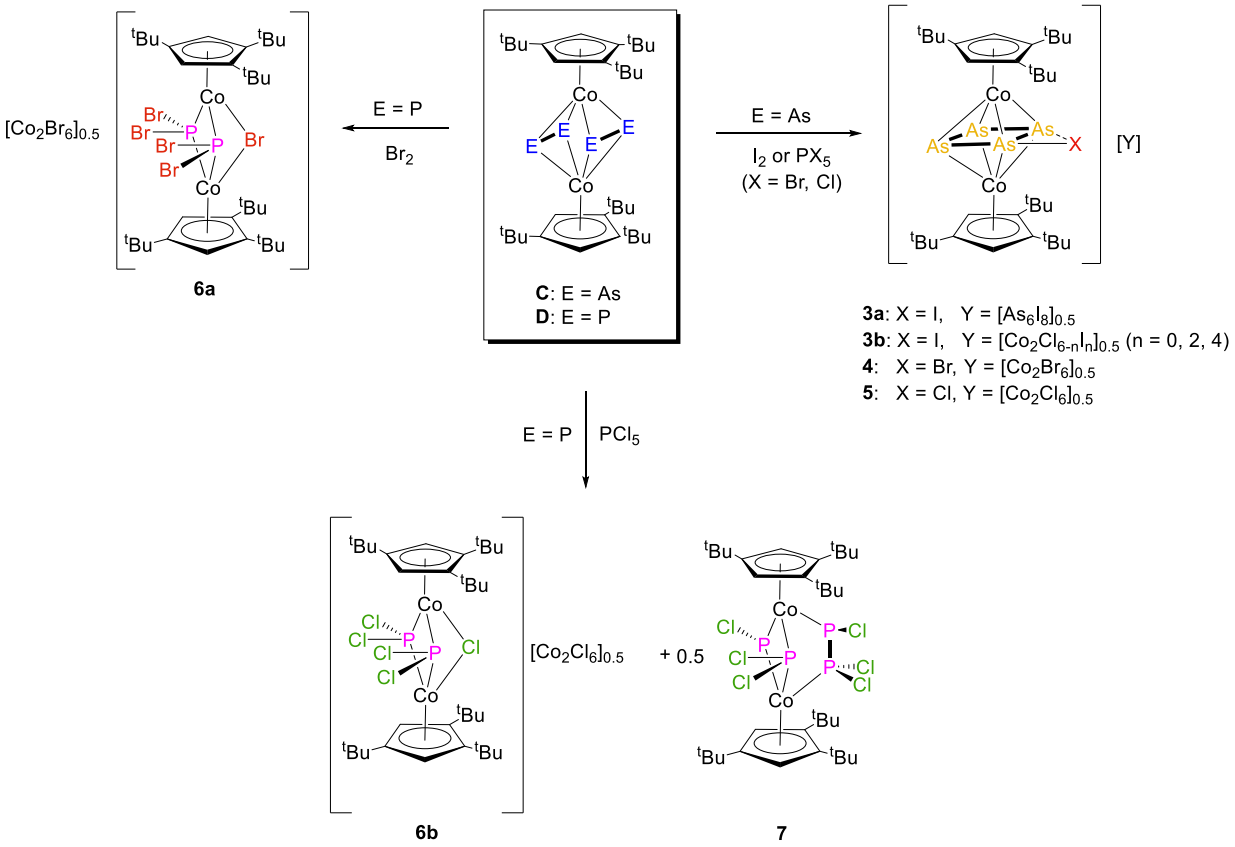


**Scheme 3.** Summary of the reactions of $[(Cp'''Co)_2(\mu,\eta^2:\eta^2\text{-}E_2)_2]$ (E = As (**C**), P (**D**)) with $X_2$ (X = I, Br) and $PCl_5$.

The reaction of **C** with an excess of halogen or halogen sources ($I_2$, $PX_5$, X = Br, Cl) afforded the isolation of the three isostructural compounds $[(Cp'''Co)_2(\mu,\eta^4:\eta^4\text{-}As_4I)][As_6I_8]_{0.5}$ (**3a**), $[(Cp'''Co)_2(\mu,\eta^4:\eta^4\text{-}As_4Br)][Co_2Br_6]_{0.5}$ (**4**) and $[(Cp'''Co)_2(\mu,\eta^4:\eta^4\text{-}As_4Cl)][Co_2Cl_6]_{0.5}$ (**5**, Scheme 3). All of them bear a strongly distorted cyclic $As_4X$ ligand, with one long As-As bond, whose presence was proved by DFT calculations. In the case of the P-analogue **D**, the $^{31}P$ NMR spectrum of the reaction solution with $I_2$ or $PBr_5$ was empty. For the $I_2$, the only products detected at room temperature were the complex $[Cp'''CoI_2]$ and $P_2I_4$. Following the reaction of **D** with $I_2$ at variable temperature by $^{31}P$ NMR spectroscopy, it was possible to observe, between 213 and 233 K, the formation of a diamagnetic species which decomposes with the increasing of the temperature and that could not be isolated so far. On the other hand, when **D** was reacted with $Br_2$ at low temperature, the ionic complex $[(Cp'''Co)_2(\mu\text{-}PBr_2)_2(\mu\text{-}Br)][Co_2Br_6]_{0.5}$ (**6a**, Scheme 3) could be isolated. The Cl-analogue of the latter, $[(Cp'''Co)_2(\mu\text{-}PCl_2)_2(\mu\text{-}Cl)][Co_2Cl_6]_{0.5}$ (**6b**), was isolated at room temperature, when $PCl_5$ was used as the halogen source, together with the neutral compound $[(Cp'''Co)_2(\mu\text{-}PCl_2)(\mu\text{-}PCl)(\mu,\eta^1:\eta^1\text{-}P_2Cl_3]$ (**7**, Scheme 3). Intrigued by

the idea of finding an alternative way to achieve the formation of E-X bonds, avoiding the harsh conditions of the halogenation, we decided to react the ionic species $[(Cp'''Co)_2(\mu,\eta^4{:}\eta^4\text{-}E_4)][TEF]_2$ (E = As (**8**), P (**9**)) with nucleophilic halides, to "quench" their Lewis acidity (Scheme 4).

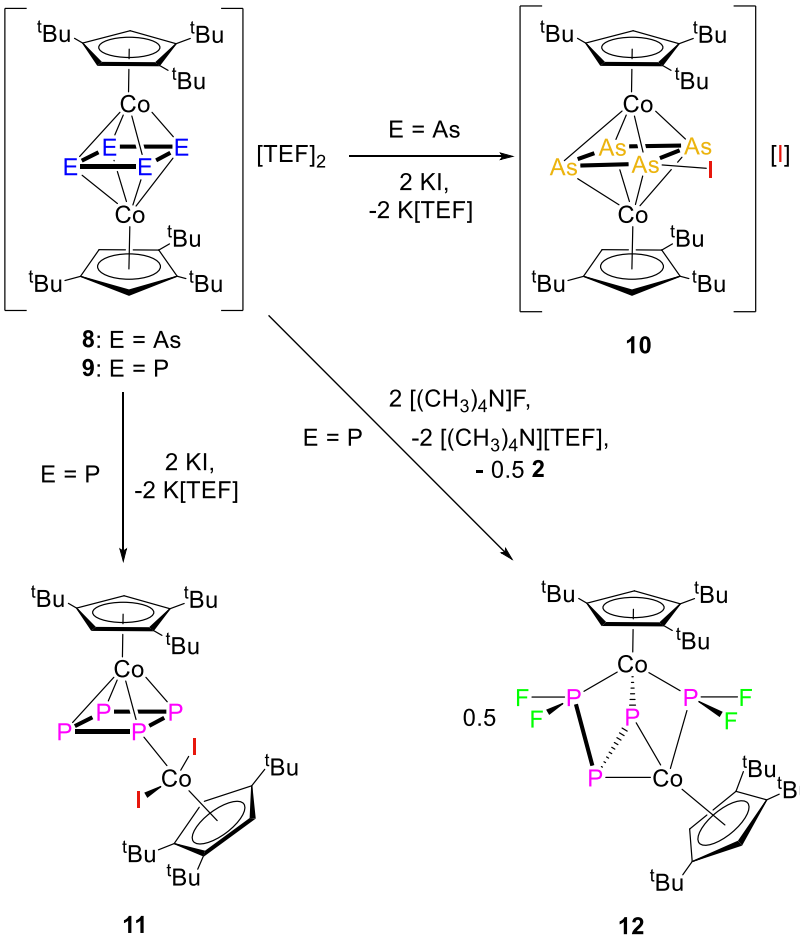


**Scheme 4.** Summary of the reactions of $[(Cp'''Co)_2(\mu,\eta^4{:}\eta^4\text{-}E_4)][TEF]_2$ (E = As (**8**), P(**9**)) with KI and $[(CH_3)_4N][TEF]$.

The reaction of **8** with KI afforded $[(Cp'''Co)_2(\mu,\eta^4{:}\eta^4\text{-}As_4I)][I]$ (**10**, Scheme 4), the analogue of **3a**, with very similar As-As bond lengths but a different anion. When the phosphorus analogue **9** was reacted with KI, the new compound $[(Cp'''Co)(Cp'''CoI_2)(\mu,\eta^4{:}\eta^1\text{-}P_4)]$ (**11**, Scheme 4) could be isolated, resulted from the iodination of one of the Co atoms. Due to the promising results obtained with KI, the next step was to use a nucleophilic fluorinating agent such as ($[(CH_3)_4N]F$), to overcome the use of stronger fluorine sources like $XeF_2$ and $PF_5$, which in previous works led only to decomposition of the starting material, to form transition metal complexes bearing P-F bonds. The reaction of **9** with ($[(CH_3)_4N]F$) proceeded as a disproportionation of **9** into **D** and $[(Cp'''Co)_2(\mu\text{-}PF_2)(\mu,\eta^2{:}\eta^1{:}\eta^1\text{-}P_3F_2)]$ (**12**, Scheme 4), with the latter being the first example of a complex bearing a $P_3F_2$ ligand coordinated to a transition metal.

To summarize, the products of the halogenation of **C** are somehow comparable with the monocations formed with its one electron oxidation, even if the mechanism of their formation is different. On the other hand, the halogenation of **D** leaded to completely different results, revealing that the nature of the pnictogen ligand affects the reactivity towards the halogens, contrarily to the response of the same compounds to the one or two electron oxidation. Additionally, it was shown that an alternative and milder way to the formation of new E-X bonds could be achieved by reacting the ionic species **8** and **9** with nucleophilic halides.

## 8.4 Halogenation of the heterobimetallic triple-decker complexes [(Cp*Fe)(Cp'''Co)(μ,η$^5$:η$^4$-E$_5$)] (E = P, As)

As the last substrates of this work, triple-decker complexes bearing two different metal fragments {Cp*Fe} and {Cp'''Co} were selected. Therefore, the halogenation of [(Cp*Fe)(Cp'''Co)(μ,η$^5$:η$^4$-E$_5$)] (E = P (**E**), As (**F**)) was followed. The reaction of **E** with $I_2$ and $Br_2$ afforded the isostructural ionic complexes [(Cp*Fe)(Cp'''Co)(μ,PI)(μ,η$^2$:η$^1$:η$^1$-$P_4I_4$)][$I_3$] (**2**, Scheme 5) and [(Cp*Fe)(Cp'''Co)(μ,PBr)(μ,η$^2$:η$^1$:η$^1$-$P_4Br_4$)][$FeBr_4$] (**3**, Scheme 5), respectively. When the halogen source was $PCl_5$, the reaction led to [(Cp*Fe)(Cp'''Co)(μ,$PCl_2$)(μ,η$^2$:η$^1$:η$^1$-$P_4Cl_4$)] (**4**, Scheme 5), which represents the neutral analogue of **2** and **3** with the central bridging PX ligand (X = I, Br) replaced by a $PCl_2$ unit, and to the compound [(Cp*Fe)(Cp'''Co)(μ,$PCl_2$)$_2$(μ,η$^1$:η$^1$-$P_2Cl_3$)] (**5**, Scheme 5). Compounds **2**-**4** bear all an unprecedented $FeCoP_5$ nortricyclane-like core. The reaction of the heavier homologue **F** towards $I_2$ and $Br_2$ leads to two isostructural compounds, [(Cp'''Co)$_2$(μ,η$^4$:η$^4$-$As_4I$)][$FeI_4$] (**7**, Scheme 5) and [(Cp'''Co)$_2$(μ,η$^4$:η$^4$-$As_4Br$)][$FeBr_4$] (**9**, Scheme 5). Additionally, with $I_2$, the trinuclear compound [(Cp*Fe)(Cp'''Co)$_2$(μ$_3$,η$^4$:η$^4$-$As_6$)][$FeI_4$] (**8**, Scheme 5) could be isolated. **7** and **9** include an homometallic cation analogue to the one observed for the halogenation products of **C**. The reaction of **F** with $PCl_5$ resulted in the ionic compound [(Cp*Fe)(Cp'''Co)(μ,η$^5$:η$^5$-$As_5$)][$FeCl_4$]$_2$ (**10**, Scheme 5) which bears a planarized *cyclo*-$As_5$ ligand but no As-Cl bonds. The dication of **10** is comparable to the one formed by the two electron oxidation of **F**. To conclude, the halogenation of the heterobimetallic triple-decker complexes **E** and **F** has shown that the nature of the pnictogen atom affects the products formed, in contrast to what observed for their two electrons oxidation. For both species, the reactivity towards $I_2$ and $Br_2$ is comparable, while a different result is observed when a chlorine source is used.

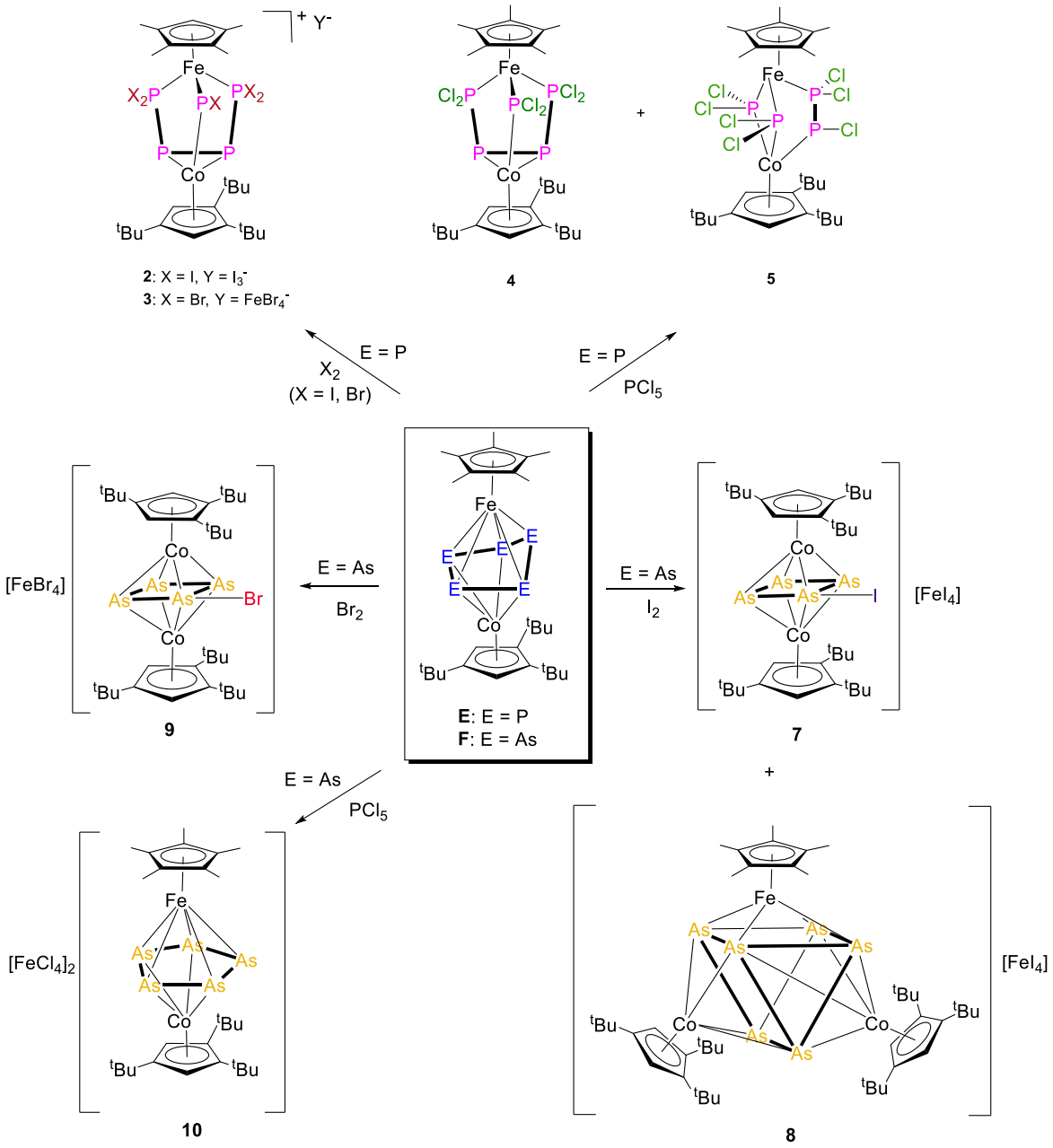


**Scheme 5.** Summary of the reactions of [(Cp*Fe)(Cp'''Co)(μ,η$^5$:η$^4$-E$_5$)] (E = P (**E**), As (**F**)) with $X_2$ (X = I, Br) and $PCl_5$.

## 8.5 Influence of the $E_n$ ligand on the halogenation reactions

As mentioned at the beginning of this chapter, the $E_n$ ligand involved in the halogenation reactions was the variable with the highest influence on the different products obtained. It is not possible to find a general trend based on the halogen used because the outcome was always different from one polypnictogen complex to the other. While in some cases the reactivity of the respective $E_n$ ligand compound was similar towards $Br_2$ and $Cl_2$ sources but completely different with $I_2$ (*e.g.* with **A** and **D**), in other cases it was comparable to $I_2$ and $Br_2$ and different towards $PCl_5$ (*e.g.* with **E** and **F**), or the same with all the halogens

(*e.g*. with **C**). On the other hand, with **B** the reactivity was different towards all the halogen sources, with the formation of similar products among the iodinated or chlorinated derivatives or among the brominated and chlorinated ones. The halogenation of the tetrahedrane complex **A**, compared to **B**, has a higher chemoselectivity. The halogenation of the triple decker complexes led in general to a large number of products, especially when $PCl_5$ was involved. Specifically, for **B**, it was observed that the chlorination reaction requires a lower temperature to isolate some of the products. The investigation of this reactivity for compounds **C**-**F** showed that the nature of the pnictogen ligand affect the final products, contrarily to what observed for the one- or two-electron oxidation of the same compounds.

In conclusion, the halogenation can be considered as an additional tool for the synthesis of new functionalized $E_n$ ligand complexes, whose related difficulties (high number of products, low yields) can be partly “balanced” by the opportunity of further functionalization of the products obtained.

[1] L. Dütsch, M. Fleischmann, S. Welsch, G. Balázs, M. Scheer, *Angew. Chem. Int. Ed*. **2018**, *57*, 3256-3261.
[2] M. V. Butovskiy, G. Balázs, M. Bodensteiner, E. V. Peresypkina, A. V. Virovets, J. Sutter, Manfred Scheer, *Angew. Chem. Int. Ed*. **2013**, *52*, 2972 –2976.
[3] M. Fleischmann, F. Dielmann, G. Balázs, M. Scheer, *Chem. Eur. J*. **2016**, *22*, 15248-15251
[4] M Piesch, C. Graβl, M. Scheer, *Angew. Chem. Int. Ed*. **2020**, *59*, 7154-7160.
[5] M. Piesch, S. Reichl, C. Riesinger, M. Seidl, G. Balázs, M. Scheer, *Chem. Eur. J*. **2021**, *27*, 9129-9140.
[6] H. Brake, E. V. Peresypkina, A. V. Virovets, M. Piesch, W. Kremer, L. Zimmermann, Ch. Klimas, M. Scheer, *Angew. Chem. Int. Ed.* **2020**, *59*, 16241-16246.

# 9 Appendix

## 9.1 Thematic List of Abbreviations

### NMR Spectroscopy

| | |
|---|---|
| NMR | Nuclear Magnetic Resonance |
| δ | chemical shift |
| ppm | part per million |
| Hz | Hertz, s-1 |
| *J* | coupling constant, Hz |
| s | singlet |
| d | doublet |
| t | triplet |
| m | multiple |
| br | broad |
| $\omega_{1/2}$ | half width at full maximum, Hz |
| VT | variable temperature |
| COSY | Correlated Spectroscopy |
| TMS | Tetramethylsilane, Si(CH3)4 |

### Mass Spectrometry

| | |
|---|---|
| MS | mass spectrometry |
| $[M]^+$ | molecular ion peak |
| m/z | mass to charge ratio |
| LIFDI | liquid injection field desorption ionization |
| FD | field desorption |
| ESI | electro spray ionization |
| EI | electron impact |

### IR Spectroscopy

| | |
|---|---|
| IR | infrared spectroscopy |
| ν̃ | wavenumber |
| br | broad |

### Solvents

| | |
|---|---|
| thf | tetrahydrofuran, $C_4H_8O$ |
| tol | toluene, $C_7H_8$ |
| $CH_2Cl_2$ | dichloromethane |
| CH3CN | acetonitrile |

### Ligands and substituents

| | |
|---|---|
| R | organic substituent |
| Me | Methyl, $-CH_3$ |
| Et | Ethyl, $-CH_2CH_3$ |
| 18-C-6 | 18-Crown-6, $[C_2H_4O]_6$ |
| *$^t$Bu* | *tert*-Butyl, $-C_4H_9$ |
| Cp | cyclopentadienyl, $\eta^5$-$C_5H_5$ |
| Cp* | $\eta^5$-$C_5Me_5$ |
| Cp''' | $\eta^5$-$C_5H_2{}^tBu_3$, 1,2,4-tris-tert-butylcyclopentadienyl |

### Other

| | |
|---|---|
| Å | Armstrong, 1 Å =$1\cdot10^{-10}$ m |
| T | temperature |
| K | Kelvin |
| °C | Degree Celsius |
| D | distance |
| r.t. | room temperature |
| M | metal |
| L | ligand |
| DFT | density functional theory |
| VE | valence electrons |
| E | group 15 element |

## Acknowledgements

Now that I am at the end of this experience, I would like to thank all the people who contributed to the realization of this thesis.

First, Prof. Dr. Manfred Scheer for giving me the opportunity to join his working group, working on this interesting research topic and for his advice and supervision in the realization of this project.

Dr. Gábor Balázs, for helping and guiding me in the research project with so much patience during all these years, for listening and always taking the time to discuss any problem.

Dr. Fabian Spitzer, thank you for welcoming me, together with Susi, with so much affection, for introducing me to the research project and to the life of the working group.

Dr. Michael Seidl, for all his endless work in refining all the structures, but above all for being a dear friend.

Dr. Julian Müller, for his invaluable help in the laboratory but especially for the nice times together.

Dr. Martin Piesch, for always finding the time to answer my questions and for all his advice.

All the people from the staff of the Central Analytical Services of the University of Regensburg: X-ray, MS, EA and NMR department. Especially, Tuan Anh Nguyen, Annette Schramm, Georgine Stühler, Barbara Baumann, Josef Kiermaier and Wolfgang Söllner for the countless analytics measurements of the samples.

All the colleagues, past and present, of the Scheer group, Schotti, Petra, Martina, Barbara and Mina, for these years together.

All the member of the Bauer group. Noel, thank you for your sincere friendship.

All the amazing people that this experience has allowed me to meet, Ola and Darek, Giulia and Claudia, for all the good memories we have created here.

Andrea, for being there in the hardest part, making it easier.

My whole family, for constantly loving and supporting me.

Miky, for sharing the ups and downs of the entire journey, for being my safe place and to genuinely share the joy of this achievement.

Finally, Nicolò. Thank you for another adventure together and for making beautiful every day we spend together, no matter what happens in the world.